NUREG/CR-4551
SAND86-1309
Vol. 2, Rev. 1. Part 4

Evaluation of Severe Accident Risks: Quantification of Major Input Parameters

Experts' Determination of Source Term Issues

Prepared by
F. T. Harper, R. J. Breeding, T. D. Brown, J. J. Gregory, H. N. Jow,
A. C. Payne, E. D. Gorham, C. N. Amos, J. Helton, G. Boyd

Sandia National Laboratories
Operated by
Sandia Corporation

Prepared for
U.S. Nuclear Regulatory Commission

NUREG/CR-4551
SAND86-1309
Vol. 2, Rev. 1, Part 4

Evaluation of Severe Accident Risks: Quantification of Major Input Parameters

Experts' Determination of Source Term Issues

Prepared by
F. T. Harper, R. J. Breeding, T. D. Brown, J. J. Gregory, H. N. Jow,
A. C. Payne, E. D. Gorham, C. N. Amos, J. Helton, G. Boyd

Sandia National Laboratories
Operated by
Sandia Corporation

Prepared for
U.S. Nuclear Regulatory Commission

AVAILABILITY NOTICE

Availability of Reference Materials Cited in NRC Publications

Most documents cited in NRC publications will be available from one of the following sources:

1. The NRC Public Document Room, 2120 L Street, NW., Lower Level, Washington, DC 20555

2. The Superintendent of Documents, U.S. Government Printing Office, P.O. Box 37082, Washington, DC 20013-7082

3. The National Technical Information Service, Springfield, VA 22161

Although the listing that follows represents the majority of documents cited in NRC publications, it is not intended to be exhaustive.

Referenced documents available for inspection and copying for a fee from the NRC Public Document Room include NRC correspondence and internal NRC memoranda; NRC bulletins, circulars, information notices, inspection and investigation notices; licensee event reports; vendor reports and correspondence; Commission papers; and applicant and licensee documents and correspondence.

The following documents in the NUREG series are available for purchase from the GPO Sales Program: formal NRC staff and contractor reports, NRC-sponsored conference proceedings, international agreement reports, grant publications, and NRC booklets and brochures. Also available are regulatory guides, NRC regulations in the *Code of Federal Regulations*, and *Nuclear Regulatory Commission Issuances*.

Documents available from the National Technical Information Service include NUREG-series reports and technical reports prepared by other Federal agencies and reports prepared by the Atomic Energy Commission, forerunner agency to the Nuclear Regulatory Commission.

Documents available from public and special technical libraries include all open literature items, such as books, journal articles, and transactions. *Federal Register* notices, Federal and State legislation, and congressional reports can usually be obtained from these libraries.

Documents such as theses, dissertations, foreign reports and translations, and non-NRC conference proceedings are available for purchase from the organization sponsoring the publication cited.

Single copies of NRC draft reports are available free, to the extent of supply, upon written request to the Office of Administration, Distribution and Mail Services Section, U.S. Nuclear Regulatory Commission, Washington, DC 20555.

Copies of industry codes and standards used in a substantive manner in the NRC regulatory process are maintained at the NRC Library, 7920 Norfolk Avenue, Bethesda, Maryland, for use by the public. Codes and standards are usually copyrighted and may be purchased from the originating organization or, if they are American National Standards, from the American National Standards Institute, 1430 Broadway, New York, NY 10018.

NUREG/CR-4551
SAND86-1309
Vol. 2, Rev. 1, Part 4

Evaluation of Severe Accident Risks: Quantification of Major Input Parameters

Experts' Determination of Source Term Issues

Manuscript Completed: May 1992
Date Published: June 1992

Prepared by
F. T. Harper, R. J. Breeding, T. D. Brown, J. J. Gregory, H. N. Jow,
A. C. Payne, E. D. Gorham, C. N. Amos[1], J. Helton[2], G. Boyd[3]

Sandia National Laboratories
Albuquerque, NM 87185-5800

Prepared for
Division of Safety Issue Resolution
Office of Nuclear Regulatory Research
U.S. Nuclear Regulatory Commission
Washington, DC 20555
NRC FIN A1228

[1]Science Applications International Corporation, Albuquerque, NM
[2]Arizona State University, Tempe, AZ
[3]Safety and Reliability Optimization Services, Inc., Knoxville, TN

ABSTRACT

This report records part of the vast amount of information received during the expert judgment elicitation process that took place in support of the NUREG-1150 effort sponsored by the U.S. Nuclear Regulatory Commission. The results of the Source Term Expert Panel are presented in this part of Volume 2 of NUREG/CR-4551. The Source Term Panel considered eight issues:

1. In-vessel fission product release and retention;

2. Ice condenser decontamination factor at Sequoyah;

3. Revolatilization from the Reactor Coolant System/Reactor Pressure Vessel;

4. Core-Concrete Interaction fission product release;

5. Release of Reactor Coolant System and Core-Concrete Interaction species from containment;

6. Late sources of iodine from water pools;

7. Reactor Building decontamination factor at Peach Bottom;

8. Release during direct containment heating.

This report begins with a brief discussion of the methods used to elicit the information from the experts. The information for each issue is then presented in five sections: (1) a brief definition of the issue, (2) a brief summary of the technical rationale supporting the distributions developed by each of the experts, (3) a brief description of the operations that the project staff performed on the raw elicitation results in order to aggregate the distributions, (4) the aggregated distributions, and (5) the individual expert elicitation summaries. The individual expert elicitation summaries were written soon after the elicitation and were sent to the experts for review. They represent the raw results as received directly from the experts.

CONTENTS

FIGURES

Issue 1

FIGURES (Continued)

FIGURES (Continued)

FIGURES (Continued)

Issue 5

FIGURES (Continued)

FIGURES (Continued)

TABLES

TABLES (Continued)

TABLES (Continued)

TABLES (Continued)

TABLES (Continued)

TABLES (Continued)

TABLES (Continued)

TABLES (Continued)

TABLES (Continued)

TABLES (Continued)

TABLES (Continued)

TABLES (Continued)

Issue 8

FOREWORD

This is one of many documents that constitute the technical basis for the NUREG-1150 document produced by the NRC Office of Nuclear Regulatory Research. This document's purpose is to present the results of the elicitations performed by the Source Term Expert Panel. The document consists of the distributions and associated technical rationale provided by the expert panel for the phenomenological questions posed by the NUREG-1150 analysts.

Figure 1 identifies all the documents that present the results of the accident progression analysis, the source term analysis, the consequence analysis, and the overall risk integration. Three interfacing programs performed this work: the Accident Sequence Evaluation Program (ASEP), the Severe Accident Risk Reduction Program (SARRP), and the PRA Phenomenology and Risk Uncertainty Evaluation Program (PRUEP). Table 1 is a list of all of the original primary documentation (published in 1987) and the corresponding revised documentation that supports the current version of NUREG-1150.

The current NUREG/CR-4551 covers the analysis included in the original NUREG/CR-4551 and NUREG/CR-4700. The accident progression event trees originally documented in NUREG/CR-4700 are now documented in the appendices of Volumes 3 to 7 of NUREG/CR-4551.

Originally, NUREG/CR-4550 was published without the designation "Draft for Comment." Thus, the final revision of NUREG/CR-4550 is designated Revision 1. The label Revision 1 is used consistently on all volumes, including Volume 2 which was not part of the original documentation. NUREG/CR-4551 was originally published as a "Draft for Comment"; so, in its final form, no Revision 1 designator is used to maintain consistency with NUREG-4550 documents.

There are several other reports published that are closely related to NUREG/CR-4551. These are:

NUREG/CR-5380, SAND88-2988, S. J. Higgins, "A User's Manual for the Postprocessing Program PSTEVNT," Sandia National Laboratories, Albuquerque, NM, November 1989.

NUREG/CR-5360, SAND89-0943, H.-N. Jow, W. B. Murfin, and J. D. Johnson, "XSOR Codes User's Manual," Sandia National Laboratories, Albuquerque, NM, 1989.

NUREG/CR-4624, BMI-2139, R. S. Denning et al., "Radionuclide Release Calculations for Selected Severe Accident Scenarios," Volumes I-V, Battelle Memorial Institute, Columbus, OH, 1986.

NUREG/CR-5062, BMI-2160, M. T. Leonard et al., "Supplemental Radionuclide Release Calculations for Selected Severe Accident Scenarios," Battelle Memorial Institute, Columbus, OH, 1988.

NUREG/CR-5331, SAND89-0072, S. E. Dingman et al., "MELCOR Analyses for Accident Progression Issues," Sandia National Laboratories, Albuquerque, NM, 1989.

NUREG/CR-5253, SAND88-2940, R. L. Iman, J. C. Helton, and J. D. Johnson, "PARTITION: A Program for Defining the Source Term/Consequence Analysis Interfaces in the NUREG-1150 Probabilistic Risk Assessments User's Guide," Sandia National Laboratories, Albuquerque, NM, May 1989.

NUREG/CR-5382, SAND88-2695, J. C. Helton et al., "Incorporation of Consequence Analysis Results into the NUREG-1150 Probabilistic Risk Assessments," Sandia National Laboratories, Albuquerque, NM, 1989.

NUREG/CR-5174, SAND88-1607, J. Michael Griesmeyer and L. N. Smith, "A Reference Manual for the Event Progression Analysis Code (EVENTRE)," Sandia National Laboratories, Albuquerque, NM, September 1989.

NUREG/CR-5262, SAND88-3093, R. L. Iman, J. D. Johnson, and J. C. Helton, "A User's Guide for the Probabilistic Risk Assessment Model Integration System (PRAMIS)," Sandia National Laboratories, Albuquerque, NM, May 1990.

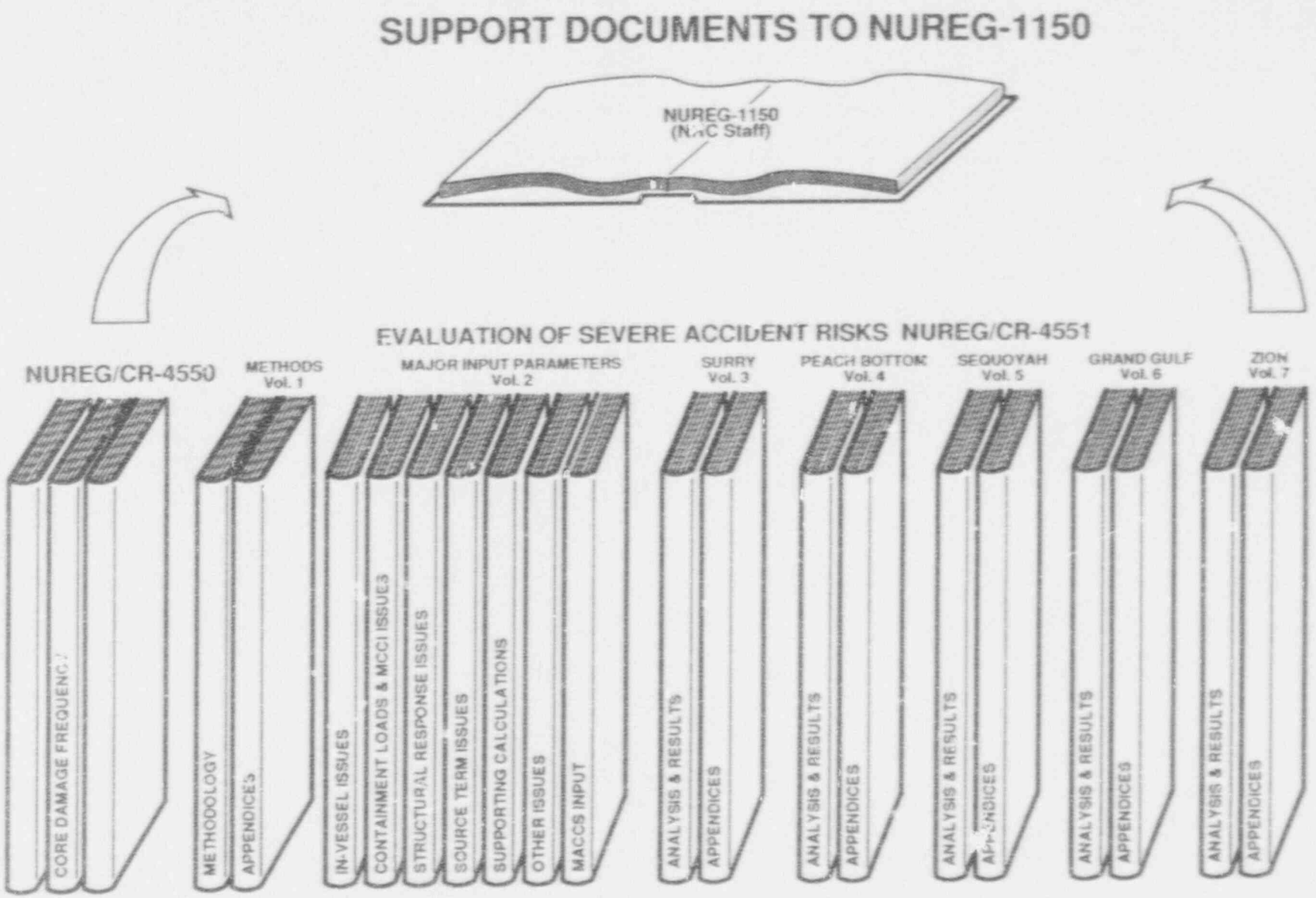

Figure 1. Back-End Documentation for NUREG-1150.

Table 1 NUREG-1150 Analysis Documentation

Original Documentation

NUREG/CR-4550		NUREG/CR-4551		NUREG/CR-4700	
Analysis of Core Damage Frequency From Internal Events		Evaluation of Severe Accident Risks and the Potential for Risk Reduction		Containment Event Analysis for Potential Severe Accidents	
Vol.	1 Methodology	Vol.	1 Surry Unit 1	Vol.	1 Surry Unit 1
	2 Summary (Not Published)		2 Sequoyah Unit 1		2 Sequoyah Unit 1
	3 Surry Unit 1		3 Peach Bottom Unit 2		3 Peach Bottom Unit 2
	4 Peach Bottom Unit 2		4 Grand Gulf Unit 1		4 Grand Gulf Unit 1
	5 Sequoyah Unit 1				
	6 Grand Gulf Unit 1				
	7 Zion Unit 1				

Revised Documentation

NUREG/CR-4550, Rev. 1, Analysis of Core Damage Frequency		NUREG/CR-4551, Rev. 1, Eval. of Severe Accident Risks	
Vol.	1 Methodology	Vol.	1 Part 1, Methodology; Part 2, Appendices
	2 Part 1 Expert Judgment Elicit. Expert Panel		2 Part 1 In-Vessel Issues
	Part 2 Expert Judgment Elicit. Project Staff		Part 2 Containment Loads and MCCI Issues
			Part 3 Structural Issues
			Part 4 Source Term Issues
			Part 5 Supporting Calculations
			Part 6 Other Issues
			Part 7 MACCS Input
	3 Part 1 Surry Unit 1 Internal Events		3 Part 1 Surry Analysis and Results
	Part 2 Surry Unit 1 Internal Events App.		Part 2 Surry Appendices
	Part 3 Surry External Events		
	4 Part 1 Peach Bottom Unit 2 Internal Events		4 Part 1 Peach Bottom Analysis and Results
	Part 2 Peach Bottom Unit 2 Int. Events App.		Part 2 Peach Bottom Appendices
	Part 3 Peach Bottom Unit 2 External Events		
	5 Part 1 Sequoyah Unit 1 Internal Events		5 Part 1 Sequoyah Analysis and Results
	Part 2 Sequoyah Unit 1 Internal Events App.		Part 2 Sequoyah Appendices
	6 Part 1 Grand Gulf Unit 1 Internal Events		6 Part 1 Grand Gulf Analysis and Results
	Part 2 Grand Gulf Unit 1 Internal Events App.		Part 2 Grand Gulf Appendices
	7 Zion Unit 1 Internal Events		7 Part 1 Zion Analysis and Results
			Part 2 Zion Appendices

ACKNOWLEDGMENTS

The authors would like to acknowledge all of the participants in the expert judgment elicitation process including the expert panels, the normative experts, the substantive experts, and the utility and industry experts who attended the meetings. While we wrote most of the actual report, the members of the expert panels provided us with most of the technical substance. We would in particularly like to thank Steve Hora of the University of Hawaii for his role in developing the expert judgment elicitation methodology, Ralph Keeney of the University of Southern California for his assistance in directing the elicitation process, Reeta Garber of Sandia National Laboratories for preparing this report, Ann Shiver of Sandia National Laboratories for aggregating the results and visually presenting these in figures, and Timothy Wheeler for providing not only the template for this report but also for much of the prose in the introductory sections. We also appreciate the support of Joseph Murphy, Mark Cunningham, and P. K. Niyogi of the NRC.

ACRONYMS AND INITIALISMS

ADS	automatic depressurization system
AICC	adiabatic isochoric complete combustion
AIChE	American Institute of Chemical Engineers
ANL	Argonne National Laboratory
ANS	American Nuclear Society
APET	accident progression event tree
ASME	American Society of Mechanical Engineers
ATWS	anticipated transient without scram
BNL	Brookhaven National Laboratory
BPNL	Battelle Pacific Northwest Laboratory
BWR	boiling water reactor
CCI	core-concrete interaction
CDF	cumulative distribution function
CL	containment load
CRD	control rod drive
DBA	design basis accident
DCH	direct containment heating
DDT	deflagration-to-detonation transition
DOE	Department of Energy
EPRI	Electric Power Research Institute
FCI	fuel coolant interaction
FAI	Fauske and Associates, Inc.
FSAR	final safety analysis report
HPME	high pressure melt injection
IC	ice condenser
IDCOR	Industry Degraded Core Rulemaking
INEL	Idaho National Engineering Laboratory
KFK	Kernforschungszentrum, Karlsruhe
LOCA	loss-of-coolant accident
LMFBR	liquid-metal fast breeder reactor
LMR	liquid-metal reactor
LSD	least significant difference
LWR	light water reactor
MAAP	Modular Accident Analysis Program
MCCI	molten core-coolant interactions
ORNL	Oak Ridge National Laboratory
PORV	power-operated relief valve
PRA	probabilistic risk analysis
PWR	pressurized water reactor

RCP	reactor coolant pump
RCS	reactor coolant system
RPV	reactor pressure vessel
RF	release fraction
RMA	Risk Manag ment Associates
SAARP	severe accident risk reduction program
SAIC	Science Applications International Corporation
S&W	Stone and Webster
SLC	standby liquid control
SNL	Sandia National Laboratories
SRV	safety relief valve
TVA	Tennessee Valley Authority
UHI	upper head injection
USC	University of Southern California
UCHB	unconditional hydrogen burn
UP	upper plenum

1. INTRODUCTION

The United States Nuclear Regulatory Commission (NRC) has prepared NUREG-1150[1] to examine the risk of accidents in a selected group of nuclear power plants. The three main objectives of NUREG-1150 are given below.

1. Prepare a current assessment of the severe accident risks of five nuclear power plants that will:

   - Provide a "snapshot" of risks reflecting plant design and operational characteristics, related failure data, and severe accident phenomenological information extant in March 1988;
   - Update the estimates of NRC's 1975 risk assessment, the Reactor Safety Study;
   - Include quantitative estimates of risk uncertainty, in response to a principal criticism of the Reactor Safety Study; and
   - Identify plant-specific risk vulnerabilities, in context of the NRC's individual plant examination process.

2. Summarize the perspectives gained in performing these risk analyses, with respect to:

   - Issues significant to severe accident frequencies, consequences, and risks;
   - Uncertainties for which the risk is significant and which may merit further research;
   - Comparisons with NRC's safety goals;
   - The potential benefits of a severe accident management program in reducing risk; and
   - The potential benefit of other plant modifications in reducing risk.

3. Provide a set of methods for the prioritization of potential safety issues and related research.

In support of NUREG-1150 and as part of the Accident Sequence Evaluation Program (ASEP) and the Severe Accident Risk Reduction Program (SARRP), Sandia National Laboratories (SNL) has directed the production of Level 3 probabilistic risk assessments (PRAs) for the Surry, Sequoyah, Peach Bottom, and Grand Gulf nuclear power plants. (Level 1 PRAs contain accident sequence analyses developed to the point of core damage. Level 2 PRAs include Level 1 and accident progression analyses; and Level 3 PRAs include Level 1, Level 2, and consequence analyses.) A PRA for the fifth NUREG-1150 plant, Zion, has been prepared by EG&G Idaho, Inc., of the Idaho National Engineering Laboratory (INEL) (Level 1) and Brookhaven National Laboratory (BNL) (Levels 2 and 3). Two of these analyses (Surry and Peach Bottom) include external events.

Expert judgment elicitation is an integral part of the methods used to produce the PRAs in support of NUREG-1150. Expert judgment is used where applicable experimental data or complete analyses are inadequate. Such situations are common in analysis of rare events and complicated severe accident phenomena. The purpose of this report is to provide the results and technical rationale obtained from the Source Term Panel. The expert judgment methodology is presented in detail in NUREG/CR-4551 Volume 1.

Expert judgments are expressions of opinion, based on knowledge and experience, that experts make in responding to technical problems. Specifically, the judgments represent the expert's state of knowledge at the time of response to the technical question. Expert judgment is not restricted to the experts' answer but includes the experts' mental processes (definitions, assumptions, and algorithms) for arriving at answers.

Expert judgment is necessarily used in technical fields. Because these judgments are often implicit, they are sometimes not acknowledged as being expert judgments. For example, expert judgment is frequently used implicitly, even unconsciously, when researchers make decisions about defining problems, establishing boundary conditions, or screening data. By contrast, expert judgment can be obtained explicitly, through formal processes.

Risk assessment frequently needs explicit expert judgment as a source of data, particularly if one or more of the following situations exist:

1. No other data (analytical or experimental) for predicting the outcome of phenomena are available;

2. High variability characterizes the data;

3. Experts question the applicability of the data;

4. Existing data need to be supplemented, interpreted, or incorporated with model or code calculations;

5. Analysts need to determine the state of knowledge about what is currently known, what is not known, and what is worth learning.

The issue selection process consisted of accumulating an extensive list of potential issues by plant or across plants and then evaluating the significance of each issue. Expert panel members participated in the issue selection by reviewing the issues selected and rejected for the expert judgment process and recommended the addition, deletion, or modification of issues from the initial list.

Eight source term issues were considered important enough to be the subject of a formal expert judgment elicitation. Table 1-1 lists these issues.

Section 2 of this report briefly outlines the expert selection process and gives a short biographical sketch of each expert. Section 3 describes the fundamental expert judgment elicitation methodology. Section 4 lists the meetings held for the Source Term Expert Panel and the people who gave

Table 1-1
Source Term Issues Considered for Expert Judgment Elicitation

	Issue	Applicable Plants
1.	Release of Fission Products from the Fuel in the Vessel and from the Vessel to the Containment	All
2.	Decontamination of Fission Products by the Ice Condenser at Sequoyah	Sequoyah
3.	Fission Products Released by Revolatilization from the Reactor Coolant System (RCS)	All
4.	Fraction of Fission Products Released During the Core-Concrete Interactions	All
5.	Release of Fission Products from Containment for Surry, Zion, Sequoyah and Grand Gulf--FCONV & FCONC	Surry Sequoyah Zion Grand Gulf
6.	BWR Late Iodine Release from the Suppression Pool and Reactor Cavity Water	Peach Bottom Grand Gulf
7.	Peach Bottom Reactor Building Decontamination Factor	Peach Bottom
8.	Radionuclide Release Associated with Pressure Driven Melt Expulsion from the Reactor Coolant System	All

presentations at the meetings. Section 5 constitutes the bulk of this report and contains a description of each issue considered, a summary of the technical rationale applied by the experts to the issue, a description of the method use to aggregate the expert's distributions, the aggregated distributions, and written accounts of each individual's response to the question. The individual expert's narrative includes the distributions and the detailed rationale behind the distributions. Each account was written by the substantive expert who assisted with the elicitation. In all cases, the experts were given ample opportunity to review these written accounts and approve them. In a few cases, the expert did not respond and were informed that their lack of response would be assumed to be tacit approval of the write-up.

REFERENCE

1. U. S. Nuclear Regulatory Commission, "Severe Accident Risks: An Assessment for Five U. S. Nuclear Power Plants," NUREG-1150, Vol. ., Office of Nuclear Regulatory Research, June 1989. (Second Draft for Peer Review)

2. EXPERT CREDENTIALS

The objective for selecting the panel members was to obtain experts with as much expertise as possible in the fields of source terms. The project attempted to include a wide diversity of expertise that encouraged alternative points of view. The selection of experts should preclude stakeholders in the findings of NUREG-1150 from participating as members of the expert panel. This led to several criteria in selecting the experts:

1. Experts should have demonstrated experience by authoring publications, hands-on experience, and consulting or managing research in the areas related to the issues;

2. Experts should represent a wide variety of experience as is obtained in universities, consulting firms, laboratories, nuclear utilities, or government agencies;

3. Experts should represent as wide a perspective of the issues as possible; and

4. Experts should be willing to be elicited under the methodology to be used.

To ensure proper representation, letters were sent to many organizations requesting nominations for experts to serve on the in-vessel, containment loads, molten core/containment interaction, structural response, and source term panels. Some of the organizations that received these letters are listed below:

Atomic Energy of Canada LTD.
Battelle Memorial Institute
Bechtel Western Power Company
Brookhaven National Laboratory
Commonwealth Edison
Electric Power Research Institute
General Electric
Idaho National Engineering Laboratory (EG&G Idaho, Inc.)
Illinois Department of Nuclear Safety
International Technology Corporation
MHB Technical Associates
New York Power Authority
NUMARC
Oak Ridge National Laboratory
Philadelphia Electric Co.
Sandia National Laboratories
Stone and Webster Engineering Corporation
Systems Energy Resources, Inc.
Tennessee Valley Authority
U.S. Nuclear Regulatory Commission
Virginia Electric Power Co.
Westinghouse Electric Corp.

It was impossible to satisfy each criterion entirely for every expert/issue combination. Nevertheless, we were pleased with the high quality and objectivity of the experts. The experts chosen for the source term issues were:

Peter Bieniarz	Risk Management Associates
Andrzej Drozd	Stone and Webster Engineering Corporation
James Gieseke	Battelle Columbus Laboratories
Robert Henry	Fauske & Associates
Thomas Kress	Oak Ridge National Laboratory
Y. H. (Ben) Liu	University of Minnesota
Dana Powers	Sandia National Laboratories
Richard Vogel	Electric Power Research Institute
David Williams	Sandia National Laboratories

Brief biographical sketchs of the experts are presented below.

Source Term Expert Panel

PETER P. BIENIARZ. Peter Bieniarz is President of Risk Management Associates, Inc. He has been heavily involved in the severe accident analysis field from both the PRA and fission product behavior ends. As part of his work, Mr. Bieniarz has been either involved in or directed several PRA's and has developed several analytical methods for calculating the progression of severe accidents. Prior to establishing Risk Management Associates, Mr. Bieniarz was the General Manager of the Albuquerque office of Energy, Inc., and Senior Technical Consultant with Pickard Lowe and Garrick, Inc.

ANDRZEJ DROZD. Andrzej Drozd is a Senior Nuclear Technology Engineer at Stone and Webster Engineering Corporation (S&W). He holds both a M.S. degree in Mechanical Engineering from Warsaw Polytechnic, Poland, and a M.S. degree in Nuclear Engineering from Rensselaer Polytechnic Institute (RPI) in Troy, New York. At S&W he is currently assigned to the Source Term Project. In this position he is responsible for developing methodologies for thermal-hydraulic and fission product transport analyses for severe accidents. He performed calculations for the LACE and DEMONA experiments as well as for OECD/GREST code comparison exercise. He was also responsible for the sodium fire studies performed by S&W for the FFTF power addition and was involved in the licensing hearings of a BWR Mark II plant. Having been awarded an International Atomic Energy Agency (IAEA) fellowship he was assigned for one year to the CNEN-CSN Laboratory at Cassacia, Italy. While in Poland, he was involved in LOCA analyses at the Institute for Nuclear Research. Also, he served as a member of the Technical Program Committee and Session Chairman at 3rd International Meeting on Reactor Thermal Hydraulics, Newport, RI, October 1985.

JAMES A. GIESEKE. Dr. Gieseke manages the Environmental Physics and Chemistry Section at Battelle's Columbus Laboratories. The technical make-up of this section is quite diverse with emphases being placed on technical areas of atmospheric chemistry, particulate technology, process and environmental engineering, geochemistry, and water quality. In addition to his management duties, Dr. Gieseke specializes in research related to the dynamics of aerosol particles. He is an expert in a wide variety of disciplines including: particle formation; interaction of particles with gases and with other particles; design of particle sampling and collection equipment; and, in particular, the analyses of gas and particle behavior during transport by gas flows.

In various analytical and experimental programs sponsored by the U.S. Nuclear Regulatory Commission over the past 14 years, he has performed and managed studies concerned with the nature of fission product release from the core region and subsequent aerosol behavior within enclosed vessels and along various flow paths for use in reactor safety analyses. These studies have included the development of models for predicting the behavior of concentrated aerosols undergoing simultaneous agglomeration, sedimentation, and deposition on surfaces, as well as the interaction of fission product vapors with system and particle surfaces. In related studies, he has directed experimental measurements of the nature of highly agglomerated aerosols as well as their transport and deposition.

Dr. Gieseke is a member of the Air Pollution Control Association, American Chemical Society, American Association for Aerosol Research, American Institute of Chemical Engineers, Ohio Academy of Science, Alpha Chi Sigma, Sigma Xi, and Phi Lambda Upsilon. He is author or co-author of more than 60 technical papers.

ROBERT HENRY. Biographical sketch not available.

THOMAS KRESS. Biographical sketch not available.

BENJAMIN Y. H. LIU. Benjamin Y. H. Liu is a Professor of Mechanical Engineering and the Director of the Particle Technology Laboratory and Environmental Division, University of Minnesota. He received his B.S.M.E. degree from the University of Nebraska and his Ph.D. from the University of Minnesota, both in Mechanical Engineering. His main research focus has been in the science and technology of small airborne particles (aerosols) on which he has published approximately 240 papers and four books. He is well known for his research on the basic property and behavior of airborne particles and methods for aerosol generation, measurement, sampling and analysis. He has served on various governmental committees dealing with small airborne particles. He is the President of the American Association for Aerosol Research and an Editor-in-Chief of the journal, Aerosol Science and Technology. He is a Fellow of the American Society of Mechanical Engineers, a Fellow of the American Association for the Advancement of Science, a Guggenheim Fellow and the recipient of a Senior U.S. Scientist Award from the Alexander von Humboldt Foundation of West Germany. He is a member of the National Academy of Engineering.

DANA POWERS. Dr. Powers obtained a B. S. in Chemistry in 1970 from the California Institute of Technology and a Ph.D. in Chemistry, Chemical Engineering, and Economics in 1975 from the California Institute of Technology.

During the period of 1974-1981, Dr. Powers was a Member of the Technical Staff in the Chemical Metallurgy Division of Sandia National Laboratories. In this capacity, he conducted research on fabrication of thick-film electrical circuits, uniaxial pressing of metal powders, pyrometallurgical materials, security of nuclear materials, and analytic representations of phase relations in materials. On behalf of the U.S. Nuclear Regulatory Commission, Dr. Powers initiated an experimental study of the interactions of reactor core materials with structural concrete.

From 1981 to the present, Dr. Powers has been the supervisor of the Severe Accident Phenomenology Division of Sandia National Laboratories. He has directed and conducted experimental studies of high-temperature melt interaction with concrete, interactions of molten sodium with structural materials, design of core retention devices, interactions of molten core materials with air and water, high-temperature chemistry of radionuclides, groundwater leaching of radionuclides, and the sampling and characterization of high concentration aerosols. Dr. Powers is also responsible for the development of computer models used in reactor risk studies to describe fission product chemistry under reactor accident conditions and core debris interactions with concrete. Dr. Powers has directed quantitative studies of uncertainty in models of reactor accident phenomena and safety studies of research reactors.

Dr. Powers has served as a consultant for the Advisory Committee on Reactor Safeguards, the Rogovin and Kemeny Commissions on the reactor accident at Three Mile Island, and the International Atomic Energy Agency. He has also served on the National Academy of Sciences Committee to Assess Safety and Technical Issues at DOE Reactors, the Steering Committee for Chemical Processes and Products in Severe Nuclear Reactor Accidents, and the Panel on Cooperation with the USSR on Reactor Safety. Dr. Powers has been a member of the Department of Energy's Advisory Committee on Nuclear Facility Safety since 1988.

RICHARD VOGEL. Dr. Vogel was Manager of the Source Term Program until April 4, 1988, in the Nuclear Power Division at the Electric Power Research Institute (EPRI) in Palo Alto, California. Since that time, he has been a Senior Scientific Advisor to that program. Dr. Vogel joined the Institute in 1980.

Before joining the Institute, Dr. Vogel was employed by Exxon Nuclear. His last position was as Manager of the Research Department. In this capacity, he participated in various R&D programs and was responsible for the administration of Battelle Northwest work carried out for Exxon Nuclear.

From 1949 to 1973, Dr. Vogel held various positions of increasing responsibility for Argonne National Laboratory in Argonne, Illinois. He began as a Senior Chemist and became Associate Division Director of the Chemical Engineering Division in 1954. Dr. Vogel was Division Director of Chemical Engineering from 1963 until 1973.

Dr. Vogel received his B.S. degree in Chemistry from Iowa State University in 1939. He received an M.S. degree in Biophysical Chemistry from Pennsylvania State University in 1941. Dr. Vogel received both an A.M. (1943) and a Ph.D. (1946) in Chemistry from Harvard University. From 1946 to 1949 Dr. Vogel was an Assistant Professor of Physical Chemistry at the Illinois Institute of Technology in Chicago. Dr. Vogel is a member of the American Chemical Society and a fellow of the American Nuclear Society. In 1982, he received the American Institute of Chemical Engineering Robert E. Wilson Award in nuclear chemical engineering.

DAVID WILLIAMS. David C. Williams received a B.S. in Chemistry from Harvard in 1957 and a Ph.D in Nuclear Chemistry from MIT in 1962. During the next four years, he did postdoctoral research in nuclear structure physics at Princeton, NJ, and at Los Alamos National Laboratory, New Mexico. Since 1966, he has been a member of the technical staff at Sandia National Laboratories in Albuquerque, New Mexico. Major work areas at Sandia have included safety of radioisotopic power supplies used in the space program, hardening and vulnerability studies for nuclear warheads, LMFBR core disruptive accident analysis, and light water reactor (LWR) severe accident analysis. In the LWR safety field, his specialities have included severe accident source terms and containment loads resulting from severe accidents, including assessment of uncertainties in source terms and containment loads. In March of 1987, he was designated a Distinguished Member of the Technical Staff at Sandia. He is a member of the New Production Reactor Engineering Development Division.

3. METHODOLOGY

3.1 Introduction

This section contains a summary of the methodology used to elicit expert judgment from the expert panels. An in-depth discussion of the methodology is contained in Volume 1 of NUREG/CR-4551.

The methodology used in the expert judgment process for NUREG-1150 was designed to obtain subjective estimates of unknown physical quantities and frequencies in a manner that best uses the available expertise and accurately reflects the collective uncertainty about these values. Several principles guided the development of the methods:

1. The assessments should be limited to issues on which alternative sources of information such as experimental or observational data, or validated computer models are not available.

2. The issues analyzed using expert judgment should have the potential to make a significant impact on the estimates of risk and uncertainty in risk.

3. The decomposition of complex issues into simpler assessments is made in order to improve the quality of the resulting information.

4. Issues should be presented to the experts without ambiguity and without the potential for preconditioning or biasing responses.

5. Experts should be trained in the practice of expressing knowledge and beliefs as probability distributions.

6. Discussion of issues and alternative beliefs should take place in structured and controlled meetings that encourage the exploration of alternative beliefs while inhibiting pressure to conform.

7. Elicitation of expert opinion should be conducted using techniques and instruments that reflect the state of the art in subjective probability assessment.

8. The aggregation of judgments from various experts should preserve the uncertainty that exists among alternative points of view. Equal weight should be assigned to the assessment for each expert to represent the uncertainty completely.

NUREG-1150 does not attempt to reduce uncertainty in risk analysis, nor is it an attempt to find a best estimate. This study is an attempt to produce an unbiased picture of uncertainty in risk. The study tries to discover the range in risk inherent in the range of plausible assumptions about phenomenology and initial and boundary conditions. The risk corresponding to the most (subjectively) plausible assumptions has a higher likelihood of being accepted by a randomly chosen expert in accident phenomena. The risk

corresponding to less plausible assumptions nevertheless has some likelihood of being accepted by any expert, and may indeed be the most acceptable for some experts. Experts are sometimes wrong, and the "true" risk could lie outside the ranges found in this study.

3.2 Steps to Elicit Expert Judgment

The principles identified above, the criticism of the draft NUREG-1150 expert judgment efforts, and the findings of precursor studies employing expert judgment[1,2] provided guidance for the design of the NUREG-1150 expert judgment elicitation process. The process evolved into ten steps:

1. Selection of issues;
2. Selection of experts;
3. Elicitation training;
4. Presentation and review of issues;
5. Preparation of expert analyses by panel members;
6. Discussion of analyses;
7. Elicitation;
8. Recomposition and aggregation;
9. Review by the panel of experts;
10. Documentation.

The methodology was implemented in a three-meeting format, with much additional work being accomplished between meetings. Steps 1 and 2 were accomplished before the first meeting of the expert panel. Step 3, elicitation training, took place in the first meeting, which lasted one-half day. The presentation and review of issues, Step 4, was done during the second meeting, which, in order to reduce travel costs, took place immediately after the first meeting. Step 5 was accomplished between the second and third meetings (in some cases the expert panels met for additional discussions during this time). Discussion and elicitation, Steps 6 and 7, occurred in the third meeting, which usually took place three months after the first and second meetings (the accident sequence frequency group and the structural response group met two months after the first two meetings). The final steps, 8, 9, and 10, were accomplished after the third meeting.

3.3 Selection of Issues

The NUREG-1150 program attempts to show the range and distribution of risk due to uncertainty in the inputs. Some of this uncertainty is phenomenological, some is stochastic, and some is because of limited background of data. There are an enormous number of input points, and all are uncertain to some extent. It was thus impossible to treat all questions and issues with the same degree of thoroughness. The criteria used to select issues for detailed uncertainty analysis were:

- High impact on risk. If an issue was highly uncertain, but variation across its entire range would not cause a big change in risk, there would be little need for a detailed treatment. The likely impact on risk was determined by the outcome seen in the draft version of NUREG-1150, by smaller scale side calculations, by the opinions of the expert panels, and by examination of previous PRAs.

- Interest within the reactor safety community. Some issues were thought not to be major determinants of uncertainty in risk, but had nevertheless been the subject of intense investigation and debate.

- To improve on the treatment in Draft NUREG-1150. Some issues had not appeared to be important in the draft version; however, it was recognized that the treatment there was less than optimum. Such issues were included to determine whether an improved treatment would change those insights.

- The issue was uncertain. Even if an issue is important for the magnitude of risk, if the outcome is certain there is no impact on the uncertainty in risk.

Issues meeting any of these criteria were listed by the NUREG-1150 staff. The preliminary list of issues was presented to a panel of experts, along with reasons for their inclusion. A list of other issues was also presented, along with reasons for their exclusion. The expert panel was asked to review the list of issues, and to add or delete issues. The expert panels were the same ones that would be asked for quantification of the uncertain issues. An understanding of the limited time and resources available generally militated against an unwarranted or overly generous expansion of the issues.

Those issues that were selected for quantification by the external expert panels fell into three broad classes: uncertain issues affecting the sequence frequency calculation, uncertain issues affecting the response of the containment and its systems, and uncertain issues affecting the radiological source term. There were more issues affecting containment than for the other classes, and there was a further breakdown into issues related to the in-vessel phenomenology, containment loads, structural response, and molten core-concrete interactions. Tables 3-1 through 3-5 show the issues presented to the containment and radiological source term expert panels, along with the reasons for including the issue.

Table 3-1
Issues Presented to the In-Vessel Panel

Issue No.	Title	Reason for Inclusion
1	Temperature-induced PWR hot leg failure	Large hot leg failure could preclude direct containment heating; depressurizes RCS and precludes SGTR
2	Temperature-induced PWR SGTR	SGTR gives direct path to environment, with large release of radionuclides
3	In-vessel hydrogen production in BWRs	Hydrogen burning has potential for causing release to environment
4	Temperature-induced bottom head failure in BWRs	Mode of bottom head failure determines subsequent accident progression
5	In-vessel hydrogen production in PWRs	Hydrogen burning has potential for causing release to environment
6	Temperature-induced bottom head failures in PWRs	Mode of bottom head failure determines subsequent accident progression

Table 3-2
Issues Presented to the Containment Loads Panel

Issue No.	Title	Reason for Inclusion
1	Hydrogen phenomena at Grand Gulf	Early failure of drywell or wetwell has potential for causing large source term
2	Hydrogen burn at vessel breach at Sequoyah	Early failure of containment or bypass of ice condenser has potential for causing large source term
3	BWR reactor building failure due to hydrogen burns	Bypass of reactor building has potential for increasing source terms
4	Loads at vessel breach at Grand Gulf	Failure of containment at vessel breach has potential for causing large source terms
5	Loads at vessel breach at Sequoyah	Same as Issue 4
6	Loads at vessel breach at Surry.	Same as Issue 4
7	Loads at vessel breach at Zion	Same as Issue 4

Table 3-3
Issues Presented to the Structural Response Panel

Issue No.	Title	Reason for Inclusion
1	Static failure pressure and mode at Zion	Containment failure is the most important determinant of source terms
2	Static failure pressure and mode at Surry	Same as Issue 1
3	Static failure pressure and mode at Peach Bottom	Same as Issue 1
4	Reactor Building bypass at Peach Bottom	Bypass of Reactor Building has potential for allowing large release of radionuclides
5	Static failure pressure and mode at Sequoyah	Same as Issue 1
6	Ice condenser failure due to detonations at Sequoyah	Failure or bypass of ice condenser has potential for large source terms
7	Drywell and wetwell failure due to detonations at Grand Gulf	Failure of drywell bypasses suppression pool. Failure of wetwell allows large release to environment
8	Pedestal failure due to erosion at Grand Gulf	Pedestal failure is a major factor in subsequent accident progression

Table 3-4
Issues Presented to the Molten Core-Concrete Interaction Panel

Issue No.	Title	Reason for Inclusion
1	Mark I drywell melt-through at Peach Bottom	Drywell meltthrough bypasses suppression pool; controversial issue
2	Mark II containment failure via pedestal failure at Grand Gulf	Pedestal failure could lead to early containment failure; controversial issue

Table 3-5
Issues Presented to the Source Term Panel

Issue No.	Title	Reason for Inclusion
1	In-vessel fission product release and retention	Release and retention are major determinants of source term
2	Ice condenser DF at Sequoyah	Ice condenser is principal decontamination mechanism in blackouts
3	Revolatilization from RCS/RPV	Revolatilization could negate effects of high retention; highly uncertain issue
4	CCI release	If in-vessel release is low, CCI release could be high; uncertain issue
5	Release of RCS and CCI species from containment	Aerosol agglomeration may be major source of cleanup in blackout; highly uncertain issue
6	Late sources of iodine at Grand Gulf	Appeared as important issue in Draft NUREG-1150
7	Reactor Building DF at Peach Bottom	Natural decontamination processes could reduce source term; uncertain and controversial issue
8	Release during direct containment heating	Uncertain and controversial issue; direct heating is also associated with early containment failure

3.4 Selection of Experts

Experts were chosen to ensure a balance of viewpoints. To this end, experts from industry groups, engineering and consulting firms, the federal government, and the national laboratories were included in the panel. A brief summary of their credentials has been presented in Section 2.

3.5 Elicitation Training

Training in probability assessment techniques is an integral part of the expert opinion methodology used in NUREG-1150. Each panel of experts that participated in the expert opinion process attended a half-day training session. This session constituted the first meeting of each panel. The training was given by consultants from the field of probability assessment and decision analysis. The trainer for the Source Term Panel was Professor Ward Edwards of the University of Southern California.

The purpose of training in probability assessment is to facilitate the elicitation process. Experts in various fields of science are often not trained in probability theory and the techniques of probability elicitation. The expertise possessed by the scientists and engineers on the panels is called substantive expertise and thus they are called substantive experts. Expertise about probability elicitation is called normative expertise and the participants in the expert opinion process schooled in probability assessment are known as normative experts. Both substantive expertise (knowledge of the problem domain being studied) and normative expertise (knowledge of techniques for encoding beliefs into probability distributions) are required for a successful expert opinion process.

During probability training, experts are exposed to various techniques for probability elicitation and the difficulties that accompany probability elicitation. Once trained, substantive experts are better able to express their knowledge in the form of probabilities and the resulting elicitations will be of a better quality. The resulting assessments are better calibrated in the sense that they accurately reflect the expert's knowledge and uncertainty. A by-product of the training is that the experts become more comfortable with the concept of subjective probability and more confident in expressing their beliefs in probability distributions.

Another benefit of training is that the time spent by the experts preparing for the issues is used more effectively because the experts can direct their analyses to the questions that must be addressed in the elicitation sessions. Furthermore, the elicitation sessions run smoothly since the normative and substantive experts are working with the same definitions and the same understanding of the desired product.

3.5.1 Training Topics

The training sessions conducted for NUREG-1150 covered several related topics. These topics included the expert opinion process itself and the need for expert opinion, the elicitation techniques for the probabilities

of various types of quantities and events or phenomena, the psychological aspects of probability assessments, and the decomposition of complex issues.

Each training session began with an overview of the goals of the expert opinion process and background material on the development of that process. The process was reviewed in some detail so that the substantive experts would be aware of what would be required of them and how their elicitations would be used. Because the formalized use of expert opinion was new to many of the participants, some were initially uneasy with the concept of expert opinion and the uses that it might be put to. Gaining the confidence of these experts through familiarization with the process was essential to the success of the expert opinion effort.

There are many different types of assessments that might be required of the experts. The type of assessment depends upon the nature of the physical quantity or phenomena under study. During the training sessions, the experts were introduced to assessment instruments for continuous quantities, discrete quantities, zero-one events, and dependent events. At appropriate points in the training, the experts were asked to make assessments using the methods under discussion. Using practice assessments develops confidence and ensures that the substantive experts understand the tasks that they will be required to perform. In order to make the training more interesting and more relevant, examples were used that reflected nuclear power risk issues.

Since many of the assessments would require the development of a probability distribution for a continuous quantity, the experts were given training in both the direct assessment techniques (assessing probabilities of given intervals of values) and bisection techniques (assessing values of the variable having given cumulative probabilities) for continuous variables. Later, in the elicitation sessions, these techniques would be used interchangeably by the normative experts.

A discussion of stochastic and parametric uncertainties and how they are differentiated in an uncertainty analysis was also provided. The concept of calibration of experts and calibration functions was also introduced. However, mathematical calibration of experts was not attempted in the NUREG-1150 expert opinion process.

Psychological aspects of probability elicitation received much attention in the training because failure to recognize and deal with psychological biases can impair the quality of the resulting assessments. One of the psychological aspects discussed is the tendency to give subjective probability distributions that are too narrow and thus understate the uncertainty or, conversely, overstate knowledge. This phenomena is often called "overconfidence," since the effect is that expressed probability distribution expresses greater certainty than is warranted. Other psychological aspects of subjective probability assessment that were discussed include anchoring, which is the tendency to assume an initial position and fail to give sufficient credit to other sources of information; representativeness, which is the tendency to give too much credit to other situations that are similar in some aspects but not

others; the tendency to overestimate the probabilities of rare events; and and problems with group behavior such as personality dominance. Whenever possible, examples of these difficulties were presented and the experts being trained were asked to participate in demonstrations.

At the end of the training session the participants were given an assessment training quiz containing 16 assessment tasks using the direct and bisection methods of assessment. The participants were asked to complete the training quiz during that evening and return the next morning to discuss the results. The purpose of the training exercise was two-fold: to give the substantive experts experience with the elicitation instruments and to provide feedback on the quality of the individual's assessments. As expected, most participants found that their assessed distributions expressed overconfidence. Once aware of this tendency, it is easier for the substantive experts to correct for this bias.

Problem decomposition was the last major segment of the training session. Problem decomposition is the process of creating a model of a complex assessment that allows the experts to make a series of simpler assessments. The simpler assessments are mathematically recomposed through the model. The net result is that the resulting probability distribution is a better expression of the expert's knowledge than if the expert had been asked to make an assessment of the initial issue without the aid of a decomposition.

Training in decomposition was conducted by presenting examples of decompositions that had been developed for the NUREG-1150 study. Several types of decompositions were shown and the process of recombining the assessments was discussed. Comments from the participants indicated that the use of problems from the nuclear safety area enhanced the value of the decomposition training.

3.6 Presentation of Issues

During the second meeting, plant analysts presented the issues to the expert panel. The purposes of the presentations were to ensure that there was a common understanding of the issue being addressed; ensure that the experts would be responding to the same elicitation question; permit unimportant issues to be excluded and important issues to be included; allow modification or decomposition of the issue; and provide a forum for the discussion of alternative data sources, models, and forms of analysis.

Each presentation included a suggested decomposition of the problem. Problem decomposition has been used in the NUREG-1150 expert judgment process as a mechanism to improve the quality of the subjective assessments. Problem decomposition improves the quality of assessments by structuring the analysis so that the expert is required to make a series of simpler assessments rather than one complex assessment. Experimental studies[3,4] have shown that decomposition often improves the accuracy of assessments. Improvement occurs because the experts are responding to questions that are less difficult to answer. The experts must state their reasoning explicitly by being more introspective about their assumptions of the analysis and thus consider alternatives that they might otherwise

ignore. Some improvement may be due to cancellation of errors which occurs when errors of underestimation are offset by comparable errors of overestimation. Decomposition also provides a form of self documentation since the expert's thought process is made explicit in the decomposition.

Plant analysts usually presented the suggested decompositions without suggested probabilities or distributions to avoid preconditioning or biasing the experts. For many of the issues, the proposed decomposition brought about lively discussions that illuminated the alternative approaches to analyzing the issue. The plant analysts also presented data sources, models, and reports that were relevant to the issue, and provided references to other sources of information.

Capturing uncertainty in the experts' opinions requires that the various experts be permitted to follow alternative analyses. Since the process was designed to take advantage of the diversity of approaches, experts were encouraged to seek their own decompositions or to modify decompositions that were suggested by the analysts. Criticism of the decompositions was encouraged and the experts were assisted in producing decompositions that better matched their interpretations of the issues.

3.7 Preparation and Discussion of Analyses

Two or three months were allowed between the initial presentations of the issues and the elicitation sessions. During this period, the experts studied the issues. Some experts chose to alter the proposed decompositions or create new decompositions and made preliminary evaluations of the subjective probabilities represented in their decompositions of the issues. The elicitation meeting provided a forum for discussion of alternative views of the issue. Presentations from both the panel members and invited observers of the meetings were encouraged. These sessions generated a substantial amount of discussion and interchange of information that often led the experts to make revisions of their prepared analyses. In some instances, the panel members prepared documentation that amounted to brief reports. It became apparent in the elicitation sessions that this interchange was an important source of information for the experts.

3.8 Elicitation

The discussion of each issue was followed by elicitation meetings between each expert and a team composed of one normative analyst and one substantive analyst. Documentation of the experts' assumptions and reasoning was produced during the elicitation meetings. However, in a few cases where there were more experts to be elicited than available normative experts, two experts were elicited in a single session.

The elicitation sessions served several purposes. The first was to obtain from the experts the decomposition and assessments of the problems. The experts were required to explain their thinking to the assessment team of one normative and one substantive expert. During the discussion of the elicitation process, the expert being elicited was questioned about stated

beliefs and asked to reflect on, and explain the reasoning behind, the values that he or she had provided. In many cases, the resulting decompositions and probability distributions differed somewhat from the initial assessments.

The role of the normative experts was to assist the expert in codifying the experts' beliefs and to ensure that the assessment was complete and consistent in a probabilistic sense so that the assessments could be recomposed at a later time. Normative experts have the ability to draw from the experts the important details being elicited. Their talent for becoming involved in the technical aspects of issues, which are not their basic area of expertise, is a crucial factor in facilitating the experts' abilities to develop logically consistent assessments. Such individuals are necessary in any expert judgment elicitation process.

The role of the substantive expert was to assist the expert by answering questions related to the issue and to ensure that technical reasoning was complete and to the point. He also served as a technical advisor to the normative expert to assist him in questioning the expert in a direction consistent with the technical needs and constraints of the plant analysis teams.

Much of the documentation of the experts' assumptions and reasoning was completed during the assessment meetings. However, some follow-up work was necessary after the elicitation sessions to fill in voids in the logic provided by the experts, or to obtain values that were incomplete.

Documentation of the elicitations is provided in Section 5 of this report. Note that while the experts participating for each issue are identified, the individual assessments are kept anonymous, and the experts are identified as Experts A, B, C, etc.

3.9 Recomposition and Aggregation of Results

Each member of the expert panels produced a distribution for each case of each issue. For some issues, several dependent variables were requested, and a separate distribution was elicited for each variable. If all the experts had worked with identical case structures, and if all had produced their results in the same form, the task of aggregation would have been simply a matter of taking the numerical average of all the distributions for each case. However, some experts used idiosyncratic case structures. On some issues, the experts expanded the case structure beyond what was tractable in the accident progression event trees or the XSOR codes. On some issues, experts gave their results in different forms.

For the purposes of aggregation it was absolutely required that the case structure be small enough to fit into the containment event trees and XSOR codes and that the case structure and dependent variables be the same between experts. If the case structure was impractically large and complex, it was reduced if possible by an analysis of variance (ANOVA). The ANOVA compared the variance in the dependent variable attributable to the differences between cases and the variance attributable to the

differences among experts to the unexplained variance in the dependent variable. For many issues it was found that the differences between cases were not significant compared to the differences between experts, that is, that the large and complex case structure had little effect on the dependent variable. A mathematical procedure was then used to determine which of the cases could be safely combined.

If different experts used different cases, they were first encouraged to resolve their differences; if they failed to do so it was necessary to find some common ground. The cases common to all experts were of course retained. The remaining cases were inspected, and the most important ones were retained. If an expert did not have one of these cases, but did have a closely analogous case, the analog was used for the missing case. If the expert did not have a case closely related to the missing case, then the average of the case for all other experts was used for his missing case. It was recognized that this procedure would reduce the range of uncertainty, so the substitution was resorted to as little as possible. For some issues, missing data could be filled in by interpolation or ratios of existing cases.

If the experts produced different dependent variables, some analysis was required to put all the outputs into the same form. Whenever this was done the experts involved might find the final form of their data difficult to reconcile with what had been produced in the elicitation. Therefore, analytical alteration of results was resorted to as little as possible, and attempts were made to explain the reasons for and methods of analysis to the experts.

After each of the experts' distributions was in the same format, they were aggregated by averaging. The experts' outputs were almost always in the form of cumulative distribution functions (CDFs), that is, curves or tables of the probability that the independent variable would be no greater than some specific value. The aggregation was carried out by averaging all the experts' probability values for each value of the independent variable. The aggregated results were thus also CDFs.

3.10 Review

Following the recomposition of the assessments and the modification of the documentation accompanying each assessment, the written analyses of each issue were returned to each panel expert, normative expert, and substantive expert associated with the issue for review. This review process ensured that potential misunderstandings were identified and resolved and that the documentation, which is given in Section 5 of this report, correctly reflects the judgment of the experts involved.

3.11 Documentation

Clear, comprehensive documentation is crucial for ensuring that the expert opinion process is accepted as credible. There must be no question as to the openness and impartiality of the process. Users and reviewers of the results must be able to trace the development of aggregated assessments from the information presented to the experts to the rationale that

motivates each expert to generate his particular assessments, and through the process of aggregating the individual assessments into a final result, including any manipulation of the assessments needed for aggregation. To this end, the issue discussions were recorded on video cassette. Such recording provides evidence of the exact conversations and presentations made before the panel. Written notes were taken by both the normative and substantive experts. Each expert was encouraged to personally document his rationale for his elicitation immediately at the end of the session. By far the most important documentation is each expert's in-depth discussion of his reasoning for his assessments. The discussion should contain the technical foundation of information (experience, issue presentation, existing data or analyses) from which the rationale for the assessment is derived.

REFERENCES

1. A. Mosleh, V. M. Bier, and G. Apostolakis, "Methods for the Elicitation and Use of Expert Opinion in Risk Assessment," Pickard, Lowe & Garrick, Inc., NUREG/CR-4962, PLG-0533, August 1987.

2. A. Tversky and D. Kahneman, "Judgement under Uncertainty: Heuristics and Biases," Science, 185, pp. 1124-31, 1974.

3. J. S. Armstrong, Long-Range Forecasting: From Crystal Ball to Computer, John Wiley & Sons, New York, 1985.

4. J. S. Armstrong, W. B. Denniston, and M. M. Gordon, "The Use of the Decomposition Principle in Making Judgments," Organizational Behavior and Human Performance, 14, pp. 257-63, 1975.

4. ELICITATION MEETINGS

The first two meetings (the elicitation training and the presentation and review of the technical issues) for the Source Term Expert Panel were held on January 12 and 13, 1988. Presentations to the Source Term Panel were made by the following people:

Nestor Ortiz, SNL
Ward Edwards, USC
Frederick Harper, SNL
Elaine Bergeron, SNL
Roger Breeding, SNL
Ed Warman, Stone & Webster
Dana Powers, SNL
James Davis, New York Power Authority
William Camp, SNL
Walt Murfin, Technadyne
Dave Williams, SNL
Herschel Specter, New York Power Authority
Edward Fuller, EPRI
Ken Bergeron, SNL
Hong Nian Jow, SNL
Thomas Kress, ORNL
Chris Amos, SAIC
John Kelly, SNL

There were two interim meetings prior to the Source Term elicitation meeting. The elicitation meeting for the Source Term Expert Panel was held on April 12 to 15. Presentations at these meetings were made to the panel by several of the above people and by the following people:

M. Khatib-Rahbar, BNL
Rudy Sher, EPRI

Normative experts for Source Term elicitation sessions were:

Ralph Keeney, USC
Detlof von Winterfeldt, USC
Richard John, USC.

5. ISSUE DESCRIPTIONS AND ELICITATION RESULTS

The results of the expert panel elicitations are presented in detail here. A brief description of each issue is given, the individual expert assessments and their rationale are discussed, and the aggregated results or resolutions for each issue are presented.

5.1 Issue 1. Release of Fission Products from the Fuel in the Vessel and from the Vessel to the Containment

Summary of Expert Panel's Assessment of Source Term Issue 1--FCOR AND FVES

Experts consulted: Peter Bieniarz, Risk Management Associates; Robert Henry, Fauske and Associates; Thomas S. Kress, Oak Ridge National Laboratory; Dana Powers, Sandia National Laboratories.

To quantify Issue 1, each expert was asked to respond to the following four questions:

1. What distributions characterize the uncertainty in the release of fission products from the fuel to the vessel?

2. What distributions characterize the uncertainty in the release of fission products from the vessel to the containment?

3. Is there a correlation between these distributions?

4. If so, what is it?

Issue Description

$FCOR_i$ represents the fraction of radionuclide group i in the initial core inventory that is released from the fuel to the vessel before the vessel fails. $FVES_i$ represents the fraction of radionuclide group i released from the fuel in the vessel that is released from the vessel at, or before, vessel failure. The release at vessel failure includes the blowdown period and extends until the reactor coolant system (RCS) reaches the same pressure as the containment. Material deposited in the vessel before breach and remaining until well after vessel breach to be released later through revaporization or resuspension is accounted for in another parameter and is not included in FVES.

A distribution is required for both FCOR and FVES for each of the nine radionuclide groups:

- Noble or inert gases (xenon, krypton);
- Halogens (iodine, bromine);
- Alkali metals (cesium, rubidium);
- Tellurium group (tellurium, selenium, antimony);
- Barium;
- Strontium;

- Noble metals (ruthenium, molybdenum, palladium, rhodium, technetium);
- Lanthanides (lanthanum, neodymium, niobium, europium, yttrium, praseodymium, promethium, samarium, zirconium);
- Cerium group (cesium, neptunium, plutonium).

The issue description presented to the expert panel contained a suggested case structure for this issue. For FCOR, it was proposed that there was no dependence upon the accident sequence. For FCOR only two cases were proposed--pressurized water reactor (PWR) and boiling water reactor (BWR). It was proposed that FVES depended upon the pressure in the vessel as well as upon the type of reactor. Thus, for FVES, four cases were proposed for the PWRs, and three cases were proposed for the BWRs:

PWR-1--Setpoint pressure (2500 psia, blackout, RCS intact)
PWR-2--High pressure (600 to 2000 psia, S_3 break)
PWR-3--Intermediate pressure (200 to 600 psia, S_2 break)
PWR-4--Low pressure (below 200 psia, large break).

BWR-1--Fast, high pressure (TBUX, blackout)
BWR-2--Fast, low pressure (TBU, blackout)
BWR-3--Slow, high pressur (TCUX, failure to scram).

NOTE: The pressure indicated refers to reactor coolant system pressure and the TBUX, TBU, TCUX, S_2, S_3 blackout designators refer to the type of sequence as defined by NUREG/CR-4550.

Summary of Experts' Rationale

Four members of the source-term panel considered this issue. However, Expert A was unable to complete his elicitations for FVES. Thus, elicitations were obtained from four experts for FCOR and from three experts for FVES.

The conclusions of the four experts for FCOR are given in the descriptions of individual elicitations. Two experts concluded that there were no significant differences between PWRs and BWRs as far as FCOR was concerned, and each provided one table that applied to both types of reactors. The other two utilized the proposed case structure but also considered a high zirconium oxidation in-vessel subcase and a low zirconium oxidation in-vessel subcase for FCOR.

The conclusions of the three experts for FVES are given in the descriptions of the individual elicitations. The panel agreed before the elicitation that cases PWR-2 and PWR-3 could be considered together, so the proposed case structure for FVES was reduced to six before the elicitations. The three experts providing values for FVES agreed that all the inert gases would escape from the vessel in all cases. One expert concluded that all the fission products except the noble gases would condense to form aerosols, and he provided one curve for aerosols, which applies to all the radionuclide groups except the noble gases for each of the six proposed cases. The second expert distinguished among inert gases, iodine, cesium, tellurium, and aerosols. He condensed the proposed number of cases. The

third expert distinguished between the radionuclide groups in a manner similar to that of the second expert, but he expanded the proposed case structure by distinguishing between high and low zirconium oxidation in the vessel for some of the six cases.

Expert A based his analysis for FCOR upon the experimental work on the release of fission products from fuel. He concluded that the results for cesium could be well represented by an equation similar to the diffusion equation and that the constants in the solution could be determined from the data. He obtained release rates for the other fission products by "relative volatilities." The results of applying this method of calculating release rates agree reasonably well with experiments. He then wrote a computer program to vary the temperature rise with time over a range of reasonable scenarios, keeping track of the amount of each fission product released. Expert A provided FCOR values for both high and low zirconium oxidation in the vessel for both types of reactors. Expert A declined to provide any values for FVES.

Expert B based his conclusions for FCOR and FVES on a large number of MAAP[B-1] runs for various accident scenarios. He also relied on the evidence from TMI-2. The MAAP results served as the basis for his conclusions, but he included uncertainty for phenomena not modeled in MAAP and phenomena that MAAP currently does not treat in sufficient detail. For example, Expert B felt that MAAP sometimes overestimated the releases of certain nuclide groups because the process of core collapse imposed physical limitations on other processes that MAAP does not consider adequately at this time. Expert B felt that neither the reactor type nor the amount of zirconium oxidation in core had a significant effect on FCOR. He also felt that the amount of zirconium oxidation before vessel failure did not significantly affect FVES. He viewed the important factor to be the hold-up time in the vessel: the longer the hold-up time, the more deposition, agglomeration, etc. Thus, for FVES, he grouped the PWR-1 and BWR-1 cases together, and he grouped the PWR-2, PWR-3, PWR-4, and BWR-2 cases together. He provided a separate distribution for case BWR-3, as the control rod drive (CRD) flow has a definite effect. Expert B considered iodine, cesium, tellurium, and aerosols separately. Although he provided separate columns for tellurium and nonvolatiles, the values in those columns were identical in all cases.

Expert C concluded that even if the dependency of the fission product release rates on temperature were much better known, the release rates, and thus FCOR, could not be much better predicted because the variations of the temperatures in the core by time and location are not well known, especially after the onset of relocation. The extent of metal oxidation is also a significant uncertainty. Relocation not only changes the surface to volume ratio, but it alters the H_2/H_2O ratio, which in turn affects the diffusion and transport rates of the fission products. Thus, the current models, which largely depend upon Arrhenius-type equations, have definite limitations. The Source Term Code Package (STCP), for example, tends to overpredict FCOR because it treats the formation of eutectics and the gradual relocation of the core poorly. Expert C provided FCOR values for both high and low zirconium oxidation in the vessel for PWRs and BWRs. Expert C thought that the biggest problem with the code predictions of FVES was the failure to account for all the important chemical forms and the

changes between them. For example, deposited CsOH may change to a silicate or borate form. This uncertainty of chemical form and transformation is thought by Expert C to be more important than the uncertainty in other important factors such as residence time, gas temperatures, and flow rates. Expert C considered iodine, cesium, tellurium, and aerosols separately. For cases PWR-1, BWR-1, and BWR-2, he provided separate tables for high and low zirconium oxidation in the vessel. Since he was the only expert to make a distinction on the amount of zirconium oxidation in the vessel, this dependency would not be significant in the aggregate distributions. Thus, an average of Expert C's high and low zirconium oxidation cases was used for the three cases in which he made this distinction.

Expert D did not consider the amount of zirconium oxidation in the vessel or the type of reactor to be important for FCOR; he provided one set of values for FCOR for both PWRs and BWRs. He thought that all the noble or inert gases (xenon and krypton) would escape from the fuel and did not provide a curve for this nuclide group. For tellurium, he concluded that the data were so ambiguous and conflicting that he could not support any particular distribution for tellurium. He thus specified that a uniform distribution between zero and one be used. Expert D's distributions for FCOR are shown in Figure 1-1.

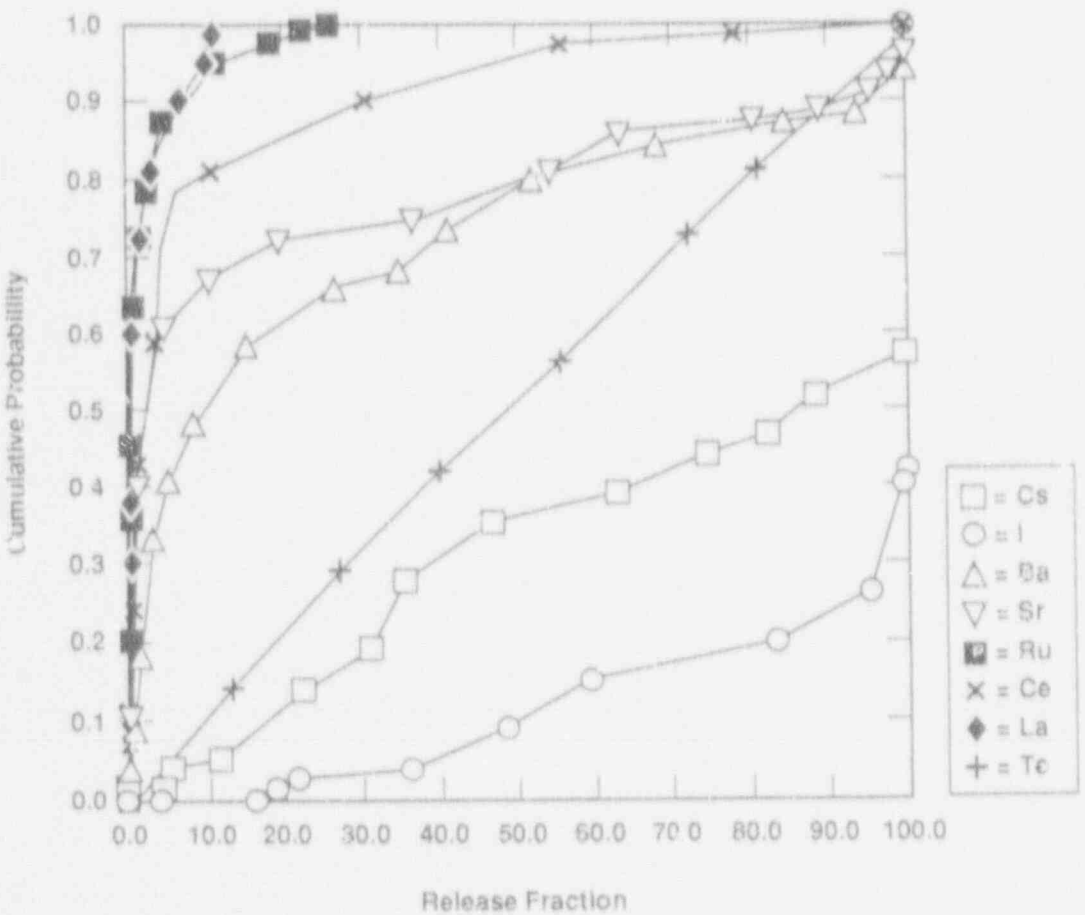

Figure 1-1. FCOR Distributions.

For FVES, Expert D concluded that before release from the RCS, the fission products would encounter low enough temperatures that all the radionuclides except the noble gases would condense to form aerosols. He thus provided one curve for FVES for each of the six proposed cases (Figure 1-2). The curve for each case applies to all the radionuclide groups except the noble gases. Expert D obtained these curves by using the aerosol sampling and transport efficiency calculation (ASTEC) code to calculate aerosol deposition along the flow path. For the calculations, he took the predominant sources of uncertainty to be:

- Mean particle size;
- Geometric standard deviation of the particle size distribution;
- Location of the break in the RCS;
- Molar flow through the RCS;
- Pressure in the RCS; and
- Temperature difference between the gas and the walls of the RCS.

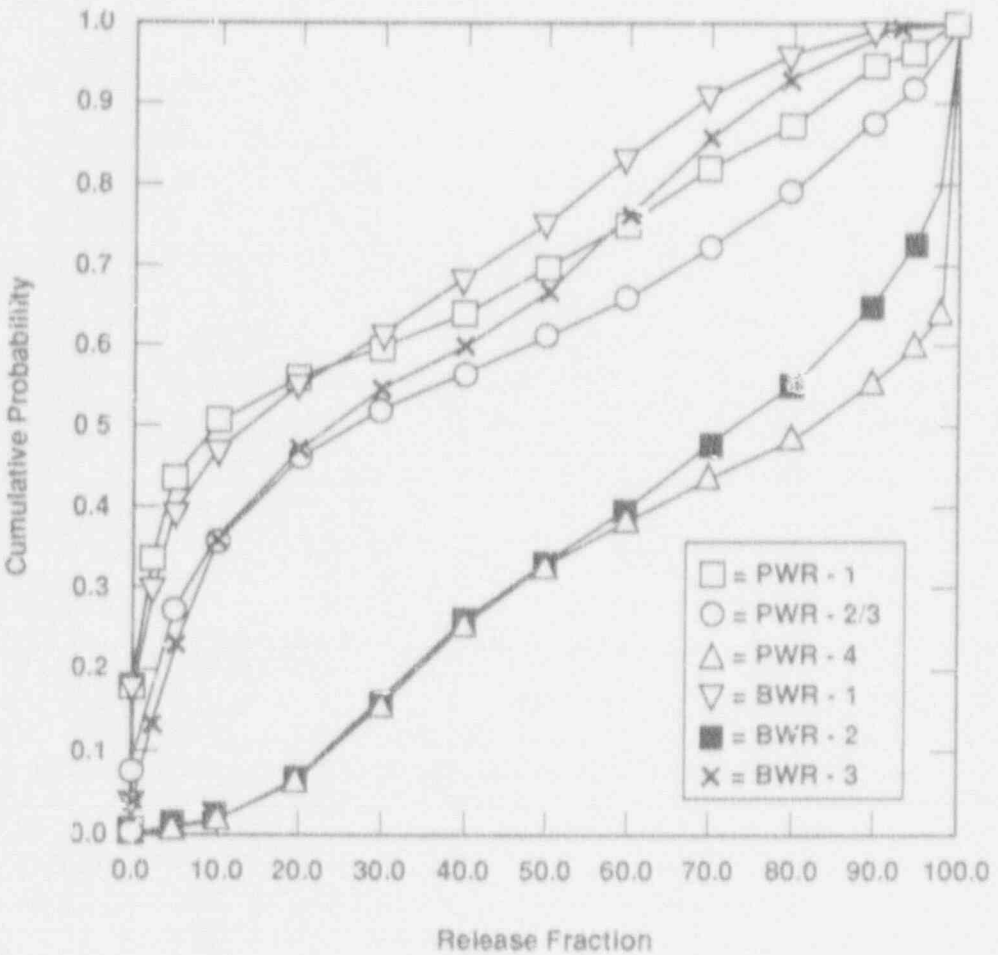

Figure 1-2. FVES Distributions.

The differences between the cases were small; a superior case structure would have been based on the location of the break(s) in the RCS. However, for any case structure the uncertainties in the particle size distribution would have been sufficient to produce relatively broad distributions, such as those shown in Figure 1-2.

A noble gas release fraction value of 1.0 was used for the FVES aggregation (with the permission of the expert). The noble gas release fractions originally supplied by the expert (presented in Tables B-2, B-3, and B-4) applied to release before vessel breach.

Method of Aggregation

All aggregation was performed by averaging based on the release fraction. That is, for each value of FCOR or FVES for which any expert gave a cumulative probability, an average was formed of the cumulative probabilities of all the experts. This usually involved interpolating values for some of the experts. This method of averaging preserves the tails of the individual distributions, which averaging based upon the cumulative distribution function does not.

In his tables of results for FCOR, Expert A provided only the 0.1% value and the 99.9% value for the last five radionuclide groups and stipulated that a "uniform distribution" be drawn between them. He did not specify whether the distribution was to be arithmetically uniform or logarithmically uniform. The difference between the two endpoints ranged from a factor of 10 to a factor of 500. In the absence of any definitive instructions, a logarithmically uniform distribution was used when the ratio between the upper and lower bound was 50 or more. An arithmetically uniform distribution was used otherwise.

Regarding the elicitation of Expert B, several assumptions were made. First, he gave values for lower limit, 90% confidence, 50% confidence, 10% confidence, and upper limit without defining either lower or upper limit. Since some numerical value was required, 1% was assigned to lower limit, and 99% was assigned to upper limit. Secondly, Expert B did not always supply a value for his upper limit. The tables he supplied had tellurium, for nonvolatiles in Tables B-2 and B-4, and for all upper limit entries in Table B-3. Actual values were required for this analysis. The values for these entries in Tables B-2, B-3, and B-4 were supplied by extrapolation. For the tellurium and nonvolatiles curves in Tables B-2 and B-4, 2% was based on similarity with Expert B's cesium curve and the reasonableness of the result on a log plot. For the upper limit values in Table B-3, 70% for iodine and 50% for the other radionuclide groups were selected on the basis of symmetry between the upper and low ends of the curves.

Expert D provided tables defining each curve in his elicitation. The tables for FCOR were not regular in release fraction or in cumulative probability and each contained between 8 and 16 entries. The values in Table 10 were obtained from these curves by interpolation. Table 10 was created for this summary only; the actual tabular values supplied by Expert D were used as input to the program that performed the aggregation. Extrapolations were made to obtain release fractions at 0.0 and 1.0. These extrapolations were approved by Expert D.

For FVES, Expert D supplied for each curve (case) a table that was regular in the release fraction, a plot of the cumulative probability, and a plot of the probability density. The actual tabular values for FVES supplied by Expert D were used as input to the program that performed the aggregation. Extrapolations were made to obtain release fractions at 0.0 and 1.0. These extrapolations were approved by Expert D.

The aggregate distributions for FCOR are given in Tables 1-1 through 1-4 of this summary and plotted in Figures 1-3 through 1-6. The aggregate distributions for FVES are given in Tables 1-5 through 1-10 of this summary and plotted in Figures 1-7 through 1-12.

Table 1-1
Fractional Release from Vessel (%) FCOR
Case PWR-1--High, Zirconium Oxidation Aggregate

Nuclide Group	Cumulative Probability								
	0.000	0.010	0.050	0.250	0.500	0.750	0.950	0.990	1.000
Xenon, Krypton	9.936	16.265	41.968	80.323	92.049	99.[illegible]1	99.983	99.995	100.000
Iodine, Bromine	9.922	13.916	26.438	55.733	75.048	9[illegible]1	100.000	100.000	100.000
Cesium, Rubidium	3.[illegible]00	6.055	17.423	41.747	61.568	88.781	100.000	100.000	100.000
Tellurium, Antimony	0.000	0.300	1.798	9.748	33.084	59.380	91.384	98.636	100.000
Barium	0.000	0.022	0.118	0.419	0.858	3.008	52.448	100.000	100.000
Strontium	0.000	0.003	0.025	0.211	0.639	1.764	51.659	100.000	100.000
Ruthenium, etc.	0.000	0.000	0.000	0.005	0.456	1.988	8.088	14.033	26.609
Lanthanum, etc.	0.000	0.000	0.000	0.002	0.010	0.118	2.143	9.979	11.054
Cerium, etc.	0.000	0.000	0.000	0.002	0.015	0.303	8.540	50.951	100.000

Table 1-2
Fractional Release from Fuel (%) FCOR
Case PWR-2--Low, Zirconium Oxidation Aggregate

Nuclide Group	Cumulative Probability								
	0.000	0.010	0.050	0.250	0.500	0.750	0.950	0.990	1.000
Xenon, Krypton	7.971	9.880	17.590	60.476	90.000	99.905	99.983	99.998	100.000
Iodine, Bromine	1.987	3.253	8.394	37.105	69.470	91.035	100.000	100.000	100.000
Cesium, Rubidium	0.983	2.410	6.703	30.309	58.536	83.007	100.000	100.000	100.000
Tellurium, Antimony	0.000	0.226	1.265	7.579	18.585	46.087	88.729	98.220	100.000
Barium	0.000	0.011	0.022	0.174	0.845	2.744	52.448	100.000	100.000
Strontium	0.000	0.003	0.015	0.078	0.402	1.336	51.659	100.000	100.000
Ruthenium, etc.	0.000	0.000	0.000	0.005	0.204	1.228	5.812	14.033	26.609
Lanthanum, etc.	0.000	0.000	0.000	0.002	0.010	0.095	2.141	9.979	11.054
Cerium, etc.	0.000	0.000	0.000	0.002	0.015	0.249	8.540	50.951	100.000

Table 1-3
Fractional Release from Fuel (%) FCOR
Case BWR-1--High Zirconium Oxidation
Aggregate

Nuclide Group	Cumulative Probability								
	0.000	0.010	0.050	0.250	0.500	0.750	0.950	0.990	1.000
Xenon, Krypton	4.972	7.349	16.988	55.714	90.000	98.905	99.983	99.998	100.000
Iodine, Bromine	2.981	4.880	12.530	33.865	73.531	85.512	100.000	100.000	100.000
Cesium, Rubidium	1.977	3.253	7.046	26.047	58.536	88.761	100.000	100.000	100.000
Tellurium, Antimony	0.000	0.300	1.811	7.050	15.334	58.525	91.364	98.636	100.000
Barium	0.000	0.022	0.118	0.418	0.858	3.006	52.448	100.000	100.000
Strontium	0.000	0.003	0.025	0.211	0.639	1.764	51.659	100.000	100.000
Ruthenium, etc.	0.000	0.000	0.000	0.005	0.456	1.988	8.088	14.033	26.699
Lanthanum, etc.	0.000	0.000	0.000	0.002	0.010	0.118	2.143	9.979	11.054
Cerium, etc.	0.000	0.000	0.000	0.002	0.015	0.303	8.540	50.951	100.000

Table 1-4
Fractional Release from Fuel (%) FCOR
Case BWR-2--Low Zirconium Oxidation
Aggregate

Nuclide Group	Cumulative Probability								
	0.000	0.010	0.050	0.250	0.500	0.750	0.950	0.990	1.000
Xenon, Krypton	1.987	3.253	8.394	4..428	90.000	99.905	99.983	99.998	100.000
Iodine, Bromine	0.599	0.663	0.920	16.200	69.470	91.035	100.000	100.000	100.000
Cesium, Rubidium	0.499	0.578	0.900	8.820	58.536	83.007	100.000	100.000	100.000
Tellurium, Antimony	0.000	0.294	0.732	4.938	14.051	46.087	88.779	98.220	100.000
Barium	0.000	0.011	0.022	0.174	0.645	2.744	52.448	100.000	100.000
Strontium	0.000	0.003	0.015	0.078	0.402	1.336	51.659	100.000	100.000
Ruthenium, etc.	0.000	0.000	0.000	0.005	0.204	1.228	5.812	14.033	26.699
Lanthanum, etc.	0.000	0.000	0.000	0.002	0.010	0.095	2.141	9.979	11.054
Cerium, etc.	0.000	0.000	0.000	0.002	0.015	0.249	8.540	50.951	100.000

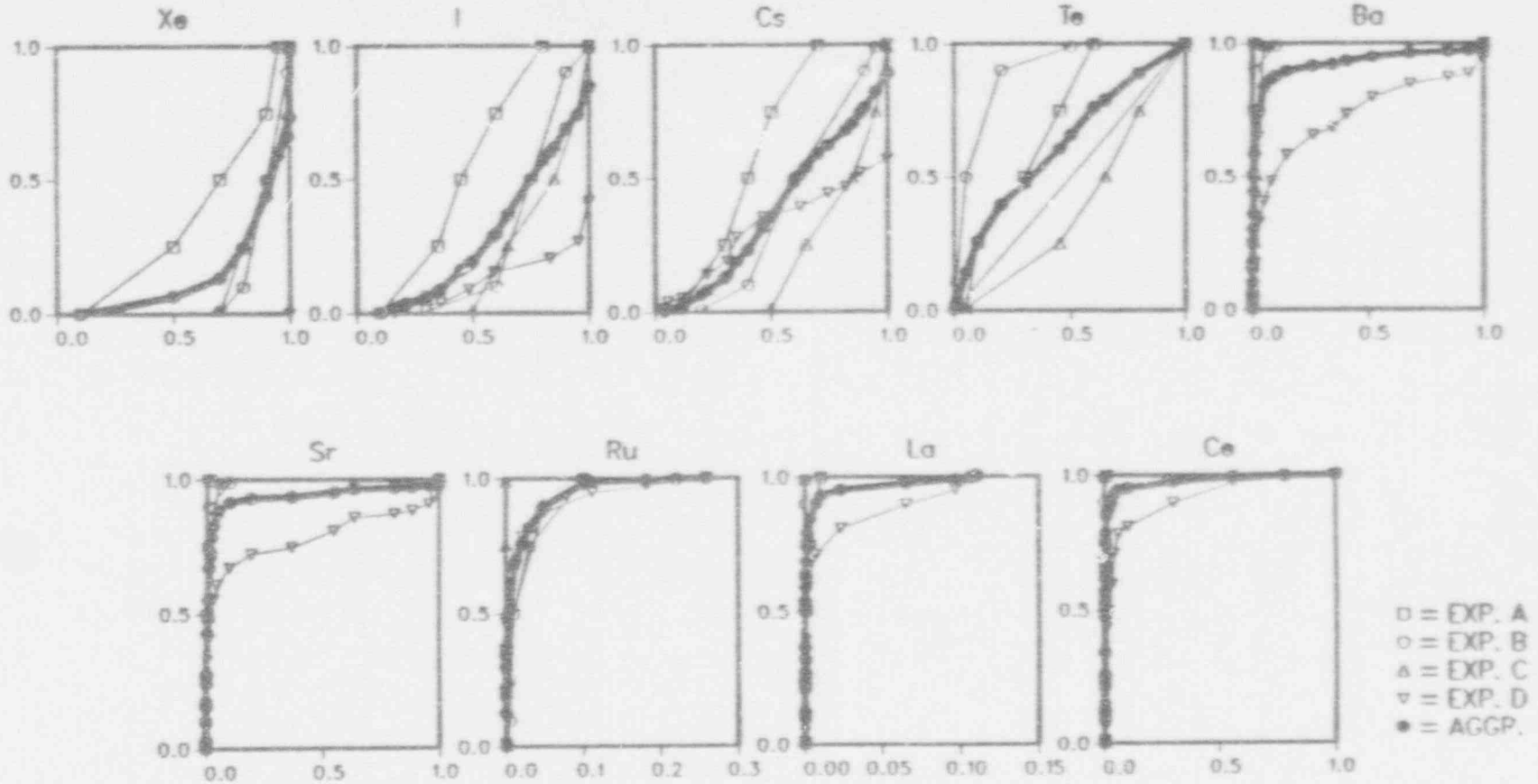

Figure 1-3. FCOR, Case PWR-1, high zirconium oxidation. Release fraction (abscissa) by cumulative probability (ordinate).

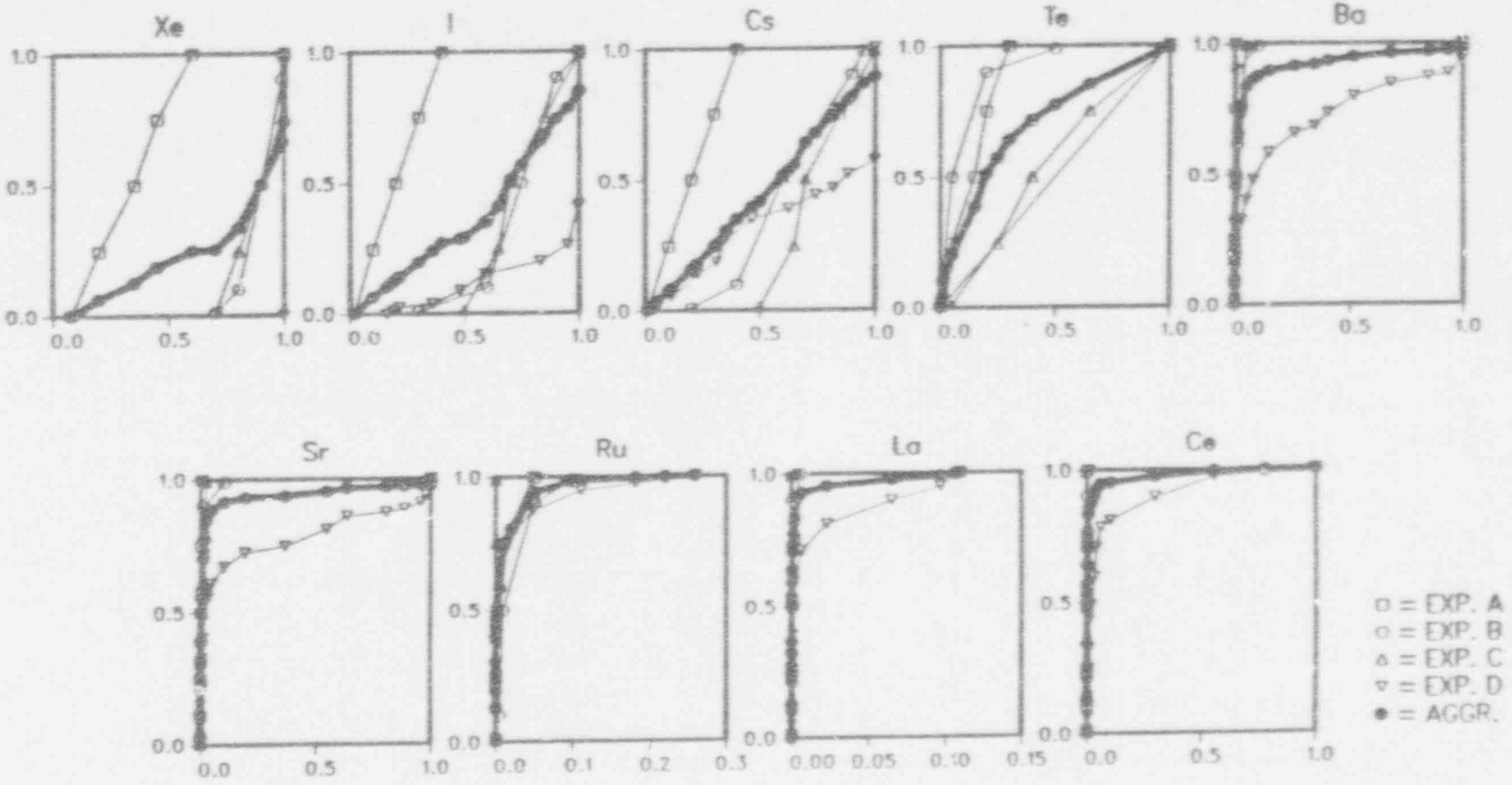

Figure 1-4. FCOR, Case PWR-2, low zirconium oxidation. Release Fraction (abscissa) by cumulative probability (ordinate).

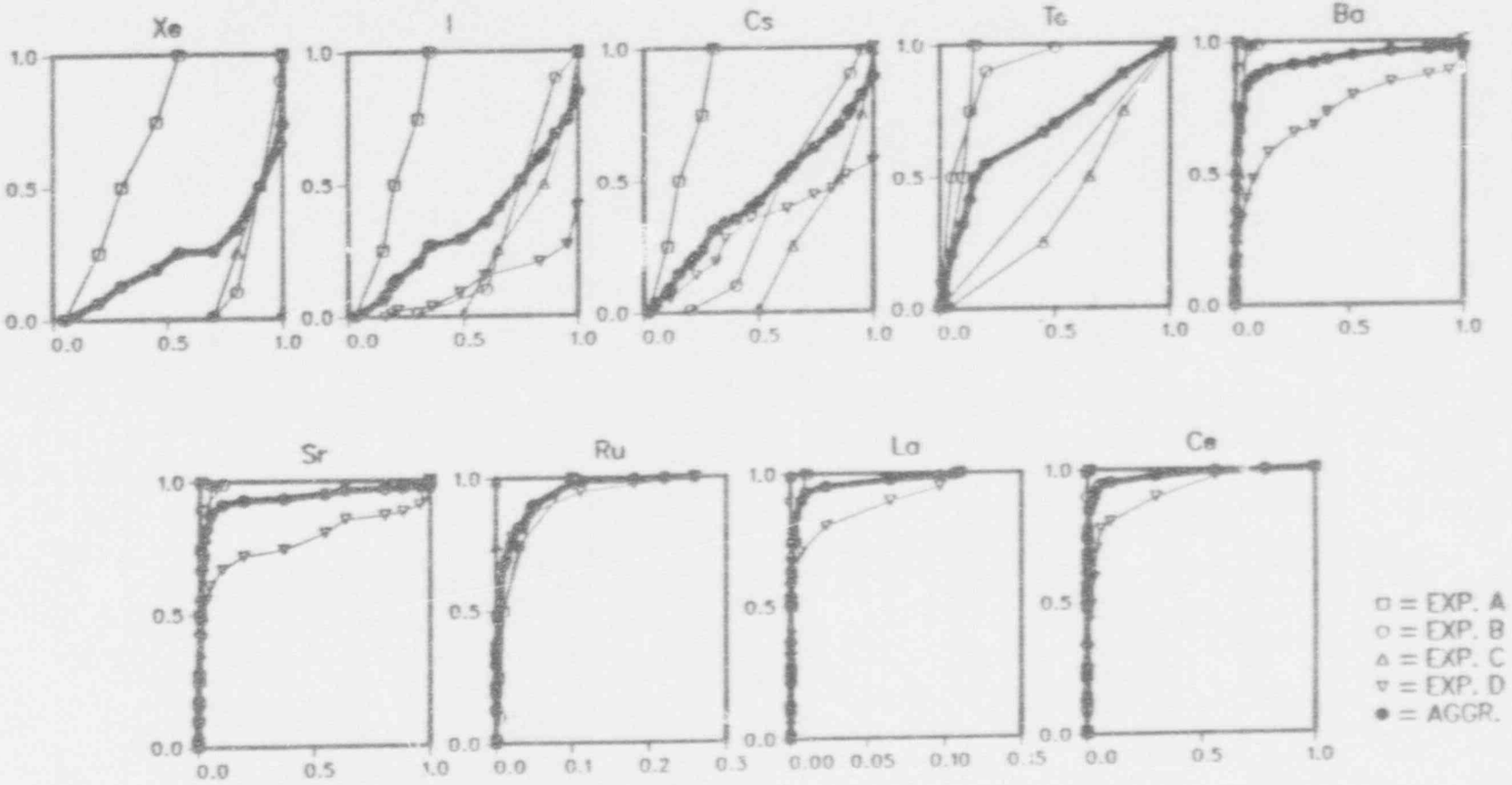

Figure 1-5. FCOR, Case EWR-1, high zirconium oxidation. Release fraction (abscissa) by cumulative probability (ordinate).

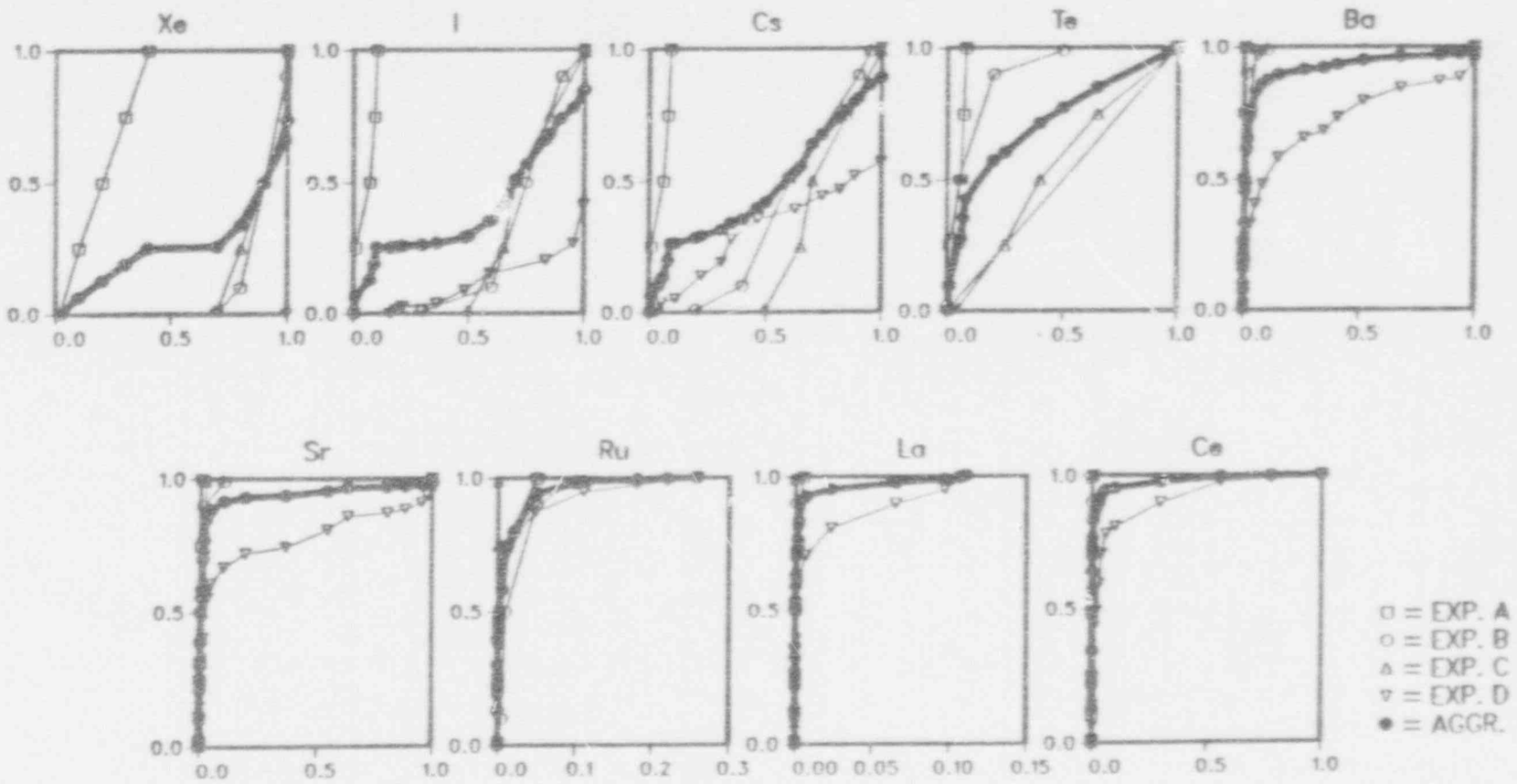

Figure 1-6. FCOR, Case BWR-2, low zirconium oxidation. Release fraction (abscissa) by cumulative probability (ordinate).

Table 1-5
Fractional Release from Vessel (%) FVES
Case PWR-1--Setpoint Pressure
Aggregate

Nuclide Group	Cumulative Probability								
	0.000	0.010	0.050	0.250	0.500	0.750	0.950	0.990	1.000
Xenon, Krypton	100.000	100.000	100.000	100.000	100.000	100.000	100.000	100.000	100.000
Iodine, Bromine	0.000	0.000	0.001	0.931	8.609	35.188	77.143	95.833	100.000
Cesium, Rubidium	0.000	0.000	0.001	0.513	4.248	35.188	77.143	95.833	100.000
Tellurium, Antimony	0.000	0.000	0.001	0.183	2.803	18.408	76.000	95.833	100.000
Barium	0.000	0.000	0.001	0.183	2.803	17.974	76.000	95.833	100.000
Strontium	0.000	0.000	0.001	0.183	2.803	17.974	76.000	95.833	100.000
Ruthenium, etc.	0.000	0.000	0.001	0.183	2.803	17.974	76.000	95.833	100.000
Lanthanum, etc.	0.000	0.000	0.001	0.183	2.803	17.974	76.000	95.833	100.000
Cerium, etc.	0.000	0.000	0.001	0.183	2.803	17.974	76.000	95.833	100.000

Table 1-6
Fractional Release from Vessel (%) FVES
Case PWR-2,3--High and Intermediate Pressure
Aggregate

Nuclide Group	Cumulative Probability								
	0.000	0.010	0.050	0.250	0.500	0.750	0.950	0.990	1.000
Xenon, Krypton	100.000	100.000	100.000	100.000	100.000	100.000	100.000	100.000	100.000
Iodine, Bromine	0.000	0.003	1.088	19.547	41.040	60.764	89.121	99.219	100.000
Cesium, Rubidium	0.000	0.003	0.895	13.082	29.469	58.548	89.121	99.219	100.000
Tellurium, Antimony	0.000	0.003	0.804	11.615	24.843	42.903	88.806	99.219	100.000
Barium	0.000	0.003	0.858	12.576	23.813	37.186	86.977	99.219	100.000
Strontium	0.000	0.003	0.858	12.576	23.813	37.186	86.977	99.219	100.000
Ruthenium, etc.	0.000	0.003	0.858	12.576	23.813	37.186	86.977	99.219	100.000
Lanthanum, etc.	0.000	0.003	0.858	12.576	23.813	37.186	86.977	99.219	100.000
Cerium, etc.	0.000	0.003	0.858	12.576	23.813	37.186	86.977	99.219	100.000

Table 1-7
Fractional Release from Vessel (%) FVES
Case PWR-4--Low Pressure
Aggregate

Nuclide Group	Cumulative Probability								
	0.000	0.010	0.050	0.250	0.500	0.750	0.950	0.990	1.000
Xenon, Krypton	100.000	100.000	100.000	100.000	100.000	100.000	100.000	100.000	100.000
Iodine, Bromine	0.000	2.500	11.502	31.079	51.631	86.524	99.314	99.902	100.000
Cesium, Rubidium	0.000	1.111	7.199	20.402	40.150	86.524	99.314	99.902	100.000
Tellurium, Antimony	0.000	0.588	4.041	16.682	33.295	66.713	99.167	99.833	100.000
Barium	0.000	0.588	4.041	16.682	33.295	61.773	99.167	99.833	100.000
Strontium	0.000	0.588	4.041	16.682	33.295	61.773	99.167	99.833	100.000
Ruthenium, etc.	0.000	0.588	4.041	16.682	33.295	61.773	99.167	99.833	100.000
Lanthanum, etc.	0.000	0.588	4.041	16.682	33.295	61.773	99.167	99.833	100.000
Cerium, etc.	0.000	0.588	4.041	16.682	33.295	61.773	99.167	99.833	100.000

Table 1-8
Fractional Release from Vessel (%) FVES
Case BWR-4--TBUX (Fast, High Pressure)
Aggregate

Nuclide Group	Cumulative Probability								
	0.000	0.010	0.050	0.250	0.500	0.750	0.950	0.990	1.000
Xenon, Krypton	100.000	100.000	100.000	100.000	100.000	100.000	100.000	100.000	100.000
Iodine, Bromine	0.000	0.002	0.008	0.962	8.598	33.205	78.635	96.134	100.000
Cesium, Rubidium	0.000	0.002	0.008	0.509	3.323	31.596	79.068	96.271	100.000
Tellurium, Antimony	0.000	0.001	0.005	0.191	3.323	30.725	78.222	96.000	100.000
Barium	0.000	0.001	0.005	0.191	3.323	25.209	76.746	95.484	100.000
Strontium	0.000	0.001	0.005	0.191	3.323	25.209	76.746	95.484	100.000
Ruthenium, etc.	0.000	0.001	0.005	0.191	3.323	25.209	76.746	95.484	100.000
Lanthanum, etc.	0.000	0.001	0.005	0.191	3.323	25.209	76.746	95.484	100.000
Cerium, etc.	0.000	0.001	0.005	0.191	3.323	25.209	76.746	95.484	100.000

Table 1-9
Fractional Release from Vessel (%) FVES
Case BWR-2--TBU (Fast, Low Pressure)
Aggregate

Nuclide Group	Cumulative Probability								
	0.000	0.010	0.050	0.250	0.500	0.750	0.950	0.990	1.000
Xenon, Krypton	100.000	100.000	100.000	100.000	100.000	100.000	100.000	100.000	100.000
Iodine, Bromine	0.000	0.592	4.142	22.818	40.703	63.025	98.558	99.712	100.000
Cesium, Rubidium	0.000	0.334	2.341	13.673	30.000	60.328	98.558	99.712	100.000
Tellurium, Antimony	0.000	0.334	2.341	13.673	26.901	58.562	98.558	99.712	100.000
Barium	0.000	0.334	2.341	12.776	25.927	58.008	98.558	99.712	100.000
Strontium	0.000	0.334	2.341	12.776	25.927	58.008	98.558	99.712	100.000
Ruthenium, etc.	0.000	0.334	2.341	12.776	25.927	58.008	98.558	99.712	100.000
Lanthanum, etc.	0.000	0.334	2.341	12.776	25.927	58.008	98.558	99.712	100.000
Cerium, etc.	0.000	0.334	2.341	12.776	25.927	58.008	98.558	99.712	100.000

Table 1-10
Fractional Release from Vessel (%) FVES
Case BWR-3-- X (Slow, High Pressure CRD)
Aggregate

Nuclide Group	Cumulative Probability								
	0.000	0.010	0.050	0.250	0.500	0.750	0.950	0.990	1.000
Xenon, Krypton	100.000	100.000	100.000	100.000	100.000	100.000	100.000	100.000	100.000
Iodine, Bromine	0.000	0.008	1.802	8.933	27.925	54.523	94.504	99.213	100.000
Cesium, Rubidium	0.001	0.008	0.758	5.187	24.557	63.353	89.885	98.507	100.000
Tellurium, Antimony	0.000	0.002	0.010	0.488	10.261	38.296	69.677	87.778	98.326
Barium	0.000	0.002	0.010	0.476	7.756	28.652	69.677	87.778	98.326
Strontium	0.000	0.002	0.010	0.476	7.756	28.652	69.677	87.778	98.326
Ruthenium, etc.	0.000	0.002	0.010	0.476	7.756	28.652	69.677	87.778	98.326
Lanthanum, etc	0.000	0.002	0.010	0.476	7.756	28.652	69.677	87.778	98.326
Cerium, etc.	0.000	0.002	0.010	0.476	7.756	28.652	69.677	87.778	98.326

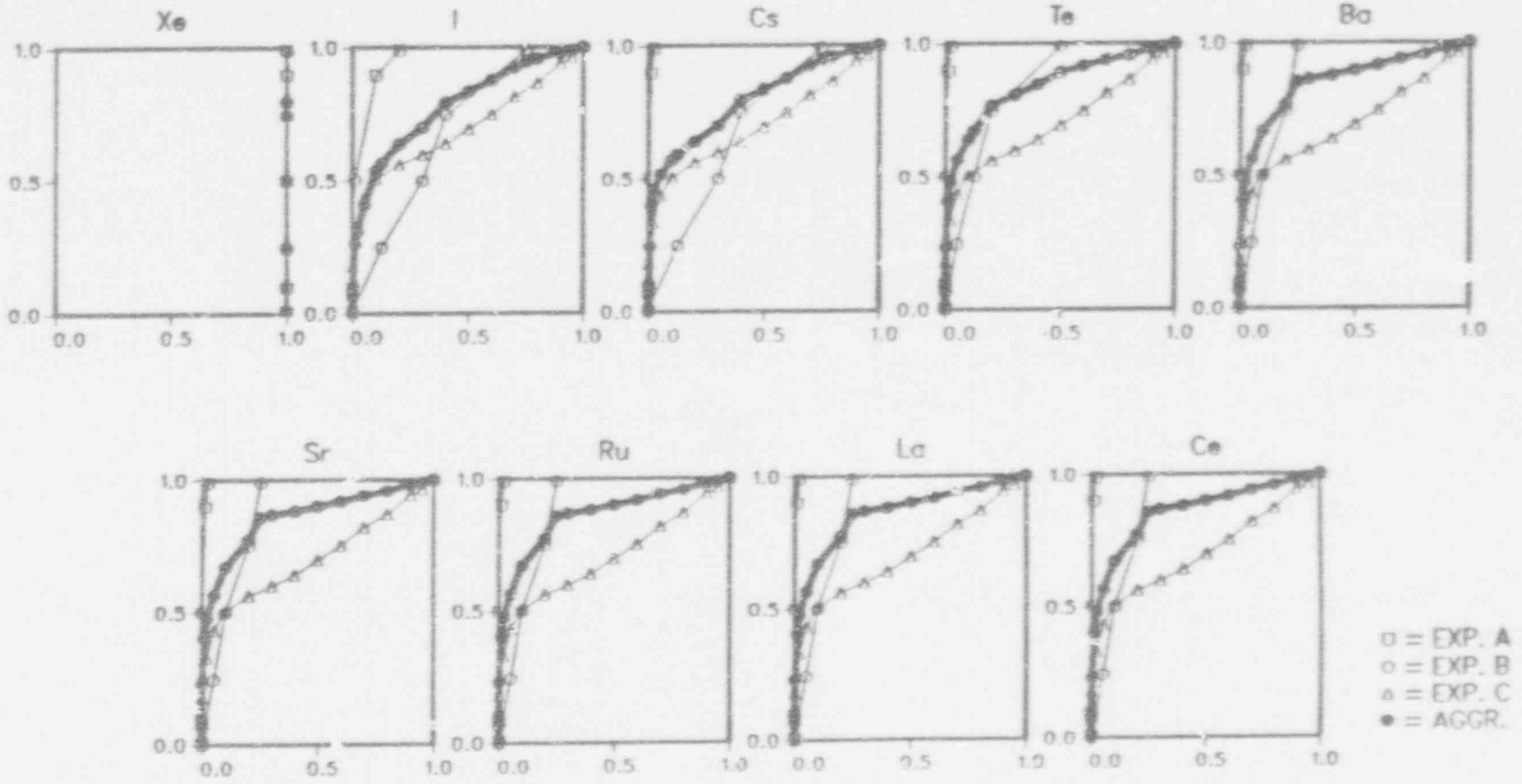

Figure 1-7. FVES, Case PWR-1, Setpoint pressure. Release fraction (abscissa) by cumulative probability (ordinate).

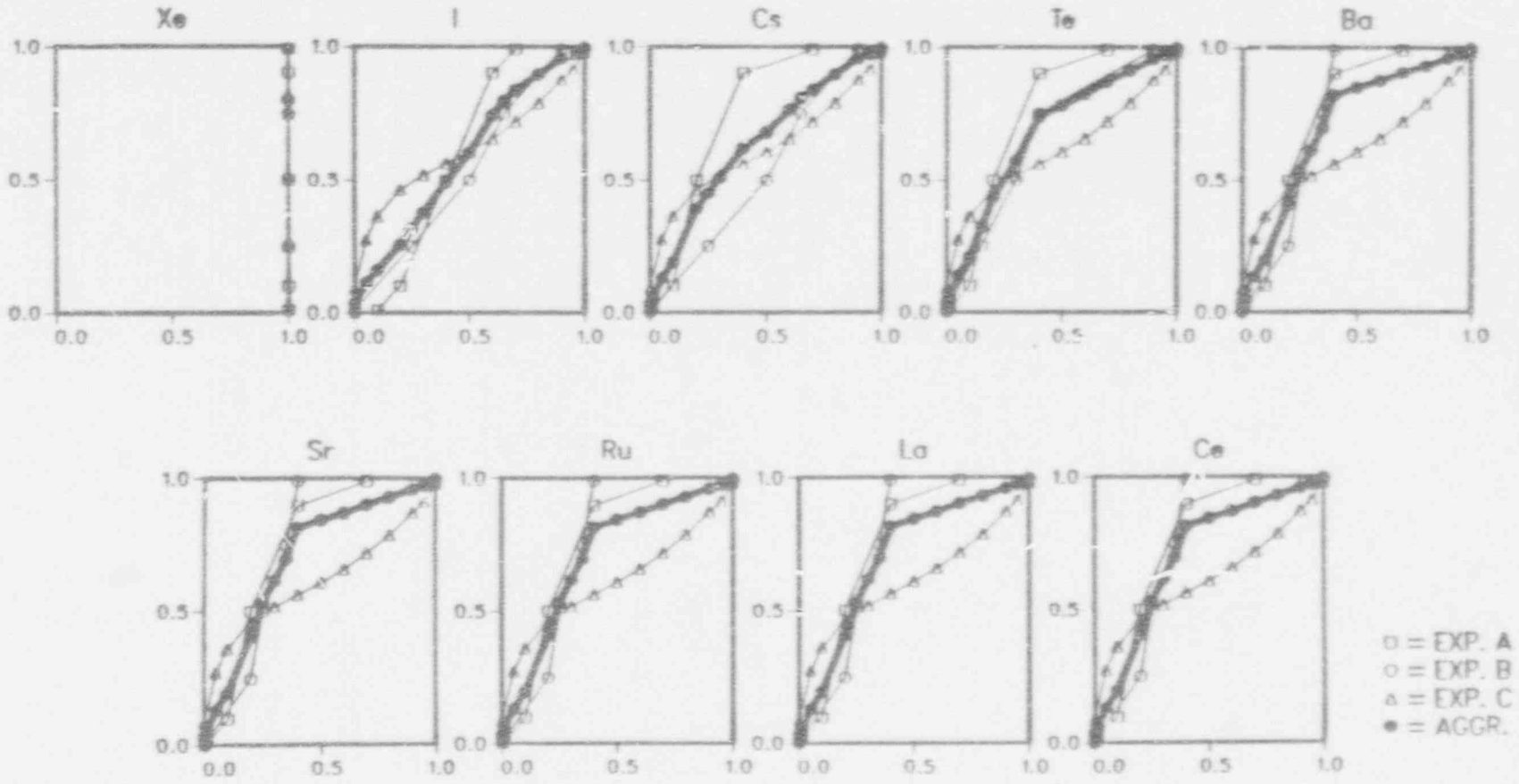

Figure 1-8. FVES, Case PWR-2/3, high and intermediate pressure. Release fraction (abscissa) by cumulative probability (ordinate).

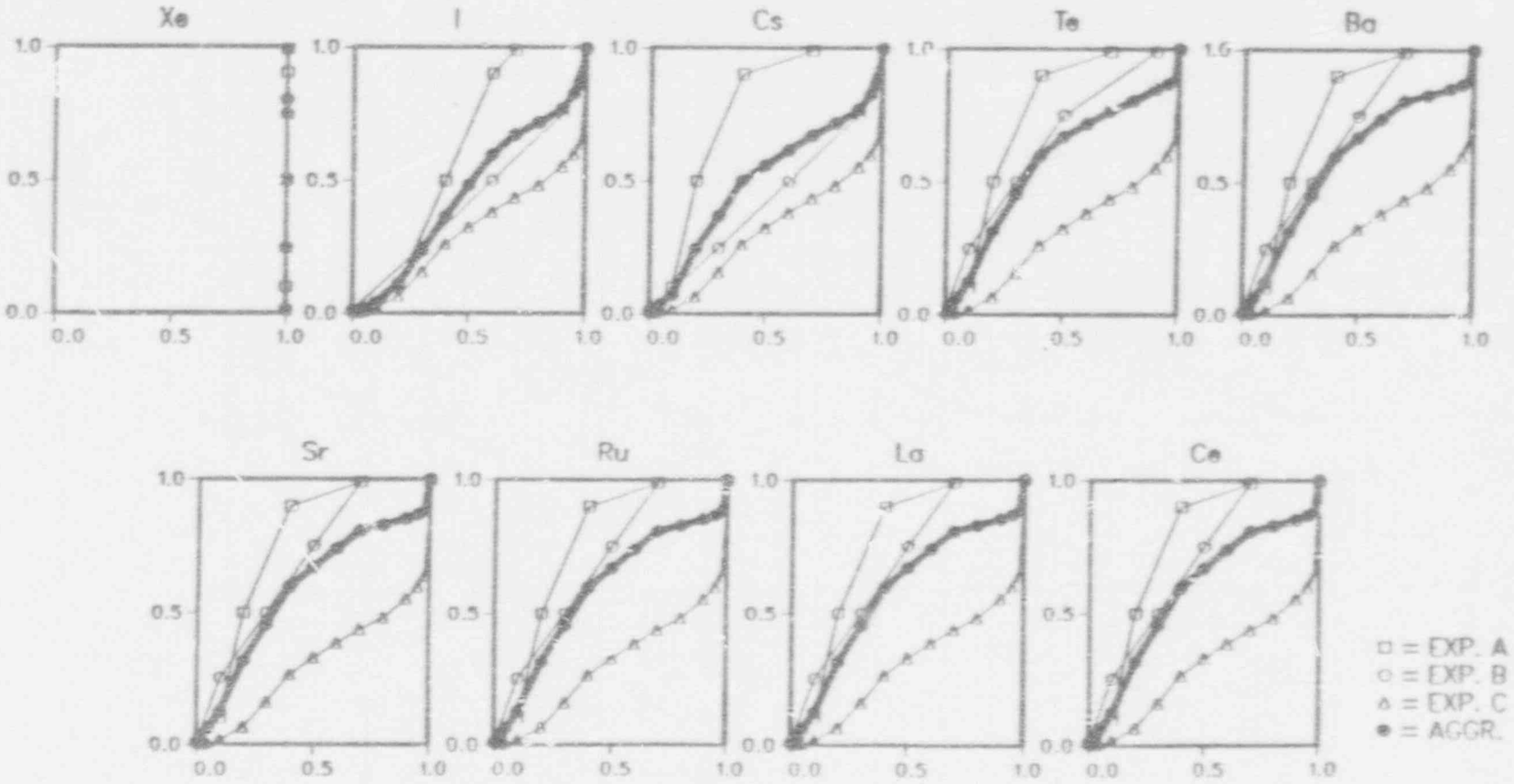

Figure 1-9. FVES, Case PWR-4, low pressure Release fraction (abscissa) by cumulative probability (ordinate).

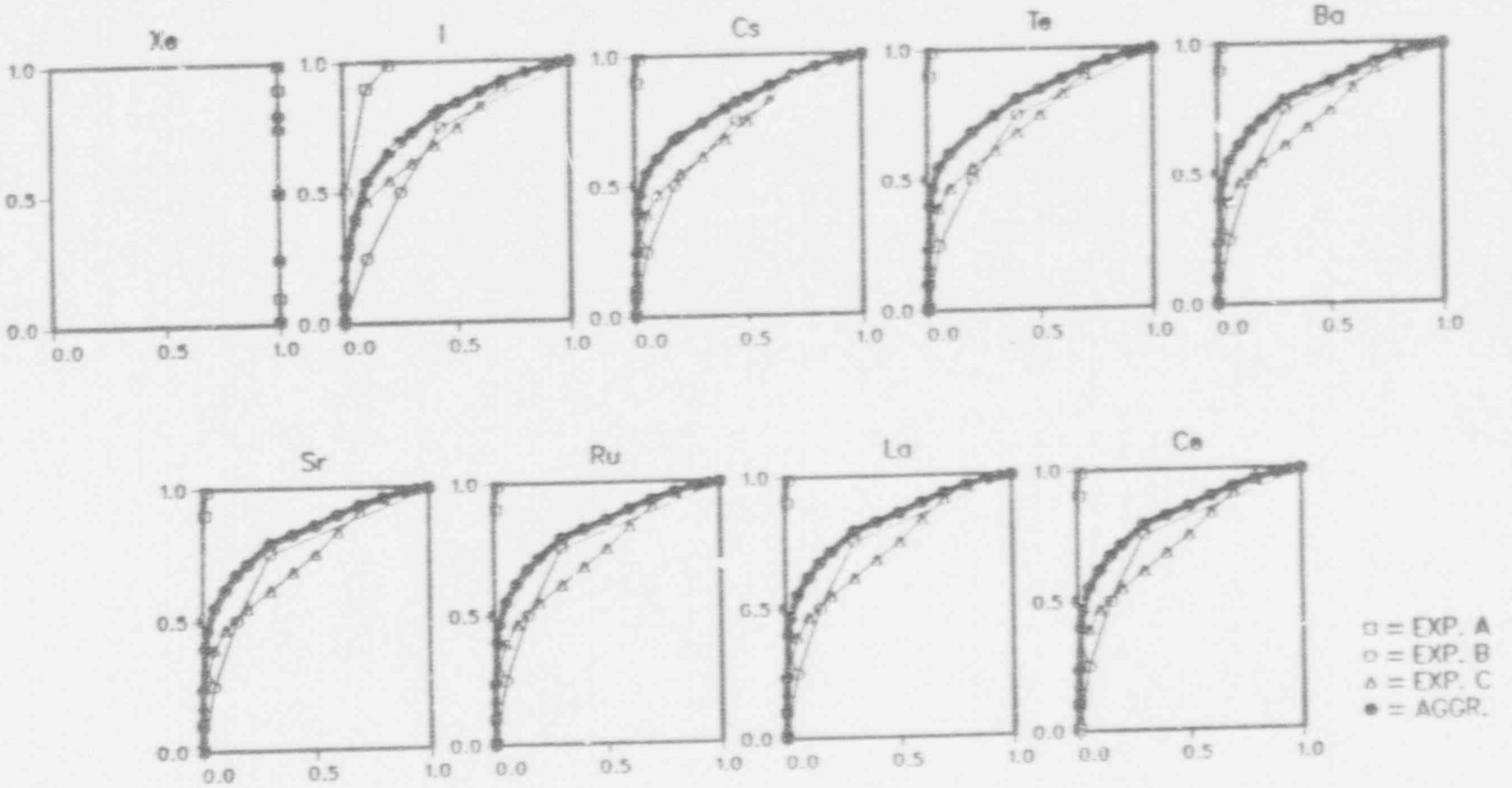

Figure 1-10. FVES, Case BWR-1, TBUX fast, high pressure. Release fraction (abscissa) by cumulative probability (ordinate).

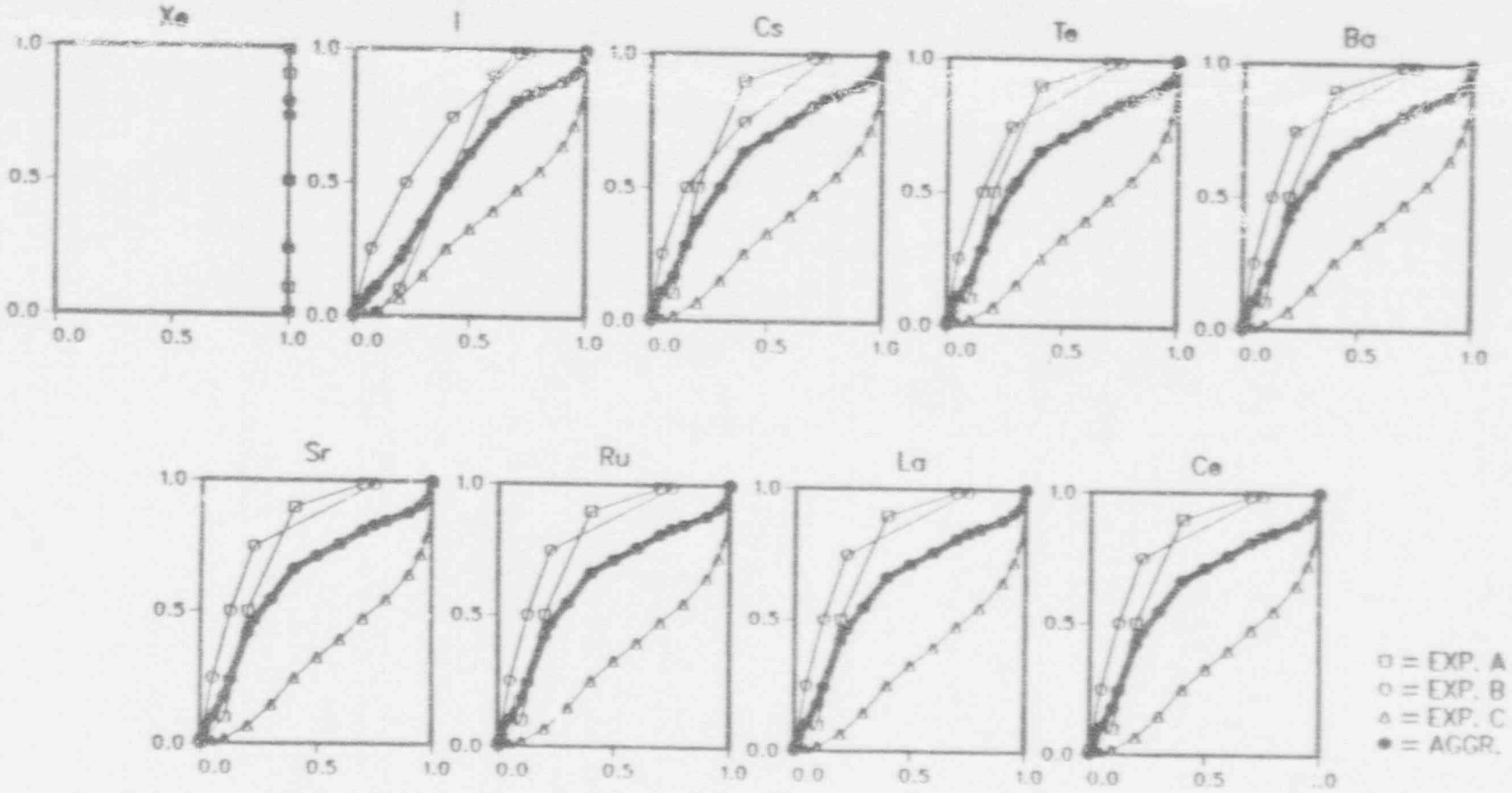

Figure 1-11. FVES, Case BWR-2, TBU fast, low pressure. Release fraction (abscissa) by cumulative probability (ordinate).

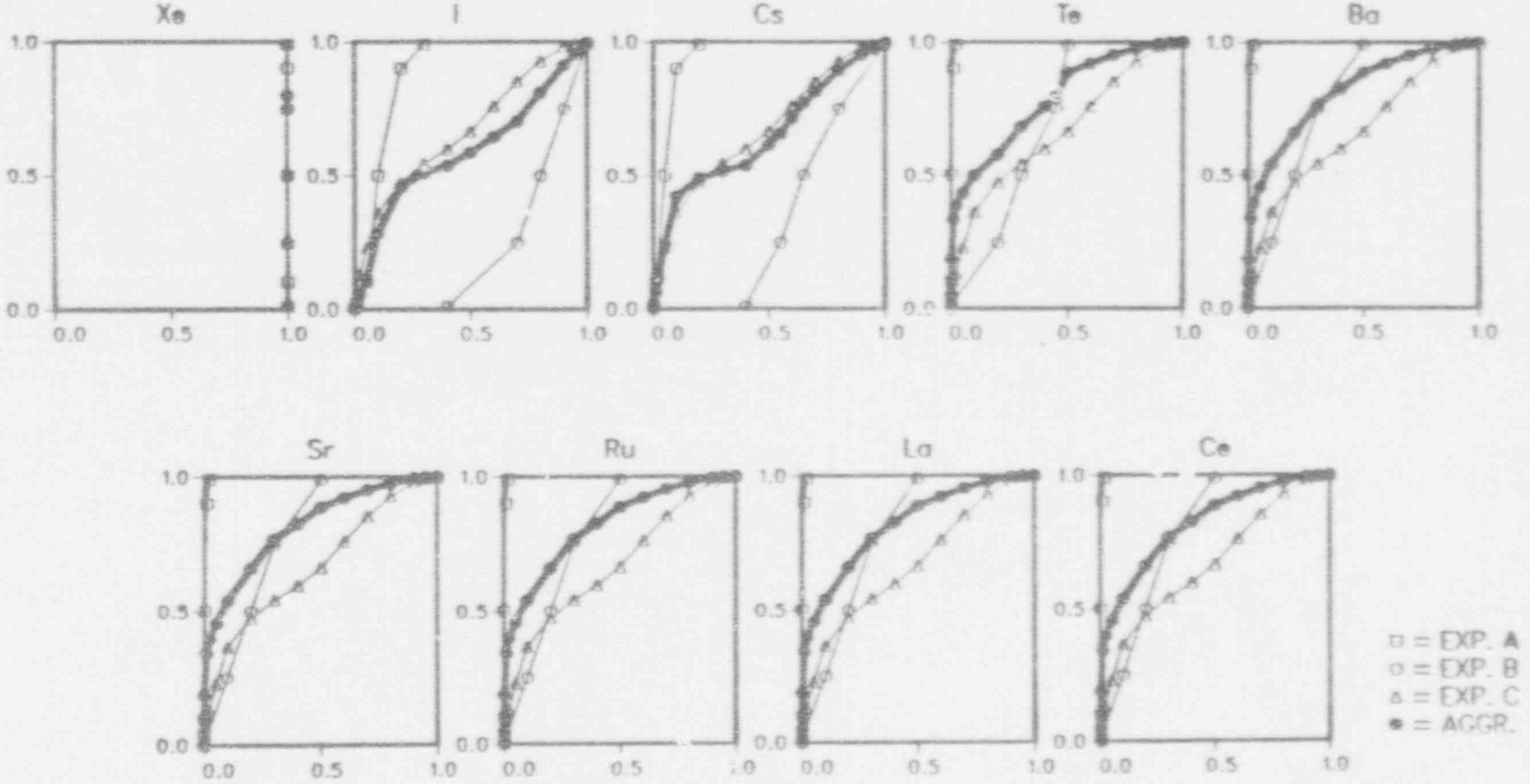

Figure 1-12. FVES, Case BWR-3, TCUX slow, high pressure, CRD. Release fraction (abscissa) by cumulative probability (ordinate).

Individual Elicitations for Issue 1

Expert A's Elicitation

Issue 1. Release of Fission Products from the Fuel in the Vessel and from the Vessel to the Containment

The next several pages (including Figures A-1 and A-2) present Expert A's rationale for FCOR in his own words. To provide a means for considering different rates of heatup and to integrate easily his decomposition, he used a computer program of several hundred lines. A listing of this program is available in the detailed elicitation notes.

Description of Expert A's Rationale/Methodology

I believe that the release of fission products from fuel is influenced by the following:

- The fission product species diffusion and volatility characteristics;
- Fuel heatup rates;
- The temperature at which melting (liquefaction) occurs;
- The time at temperature before relocation and cooling;
- The degree of clad oxidation (for Te and possibly Ba and Ru);
- Oxidation of fuel;
- Liquefaction.

And on a whole core basis:

- The melt progression characteristics (fractions of core involved).
- Surface/volume ratios.
- Quenching effects.

If one focuses only on a piece of fuel, say a unit mass, then the ORNL experiments indicate that the release of fission products generally can be correlated by a diffusive-like relationship:

$$\frac{dc}{dt} = DV^2C$$

where

$$D = D_0 e^{-\frac{Q}{T}}.$$

Best-fitting this type of relationship to the ORNL cesium release data gives:

- Equivalent spherical length parameter = 6 μ
- D_o = .0000763 cm^2/s
- Q = 74300 cal/mol.

A typical comparison of the predicted release pattern using these parameters to the experiments is shown in Figure A-1.

"Relative volatility" considerations extracted from the data on the release of the other fission product species as shown on Figure A-2 can be used to extend the model to the species of interest. The rationale for this is as follows:

Note on Figure A-2 that Dick Lorenz has correlated a great quantity of fission product release data and has shown that the release rate (fraction/unit time) can consistently be correlated with a "relative volatility" (RV) according to

$$\text{Release rate} = Ae^{B(RV)}.$$

Therefore, if the release rate of cesium, for example, is known, the release rates for another species, i, can be determined as

$$(\text{Release rate})_i = Ae^{B(RV_{Cs})\ \frac{(RV_i)}{(RV_{Cs})}}.$$

But since the release of cesium has been correlated by our model as

$$= D_o e^{-Q/T},$$

then the release rate of species i should be

$$(\text{Release rate})_i = Ae^{-(Q/T)\ \frac{(PV_i)}{(RV_{Cs})}}.$$

The values used for the species "relative volatilities" are summarized below as taken from Figure A-2.

Species	RV
1. NG	(Unknown)(determined from ORNL Kr data ~ 1.1)
2. I	1.03
3. Cs	1.00
4. Se, Sa	.68
5. Ba	.42
6. Sr	.34
7. Rn...	.25
8. La, cm	.14
9. Ce,...	.085

The release of tellurium is a special case. It is here assumed to be released from the UO_2 matrix in the same relative amounts as for iodine except that it is held up in any unoxidized zircaloy until the local level of oxidation exceeds 95%.

The "diffusive-like" correlation with the relative volatilities was programmed for solution with arbitrary thermal transients on a PC and the program given the name KREL.

For the purposes of this exercise in determining limits and distributions on the release, the existing code calculations and experimental data Power Burst Facility ([PBF], NRU) were examined to establish generalized "bounding" representative thermal transients during accident sequences. It was observed that, in general, these can be described in three phases:

1. A relatively slow rise in temperature to a value of about 1750 K.

2. A faster rise in temperature (depending on the rate of Zr oxidation) from 1750 K to some "melt" temperature.

3. A hold for some time at the "melt" temperature to liquefy the fuel and allow it to relocate to cooler regions.

Examination of the existing code calculations and additional "hand" calculations made here established the following "bounding" values for the three phases:

Phase 1 - slow rise:

- Fastest ramp is about 0.5 K/s (adiabatic at appropriate decay heat levels).

- Slowest ramp depends on the level of cooling but is generally observed to not be less than 0.1 K/s.

Phase 2 - oxidation driven heat-up:

Examination of the various BMI-2104, MELPROG, SCDAP, BWRSAR, MELCOR, and other calculations as well as observation of experiments (PBF, NRU, ACRR) shows that this ramp varies from about 10 K/s to about 40 K/s.

Phase 3 - representative melt temperature:

Examination of experimental data (ORNL, PBF, ACRR) indicates this value can be as low as 2275 K but generally does not exceed 2700 K (although UO_2 melt temperature = 3200 K).

Phase 3 - hold at melt temperature:

Melting fuel elements require an energy input equivalent to 661 K increase in temperature. The hold time must be consistent with the amount of time required to insert this amount of additional energy at the specified heat-up rate.

It is obvious, then, that the maximum release from a segment of fuel will be obtained from KREL under conditions of:

- Slowest phase-1 heat-up (0.1 K/s up to 1750 K).
- Slowest phase-2 heat-up (10. K/s from 1750 K to Tmelt).
- Highest assumed Tmelt (2700 K).
- Hold time consistent with 10 K/s heat-up rate.

The minimum release will be obtained by:

- Fastest phase-1 heat-up (0.5 K/s up to 1750 K).
- Fastest phase-2 heat-up (40 K/s from 1750 K to Tmelt).
- Lowest value for Tmelt (2275 K).
- Hold time consistent with 40 K/s heat-up rate.

A best guess choice is more difficult to make. My selection to be representative of all the observed behavior is to use a 50-50 combination of the heat-up rates but to select a melt temperature of 2700 K.

On a core-wide basis, the overall release will depend on the integrated behavior of the various local transients (i.e., what portions undergo what transients). For this exercise, we are not given specific sequences with adequate descriptions of the core-wide global melting process. We are asked to characterize the releases under four general conditions:

- PWRs at high oxidation levels
- PWRs at low oxidation levels
- BWRs at high oxidation levels
- BWRs at low oxidation levels.

I believe that the oxidation level is a good general indicator of the overall "energetics" of the accident progression especially for the high temperature phases. That is, the Zr oxidation is believed to be the dominant energy input at temperatures exceeding 1750 K.

The question is how to translate a given level of Zr oxidation into the extent of core participation in the previously defined bounding thermal transients.

This was rationalized as follows:

If a given melting temperature (Tmelt) is presumed, then the amount of energy input into unit mass of the fuel element that will be required to heat from 1750 K to Tmelt plus adding the additional amount of melting energy is given by

$$E = MC_p\Delta T = [M_{fuel}\ Cp_f + M_c\ Cp_c][Tmelt - 1750 + 661].$$

A general value for the energy released during Zr/steam oxidation is about 2762 BTU/lb of Zr reacted.

Therefore, the required amount of Zr reaction to provide all of this energy is $M_{Zr\ reaction} = E/2762$.

The required fraction of the clad to be oxidized to provide the energy for the particular specified thermal transient (assuming negligible heat losses) is

$$f_c = \frac{M_{Zr\ reaction}}{M_c} = \frac{\left[\frac{M_f}{M_c}\ Cp_f + Cp_c\right]\left[Tmelt - 1750 + 661\right]}{2762}.$$

Typically for both BWR and PWR: $\frac{M_f}{M_c} = 4.88$

$Cp_f = 0.12$ BTU/lb °F

$Cp_c = 0.08$ BTU/lb °F.

These relationships determine the required fraction of clad oxidation to produce the specified thermal behavior. However, we are given as a "sequence" condition, the overall integrated core-wide Zr oxidation level. To be consistent with the specified thermal transient, then we must have a specific value for the fraction of the core involved in the transient that would result in this specified oxidation level.

For PWRs, in which the only Zr involved is the clad, the fraction of core involvement, F_x, to give a specified oxidation level, f_{ox}, must be:

$$F_x = f_{ox}/f_c.$$

For BWRs, the situation is a little more complicated because of the presence of significant Zr in the channel boxes. (It is assumed that the sequence-specified oxidation level includes oxidized channel boxes as well as oxidized clad.) Therefore, the BWR case is rationalized as follows:

The fraction of clad oxidation, f_c, required for the prescribed thermal transient is the same as for the PWR:

$$f_c = \left[\left(\frac{M_b}{M_c}\right) Cp_f + Cp_c\right] [Tmelt - 1750 + 661] / 2762.$$

If we now assume that the ratio of channel box oxidation to clad oxidation is equal to the ratio of surface areas, A_b/A_c, then the fraction of channel box oxidation, f_b, is given by

$$f_b = f_c \left(\frac{A_b}{A_c}\right) R_o \quad \text{where } R_B = \text{ratio of mass of Zr in the clad to that in the channel box, } M_c/M_b$$

$R_B = .73$ and $(A_b/A_c) = .22$.

Therefore the total fraction of Zr reacted to produce the given transient is

$$f_{tot} = f_c + f_b, \text{ and}$$

as with the PWR, the fraction of core involvement, F_x, to produce the transient and to produce the specified level of overall Zr oxidation is given by

$$F_x = f_{ox}/(f_c + f_b).$$

The various core involvement fractions for the specified levels of oxidation and the specified bounding and best guess thermal transients are summarized below:

Case	Tmelt (K)	Overall Zr Oxidation Level (f_{ox})	Fraction of Clad Oxidized (f_o)	Core Involvement Fraction (F_z)
PWR HIGH				
Hi - Hi	2700	84	0.70	1.00
Hi - Lo	2275	36	0.51	0.71
Nominal	2700	60	0.70	0.86
PWR LOW				
Lo - Hi	2700	36	0.70	0.51
Lo - Lo	2375	14	0.51	0.27
Nominal	2700	25	0.70	0.36
BWR HIGH				
Hi - Hi	2700	39	0.70	0.48
Hi - Lo	2275	25	0.51	0.31
Nominal	2700	32	0.70	0.40
BWR LOW				
Lo - Hi	2700	12	0.70	0.15
Lo - Lo	2275	8	0.51	0.10
Nominal	2700	10	0.70	0.12

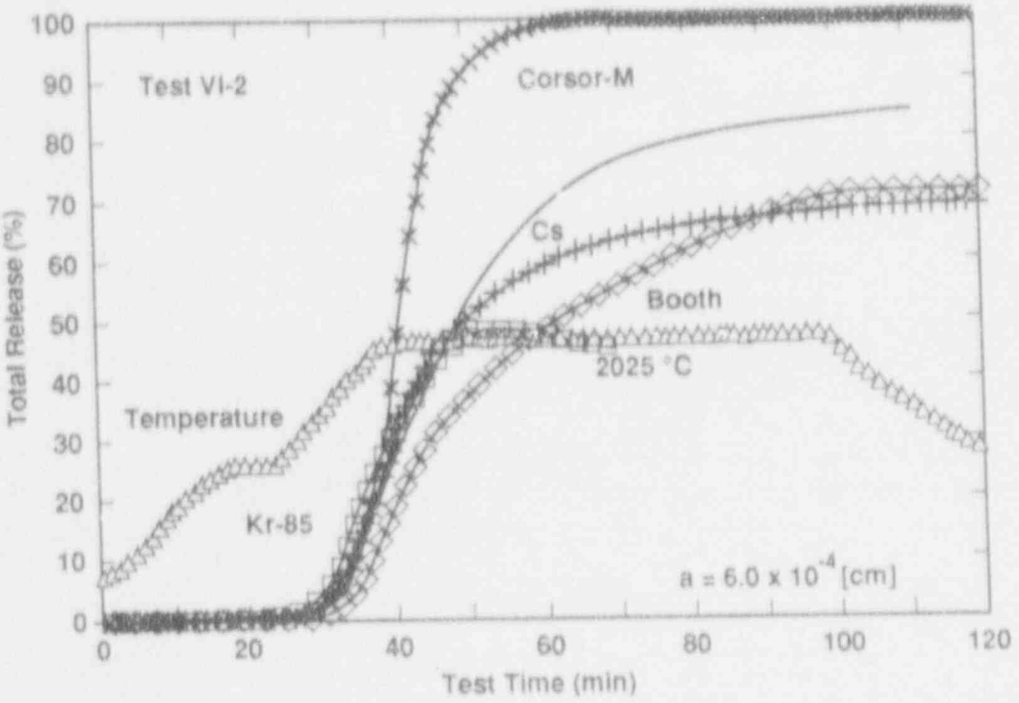

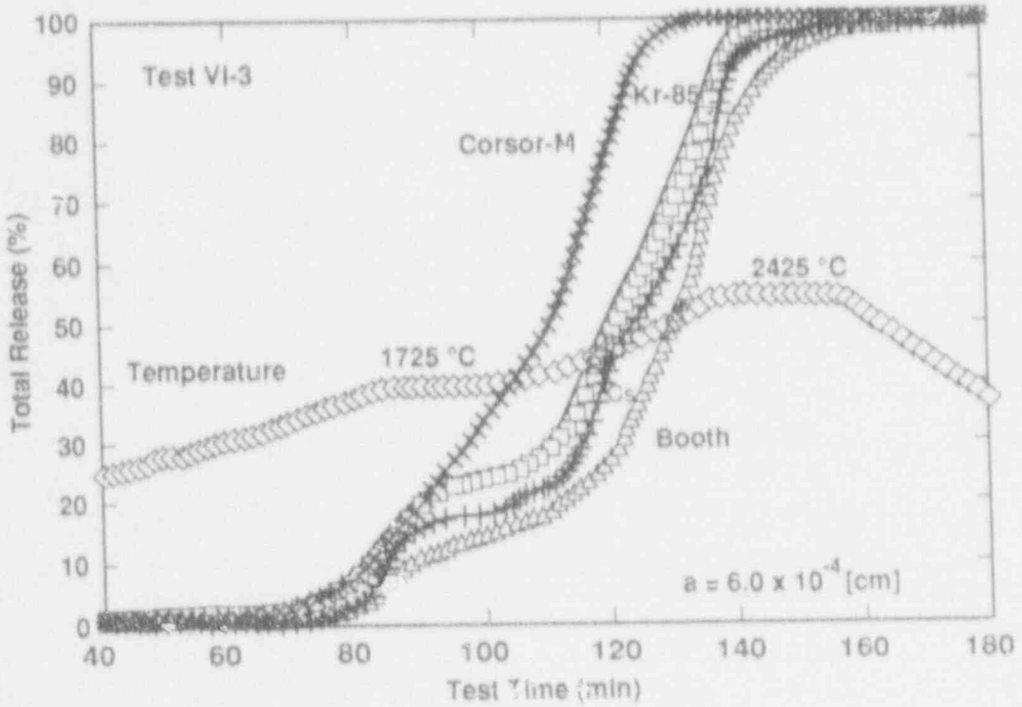

Figure A-1. Krypton and Cesium Releases.

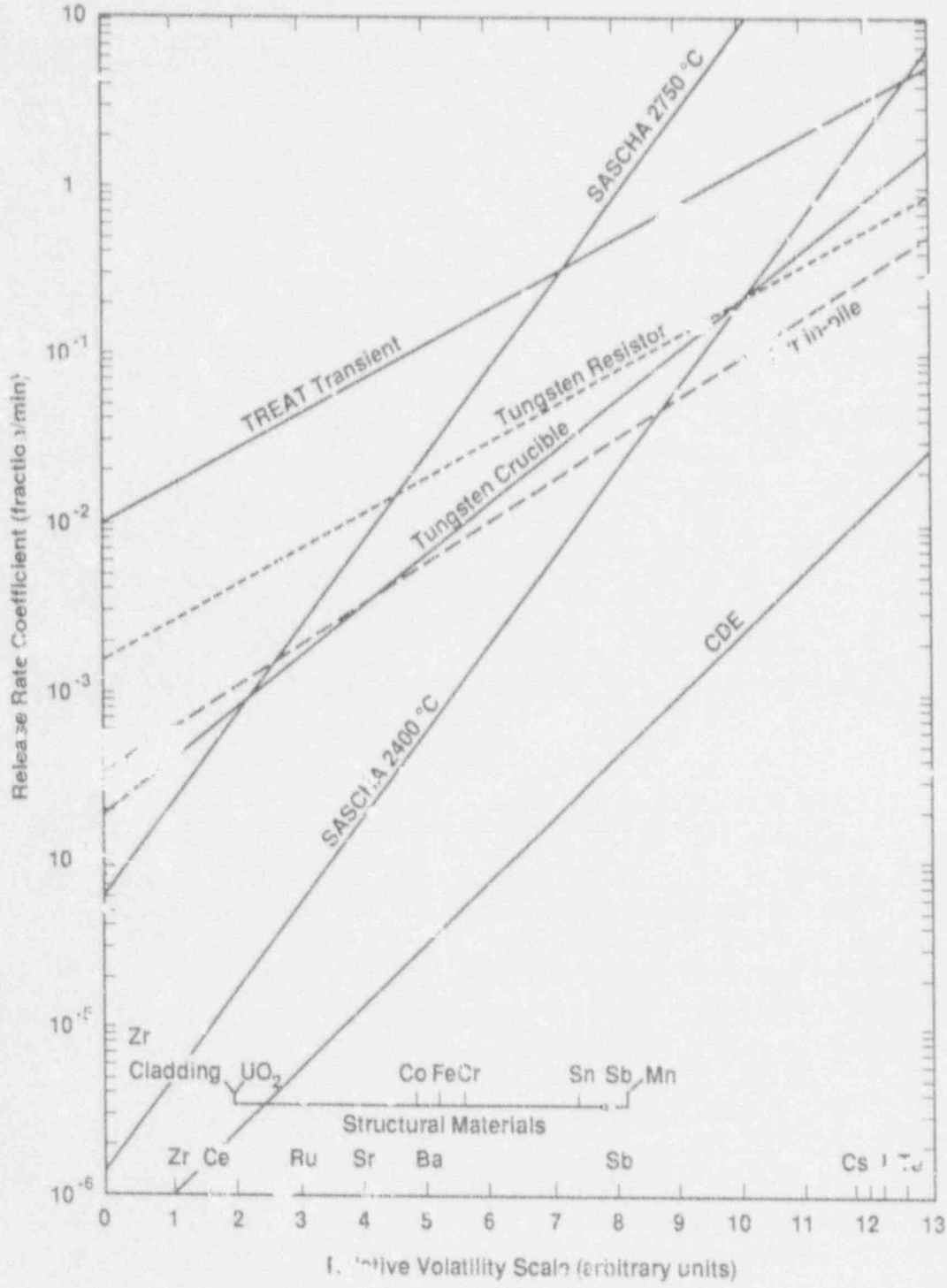

Figure A-2. Relative Volatility Considerations.

Results of Expert A's Elicitation

Expert A's conclusions about FCOR are contained in Tables A-1 through A-4. He provided five points defining a cumulative distribution for radionuclide groups 1 through 4. For groups 5 through 9, he provided only the lower and upper bounds (0.1% and 99.9% values). He stated that a uniform distribution should be used between these points. As the difference between the two endpoints ranges from a factor of 10 to a factor of 500, it is not clear whether Expert A had a uniform arithmetic distribution or a uniform logarithmic distribution in mind.

He felt that not all of the noble gases would be released from the fuel before vessel breach because some of the rods on the periphery of the core would remain relatively cool during the core melt. For the other radionuclide groups, he obtained his midpoint by assuming that half the core heated up from 1750 K to 2700 K quickly and the other half heated up slowly. The results of this approximation compared reasonably well with CORSOR results.

Expert A had difficulty obtaining realistic heatup rates for the core. Only MELPROG has core heatup as a function of radius, and very few MELPROG results are available. Using average core temperature to determine release rates is inadequate because of the strong temperature dependence for most of the nuclide groups.

Expert A obtained his upper bounds by assuming a slow heatup, a high melting temperature, high volatility, a zirconium oxidation at the upper end of the range, and a large fraction of the core molten. For his lower bounds, he assumed the opposite: a fast heatup, a low melting temperature, low volatility, a zirconium oxidation at the lower end of the range, and a small fraction of the core molten.

Expert A concluded that the releases for the fuel for the BWRs would be less than for the PWRs, mainly because the peripheral cold region is larger in the BWRs. The BWR power profile is steeper at the edge, and the channel boxes restrict radial natural circulation during core melt.

Table A-1
Fractional Release (%) from Fuel to Vessel--FCOR
Case 1--PWR with High Zirconium Oxidation

Nuclide Group	Cumulative Probability 0.1%	25%	50%	75%	99.9%
1. Xenon, Krypton	10.0	50.0	70.0	90.0	95.0
2. Iodine, Bromine	10.0	35.0	5.0	60.0	80.0
3. Cesium, Rubidium	10.0	30.0	1.0	50.0	70.0
4. Tellurium, Antimony, Selenium	5.0	10.0	30.0	45.0	60.0
5. Barium	0.1	0.25*	0.5*	0.75*	1.0
6. Strontium	0.1	0.25*	0.5*	0.75*	1.0
7. Ruthenium, etc.	0.1	0.3*	1.0*	3.0*	10.0
8. Lanthanum, etc.	0.01	0.03*	0.1*	0.3*	1.0
9. Cerium, etc.	0.01	0.03*	0.1*	0.3*	1.0

*Interpolated values

Table A-2
Fractional Release (%) from Fuel to Vessel--FCOR
Case 2--PWR With Low Zirconium Oxidation

Nuclide Group	Cumulative Probability 0.1%	25%	50%	75%	99.9%
1. Xenon, Krypton	8.0	20.0	35.0	45.0	60.0
2. Iodine, Bromine	2.0	10.0	20.0	30.0	40.0
3. Cesium, Rubidium	1.0	10.0	20.0	30.0	40.0
4. Tellurium, Antimony, Selenium	0.1	5.0	15.0	20.0	30.0
5. Barium	0.01	0.03*	0.07*	0.19*	0.5
6. Strontium	0.01	0.03*	0.07*	0.19*	0.5
7. Ruthenium, etc.	0.01	0.05*	0.22*	1.05*	5.0
8. Lanthanum, etc.	0.01	0.03*	0.07*	0.19*	0.5
9. Cerium, etc.	0.01	0.03*	0.07*	0.19*	0.5

*Interpolated values

Table A-3
Fractional Release (%) from Fuel to Vessel--FCOR
Case 3--BWR with High Zirconium Oxidation

Nuclide Group	Cumulative Probability 0.1%	25%	50%	75%	99.9%
1. Xenon, Krypton	5.0	20.0	30.0	45.0	55.0
2. Iodine, Bromine	3.0	15.0	20.0	30.0	35.0
3. Cesium, Rubidium	2.0	10.0	15.0	25.0	30.0
4. Tellurium, Antimony, Selenium	2.0	5.0	10.0	13.0	15.0
5. Barium	0.1	0.25*	0.5*	0.75*	1.0
6. Strontium	0.1	0.25*	0.5*	0.75*	1.0
7. Ruthenium, etc.	0.1	0.3*	1.0*	3.0*	10.0
8. Lanthanum, etc.	0.01	0.03*	0.1*	0.3*	1.0
9. Cerium, etc.	0.01	0.03*	0.1*	0.3*	1.0

*Interpolated values

Table A-4
Fractional Release (%) from Fuel to Vessel--FCOR
Case 4--BWR with Low Zirconium Oxidation

Nuclide Group	Cumulative Probability 0.1%	25%	50%	75%	99.9%
1. Xenon, Krypton	2.0	10.0	20.0	30.0	40.0
2. Iodine, Bromine	0.6	1.0	7.0	9.0	10.0
3. Cesium, Rubidium	0.5	1.0	6.0	8.0	9.0
4. Tellurium, Antimony, Selenium	0.5	1.0	6.0	7.0	8.0
5. Barium	0.01	0.03*	0.07*	0.19*	0.5
6. Strontium	0.01	0.03*	0.07*	0.19*	0.5
7. Ruthenium, etc.	0.01	0.05*	0.22*	1.05*	5.0
8. Lanthanum, etc.	0.01	0.03*	0.07*	0.19*	0.5
9. Cerium, etc.	0.01	0.03*	0.07*	0.19*	0.5

*Interpolated values

Expert B's Elicitation

Issue 1. Release of Fission Products from the Fuel in the Vessel and from the Vessel to the Containment

Description of Expert B's Rationale/Methodology

Most of Expert B's contributions were derived from a wide array of MAAP[B-1] runs of various accident scenarios. While the MAAP runs were the basis for input, the expert's distributions included uncertainty because of phenomena other than those specifically represented in MAAP. Note that the MAAP runs did not directly translate into the points on his distribution, and some MAAP analyses would possibly give results outside this expert's uncertainty ranges. This is possible because of this expert's knowledge that MAAP can overstate the releases as a result of phenomena not modeled, such as limitations imposed on other physical events by the process of core collapse.

Expert B did not believe that the distinction between cases depending on the level of zirconium oxidation was necessary; thus, that aspect of the originally defined case structure is excluded here. This decision was based on his observation that the zirconium dependence was not of great significance for the parameters considered here.

Finally, Expert B cautioned that the elicitation of input in this manner (limited distinction of scenarios) necessitates a careful examination of the results and possible reiteration. If, for example, one type of scenario dominated the results, the uncertainty in this issue may be overstated.

Results of Expert B's Elicitation: FCOR

Expert B did not believe that it was necessary to distinguish the uncertainty ranges for the BWRs and PWRs for this variable. Therefore, with no dependencies on zirconium oxidation or RCS pressure, only one set of values was provided (Table B-1).

Sources of Uncertainty: FCOR

Expert B discussed the factors most affecting his selection of uncertainty ranges for each of the individual groups. For the noble gases, the uncertainty is not large, and the range of values represents the uncertainty of not being able to specify the exact nature of the meltdown. The iodine values represent primarily cesium iodide. This uncertainty range was derived from the MAAP code results, integrated with the evidence from the Three Mile Island (TMI) accident. Expert B also broadened this distribution somewhat to account for the other states of iodine. The cesium distribution is also based on MAAP, but it has been more strongly affected by Expert B's review of TMI data, which shows that cesium remained

Table B-1
Values of FCOR for Radionuclide Groups*

Distribution	Noble Gases	(CsI)	Cs	Te	(SrO)	(MoO_2)	(Ba_2)
Lower Limit	0.70	0.30	0.20	0.0	1×10^{-5}	1×10^{-3}	1×10^{-4}
90% Confidence**	0.80	0.60	0.40	0.01	1×10^{-4}	5×10^{-3}	1×10^{-3}
50% Confidence	0.90	0.75	0.60	0.05	1×10^{-3}	0.01	5×10^{-3}
10% Confidence	0.99	0.90	0.90	0.20	0.01	0.05	0.01
Upper Limit	1.0	1.00	0.95	0.50	0.10	0.10	0.10

*Expert B divided the groups somewhat differently. Specific species were used for the nonvolatiles. Lanthanum and cesium releases were estimated to be less than 1×10^{-4} and were not included in the uncertainty elicitation.

**The confidence level is the likelihood of an equal or greater FCOR value than the level indicated. For example, there is a 90% chance that FCOR is greater than or equal to 0.8 for iodine.

in portions of the core that had experienced very high temperatures during the accident. It is therefore reasonable to assume that there are mechanisms that could limit the amount of cesium release.

The tellurium release is low because the tellurium gets bound up with unreacted zirconium clad. There is no dependence on the amount of zirconium oxidation, however, because there is so much cladding that even a very small unreacted portion would control the tellurium release. The uncertainty range is dominated by the uncertainty of the exact nature of the meltdown progression, but it is also broadened by the potential for unknown chemical states.

For the nonvolatiles, Expert B provided separate ranges for different species. Expert B also suggested that these could be combined, if expedient to do so, into a single uncertainty range (that provided for strontium oxide) to apply to all nonvolatiles. The uncertainty in the nonvolatile releases is from uncertainty in the exact scenario. The ranges are wide, reflecting the ranges of MAAP results for different scenarios. The distributions are similar, although the MAAP results indicate slightly higher volatility for molybdenum oxide. The lanthanum and cesium releases were thought to be too small to be significant.

Results of Expert B's Elicitation: FVES

The FVES values were provided with a case structure, although Expert B required only two pressure regimes rather than the three suggested. Note that the pressure regime was assumed to be defined by the pressure at the time of lower head failure. All scenarios involving induced ruptures

should use the lower pressure values, since the time at low pressure will dominate the process and the larger release would be expected. The high and low pressure cases were construed to have the same uncertainty ranges for either the PWR or the BWR, with only case 3 for the BWR requiring a special distribution. Expert B's inputs for each of the cases are given in Tables B-2 through B-4.

Table B-2
FVES PWR Case 1, High Pressure (P=17 Mpa)
or BWR Case 1 (TBUX)

	Values of FVES for Radionuclide Groups*				
Distribution	Noble Gases	Cesium Iodide (CsI)	Cesium	Tellurium	Nonvolatiles
Lower Limit	0.01	1×10^{-4}	1×10^{-4}	1×10^{-5}	1×10^{-5}
90% Confidence*	0.1	1×10^{-3}	1×10^{-3}	1×10^{-4}	1×10^{-4}
50% Confidence	0.5	0.01	5×10^{-3}	1×10^{-3}	1×10^{-3}
10% Confidence	0.9	0.1	0.01	0.01	0.01
Upper Limit	1.0	0.2	0.02	0.02	0.02

*The confidence level is the likelihood of an equal or greater FVES value than the level indicated.

Table B-3
FVES PWR Cases 2 and 3, Intermediate or Low Pressure
or BWR Case 2 (TBU)

	Values of FVES for Radionuclide Groups*				
Distribution	Noble Gases	Cesium Iodide (CsI)	Cesium	Tellurium	Nonvolatiles
Lower Limit	0.4	0.1	0.01	0.01	0.01
90% Confidence*	0.6	0.2	0.1	0.1	0.1
50% Confidence	0.9	0.4	0.2	0.2	0.2
10% Confidence	0.99	0.6	0.4	0.4	0.4
Upper Limit	1.0	0.90	0.7	0.7	0.7

*The confidence level is the likelihood of an equal or greater FVES value than the level indicated.

Table B-4
FVES BWR Case 3, High Pressure with CRD Flow (TCUX)

	Values of FVES for Radionuclide Groups*				
Distribution	Noble Gases	Cesium Iodide (CsI)	Cesium	Tellurium	Nonvolatiles
Lower Limit	0.01	0.01	1×10^{-3}	1×10^{-5}	1×10^{-5}
90% Confidence*	0.1	0.05	0.02	1×10^{-4}	1×10^{-4}
50% Confidence	0.5	0.1	0.05	1×10^{-3}	1×10^{-3}
10% Confidence	0.9	0.2	0.1	0.01	0.01
Upper Limit	1.0	0.3	0.2	0.02	0.02

*The confidence level is the likelihood of an equal or greater FVES value than the level indicated.

Sources of Uncertainty: FVES

As with the FCOR inputs, Expert B provided the factors that most affected his uncertainty range for each of the radionuclide groups. For the BWR and PWR high pressure cases, the results are driven by the scenario's long hold-up times, resulting in high aerosol deposition. For the noble gases, the uncertainty is due almost solely to the uncertainty of whether the instrument tubes will fail; thus, this result is heavily influenced by the TMI insights concerning failed instrument tubes. For iodine, the uncertainty includes uncertainty in chemical states, as well as in the scenario (whether the instrument penetrations fail). Thus, the lower bound would be a stable cesium iodide and no penetration failures. The cesium distribution is further affected by the possibility of surface reactions for CsOH; hence, the cesium distribution is different from the iodine distribution. The tellurium range reflects the element's strong affinity for metals and low revaporization potential. The low FVES values for tellurium reflect Expert B's belief that what escapes the fuel will very likely find other metal before getting out of the vessel. Finally, the nonvolatiles all have the same distribution as tellurium because all are governed by aerosol physics rather than by any species-dependent quality.

For all of the lower pressure cases, the same uncertainty distributions apply. As noted above, these cases also apply to all cases of induced rupture, even if the system was at high pressure for some time before rupture. FVES for these cases is driven by the fact that there is a hole in the system and the residence time is low. There is a dependence on where the location of the hole in the system, and the uncertainty in this is factored into Expert B's distributions. The noble gas range is small, since most would likely escape through the hole in the system. The iodine releases are higher than in the high pressure cases because of the reduced residence time. Once again, the iodine distribution included the uncertainty because of the possibility of alternative chemical states.

Revaporization also affects the iodine release uncertainty. The cesium range is somewhat different than the iodine range because compounds other than cesium iodide could be involved. The cesium distribution reflects the fact that release would be governed by the aerosol deposition rate. For tellurium and the nonvolatiles, the process is completely governed by the aerosol deposition physics, and the uncertainty in that process overrides any species dependencies.

The only BWR distribution provided separately was for the case of high pressure with CRD flow. For this case, MAAP runs on similar sequences provided most of the background for Expert B to select distributions. The noble gas results are the same as for the other high pressure cases. The iodine distribution has been altered to reflect the possibility of increased residence time in this case. As with the other cases, the uncertainty is also affected by the revaporization and the potential for decomposition. For cesium, the distribution is changed to reflect the possibility of more effective retention caused by the CRD flow. The nonvolatiles and tellurium reflect Expert B's judgment of effective deposition and no revaporization.

Correlations with Other Variables

As provided by Expert B, the only correlations required for these variables are in the case structure.

REFERENCE

B-1. Fauske and Associates, Inc., "MAAP Modular Accident Analysis Program User's Manual," Vols. I and II, IDCOR Technical Report 16.2-3, February 1987.

Expert C's Elicitation

Issue 1. Release of Fission Products from the Fuel in the Vessel and from the Vessel to the Containment

Description of Expert C's Rationale/Methodology

Expert C relied heavily on code calculations to support these results. Uncertainty ranges were produced from both code sensitivity studies and physical reasoning that considered deficiencies in the models for in-vessel release and transport of fission products that were implemented in the codes. The following sources of information were cited:

- STCP results;
- QUASAR study conducted by Brookhaven National Laboratory (BNL);
- QUEST study conducted by SNL;
- Assessment of the CORSOR and TRAP-MELT codes by ORNL;
- Calculations made with the MARCH-RMA code.

The discussion that follows is derived primarily from Expert C's written notes.

Expert C developed a case structure. He felt that he could not distinguish between PWRs and BWRs for the release from fuel in the vessel (FCOR). However, he felt that release from fuel correlated with the extent of in-vessel zircaloy oxidation. Thus, results were provided for high in-vessel zirconium oxidation (defined as 50% or greater oxidation of the fuel cladding, corresponding to 20% or greater total zircaloy oxidation in a BWR) and for low zirconium oxidation. In the determination of the release of fission products from the vessel (FVES), he felt that the extent of zircaloy oxidation was important. Cases were added for BWRs and PWRs when high system pressure was present. While Expert C could not distinguish between PWR cases with the system at the setpoint pressure and simply high system pressures (PWR Cases 1 and 2), a distinction based on the extent of in-vessel zircaloy oxidation was made. For BWRs, Cases 1 and 2 were subdivided based on the extent of in-vessel zircaloy oxidation. Case 3 for the BWR was not subdivided, since it was believed that this case would always result in extensive zircaloy oxidation. Figure C-1 shows the resulting case structure.

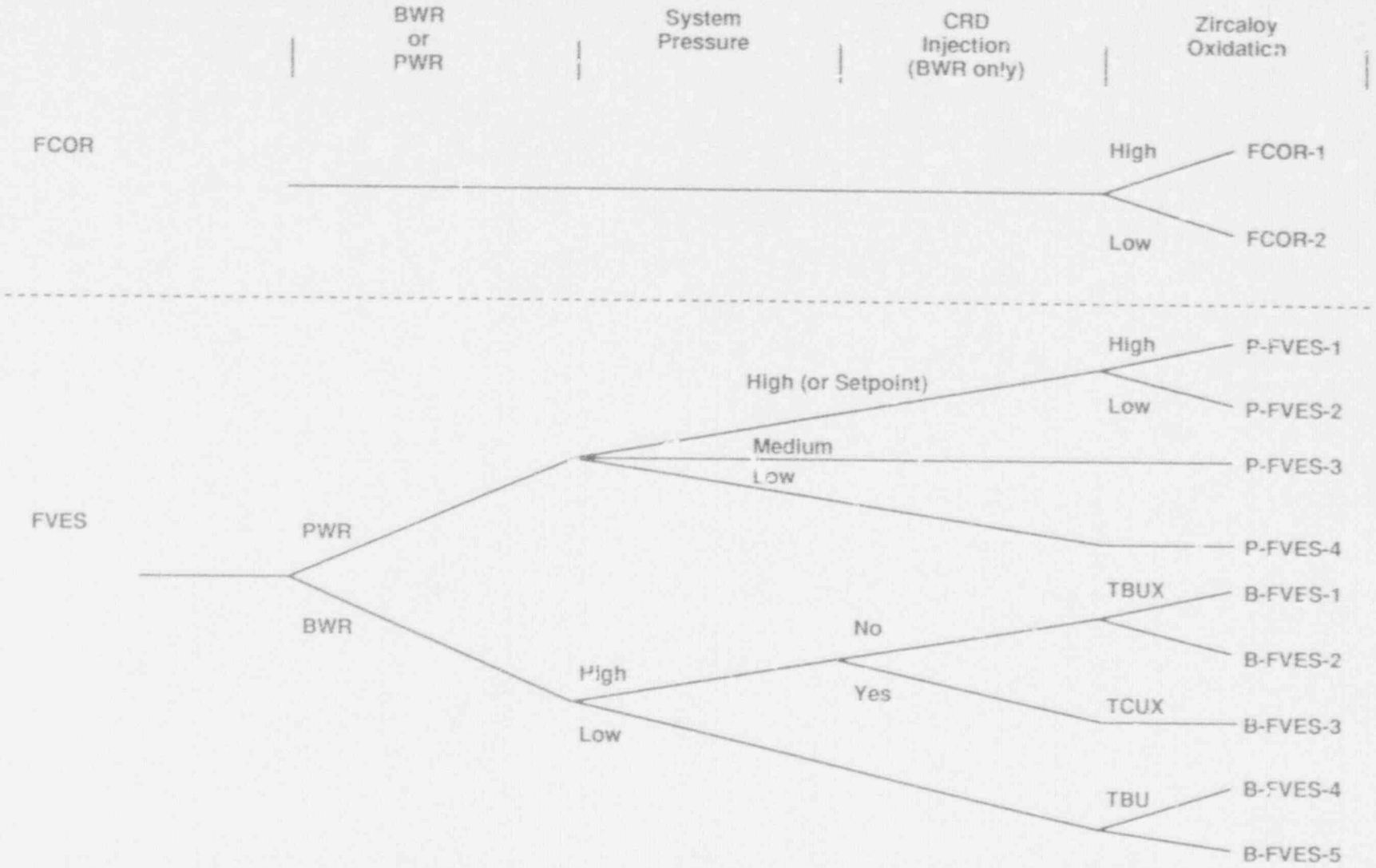

Figure C-1. Case Structure for Expert C's Elicitation.

Fraction of Fuel Inventory Released in the Vessel (FCOR)

Expert C stated that the models used in contemporary severe accident analysis codes considered by him employ the Arrhenius equation. This equation represents the temperature dependence of the release rate of fission products. There are several factors other than temperature that can influence the release rates of fission products. The most prominent are

- Fuel, structure, and aerosol chemistry;
- Condensed phase transport;
- Boundary layer transport;
- Coolant velocity effects;
- Fuel geometry (surface-to-volume ratio).

Expert C stated that the Arrhenius equation can represent some but not all important temperature dependencies. No simple $e^{-A/T}$ expression can represent the temperature dependence of releases. Moreover, many of the factors listed above are also dependent on system pressure, chemical potentials, and flow velocities.

In addition to these factors, Expert C believed that there is a significant uncertainty in the prediction of the fuel temperatures and the extent of local oxidation during core degradation. The inability of codes to predict reliable fuel temperature history stems from the lack of sufficiently mechanistic and validated core damage and degradation models. Note that even if there were excellent fission product release models, the boundary conditions and the parameters fed into these well-understood release models would be highly uncertain. Therefore, the lack of these fission product release models did not concern Expert C. What did concern him is the inability to predict better the core damage and melt progression.

The present methodology employed by severe accident codes uses the Arrhenius equation to relate the release rates of the fission products to nodal temperature. The applicability of this approach may be argued successfully only up to the point at which relocation of molten zirconium-uranium dioxide eutectics begins to take place. At that time, the nodal temperature of the remaining uranium and zirconium oxides changes, as does the temperature of the relocated solution, which refreezes onto the lower portion of the rod. This relocation changes the surface-to-volume ratio of the involved nodes and also affects the diffusion and transport of the fission products. The relocation of the zirconium oxides also affects the hydrogen-to-steam ratio, which significantly affects the release rate of fission products such as barium and molybdenum.

The current analyses with the STCP overpredict the maximum temperature in the core and do not account well for the formation of eutectics and gradual core relocation. Accounting for these processes would probably reduce the release rates. Simultaneously, the persistence of these slower release rates would be greater. Expert C believes that the overall effect will be to reduce the total quantity of fission product released from the fuel.

In the PWR cases for which there is discharge of upper head injection (UHI) or accumulators to the vessel before vessel breach, an enhanced release of fission products would be expected.

The effect of losing geometry was seen to have a far greater impact on the release of fission products than the differences between a PWR and a BWR. Thus, the cases were combined. Zirconium oxidation is a significant energy source during core degradation. High levels of oxidation imply higher core temperatures overall and thus higher releases. Higher core temperatures would increase the release of iodine, cesium, barium, and strontium. The effect of high temperatures on other radionuclides was not seen to be as important. Tellurium releases also increase when more zirconium is oxidized, but this is because less zirconium is available for the formation of tellurides.

For the cerium, ruthenium, and lanthanide groups, Expert C stated that the uncertainty in the in-vessel release was large but that the absolute magnitudes of the releases were so small that they warranted little attention.

Fraction of In-Vessel Releases Escaping to the Containment

Expert C stated that the retention of fission products by the RCS or reactor pressure vessel (RPV) depends principally on the following factors:

- Chemical interactions between radionuclides and structures;
- Residence time;
- Carrier gas and structure temperatures (governed by core blockage formation and steam flow rates);
- Ratio of structural surface area to gas volume.

These factors depend in turn on the accident sequence and can vary widely, depending on the underlying uncertainties in the thermal-hydraulic analysis of each accident sequence.

During an accident, fission products released from the core will be transported to the rest of the primary system by the mixture of steam and hydrogen exiting the core. Depending upon when fission product release occurs, the temperature of this carrier gas may be quite high (1650 to 2200 K). During the early stages of the accident, when the carrier gas is relatively cool, the volatile fission products (iodine, cesium, and tellurium) transported out of the core region are removed from this gas stream by condensation onto the cool structures or condensation onto the entrained aerosols (presumably isothermal with the carrier gas), and are subsequently deposited (to some extent) onto primary system surfaces. The aerosols transported out of the core, both fission product and inert, are removed from the gas stream by several mechanisms, such as sedimentation thermophoresis, turbulent or laminar diffusion, and other means. Thus, during the early stages of an accident, high retention of the fission products released from the core would be expected.

As the accident progresses, the structures in the path of the carrier gas become hotter because of heat transfer from the carrier gas and heating from fission product decay of the deposits. If the temperatures of the structures, and thus the deposited matter, become sufficiently high, revaporization of the volatiles not chemisorpted may take place. The extent of this revaporization depends greatly on the chemical form of the deposited species. For example, the deposited CsOH may not remain as pure CsOH but rather may combine with impurities in the stainless steel or boric acid to produce cesium silicates or cesium borates, respectively. In this example, the chemical reactions produce less volatile species. However, little is known of the chemical effects of the ambient atmosphere or structural impurities on the subsequent form and the volatility of the deposited species. The tendency based on the limited information available, is to expect less volatile forms and thus to reduce the volacility of the species. Expert C therefore believes that revaporization of deposited fission products will be hindered by chemistry aspects. Furthermore, it is Expert C's opinion that the uncertainty in this area overshadows the other factors specified earlier. The lack of data and adequate models to account for chemistry of the deposits is a very serious deficiency in the available models.

The residence time of the fission products inside the reactor system is directly related to the flow rate of the gas mixture leaving the reactor core and, during low through-flow periods, to the natural circulation established. The through-flow is dependent on the accident sequence. During the early stage of the accident, the composition of the carrier gas will be mostly steam, and the flow rate will be basically equal to the steaming rate of the core. When the core heats up and hydrogen begins to be produced, the flow rate diminishes as steam begins to be consumed by zirconium oxidation. The uncertainties of core degradation and relocation then become significant and influence the fission product behavior. The zirconium-uranium oxide relocation and the possible subsequent formation of core blockages affect not only the flow rate of gases leaving the core but also their composition (steam-to-hydrogen ratio) and, to a much greater extent, their temperature. With a completely blocked core, the average core exit gas temperature will be considerably cooler than for a partially blocked core. The cooler gases will allow the primary system structures to remain cooler, and thus the retention of fission products will be much higher, owing to reduced revolatilization.

The structural surface-to-gas volume ratio plays an important role in fission product retention by the reactor system, given that the carrier gas temperature is not hot enough to result in revaporization. The volatile species condense readily onto the surfaces offered by the aerosols. The surface area of these aerosols is much greater than that of the primary system structures. Thus, if the carrier gas and therefore the aerosols are cool, the volatiles will readily condense onto the aerosol surfaces. The aerosols, depending on the carrier gas flow rates and the existence of natural circulation flows, deposit primarily by gravitational settling and impaction, taking with them the condensed volatiles. The existence of sufficient aerosols to facilitate this behavior is uncertain. Also uncertain is the aerosol physics inside the primary system. Experiments conducted during the LACE program (LA3 tests) indicate that computer codes

tend to underpredict greatly the removal of flowing aerosols inside mock reactor system piping.

If the carrier gas temperatures become high, as with a partially blocked or unblocked core, the aerosol behavior becomes less critical until the gas (and thus the aerosol) loses some of its energy. This may happen in upstream volumes of the primary system (particularly a PWR RCS) where the aerosol particle sizes may be small because larger particles would have settled in earlier volumes. The deposition rate of the smaller particles depends not only on their terminal velocities, but also on the agglomeration rate of the smaller particles and on the through-flow rate of the gases.

Expert C believes that retention of volatile fission products in the primary system is generally inversely correlated with in-vessel zirconium oxidation. Higher zirconium oxidation produces higher temperature within the primary system and thus greater revolatilization. Primary system pressure affects retention through its effect on the carrier gas flow rate. High pressures lead to lower (volumetric) flow rates and thus greater aerosol retention. Thus, both volatile and nonvolatile fission products are affected. Tellurium retention is governed by chemisorption and thus is less impacted by zircaloy oxidation and primary system pressure than are the other species. Some small effect of residence time (i.e., system pressure) is expected.

In general, retention in BWRs is lower than that in PWRs because of the reduced mass of primary system structures in BWRs. The reduced mass leads to higher temperatures, promoting revolatilization. Much of the primary system retention in BWRs occurs in the safety/relief valve tailpipes.

Observations by Expert C for specific cases are provided in Table C-1. (Case designations are shown in Figure C-1.) Expert C believes that there is no correlation between FCOR and FVES except that from the effect of zircaloy oxidation, which is already reflected in his case structure.

Table C-1
Observations on In-Vessel Retention for Specific Cases

Case Designator	Description	Observations
P-FVES-1	PWR, high pressure, high zircaloy oxidation	Low carrier gas flow but high gas temperatures. Competing effects add to the uncertainty. Steam generated by core slump may sweep material into cooler portions of RCS, enhancing retention. Timing of core slump relative to when revolatization occurs adds to the uncertainty.
P-FVES-2	PWR, high pressure, low zircaloy oxidation	Retention improved relative to previous case because of lower temperatures.
P-FVES-3	PWR, intermediate pressure, little impact from zircaloy oxidation level	Few calculations available and thus greater uncertainty. Higher gas flow rates reduce retention relative to previous cases. Little natural circulation can develop because of system leak. Tellurium is efficiently retained because of chemisorption. Flow rather than temperature controls retention, so no dependence on zircaloy oxidation was noted.
P-FVES-4	PWR, low pressure, little impact from zircaloy oxidation level	Little or no core through flow. Fission products stay in core region until core slump occurs. High flows at core slump tend to sweep fission products out. However, structure temperatures are low. Competing effects lead to high uncertainty.
B-FVES-1	BWR, high pressure, high zircaloy oxidation (TBUX)	Generally high retention due to low flow rates. Changes in chemical form of cesium and iodine tend to increase retention over code predictions.

Table C-1. (Continued)

Case Designator	Description	Observations
B-FVES-2	BWR, high pressure, low zircaloy oxidation (TBUX)	Increased retention over previous case because lower temperatures
B-FVES-3	BWR, high pressure, injection from control rod drive hydraulic system leads to high zircaloy oxidation (TCUX). (Use B-FVES-2 if in-vessel experts think low oxidation possible.)	Low residence time because of high steam flows. High structure temperatures expected. Retention of volatiles is low. Tellurium chemisorption is still expected.
B-FVES-4	BWR, low pressure, high zircaloy oxidation (TBU)	Low flows and low temperatures. Indistinguishable from B-FVES-1.
B-FVES-5	BWR, low pressure, low zircaloy oxidation (TBU)	Low flows and low temperature. Retention of tellurium particularly efficient enhanced by very low flows

Results of Expert C's Elicitation

Fraction of Fuel Inventory Released In-Vessel (FCOR)

Results for high in-vessel zircaloy oxidation are provided in Table C-2. Table C-3 provides the results for low in-vessel zircaloy oxidation. Figures C-2 and C-3, respectively, display these high and low results graphically (except for ruthenium and lanthanum, which are too low for appropriate display).

Table C-2
FCOR for High In-Vessel Zirconium Oxidation

Radionuclide Group	Distribution (%)				
	1	25	50	75	99
Cesium and Iodine	0.50	0.65	0.85*	0.95	1.00
Tellurium	0.05	0.45	0.65	0.80	1.00
Barium	0.00	0.01	0.02	0.03	0.05
Strontium	0.00	0.005	0.015	0.02	0.05
Ruthenium	1×10^{-7}**	--	1×10^{-3}	--	0.01***
Lanthanum	1×10^{-7}**	--	1×10^{-3}	--	0.01***

*Median is adjusted downward from typical code predictions to account for the possibility that fuel relocation begins at lower temperatures than currently believed because of the formation of low-melting-temperature eutectics.

**5th percentile

***95th percentile

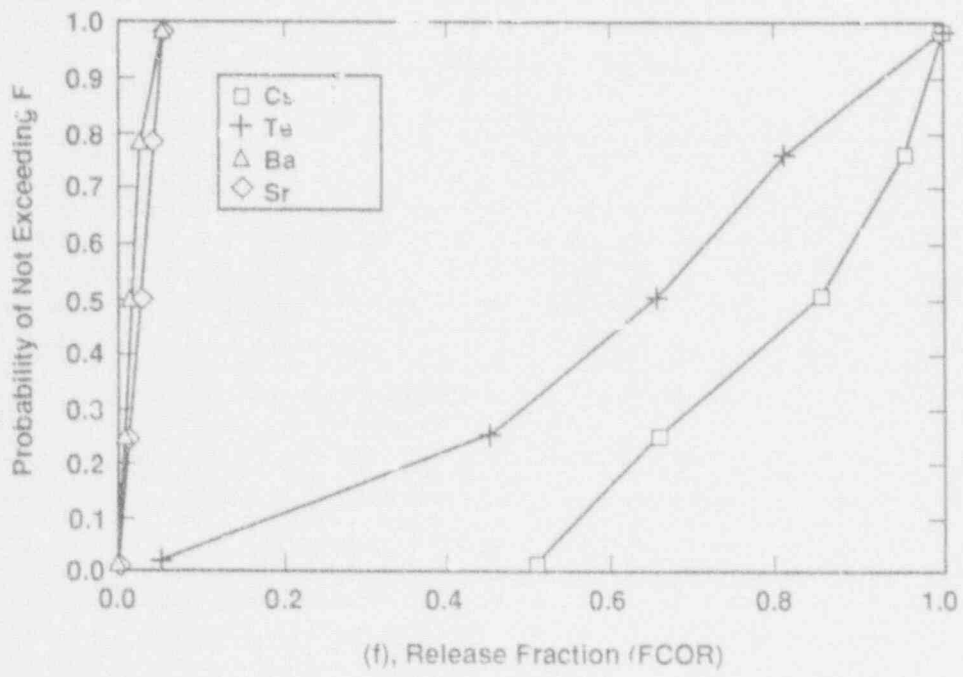

Figure C-2. Release from Fuel in the Vessel (FCOR); PWR and BWR High Zirconium Oxidation.

Table C-3
FCOR for Low In-Vessel Zirconium Oxidation

Radionuclide Group	Distribution (%)				
	1	25	50	75	99
Cesium and Iodine	0.50	0.65	0.70	0.85	1.00
Tellurium	0.50	0.25	0.40	0.65	1.00
Barium	0.00	0.005	0.015	0.025	0.05
Strontium	0.00	0.005	0.01	0.015	0.02
Ruthenium	1×10^{-7}*	--	1×10^{-3}	--	0.01**
Lanthanum	1×10^{-7}*	--	1×10^{-3}	--	0.01**

*5th percentile
**95th percentile

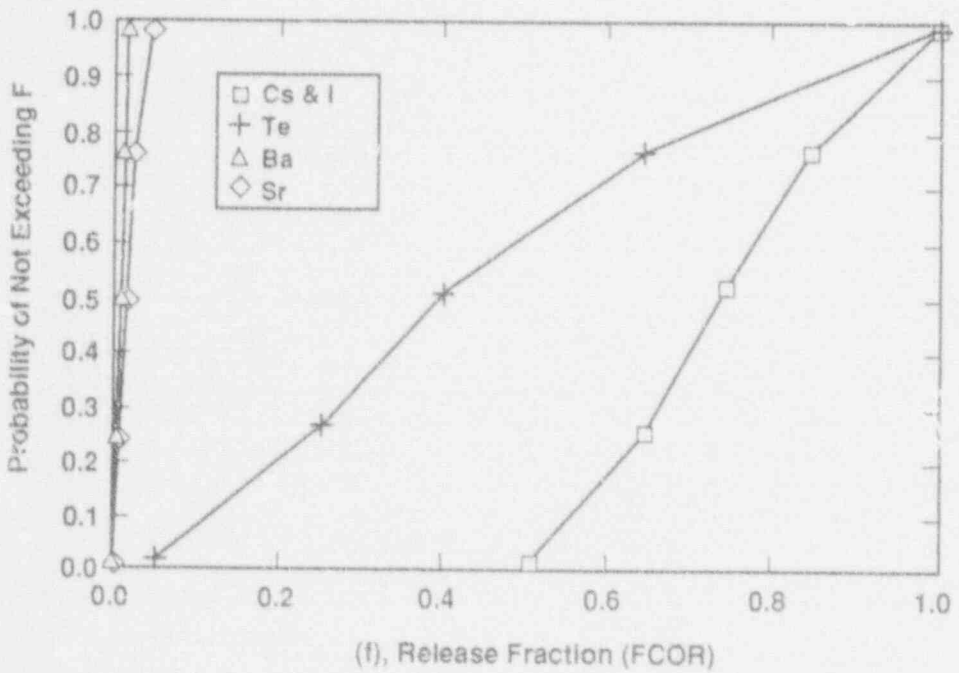

Figure C-3. Release from Fuel in the Vessel (FCOR); PWR and BWR Low Zirconium Oxidation.

Fraction of Release from Fuel Released from the Vessel (FVES)

Expert C provided these results in terms of a retention factor (i.e., 1-FVES). The results below have been translated to release factors (i.e., FVES is reported). Values are given for iodine and cesium together for PWRs (Expert C could not differentiate between these two radionuclide groups), tellurium, and aerosols. The aerosol category includes all other radionuclide groups plus inert aerosols.

Results for a PWR at high pressure with high in-vessel zircaloy oxidation are provided in Table C-4. Table C-5 is for a high-pressure PWR with low in-vessel zircaloy oxidation. Figures C-4 and C-5 show these results graphically.

Table C-4
FVES for a High Pressure PWR with High In-Vessel Zirconium Oxidation

Radionuclide Group	Distribution (%)				
	1	25	50	75	99
Cesium & Iodine	0.00	0.15	0.35	0.45	0.75
Tellurium	0.00	0.05	0.15	0.20	0.50
Aerosols	0.00	0.05	0.10	0.20	0.25

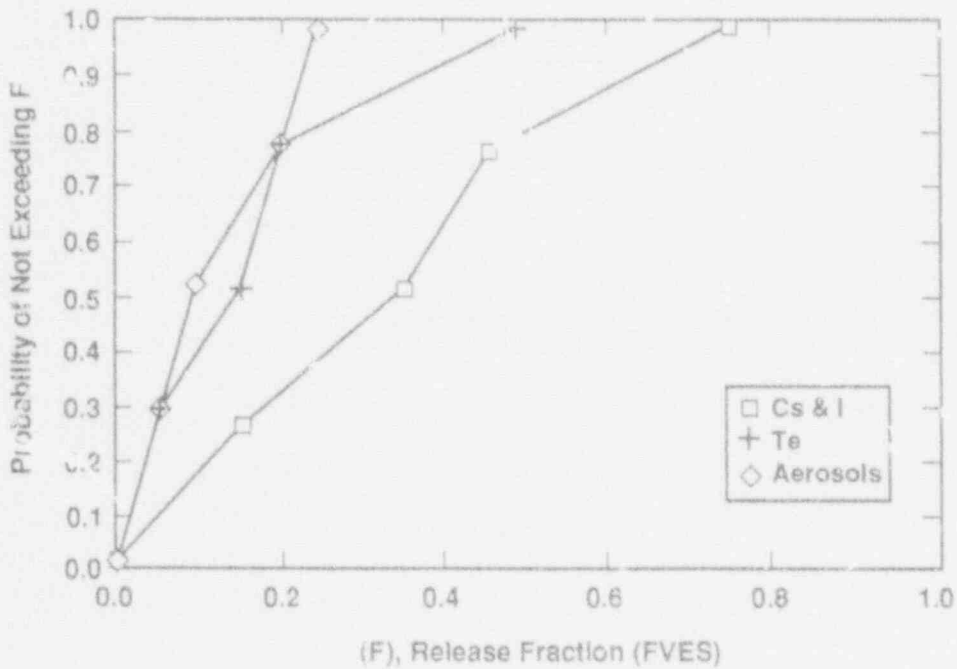

Figure C-4. Fractional Release from Primary (FVES); High Pressure PWR, High Zirconium Oxidation.

Table C-5
FVES for a High-Pressure PWR with Low In-Vessel Zr Oxidation

Radionuclide Group	Distribution (%)				
	1	25	50	75	99
Cesium & Iodine	0.00	0.10	0.25	0.35	0.75
Tellurium	0.00	0.05	0.10	0.20	0.50
Aerosols*	0.00	0.05	0.10	0.20	0.25

* Same as for Case P-FVES-1

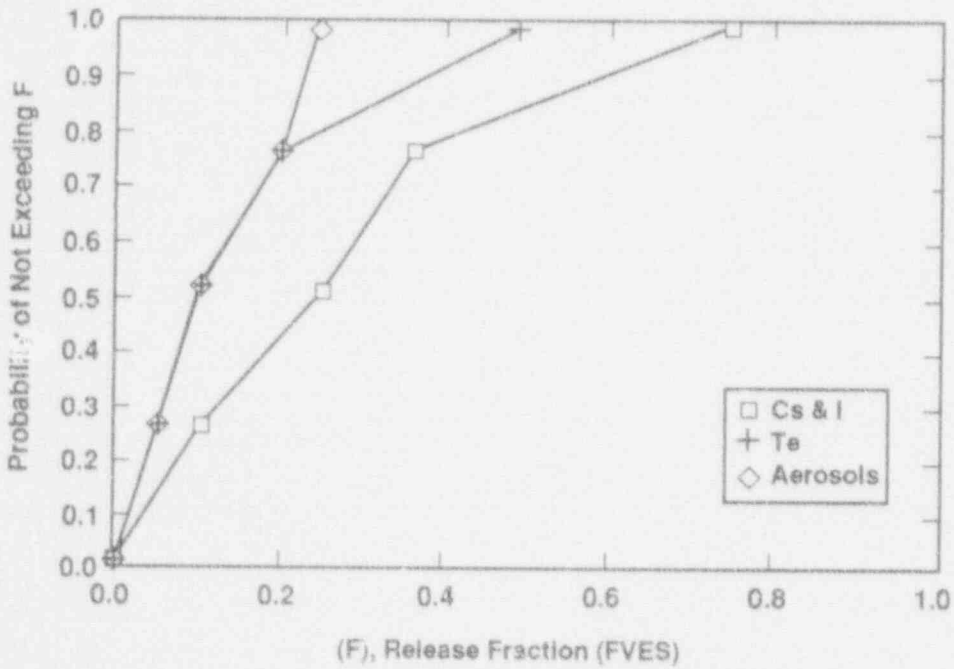

Figure C-5. Fractional Release from Primary (FVES); High Pressure PWR, Low Zirconium Oxidation.

Tables C-6 and C-7, as well as Figures C-6 and C-7, provide results for PWRs at intermediate and low pressure, respectively. These results are independent of the level of in-vessel zircaloy oxidation.

Table C-6
FVES for an Intermediate Pressure PWR

Radionuclide Group	Distribution (%)				
	1	25	50	75	99
Cesium & Iodine	0.00	0.25	0.50	0.65	0.90
Tellurium	0.00	0.15	0.30	0.40	0.90
Aerosols	0.00	0.20	0.25	0.35	0.40

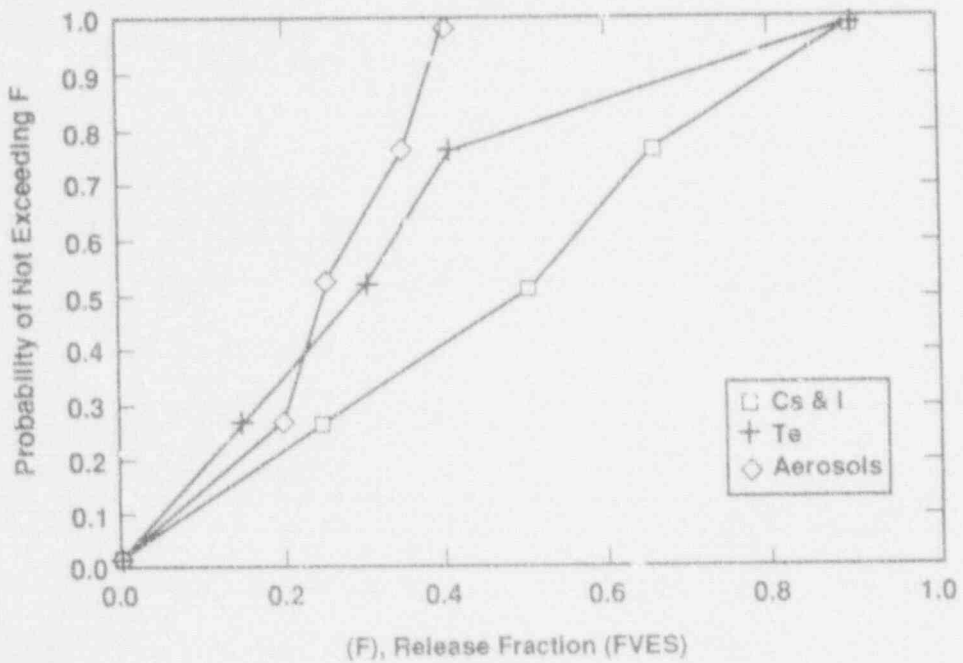

Figure C-6. Fractional Release from Primary (FVES); Intermediate Pressure PWR.

Table C-9
FVES for a High Pressure BWR (TBUX) with
Low In-Vessel Zirconium Oxidation

Radionuclide Group	Distribution (%)				
	1	25	50	75	99
Iodine	0.00	0.10	0.20	0.35	1.00
Cesium	0.00	0.05	0.15	0.30	1.00
Tellurium*	0.00	0.05	0.20	0.40	1.00
Aerosols*	0.00	0.05	0.15	0.30	1.00

* Same as for Case B-FVES-1

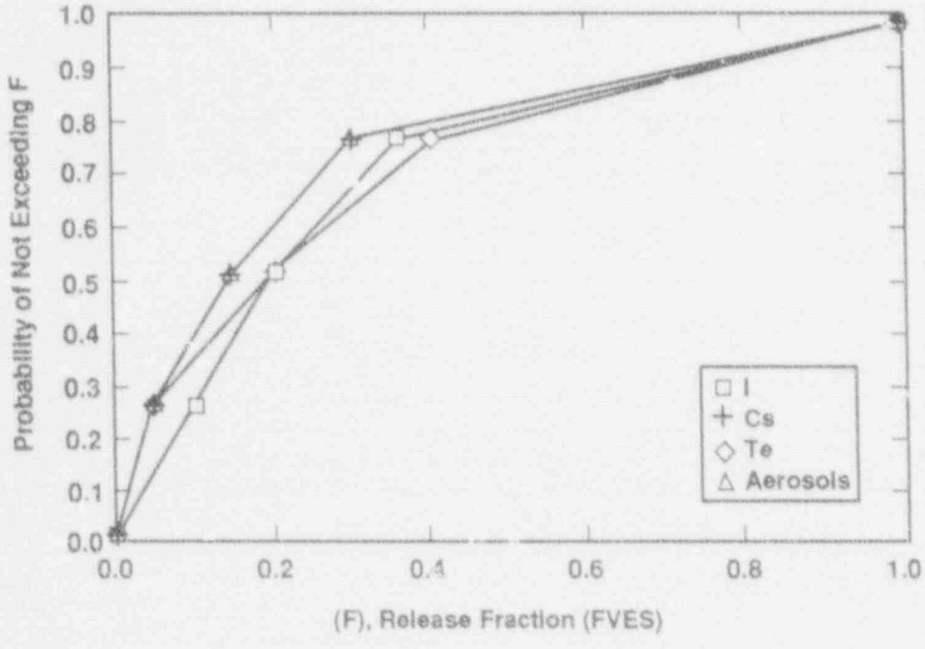

Figure C-9. Fractional Release from Primary (FVES);
BWR TBUX with Low Oxidation

Table C-10 and Figure C-10 provide the results for a low-pressure BWR with low in-vessel zircaloy oxidation. Expert C indicated that for high zircaloy-oxidation cases, system pressure had a small impact, and thus Cases B-FVES-1 and B-FVES-3 were essentially identical in this respect.

Table C-10
FVES for a Low Pressure BWR (TBU) with Low
In-Vessel Zirconium Oxidation

Radionuclide Group	Distribution (%)				
	1	25	50	75	99
Iodine	0.00	0.05	0.15	0.25	0.50
Cesium	0.00	0.05	0.10	0.20	0.50
Tellurium*	0.00	0.05	0.10	0.15	0.50
Aerosols*	0.00	0.05	0.10	0.15	0.50

* Same as for Case B-FVES-1

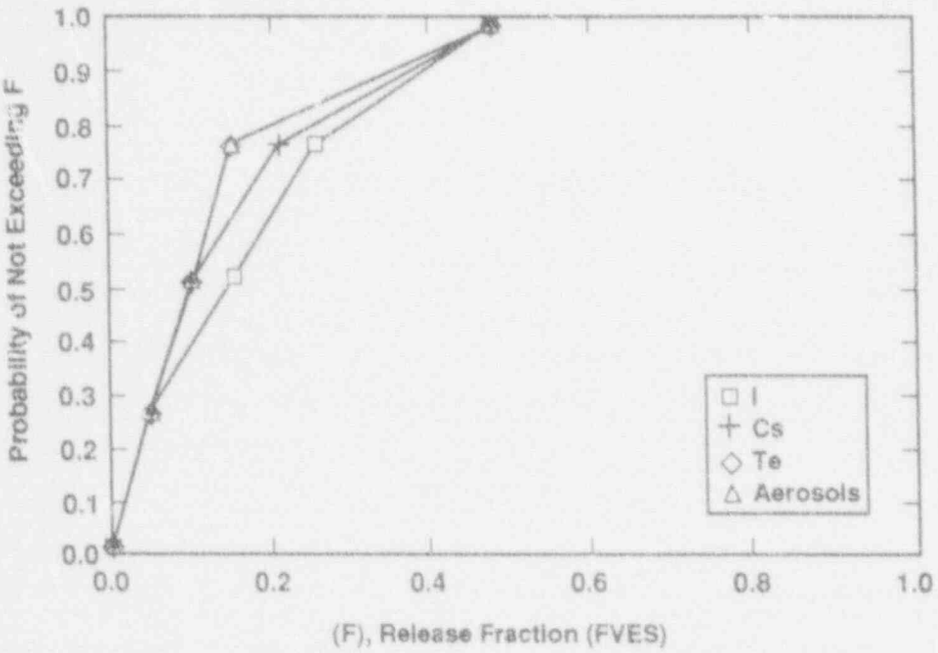

Figure C-10. Fractional Release From Primary (FVES); BWR TBU with Low Zirconium Oxidation.

Table C-11 and Figure C-11 provide the results for a high pressure BWR with injection from the CRDHS.

Table C-11
FVES for a High Pressure BWR (TBU) with CRDHS Injection

Radionuclide Group	Distribution (%)				
	1	25	50	75	99
Iodine	0.40	0.70	0.80	0.90	1.00
Cesium	0.40	0.55	0.65	0.80	1.00
Tellurium*	0.00	0.20	0.30	0.45	0.50
Aerosols*	0.00	0.10	0.20	0.30	0.50

* Same as for Case B-FVES-1

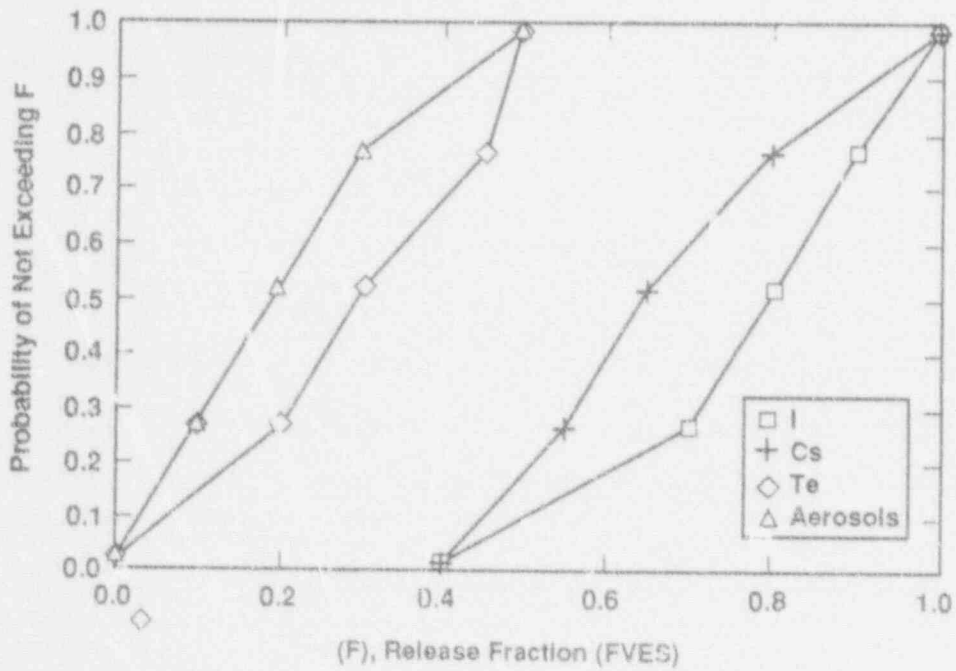

Figure C-11. Fractional Release from Primary (FVES); BWR TCUX (High Pressure and Injection).

Sources of Uncertainty

Fraction of Fuel Inventory Released in the Vessel (FCOR)

Expert C felt that the dominant contributor to uncertainty in FCOR was the effect of material relocation on the core geometry (i.e., the fuel surface-to-volume ratio). He felt that more detailed mechanistic modeling of melt relocation could reduce these uncertainties. Prediction of fuel temperature history is a related uncertainty.

Fraction of In-Vessel Releases Escaping to the Containment

Expert C felt that changes in the chemical form of fission products within the primary system are the dominant sources of uncertainty. Such changes are known to occur, but they have not been adequately studied. He felt that further research in this area could reduce uncertainties. Gas flow velocity uncertainties and, in particular, the effect of natural circulation flows were also seen as contributors to uncertainty.

1

IMAGE EVALUATION TEST TARGET (MT-3)

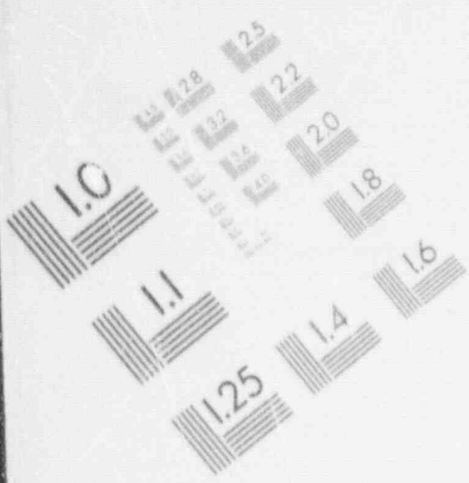

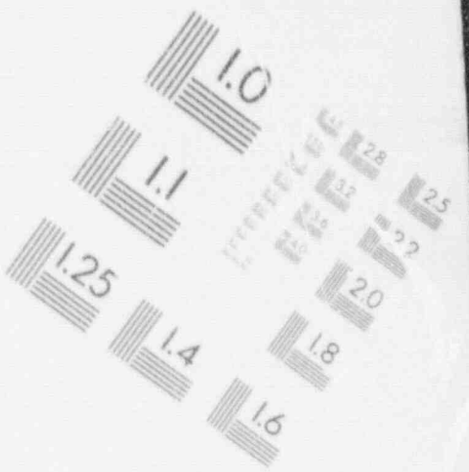

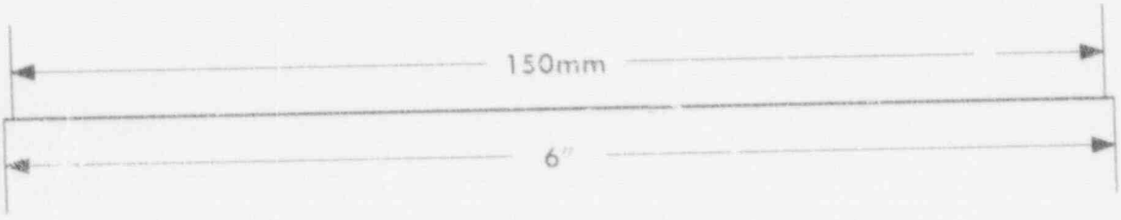

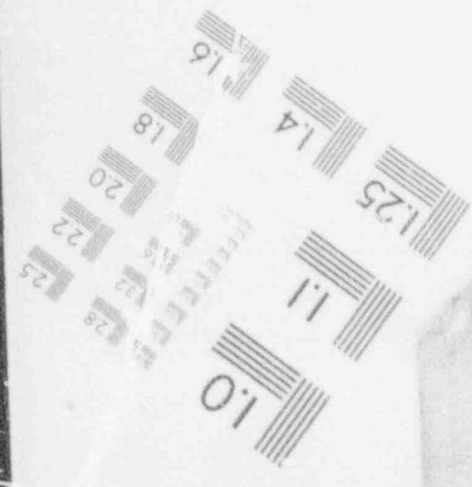

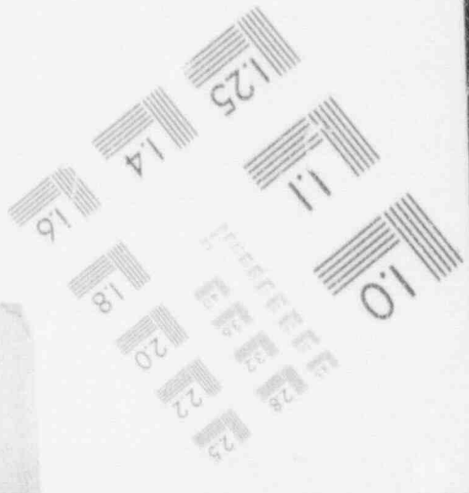

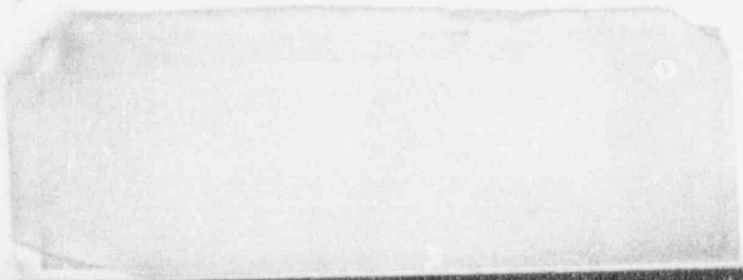

1

IMAGE EVALUATION
TEST TARGET (MT-3)

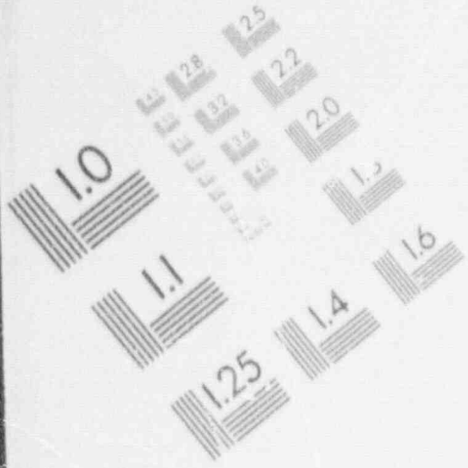

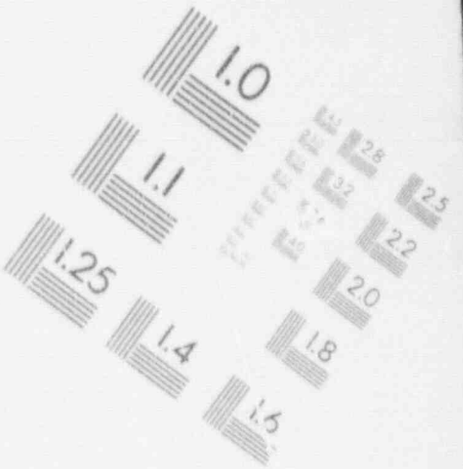

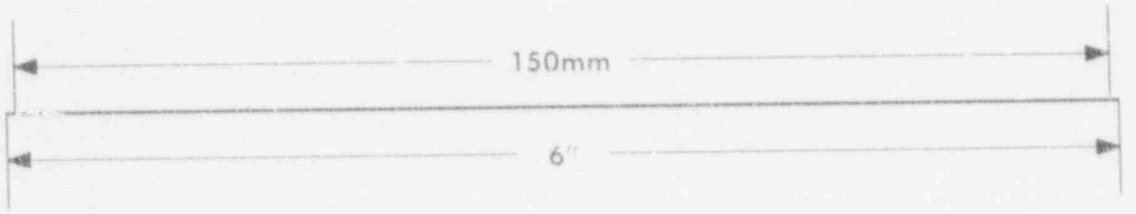

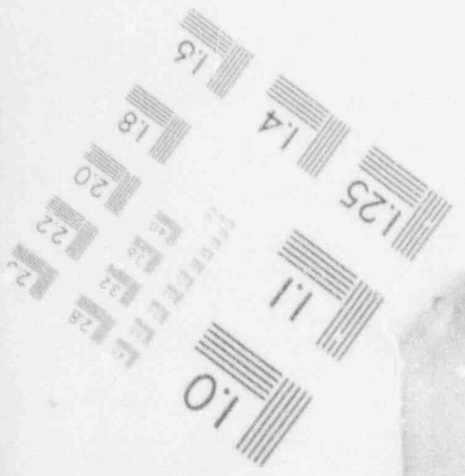

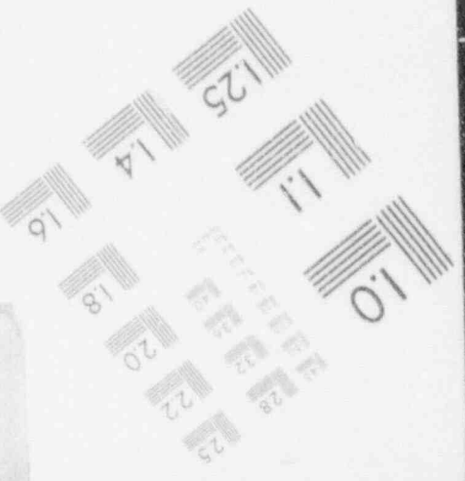

Expert D's Elicitation

Issue 1. Release of Fission Products from the Fuel in the Vessel and from the Vessel to the Containment

Expert D provided considerably more documentation than is appropriate for this section. The elicitation appears in its entirety in NUREG/CR-4551, Vol. 2, Part 5.

5.2 Issue 2. Decontamination of Fission Products by the Ice Condenser at Sequoyah

Summary and Aggregation of Expert Panel's Assessment of Source Term Issue 2: Decontamination of Fission Products by the Ice Condenser at Sequoyah

Experts Consulted: James Gieseke, Battelle Memorial Institute (BMI); Ben Y. H. Liu, University of Minnesota; Richard Vogel, Electric Power Research Institute (EPRI).

Issue Description

What distributions characterize the uncertainty in decontamination of fission products by the ice condenser at Sequoyah? In the parametric equation utilized by the source term calculation, the ice condenser decontamination factor (DF) variables are $DFICV_i$ and $DFICC_i$ for radionuclide group i. The DF variable for RCS releases is DFICV, and that applied to CCI releases is DFICC. The DF is set equal to 1 for noble gases and the organic iodide species, and is also set equal to 1 for all radionuclide groups if the ice is melted from the ice condenser. The cases to be considered include the following:

Case 1. Air return fans operating, no containment failure within 1 hour of release, no direct containment heating (DCH), multiple passes through ice condenser, low steam concentrations at ice condenser inlet.

Case 2. Air return fans operating, early containment failure in upper compartment, no DCH, single pass through ice condenser, low steam concentrations at ice condenser inlet.

Case 3. Air return fans not operating, no DCH, single pass through ice condenser, high steam concentrations at ice condenser inlet.

Case 4. DCH event, single pass through ice condenser, high steam concentration at ice condenser inlet, and high velocity gas through ice condenser.

Summary of Experts' Rationale

Expert A based his results on code calculations made by the STCP[A-1, A-2, A-3] and supplemented this information with his general knowledge of aerosol behavior. He explained that the particles smaller than 0.1μ and particles larger than 0.5μ are removed more efficiently than are particles in the 0.1 to 0.5μ range. The additional removal mechanisms that act on the smaller particles are Brownian diffusion and thermophoresis, while the additional removal mechanisms that act on the larger particles are impaction and sedimentation. The upper bound DF would require that there be very few particles in the 0.1 to 0.5μ range.

Two factors that could reduce the ice DF are preferential passage through channels in the ice condenser and compaction of the ice (reducing the surface area available for deposition). The expert felt that both were likely in a full-scale ice condenser and would tend to make the high DFs of 25 to 40 observed in the laboratory very unlikely in a reactor accident.

Expert A used the code calculations and experimental observations to get single pass aerosol DFs. He then took into consideration the behavior during multiple passes through the ice condenser; the DFs observed on subsequent passes are always less than on the preceding pass.

Expert B based his assessment largely on the ICEDF code written by BPNL and previous STCP calculations[B-1, B-2] (ICEDF is part of the STCP suite of codes). He also used the empirically derived equation presented by Expert C that approximates the ICEDF code and considers the parameters of steam concentration, aerosol size, number of passes through the ice condenser, and the presence or absence of ice. He used the DCH CONTAIN calculations as a basis for Case 4.

Expert B adjusted the values obtained from the above sources if he believed some effects were not adequately treated in the calculations: (1) condensation on aerosol particulates (would increase the DF), (2) flow velocity, (3) flow recirculation, (4) channeling within the ice condenser, (5) hydrogen burn rearrangement of the ice beds, (6) impaction mechanism of aerosol removal (most codes overpredict the DF), and (7) condensation (most codes underpredict DF).

Expert C performed a parametric study using an approximate empirical equation that he developed:

$$DF_{tot} = \left\{ (1 - f\alpha) \left(\Sigma_k \frac{X_k}{DF_k} \right)^n \right\}^{-1} ,$$

where

- f = 1, ice present; = 0, no ice present,
- α = volume fraction of steam in the carrier gas,
- n = number of passes through the ice condenser,
- X_k = mass fraction of aerosols in the size range k,
- DF_k = decontamination factor for a single pass of aerosol particles of size k with only noncondensible carrier gas.

The derivation of the equation was based upon work performed at Battelle's Pacific Northwest Laboratory (BPNL) (the ICEDF code). The parameters varied were aerosol size, fraction of the ice remaining, carrier gas steam fraction, number of passes through the ice condenser, and time. Two time regimes were considered: the time in which primary system releases occur and the time during which the core-concrete interaction releases occur.

Expert C believed that the driving force for ice condenser DF is steam condensation. Aerodynamic particle size distributions for Cases 1, 2, and 3 were obtained from Reference C-2. For Case 4, the DCH case, Expert C obtained particle size distributions from the Sandia Surtsey DCH-2 Test.

Aggregated Results

Values in Tables 2-1 through 2-6 are cumulative probabilities.

Table 2 1
Case 1: RCS and CCI Releases

DF	Aggregate	Expert A	Expert B	Expert C
1.000	0.000	0.000	0.000	0.001
1.100	0.009	0.001	0.001	0.026
1.300	0.127	0.056	0.250	0.076
1.600	0.263	0.139	0.500	0.150
2.000	0.357	0.250	0.571	0.250
3.000	0.528	0.500	0.750	0.333
5.000	0.666	0.583	0.916	0.500
6.000	0.750	0.625	0.999	0.625
7.000	0.806	0.667	1.000	0.750
9.000	0.887	0.750	1.000	0.910
10.000	0.917	0.762	1.000	0.990
30.000	1.000	0.999	1.000	1.000

Table 2-2
Case 2: RCS Releases

DF	Aggregate	Expert A	Expert B	Expert C
1.000	0.001	0.001	0.000	0.001
1.050	0.047	0.126	0.001	0.013
1.100	0.109	0.250	0.051	0.026
1.250	0.255	0.500	0.200	0.063
1.300	0.281	0.517	0.250	0.076
1.500	0.403	0.583	0.500	0.126
2.000	0.528	0.750	0.583	0.250
3.000	0.694	0.999	0.750	0.333
5.000	0.805	1.000	0.916	0.500
6.000	0.875	1.000	0.999	0.625
7.000	0.917	1.000	1.000	0.750
10.000	0.997	1.000	1.000	0.990

Table 2-3
Case 2: CCI Releases

DF	Aggregate	Expert A	Expert B	Expert C
1.000	0.001	0.001	0.000	0.001
1.050	0.047	0.126	0.001	0.013
1.100	0.109	0.250	0.051	0.026
1.250	0.255	0.500	0.200	0.063
1.300	0.281	0.517	0.250	0.076
2.000	0.500	0.750	0.500	0.250
3.000	0.694	0.999	0.750	0.333
5.000	0.805	1.000	0.916	0.500
6.000	0.875	1.000	0.999	0.625
7.000	0.917	1.000	1.000	0.750
10.000	0.997	1.000	1.000	0.990

Table 2-4
Case 3: RCS Releases

DF	Aggregate	Expert A	Expert B	Expert C
1.000	0.000	0.001	0.000	0.000
1.100	0.017	0.051	0.001	0.000
1.500	0.101	0.250	0.053	0.000
2.000	0.206	0.500	0.119	0.000
3.000	0.333	0.750	0.250	0.000
5.000	0.458	0.999	0.375	0.000
7.000	0.500	1.000	0.500	0.000
10.000	0.584	1.000	0.750	0.001
20.000	0.683	1.000	0.999	0.050
28.000	0.833	1.000	1.000	0.500
36.000	0.967	1.000	1.000	0.900
42.000	0.997	1.000	1.000	0.990

Table 2-5
Case 3: CCI Releases

DF	Aggregate	Expert A	Expert B	Expert C
1.000	0.017	0.001	0.000	0.050
1.100	0.045	0.051	0.001	0.082
1.500	0.191	0.250	0.112	0.211
2.000	0.374	0.500	0.250	0.371
2.400	0.472	0.600	0.317	0.500
3.000	0.689	0.750	0.417	0.900
3.500	0.752	0.812	0.500	0.945
4.000	0.797	0.875	0.528	0.990
5.000	0.861	0.999	0.583	1.000
8.000	0.917	1.000	0.750	1.000
20.000	1.000	1.000	0.999	1.000

Table 2-6
Case 4: RCS and CCI Releases

DF	Aggregate	Expert A	Expert B	Expert C
1.000	0.000	0.001	0.000	0.000
1.200	0.017	0.051	0.001	0.000
2.000	0.167	0.250	0.250	0.000
2.100	0.200	0.275	0.267	0.058
2.350	0.248	0.338	0.308	0.099
2.790	0.361	0.448	0.382	0.255
3.000	0.400	0.500	0.417	0.282
3.500	0.463	0.542	0.500	0.347
6.000	0.724	0.750	0.750	0.673
6.380	0.745	0.761	0.753	0.722
15.000	0.884	0.999	0.816	0.838
15.690	0.889	1.000	0.821	0.847
29.700	0.942	1.000	0.924	0.903
40.000	0.974	1.000	0.999	0.923
63.500	0.989	1.000	1.000	0.967

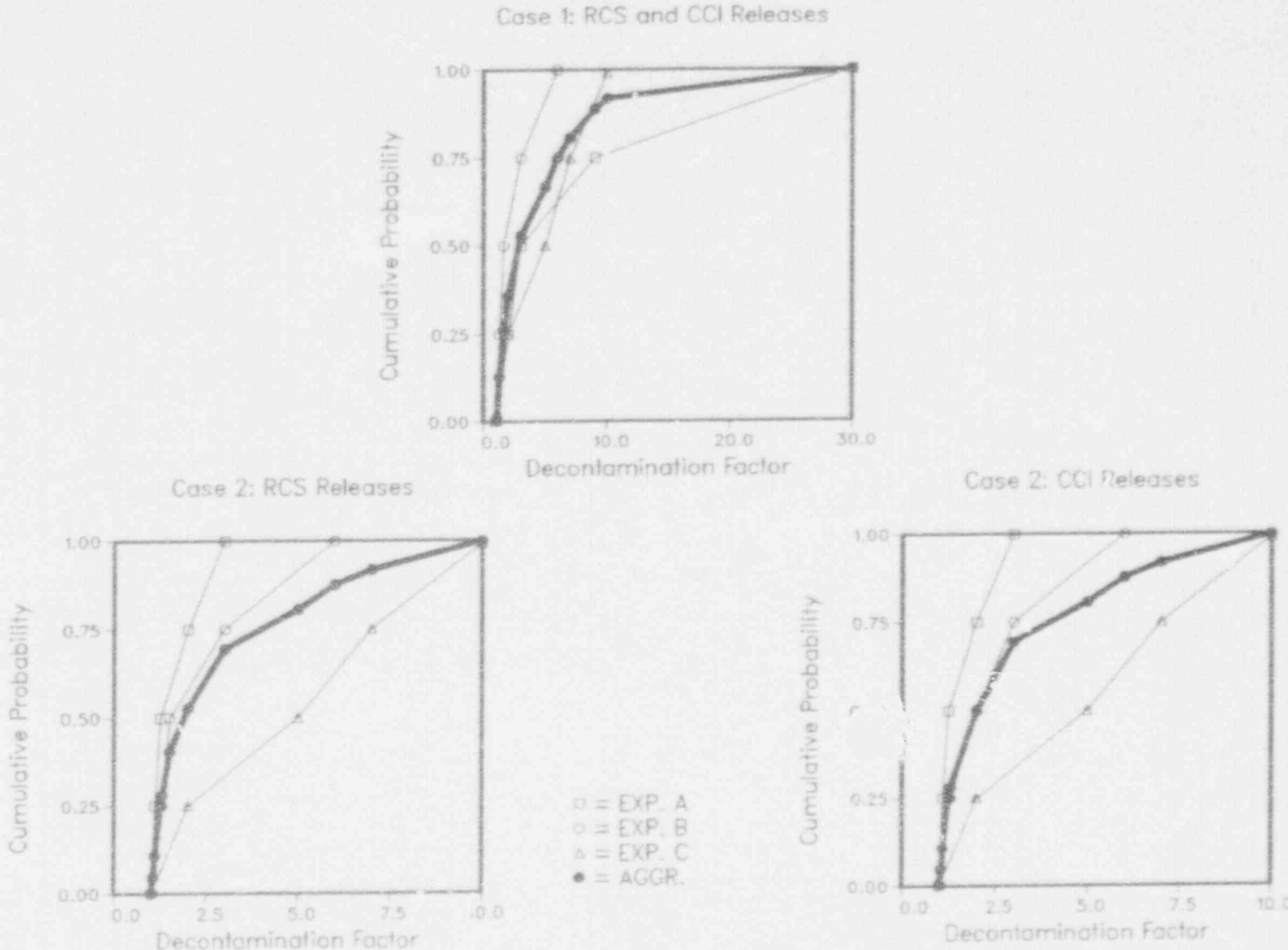

Figure 2-1. Case 1: RCS and CCI Releases (top); Case 2: RCS Releases (left); Case 2: CCI Releases (right).

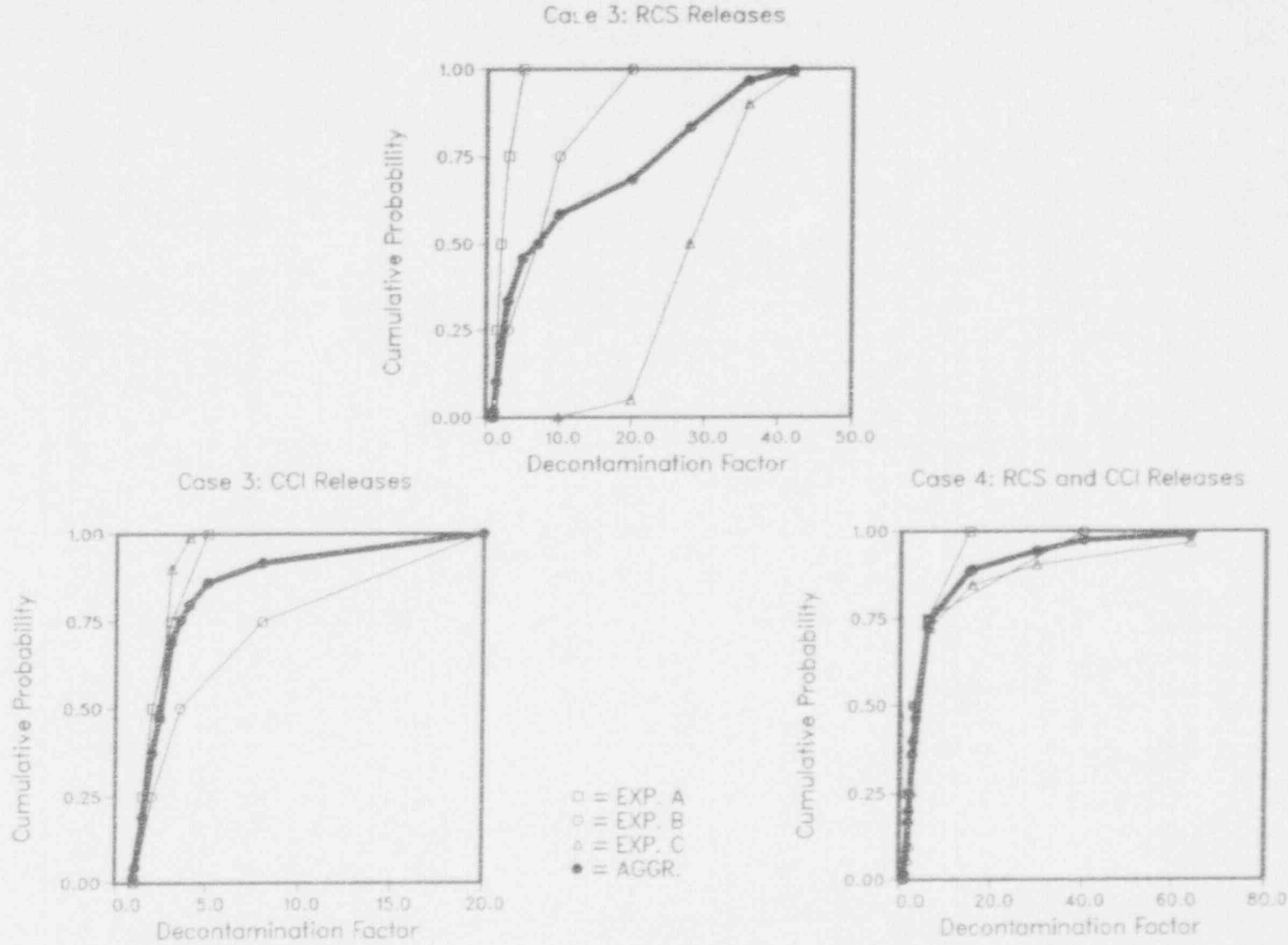

Figure 2-2. Case 3: RCS Releases (top); Case 3: CCI Releases (left); Case 4: RCS and CCI Releases (right).

Individual Elicitations for Issue 2

Expert A's Elicitation

Decontamination of Fission Products by the Ice Condenser at Sequoyah

Description of Expert A's Rationale/Methodology

Expert A based his results on his extensive knowledge of aerosol behavior in general and on the results of calculations by the STCP[A-1,A-2,A-3] and other codes. He also used the results that were reported in an unpublished document supplied by another panel member. He noted that the code results show a wide range for the ice condenser DF, from 1.01 to 25. Expert A assumed that a low steam fraction meant that the steam mole fraction was in the 5 to 20% range, while a high steam case meant that the steam mole fraction was 50% or greater.

Expert A pointed out that particles smaller than 0.1μ and particles larger than 0.5μ are removed more efficiently than are particles in the 0.1μ to .5μ range. Particles with diameters in this range are always the most difficult to remove, whether by natural or engineered means. Below 0.1μ, Brownian diffusion and thermophoresis are effective removal mechanisms. Above 0.5μ, impaction and sedimentation are effective. One factor required to obtain Expert A's upper bound DF values is that there be very few particles in the 0.1μ to 0.5μ range.

Expert A decided that he could not distinguish between hygroscopic and nonhygroscopic aerosols, since other unknowns, such as the exact steam concentration or the amount of channeling, had much larger effects than whether the particles were hygroscopic. Thus, he had one curve for ice condenser DF for each of the four cases.

The other factors in determining the upper bound DFs are a lack of channeling, uniform steady flow through the ice condenser, and a large ice surface area. Channeling is particularly difficult to avoid because of its inherent positive feedback nature. That is, if a channel starts to open, the increased flow through that part of the ice bed tends to melt the ice preferentially in that area, thus increasing the size of the channel and causing more flow and more melting in the area. In the real world, where ideal small-scale laboratory conditions are very difficult to obtain, it seems unlikely that channeling, to some extent, can be avoided. Some areas are certain to get more flow than others, and increased melting in these areas will ensure that flows increase in these areas disproportionately. Compaction of the ice over time, especially in the bottom of the baskets, also seems difficult to avoid and may significantly reduce the surface area of the ice. When all these factors are considered, the high DFs of 25 to 40 sometimes observed in the laboratory are not likely to be observed in a reactor accident.

Expert A's method used the calculations and tests to get single pass aerosol penetration values. The DFs observed on subsequent passes through the ice condenser are always less than on the preceding pass, but this can be accounted for by using an effective number of passes rather than the

actual number. (The effective number of passes is the number of passes required to get the total decontamination factor, assuming that each is as effective as the first pass.) From the Battelle STCP calculations, he observed that ice condenser DFs were usually in the range of 2 to 5. This agrees well with five effective passes and single pass penetration values around 0.80. Expert A would expect both these numbers, based on experiments and other code results.

Considering the likelihood of some channeling, some reduced ice surface area from compaction, and unsteady, nonuniform flow, Expert A concluded that a DF of 3 was his midpoint value for the low-steam, multiple-pass case and for the high-steam, single-pass case.

Results of Expert A's Elicitation

Expert A gave the following ice condenser DF table, which contains his results for all four cases.

Table A-1
Ice Condenser DF

	Cumulative Probability				
	0.001	0.25	0.50	0.75	0.999
Case 1	1.1	2.0	3.0	9.0	30.0
Case 2	1.0	1.1	1.25	2.0	3.0
Case 3	1.0	1.5	2.0	3.0	5.0
Case 4	1.0	2.0	3.0	6.0	15.0

The lower bounds are approximately the same and assume that the ice condenser is essentially ineffective. Either a hydrogen detonation has made the ice condenser nonfunctional, or channeling is so severe that aerosol removal is negligible.

Case 1

This case has multiple passes through the ice condenser because the fans are operating, there is no DCH, and the steam fraction is low. Expert A determined his midpoint DF of 3.0 as described above. A large amount of uncertainty is in this value because the steam fraction and the particle size are not well known. For 5% steam, particle size is very important; for 20% steam the particle size has only some importance; and for 50% steam the particle size is completely irrelevant. As the low steam case includes both the 5% and the 20% steam fractions, this leads to considerable uncertainty. Expert B determined his upper bound by assuming that there was no channeling, steady and uniform flow, little or no ice surface reduction by compaction, and very few particles in the 0.1μ to 0.5μ range. In the unlikely event (99.9%) that all these conditions were met, then DFs around 30 like those found in carefully controlled laboratory experiments could be realized. Expert A obtained his 25% and 75% values by taking

geometric means using the 0.1%, 50% and 99.9% values and then seeing whether the resulting quartiles seemed reasonable. Some of the geometric means for the 25% and 75% values were adjusted up or down slightly in the rounding off process to obtain quartile points that seemed more reasonable.

Case 2

Even though the fans are operating, this case has few passes through the ice condenser, since the containment is failed in the upper compartment. There is no DCH, and the steam fraction is low. Expert A determined his midpoint DF of 1.25 by assuming that one pass through the ice condenser is all that really can be counted on, and an 80% penetration for one pass is in the middle of the reported range. While a small failure size might result in two to five passes for some of the gas, channeling is also possible. The one will increase the removal, while the other will reduce it. For the midpoint, Expert A figured they would effectively cancel out. The upper bound was obtained by assuming that five effective passes with a single pass penetration of 80% were the most that could be expected under any conditions with a failure in the upper compartment. The 25% and 75% values were obtained by geometric averaging as discussed above.

Case 3

This case has a high steam fraction, but the fans are not operating. Thus, there is only one pass through the ice condenser and no DCH. Expert A felt that the high steam fraction would enhance aerosol removal more than the lack of multiple passes forced by the fans would degrade the removal. Therefore, the DFs for this case fall between those for Case 1 and Case 2, and are closer to Case 2 than to Case 1. He determined the midpoint DF of 2 by adjusting the Case 2 penetration (0.80) downward to 0.50. The upper bound was obtained similarly.

Case 4

This case has a very high steam fraction, DCH, and only one pass through the ice condenser. The high steam fraction could lead to very high DFs if channeling or a hydrogen detonation (from the high hydrogen concentration in this case) does not compromise the integrity and functionality of the ice condenser. The DFs for this case also fall between those for Case 1 and Case 2, but are closer to Case 1 than to Case 2. Expert A thought the midpoint DF of 3 should apply to this case as well as to Case 1 but that the upper bound should be lower because multiple passes were not possible. Thus, the 99.9% DF was obtained by adjusting the Case 1 value downward.

Sources of Uncertainty

The largest single source of uncertainty is in the steam fraction. The large and small fractions used here encompass a wide range, and for the lower steam fractions, the removal effectiveness is sharply dependent on the steam fraction. Also important in determining the uncertainty are channeling, type of flow, and reduced ice surface area (discussed above). The effects of aerosol densities and the temperature of the gas coming into the ice condenser are small compared to the other uncertainties.

REFERENCES

A-1. J. A. Gieseke et al., "Radionuclide Release Under Specific LWR Accident Conditions, Vol. IV: PWR Ice Condenser Design," BMI-2104, Battelle Memorial Institute, 1984.

A-2. R. S. Denning et al., "Radionuclide Release Calculations for Selected Severe Accident Scenarios," Vols. I-V, NUREG/CR-4624, BMI-2139, Battelle Memorial Institute, 1986.

A-3. M. T. Leonard et al., "Supplemental Radionuclide Release Calculations for Selected Severe Accident Scenarios," NUREG/CR-5062, BMI-2160, Battelle Memorial Institute, 1987.

Expert B's Elicitation

Decontamination of Fission Products by the Ice Condenser at Sequoyah

Description of Expert B's Rationale/Methodology

Expert B largely relied upon knowledge of, and familiarity with, the ICEDF code written by BPNL, and has performed various calculations with the code. Previous STCP calculations[B-1,B-2,B-3] were utilized as base values for the assessment; for ice condenser containments, the STCP code suite utilizes the ICEDF code within its framework. Conditions from the calculations were matched to those in the specified cases to obtain base values for the assessed distributions.

Expert B also utilized the Electric Power Research Institute (EPRI) approximation equation that was distributed by another panel expert. The equation is empirically derived and approximates results of calculations from the ICEDF code, considering the parameters of steam concentration, mass fraction of aerosols in various size ranges, number of passes through the ice condenser, and the presence or absence of ice. The CONTAIN calculations performed at Sandia for DCH in an ice condenser containment[B-4] were utilized as a basis for Case 4.

Base values were adjusted if Expert B believed certain effects were neglected in the calculations, and consideration of uncertainty was incorporated into the ranges provided for the assessment. It was judged that one of the decontamination effects routinely neglected in the ICEDF code is condensation of aerosol particulate. Consideration of this effect increases the base value DF. Some of the uncertainties in the modeling include flow velocity, flow recirculation and channeling within the ice condenser, and hydrogen burn rearrangement of the ice beds. Expert B also thinks that most codes overpredict the impaction mechanism of aerosol removal, and underpredict condensation, which was judged to be the dominant mechanism in decontamination of fission products within an ice condenser.

For the assessment, Expert B considered the initial findings of the experimental result/ICEDF[B-5] code prediction comparison being performed at BPNL. The code underpredicts deposition in the lower part of the ice condenser. The experiments show a higher melting rate in the lower part of the condenser, and experimental conditions demonstrate a maldistribution of the temperature field across the flow channels within the condenser. The model used in the ICEDF code assumes a single, well-mixed node; further nodalization could provide higher DFs but would probably predict channel meltings that would then decrease the DF. The BPNL results have demonstrated recirculation flows within the ice condenser even when the air return fans are operating.

Results of Expert B's Elicitation

For all the cases provided, the median value was usually based on a particular calculation with adjustments for certain considerations. The

lower end of each distribution accounts for effects such as channeling, early melting of ice, and rearrangement of ice because of hydrogen deflagrations. The upper end of each distribution accounts for intact effective ice configuration, fission product release synchronized with steam release, and conditions generally conducive to aerosol removal from the gas flow.

Case 1

The assumptions in the case assessment were 10% steam concentration at the ice condenser inlet, five to ten effective passes through the ice condenser, and DF values obtained before vessel failure. The BMI sequences used in determining the base, or 50 percentile, were S_3HF_1 and S_3HF_2, which for all fission product groups provided DF values on the order of 1.56. The EPRI empirical equation distributed by Expert C provided a value of 2.7 for the DF. The resulting distribution supplied for primary system and core-concrete interaction releases is as follows:

Cumululative Probability	0.001	0.25	0.50	0.75	0.999
DF	1.1	1.3	1.6	3.0	6.0

Case 2

The assumptions in the case assessment were 10% steam concentration, a single pass through the ice condenser, and DF values obtained after vessel failure. The BMI sequences used in determining the base were again S_3HF_1 and S_3HF_2, and for the primary system releases, they provided values ranging from 1.36 to 1.52. The resulting distribution for the primary system releases group is

Cumulative Probability	0.001	0.25	0.50	0.75	0.999
DF	1.05	1.3	1.5	3.0	6.0

The BMI sequence DF values for the CCI releases ranged from 1.65 to 2.50. The empirical equation provided a value of 1.1 when utilizing particulate size distributions for the CCI releases. The resulting distribution for the primary system release group is

Cumulative Probability	0.001	0.25	0.50	0.75	0.999
DF	1.05	1.3	2.0	3.0	6.0

Case 3

The assumptions in the case assessment were 80 to 90% steam concentration, a single pass through the ice condenser, and DF values obtained after vessel failure. The BMI sequence utilized in determining the base values was the TB sequence, and for the primary system releases, the DF values ranged from 5.42 to 6.59. These values should be higher, however, when condensation on particles is considered, and the values were adjusted accordingly for the median of the distribution. The empirical equation provided values ranging from 1.03 to 10, with certain parameters varied. The resulting distribution for the primary system releases groups is

Cumulative Probability	0.001	0.25	0.50	0.75	0.999
DF	1.1	3.0	7.0	10.0	20.0

For the CCI releases the DF values are lower because the CCI releases occur when less steam is in the lower compartment. The DF values in the BMI TB sequence ranged from 3.35 to 4.85. The resulting distribution for the CCI releases is:

Cumulative Probability	0.001	0.25	0.50	0.75	0.999
DF	1.1	2.0	3.5	8.0	20.0

Case 4

The assumptions in the case assessment were 100% steam concentration, a single pass through the ice condenser, and DF values obtained after vessel failure. The only source of information that Expert B used in this case was the Sandia CONTAIN[B-4] calculation for DCH. The high steam concentration and lower residence times because of high velocities increase DF values for the entire distribution in this case. Expert B believed that the impaction removal efficiency for the 10μ particles in the CONTAIN calculation was too optimistic and lowered the median as a result. Expert B also felt that thermophoretic effects are the force driving the decontamination process in a DCH event because of the large temperature gradient between the gas and the ice; with this in mind, the upper end of the distribution was increased. The resulting distribution for both primary system and CCI releases is:

Cumulative Probability	0.001	0.25	0.50	0.75	0.999
DF	1.2	2.0	3.5	6.0	40.0

Sources of Uncertainty

Expert B believed that a large source of uncertainty was in the sequence definition, that is, the boundary conditions for the problem. This uncertainty includes the level of steam concentration in the ice condenser inlet, and also the timing of the radionuclide release with respect to the steam concentration. Other uncertainties include the degree of condensation on particulate, velocity and temperature distributions within the ice condenser, the degree of flow recirculation and channeling, and the effect of hydrogen phenomena on the rearrangement of the ice bed.

REFERENCES

B-1. J. A. Gieseke et al., "Radionuclide Release Under Specific LWR Accident Conditions," Volume IV: PWR Ice Condenser Design, BMI-2104, Battelle Memorial Institute, 1984.

B-2. R. S. Denning et al., "Radionuclide Release Calculations for Selected Severe Accident Scenarios," Vols. I-V, NUREG/CR-4624, BMI-2139, Battelle Memorial Institute, 1986.

B-3. M. T. Leonard et al.,"Supplemental Radionuclide Release Calculations for Selected Severe Accident Sequences," NUREG/CR-5062, BMI-2160, Battelle Memorial Institute, 1987.

B-4. D. C. Williams et al., "'Quick Look' CONTAIN Calculations for the D. C. Cook Ice Condenser Plant," Addendum to Appendix C, Volume 2, NUREG/CR-4551, SAND86-1309, Sandia National Laboratories, February 1987. (Draft for comment)

B-5. L. D. Kannberg, "Preliminary Results of Experiments on Aerosol Deposition in Ice Condensers," Transactions of the 5th Water Reactor Safety Meeting, Gaithersburg, MD, October 26-29, 19[illegible].

Expert C's Elicitation

Decontamination of Fission Products by the Ice Condenser at Sequoyah

Description of Expert C's Rationale/Methodology

Expert C developed an approximate empirical equation to calculate ice condenser DFs based on the parametric variables of aerosol size distribution, a parameter representing whether or not ice remains, carrier gas steam fraction, and number of passes through the ice condenser. The equation was based upon work at Battelle's Pacific Northwest Laboratory (BPNL). The equation approximates results of the ICEDF code and uses certain simplified assumptions from the code, as well as information and analysis from the BPNL document NUREG/CR-3248.[C-1] The ICEDF code invokes standard aerosol deposition mechanisms in addressing the problem of calculating DFs in an ice condenser. The NUREG/CR-3248 document details analyses at BPNL for fission product scrubbing in ice condensers.

The approximate equation was used in a parametric study in which the variables treated were ice/no ice, steam concentration, passes through the condenser, particle size, and time. The two time regimes were characteristic of primary system releases and core-concrete interaction (CCI) releases. The time element is manifested implicitly in the variables of particle size and carrier gas steam content; therefore, time was not treated as an explicit independent variable in the approximate equation. The equation is described as follows:

$$DF_{tot} = \left\{ (1 - f\alpha) \left(\Sigma_k \frac{X_k}{DF_k} \right)^n \right\}^{-1} ,$$

where

- f = 1, ice present; = 0, no ice present,
- α = volume fraction of steam in the carrier gas,
- n = number of passes through the ice condenser,
- X_k = mass fraction of aerosols in the size range k,
- DF_k = decontamination factor for a single pass of aerosol particles of size k with only noncondensible carrier gas.

A single effective pass was assumed for assessment of the distribution medians because continual release of fission products results in an average of only one effective pass through the ice condenser. The effect of multiple passes in the ice condenser was accounted for in the upper ends of the distributions.

Expert C believed that the driving force for ice condenser DF is steam condensation. Thus, with no dependency on the number of passes through the condenser and a large dependency on steam condensation, the cases were

classified as either having low steam concentrations (50%, Cases 1 and 2), or high steam concentrations (90%, Cases 3 and 4). Because of the nature of the DCH phenomenology, the cases with high steam concentrations were then classified as with DCH, Case 4, or without DCH, Case 3.

Originally, Expert C supplied separate information for primary releases and CCI releases for all the cases. The CCI release distributions for ice condenser DF had originally been based on calculations that assumed no ice in the condenser and very low steam concentrations (10%) in the carrier gas. The values for DF were therefore approximately 1.0. When it was noted that ice is still present for most of the CCI release and that the DF was set equal to 1.0 when the ice is melted or totally bypassed, the distributions for Cases 1, 2, and 4 for the primary system were deemed sufficient for the CCI releases. For Case 3, a separate distribution was provided for the CCI releases because of the wide disparity in the steam content between the primary system releases and the CCI releases.

Aerodynamic particle size distributions for all but Case 4 were obtained from the calculation[C-2] for the S_3HF accident sequence at Sequoyah. For Case 4, the DCH case, Expert C based his assessment on aerodynamic particle size and requested that Sandia Surtsey Test particle size results be used to qualify the distribution. Impactor data obtained during the DCH-2 test[C-3] were used. The data indicate a unimodal aerosol distribution of less than 10 μm aerodynamic equivalent diameter with a mass mean diameter between 1 and 2 μm. Attachment C-1 describes the method used to obtain the distribution for aerodynamic equivalent diameter. The distribution is

Cumulative Probability	0.058	0.099	0.255	0.722	0.847	0.903	0.967
Aero. Dia. (μm)	0.4	0.7	1.1	2.5	4.5	6.4	10.3

The decontamination of the aerosol-laden gases in Case 4 was specified by Expert C to be obtained from Table 4 in NUREG/CR-3248. The predicted DF is a function of aerodynamic particle diameter:

Aerodynamic Particle Dia. (μm)	Case 4-DF $\epsilon F = 0.3$ $X_1 = 0.5; X_2 = 2.05$
0.001	203.1
0.01	11.2
0.10	2.3
0.40	2.1
1.0	2.6
2.0	4.5
4.0	12.0
8.0	41.5
10.0	63.5
20.0	248.9
50.0	1529.5
100.0	6064.0

The gas flow rate = 18.9 m^3/s, T = 293 K, P = 1 atm; $\mu = 1.8 \times 10^{-4}$ poise, ϵ = fraction of bed filled with ice, F = fraction of ice surface available

for sedimentation, and X = mole fraction of gas that is steam where i is the inlet gas and o is the outlet gas.

Results of Expert C's Elicitation

For Cases 1 and 2, all radionuclide groups, the distribution for the ice condenser DF is as follows:

Cumulative Probability	0.001	0.25	0.50	0.75	0.99
DF	1.0	2.0	5.0	7.0	10.0

For Case 3 primary system releases, the distribution for the ice condenser DF is as follows:

Cumulative Probability	0.001	0.25	0.50	0.75	0.99
DF	10.0	20.0	28.0	36.0	42.0

For Case 3 CCI releases, the distribution for the ice condenser DF is as follows:

Cumulative Probability	0.001	0.25	0.50	0.75	0.99
DF	1.0	1.0	2.0	3.0	4.0

For Case 4, all radionuclide groups, the distribution for the ice condenser DF is as follows:

Cumulative Probability	0.058	0.099	0.255	0.722	0.847	0.903	0.967
DF	2.1	2.4	2.8	6.4	15.7	29.7	63.5

Sources of Uncertainty

Expert C believed that a large part of the uncertainty in this issue is in the sequence definition. The boundary conditions for the problem definition itself are not well defined. There is uncertainty associated with the timing of the releases with respect to steam concentration in the lower compartment and also with respect to the amount of ice left in the ice condenser. There is also uncertainty concerning the aerosol size distributions of the releases. The process of fission product decontamination by the ice condenser is pretty well understood, but the boundary conditions pose the largest amount of uncertainty to the issue.

Suggested Methods for Reducing Uncertainty

Expert C feels that after the top sequences affecting risk are determined in the Sequoyah NUREG-1150 analysis, there should be some effort devoted to executing mechanistic analyses for those sequences. The analyses should focus on the uncertain phenomena in a more detailed fashion to help resolve some of the existing uncertainty.

Attachment C-1

DCH-2 Aerosol Size Distribution

The distribution for the aerosol particle size distribution was obtained from the data in the DCH-2 test result report. The data were digitized and plotted:

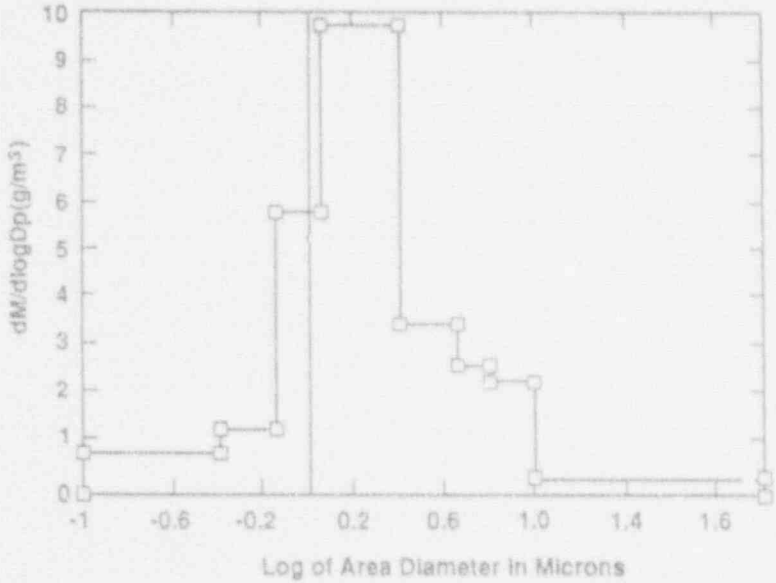

The area under the curve of the discrete ranges was obtained and then normalized to the total area under the curve. From each normalized integral, a cumulative distribution was obtained:

Log of Particle Size	Particle Size (micron)	dM/dlogDp (g/m^3)	Particle Range (micron)	Integral of Specified Range	Normalized Integral	Cumulative Distribution
-1.000	0.100	0.000				
-1.000	0.100	0.681	.1 -- .4	0.416	0.058	0.058
-0.389	0.409	0.681				
-0.389	0.409	1.209	.4 -- .7	0.301	0.042	0.099
-0.139	0.725	1.209				
-0.139	0.725	5.823	.7 -- 1.1	1.125	0.155	0.255
0.054	1.132	5.823				
0.054	1.132	9.823	1.1 -- 2.5	3.386	0.468	0.722
0.399	2.503	9.823				
0.399	2.503	3.492	2.5 -- 4.5	0.905	0.125	0.847
0.658	4.547	3.492				
0.658	4.547	2.647	4.5 -- 6.4	0.401	0.055	0.903
0.809	6.446	2.647				
0.809	6.446	2.302	6.4 -- 10.3	0.467	0.065	0.967
1.012	10.285	2.302				
1.012	10.285	0.240	10.3 -- 100.	0.237	0.033	1.000
2.000	100.000	0.240				
2.000	100.000	0.000				

REFERENCES

C-1. W. K. Winegardner et al., "Studies of Fission Product Scrubbing within Ice Compartments," NUREG/CR-3248, PNL-4691. Battelle Pacific Northwest Laboratory, 1983.

C-2. M. T. Leonard et al., "Supplemental Radionuclide Release Calculations for Selected Severe Accident Sequences," NUREG/CR-5062, BMI-2160. Battelle Memorial Institute, 1987.

C-3. W. W. Tarbell et al., "DCH-2: Results from the Second Experiment Performed in the Surtsey Direct Heating Test Facility," NUREG/CR-4917, SAND87-0976, Sandia National Laboratories, 1988.

5.3 Issue 3. Fission Products Released by Revolatilization from the RCS

Summary and Aggregation of Expert Panel's Assessment of Source Term Issue 3: FLATE1 and FLATE2

Experts Consulted: Peter Bieniarz, Risk Management Associates; Andrzej Drozd, Stone & Webster Engineering Corporation; Robert Henry Fauske and Associates; Dana Powers, Sandia National Laboratories.

Issue Description

What distributions characterize the uncertainty in the fraction of radionuclides that remain in the RCS after vessel breach and are then released to containment? The radionuclides may be released as a result of material released from the fuel in the vessel, deposited in the RCS, and then revaporized and released from the RCS during and after vessel breach or volatilization of material remaining in the RCS reactor pressure vessel (RPV) after vessel breach (0 to 20% of the fuel rods may be unmelted but fractured).

In the parametric equation used for the source term calculations, the revolatilization variables are $FLATE1_i$ and $FLATE2_i$ for radionuclide group i. The variables represent the fraction of the material available for each process that ultimately becomes volatile: $FLATE1_i$ is multiplied by the fraction of the nuclide group i originally released from the core in-vessel and not released from the vessel and $FLATE2_i$ is multiplied by the fraction of the nuclide group i not released from the core in the vessel and also retained in the vessel after breach. FLATE1 and FLATE2 can be the same. The cases originally considered include the following:

Case 1. PWR with a ruptured RPV and a rupture in the RCS piping

Case 2. PWR with a ruptured RPV and intact RCS piping

Case 3. BWR with a ruptured RPV, an intact piping system, and low drywell temperature

Case 4. BWR with a ruptured RPV, an intact piping system, and high drywell temperature

Sprays are always assumed to be recovered in 24 h from core damage (there are no drywell sprays in the Grand Gulf containment).

Summary of Experts' Rationale

Expert A used MARCH-RMACT calculations (a modified version of the STCP) as his primary aid to evaluate this issue. He also referred to information from the Brookhaven National Laboratory's (BNL's) QUASAR study, revaporization studies at SNL, and source term safety assessment work for the Indian Point Nuclear Power Plant.

Expert A pointed out that the revaporization of fission products from reactor pressure vessel and RCS surfaces depends on the temperature of the surfaces and the heat and mass transfer between the vessel and the containment. He felt that the natural circulation between the hot and cold regions of the RPV/RCS could transport the revolatilized materials to cooler regions of the RCS where they might be deposited (avoiding release to the containment.)

In the case of BWRs, the revolatilization will be dependent on the drywell temperature and the chemistry aspects of the deposited materials. For 24 h, the drywell temperature would be low enough to keep the reactor vessel walls cool enough to prevent revaporization. Even in the event of high drywell temperatures, natural circulation within the reactor system and the chemistry of the surfaces would prevent significant revolatilization. The tellurium and aerosol nuclide groups will not revolatilize because no highly reducing gases are in the BWR system; iodine and cesium are the only species with the potential to revolatilize.

Expert A felt that there would be less revolatilization for a breach in the PWR involving one hole than in the BWRs because the containment temperatures would be lower and the thermal mass in the RCS would be higher. Revolatilization is higher if there are two RCS breaches (e.g., in the vessel and in the hot leg) because the RCS is hotter than if there were only one breach and because natural circulation is set up between the RCS and the containment. The Expert felt that there was a very low probability that the material not released in the RCS/RPV would revolatilize and provided zero values for FLATE2.

Expert B based his elicitation on the results of MAAP calculations for several different sequences for both BWRs and PWRs. The major contributor to revaporization in BWRs is the early revaporization release within a few hours of vessel breach, dominated by vaporizing water held in the downcomer region and flushed out of the vessel.

The Expert stated that the CsOH is more tightly bound by the surface of the reactor vessel structure than cesium iodine, and he would therefore expect higher revaporization rates for iodine than cesium. The expert did not differentiate between FLATE1 and FLATE2.

Expert C developed a mechanistic model for the phenomenon of revaporization of radionuclides deposited on RCS structures. Parametric quantities within the model were varied through use of a Monte Carlo sampling scheme. The uncertain parameters included variables related to initial and boundary conditions, decay heating rates, chemical speciation of the radionuclides, chemical and thermophysical properties, geometry of the degraded core, configuration of the system, chemical environment in the reactor system, degradation of materials, and thermal and hydraulic conditions. The three parts of the model and some of the uncertainties considered for each part are listed below.

1. Estimation of the vapor phase and system surface temperatures:

   - Depth and thermophysical properties of the porous oxide layer that coats the inside of the RCS piping;

- Properties and depth of the RCS piping insulation;
- Ambient temperatures of containment;
- Decay heating rates;
- Gas and surface emissivities;
- Correlations for heat transfer coefficients; and
- Length of piping.

2. Estimation of the flow velocities through the piping system:
   - Vessel hole size;
   - Length of piping before the break;
   - Diameter of piping break;
   - Length of the fuel remaining in the core and inside diameter of core annulus;
   - Hydraulic parameters (loss coefficients and friction factor);
   - Thermophysical properties of the gas (conductivity, heat capacity, and viscosity); and
   - Parameters for core debris.
3. Estimation of the equilibrium partial pressure of the vapor species:
   - Uncertainties in the chemistry of each radionuclide were varied.

Expert D used a simple model to estimate the amount of revolatilization than can be expected:

$$REVOL = (F_{DV} - F_{HL})$$

where

F_{DV} = fraction of cesium, iodine, and tellurium inventory deposited in the RCS/RPV before vessel breach,

F_{HL} = ratio of cesium, iodine, and tellurium inventory decay heat to RCS/RPV heat losses.

Although many other parameters had an impact on revolatilization (gas temperature, structure temperature, fission product flow rate, chemical binding, and others), the driving force is "local" decay heat. He used Risk Management Assessment (RMA) analyses of the TMLB accident sequence for Surry to estimate the heat rejection capabilities of the RCS/RPV. He also used ORIGEN2 calculations to provide decay heat values.

The Expert pointed out that in the BWR cases, high drywell temperature could reduce the amount of RCS/RPV heat rejected to the containment and would increase revolatilization. He felt that PWR Case 2 was similar to the BWR high drywell temperature case and that the PWR Case 1 was similar to the BWR low temperature case.

Expert D felt that it was unlikely that the nonvolatiles would be released from the fuel before vessel breach, and therefore, they would not be available to be revolatilized after vessel breach. Consequently, he considered only revolatilization of cesium, iodine, and tellurium.

Method of Aggregation

Case Structure Modification

The original case structure was redefined after reviewing the elicitation summaries of four experts on this panel as follows:

1. **PWR Case Structure**. Only Expert B did not follow the original PWR case structure. He made two subcases for PWR Case 2: two holes with water in the containment and two holes without water in the containment. Therefore, it was necessary to create three cases to average distributions for the PWR.

   Case 1: one opening after vessel breach,

   Case 2: two openings after vessel breach (i.e., consequential pipe break) and no water in containment, and

   Case 3: two openings after vessel breach and water in containment.

2. **BWR Case Structure**. Three experts used the original BWR case structure. Experts A and C assigned the same distribution to the two BWR cases. Expert D assigned different distributions to the two BWR cases, but the difference between the two distributions was not significant. Expert B used a different case structure for the BWR cases. For the station blackout sequences (TBUX or TBU) in which there is no water injection capability after vessel breach, he considered revaporization release of iodine and cesium. For the high pressure anticipated transient without scram (ATWS) sequence TCUX, the low pressure injection systems would become available for injecting water into the reactor vessel. Expert B argued that this would cool the reactor vessel and result in no revaporization release for TCUX sequence.

   For the station blackout sequences, Expert B also provided different distributions for the EARLY PHASE (within a few hours after vessel breach) and the LATE PHASE (from a few to 24 h after vessel breach). The LATE PHASE applies to the high drywell

temperature condition. For the saturated or low drywell temperature condition, the LATE PHASE revaporization becomes 0.

Since PBSOR and GGSOR do not have time dependent source term capability, these two phases of Expert B's release fractions were added together for the station blackout sequences with high drywell temperature.

Therefore, there are three cases for the BWR:

Case 1. No water injection after vessel breach (TBUX or TBU) and high drywell temperature,

Case 2. No water injection after vessel breach (TBUX or TBU) and low drywell temperature, and

Case 3. Water injection available after vessel breach (e.g., TCUX)

Radionuclide Groups Considered

Experts A and B only considered revaporization releases for iodine and cesium groups. Expert D stated that tellurium group would behave like iodine and cesium groups as far as revaporization release. Expert C calculated revaporization release distributions for iodine, cesium, tellurium, strontium, ruthenium, and barium. However, the median values of revaporization release for strontium, ruthenium, and barium calculated by Expert C were rather small. Therefore, three groups were considered in the revaporization release: iodine, cesium, and tellurium.

Assumptions Used in Averaging Distributions

- For those experts who did not assign values for the two endpoint probabilities (i.e., 0 and 1), linear extrapolation was used to obtain these endpoints.
- The arithmetic mean is used for calculating the average frequency among different experts for a given value of revaporization fraction.
- Linear interpolation is used to obtain the values between the expert assessed points.

Aggregated Results

The aggregation for each PWR case is given in Tables 3-1 to 3-3 and for each BWR case in Table 3-4 to 3-6. These results are then plotted in Figures 3-1 to 3-6.

Table 3-1
Aggregate for PWR Case 1. One Opening after Vessel breach

	Fractiles								
Nuclide	0.000	0.010	0.050	0.250	0.500	0.750	0.950	0.990	1.000
Iodine	0.000	0.000	0.000	0.011	0.045	0.102	0.439	0.800	1.000
Cesium	0.000	0.000	0.000	0.011	0.023	0.072	0.171	0.248	0.750
Tellurim	0.000	0.000	0.000	0.000	0.000	0.024	0.209	0.413	0.800

Table 3-2
Aggregate for PWR Case 2. Two Openings after Vessel Breach, Dry

	Fractiles								
Nuclide	0.000	0.012	0.050	0.250	0.500	0.750	0.950	0.990	1.000
Iodine	0.000	0.000	0.000	0.044	0.170	0.305	0.715	0.920	1.000
Cesium	0.000	0.000	0.000	0.025	0.113	0.274	0.700	0.912	1.000
Tellurium	0.000	0.000	0.000	0.000	0.000	0.077	0.628	0.890	1.000

Table 3-3
Aggregate for PWR Case 3. Two Openings after Vessel Breach, Wet

	Fractiles								
Nuclide	0.000	0.010	0.050	0.250	0.500	0.750	0.950	0.990	1.000
Iodine	0.000	0.000	0.000	0.000	0.060	0.268	0.715	0.920	1.000
Cesium	0.000	0.000	0.000	0.000	0.025	0.251	0.700	0.912	1.000
Tellurium	0.000	0.000	0.000	0.000	0.000	0.077	0.628	0.890	1.000

Table 3-4
Aggregate for BWR Case 1. Station Blackout, High Temperature

	Fractiles								
Nuclide	0.000	0.010	0.050	0.250	0.500	0.750	0.950	0.990	1.000
Iodine	0.000	0.000	0.000	0.030	0.115	0.306	0.557	0.800	1.000
Cesium	0.000	0.000	0.000	0.001	0.051	0.132	0.284	0.535	0.750
Tellurium	0.000	0.000	0.000	0.000	0.000	0.024	0.224	0.413	1.000

Table 3-5
Aggregate for BWR Case 2. Station Blackout, Low Temperature

	Fractiles								
Nuclide	0.000	0.010	0.050	0.250	0.500	0.750	0.950	0.990	1.000
Iodine	0.000	0.000	0.000	0.030	0.114	0.261	0.456	0.800	1.000
Cesium	0.000	0.000	0.000	0.001	0.050	0.122	0.236	0.438	0.750
Tellurium	0.000	0.000	0.000	0.000	0.000	0.024	0.209	0.413	1.000

Table 3-6
Aggregate for BWR Case 3. Station Blackout, TCUX

	Fractiles								
Nuclide	0.000	0.010	0.050	0.250	0.500	0.750	0.950	0.990	1.000
Iodine	0.000	0.000	0.000	0.011	0.045	0.102	0.439	0.800	1.000
Cesium	0.000	0.000	0.000	0.001	0.023	0.072	0.171	0.248	0.750
Tellurium	0.000	0.000	0.000	0.000	0.000	0.024	0.209	0.413	1.000

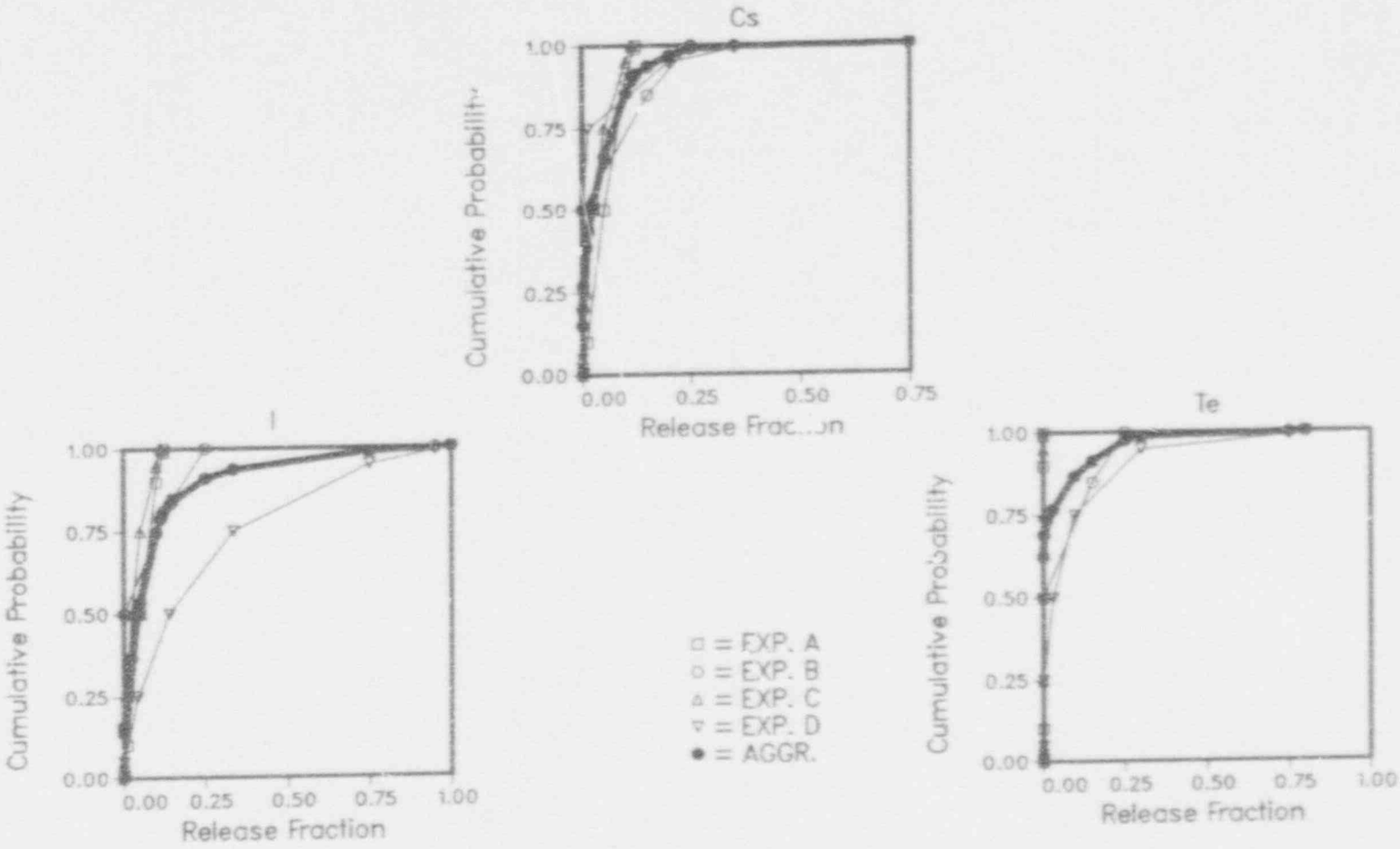

Figure 3-1. Case 1: PWR One Opening; Revaporization Release Fraction for Iodine (A); Cesium (B); Tellurium (C).

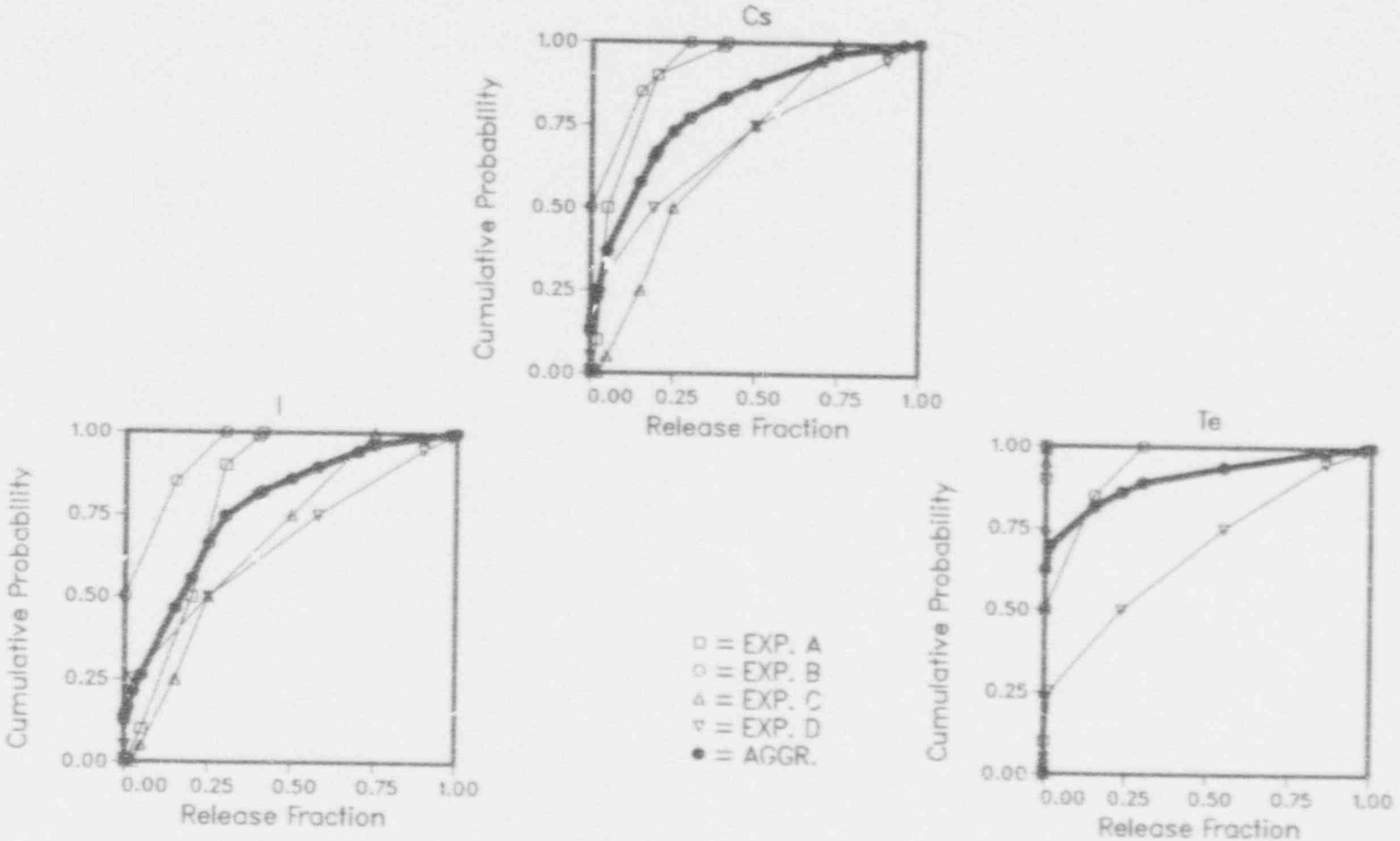

Figure 3-2. Case 2: PWR Two Openings, Dry; Revaporization Release Fraction for Iodine (A); Cesium (B); Tellurium (C).

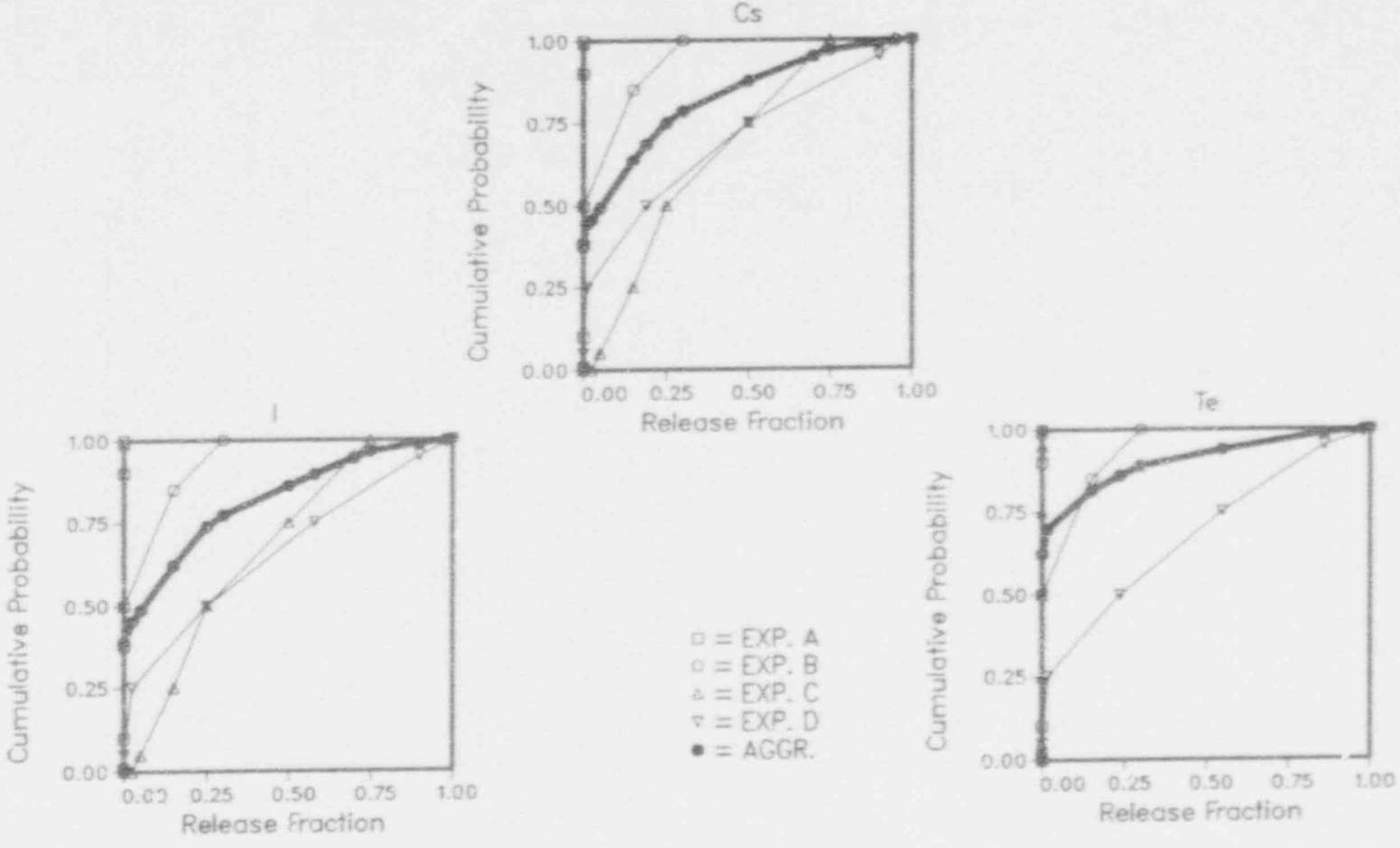

Figure 3-3. Case 2: PWR Two Openings, Wet; Revaporization Release Fraction for Iodine (A); Cesium (B); Tellurium (C).

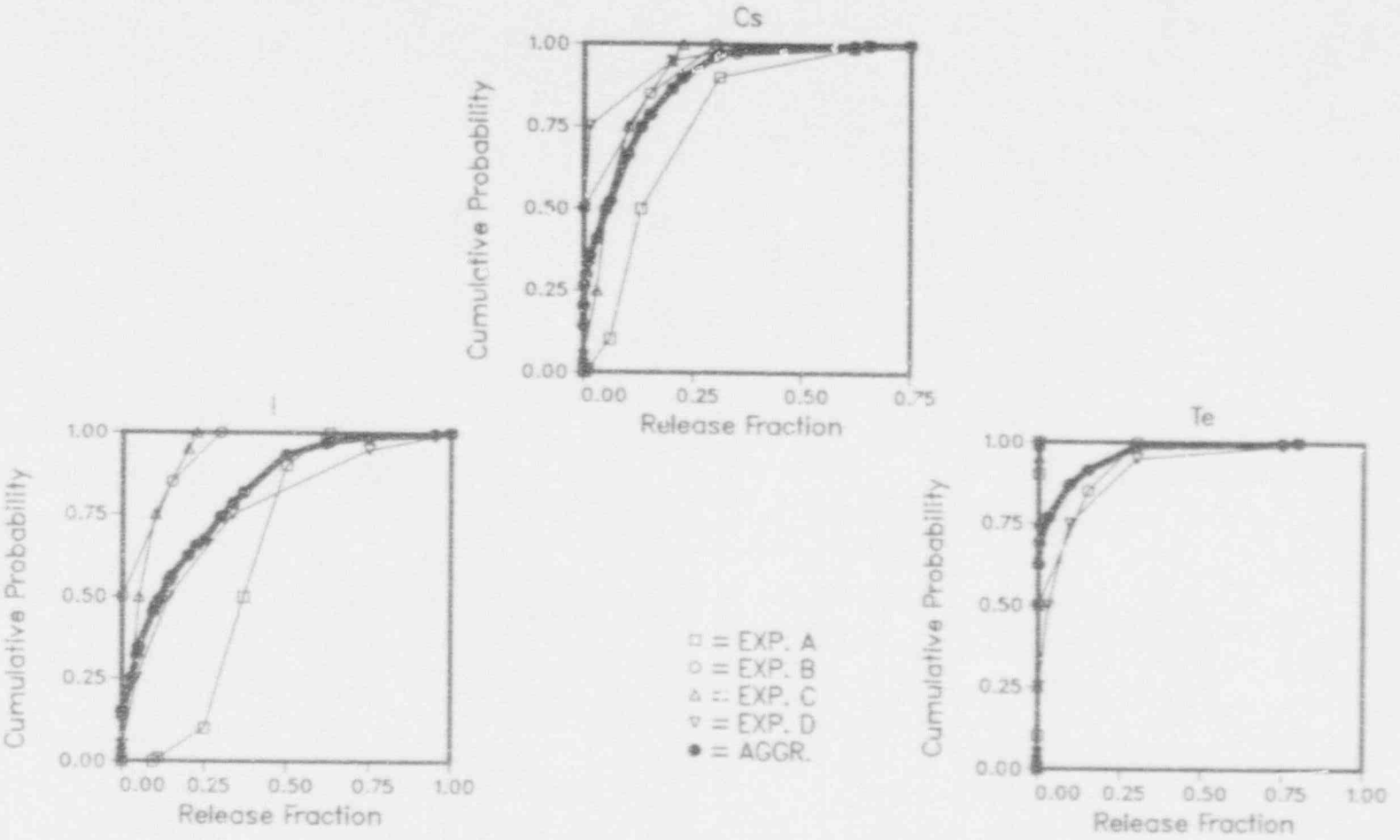

Figure 3-4. Case 1: BWR Station Blackout, High temperature; Revaporization Release Fraction For Iodine (A); Cesium (B); Tellurium (C).

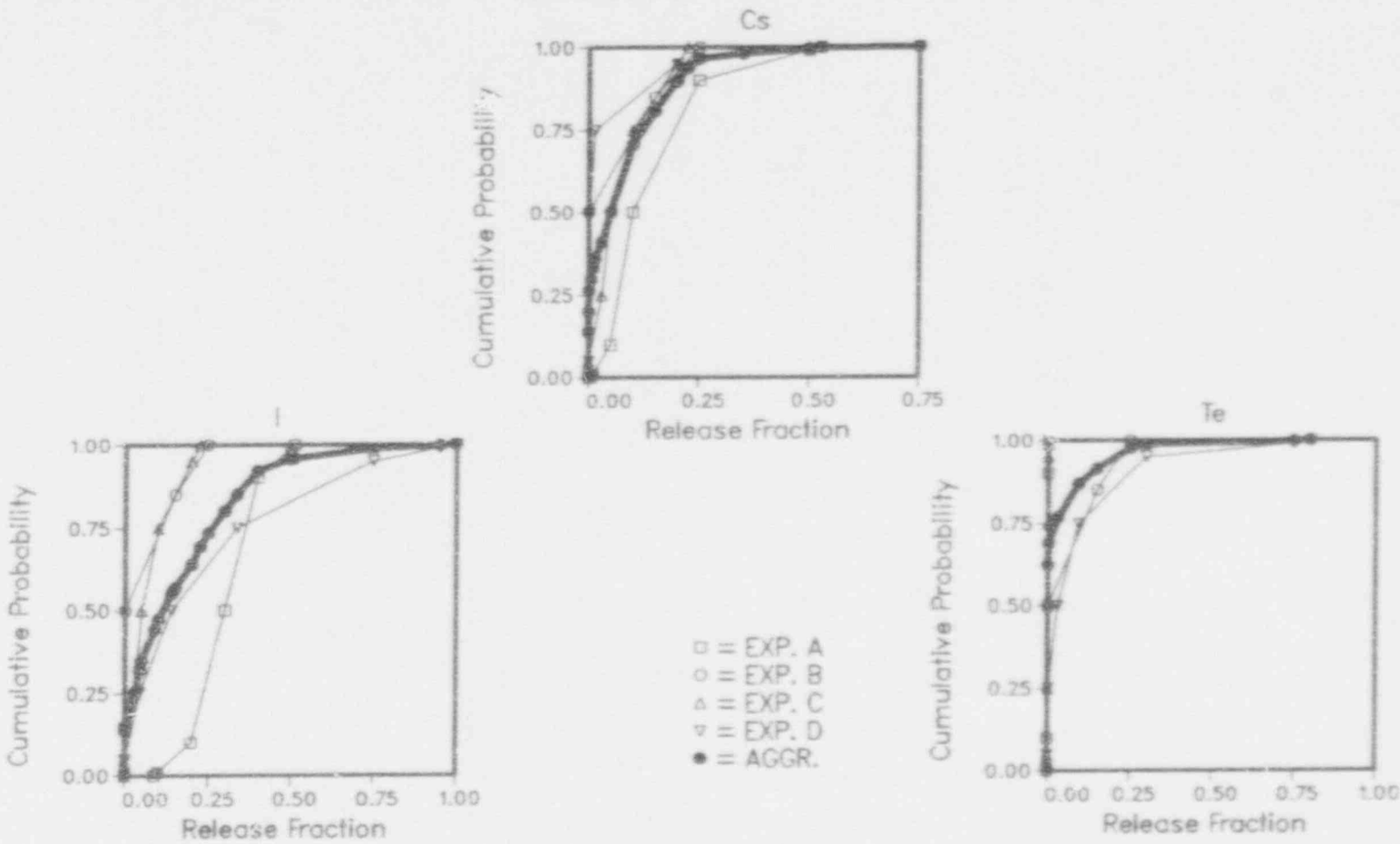

Figure 3-5. Case 1: BWR Station Blackout, Low Temperature; Revaporization Release Fraction for Iodine (A); Cesium (B); Tellurium (C).

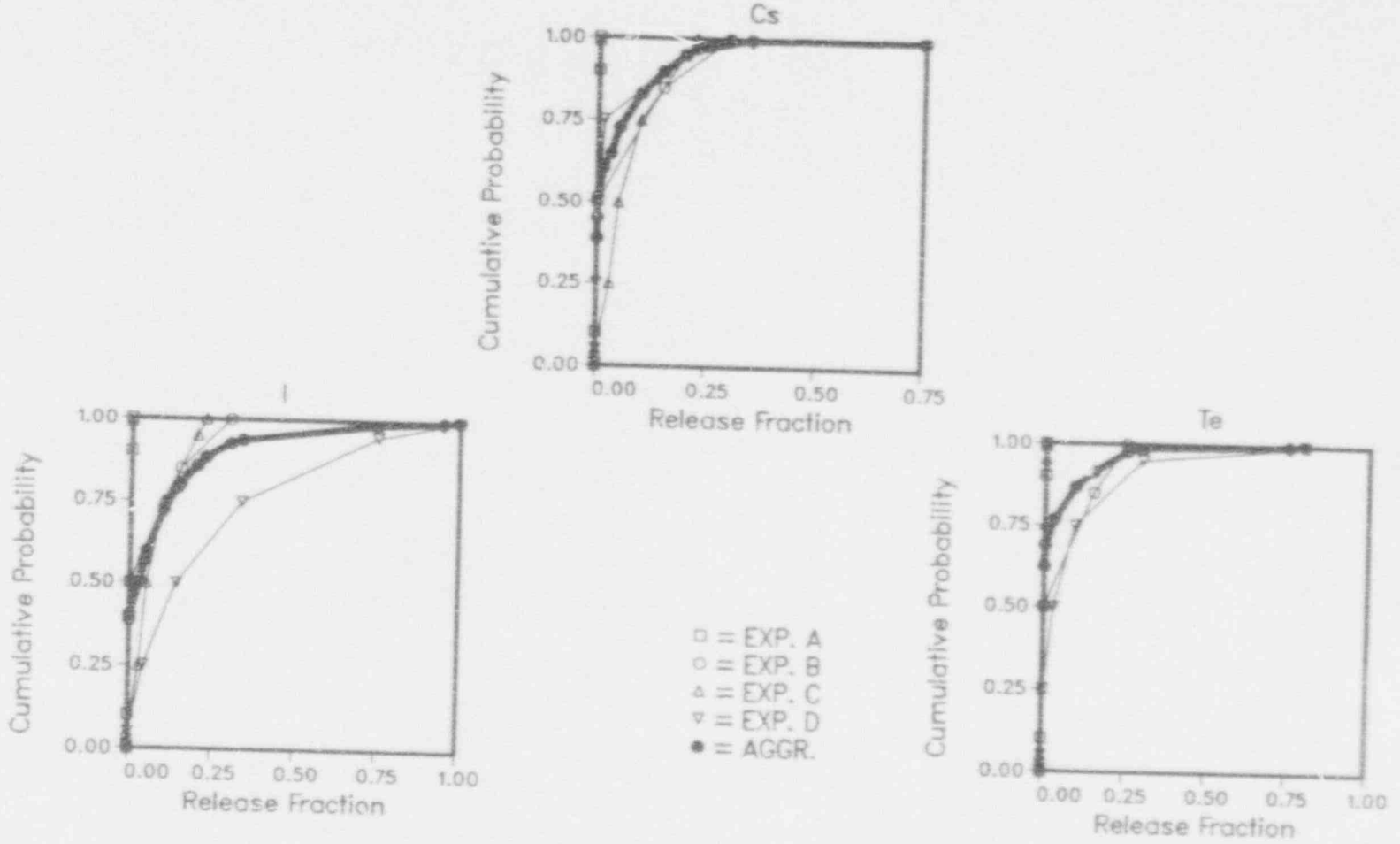

Figure 3-6. Case 3: BWR Station Blackout, TCUX; Revaporization Release Fraction for Iodine (A); Cesium (B); Tellurium (C).

Individual Elicitations for Issue 3

Expert A's Elicitation

Fission Products Released by Revolatilization from the RCS FLATE1 and FLATE2

Description of Expert A's Rationale/Methodology

Expert A ran a series of 10 calculations with MARCH-RMAMCT (a modified version of the STCP)[A-1] in order to aid in the quantification of this issue. Information from the QUASAR study (unpublished draft) at BNL,[A-2] and, to a lesser degree, References A-3, A-4, and A-5 were also used. Expert A provided a detailed description, supplemented with discussion, of the rationale used to formulate distributions for this issue.

FLATE1

The revolatilization of fission products deposited in the reactor system depends on the temperature response of the reactor system. Following vessel failure, the materials deposited on the structures can be revaporized only if their temperature increases enough. Also, even if the materials revaporize, outflow from the vessel to the containment has to exist for these materials to become part of the source term. The natural circulation between the hot and cold regions of the reactor vessel could transport the revolatilized materials to cooler regions where they might be deposited. Overall, the amount of revolatilization will depend on the heat transfer between the containment and the reactor system.

In the case of the BWRs, the revolatilization will be entirely dependent on (1) drywell temperature and (2) chemistry of the deposited materials. With the exception of Grand Gulf, containment spray would be available by 24 h after the start of the event. Before 24 h, the drywell temperature would be low enough to prevent revaporization. Even if the drywell temperature was high enough, as in the case of an early blackout sequence, the chemistry aspects and the natural circulation in the system would prevent significant revolatilization. Regardless of the presence of drywell sprays, natural circulation in the reactor system causes revaporization and settling within the system itself, rather than outside the system. For BWRs, the tellurium and aerosol nuclide groups will not revolatilize because there are no highly reducing gases in the BWR system; iodine and cesium are the only species that revolatilize.

In the case of the PWRs, the temperature in the containment would be lower than in the BWR case. Moreover, the thermal mass of the PWR is considerably larger than that of the BWR. As with the BWRs, only iodine and cesium are revolatilized for the PWRs. For a single opening in the vessel, the RCS remains cooler than when there are two openings in the vessel. Efficient natural circulation flow within the system is established, preventing release of whatever revolatilized fission products may be in the gas phase. If a second opening exists in the system, such as in the hot leg, a natural convection flow is established between the hot cavity and the containment. This hot through-flow consisting of reducing gases may revolatilize the volatiles and carry them to the containment. However, the chemistry of the deposited materials may discourage this.

FLATE2

The volatilization of material never released in the RCS/RPV, such as unmelted fuel rods within fractured clad, has such a low probability that this value is included within the uncertainty of the FLATE1 distribution. As such, a distribution was not provided for FLATE2, which is considered to be a zero value.

Results of Expert A's Elicitation

BWR Cases 1 and 2

For the nuclide groups cesium and iodine, the distribution for FLATE1 is the following:

Cumulative Probability	0.05	0.25	0.50	0.75	0.95
FLATE1 (%)	0.0	3.0	5.0	10.0	20.0

For the remaining nuclide groups, FLATE1 = 0, no distribution; and for all nuclide groups, FLATE2 = 0, no distribution.

PWR Case 1

For the nuclide groups cesium and iodine and a single opening in the RCS, the distribution for FLATE1 is the following:

Cumulative Probability	0.05	0.25	0.50	0.75	0.95
FLATE1 (%)	0.0	1.0	2.5	5.0	10.0

For the remaining nuclide groups, FLATE1 = 0, no distribution; and for all nuclide groups, FLATE2 = 0, no distribution.

PWR Case 2

For the nuclide groups cesium and iodine and two openings in the RCS, the distribution for FLATE1 is the following:

Cumulative Probability	.05	.25	.50	.75	.95
FLATE1 (%)	5.0	15.0	25.0	50.0	70.0

For the remaining nuclide groups, FLATE1 = 0, no distribution; and for all nuclide groups, FLATE2 = 0, no distribution.

Sources of Uncertainty

Expert A believes that the uncertainty for this issue involves the:

- Chemical form of the deposited material;
- Temperature of the reactor system;
- Presence of natural circulation within the reactor system;
- Possibility of natural circulation between the reactor cavity and the reactor vessel.

The first uncertainty results from lack of specific data and inadequate modeling of the potential chemical changes of the deposited materials. Expert A feels that the chemical form of the deposited species is most likely to favor the formation of less volatile species.

The second uncertainty depends upon the amount of energy deposited in the reactor system. This energy can be obtained from several sources, including the decay energy from the deposited fission product materials and the energy transported from the containment to the reactor system surfaces. The energy transport from containment is similarly dependent upon uncertain phenomena including atmospheric temperatures resulting from CCI, energy transport from the corium surface to the atmosphere, and the heat transfer to the reactor system through degrading or degraded insulation.

The third uncertainty relates mainly to the mode of core degradation. This includes whether blockages are formed within the vessel, as well as the subsequent development of natural circulation within the vessel. Another uncertainty is the circulation pattern of any natural circulating flows. Natural circulation can affect the subsequent settling or redeposition of revolatilized material.

The fourth uncertainty is dependent upon the size of the reactor vessel breach, the pressurization rate of the reactor vessel volume with respect to the containment, and the establishment of natural circulation paths within the reactor system. Expert A believes that a natural circulation path between the cavity region and the vessel is not likely. For a PWR, this is because the circulation would more likely develop between the cavity and the much larger, unobstructed path to the containment volume. For a BWR, the path between the cavity and the vessel is heavily obstructed by structural mesh that would interfere with circulation into the vessel.

REFERENCES

A-1 P. P. Bieniarz and R. E. Deem, "Analysis of a BWR Mk1 Utilizing Advanced BMI-2104 Computational Techniques to Calculate Source Terms," IAEA-SM-281/48, in Source Term Evaluation for Accident Conditions. Vienna: International Atomic Energy Authority, 1986.

A-2 M. Khatib-Rahbar et al., "On the Uncertainties in Core Melt Progression, Fission Product Release and Pressurization Loads for a BWR with Mark Containment," Technical Report A-3286, Brookhaven National Laboratory, February 20, 1988. (Draft for Comment)

A-3 D. A. Powers and P. P. Bieniarz, "Influence of Chemical Form on Cesium Revaporization from the Reactor Coolant System," Proceedings of the Symposium on Chemical Phenomena Associated with Radioactive Releases During Severe Nuclear Plant Accidents, NUREG/CP-0078, Washington, DC, 1987.

A-4 D. A. Powers and R. M. Elrick, "Interactions of the Radionuclide Vapors with Surfaces During Transport Through the Reactor Coolant System," Proceedings of a Workshop on Chemical Processes and Products During Reactor Accidents. Captiva Island, FL, 1987.

A-5 Risk Management Associates and New York Power Authority, "Source Term Safety Assessment of Radionuclide Releases Under Severe Accident Conditions at Indian Point 3 Nuclear Power Plant," 1984.

Expert B's Elicitation

Fission Products Released by Revolatilization from the RCS FLATE1 and FLATE2

Description of Expert B's Rationale/Methodology

Expert B did not differentiate between revolatilization release from previously deposited fission products and volatilization release from fuel remaining in the reactor vessel. The release fractions that the expert gave during elicitation included considerations of both contributions.

The case structure for PWRs (i.e., one hole and two holes) was used by the expert. However, he did not use the BWR case structure suggested during the elicitation meeting. Instead, he used the BWR case structure discussed at the previous source term experts' meetings. The drywell temperature would affect only the late revaporization release. The expert stated that the major contributor of revaporization in BWRs is from the early revaporization release within a few hours after vessel breach, which is dominated by vaporizing water held in the downcomer region and flushing it out of the vessel after vessel breach.

He stated that the CsOH is more tightly bound by the surface of the reactor vessel structure than cesium iodide. Therefore, he would expect higher value of revaporization fraction for iodine than that for cesium.

The approach used was the result of MAAP calculations of a variety of accident sequences for both the PWR and the BWR systems.

Results of Expert B's Elicitation

Since Expert B did not differentiate between FLATE1 and FLATE2, the uncertainty distribution functions given include both FLATE1 and FLATE2.

PWR Case 1: Single Hole--TMLB Sequence

The characteristics of this case are:

- Single opening in RCS;
- Circulation flows distribute material;
- RCS heat loss;
- Containment pressurizing.

The expert explained that there would be little or no revaporization for this case. Surface reactions are the one uncertainty for this case. However, the expert concluded that this uncertainty would more tightly bind the material deposited on the structure surface and hence reduce the fraction revaporized. Table B-1 shows the probability distributions of iodine and cesium revolatilization release fractions for this case.

Table B-1
Cumulative Distribution Function of FLATE
PWR Case 1: One Opening

Cumulative Probability (%)	Cesium Iodide (CsI)	Cesium (CsOH)
1	0.001	0.001
10	0.01	0.01
50	0.05	0.05
90	0.1	0.1
99	0.12	0.12

PWR Case 2: Two Holes--Consequential Pipe Rupture (Hot Leg) with No Water in the Containment

The characteristics of this case are:

- Multiple openings in RCS;
- Circulation flows distribute material;
- No water in containment;
- Some fuel could be held up in the RPV.

Expert B concluded that there would be some revaporization for this case but it would not be extensive. Table B-2 shows the probability distributions of iodine and cesium revolatilization release fractions for this case.

Table B-2
Cumulative Distribution Function of FLATE
PWR Case 2: Two Openings, Dry

Cumulative Probability (%)	Cesium Iodide (CsI)	Cesium (CsOH)
1	0.01	0.01
10	0.05	0.02
50	0.2	0.05
90	0.3	0.2
99	0.4	0.4

PWR Case 3: Two Holes--LOCA or Consequential LOCA with Water in the Containment

This case is the same as PWR Case 2, except that there is water in the containment floor. Expert B stated that for this case, the water in the containment provides an extensive heat sink. Therefore, he concluded that the extensive heat loss from the RCS results in no revaporization.

BWR Case 1: TBUX--Station Blackout, High Pressure

The characteristics of this case are:

- Single opening in RCS;
- Circulation flows distribute material;
- RCS heat losses;
- Containment pressurizing;
- Vaporization of water held up in the vessel downcomer.

For this case, the revolatilization release would be larger than those for the previous two PWR cases. The first and dominant contributor is from the initial blowdown after vessel breach. There would be a substantial amount of water in the downcomer regions of the reactor vessel at the time of vessel breach. This water would be vaporized and flushed out of the vessel within a few hours after vessel breach and provide a mechanism for fission products revaporization. Table B-3 shows the probability distributions of iodine and cesium release fractions for the early revaporization phase.

Table P-3
Cumulative Distribution Function of FLATE
BWR Case 1: TBUX--Early Phase

Cumulative Probability (%)	Cesium Iodide (CsI)	Cesium (CsOH)
1	0.1	0.01
10	0.2	0.05
50	0.3	0.1
90	0.4	0.25
99	0.5	0.5

Longer term revaporization release to containment will occur if the drywell temperature becomes hot after vessel breach (from a few hours to about 24 h). Expert B stated that the release fraction for the later phase of revaporization would be about one quarter that of the early phase. Table B-4 shows the probability distributions of iodine and cesium revolatilization release fractions for the late revaporization release because of high drywell temperature.

Table B-4
Cumulative Distribution Function of FLATE
BWR Case 1: Late Phase

Cumulative Probability (%)	Cesium Iodide (CsI)	Cesium (CsOH)
1	0.01	0.001
10	0.05	0.01
50	0.07	0.03
90	0.1	0.06
99	0.12	0.12

BWR Case 2: TCUX--ATWS Sequence, High Pressure

The low pressure systems should be available after vessel breach. The low pressure injection systems could provide cooling to the reactor vessel; therefore, no revaporization would occur.

BWR Case 3: TBU--Station Blackout Sequence, Low Pressure

This case is similar to BWR Case 1: TBUX, except that there is less water in the downcomer at the time of vessel breach. The same uncertainty distributions as for BWR Case 1: TBUX were used.

Sources of Uncertainty

Expert B identified the following key issues in considering the uncertainty of revolatilization from the RCS after vessel breach:

- Fraction of fission products deposited;
- Structure masses;
- Circulation flows;
- Chemical state of deposited fission products;
- Primary system heat losses or gains;
- Aerosol transport and deposition;
- Containment pressurization;
- Core left in the RCS;
- Water remaining in the RCS.

Correlations with Other Variables

Even though the Expert did not explicitly correlate this source term issue with any other issues, he indicated that the amount of fission products deposited (i.e., 1-FVES) was used as part of the information in his assessment. He indicated that larger deposition would result in larger revaporization. The MAAP calculations showed that the high pressure sequences in PWR Case 1 (TMLB) would have higher fission product deposition

than the intermediate/low pressure sequences in PWR Case 2. Therefore, even though PWR Case 1 has only one hole, the expert assigned the same 50th percentile value to cesium for both PWR Cases 1 and 2.

Therefore, the expert used a negative correlation between parameter FLATE and FVES.

Suggested Methods for Reducing Uncertainty

None.

Expert C's Elicitation

Fission Products Released by Revolatilization From the RCS FLATE1 and FLATE2

Description of Expert C's Rationale/Methodology

Expert C conducted the assessment for revaporization of radionuclides deposited on RCS structures (FLATE1) and noted that late time release of radionuclides from the residual fuel (FLATE2) needs to be recognized elsewhere. A mechanistic model for the phenomenon of revaporization was developed, and parametric quantities within the model were varied through use of a Monte Carlo sampling scheme. The uncertainty parameters included variables related to initial and boundary conditions, decay heating rates, and chemical speciation of the radionuclides, chemical and thermophysical properties, geometry of the degraded core, configuration of the system, chemical environment in the reactor system, degradation of materials, and thermal and hydraulic conditions and models. The analyses and justifications used to conduct the assessment are documented in their entirety in Part 5 of this volume, and will only be summarized here.

Expert C chose to model the uncertainty for the issue through distinct parametic quantities and not in the integral quantity. He felt that ad hoc estimation of the ranges of an integral quantity is arbitrary, qualitatively based upon intuition, and not easily justified. The approach of Expert C, however, lends itself to the evaluation of the sensitivity of the integral quantity upon a microscopic quantity. The uncertainty range of the microscopic parameter has been studied and established with a significant and justifiable basis.

The initial and boundary conditions for the source term estimates are heavily dependent upon the accident progression up to the revaporization process. Therefore, three steps were used in developing the mechanistic model:

1. Estimation of the vapor phase and system surface temperatures;
2. Estimation of the flow velocities through the piping system; and
3. Estimation of the equilibrium partial pressure of the vapor species.

The accident situation for the four cases of the revaporization problem was explained as follows:

> The reactor vessel has been breached by core debris. Residual fuel remains in the core region. Gases are drawn through the breach, through the fuel and then flow along the piping system. The remaining fuel heats the gases to drive the flow. Radionuclides along the piping system may also heat the gases or the piping system may act as a heat sink. A second breach in the piping system allows the gas flow to escape. Since the results are to be applicable to arbitrary accidents,

dimensions of the breaks and the length of the flow pathway are considered uncertain.

Surface Temperatures in the Reactor Coolant System

The inner surface of the stainless steel piping in the reactor coolant system is, in normal operation, corroded and coated with a magnetite layer. During an accident, the corrosion increases because of steam oxidation and boric acid, enlarging the depth of the oxide layer. The exact depth and thermophysical properties of this porous oxide layer are not known and were varied in the execution of the analysis. The radionuclides are deposited on top of the oxide layer and, for this analysis, were assumed to be spread uniformly over 6.6×10^6 cm^2. Initially, the deposition will probably not be uniform, but continual vaporization and redeposition will even the distribution by the time the net revaporization is of interest. The layer of radionuclides was considered to create no thermal resistance to heat transfer.

The exterior of the piping may be covered with insulation that during the accident degrades somewhat. The properties and depth of the insulation were uncertainty parameters in the analysis. The ambient temperature range in containment is different for PWRs and BWRs. For a PWR, the long-term, quasi-steady temperature (ignoring transients) will not exceed the saturation temperature of water at the maximum pressure attainable in containment. The temperature may be lower because of engineered safety features such as cooling of the atmosphere by the ice condenser or sprays. For a BWR, the drywell temperatures could possibly be higher. Because of the uncertainty of the ambient temperature, it was yet another parameter varied in the analysis for the separate cases.

Heat transport from the gas to the pipe was modeled as the sum of the convective and radiative components. The vaporization of radionuclides from the pipe surface was considered negligible and not included in the model. Decay heating from the deposited radionuclides was considered, however, and included in the steady-state transfer of heat through the system. Decay heat from the radionuclides and/or heating from the gas is conducted from the inner layer of radionuclides through the corrosion layer, metal pipe, and insulation. Because of the decay heating contribution, the gas within the RCS is sometimes heated and sometimes cooled.

For the length of piping from the reactor vessel to the break, the axial temperature distribution in the pipe was determined with a 10 node model, after coupling with the flow model to obtain the gas temperature. Uncertainties in the model include decay heating rates, gas and surface emissivities, correlations for heat transfer coefficients, length of piping, and those parameters mentioned above.

Flow Through the Ruptured Coolant System

The flow in the RCS is induced by buoyant effects from heating of the gases and is resisted by the viscous forces in the system that include friction, and entrance and exit effects. The total pressure drop through the entire

system is approximately zero; thus, the pressure rise from thermal effects is offset by the pressure drop from viscous forces. The pressure drop in the system is the result of:

- Entrance effects at the rupture in the reactor vessel;
- Exit losses at the rupture in the piping system;
- Entrance effects to the piping system;
- Friction losses during flow through the piping system;
- Friction losses during flow through the residual core material.

For the analysis, it was assumed that the residual fuel is present as rod stubs arrayed in an annulus and the flow through the annulus is laminar. Although the debris may be in a rubble bed, only a fraction of the total flow would actually pass through the bed. The low flow through the bed would cause little cooling, and the bed would reheat, melt, and leave a geometry similar to the assumed geometry.

Heat transport from the core region to the gas was modeled as the sum of the convective and radiative components. The mode of convective heating is natural convection and was treated as such. The gases passing through the system contain optically active gases such as carbon dioxide and water and will be laden with aerosols produced in CCI. The gas can therefore be considered as optically thick. Thus, for the analysis, the heat transfer from the core to the gas was approximated by an expression for radiative exchange between parallel plates.

For this phase of the analysis, there were many uncertainty parameters that include the boundary conditions of temperature, pressure, and composition of the gas drawn into the system as well as the temperature of the core debris. Physical parameters were varied such as vessel hole size, length of piping before the break, diameter of the piping break, and length of the fuel remaining in the core, as well as the inside diameter of the core annulus. Uncertainty was associated with the hydraulic parameters of loss coefficients and friction factor, and the thermophysical properties of the gas including conductivity, heat capacity, and viscosity (any effects of aerosols on the properties were neglected). The correlation for the convective heat transfer coefficient incorporated uncertainty ranges, and the parameters for core debris and gas emissivities were also varied.

Radionuclide Chemistry

The uncertainties in the chemistry of the radionuclides will be discussed for each radionuclide. Cesium, iodine, tellurium, ruthenium, barium, strontium, cerium, and lanthanum were considered in the analysis.

Cesium. It cannot be assumed that cesium is deposited on the RCS surfaces in the form of pure CsOH. It may chemically react with other species deposited on the surface and form products such as cesium borate, cesium ferrate, cesium phosphate, cesium manganate, cesium silicate, cesium tellurate, cesium molybdate, cesium uranate, or cesium zirconate. It might react with the carbon dioxide produced during CCI to form cesium carbonate. Any reaction results in substantial reduction of its activity. For the analysis, the deposited cesium was assumed to be in the form of cesium

borate. The uncertainties in the vapor pressures of the vaporization of $CsBO_2$ were ascribed to the uncertainties in the enthalpy of formation of the gaseous species and also the activity of the condensed $CsBO_2$.

Iodine. There is much evidence that little iodine is retained in the RCS during core degradation, because it is converted to the volatile forms of HI, I, or I_2. Although the deposited iodine might be present in the form of NiI_2 or AgIodine, it was assumed for the analysis that whatever iodine is retained in the system was CsI; hence, its activity becomes reduced. The vaporization reactions that were considered neglected the oxidation process because oxygen levels will be low from oxidation of hot metals within the vessel. Uncertainties in the vapor pressures were ascribed as for cesium.

Tellurium. There is much controversy over the behavior of tellurium during core degradation; it is an issue of contention that any significant amounts are released. It has been proposed that tellurium is released from the fuel as either $Te_2(g)$ or SnTe(g), or even Cs_2Te. Te_2 vapors react readily with stainless steel to form nickel telluride or iron telluride. The deposited form of tellurium, for this analysis, was assumed to be nickel telluride because it was believed that SnTe is reactive and that the transport pathways and environments were unrealistic in the tests that show tellurium may be associated with cesium in releases. Because all the oxygen drawn into the vessel will not be available to drive the vaporization of tellurium, the oxygen potential was calculated from the iron oxide equilibrium. Uncertainties in the vapor pressures were ascribed as for cesium.

Ruthenium. Ruthenium behavior during core degradation is not yet understood. If present in a sufficiently oxidizing atmosphere, it reacts to form very volatile species, although this condition would not likely exist in the vessel. Ruthenium-bearing metallic inclusions may alloy with steel or zircaloy during core degradation. It is questionable whether there is any ruthenium to revaporize, and if there is, the question of what its chemical form will be remains. Routine thermochemical calculations show that the deposited material will be a metal in the hydrogen/steam atmosphere produced during core degradation. In the analysis, therefore, it is assumed that the deposition of ruthenium will be as a relatively pure metal particulate. As with tellurium, the oxygen potential necessary to drive the vaporization was obtained from the iron oxide equilibrium. Uncertainties in the revaporization were assumed to be adequately indicated by the uncertainty in the enthalpies of the formation of the vapor species.

Barium and Strontium. Qualitatively, the chemical features of the alkaline earths barium and strontium are similar, although quantitatively, they are not. High oxygen potentials inhibit vaporization of the alkaline earths, but the low oxygen potentials present in a reactor accident will enhance vaporization. Even if the alkaline earths are released from the fuel as metal vapors, they quickly convert to the oxides in the cooler environs of the piping system, and are thus deposited as monoxides. At elevated temperatures, they are quite reactive toward other oxides, producing zirconates and uranates. Alkaline earth oxides are also quite soluble in B_2O_3, forming borates and will react with silica to form silicates. Among

the possible chemical forms of the deposited material, the monoxide should be the most volatile and the zirconate among the least volatile. Hence, the deposited forms assumed for the analysis were split equally between the monoxides and the zirconates. Steam and hydrogen partial pressures were calculated assuming up to 0.1 atmosphere of hydrogen and the oxygen potential was dictated by the iron oxide equilibrium. Uncertainties were ascribed to the uncertainties in the enthalpy of formation of the vapor species.

Lanthanum. Lanthanum is considered to be quite refractory, being present in the fuel as the oxide, La_2O_3, and thus its release from the fuel is small. Because of its hexagonal structure, La_2O_3 that is released is not very soluble in solids deposited on the RCS surfaces. It will, however, dissolve in borates on the surfaces. It is assumed, in this analysis, that the deposited form of lanthanum is the lanthanum oxide and that its activity is 1.0. As before, the ambient oxygen potential is taken to be dictated by the iron oxide equilibrium, and uncertainties were associated with the enthalpy of formation of the vapor species.

Cerium. Cerium is considered to be present in the fuel as the oxide, CeO_2. Its activity, however is largely variable depending on the ambient oxygen potential. The deposited form of cerium dioxide was used in the analysis. Uncertainties in the vapor pressures of the vaporization of CeO_2 were ascribed to the uncertainties in the enthalpy of formation of the gaseous species and also the activity of the deposited CeO_2.

Results of Expert C's Elicitation

Case 1.

After 2,900 calculations with the Monte Carlo approach for Case 1, probability densities were obtained for the flow rate through the system, the temperature of the gas entering the piping, and the structural surface temperature at the entrance and exit of the piping. The mean value for flow rate was ~213 g-moles/s. The temperature of the gas entering the vessel was an uncertainty variable with an assumed uniform distribution and a mean value of 900 K. The mean temperature of the gas entering the piping system was ~1084 K. The mean values for the structural surface at the piping entrance and exit were determined to be ~1056 K and ~1013 K, respectively. The calculation for structural temperatures indicated that there was indeed both heating (from deposited radionuclide decay) and cooling of the gas within the piping system.

The cumulative probabilities for the first six radionuclide groups are presented for Case 1 in Table C-1.

Table C-1
Case 1. Radionuclide Revaporization

Revaporization Fraction	Cumulative Probabilities					
	Cesium	Iodine	Tellurium	Ruthenium	Strontium	Barium
10^{-7}	-	-	-	-	-	0.431
10^{-6}	-	-	-	-	-	0.490
10^{-5}	0.153	0.064	0.073	0.536	0.808	0.566
10^{-4}	0.175	0.111	0.123	0.585	0.864	0.645
10^{-3}	0.212	0.155	0.178	0.612	0.921	0.714
0.01	0.259	0.210	0.228	0.658	0.966	0.786
0.02	0.283	0.244	0.265	0.680	0.977	0.803
0.03	0.315	0.263	0.283	0.687	0.980	0.821
0.04	0.333	0.277	0.297	0.694	-	0.827
0.05	0.341	0.294	0.329	0.702	0.983	0.834
0.06	0.349	0.302	0.338	0.711	0.986	0.838
0.07	0.365	0.308	0.361	0.716	0.989	0.845
0.08	0.376	0.319	0.374	0.718	0.991	0.855
0.09	0.384	0.332	0.379	0.721	0.992	-
0.10	0.392	0.349	0.384	0.723	-	-
0.15	0.463	0.402	0.443	0.743	-	0.883
0.20	0.511	0.432	0.470	0.772	-	0.907
0.25	0.553	0.499	0.511	0.798	0.994	0.921
0.30	0.595	0.546	0.548	0.825	-	0.928
0.35	0.645	0.598	0.589	0.845	-	0.938
0.40	0.682	0.634	0.635	0.864	0.997	0.941
0.45	0.714	0.670	0.676	0.881	-	0.959
0.50	0.757	0.709	0.717	0.896	-	0.966
0.55	0.788	0.734	0.749	0.910	-	0.972
0.60	0.807	0.762	0.785	0.927	-	0.976
0.65	0.839	0.784	0.813	0.934	-	0.979
0.70	0.868	0.823	0.849	0.947	-	0.983
0.75	0.892	0.856	0.890	0.949	-	0.983
0.80	0.926	0.892	0.927	0.959	-	0.990
0.85	0.936	0.931	0.945	0.971	-	0.993
0.90	0.955	0.953	0.968	0.985	-	0.997
0.95	0.987	0.975	0.977	1.000	-	0.997
1.00	1.000	1.000	1.000	1.000	-	1.000

Several executions of the models produced release fractions for lanthanum and cerium of less than 10^{-7}. This is probably because of low piping temperatures resulting in low vapor pressures. If the piping temperatures were sufficiently high, the oxygen partial pressure was high enough to suppress release.

Cases 2, 3, and 4

The remaining three cases involve rupture of the RCS only through a single failure in the vessel. If a leak-tight RCS is assumed, the flow of radionuclides out of the vessel would entail a counter-current flow through the opening in the vessel. Natural circulation through the vessel might not even be conducive to involving flow over deposited radionuclides, and the revaporization process could thus be negligible.

Reactor coolant systems, however, leak during normal operation. This leakage is equivalent to a hole about 3 mm in diameter. This opening in the system ensures net flow through the RCS. Thus, the analysis for Case 2 was executed as for Case 1, but the parameter for the piping breach was changed and was again variable. The execution of the analyses for Cases 3 and 4 was the same as for Case 2, except that the ambient temperature values were increased accordingly. For the three cases, results for revaporization of iodine and barium showed little difference, and therefore, the results of Case 2 were applied to Cases 3 and 4. All the species, with the exception of iodine showed substantially reduced vaporization relative to Case 1. The revaporization of cesium iodine is very sensitive to the activity coefficient of cesium iodine. The results for Cases 2, 3 and 4 are presented in Table C-2.

Table C-2
Cases 2, 3, and 4. Radionuclide Revaporization

	Cumulative Probabilities					
Revaporization Fraction	Cesium	Iodine	Tellurium	Ruthenium	Strontium	Barium
10^{-7}	0.243	-	0.141	-	0.664	0.515
10^{-6}	0.276	-	0.147	-	0.809	0.580
10^{-5}	0.333	0.000	0.147	-	0.909	0.633
10^{-4}	0.391	0.000	0.166	-	0.973	0.726
10^{-3}	0.543	0.065	0.233	-	1.000	0.854
0.01	0.728	0.108	0.399	-	-	0.950
0.02	0.786	0.135	0.454	-	-	0.969
0.03	0.798	0.184	0.509	-	-	0.983
0.04	0.811	0.243	0.577	-	-	-
0.05	0.852	0.260	0.620	-	-	-
0.06	0.868	0.300	0.675	-	-	0.989
0.07	0.868	0.331	0.699	-	-	-

Table C-2 (Continued)

Revaporization Fraction	Cumulative Probabilities					
	Cesium	Iodine	Tellurium	Ruthenium	Strontium	Barium
0.08	0.876	0.371	0.724	-	-	-
0.09	-	0.401	-	-	-	-
0.10	-	0.420	-	-	-	-
0.15	0.926	0.519	0.853	-	-	0.992
0.20	0.951	0.595	0.890	-	-	-
0.25	0.967	0.654	0.920	-	-	0.997
0.30	0.988	0.700	0.957	-	-	-
0.35	0.992	0.770	0.957	-	-	1.000
0.40	0.992	0.814	0.963	-	-	-
0.45	0.996	0.848	0.963	-	-	-
0.50	0.996	0.876	0.969	-	-	-
0.55	0.996	0.897	0.976	-	-	-
0.60	0.996	0.920	0.982	-	-	-
0.65	0.996	0.932	0.988	-	-	-
0.70	0.996	0.935	0.988	-	-	-
0.75	1.000	0.952	0.988	-	-	-
0.80	-	0.958	1.000	-	-	-
0.85	-	0.958	-	-	-	-
0.90	-	0.985	-	-	-	-
0.95	-	0.994	-	-	-	-
1.00	-	1.000	-	-	-	-

Sources of Uncertainty

The uncertainty parameters, as mentioned earlier, included variables related to initial and boundary conditions, decay heating rates and chemical speciation of the radionuclides, chemical and thermophysical properties, geometry of the degraded core, system and piping configuration, chemical environment in the reactor system, degradation of materials, and thermal and hydraulic conditions and models. Expert C noted that the flow of gas through the RCS appears to affect the revaporization release, although the effect is modest for the more volatile radionuclides such as iodine. At a low flow condition, the ambient temperature has a very small effect on revaporization. Far more important seems to be the temperatures and heat transfer inside the piping system, which are again dependent upon radionuclide deposition and surface degradation on the inner surface of the piping.

Chemical phenomena and the chemical forms of the deposited radionuclides also affect the revaporization of some species, particularly the deposited form of cesium. The deposited form of iodine, however, had a much lesser effect. It would require great dilution of any iodide in other materials to significantly alter its revaporization characteristics.

Correlation With Other Variables

Expert C noted many correlations between variables used in the analysis and those developed throughout the accident progression. Some of the explicit references to correlations are provided below:

1. The ambient temperature and pressure are dependent upon DCH, hydrogen phenomena, engineered safety features, and containment failure and mode of failure;

2. Decay heating by deposited radionuclides is correlated to the amount initially deposited;

3. The radiative heat transfer to and from the aerosol-laden gas depends upon the nature of the aerosols produced (and possibly scrubbed) during CCI;

4 The temperature of the gas entering the system depends upon the nature of the CCI;

5. The molecular weight of the gas depends upon the CCI aerosols;

6. The diameter of the breach in the RPV affects the calculation.

Suggested Methods for Reducing Uncertainty

None.

Expert D's Elicitation

Issue 3: Fission Products Released by Revolatilization from the Reactor Coolant System (RCS)

Description of Expert D's Rationale/Methodology

Expert D indicated that several parameters affected the revolatilization of fission products from the RCS/RPV. These parameters included the decay heat level, gas temperature in the RCS/RPV, temperature of the structures, fission product distribution, flow rate and flow pattern in the vessel, fission product vapor pressure and chemical form, and chemical binding with structures. However, it was the expert's position that revolatilization is driven by energy distribution. He felt that the driving force is "local" decay heat.

For the PWR cases, the number of openings in the vessel affects the flow patterns in the RCS/RPV. For the one-opening case, it was likely that natural convection would evenly distribute the fission products throughout the RCS. On the other hand, for the two-opening case, it was likely that all the airborne fission products would be convected into the containment.

For the BWR cases, the temperature in the drywell affects the amount of heat rejected from the RPV. For the case in which the drywell temperature is high (and thus temperature gradient between the RPV and the drywell is small), the expert felt that the amount of energy rejected from the RPV would be small, and therefore, the RPV would stay hot. A high RPV temperature favors a relatively large amount of revolatilization. For the low drywell temperature case, a relatively large amount of heat would be rejected from the RPV, and therefore, the amount of revolatilization would be less than for the high drywell case.

The effect on revolatilization of two openings in a PWR and a high drywell temperature for the BWR would be similar. Similarly, the effect on revolatilization of one hole in a PWR would be similar to a low drywell temperature in a BWR. Therefore, the expert combined Cases 2 and 3 and Cases 1 and 4.

Expert D considered two groups of radionuclides. He grouped cesium, iodine, and tellurium into one group and nonvolatiles into a second group. The expert thought it was unlikely that the nonvolatiles would be released before vessel breach, and therefore, they would be unavailable for revolatilization after vessel breach. There is thus no revolatilization of the nonvolatiles. From here on, any reference to fission products, unless specifically stated, will refer to the first group (i.e., cesium, iodine, tellurium).

Expert D felt that revolatilization was based on the heat rejection capabilities of the RCS/RPV. Based on a heat rejection model, he expressed the revolatilizat on as:

$REVOL = (F_{DV} - F_{HL})/F_{DV}$,

where

F_{DV} = fraction of cesium, iodine, and tellurium inventory deposited in the RCS/RPV prior to vessel breach,

F_{HL} = ratio of cesium, iodine, and tellurium inventory decay heat to RCS/RPV heat losses.

This simple model was used to estimate the amount of revolatilization expected for different values of F_{DV} and F_{HL}. Based on this model, if the heat rejection capabilities are greater than the decay heat, there will be no revolatilization of fission products. To use his model, the heat rejection capabilities of the RCS/RPV and the amount of decay heat associated with the fission products were estimated. Based on RMA analysis of the TMLB accident sequence for Surry,* the heat rejection capabilities of the RCS/RPV could be as high as 3.5 MW_t. In the analysis, two levels of heat rejection were considered: 3.5 MW_t and 2 MW_t. A heat rejection level of 2 MW_t was thought to be a conservative. To estimate the level of decay heat, the expert reviewed References D-1 and D-2 to obtain a representative time of vessel failure. From these references, the vessel failure time for 38 accident sequences (six plants) were obtained. For 26 of these 38 sequences, vessel failure occurred between 2 and 5 h. Vessel failure before 2 h occurred in only two sequences. Therefore, to be conservative, a decay heat level was used that corresponded to 2 h after vessel breach. The values for decay heat were obtained from ORIGEN2 calculations performed for Surry.** From these calculations, the amounts of beta and gamma energy being released were obtained. Two levels of decay heat were considered. The first level corresponded to 100% beta and 25% gamma energy being deposited in the RCS/RPV. The expert felt that the large mass of the RCS/RPV would absorb 75% of the gamma heating. The second level corresponded to 100% of both beta and gamma energy deposited in the RCS/RPV. Four combinations were analyzed:

1. High heat rejection with low gamma heating;
2. Low heat rejection with low gamma heating;
3. High heat rejection with high gamma heating;
4. Low heat rejeccion with high gamma heating.

The results for these combinations are presented in Table D-1. Based on the expert's model, there will be no revolatilization for combination 1. The heat rejection capabilities of the RCS/RPV are sufficient to offset the decay heat of the fission products. Futhermore, combination 4 was thought extremely unrealistic because it contained both a low value for heat

---

* Andrzej Drozd, Stone & Webster Engineering Corporation, to Peter Bieniarz, RMA, Personal Communication, RMA Analysis of TMLB Accident for Surry Plant.

** Stone & Webster Engineering Corporation Calculation: 5220236-UR(B)-006-0. Relevant excerpts from this proprietary document are included in Part 5 of this volume.

rejection and a high value for gamma heating. It was the expert's opinion that the most probable range for FLATE was from 0 to 0.3 with a heavy bias towards the low end of the range.

Table D-1
Estimation of Revolatilization Base on an
RCS/RPV Heat Rejection Model
β = 1.54 MW, γ = 4.70 MW

Decay Heat (MW)	Heat Rejection (MW)	Revolatilization (FLATE)
2.70	3.5	0.0 for all F_{DV}
2.70	2.0	0.0 if $F_{DV} < 0.7$ 0.06 if $F_{DV} = 0.8$
6.24	3.5	0.0 if $F_{DV} < 0.55$ 0.3 if $F_{DV} = 0.8$
6.24	2.0	0.2 if $F_{DV} = 0.4$ 0.6 if $F_{DV} = 0.8$

Results of Expert D's Elicitation

The range for FLATE and the corresponding probabilities are presented in Table D-2.

Table D-2
Amount of Revolatilization (FLATE)

Case 1 (PWR) Case 4 (BWR)		Case 2 (PWR) Case 3 (BWR)	
FLATE	Cumulative Probability	FLATE	Cumulative Probability
0.00	0.50	0.00	0.50
0.15	0.85	0.15	0.85
0.25	1.00	0.30	1.00

Sources of Uncertainty

Expert D felt that the major source of uncertainty was the rather coarsely defined initial conditions. The uncertainties of the phenomenology were small compared to that of the initial conditions.

Correlations with Other Variables

Expert D indicated that FLATE is correlated with the fraction of cesium, iodine, and tellurium inventory deposited in the RCS/RPV before vessel breach. In the terminology of XSOR, this corresponds to roughly (1-FVES)*FCOR.

REFERENCES

D-1 J. A. Gieseke et al., "Radionuclide Release Under Specific LWR Accident Conditions," Vols. I-V, BMI-2104, Battelle Memorial Institute, 1984.

D-2 R. S. Denning et al., "Radionuclide Release Calculations for Selected Severe Accident Scenarios," Vols. I-V, NUREG/CR-4624, BMI-2139, Battelle Memorial Institute, 1986.

5.4 Issue 4. Fraction of Fission Products Released During the Core-Concrete Interactions

Summary and Aggregation of Source Term Issue 4: FCCI

Experts Consulted: Peter Bieniarz, Risk Management Associates; Robert Henry, Fauske and Associates; Richard Vogel, Electric Power Research Institute; David Williams, Sandia National Laboratories.

Issue Description

The experts were asked what distributions characterize the uncertainty in the release of fission products from the molten fuel to the containment during the core-concrete interaction (CCI).

$FCCI_i$ represents the fraction of radionuclide group i in the core debris at the time of vessel failure that is released to the containment during the CCI. The nine radionuclide groups are:

1. Noble or Inert Gases (xenon, krypton)
2. Halogens (iodine, bromine)
3. Alkali Metals (cesium, rubidium)
4. Tellurium Group (tellurium, selenium, antimony)
5. Barium (barium)
6. Strontium (strontium)
7. Noble Metals (rubidium, molybdenum, palladium, rhodium, technetium)
8. Lanthanides (lanthanum, neodymium, niobium, europium, yttrium, prasecodymium, promethium, samarium, zirconium)
9. Cerium Group (cerium, neptunium, plutonium)

A distribution is required for each radionuclide group for each case described below. The fraction of the core participating in CCI will be accounted for in the accident progression event tree. The fraction of the core participating in direct containment heating or ex-vessel steam explosions is assumed to be unavailable to participate in CCI.

Releases of the fission products from the containment and removal from the containment atmosphere by natural processes (e.g., agglomeration) and engineered processes (e.g., sprays) will be accounted for elsewhere in the source term calculation and are not considered in this issue. In particular, fission product removal by a water pool overlying the core during CCI is not to be considered in determining FCCI. FCCI should represent the release from the top surface of the core debris. Retention in the pool will be calculated separately.

Of the five plants being considered in this study, only Surry has siliceous or basaltic concrete. Sequoyah, Zion, Peach Bottom, and Grand Gulf are believed to have limestone/common sand concrete, i.e., the coarse aggregate in the concrete is limestone and the fine aggregate is common sand.

The experts were asked to consider combinations of the following initital conditions:

1. **PWRs**. High and low zirconium content in the debris, the presence of water, and the type of concrete at the plant (Surry, siliceous; Zion, limestone/common sand; Sequoyah, limestone).

2. **BWRs**. High and low zirconium content in the debris, the presence of water, the spread area, and the type of concrete (believed to be limestone/common sand for both BWRs).

Summary of Experts' Rationale

Expert A's results represent the work of two experts who collaborated. Each expert considered different aspects of the issue: one generated activity coefficients, and the other used these activity coefficients to generate the required release fractions.

Expert A's activity coefficient distributions were based on the distribution for activity coefficients predominantly on experiments done by Carl Alexander at Battelle Memorial Institute. This information was augmented by CORCON-MCD2/VANESA results and work from small-scale laboratory studies by Mike Roche at Argonne National Laboratory.

The other expert used Zion MAAP calculations to formulate Expert A's release fractions. He made no differentiation between the high and low pressure cases and the high and low zirconium cases. For the wet cases, it was assumed that the debris was eventually quenched, so that the CCI releases were assumed to occur during a quenching interval (5000 s for the nondispersed case.)

Expert B based his results on a variety of sources: the BNL Quasar study, a paper presented to the panel by Dave Williams (SNL), a summary article by Brad Burson of the Nuclear Regulatory Commission (NRC), and CORCON results (see individual elicitation notes for references). The expert did not distinguish between prompt and delayed CCI. Water in the cavity was assumed to rapidly oxidize the zirconium in the debris resulting in low levels of zirconium available for CCI in the wet cavity cases.

Expert C created a base distribution from the results of code calculations (predominantly Source Term Code Package Calculations from BMI-2104, BMI-2139, and BMI-2160). He then modified the distributions to account for uncertainties not considered in the code calculations. He accounted for mechanical aerosol release from CCI by considering the old VANESA bubble burst model, observations of SNL's WITCH experiments, and observations from the steel industry's carbon boil experience.

Method of Aggregation

Simple interpolation was performed on the results of Experts A and B to aggregate results with Expert C. In addition, several modifications and assumptions were made to aggregate the results of Expert B: PWR

Limestone/Common Sand Concrete results were used for both Sequoyah and Zion; the PWR Basaltic Concrete results were used for Surry; the BWR Limestone Concrete results were used for the BWRs, although the BWRs are thought to have limestone/common sand; high zirconium cases were used for both wet and dry cavity high zirconium cases; low zirconium cases were used for both wet and dry cavity low zirconium cases; all cesium and iodine are assumed to come out; and an insignificant fraction of the molybdenum and ruthenium is assumed to come out.

All of the operations to perform the aggregation were approved by the experts.

Aggregated Results

The results of the aggregation are presented in Figures 4-1 to 4-20.

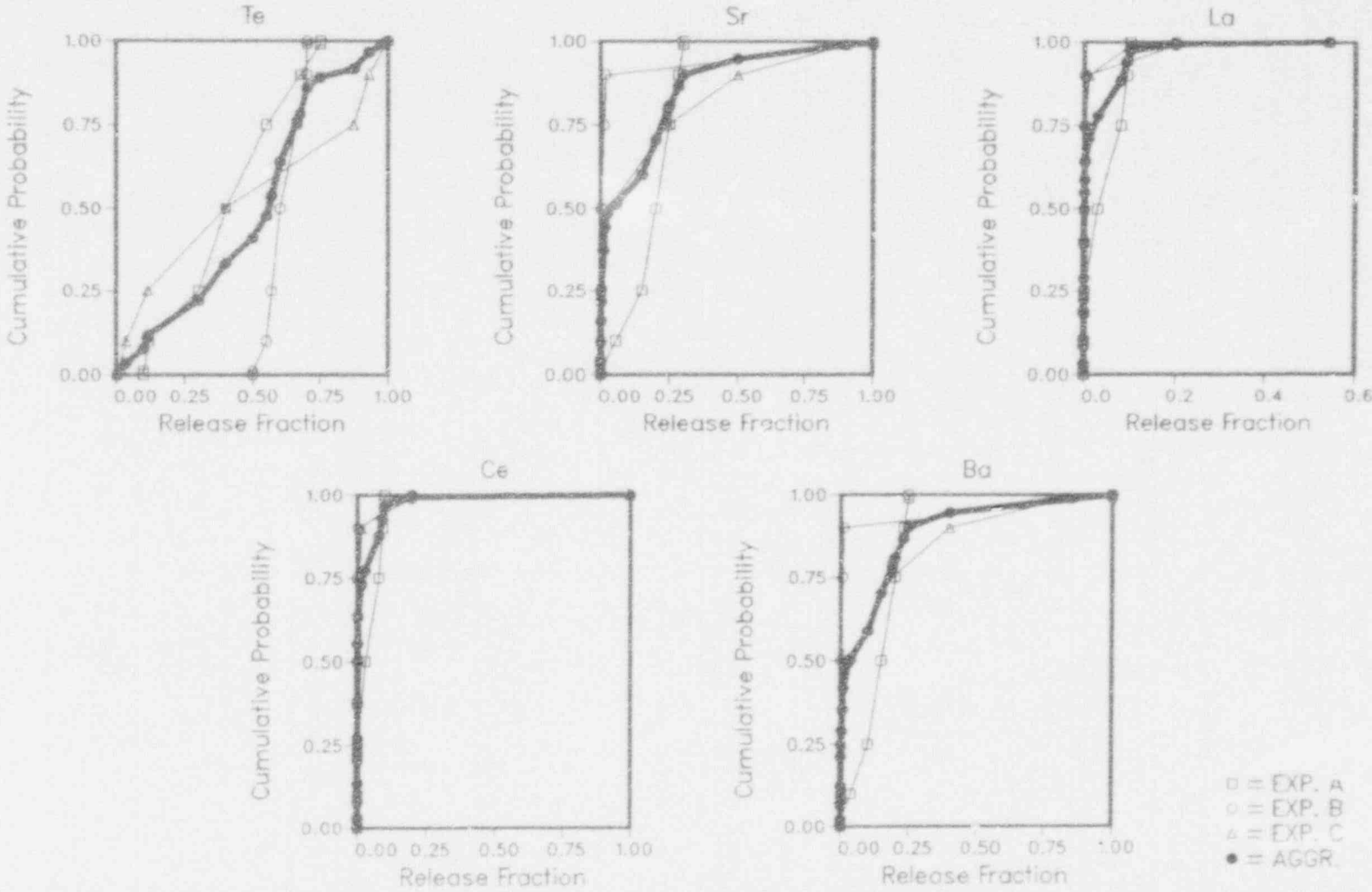

Figure 4-1. FCCI, Case 1, Zion, Dry Cavity, High Zirconium.

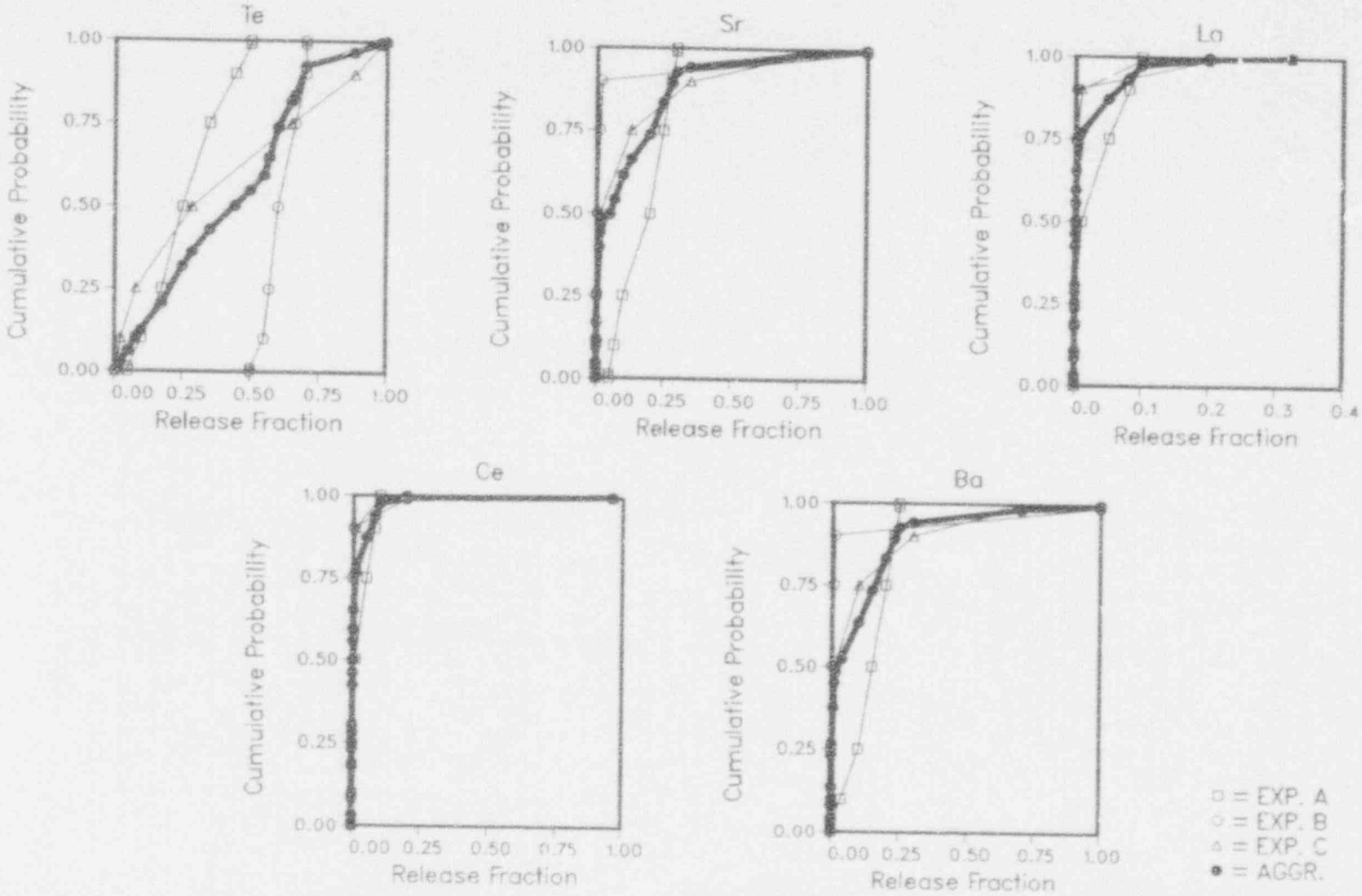

Figure 4-2. FCCI, Case 2, Zion, Dry Cavity, Low Zirconium.

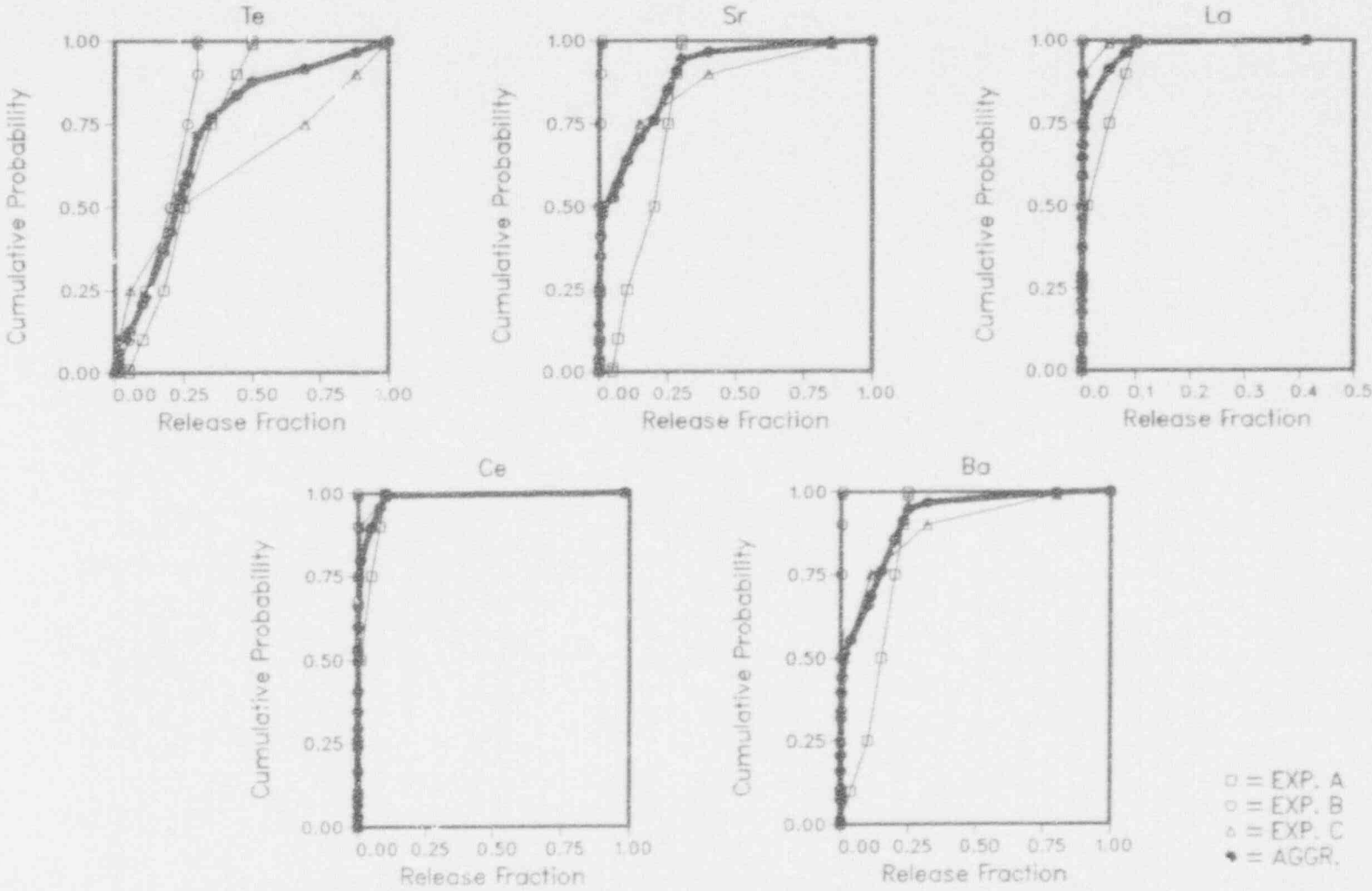

Figure 4-3. FCCI, Case 3, Zion, Wet Cavity, High Zirconium.

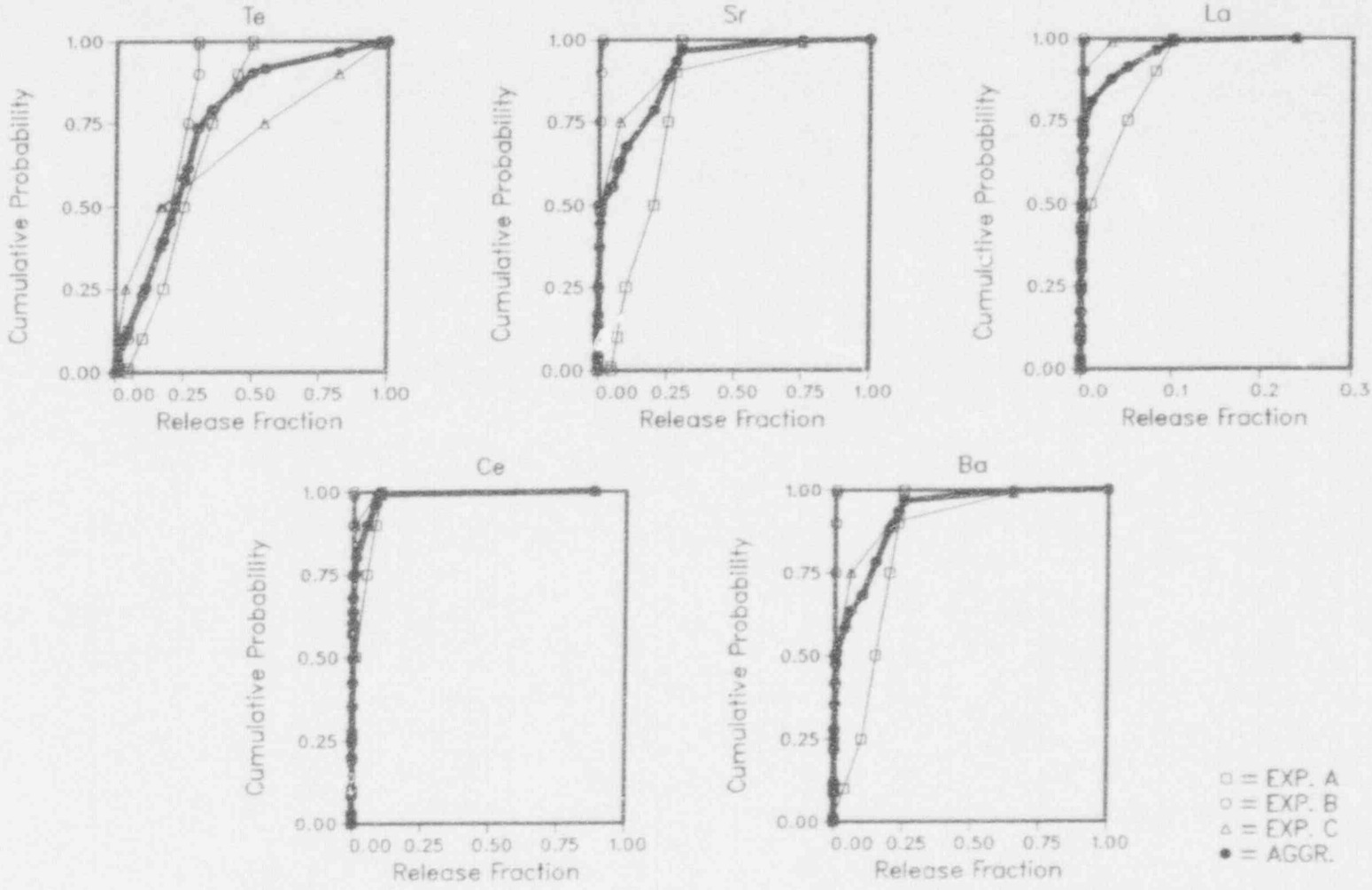

Figure 4-4. FCCI, Case 4, Zion, Wet Cavity, Low Zirconium.

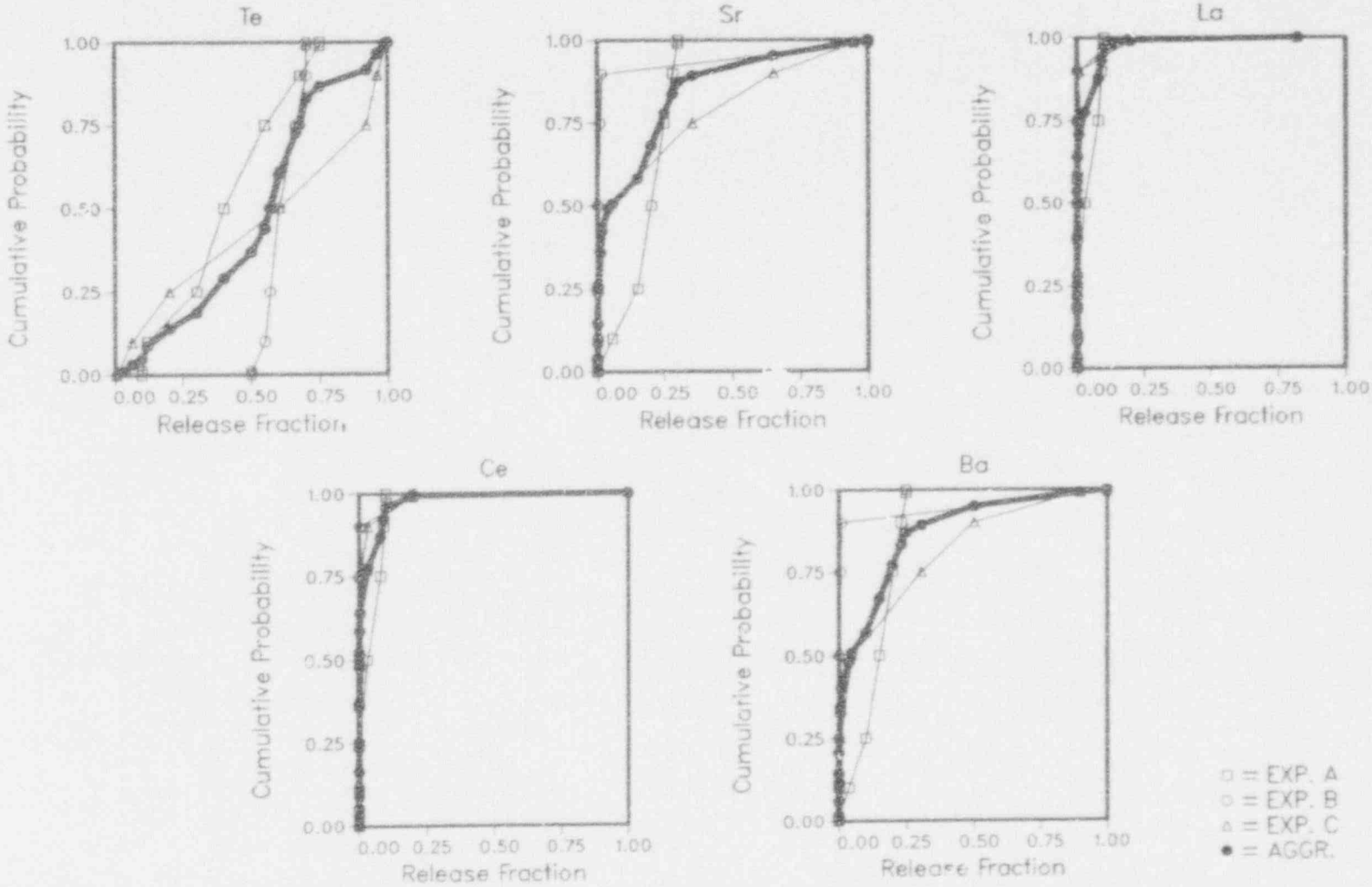

Figure 4-5. FCCI, Case 5, Sequoyah, Dry Cavity, High Zirconium.

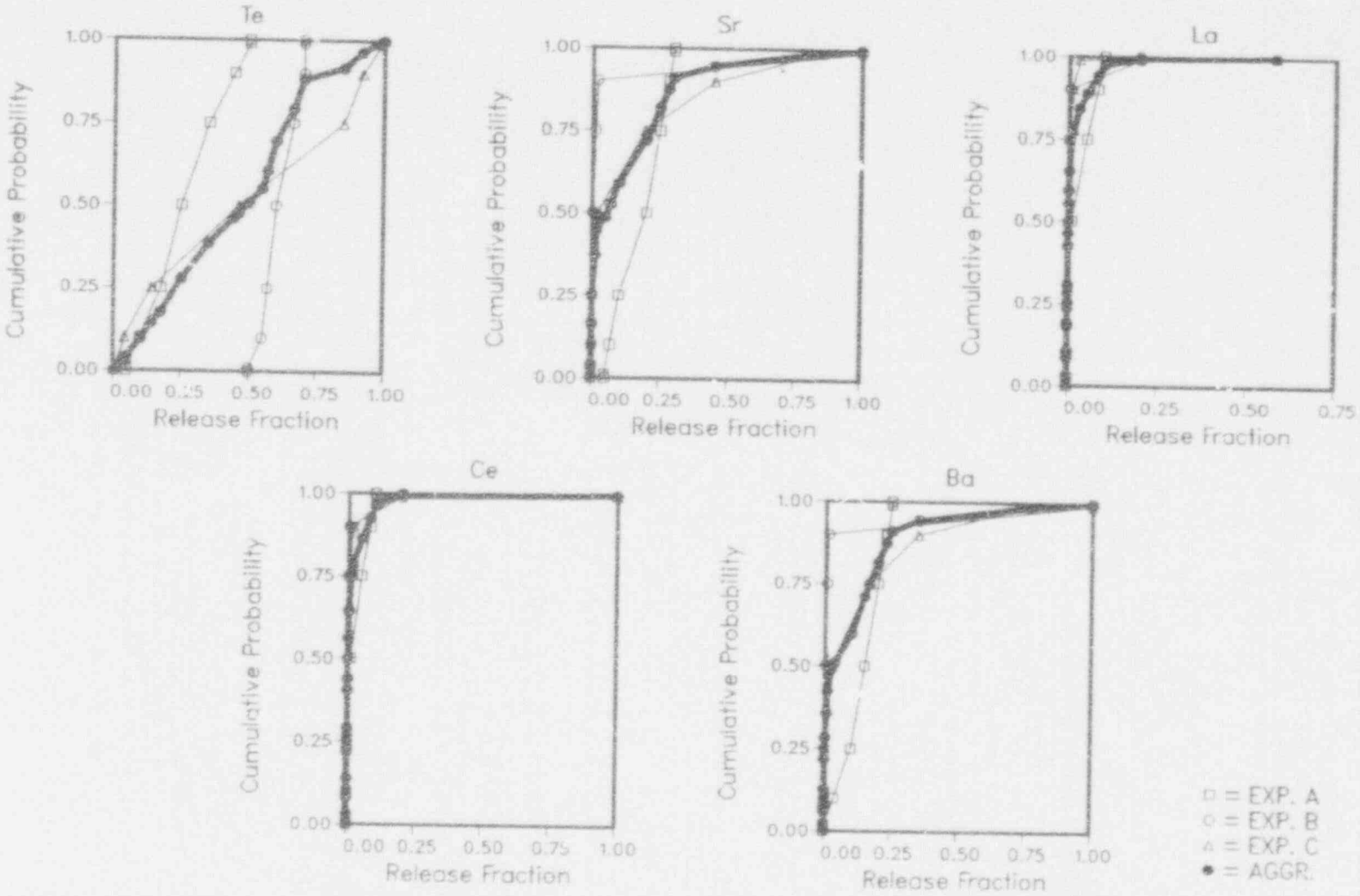

Figure 4-6. FCCI, Case 6, Sequoyah, Dry Cavity, Low Zirconium.

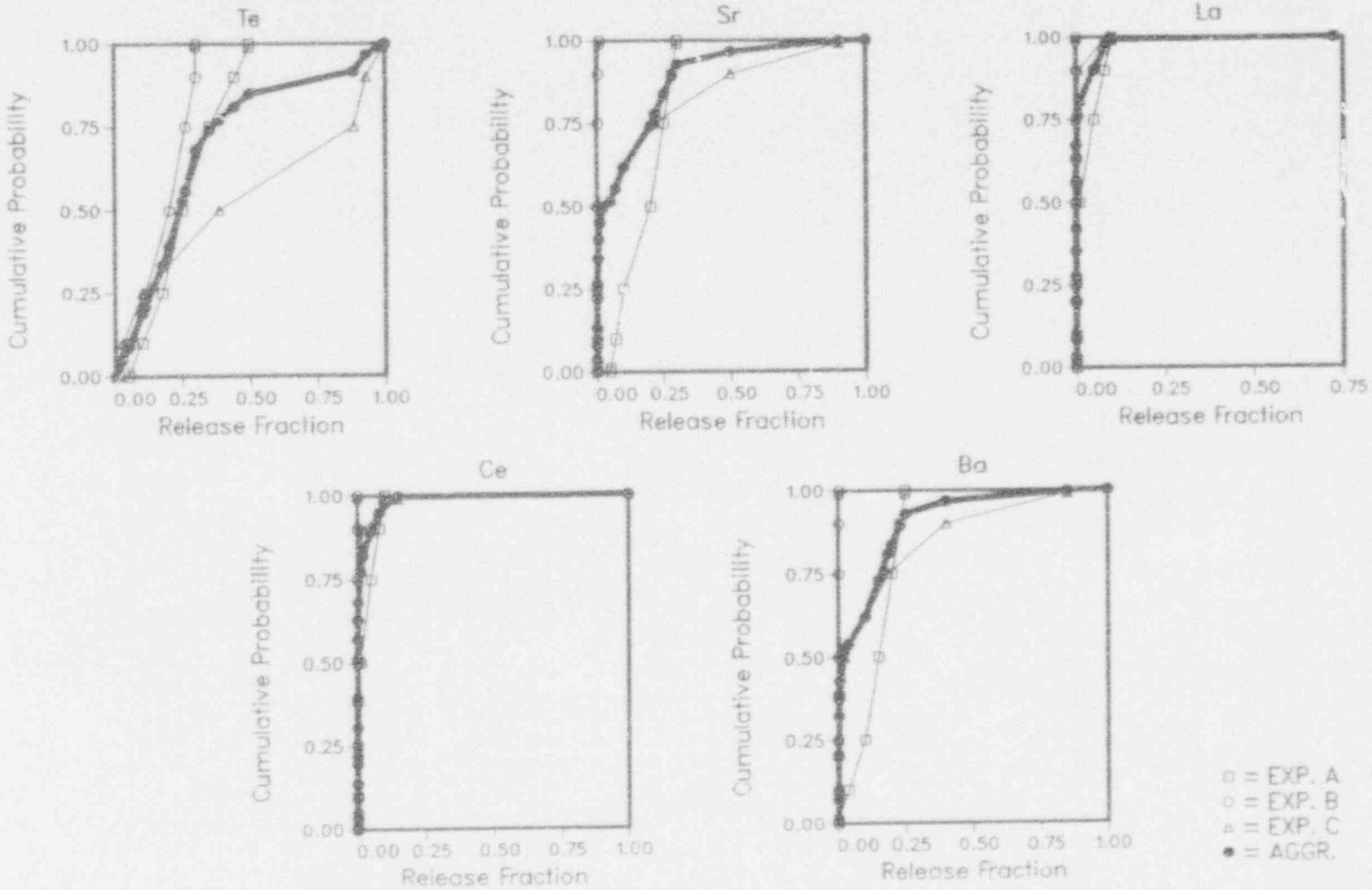

Figure 4-7. FCCI, Case 7, Sequoyah, Wet Cavity, High Zirconium.

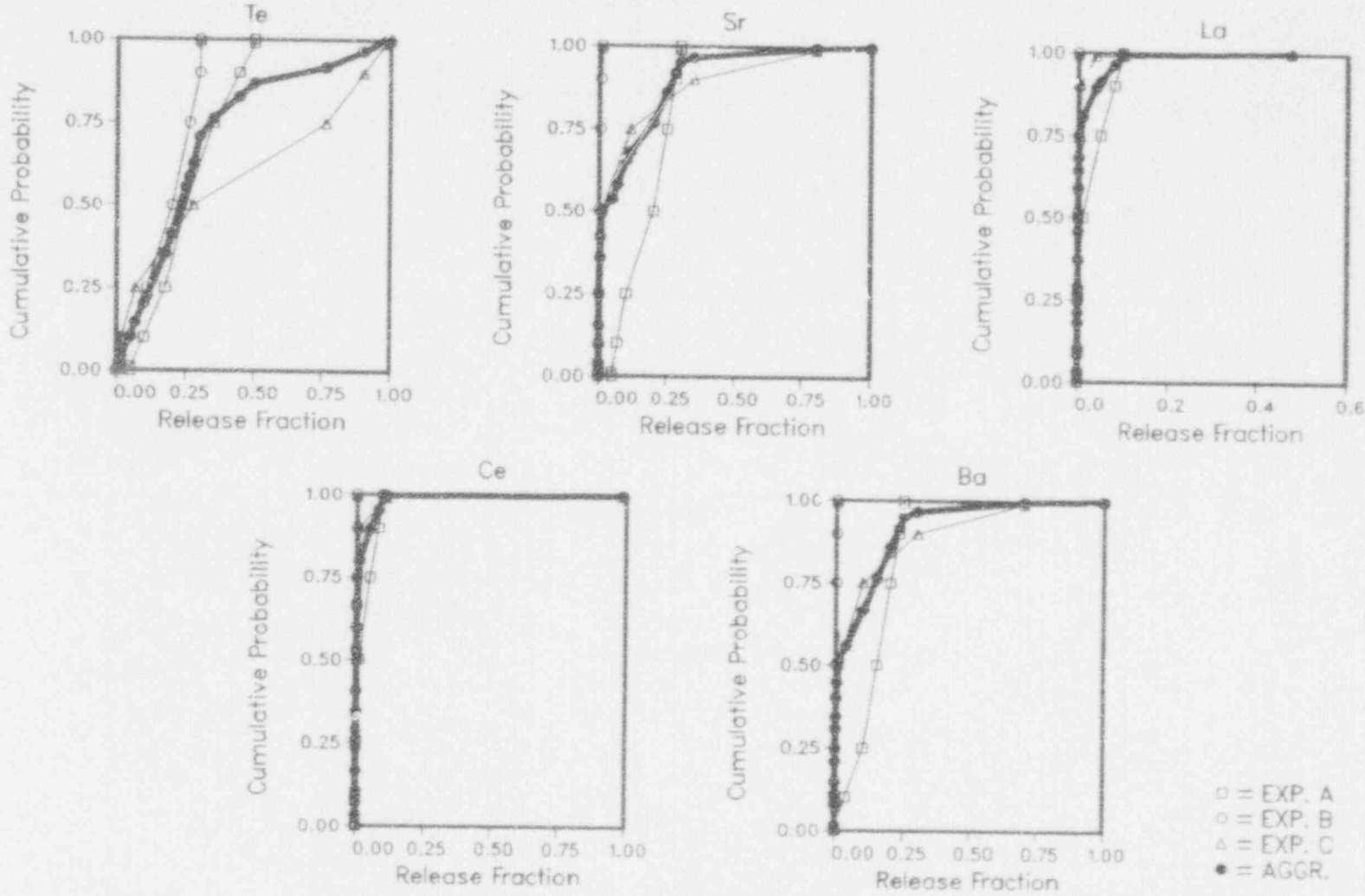

Figure 4-8. FCCI, Case 8, Sequoyah, Wet Cavity, Low Zirconium.

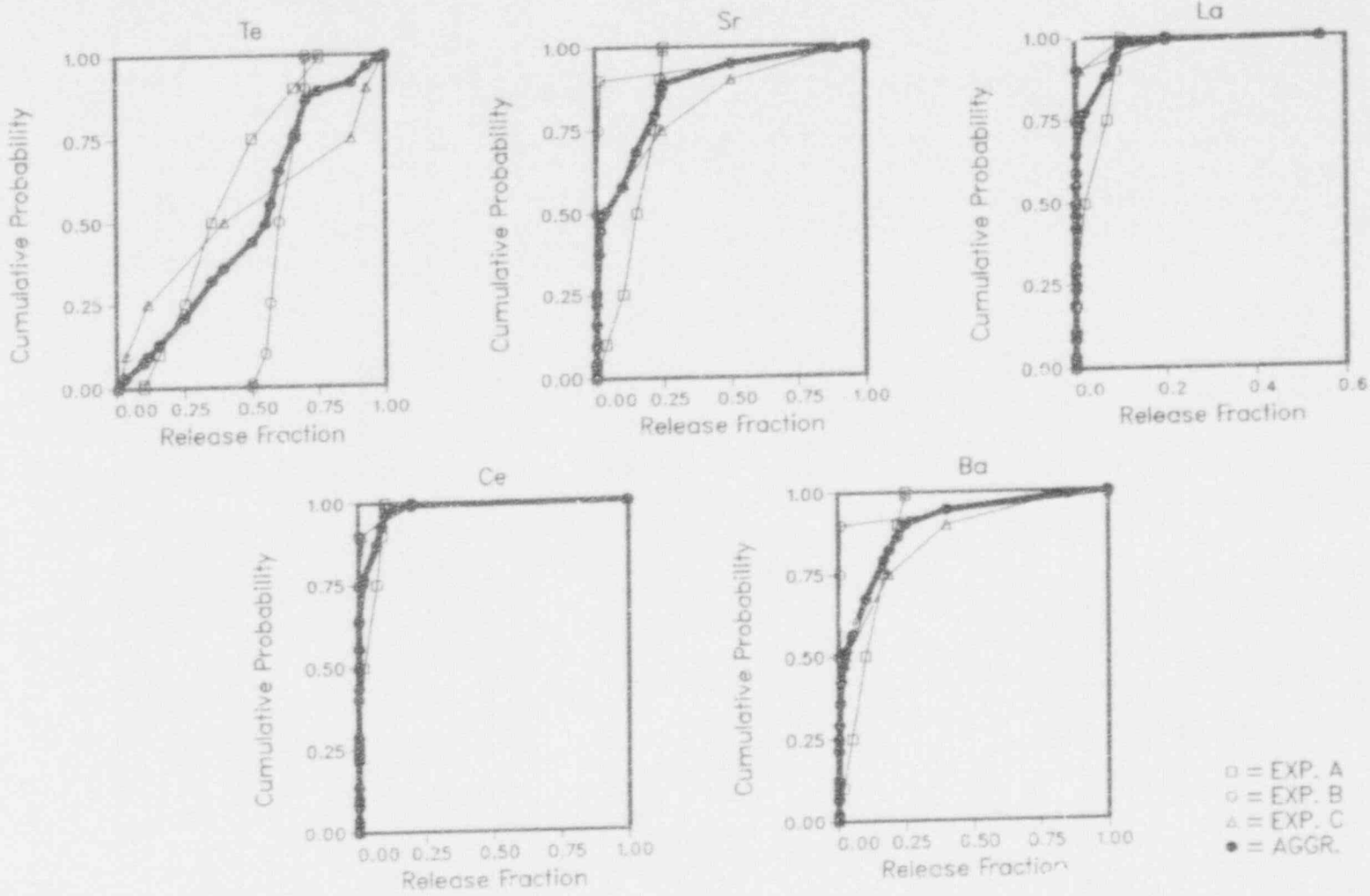

Figure 4-9. FCCI, Case 9, Surry, Dry Cavity, High Zirconium.

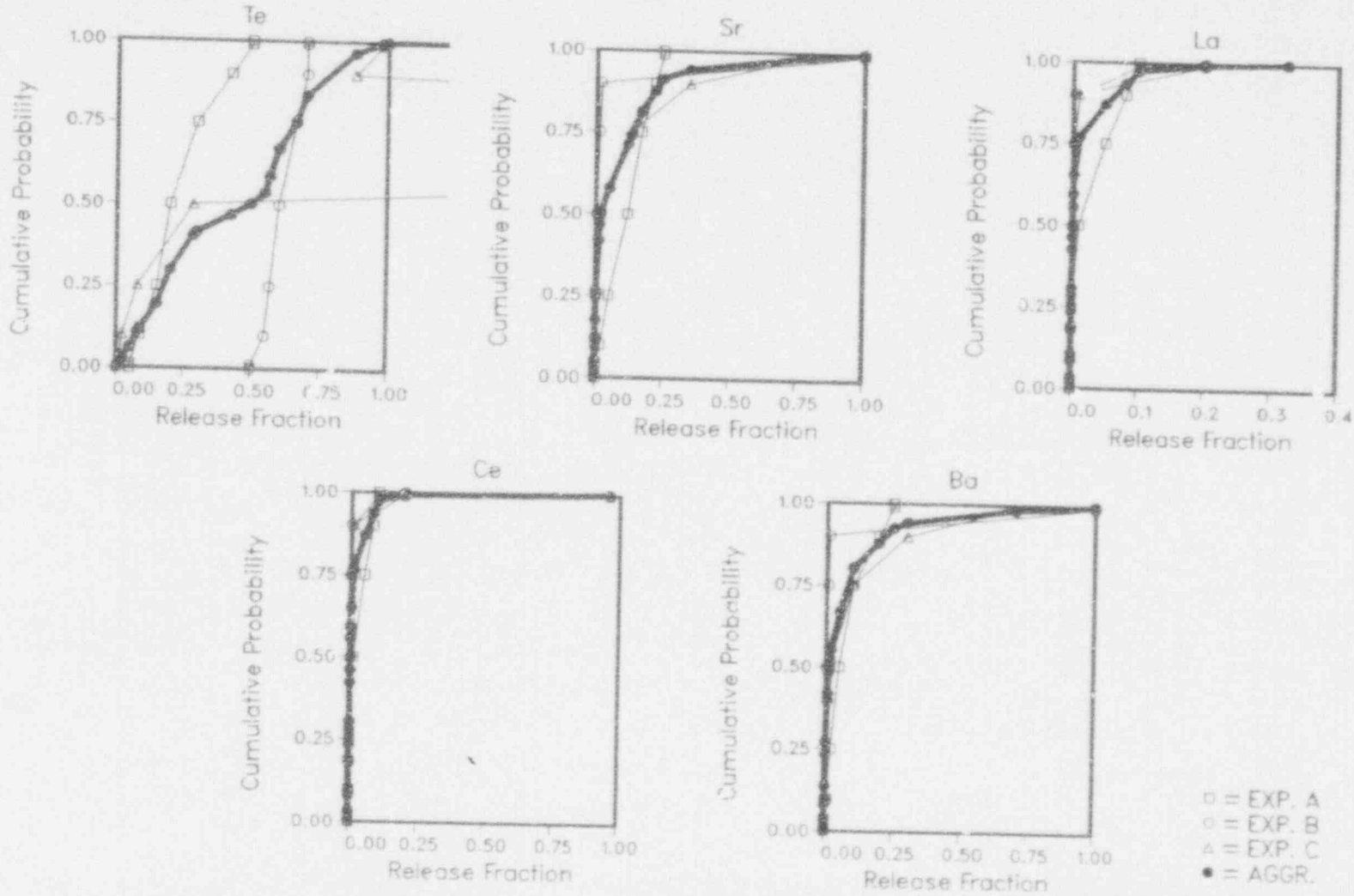

Figure 4-10. FCCI, Case 10, Surry, Dry Cavity, Low Zirconium.

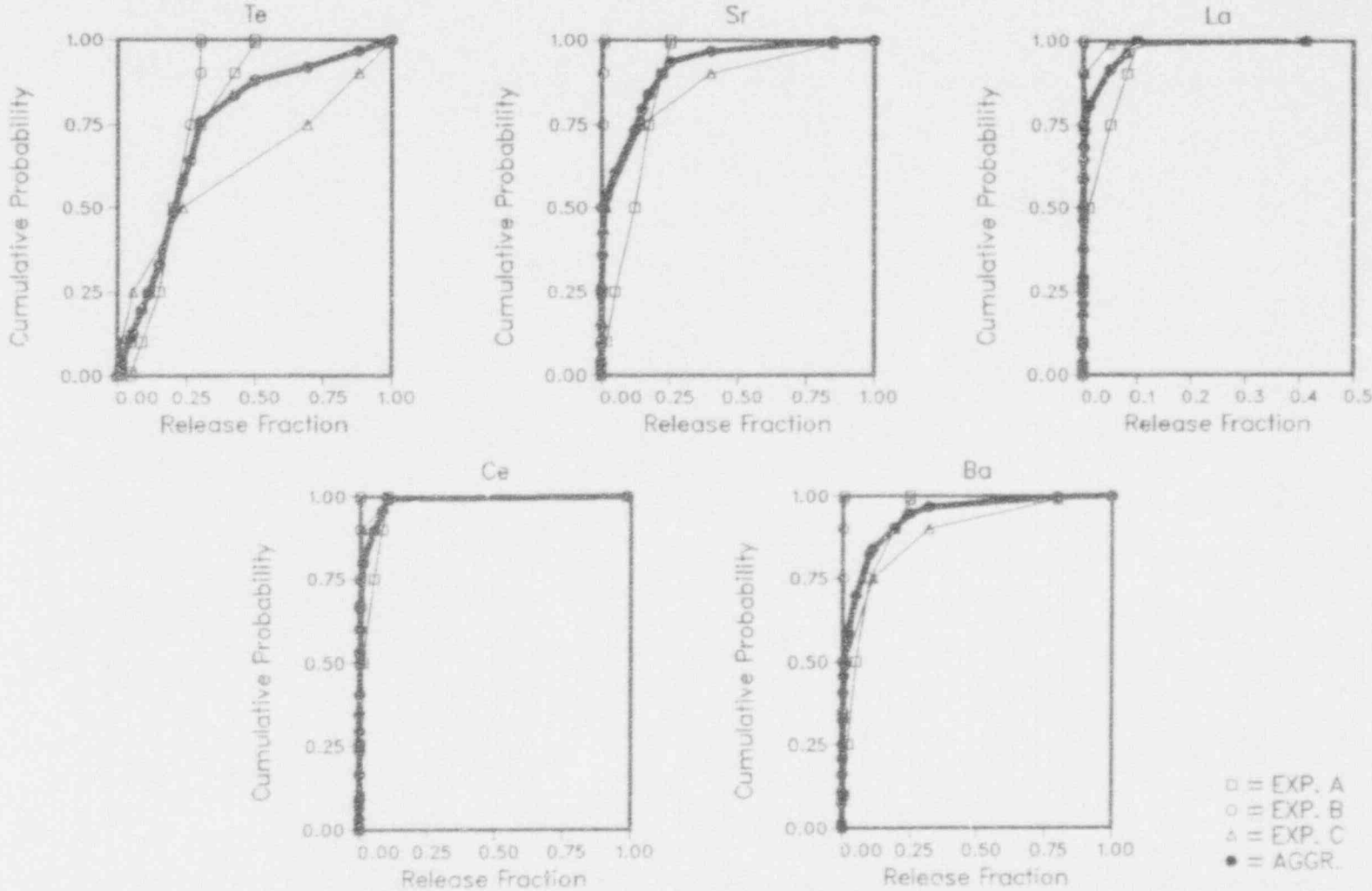

Figure 4-11. FCCI, Case 11, Surry, Wet Cavity, High Zirconium.

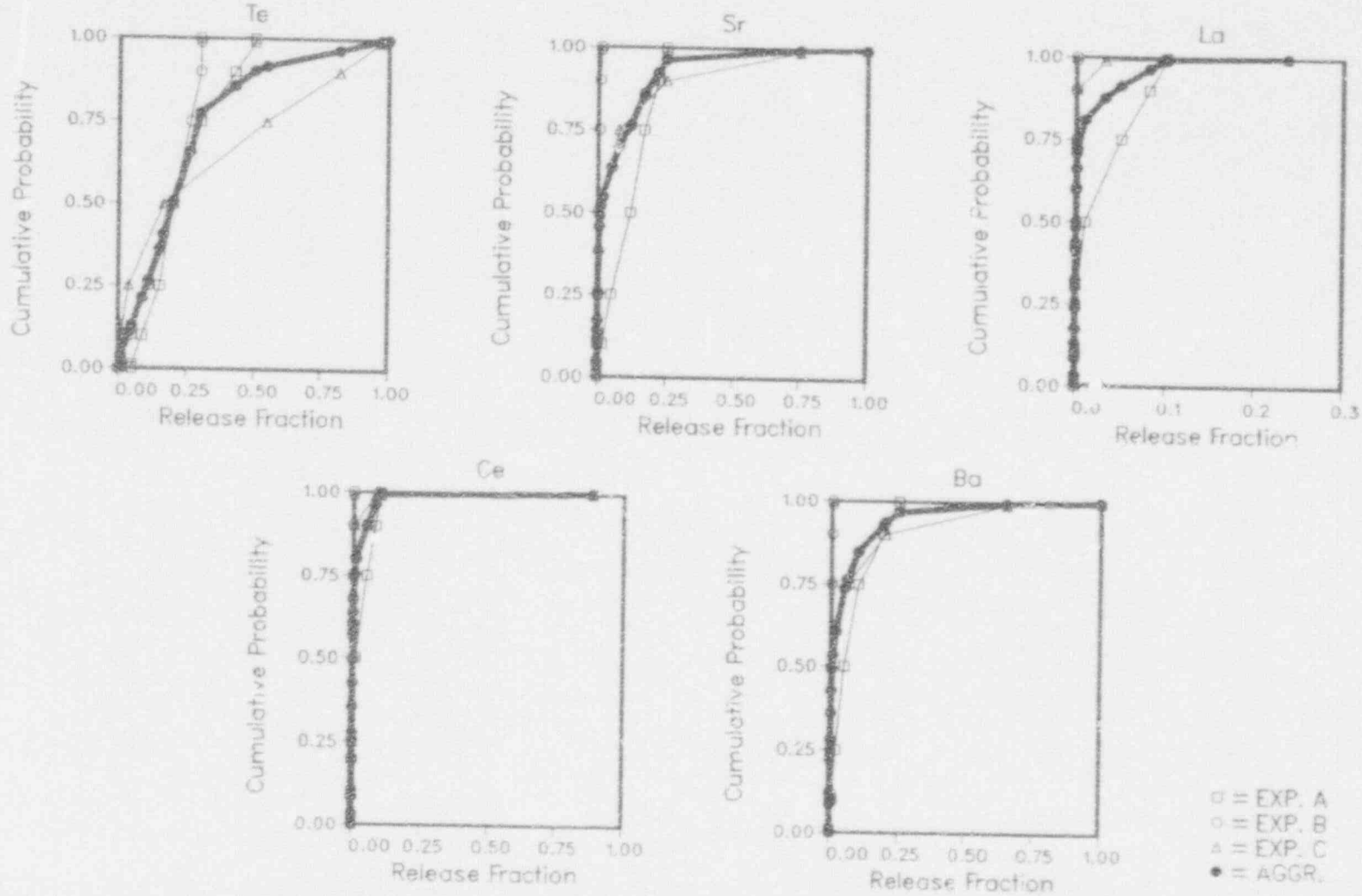

Figure 4-12. FCCI, Case 12, Surry, Wet Cavity, Low Zirconium.

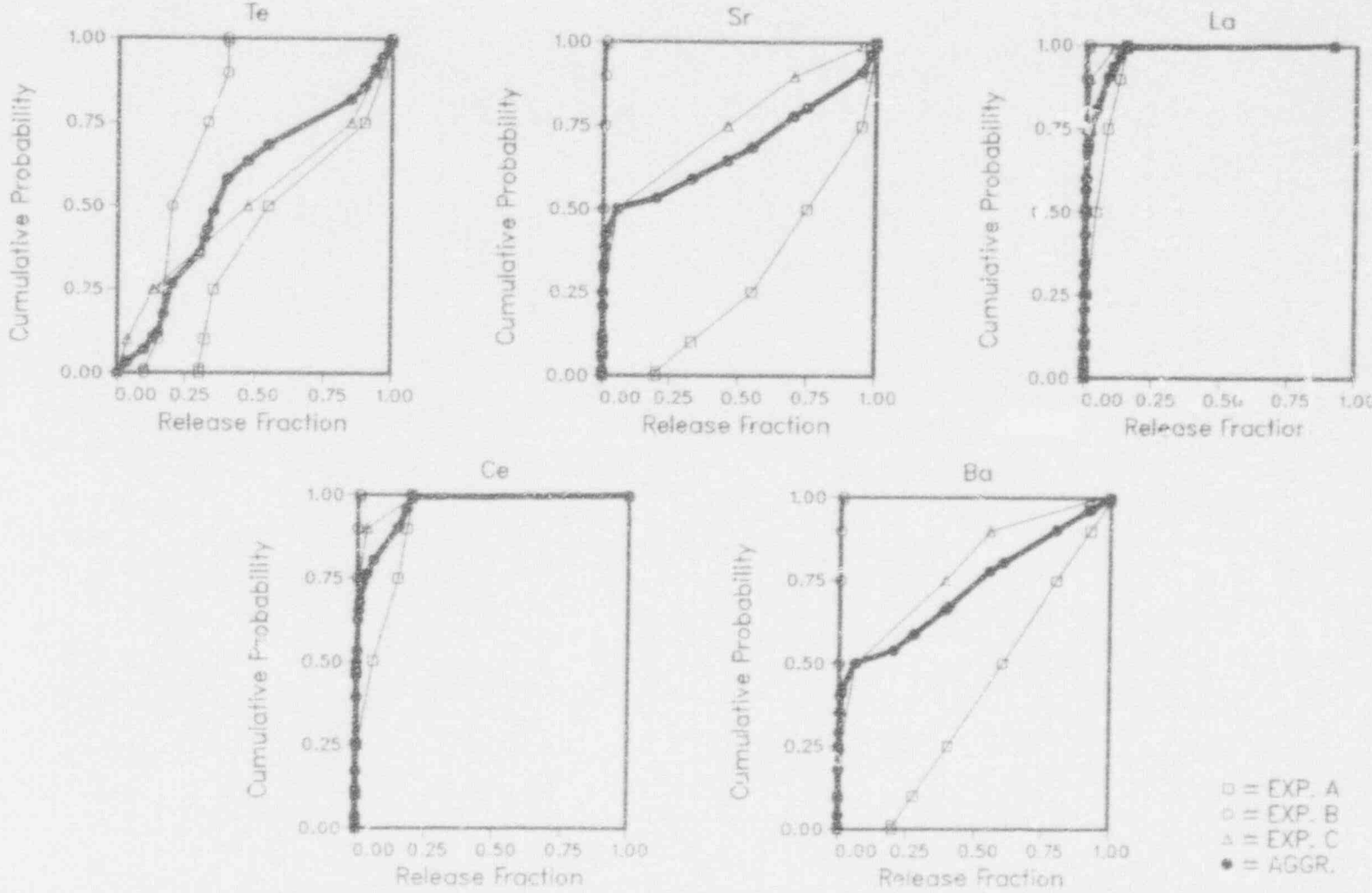

Figure 4-13. FCCI, Case 13, Peach Bottom, Dry Cavity, High Zirconium.

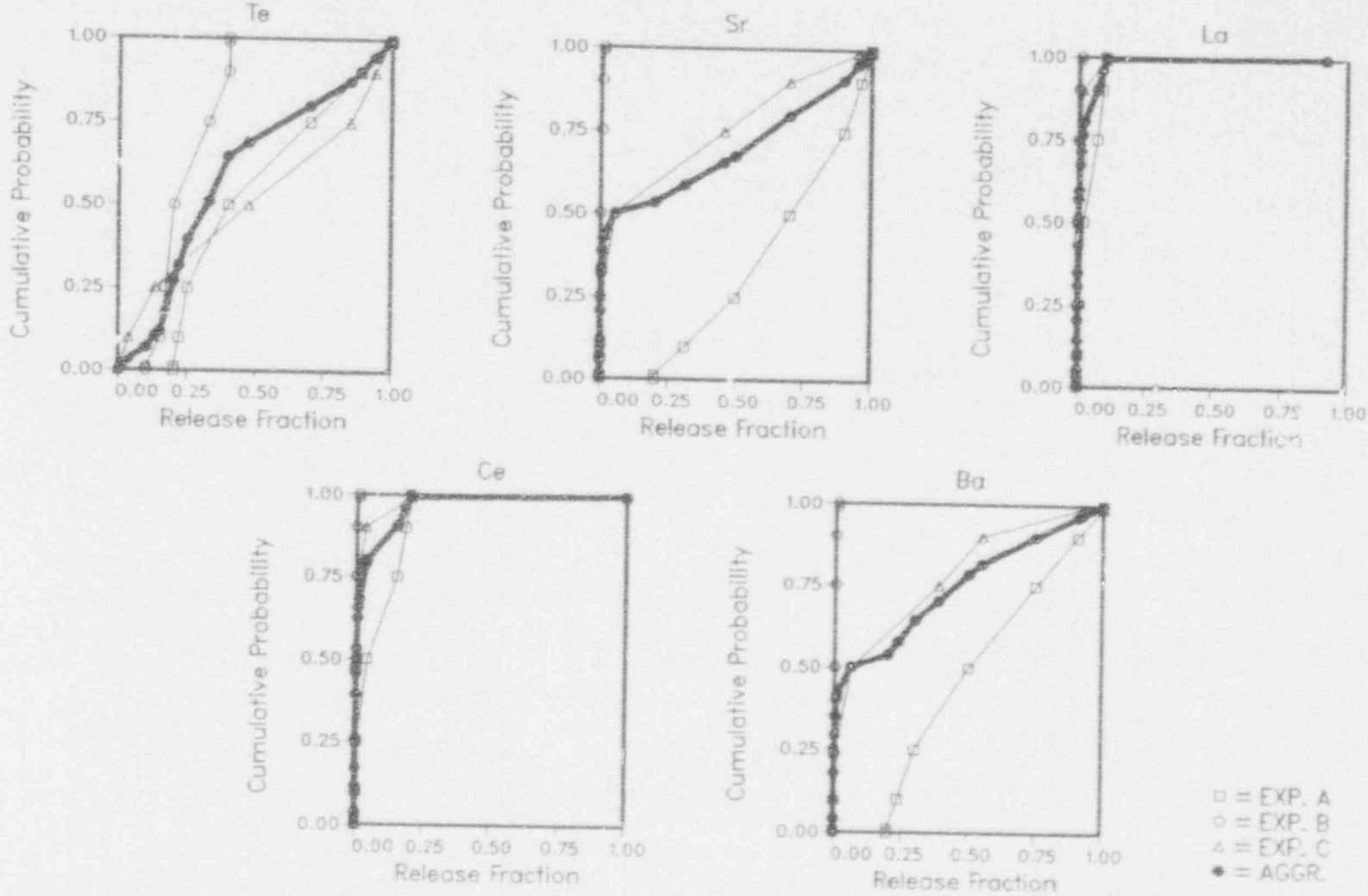

Figure 4-14. FCCI, Case 14, Peach Bottom, Dry Cavity, Low Zirconium.

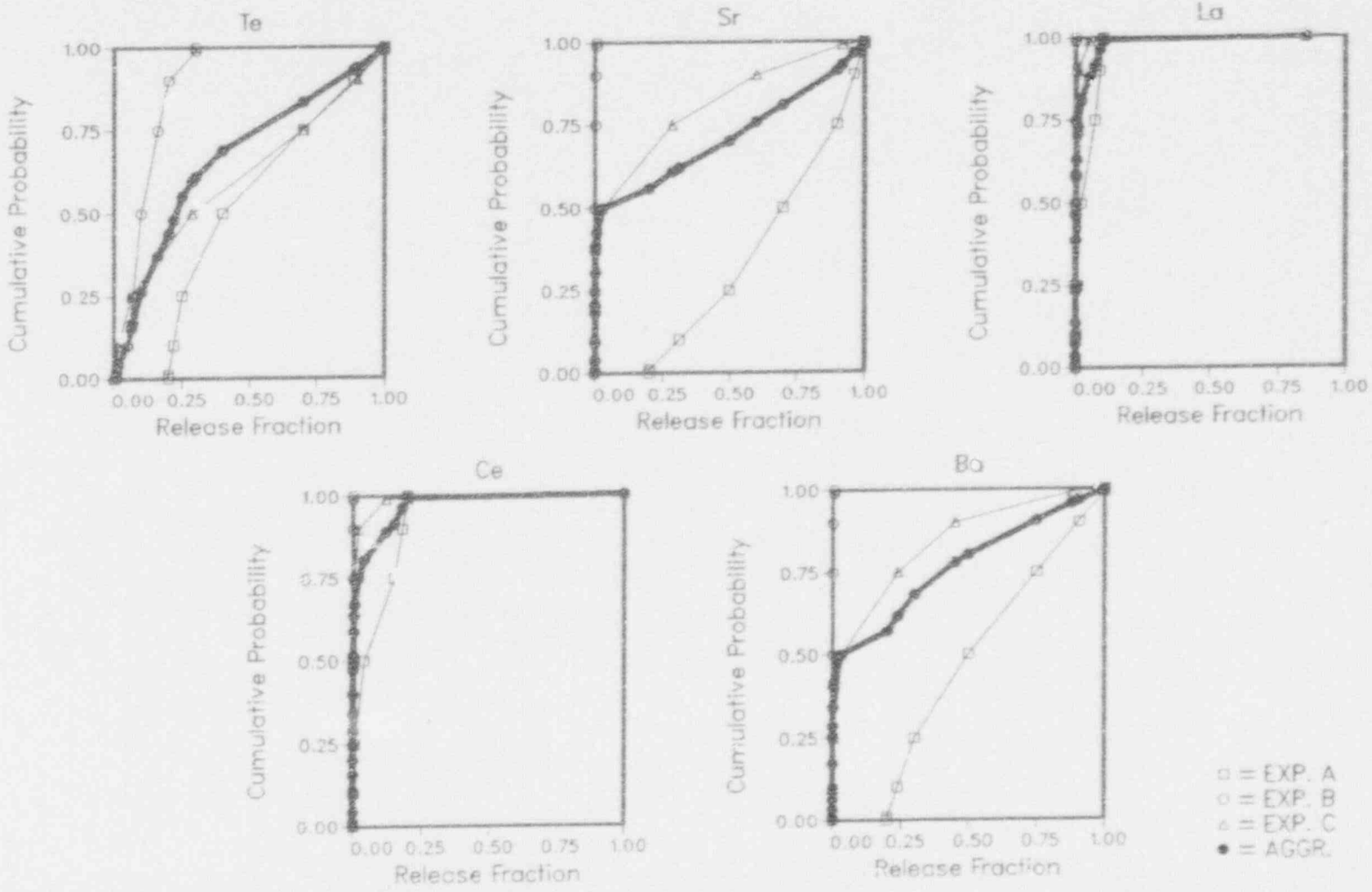

Figure 4-15. FCCI, Case 15, Peach Bottom, Wet Cavity, High Zirconium.

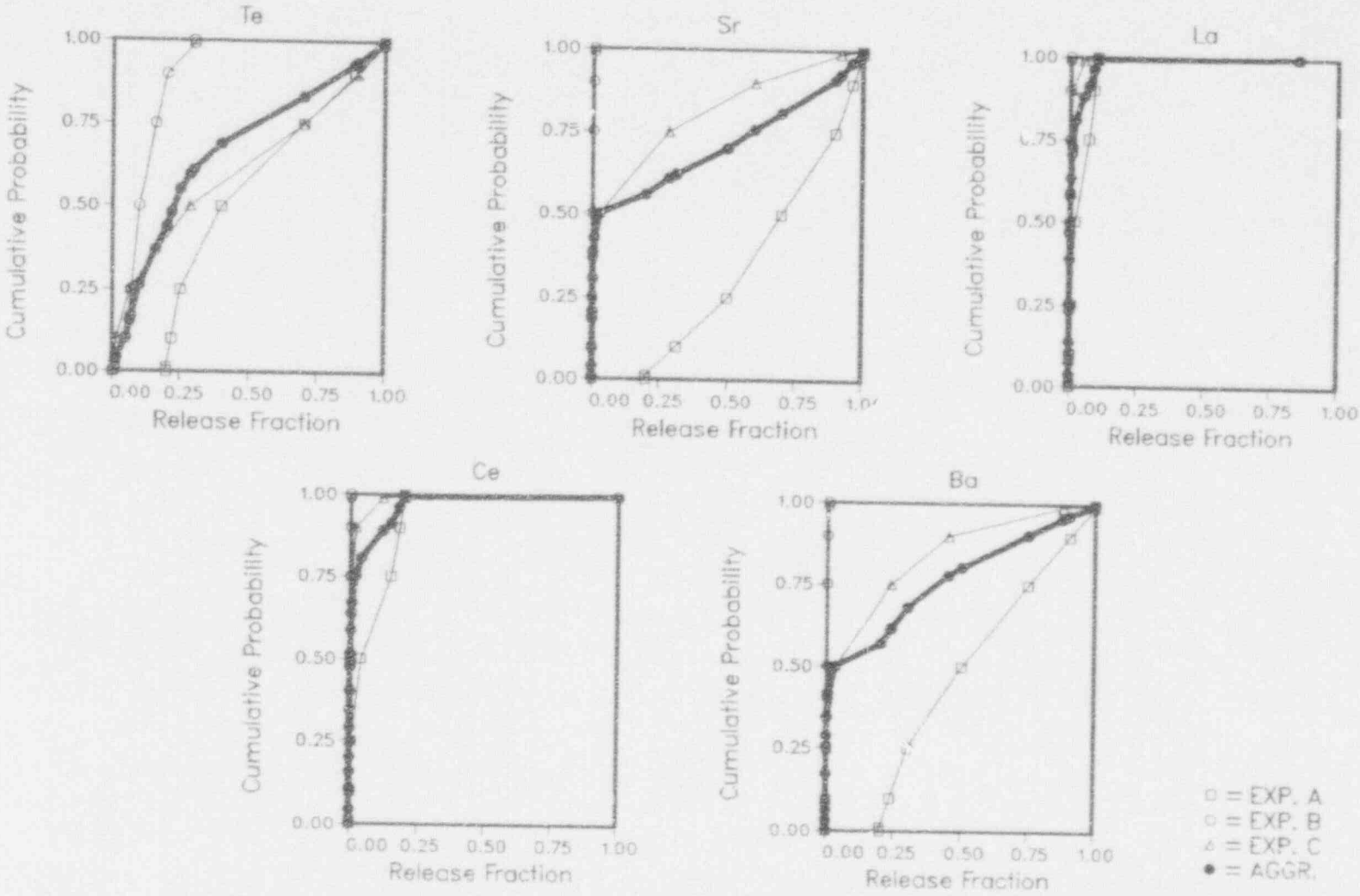

Figure 4-16. FCCI, Case 16, Peach Bottom, Wet Cavity, Low Zirconium.

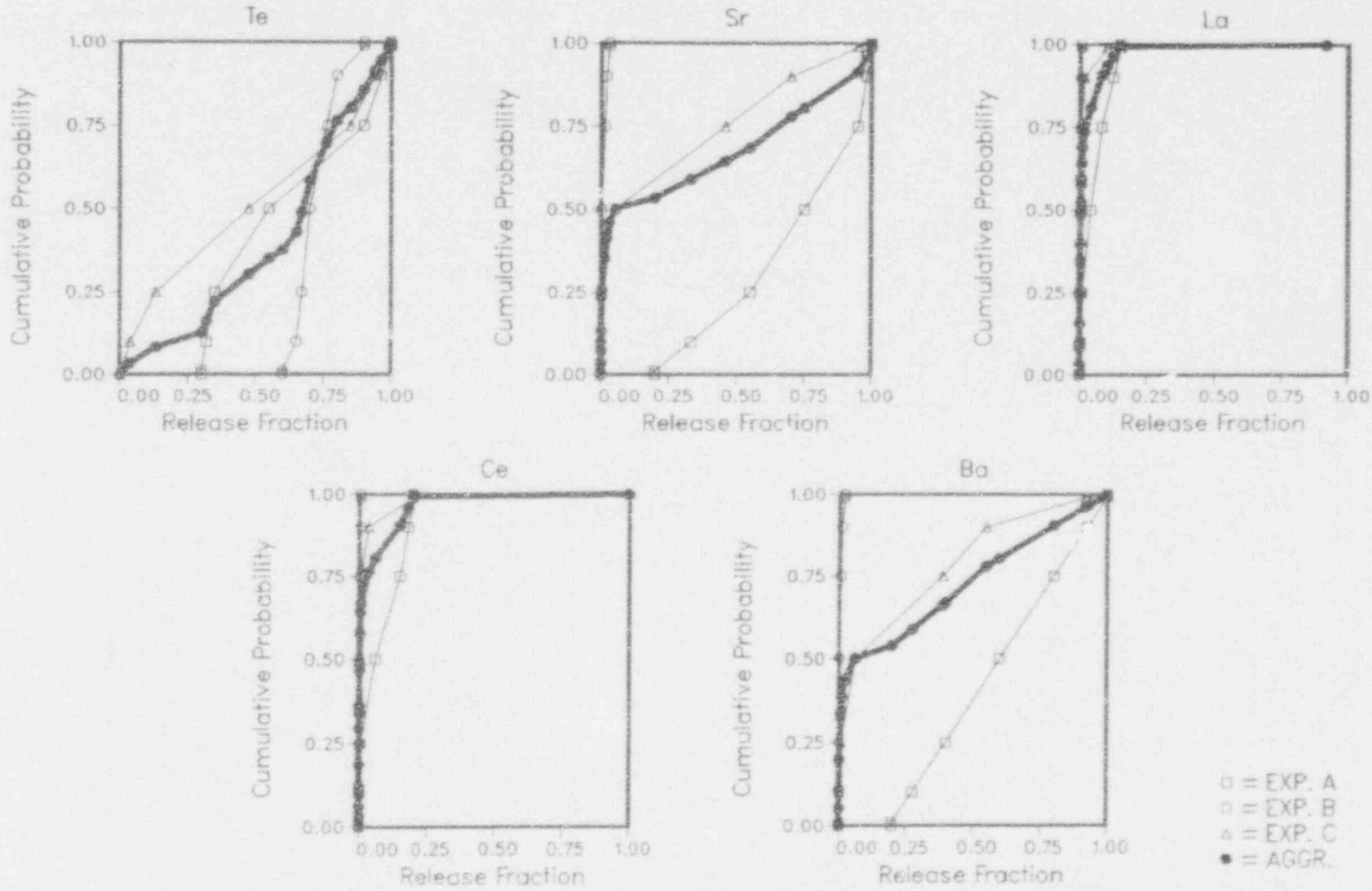

Figure 4-17. FCCI, Case 17, Grand Gulf, Dry Cavity, High Zirconium

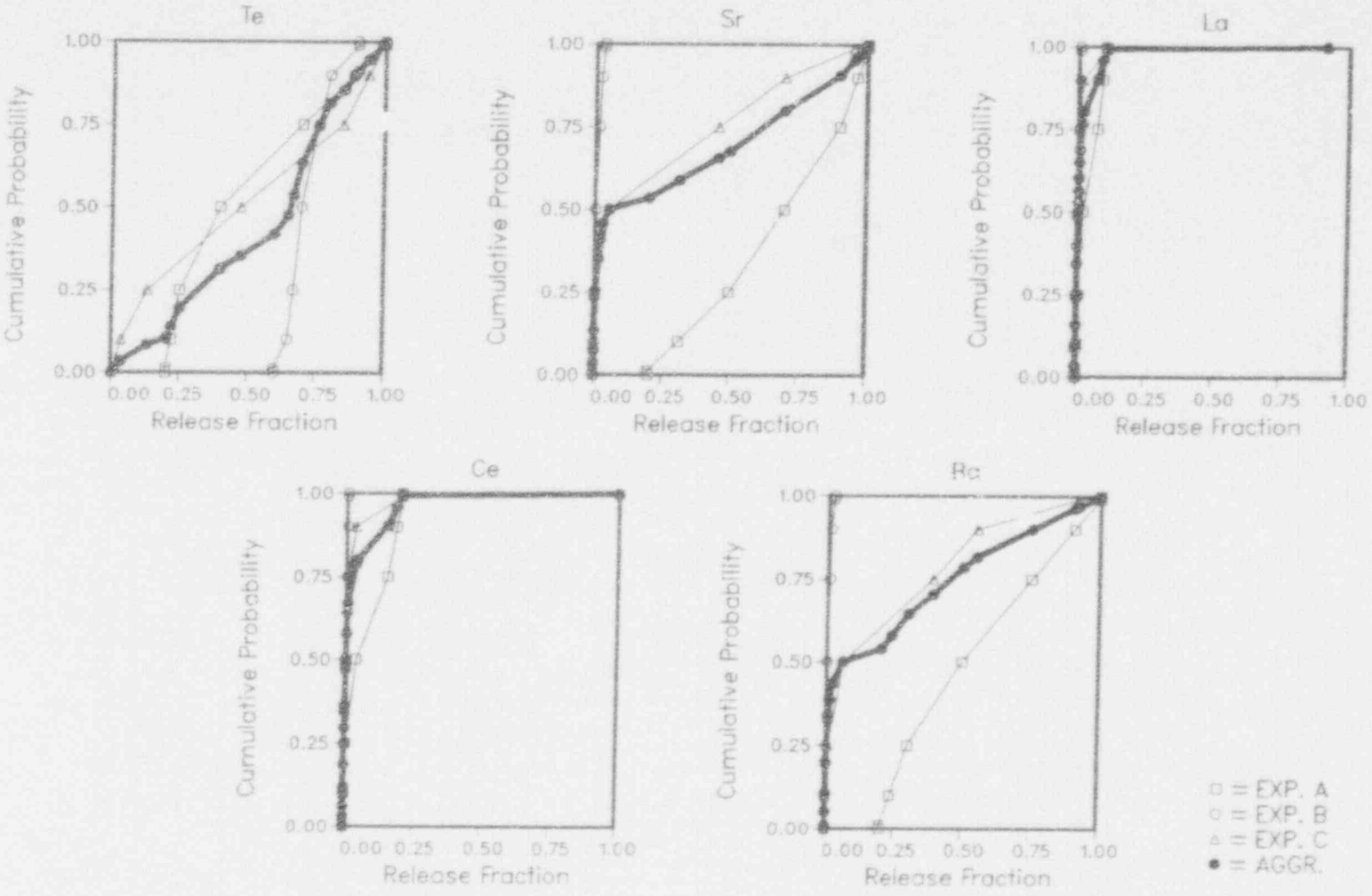

Figure 4-18. FCCI, Case 18, Grand Gulf, Dry Cavity, Low Zirconium.

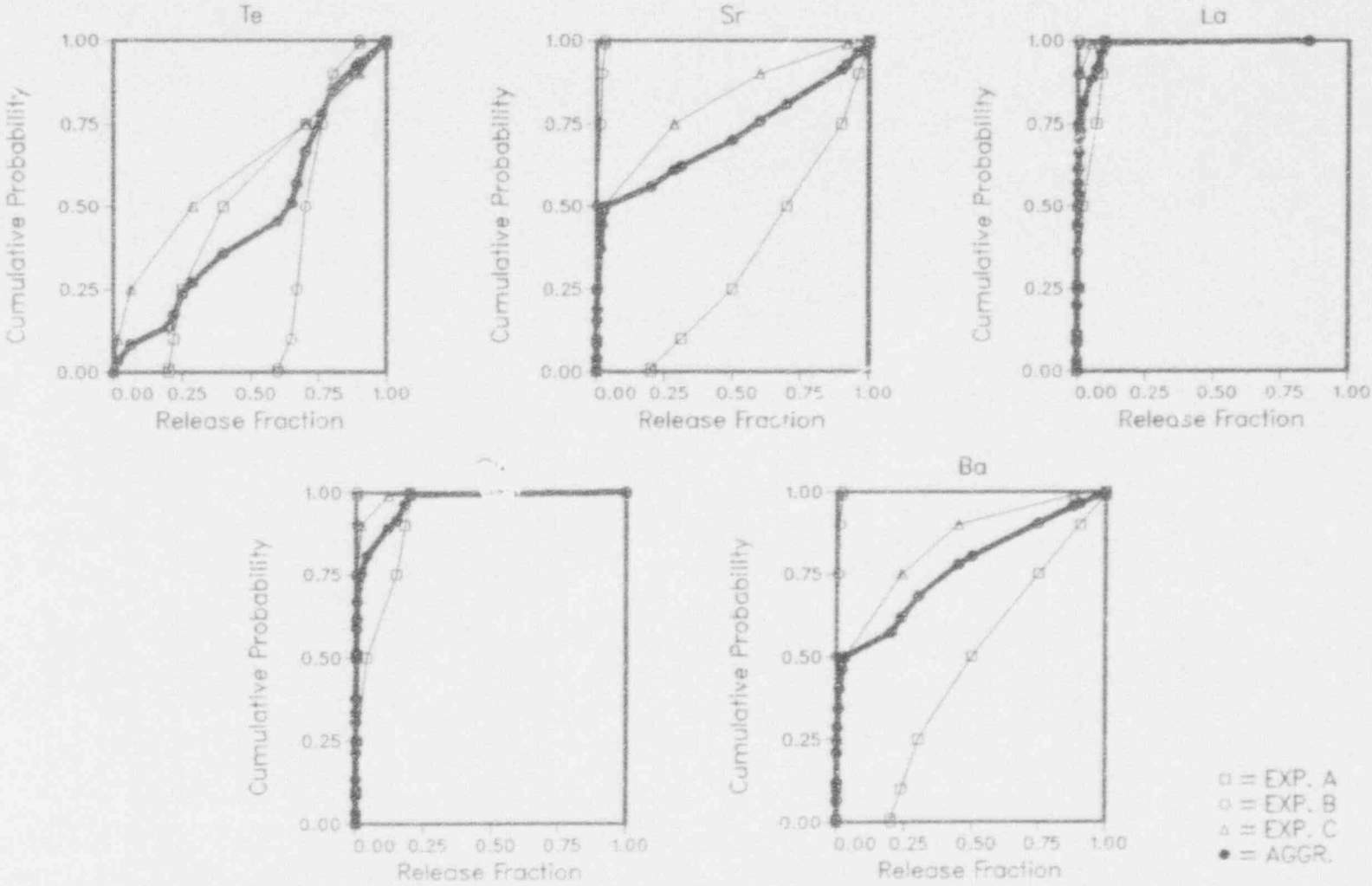

Figure 4-19. FCCI, Case 19, Grand Gulf, Wet Cavity, High Zirconium.

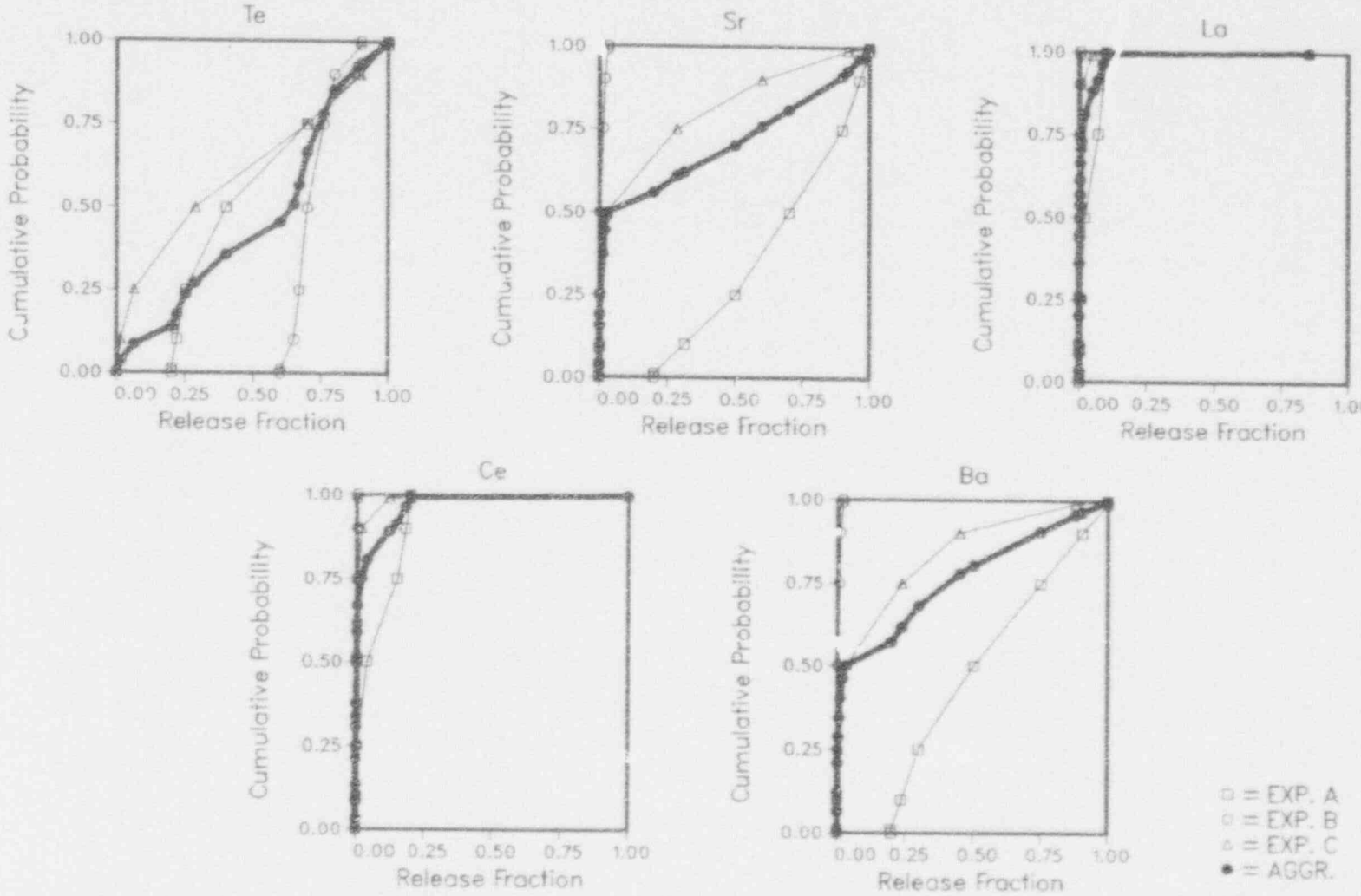

Figure 4-20. FCC1, Case 20, Grand Gulf, Wet Cavity, Low Zirconium.

Individual Elicitations for Issue 4

Expert A's Elicitation

Fraction of Fission Products Released During the Core-Concrete Interactions

Description of Expert A's Rationale/Methodology

Two experts collaborated to work on different parts of this issue: one generated the activity coefficients, and the other used these activity coefficients to generate the required release fractions.

Rationale for Activity Coefficients

Most of the rationale for the activity coefficients is presented in the attached paper given to the panel which appears later in this section. Some additional comments from the elicitation session are provided below.

The values are good for a medium amount (10 to 90%) of zirconium in the debris. The expert stated that the activity coefficients are thermodynamic equilibrium values.

Expert A stated that he suspected that the type of concrete did not impact the results. He also stated that most of the release will be within one hour.

Rationale for Release Fractions

For PWRs, the expert based his results on Zion MAAP calculations made with limestone/common sand concrete and assumed 100% of the debris in the cavity. The uncertainties in the thermal hydraulic portion of the FCCI analysis were on the order of two and three much less than those in the activity coefficients.

Expert A sent the following comments with the completed results:

> "As discussed during the elicitation, I would expect the release fractions per unit mass of debris to be different for high pressure and low pressure accident sequences. This is due to the potential for debris dispersal and the long term heat losses which affect the debris temperature and thus the fission product release rate. However, these uncertainties would be encompassed by those assigned to the activity coefficients. Thus, the values given in the tables should be used for high pressure and low pressure sequences on a per unit mass basis."

In terms of the high and low zircaloy mass for PWRs, and following the guidance given during the Committee's meetings, in my assessment the limits imposed on the unreacted zircaloy in the debris would assure that sufficient zircaloy would be available for significant reaction. Therefore, little difference in the release fractions would be expected. Consequently, the release fractions reported in the tables are the same for both high Zirc and low Zirc conditions. This is consistent with my elicitation.

For wet cavity cases, my assessment is based upon water being present at all times such that the debris would eventually be quenched. With the potential for quenching, fission product release would be terminated. Therefore, the release from debris would only occur during the core-concrete attack with simultaneous debris quenching. Depending upon the plant and the accident sequence, this would vary from a few minutes to tens of minutes. In particular, those with smaller reactor cavity configurations would require a longer interval to quench the material. This would allow for additional release to occur and has been taken into account in my assessment for the wet cavity conditions in the various plants.

Since the major release occurs during zircaloy oxidation, this release is over an interval comparable to the quenching time. This substantially complicates the analysis for a wet cavity. In particular, it emphasizes the sequence specific features such as the time required for core debris to leave the reactor vessel and enter the reactor cavity/pedestal region, i.e., minutes, tens of minutes, or hours. To make the problem tractable, I used the release rates for a non-dispersed case with a quenching interval of 5000 seconds which overstates the quenching time (understates the quenching rate). The debris temperature enters into the release in a highly non-linear manner. As an overstatement of the release during the quenching, I decreased the releases from the dry cavity case by a factor of three. This accounts for the initial rapid release in a simultaneous cool down. With the confined pedestal region for Grand Gulf, the release is sufficiently rapid that the wet and dry conditions are given the same release fractions."

Results of Expert A's Elicitation

The initial distribution for the activity coefficients can be found in the paper supplied by the first expert. The activity coefficient distributions that were obtained in the elicitation session are found in Figures A-1 to A-3.

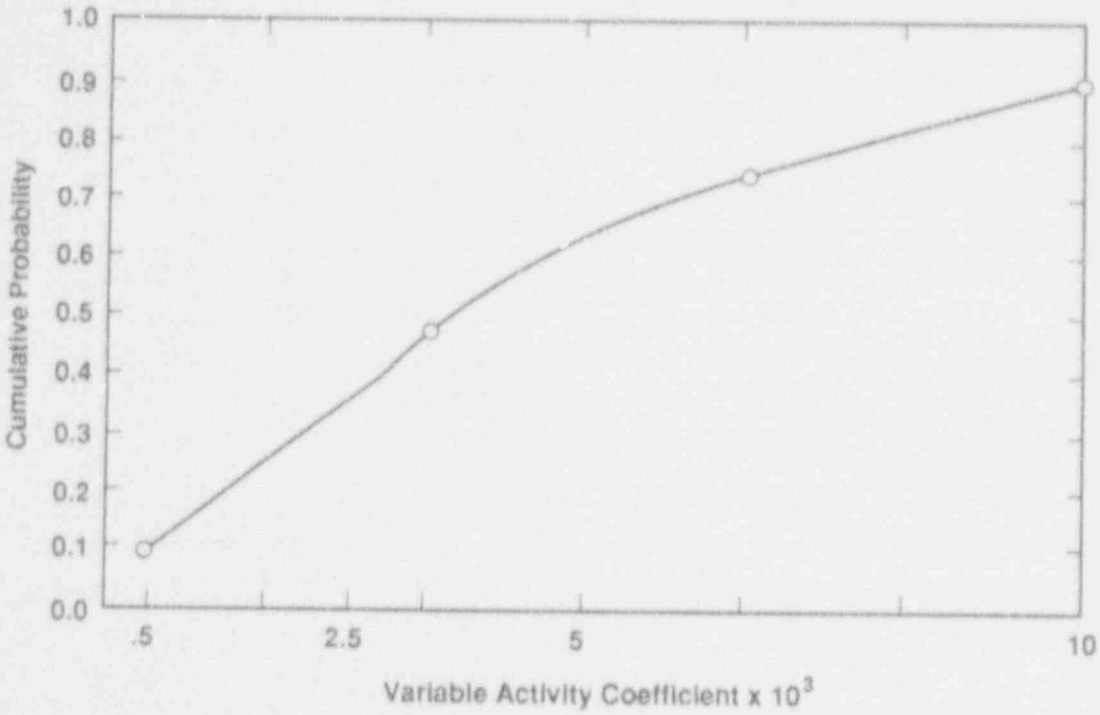

Figure A-1. Distributions for Barium and Strontium.

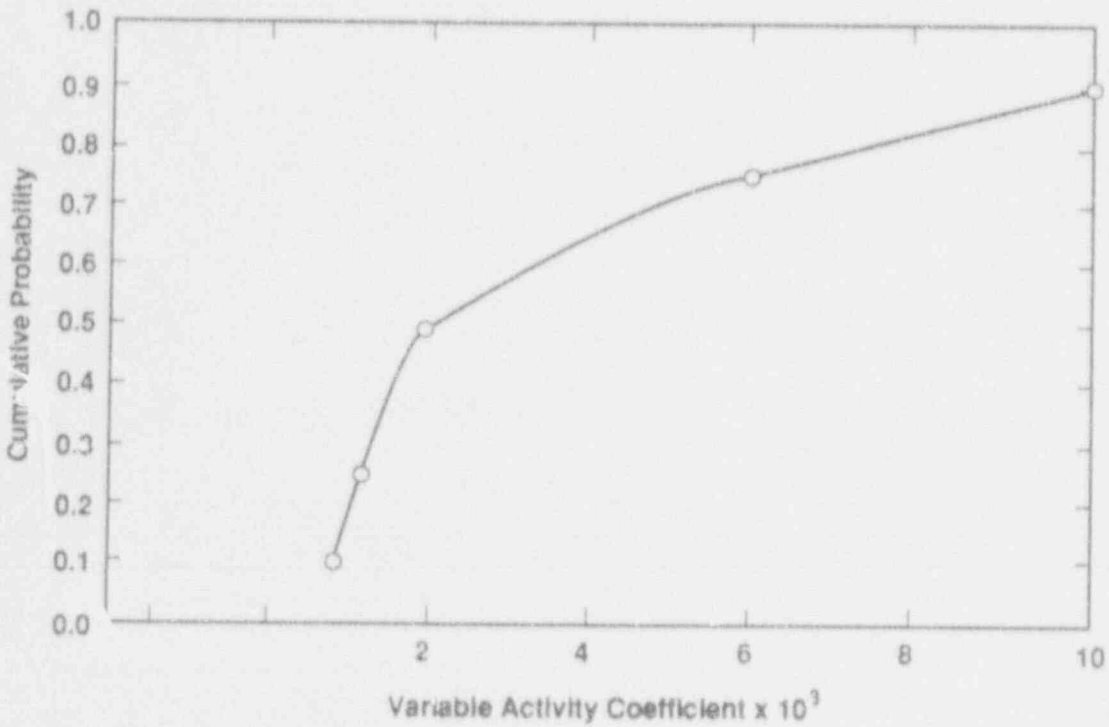

Figure A-2. Distributions for Lanthanum and Cerium.

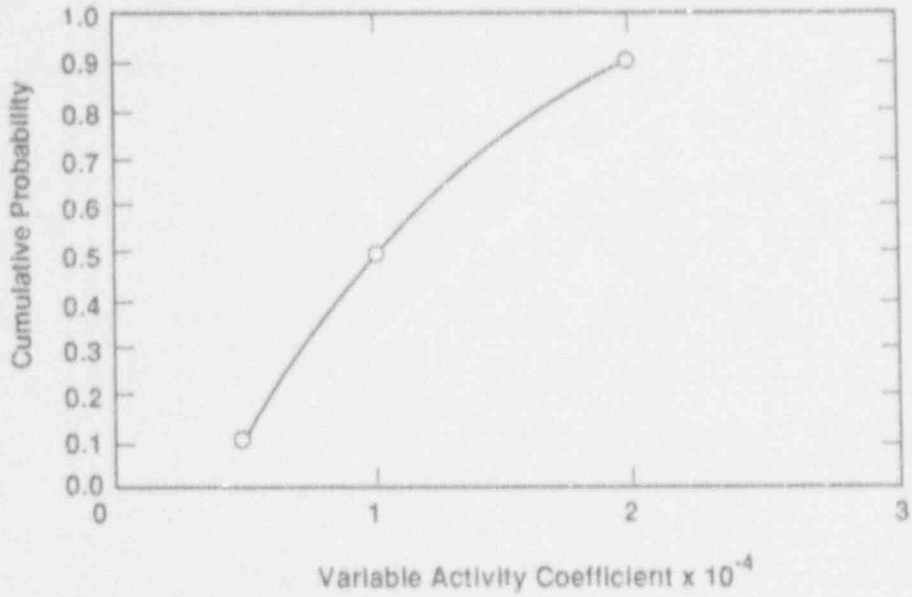

Figure A-3. Distributions for Ruthenium.

The release fraction distributions supplied by the second expert are presented in the Tables A-1 through A-5. The Sequoyah and Surry cases are the same as those for Zion. Iodine and cesium fractions are assumed to be 1.0 in all cases.

Table A-1
Case 1, Zion--Dry Cavity, High Zirconium
Case 2, Zion--Dry Cavity, Low Zirconium

Nuclide	LL	0.1	0.5	0.9	UL
Tellurium	.5	.55	.6	.7	.7
Strontium	2E-4	8E-4	1.6E-3	1.6E-2	1
Lanthanum	2E-5	2E-4	4E-4	2E-3	.2
Cerium	2E-5	2E-4	4E-4	2E-3	.2
Barium	2E-4	5E-4	1E-3	1E-2	1

Table A-2
Case 3, Zion--Wet Cavity High Zirconium
Case 4, Zion--Wet Cavity, Low Zirconium

Nuclide	LL	0.1	0.5	0.9	UL
Tellurium	1E-2	5E-2	2E-1	3E-1	3E-1
Strontium	7E-5	3E-4	5E-4	5E-3	1E-2
Lanthanum	7E-6	7E-5	1.3E-4	7E-4	1E-3
Cerium	7E-6	7E-5	1.3E-4	7E-4	1.3E-3
Barium	7E-5	1.5E-5	3E-4	3E-3	5E-3

Table A-3
Case 13, Peach Bottom--Dry Cavity High Zirconium
Case 14, Peach Bottom--Dry Cavity Low Zirconium

Nuclide	LL	0.1	0.5	0.9	UL
Tellurium	E-1	1.5E-1	2E-1	4E-1	4E-1
Strontium	7E-5	3E-4	5E-4	5E-3	E-2
Lanthanum	7E-6	7E-5	1.3E-4	7E-4	E-2
Cerium	7E-6	7E-5	1.3E-4	7E-4	E-2
Barium	7E-5	2E-4	3E-4	3E-3	E-2

Table A-4
Case 15, Peach Bottom--Wet Cavity High Zirconium
Case 16 Peach Bottom--Wet Cavity Low Zirconium

Nuclide	LL	0.1	0.5	0.9	UL
Tellurium	E-2	5E-2	E-1	2E-1	3E-1
Strontium	E-6	E-5	5E-5	E-3	5E-3
Lanthanum	E-7	E-6	5E-6	E-4	E-3
Cerium	E-7	E-6	5E-6	E-4	E-3
Barium	E-6	E-5	5E-5	E-3	5E-3

Table A-5
Case 17, Grand Gulf--Dry Cavity High Zirconium
Case 18, Grand Gulf--Dry Cavity Low Zirconium
Case 19, Grand Gulf--Wet Cavity High Zirconium
Case 20, Grand Gulf--Wet Cavity Low Zirconium

Nuclide	LL	0.1	0.5	0.9	UL
Tellurium	6E-1	6.5E-1	7E-1	8E-1	9E-1
Strontium	2E-4	5E-4	2E-3	2E-2	3E-2
Lanthanum	4E-5	E-4	4E-4	4E-3	5E-3
Cerium	4E-5	E-4	4E-4	4E-3	5E-3
Barium	E-4	5E-4	E-3	E-2	2E-2

Sources of Uncertainty

A large source of the uncertainty for the activity coefficients was the question whether hydroxides exist for lanthanum, barium, and strontium. As the amount of hydroxide increases, the activity coefficients increase.

The entire uncertainty in FCCI is driven by the uncertainty in the activity coefficients.

Attachment to Expert A's Written Elicitation

Rationale for Activity Coefficients

This issue is concerned with the estimation of FCCI under various conditions. $FCCI_i$ represents the fraction of the radionuclide group i in the core material at the time of breach which is released to the containment during the CCI.

These fractions are generally calculated by the combined CORCON-MOD2/VANESA code. There are two areas in these calculations with which we are uncomfortable. First, the VANESA code uses ideal solution concepts which means that the activity coefficients are assumed to be 1. These activity coefficients should be measured under controlled conditions. This is a very difficult experiment. The second area is the estimation of temperature of the corium-concrete reaction mixture.

With regard to the first area there is little experimental data. The second potential problem area, the temperature, involves the oxidation of zirconium in a molten oxide media by steam and of special importance, heat transfer considerations of a complicated nature. I have talked with one of the other experts on the panel, and he shares my general views but is much more proficient in the heat transfer area than I. Therefore, I will defer to him in the development of the detailed case in this area. In general, however, any decrease in temperature should be reflected in an almost exponential way by decreasing the release fractions as corrected by modified activity coefficients.

With these two caveats, it seems appropriate to use as a starting point the CORCON-MOD2/VANESA 101 calculations to be furnished by Dana Powers (SNL) for the various cases and suggest changes.

It is my understanding that the VANESA code permits the changing of the release fractions by directly multiplying the release fraction by the activity coefficient. The rest of this memorandum addresses the activity coefficient question.

Argonne* has very recently obtained a small amount of activity coefficient data on Sr and Ba. These data are at an oxidation potential characteristic of the absence of zirconium. Therefore, the data may not be applicable to accident cases. These data were reported at the Captiva Island meeting in December. In the Argonne view, a complicating factor is the presence of Ba and Sr as the dissolved zirconates rather than as dissolved oxides (really ions). If calculations using SOLGASMIX to predict the amount vaporized in the Argonne transpiration experiments at 2150 K are carried out, the predictions and results in mg are as follows:

---

*There are two groups at Argonne working on this problem. The work reported here is from small-scale laboratory studies carried out by Mike Roche.

	Calculated Not Assuming Zirconates	Calculated Assuming Zirconates	Experimentally Observed
Sr	0.122	.003	.018
Ba	0.216	.006	.006

Thus one may estimate the activity coefficients as follows:

Sr $.003/.122 = 2.5 \times 10^{-2}$
Ba $.006/.216 = 2.8 \times 10^{-2}$.

These numbers would then be our activity coefficients for the system in the absence of zirconium, and it can be seen that the amount experimentally vaporized agrees roughly with assuming that zirconates are decreasing the volatility of the barium and strontium. It should be mentioned that these experiments were carried out in the presence of limestone concrete. The presence of silicates might further decrease activity coefficients.

With regard to lanthanum in a system not containing zirconium metal, assuming an activity coefficient of 1, the calculated transport was 0.013 mg. The measured transport was < 0.002. Thus one might very roughly estimate an activity coefficient of less than .002/.013 = .15.

Other species of interest are tellurium, cerium, rubidium, iodine, and cesium. In the cases of tellurium, cesium and iodine, there seems to be ample evidence that tellurium is very readily volatilized as would also be the case for cesium and iodine. Therefore there seems to be no good reason to assume any hindering of volatilization. In the cases of Ru and Ce there are no data from the Argonne small-scale laboratory group yet.

In most accident scenarios, the core-concrete reaction initially takes place in the presence of zirconium metal. Thus the oxidation potential is quite low. This is really the regime of importance since the fission products are released during the period when zirconium is present. We badly need more experimental data in this regime. Two groups at Argonne are working on the problem. One group is using transpiration experiments on a small scale. The data previously cited comes from this group. The other effort involves experiments on a 30 kg scale. These data are not yet in a usable form.

Carl Alexander is carrying out experiments at Battelle Memorial Institute to measure activity coefficients. These experiments seem to be in a proper oxidation potential regime. The date was reported at the Captiva Island meeting in December 1987. This information was augmented by extensive telephone conversations with Carl. One particularly interesting set of experiments done at 2400 K using mass spectroscopic techniques involves an oxygen to metal ratio of 1.5. A mixture of ZrO_2, UO_2, and Zr was used with Ru, Ba, Sr, Y, La, Sm and Ce added (0.3 to 1 atom percent).

Activity coefficients for some of the interesting elements at 2400 K are as follows:

Ba: 10^{-3}
Sr: 10^{-3}
La: 2×10^{-3}
Ce: 2×10^{-3}
Ru: very low (barely detectable).

The question of volatile hydroxides was discussed since this mass spectroscopic approach involves no steam. It was Carl's opinion that the hydroxides would not become stable until lower temperatures, perhaps in the neighborhood of 1900 K. However, there seems to be some difference of opinion among experts on this subject so the activity coefficients are "tilted" toward the high end.

Based on these rather thin experimental data, the following uncertainties in the activity coefficients are estimated at 2400 K:

Probability of Being Correct	0.25	.5	.25
Ba	10^{-2}	10^{-3}	5×10^{-4}
Sr	10^{-2}	10^{-3}	5×10^{-4}
La	10^{-2}	2×10^{-3}	10^{-3}
Ce	10^{-2}	2×10^{-3}	10^{-3}
Ru	2×10^{-4}	10^{-4}	5×10^{-5}
Cs	1	.9	.8
I	1	.9	.8
Te	1	.9	.8

Expert B's Elicitation

Fraction of Fission Products Released During the Core-Concrete Interactions

Description of Expert B's Rationale/Methodology

Expert B used the results of the QUASAR study[B-1] for the plants which had limestone concrete. For all plants he referred to the panel presentation by Williams,* and Burson's summary article.[B-2] He also used results from the CORCON module, which is incorporated in several different computer codes.

Expert B defined six cases:

1. PWR--Basalt Concrete, High Zirconium Oxidation in the Vessel
2. PWR--Basalt Concrete, Low Zirconium Oxidation in the Vessel
3. PWR--Limestone/Common Sand Concrete, High Zirconium Oxidation In the Vessel
4. PWR--Limestone/Common Sand Concrete, Low Zirconium Oxidation In the Vessel
5. BWR--Limestone Concrete, High Zirconium Oxidation in the Vessel
6. BWR--Limestone Concrete, Low Zirconium Oxidation in the Vessel.

He made no distinction between whether the CCI was prompt or delayed. If the cavity was full of water, Expert B believed that the unoxidized zirconium in the molten core debris would oxidize rapidly once the debris contacted the water. Thus, the low zirconium oxidation cases in the vessel with water in the cavity should be treated as high zirconium oxidation in the vessel. Note that low zirconium oxidation in the vessel implies high unoxidized zirconium fraction in the core debris, and that high zirconium oxidation in-vessel implies low unoxidized zirconium fraction in the core debris. To avoid confusion, the terms "Low Zirconium" and "High Zirconium" will not be used.

Of the nine radionuclide groups, the core debris is not expected to contain significant amounts of the noble gases, so no distribution was provided for that group. Expert B stated that all the iodine and cesium would be released from the melt for all cases, so no distributions were provided for those groups either. Expert B considered the lanthanum and cerium groups

---

*D. C. Williams and A. W. Shiver, "Some Uncertainties in Radionuclide and Aerosol Release During Core-Concrete Interactions," Presentation to the Source Term Panel, March 15, 1988.

together for the PWRs. Thus, for the PWRs, he provided distributions for four groups: tellurium, barium, strontium, and lanthanum/cerium. For the BWRs he provided distributions for five groups: tellurium, barium, strontium, lanthanum, and cerium. Expert B did not provide distributions for the ruthenium radionuclide group because he felt that there was insufficient information on which to base an estimate and that the releases would be very low.

Results of Expert B's Elicitation

Expert B's conclusions about FCCI are contained in Tables B-1 through B-6. A discussion of each of Expert B's six cases follows.

Case 1. PWR--Basalt Concrete, Low Unoxidized Zirconium Fraction in Debris

For tellurium, Expert B selected his midpoint, 20% release, from CORCON results.* He reasoned that it would be impossible to get more than 50% of the tellurium released, since the outgassing of the concrete will be relatively small and the period of concrete attack relatively short. This value formed his upper bound (99 percentile value). For his lower bound, he thought there could be as little as 5% of the tellurium released if the oxidic material came out of the vessel first and the tellurium came out with the metallic fraction later. When the tellurium leaves the vessel, the oxides have already quenched and cooled off, and there is no immediate reheat. Much of the unoxidized metal may remain unoxidized in this scenario.

The release of the barium group is more affected by temperature than is the tellurium release. The more reducing the atmosphere, the more barium is released. With basaltic concrete and a low zirconium fraction in the melt, little outgassing of the concrete is expected, and the barium release rates should be relatively low. Similar reasoning applies to the strontium group and the lanthanum/cerium groups.

Table B-1
Fractional Release (%) from CCI
Case 1. PWR--Basaltic Concrete, Low Zirconium in Debris

	Cumulative Probability (%)				
Nuclide	1	25	50	75	99
Tellurium	5	15	20	30	50
Barium	0	2	5	10	25
Strontium	0	5	12	17	25
Lanthanum/cerium	0.01	0.05	1	5	10

*CORCON results supplied privately by Dana Powers of Sandia National Laboratories.

Case 2. PWR--Basalt Concrete, High Unoxidized Zirconium Fraction in Debris

As there is more zirconium to oxidize during the CCI, higher temperatures may be expected in this case than in Case 1. As the aggregate is all basalt, however, only a little more gas will be produced. The middle three points of the tellurium, barium, and strontium distributions are all higher than for Case 1 to account for the higher temperatures. The upper bound of the tellurium distribution increases to 75% released. The same upper bound as in Case 1 is retained for barium and strontium, since there would not be enough gas generated to release more than a quarter of the fission products in these radionuclide groups.

Table B-2
Fractional Release (%) from CCI
Case 2. PWR--Basaltic Concrete, High Zirconium in Debris

	Cumulative Probability (%)				
Nuclide	1	25	50	75	99
Tellurium	10	25	35	50	75
Barium	0	5	10	17	25
Strontium	0	10	15	22	25
Lanthanum/cerium	0.01	0.05	2	7	10

Case 3. PWR--Limestone/Common Sand Concrete, Low Unoxidized Zirconium Fraction in Debris

Compared to Case 1, a great deal more gas evolved in this case because of the decomposition of the limestone aggregate. Expert B moved the middle three points of his tellurium distribution up somewhat to account for the extra gas production. The endpoints of the tellurium distribution, however, are not affected by the amount of gas generated and are the same as in Case 1. The middle portions of the barium and strontium distributions are significantly increased relative to Case 1 because of the increased amount of gas released. The lanthanum/cerium distribution remains the same as in Case 1. The amount of gas liberated should have a relatively small effect on the release of these fission products. The range for these groups is already so wide that the effects of concrete composition are included. The uncertainty in the oxidation potential and the activity coefficients overshadows the effects of concrete composition.

Table B-3
Fractional Release (%) from CCI, Case 3,
PWR--Limestone/Common Sand Concrete, Low Zirconium in Debris

	Cumulative Probability (%)				
Nuclide	1	25	50	75	99
Tellurium	5	17.5	25	35	50
Barium	0	10	15	20	25
Strontium	5	10	20	25	30
Lanthanum/cerium	0.01	0.05	1	5	10

Case 4. PWR--Limestone/Common Sand Concrete, High Unoxidized Zirconium Fraction in Debris

The upper bounds are similar to those in Case 2 since they depend only weakly on the amount of gas generated. The middle portions of the distributions for tellurium, barium, and strontium are all higher than in Case 2 because of the increased amount of gas generated by the concrete decomposition. Of the four PWR cases, the release fractions are highest in this one.

Table B-4
Fractional Release (%) from CCI, Case 4,
PWR--Limestone/Common Sand Concrete, High Zirconium in Debris

	Cumulative Probability (%)				
Nuclide	1	25	50	75	99
Tellurium	10	30	40	55	75
Barium	0	10	15	20	25
Strontium	0	15	20	25	30
Lanthanum/cerium	0.01	0.1	3	8	10

Case 5, BWR--Limestone Concrete, Low Unoxidized Zirconium Fraction in Debris

Expert B felt that his distributions were wide enough to encompass the uncertainty in the concrete composition at Peach Bottom. Expert B expects the unoxidized metals to come out first following vessel failure in a BWR, so it is quite conceivable that all the tellurium could be "cooked out" of the metallic fraction of the debris by the hot oxide coming out after the metal. His midpoint (40%) is based on CORCON results adjusted upward to

account for deficiencies. The lower bound, 20% released, allows for the possibility that the initial discharge from the vessel is a metal-oxide mixture. The barium and strontium releases are much higher than in the PWR cases. The BWR core contains much more zirconium than the PWR core, so there will be more zirconium to oxidize during the CCI. In addition to the higher temperatures, the aggregate is all limestone, and amount of gas generated will be large. The barium and strontium release fractions are more dependent upon temperature than are the tellurium release fractions. As for tellurium, the upper bounds for the barium and strontium groups are 100% release. The cerium and lanthanum radionuclide groups are separated in the BWR cases because of the temperature dependence.

Table B-5
Fractional Release (%) from CCI.
Case 5. BWR--Limestone Concrete, Low Zirconium in Debris

	Cumulative Probability (%)				
Nuclide	1	25	50	75	99
Tellurium	20	25	40	70	100
Barium	20	30	50	75	100
Strontium	20	50	70	90	100
Lanthanum	0.1	0.7	2	7	10
Cerium	0.1	0.5	4	15	20

Case 6. BWR--Limestone Concrete, High Unoxidized Zirconium Fraction in Debris

The release fractions are generally somewhat higher than in Case 5 to account for the higher temperatures that result from the large amount of unoxidized zirconium in the core debris.

Table B-6
Fractional Release (%) from CCI.
Case 6. BWR--Limestone Concrete, High Zirconium in Debris

	Cumulative Probability (%)				
Nuclide	1	25	50	75	99
Tellurium	30	35	55	90	100
Barium	20	40	60	80	100
Strontium	20	55	75	95	100
Lanthanum	0.1	0.8	4	8	15
Cerium	0.1	0.5	6	15	20

Sources of Uncertainty

Expert B felt that the uncertainty in the distributions for FCCI was largely because of uncertainties in the oxidation potentials and the activation coefficients.

REFERENCES

B-1. "On the Uncertainties in Core Melt Progression, Fission Product Release, and Pressurization Loads for a BWR with a Mark I Containment," Technical Report, Brookhaven National Laboratory, February 20, 1988.

B-2. S. B. Burson, "Core-Concrete Interactions," Section 5 of Uncertainty Papers on Severe Accident Source Terms, NUREG-1265, U.S. Nuclear Regulatory Commission, Washington, DC, 1987.

Expert C's Elicitation

Fraction of Fission Products Released During the Core-Concrete Interactions

Description of Expert C's Rationale/Methodology

Expert C considered both thermochemical vaporization and mechanical aerosolization processes in evaluating the release associated with core-concrete interactions. Of the two, he believed that vaporization had the greater potential to yield large release fractions, and he felt that it was more amenable to detailed analysis. Hence, he devoted most of his efforts to assessing the vaporization release. Expert C developed separate distributions (CDFs) for the vaporization release and for the mechanical aerosol release. In developing the final distribution for the CCI release for each fractile, Expert C used the higher of the vaporization release fraction or the mechanical aerosolization release fraction corresponding to his distributions.

Vaporization Release

Expert C analyzed CCI releases in terms of the parameter $FCCI_i$, which is defined, for each radionuclide group i, as the ratio (radionuclide released from the melt)/(radionuclide in the melt at the time of CCI onset). For the vaporization contribution to $FCCI_i$, Expert C felt it was necessary to address two fundamental considerations:

1. Many calculations with mechanistic accident analysis codes (the STCP, MAAP, etc.) have been performed for a variety of accident sequences. Expert C believed that these codes combine evaluation of the boundary and initial conditions for CCI with treatments of many phenomenologies involved in CCI to a degree that no simple stand-alone, separate-effects calculations could match. Hence, he believed that any uncertainty methodology should incorporate the information represented by the code calculations as directly as possible. (Expert C noted that in the VANESA calculations, mechanical aerosol generation was quite minor compared with vaporization except when total releases were extremely small; hence, he assumed the code results to be representative of the vaporization contribution to $FCCI_i$.)

2. Despite the value of the code calculation, Expert C also believed that there are some important uncertainties in them because of phenomenological uncertainties in both the CCI modeling and the modeling of the processes that determine the boundary/initial conditions for CCI (e.g., the in-vessel melt progression). Hence, any uncertainty methodology should explicitly take into account the more important modeling uncertainties that might affect the code results. Since these uncertainties involve limitations of the code models themselves, some of them are not readily investigated simply by performing sensitivity studies with the codes, even if it were feasible to perform any desired number of such sensitivity studies.

To meet these needs, Expert C devised a two-step process for developing uncertainty distributions for $FCCI_i$. The first step was to develop what he called a "base distribution" using the results of code calculations. He relied primarily upon STCP calculations[C-1,C-3] and calculations with stand alone versions of the CORCON and VANESA codes[C-4,*] (which constitute the CCI modules in the STCP), although he also considered some MAAP code results.** Many code results used by Expert C and the base distributions he estimated from them, are summarized in the Results of Expert's Elicitation section of this document.

The second step was to make substantial changes to the base distribution to account for the uncertainties that he believed could have potentially important effects upon the code calculations. Expert C reasoned that for small release fractions, $FCCI_i$ would be proportional to the time integral of the quantity $P_{vi}(dV_g/dt)$, where P_{vi} is the effective vapor pressure of radionuclide species i and dV_g/dt is the volumetric rate at which gas sparges. Expert C felt that P_{vi} was uncertain by orders of magnitude, while CCI experiments indicated that the codes generally did a reasonably good job of predicting the concrete ablation rate (which controls gas sparging rates); hence, he emphasized the uncertainties in P_{vi} and assumed that the uncertainty a given effect could introduce in $FCCI_i$ would be proportional to its effect upon P_{vi}.

When the release fractions were large, Expert C modified his approach to take into account the reduction in vaporization rates as the melt becomes depleted in the vaporizing species. In most cases of interest, Expert C noted that vapor pressures calculated by the VANESA code were approximately proportional to the concentration remaining in the melt. This leads to a simple exponential decay in vaporization rate with time, other parameters remaining constant. Hence, Expert C defined a "release parameter" $RCCI_i$, related to $FCCI_i$ by

$$FCCI_i = 1 - \exp(-RCCI_i). \qquad \text{Eq. (1)}$$

He then converted his base distribution for $FCCI_i$ into an equivalent distribution for $RCCI_i$ and analyzed the effects of the various uncertainties in terms of the factors by which they might alter P_{vi}, with emphasis on their effects during the time period that dominated the releases in the code calculations. He then assumed that these effects would alter $RCCI_i$ by the same factors.

The uncertainties considered by the expert were the following:

1. Uncertainty in the amount of unoxidized zirconium in the melt;

---

*D. C. Williams and D. A. Powers, "Some Uncertainties in Radionuclide Release during Core-Concrete Interactions," SAND87-2558A, presented at the Second Symposium on Nuclear Reactor Severe Accident Chemistry, Third Chemical Congress of North America, Toronto, Canada, June 5-10, 1988.

**E. L. Fuller, Presentation to Source Term Panel, Albuquerque, New Mexico, January 12-14, 1988; E. L. Fuller to D. C. Williams, Letters on Peach Bottom MAAP Analysis for Station Blackout, March 14, 1988 and March 28, 1988.

2. Uncertainties in the radionuclide chemical speciation in the melt;

3. Uncertainty in the oxygen potential characterizing the oxidic phase of the melt;

4. Uncertainty in the effects of water overlying the melt;

5. Uncertainty in the temperature of the melt during the time of maximum vaporization. This uncertainty includes uncertainty in debris temperature at vessel breach (VB) and also includes other factors, e.g., heat generation by oxidation of metallic zirconium in the melt;

6. Uncertainty in the concrete type, and in the effect of concrete type upon the releases (virtually all available BWR STCP calculations assumed a high-limestone concrete, while information provided to the experts shortly before their elicitations indicated that the concrete type is actually LS/CS in the BWR plants considered);

7. Uncertainty in the free energies of formation of the various species involved in vaporization of a given radionuclide;

8. Uncertainty in the activity coefficients of radionuclide species in the melt;

Expert C did not believe that all these uncertainties were necessarily important for all radionuclide species or for all cases considered. Hence, the number of uncertainties he treated in any one analysis was less than the eight listed above. Information on the uncertainties considered for individual cases is given in the summary of the results of the elicitation.

For each uncertainty considered in a particular analysis, Expert C defined a small number (usually three or four) of discrete levels; i.e., he selected three or more values for a parameter representing the uncertainty. For the CCI analysis, this parameter was the factor R by which the uncertainty could alter P_{vi} and, hence, alter $RCCI_i$. He then assigned a weight W to each level, i.e., a subjective probability that the parameter R would take on a value close to the value representing each level.

In developing his distributions for the R values, Expert C employed stand-alone thermochemical calculations using the VANESA data base to assess the effects of uncertainties in condensed phase speciation, melt temperature, and oxidic phase oxygen potential. He used a number of CORCON/VANESA calculations performed specifically for his elicitation, to assess the possible effects of uncertainty in melt zirconium content and uncertainties associated with the concrete type.* Uncertainties in free energies and activity coefficients were directly converted into corresponding

---

*D. C. Williams and D. A. Powers, "Some Uncertainties in Radionuclide Release During Core-Concrete Interactions," SAND87-2558A, presented at the Second Symposium on Nuclear Reactor Severe Accident Chemistry, Third Chemical Congress of North America, Toronto, Canada, June 5-10, 1988.

uncertainties in vapor pressures. R-value distributions for the effect of overlying water were essentially subjective.

The R values developed by Expert C are multiplication factors, which may be applied directly to the $RCCI_i$ distributions that he derived from the code calculations. The base CDF for $RCCI_i$ was modified using a "decomposition tree" structure that allowed for all possible combinations of the levels defined for all the uncertainties to be considered. Each of the endpoints of the tree yields a reproduction of the base CDF for $RCCI_i$ shifted by an amount equal to the product of the R values assigned to the branches corresponding to the particular path taken through the tree. The weight assigned to this endpoint is equal to the product of the W values assigned to each of the branch points. The final distribution for $RCCI_i$ was formed by combining the weighted distributions obtained for all the tree endpoints. This distribution was then converted back to a distribution for $FCCI_i$ using Eq. (1).

Expert C's decomposition tree is illustrated schematically in Figure C-1. The figure is drawn for a case in which five uncertainties are considered, with four levels defined for the first uncertainty and three levels for the other four uncertainties, yielding 324 endpoints for the entire tree. Each branch point is associated with an (R,W) pair. The superscripts in the figure refer to the 1st, 2nd, ..., 5th uncertainty considered. The subscript refers to the level chosen for that uncertainty. A given path through the tree can be represented by the five numbers (jklmn), where

j = level chosen for uncertainty 1,
k = level chosen for uncertainty 2,
l = level chosen for uncertainty 3,
m = level chosen for uncertainty 4,
n = level chosen for uncertainty 5.

In Figure C-1, complete paths and the corresponding (jklmn) values are shown schematically for nine of the 324 endpoints of the tree.

In principle, dependencies between the uncertainties could be taken into account by allowing the R values and/or the W values assigned at any branch point to depend upon which branch had been taken at the previous branch points. Practical considerations imposed severe limits upon the degree to which this could be done, however. Except where otherwise noted in the discussion of the elicitation results, the various uncertainties were assumed to be phenomenologically independent.

For each endpoint of the tree, a CDF for $RCCI_i$ can be generated. This CDF is

$$RCCI_i^N(P) = R^1jR^2kR^3lR^4mR^5nRCCII^0(P), \qquad \text{Eq. (2)}$$

where $RCCI_i^0(P)$ is the value of the release parameter, defined by Eq. (1) for radionuclide group i corresponding to the Pth fractile of the base distribution, while $RCCI_i^N(P)$ is the value of the release parameter.

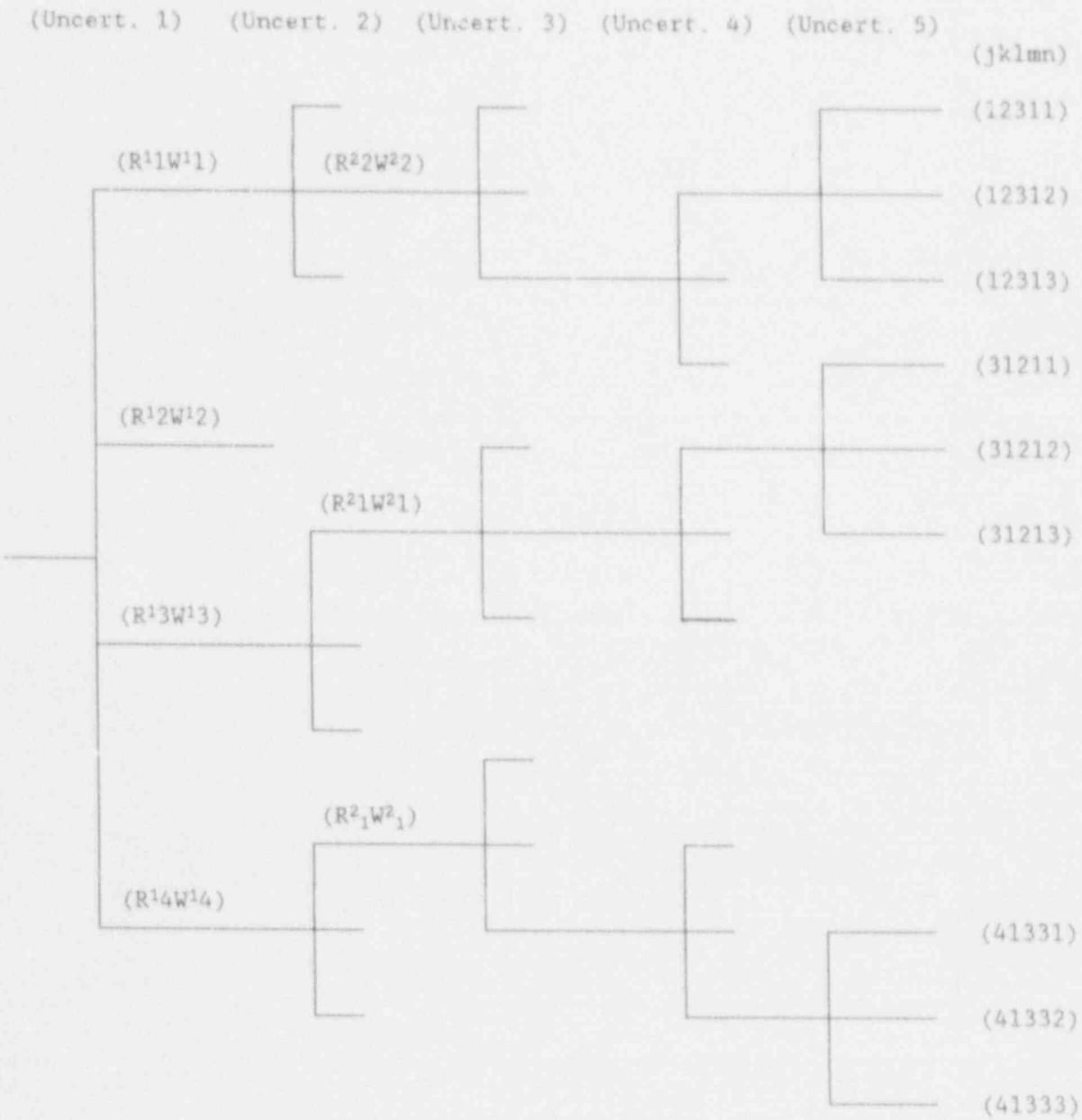

Figure C-1. Schematic of Decomposition Tree Used by Expert C.

corresponding to the Pth fractile of the distribution for the Nth endpoint of the tree. The weight assigned to this particular result (tree endpoint) is given by

$$W^N = W^1 j W^2 k W^3 l W^4 m W^5 n. \qquad \text{Eq. (3)}$$

To obtain the final combined distributions, Expert C inverted the endpoint distributions and summed the resulting weighted probabilities corresponding to a given value of $RCCI_i$, thus,

$$P(RCCI_i) = \sum_N W^N P^N(RCCI_i). \qquad \text{Eq. (4}$$

Here $P^N(RCCI_i)$ is the probability that the release parameter will be less than $RCCI_i$ for the Nth endpoint distribution, and $P(RCCI_i)$ is the probability that the release parameter will be less than $RCCI_i$ in the combined distribution. Finally, Expert C converted the combined distribution back into a distribution for $FCCI_i$, using Eq. (1).

Although it was possible, Expert C did not apply these procedures to radionuclide group 6, the "ruthenium group." This group is represented by the elements ruthenium and molybdenum in the VANESA calculations. Calculated releases were always very small for this group, usually $<10^{-5}$. The expert believed that a straightforward application of his procedures would have generated distributions that would generally be lower than the distributions the expert obtained for mechanical aerosol generation. Hence, the expert used his mechanical aerosol generation distributions for these species, with some modifications to the high end.

In the STCP calculations, noble gas, cesium, and iodine are almost always calculated to undergo quantitative release. Hence, it would not be possible to apply Expert C's standard procedure, since no base distribution for RCCI could be defined from the code calculations. Expert C believed that the release fractions for these species should be large (>50%) in most cases but acknowledged that they could be somewhat less than unity, especially under special circumstances.

Finally, Expert C emphasized that despite the use of the formalism described here, the distributions should still be viewed as being fundamentally subjective. The W values, in particular, represent subjective probabilities, and even the R values include subjective elements despite the use of code results, experimental results, and thermochemical calculations when these were available and applicable. Since the expert did consider these distributions to be subjective, he therefore revised the final results when he considered them to be unreasonable in some respect. In general, these revisions were limited to adjustments to the tails of the distributions to modify release fractions he considered to be too high or too low.

Rationale for Mechanical Aerosol Release

After calculating distributions for the vaporization release using the method described above, Expert C then considered the mechanical aerosol release and modeled a separate distribution for it. He did not allow the total release to be lower than the greater of the mechanical aerosol release and the vaporization release.

The expert used experimental data supplemented by a bubble burst model to describe the mechanical aerosol generation. The latter model neglected the aerosols entrained in the gas from the CCI that flows through the melt. He assumed mechanical aerosolization to be negligible when overlying water is present (bubble burst phenomena are not important if a crust is present).

The expert used the old VANESA default bubble burst model to form one estimate. The VANESA default assumes that for every bubble that bursts, an aerosol of 2000 particles with 1.0 μm diameter is created. The expert calculated the mass/unit volume of gas as follows:

$$M_{uv\ gas} = 2000 * \rho_p * V_p/V_b = 2000 * \rho_p * (1/6 * d_p^3 * \pi)/(1/6 * d_b^3 * \pi)$$
$$= 5.5 * 10^{-5}\ kg/m^3 \text{ at } 400\ K,$$

where

$M_{uv\ gas}$ is the aerosol mass/unit volume of gas,
ρ_p is the density of aerosol particle,
V_p is the volume of particle,
V_b is the volume of bubble,
d_p is the diameter of particle,
d_b is the diameter of bubble.

The expert stated that other more mechanistic models gave similar results, such as the correlation in the current version of VANESA. Actual measurements yield a wider range. The WITCH experiments gave a mass/unit volume on the order of 10^{-6} kg/m^3, but carbon boil experience from the steel industry reported aerosol densities of up to several hundreds of g/m^3. He also formed what he considered to be very rough upper limit estimates from the SURC4 experiments, which gave results in the range of 0.03 to 30 kg/m^3 (gas temperature = 400 K), depending upon which stage of the experiment was considered (see Table C-2).

To estimate the aerosol released by mechanical processes during CCI, Expert C multiplied the estimates of aerosol concentrations from the various sources noted above by the volume of gas CORCON calculated to be evolved during the first 12 h of CCI in the Peach Bottom TB scenario. He considered calculations that assumed both limestone and LS/CS concretes (Tables C-1 and C-2).

Table C-1
Some Mechanical Aerosol Generation Estimates

Source of Aerosol Estimate	Gases from Limestone Concrete		Gases from Limestone/Common Sand Concrete	
	Mass (kg)	Mass Fraction*	Mass (kg)	Mass Fraction*
VANESA	2.84	$1.42 * 10^{-5}$	1.08	$5.4 * 10^{-6}$
WITCH	0.0515	$2.6 * 10^{-7}$	0.0196	$9.8 * 10^{-8}$
CARBON BOIL**	155000	0.0775	870	0.0294

*Assuming $2*10^5$ kg of melt
**3100 g/m^3

Table C-2
Estimates Based Upon SURC 4 Results

Stage of SURC 4 Experiment	Gases From Limestone Concrete			Gases From Limestone/Common Sand Concrete	
	STP g/m^3	400 K g/m^3	Mass (kg)	Mass (kg)	Mass Fraction
Pre-zirconium Addition	< 0.66	< 0.45	23.2	8.81	$4.4 * 10^{-5}$
Zirconium Addition	< 43	< 29.3	1509	574	0.0029
Late period	< .045	< 0.031	1.6	0.61	$3.1 * 10^{-6}$

Based on the above information, the expert produced the following cumulative distribution (shown in Table C-3) for mechanical aerosol release fractions assuming gas volumes calculated by CORCON to be generated during the first 12 h of CCI in Peach Bottom assuming a limestone/common sand concrete.

Table C-3
Cumulative Distribution for Mechanical
Aerosol Release Fractions

Cumulative Weight	Release Fraction	Comment
0.01	10^{-8}	
0.05	10^{-7}	WITCH
0.25	$5*10^{-5}$	VANESA 1.00
0.50	$7.1*10^{-5}$	
0.75	10^{-3}	(SURC 4, upper limit)/3
0.95	0.03	Steel-making experience
0.99	0.1	

Results of Expert's Elicitation

1. BWR Results

A. Base Case Distributions for BWRs

Some of the data used by the Expert C to generate the base case distributions are presented in Table C-4 (Peach Bottom) and Table C-5 (Grand Gulf).

Table C-4
Summary of Peach Bottom FCCI Results Used by Expert C

	STCP and Stand-Alone CORCON/VANESA Results	MAAP Results
Tellurium	0.48 - 0.93; 0.966	~ 0.4
Strontium	0.62 - 0.88; 0.10, 0.95	0.18 - 0.48; 0.02
Lanthanum	0.015 - 0.07; 0.006	~ 0.02
Cerium	0.025 - 0.09; 0.006, 0.12	~ 0.02
Barium	0.44 - 0.67; 0.80	~ 0.07_5

In Table C-4, values separated by a hyphen represent a range of results that Expert C considered reasonable and representative of the cases at hand; values following the semicolon represent atypical values (e.g., sensitivity studies with extreme values of important parameters or accident sequences nonrepresentative of those of interest here). Expert C felt that the STCP-MAAP differences could be ascribed to some of the phenomenological uncertainties represented in his decomposition tree and therefore derived his base distribution primarily from the STCP results, since he believed that including the MAAP results in the base

distribution would be double counting the phenomenological uncertainties. He also noted that STCP-MAAP differences were rather small compared with his uncertainty ranges.

Table C-5
Summary of Grand Gulf FCCI Results Used by Expert C
(STCP Analyses, Reference 1)

	TC	TB	TBS
NG, Iodine, Cesium	1.0	1.0	1.0
Tellurium	0.19	0.35	0.23
Strontium	0.42	0.55	0.42
Ruthenium	3.6×10^{-7}	8.0×10^{-7}	2.5×10^{-7}
Lanthanum	0.029	0.037	0.024
Cerium	0.047	0.060	0.035
Barium	0.25	0.36	0.26

The expert stated that the data could be interpreted as implying that Grand Gulf has significantly lower releases than Peach Bottom. However, the only possibly important difference in the calculations is that the Grand Gulf cavity permits less spread of the debris. He believed that this would be expected to increase the releases, not decrease them. The expert assumed that the difference between the calculations represented typical case-to-case variability in the calculations and did not reflect actual differences between the plants. He therefore combined the two plants and produced results general to the BWRs considered in this analysis.

The base case BWR distributions produced by the expert are presented in Figure C-2.

B. **Subuncertainties Considered in BWRs.**

Seven uncertainties were considered by the expert that were not considered in the code calculations and experimental results that made up the base case distributions. The R-factor values and the respective weights assigned to them for the seven uncertainties are given below. In this issue, Expert C considered two specific questions related to VANESA's calculation of lanthanum and cerium releases, respectively: the assumption of La_2O_3 versus "$LaO_{1.5}$" and Ce (IV) oxide versus Ce(III) oxide in the condensed phase. In each case, VANESA assumes the first form, while assumption of the second can yield lower calculated releases.*

*This subject is discussed further in D. C. Williams and D. A. Powers, "Some Uncertainties in Radionuclide Release during Core-Concrete Interactions," SAND87-2558A, at the Second Symposium on Nuclear Reactor Severe Accident Chemistry, Third Chemical Congress of North America, Toronto, Canada, June 5-10, 1988.

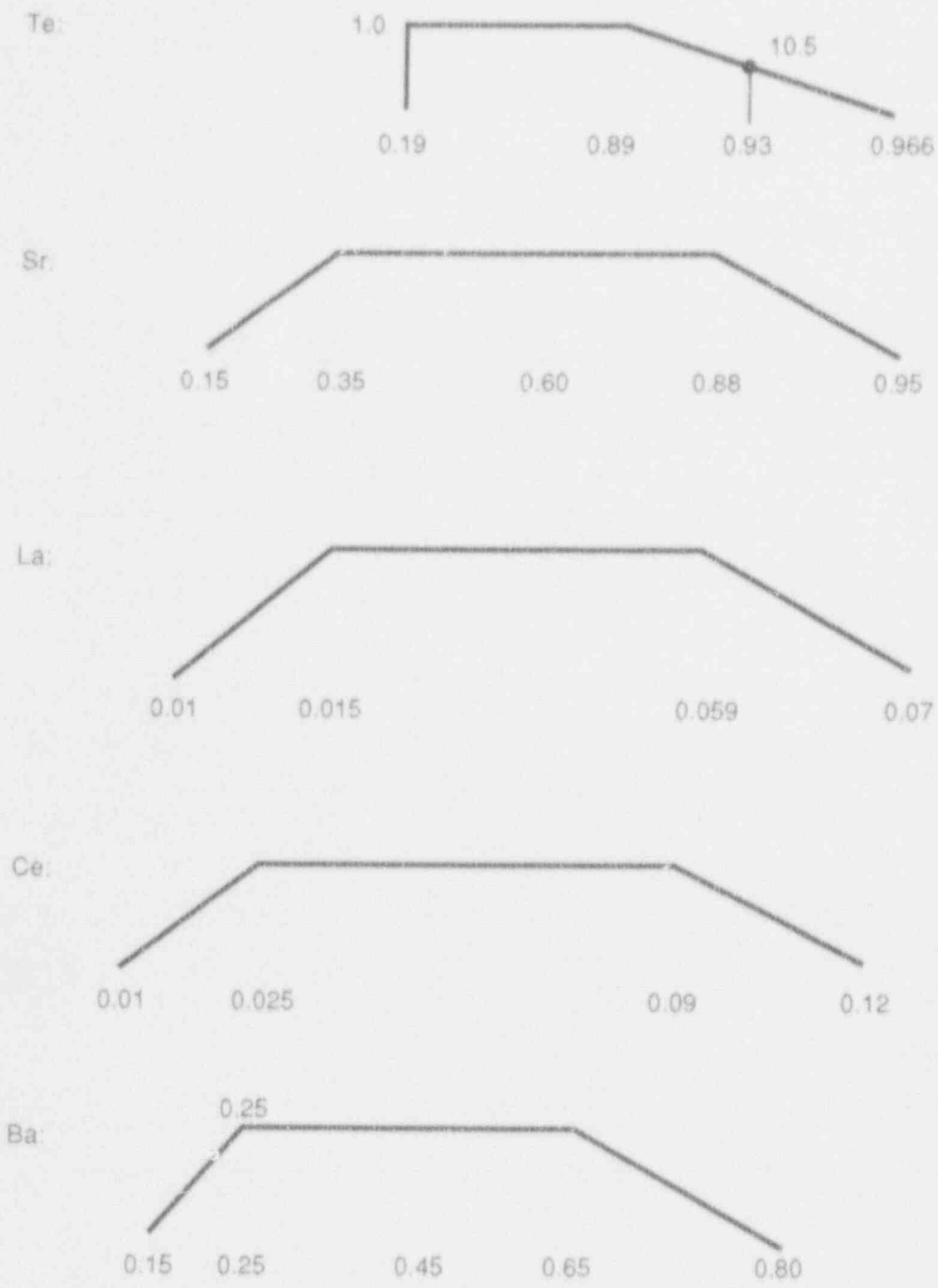

Figure C-2. BWR Base Distributions for CCI.

- Uncertainty in Condensed Phase Specification

  La R-value = 1.0, Weight (W) = 0.1
  R = 0.1, W = 0.9
  Ce R = 1.0, W = 0.2
  R = 0.0107, W = 0.8

  Lanthanum and cerium are the only species affected.

- Uncertainty in Oxygen Potential (OP) in the Oxidic Phase

  Expert C generally favors values that are close to the VANESA standard. The basis is that gas agitation likely mixes constituents during periods of maximum release.

  In Table C-6, OP is a measure of the degree to which oxygen transport from the oxide layer to the metallic layer results in oxygen potential equilibration between the layers OP=0 corresponds to complete equilibration (the VANESA assumption), while OP=1 corresponds to an H_2/H_2O ratio of 2 in the oxide layer independently of the metallic layer oxygen potential.*

Table C-6
R Values for Different Oxygen Potentials (Oxide Phase)

Nuclide	R for OP = 0.0 (Weight 0.34)	R for OP = 0.1 (Weight 0.33)	R for OP = .5-1 (Weight 0.33)	Comment
Tellurium				Unaffected by this uncertainty
Strontium	1.0	0.4	0.002	Standard condensed phase
Lanthanum	1.0	0.68	0.044	
Cerium	1.0	0.45	0.077	
Cesium	1.0	0.73	2.0	Alternate condensed phase
Barium	1.0	0.42	0.0163	

*For details see D. C. Williams and D. A. Powers, "Some Uncertainties in Radionuclide Release during Core-Concrete Interactions," SAND87-2558A, at the Second Symposium on Nuclear Reactor Severe Accident Chemistry, Third Chemical Congress of North America, Toronto, Canada, June 5-10, 1988.

- Uncertainty in Temperature

  This is calculated from vapor pressure using VANESA thermochemistry and T = 2500 ± 250 K. Values for species in the oxide layer depend somewhat on the oxygen potential. Refer to Table C-7.

Table C-7
R Values for Different Temperatures

Nuclide	R for T = 2250 (Weight 0.3)	R for T = 2500 (Weight 0.4)	R for T = 2750 (Weight 0.3)
Tellurium	0.405	1.0	2.11
Strontium	0.51	1.0	1.74
Lanthanum	0.11	1.0	6.1
Cerium	0.12	1.0	5.6
Barium	0.53	1.0	1.71

- Uncertainty in Concrete Type

  Some effects of silica are not modeled in the codes. However, there is only a marginal excess of silica over CaO in LS/CS concrete. Hence, these effects are neglected for the BWRs.

  The values that follow are based upon comparing CORCON/VANESA calculations for the Peach Bottom TB sequence with LS and LS/CS concrete.[C-1]

Table C-8
Release Parameters for Different Concrete Types

Nuclide	R for LS CON (Weight 0.33)	R for LS/CS (Weight 0.33)	R for TB CALC* (Weight 0.34)
Tellurium	1.0	0.47	0.22
Strontium	1.0	0.53	0.28
Lanthanum	1.0	0.28	0.078
Cerium	1.0	0.33	0.108
Barium	1.0	0.58	0.340

- Uncertainty in Effect of Overlying Water

  The codes (and some experiments) suggest that there is not much effect, but the codes neglect the possible effects of crust formation and the available experimental data are limited. BWR CCIs generate a lot of heat, and crust formation may be minimal.

Table C-9
R Values for Effect of Overlying Water

Nuclide	R (Weight 0.5)	R (Weight 0.3)	R (Weight 0.2)	Comment
All	1.0	0.5	0.1	All species assigned these values

- Uncertainty in Free Energies of Formation

  Expert C included in this category uncertainties in the free energies of formation of the various radionuclide vapor species, as well as uncertainties in the free energies of the condensed phase when in the pure state. He did not attempt a detailed species-by-species assessment of the available data base; rather, he relied upon the general observation that free energy uncertainties of the order of 10 kcal/g-mole are rather common in high-temperature thermodynamic data, and free energy uncertainties of this magnitude would contribute roughly an order of magnitude uncertainty in vapor pressures at CCI temperatures.

Table C-9a
R Values for Free Energy Uncertainties

Nuclide	Low Value (Weight 0.25)	Intermediate Value (Weight 0.5)	High Value (Weight 0.25)
All	0.1	1.0	10.0

- Uncertainty in Activity Coefficients

  Expert C included in this category all interactions within the melt that would introduce errors into VANESA's treatment of the melt as being an ideal solution. Again, he did not attempt a detailed species-by-species assessment, except to note that the effects of nonideality are likely smaller for the metallic phase than for the oxidic phase of the melt. Hence, he assigned a smaller range of R values for tellurium than for the other species.

Table C-9b
R Values for Activity Coefficients

Nuclide	Low Value (Weight 0.25)	Intermediate Value (Weight 0.5)	High Value (Weight 0.25)
Tellurium	0.32	1.0	3.2
Strontium, Lanthanum, Cerium, Barium	0.1	1.0	10.0

- Uncertainty in Zirconium Oxidation.

  The extent of in-vessel oxidation of zirconium is potentially significant because it affects the amount of metallic zirconium in the melt, which is known to be important to CCI. However, Expert C did not believe that in-vessel oxidation is likely to be sufficient to deplete the melt of zirconium, so all BWR melts could be considered to be zirconium rich. Hence, he did not consider uncertainties for in-vessel zirconium oxidation for BWR melts.

- Effect of Revisions to the VANESA Thermochemical Data Base.

  All the STCP calculations Expert C used to define his base distributions were performed with VANESA Version 1.0. Calculations using the more recent Version 1.01 resulted in significantly different release fractions in some cases.* By comparing vapor pressures calculated using the thermochemical data incorporated into the two code version, he concluded that changes to these thermochemical data were the principal

*D. C. Williams and D. A. Powers, "Some Uncertainties in Radionuclide Release during Core-Concrete Interactions," SAND87-2553A, presented at the Second Symposium on Nuclear Reactor Severe Accident Chemistry, Third Chemical Congress of North America, Toronto, Canada, June 5-10, 1988.

reason for the differences in the results. He felt that these changes did not reflect clearly improved new data; rather, they reflected uncertainties and ambiguities in the underlying thermochemical data base used in developing both code versions. Hence, he viewed the differences as representative of those arising because of uncertainties in the free energies, rather than one data set being "right" and the other "wrong."

These differences did not exceed the uncertainty range he had allotted to free energy uncertainties, and the expert therefore felt no need to broaden his distributions to reflect these differences. However, he believed his distributions should acknowledge the implications of the data set used by the newer code version in some degree. Hence, he shifted his base distributions for $RCCI_i$ by a factor equal to the square root of the ratio (VANESA 1.1 release)/(VANESA 1.0 release) for the Peach Bottom TB sequence; thus, for this particular analysis, the shifted release values correspond to the geometric mean of the two code results. For tellurium, lanthanum, and cerium, the respective shift factors were 1.98, 0.67, and 2.49. For strontium and barium, differences between the two code results were very small, and no shift factors were applied. (The base distributions given in the tables that follow are the unshifted values.)

C. Final BWR Distributions

The final release fraction distributions are presented in Tables C-10 to C-19.

Table C-10
BWRs: Tellurium, Dry Cavity

Cumulative Weight	Final Distribution
1.000E-02	5.402E-03
5.000E-02	1.804E-02
2.500E-01	1.315E-01
5.000E-01	4.754E-01
7.500E-01	9.200E-01
9.500E-01	9.500E-01
9.900E-01	9.900E-01

Table C-11
BWRs: Tellurium, Wet Cavity

Cumulative Weight	Final Distribution
1.000E-02	1.572E-03
5.000E-02	6.853E-03
2.500E-01	6.394E-02
5.000E-01	2.870E-01
7.500E-01	8.170E-01
9.500E-01	9.400E-01
9.900E-01	9.900E-01

Table C-12
BWRs: Strontium, Dry Cavity

Cumulative Weight	Final Distribution
1.000E-02	7.425E-06
5.000E-02	5.615E-05
2.500E-01	2.770E-03
5.000E-01	5.246E-02
7.500E-01	4.584E-01
9.500E-01	7.500E-01
9.900E-01	9.500E-01

Table C-13
BWRs: Strontium, Wet Cavity

Cumulative Weight	Final Distribution
1.000E-02	2.822E-06
5.000E-02	2.531E-05
2.500E-01	1.350E-03
5.000E-01	2.662E-02
7.500E-01	2.853E-01
9.500E-01	7.000E-01
9.900E-01	9.200E-01

Table C-14
BWRs: Lanthanum, Dry Cavity

Cumulative Weight	Final Distribution
1.000E-02	7.024E-08
5.000E-02	6.602E-07
2.500E-01	1.737E-05
5.000E-01	1.853E-04
7.500E-01	1.903E-03
9.500E-01	3.000E-02
9.900E-01	1.000E-01

Table C-15
BWRs: Lanthanum, Wet Cavity

Cumulative Weight	Final Distribution
1.000E-02	2.955E-08
5.000E-02	2.884E-07
2.500E-01	8.590E-06
5.000E-01	9.784E-05
7.500E-01	1.070E-03
9.500E-01	1.000E-02
9.900E-01	5.000E-02

Table C-16
BWRs: Cerium, Dry Cavity

Cumulative Weight	Final Distribution
1.000E-02	5.137E-07
5.000E-02	3.431E-06
2.500E-01	7.061E-05
5.000E-01	6.591E-04
7.500E-01	6.475E-03
9.500E-01	7.000E-02
9.900E-01	2.000E-01

Table C-17
BWRs: Cerium, Wet Cavity

Cumulative Weight	Final Distribution
1.000E-02	1.772E-07
5.000E-02	1.394E-06
2.500E-01	3.387E-05
5.000E-01	3.405E-04
7.500E-01	3.571E-03
9.500E-01	4.000E-02
9.900E-01	1.200E-01

Table C-18
BWRs: Barium, Dry Cavity

Cumulative Weight	Final Distribution
1.000E-02	4.668E-05
5.000E-02	3.377E-04
2.500E-01	7.077E-03
5.000E-01	6.120E-02
7.500E-01	3.874E-01
9.500E-01	6.500E-01
9.900E-01	9.200E-01

Table C-19
BWRs: Barium, Wet Cavity

Cumulative Weight	Final Distribution
1.000E-02	1.877E-05
5.000E-02	1.442E-04
2.500E-01	3.438E-03
5.000E-01	3.152E-02
7.500E-01	2.382E-01
9.500E-01	6.000E-01
9.900E-01	8.800E-01

2. PWR Results

A. **Base Case Distributions for PWRs**

Some of the data used by Expert C to generate the base case distributions are presented in Table C-20 (Surry), Table C-21 (Zion), and Table C-22 (Sequoyah).

The base distributions for Surry were built using calculations in BMI-2139,[C-1] BMI-2160[C-2] and some sensitivity calculations by Dave Bradley. The expert also considered some of the high release fractions calculated in BMI-2104.[C-3]

After evaluating the Zion data, he noted that some release fractions tended to be higher than those in recent Surry analyses, but the scenarios were different and direct comparisons of the results may not be appropriate. Running Surry TMLB' calculations with a LS/CS concrete resulted in releases similar to those for calculations using basaltic concrete with the exception of the lanthanum and cerium releases, which were somewhat lower for the LS/CS concrete. The expert therefore used the same base release distributions for the Zion and Surry releases. The predicted releases for Sequoyah tended to be higher than the predicted Surry releases. Running the Surry TMLB' analysis with a limestone concrete (as in Sequoyah) also yielded higher releases. Separate base distributions were therefore used for Sequoyah.

The base distributions used by the expert are presented in Figures C-3 and C-4.

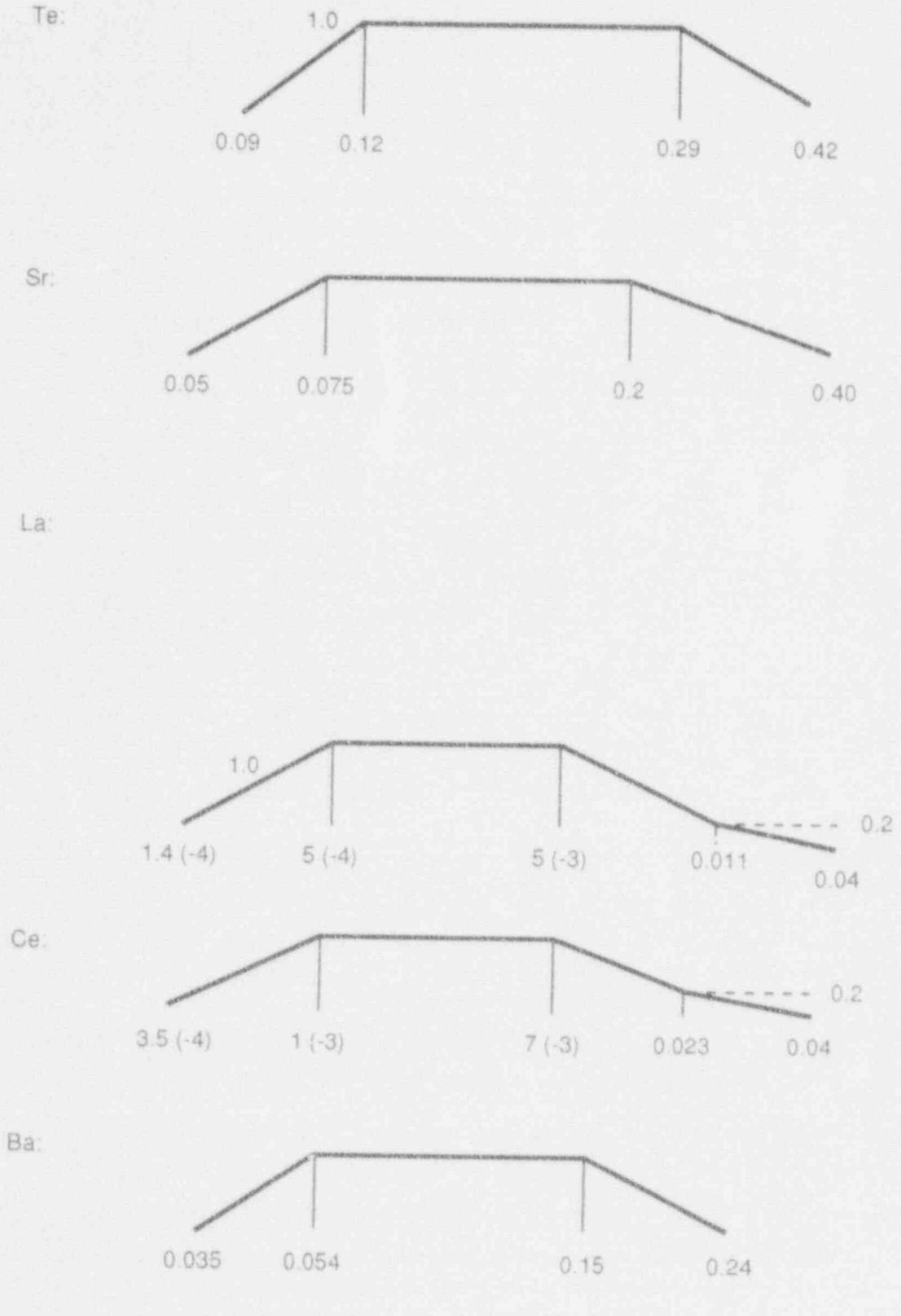

Figure C-3. Distribution for Surry and Zion.

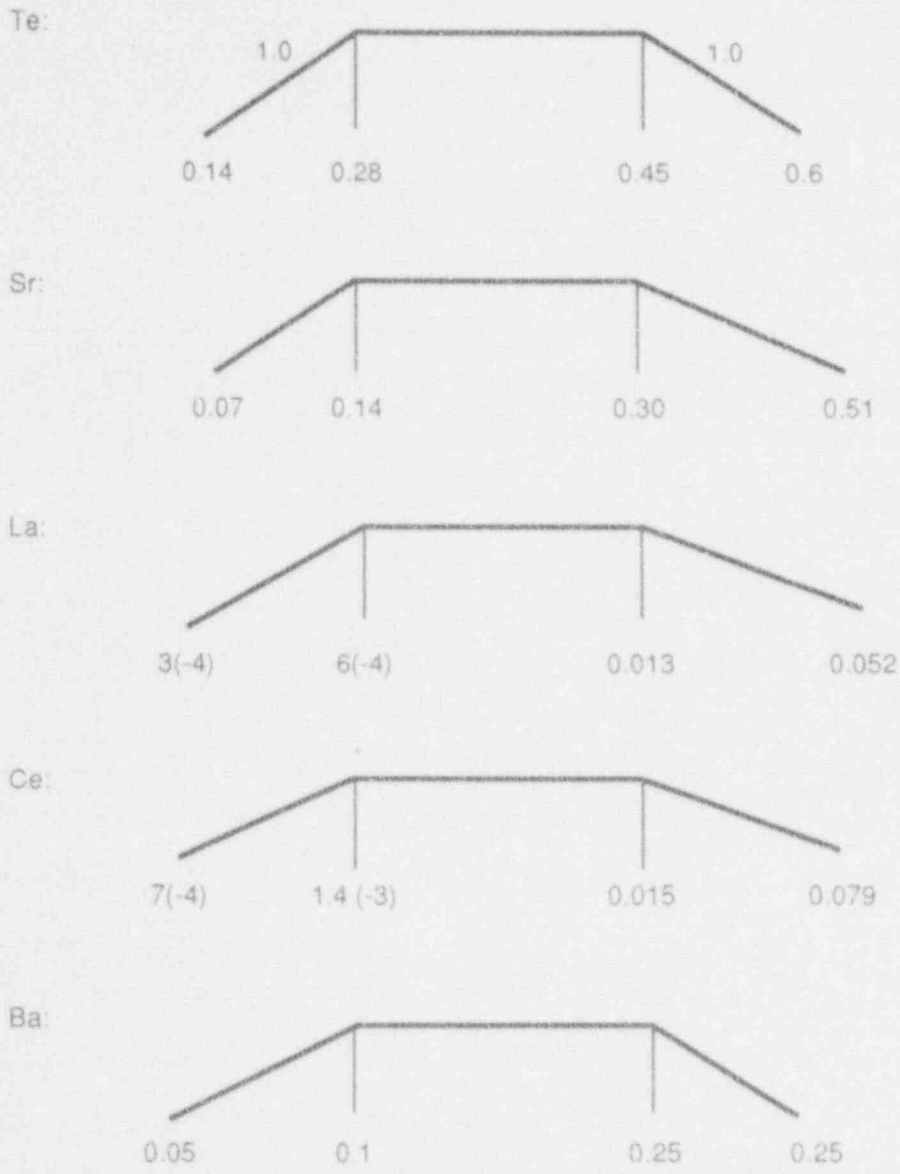

Figure C-4. Distribution for Sequoyah.

Table C-20
Previous Data on Core-Concrete Interactions
Release Fractions

Surry

	Old Surry	From BMI-2139 and BMI-2160	From Bradley Calculations
Tellurium	0.3-0.42	0.13-0.15	0.09-0 23; .29*
Strontium	0.08-0.34	0.09	0.086-0.155; 0.40*
Ruthenium		6(-7)-4(-9)	
Lanthanum	2(-4)- .04	4.2(-3)-3.7(-3)	5(-4)-5(-3); .011*
Cerium		9(-4)-1(-3)	0.001-0.007;0.023*
Barium		0.06	0.058-0.096;0.24*

*Maximum case.

Table C-21
Previous Data on Core-Concrete Interactions
Release Fractions

Zion

	From BMI-2139	Surry TMLB' with LS/CS Concrete
Tellurium	0.36-0.47	0.114
Strontium	0.10-0 34; 1.5(-4)	0.073
Ruthenium	9(-7)-3.9(-6), 2.4(-3)	
Lanthanum	5(-3)-7.4(-3); 8.7(-6)	1.4(-4)
Cerium	1.7(-3)-7.7(-3); 4.8(-7)	3.5(-4)
Barium	0.076-0.23; 1.5(-3)	0.050

Table C-22
Previous Data on Core-Concrete Interactions
Release Fractions

Sequoyah

	From BMI-2139 and BMI-2166	ACD Results	Surry TMLB'with LS/CS Concrete
Tellurium	0.3-0.7	0.22	0.28
Strontium	0.17-0.19	0.51	0.14
Ruthenium	2.5(-6)-6(-6)	8(-7)	
Lanthanum	8.0(-3)-1.3(-2)	0.052	63(-4)
Cerium	5.6(-)-1.2(-2)	0.079	1.4(-3)
Barium	0.10-0.11	0.27	0.11

B. Subuncertainties Considered in PWRs

Seven PWR uncertainties were considered by the expert which he felt were not adequately represented by the code calculations and experimental results that made up the base case distributions. The R-values and the respective weights assigned to them for the seven uncertainties are presented below.

- Uncertainty in Zirconium Oxidation

  The expert defined the high zirconium cases as having 75% unoxidized metal remaining in the debris and the low zirconium cases as 40% unoxidized metal remaining in the debris.

  For the low zirconium case the R is .707 for all radionuclides except tellurium--R for tellurium = .822. The weight for this case is 1.0.

  For the high zirconium case the R is 1.414 for all radionuclides except tellurium--R for tellurium = 1.22. The weight for this case is 1.0.

- Uncertainty in Condensed Phase Speciation

  R-values and weights are the same as given for the BWP uncertainties.

- Uncertainty in Oxygen Potential

  R-values and weights are the same as given for the BWR uncertainties.

- Uncertainty in Effect of Overlying Water

  R-values and weights are the same as given for the BWR uncertainties.

- Uncertainty in Temperature

  R-values and weights are the same as given for the BWR uncertainties.

- Uncertainty in Activity Coefficients

  R-values and weights are the same as given for the BWR uncertainties.

- Uncertainty in Free Energy

  R-values and weights are the same as given for the BWR uncertainties. The changes to the VANESA data base were also treated as was done for the BWRs.

C. **Final PWR Distributions**

The final release fraction distributions are presented in Tables C-23 to C-62.

Table C-23
Surry and Zion: Tellurium, Dry Cavity, Low Zr

Cumulative Weight	Final Distribution
1.000E-02	4.663E-03
5.000E-02	1.252E-02
2.500E-01	7.827E-02
5.000E-01	2.863E-01
7.500E-01	7.494E-01
9.500E-01	9.200E-01
9.900E-01	9.800E-01

Table C-24
Surry and Zion: Tellurium, Wet Cavity, Low Zr

Cumulative Weight	Final Distribution
1.000E-02	1.212E-03
5.000E-02	4.718E-03
2.500E-01	3.739E-02
5.000E-01	1.643E-01
7.500E-01	5.450E-01
9.500E-01	9.000E-01
9.900E-01	9.700E-01

Table C-25
Surry and Zion: Tellurium, Dry Cavity, High Zr

Cumulative Weight	Final Distribution
1.000E-02	6.963E-03
5.000E-02	1.867E-02
2.500E-01	1.147E-01
5.000E-01	3.961E-01
7.500E-01	8.737E-01
9.500E-01	9.300E-01
9.900E-01	9.900E-01

Table C-26
Surry and Zion: Tellurium, Wet Cavity, High Zr

Cumulative Weight	Final Distribution
1.000E-02	1.811E-03
5.000E-02	7.046E-03
2.500E-01	5.538E-02
5.000E-01	2.353E-01
7.500E-01	6.919E-01
9.500E-01	9.200E-01
9.900E-01	9.800E-01

Table C-27
Surry and Zion: Strontium, Dry Cavity, Low Zr

Cumulative Weight	Final Distribution
1.000E-02	1.963E-06
5.000E-02	1.527E-05
2.500E-01	6.914E-04
5.000E-01	1.346E-02
7.500E-01	1.311E-01
9.500E-01	4.500E-01
9.900E-01	8.000E-01

Table C-28
Surry and Zion: Strontium, Wet Cavity, Low Zr

Cumulative Weight	Final Distribution
1.000E-02	8.435E-07
5.000E-02	7.172E-06
2.500E-01	3.320E-04
5.000E-01	6.620E-03
7.500E-01	7.620E-02
9.500E-01	4.000E-01
9.900E-01	7.500E-01

Table C-29
Surry and Zion: Strontium, Dry Cavity, High Zr

Cumulative Weight	Final Distribution
1.000E-02	3.925E-06
5.000E-02	3.055E-05
2.500E-01	1.382E-03
5.000E-01	2.674E-02
7.500E-01	2.450E-01
9.500E-01	6.000E-01
9.900E-01	9.000E-01

Table C-30
Surry and Zion: Strontium, Wet Cavity, High Zr

Cumulative Weight	Final Distribution
1.000E-02	1.687E-06
5.000E-02	1.434E-05
2.500E-01	6.641E-04
5.000E-01	1.320E-02
7.500E-01	1.466E-01
9.500E-01	5.000E-01
9.900E-01	8.500E-01

Table C-31
Surry and Zion: Lanthanum, Dry Cavity, Low Zr

Cumulative Weight	Final Distribution
1.000E-02	1.060E-08
5.000E-02	9.621E-08
2.500E-01	5.000E-06
5.000E-01	7.100E-05
7.500E-01	1.000E-03
9.500E-01	3.000E-02
9.900E-01	1.000E-01

Table C-32
Surry and Zion: Lanthanum, Wet Cavity, Low Zr

Cumulative Weight	Final Distribution
1.000E-02	4.361E-09
5.000E-02	4.122E-08
2.500E-01	1.226E-06
5.000E-01	1.382E-05
7.500E-01	1.498E-04
9.500E-01	3.990E-03
9.900E-01	2.226E-02

Table C-33
Surry and Zion: Lanthanum, Dry Cavity, High Zr

Cumulative Weight	Final Distribution
1.000E-02	2.120E-09
5.000E-02	1.924E-07
2.500E-01	4.994E-06
5.000E-01	7.100E-05
7.500E-01	1.000E-03
9.500E-01	3.000E-02
9.900E-01	1.000E-01

Table C-34
Surry and Zion: Lanthanum, Wet Cavity, High Zr

Cumulative Weight	Final Distribution
1.000E-02	8.722E-09
5.000E-02	8.243E-08
2.500E-01	2.452E-06
5.000E-01	2.764E-05
7.500E-01	2.997E-04
9.500E-01	7.963E-03
9.900E-01	5.000E-02

Table C-35
Surry and Zion: Cerium, Dry Cavity, Low Zr

Cumulative Weight	Final Distribution
1.000E-02	9.385E-08
5.000E-02	5.729E-07
2.500E-01	1.173E-05
5.000E-01	1.070E-04
7.500E-01	1.035E-03
9.500E-01	3.000E-02
9.900E-01	1.000E-01

Table C-36
Surry and Zion: Cerium, Wet Cavity, Low Zr

Cumulative Weight	Final Distribution
1.000E-02	3.001E-08
5.000E-02	2.319E-07
2.500E-01	5.563E-06
5.000E-01	5.531E-05
7.500E-01	5.745E-04
9.500E-01	1.694E-02
9.900E-01	8.000E-02

Table C-37
Surry and Zion: Cerium, Dry Cavity, High Zr

Cumulative Weight	Final Distribution
1.000E-02	1.877E-07
5.000E-02	1.146E-06
2.500E-01	2.346E-05
5.000E-01	2.140E-04
7.500E-01	2.068E-03
9.500E-01	5.420E-02
9.900E-01	1.500E-01

Table C-38
Surry and Zion: Cerium, Wet Cavity, High Zr

Cumulative Weight	Final Distribution
1.000E-02	6.002E-08
5.000E-02	4.638E-07
2.500E-01	1.113E-05
5.000E-01	1.106E-04
7.500E-01	1.148E-03
9.500E-01	3.360E-02
9.900E-01	1.000E-01

Table C-39
Surry and Zion: Barium, Dry Cavity, Low Zr

Cumulative Weight	Final Distribution
1.000E-02	1.057E-05
5.000E-02	8.334E-05
2.500E-01	1.624E-03
5.000E-01	1.426E-02
7.500E-01	9.923E-02
9.500E-01	3.500E-01
9.900E-01	7.000E-01

Table C-40
Surry and Zion: Barium, Wet Cavity, Low Zr

Cumulative Weight	Final Distribution
1.000E-02	4.779E-06
5.000E-02	3.556E-05
2.500E-01	8.027E-04
5.000E-01	7.198E-03
7.500E-01	5.740E-02
9.500E-01	3.000E-01
9.900E-01	6.500E-01

Table C-41
Surry and Zion: Barium, Dry Cavity, High Zr

Cumulative Weight	Final Distribution
1.000E-02	2.113E-05
5.000E-02	1.667E-04
2.500E-01	3.246E-03
5.000E-01	2.831E-02
7.500E-01	1.886E-01
9.500E-01	5.000E-01
9.900E-01	8.500E-01

Table C-42
Surry and Zion: Barium, Wet Cavity, High Zr

Cumulative Weight	Final Distribution
1.000E-02	9.558E-06
5.000E-02	7.113E-05
2.500E-01	1.604E-03
5.000E-01	1.434E-02
7.500E-01	1.115E-01
9.500E-01	4.000E-01
9.900E-01	8.000E-01

Table C-43
Sequoyah: Tellurium, Dry Cavity, Low Zr

Cumulative Weight	Final Distribution
1.000E-02	8.581E-03
5.000E-02	2.312E-02
2.500E-01	1.399E-01
5.000E-01	4.628E-01
7.500E-01	8.500E-01
9.500E-01	9.500E-01
9.900E-01	9.900E-01

Table C-44
Sequoyah: Tellurium, Wet Cavity, Low Zr

Cumulative Weight	Final Distribution
1.000E-02	2.249E-03
5.000E-02	8.677E-03
2.500E-01	6.766E-02
5.000E-01	2.782E-01
7.500E-01	7.642E-01
9.500E-01	9.300E-01
9.900E-01	9.800E-01

Table C-45
Sequoyah: Tellurium, Dry Cavity, High Zr

Cumulative Weight	Final Distribution
1.000E-02	1.280E-02
5.000E-02	3.437E-02
2.500E-01	2.017E-01
5.000E-01	6.050E-01
7.500E-01	9.200E-01
9.500E-01	9.700E-01
9.900E-01	9.900E-01

Table C-46
Sequoyah: Tellurium, Wet Cavity, High Zr

Cumulative Weight	Final Distribution
1.000E-02	3.360E-03
5.000E-02	1.295E-02
2.500E-01	9.945E-02
5.000E-01	3.858E-01
7.500E-01	8.847E-01
9.500E-01	9.500E-01
9.900E-01	9.900E-01

Table C-47
Sequoyah: Strontium, Dry Cavity, Low Zr

Cumulative Weight	Final Distribution
1.000E-02	3.056E-06
5.000E-02	2.401E-05
2.500E-01	1.060E-03
5.000E-01	2.078E-02
7.500E-01	1.952E-01
9.500E-01	5.500E-01
9.900E-01	8.500E-01

Table C-47
Sequoyah: Strontium, Wet Cavity, Low Zr

Cumulative Weight	Final Distribution
1.000E-02	1.327E-06
5.000E-02	1.124E-05
2.500E-01	5.133E-04
5.000E-01	1.023E-02
7.500E-01	1.156E-01
9.500E-01	4.700E-01
9.900E-01	8.000E-01

Table C-48
Sequoyah: Strontium, Dry Cavity, High Zr

Cumulative Weight	Final Distribution
1.000E-02	6.112E-06
5.000E-02	4.802E-05
2.500E-01	2.119E-03
5.000E-01	4.112E-02
7.500E-01	3.523E-01
9.500E-01	7.000E-01
9.900E-01	9.500E-01

Table C-50
Sequoyah: Strontium, Wet Cavity, High Zr

Cumulative Weight	Final Distribution
1.000E-02	2.653E-06
5.000E-02	2.248E-05
2.500E-01	1.026E-03
5.000E-01	2.035E-02
7.500E-01	2.178E-01
9.500E-01	6.000E-01
9.900E-01	9.000E-01

Table C-51
Sequoyah: Lanthanum, Dry Cavity, Low Zr

Cumulative Weight	Final Distribution
1.000E-02	1.999E-08
5.000E-02	1.917E-07
2.500E-01	5.220E-06
5.000E-01	7.100E-05
7.500E-01	1.000E-03
9.500E-01	3.000E-02
9.900E-01	1.000E-01

Table C-52
Sequoyah: Lanthanum, Wet Cavity, Low Zr

Cumulative Weight	Final Distribution
1.000E-02	8.657E-09
5.000E-02	8.404E-08
2.500E-01	2.566E-06
5.000E-01	2.963E-05
7.500E-01	3.342E-04
9.500E-01	9.075E-03
9.900E-01	4.000E-02

Table C-53
Sequoyah: Lanthanum, Dry Cavity, High Zr

Cumulative Weight	Final Distribution
1.000E-02	3.999E-08
5.000E-02	3.835E-07
2.500E-01	1.044E-05
5.000E-01	1.130E-04
7.500E-01	1.189E-03
9.500E-01	3.028E-02
9.900E-01	1.300E-01

Table C-54
Sequoyah: Lanthanum, Wet Cavity, High Zr

Cumulative Weight	Final Distribution
1.000E-02	1.731E-08
5.000E-02	1.681E-07
2.500E-01	5.131E-06
5.000E-01	5.927E-05
7.500E-01	6.683E-04
9.500E-01	1.300E-02
9.900E-01	8.000E-02

Table C-55
Sequoyah: Cerium, Dry Cavity, Low Zr

Cumulative Weight	Final Distribution
1.000E-02	1.813E-07
5.000E-02	1.109E-06
2.500E-01	2.280E-05
5.000E-01	2.117E-04
7.500E-01	2.082E-03
9.500E-01	5.582E-02
9.900E-01	1.500E-01

Table C-56
Sequoyah: Cerium, Wet Cavity, Low Zr

Cumulative Weight	Final Distribution
1.000E-02	5.597E-08
5.000E-02	4.384E-07
2.500E-01	1.088E-05
5.000E-01	1.097E-04
7.500E-01	1.156E-03
9.500E-01	3.470E-02
9.900E-01	1.100E-01

Table C-57
Sequoyah: Cerium, Dry Cavity, High Zr

Cumulative Weight	Final Distribution
1.000E-02	3.625E-07
5.000E-02	2.217E-06
2.500E-01	4.560E-05
5.000E-01	4.235E-04
7.500E-01	4.160E-03
9.500E-01	1.085E-01
9.900E-01	2.000E-01

Table C-58
Sequoyah: Cerium, Wet Cavity, High Zr

Cumulative Weight	Final Distribution
1.000E-02	1.119E-07
5.000E-02	8.768E-07
2.500E-01	2.176E-05
5.000E-01	2.193E-04
7.500E-01	2.310E-03
9.500E-01	6.820E-02
9.900E-01	1.500E-01

Table C-59
Sequoyah: Barium, Dry Cavity, Low Zr

Cumulative Weight	Final Distribution
1.000E-02	1.829E-05
5.000E-02	1.402E-04
2.500E-01	2.782E-03
5.000E-01	2.437E-02
7.500E-01	1.661E-01
9.500E-01	4.500E-01
9.900E-01	7.700E-01

Table C-60
Sequoyah: Barium, Wet Cavity, Low Zr

Cumulative Weight	Final Distribution
1.000E-02	7.975E-06
5.000E-02	6.019E-05
2.500E-01	1.375E-03
5.000E-01	1.233E-02
7.500E-01	9.726E-02
9.500E-01	4.000E-01
9.900E-01	7.000E-01

Table C-61
Sequoyah: Barium, Dry Cavity, High Zr

Cumulative Weight	Final Distribution
1.000E-02	3.659E-05
5.000E-02	2.804E-04
2.500E-01	5.557E-03
5.000E-01	4.814E-02
7.500E-01	3.046E-01
9.500E-01	6.000E-01
9.900E-01	9.000E-01

Table C-62
Sequoyah: Barium, Wet Cavity, High Zr

Cumulative Weight	Final Distribution
1.000E-02	1.595E-05
5.000E-02	1.204E-04
2.500E-01	2.748E-03
5.000E-01	2.451E-02
7.500E-01	1.851E-01
9.500E-01	5.000E-01
9.900E-01	8.500E-01

D. Cesium and Iodine Releases for BWRs and PWRs

VANESA almost always calculates 100% release; however, this expert felt that nothing was ever 100%. The expert therefore provided the distribution for cesium/iodine release fractions in Table C-63.

Table C-63
Release Fractions for Cs and I (all cases)

Cumulative Weight	Release Fraction No Water	Release Fraction With Water
0.01	0.01	0.003
0.05	0.1	0.05
0.25	0.75	0.60
0.50	0.90	0.80
0.75	0.95	0.90
0.95	0.99	0.97
0.99	0.999	0.995

E. Molybdenum and Ruthenium Releases for BWRs and PWRs

The molybdenum and ruthenium releases are grouped together as ruthenium releases. The expert referenced VANESA calculation that usually calculate small releases (typically $<10^{-5}$) and John Brockman of Sandia. VANESA can give a significant release if $H_2O/H_2 > 1.0$; this may overestimate the effect because it does not treat $Mo \rightarrow MoO_2$ in the condensed phase. However, Brockman states that molybdenum is released in experiments with oxide melts, but not with metallic melts.

F. Since ruthenium seems extremely unlikely to volatilize during the core concrete interaction, the releases of the "Ru" group are generally not greater than the mechanical aerosol release. The distribution is presented in Table C-64.

Table C-64
Ru Group Release (all cases)

Cumulative Weight	Release Fraction No Water	Release Fraction With Water
0.01	10^{-8}	2×10^{-9} (*)
0.05	10^{-7}	2×10^{-8} (*)
0.25	5×10^{-6}	10^{-6} (*)
0.5	7.1×10^{-5}	1.4×10^{-5} (*)
0.75	10^{-3}	2×10^{-4} (*)
0.95	0.05	0.03
0.99	0.25	0.15

(*)Based on mechanical aerosol release; arbitrarily divided by 5 for net (?) case.

Sources of Uncertainty

The R and W values directly reflect the importance Expert C assigned to the uncertainties that he explicitly included in his decomposition tree discussed in connection with Figure C-1. He felt that the dominant source of uncertainty was phenomenological uncertainty (including thermochemical data uncertainties) in the models for CCIs and associated radionuclide release. He thought that the uncertainty "inherited" from the uncertainties in the in-vessel analysis was significant but less than that associated with CCI phenomenology. Uncertainty resulting from the need to group a range of accident scenarios in a single case might be nontrivial, but he expected that it would prove less than either the CCI phenomenological uncertainty or the in-vessel "inherited" uncertainty.

Correlation with Other Variables

Expert C did not specify any correlations between FCCI and other variables, other than the correlations defined by the case structure.

Suggested Methods for Reducing Uncertainty

Expert C believed that small-scale thermochemical experiments could prove quite useful in reducing the uncertainties of condensed phase speciation, free energies of formation, and activity coefficients. The other uncertainties reflect primarily uncertainties in the thermochemical boundary conditions imposed upon the vaporization process. Reducing these uncertainties will require improvements to the mechanistic models for CCI processes and the associated radionuclide releases. He felt that it might be quite difficult to resolve some of the issues involved, such as the

oxygen potential governing vaporization from the oxidic phase. Fairly large scale experiments with melts having prototypic chemistries (including especially zirconium-containing melts) will be needed for code validation. Experiments with prototypic melts will also be needed to resolve such questions as the effect of overlying water pools and mechanical aerosol generation; the latter, at least, may not require large-scale experiments (smaller-scale experiments with gas sparging may be sufficient). Reduction of the uncertainty "inherited" from the in-vessel analysis obviously requires improved modeling of the in-vessel accident progression.

The uncertainty related to concrete type in the BWRs could be resolved by definitely determining the concrete type and then rerunning at least some of the STCP calculations with the correct concrete type. (The expert felt that there has been so much confusion as to concrete type that it might be necessary to analyze chemically a sample actually taken from the cavity floor in order to be certain.)

REFERENCES

C-1. R. S. Denning et al., "Supplemental Radionuclide Release Calculations for Selected Severe Accident Scenarios," Vols. I-V, NUREG/CR-4624, BMI-2139, Battelle Memorial Institute, 1986.

C-2. M. T. Leonard et al., "Supplemental Radionuclide Release Calculations for Selected Severe Accident Scenarios," NUREG/CR-5062, BMI-2160, Battelle Memorial Institute, 1987.

C-3. J. A. Gieseke et al., "Radionuclide Release Under Specific LWR Accident Conditions," Vol. IV: PWR Ice Condenser Design, BMI-2104, Battelle Memorial Institute, 1984.

C-4. D. R. Bradley and A. W. Shiver, "Uncertainty in the Ex-Vessel Source Term Caused by Uncertainty in In-Vessel Models," in Proceedings of the International ANS/ENS Topical Meeting on Thermal Reactor Safety 3 XVII.4, San Diego, CA, February 2-6, 1986.

5.5 Release of Fission Products from Containment for Surry, Zion, Sequoyah, Peach Bottom, and Grand Gulf--FCONV & FCONC

Summary and Aggregation of Expert Panel's Assessment of Source Term Issue 5--FCONV, FCONC

Experts consulted: Andrzej Drozd, Stone & Webster Engineering Corp; James Gieseke, Battelle Memorial Institute; Thomas Kress, Oak Ridge National Laboratory; Ben Y. H. Liu, University of Minnesota; David Williams, Sandia National Laboratory.

Issue Description

This issue attempts to characterize the fraction of radionuclides released to the containment atmosphere that would be released from the containment in a containment failure. Radionuclides arising from two sources are considered: those released to the containment atmosphere at or before vessel breach and those released to the containment atmosphere subsequent to vessel breach because of core-concrete interactions (CCIs).

The fractions associated with these two sources are referred to as FCONV and FCONC, where

$FCONV = mV_{out}/mV_{in}$;

mV_{in} = mass (kg) of a radionuclide (or radionuclide class) released from the vessel to the containment atmosphere at or before vessel breach;

mV_{out} = mass (kg) of a radionuclide (or radionuclide group) released from the vessel to the containment atmosphere at or before vessel breach that is subsequently released from containment;

and

$FCONC = mC_{out}/mC_{in}$;

mC_{in} = mass (kg) of a radionuclide (or radionuclide group) released to the containment atmosphere after vessel breach because of CCI;

mC_{out} = mass (kg) of a radionuclide (or radionuclide group) released to the containment atmosphere after vessel breach because of CCI that is subsequently released from the containment.

Values for FCONV and FCONC will be determined for a number of different cases involving both PWRs and BWRs. The following terminology is used in conjunction with these cases. For FCONV, "early" means at or before vessel breach, and "late" means at least 3.5 h after vessel breach (nominally 6 h after vessel breach). For FCONC, "early" means before the start of CCI,

and "late" means after the bulk of CCI has occurred (taken to be about 3.5 h after the start of CCI). Containment failures are divided into leaks and ruptures. A "rupture" is assumed to be a breach in the containment sufficient to depressurize the containment in 2 h or less. A "leak" is assumed to be a breach in the containment that is larger than the design leakage and would arrest slow pressurization but would not depressurize the containment in less than 2 h. As such, leaks correspond to hole sizes of about 0.1 ft^2, and ruptures correspond to hole sizes of about [illegible] ft^2 to 7 ft^2 (0.65 m^2). Catastrophic ruptures in which a large part of the containment boundary is completely destroyed are not considered. Leaks that are so small that containment pressurization would not be arrested or substantially slowed are also not considered.

The following 16 cases were selected for consideration:

Case 1: FCONV, PWR, Early Containment Leak
Case 2: FCONV, PWR, Early Containment Rupture
Case 3: FCONV, PWR, Late Containment Rupture
Case 4: FCONV, Sequoyah, Early Rupture in Lower Compartment or Ice Condenser
Case 5: FCONV, BWR, Early Containment Rupture
Case 6: FCONV, BWR, Early Containment Leak
Case 7: FCONC, PWR, Early Containment Leak
Case 8: FCONC, PWR, Early Containment Rupture
Case 9: FCONC, PWR, Late Containment Rupture
Case 10: FCONC, PWR, Sequoyah, Early Rupture in Lower Compartment or Ice Condenser
Case 11: FCONC, BWR, Early Containment Leak, Saturated Pool
Case 12: FCONC, BWR, Early Containment Leak, Subcooled Pool
Case 13: FCONC, BWR, Early Containment Rupture, Saturated Pool
Case 14: FCONC, BWR, Early Containment Rupture, Subcooled Pool
Case 15: FCONC, BWR, Late Containment Leak
Case 16: FCONC, BWR, Late Containment Rupture

The values for FCONV and FCONC in the preceding cases are characterized without the inclusion of the effects of engineered safety features such as containment sprays, suppression pools, or ice condensers. Also, the possible effect of overlying water pools in scrubbing or quenching CCIs is not considered. Similarly, the effect of passage through other buildings after leaving the containment is not included. All the above effects will be considered elsewhere in the integrated analyses.

Summary of Rationale

Expert A relied on A Reference Guide on Severe Accidents, (an unpublished document that compiles insights from BMI-2104, NUREG/CR-4624, and NUREG-1150) for much of his understanding of severe accident conditions. He used BMI-2104 and BMI-2139 for estimates of the event timing and thus residence times. The expert grouped all the radionuclides together.

The most important factor in determining this issue is the residence time of the aerosols in the containment; the longer the time before CF, the smaller the release rate. Everything else is secondary, even the

difference between whether the failure is a leak or a rupture. The expert felt that the values applied to FCONV and FCONC should be the same.

The opposing effects of agglomeration and sedimentation on release rates for different dynamic shape factors reduces the importance of variance in the dynamic shape factor. "Fluffy" particles have higher settling rates, but they do not coagulate as quickly as smaller particles. Small particles do not resuspend, do coagulate, but do not settle out.

Expert A does not distinguish between the volatiles and the refractory groups. The reason for this is that a significant fraction of the volatiles are released from the fuel before vessel breach and are deposited on the surfaces of the reactor coolant system. The refractories are released from the fuel at a slower rate and a significant fraction are released after vessel breach and have a direct pathway to the containment.

The expert stated that the aerosol concentration in the containment dropped dramatically in 1 to 2 h and did not change much after that. The additional humidity does not make much difference in FCONC and FCONV. The humidity makes particles more compact. Because they are more compact, they settle out faster, but do not agglomerate as fast. Differences in containment construction do not make much difference, and fission product releases in BWRs should be as similar to those in PWRs.

Expert B used NAUA calculations done in conjunction with STCP calculations as a basis for his results. He took numbers from NAUA output as well as reports.

To distinguish between FCONC and FCONV, values for PI (particle source in vessel) and PE (particle source ex-vessel) provided by NAUA were considered. He also considered values for cerium that only come from the CCI release.

For practical considerations, only xenon, iodine, cesium, and tellurium were considered for RCS release (FCONV), and only tellurium, strontium, lanthanum, cerium, and barium are considered for ex-vessel (CCI) release (FCONC). The expert also considered the BNL uncertainty study, a calculation by Ed Fuller (EPRI) for Peach Bottom, CONTAIN calculations by Expert C, and MELCOR calculations.

The expert's distributions are intended to include uncertainties from:

- Surface area (deposition area or compartment height);
- Natural circulation;
- Hygroscopic nature of aerosols (primarily iodine and cesium groups);
- Particle shape factors (not big effect);
- H_2 burn,
- Residence time.

Expert C examined available code calculations relevant to aerosol/fission product behavior in the containment and as released from it. In most cases, these calculations were performed with the STCP or CONTAIN codes.

The expert developed a base distribution for FCONV and FCONC from the code results, and then modified these base distributions to include the effect of factors not considered by the codes.

The uncertainties not well represented by the range of the available code calculations were factored into the distribution with the use of scale factors to account for effects involving factors such as aerosol agglomeration, steam condensation, aerosol source strength, timing, shape factors, and containment volume. The final distributions were modified if they did not agree with the expert's intuition.

Expert D considered calculations performed in the CREST exercise, by SNL and by the American Nuclear Society (ANS). He also assessed the following factors listed or discussed below that could affect FCONV and FCONC.

1. Aerosol Characteristics:
   - Shape Factors
   - Distribution
   - Density
2. Residence Time (ANS parametric study showed a factor of 10 decrease in airborne fission products in 2 h):
   - Size of Breach
   - Timing of Breach.
3. Multicompartmentation (ANS parametric study and KfK DEMONA experiments show an effect of about a factor of 1.6.).
4. Effective Height (STCP and Stone and Webster studies show effect to be a factor of about two to five).
5. Thermodynamic State of Atmosphere:
   - Superheated
   - Saturated (condensing)
6. Hygroscopicity (LACE experiments show that if effect is present, it can be dominant).
7. H_2 Burn (affects 2 and 5 above, increases leakage by a factor of two).

Expert E used the EPRI modified FAI simplified aerosol algorithm and conducted an independent uncertainty analysis. The expert directly varied the following parameters in his uncertainty analysis:

1. Containment leak rates (including condensation onto walls),
2. Aerosol source rates,

3. Geometry (particularly effective containment height and containment volume),

4. Aerosol form factors (gamma and chi).

To study the impact of the timing and mode of containment failure, he varied the containment failure time and leak rates, assuming choked flow from containment failure sizes of 0.1 ft^2 to 7 ft^2. He also considered pre-existing leakage, steam condensation onto walls, and the impact of pool flashing in his calculations.

The expert considered three sources of aerosols in his analysis:

1. Aerosols released directly from the RCS (in BWRs the aerosols were passed through a suppression pool in most of the cases);

2. CCI aerosol releases;

3. Releases from the flashing of the suppression pool.

In the study, the expert assumed that the horizontal surface area available for deposition was the mean cross-sectional area of the containment multiplied by two. He varied this value from one to three in his uncertainty analysis.

The expert used BNL QUEST study values for aerosol from factors for input into his analysis.

It is the expert's opinion that the timing and mode of containment failure are the major sources of uncertainty. He also believes that the level of turbulence in containment, as it affects agglomeration, is an important uncertainty (he could not model this uncertainty explicitly).

The expert based much of the information in his sensitivity studies on EPRI research on empirical aerosol correlations. A basic assumption made by Expert E was that FCONV applies uniformly to all fission products from the RCS (except for the noble gases), and FCONC applies uniformly to fission products released during CCI.

Method of Aggregation

Eighty-two subcases were generated when all the distinguishing parameters were taken into account. The parameters by which the original 26 cases were subdivided are listed below:

1. Plant difference (Surry, Sequoyah, Zion, Peach Bottom, Grand Gulf, and La Salle);

2. Wet and dry cavities for the PWRs,

3. Containment failure in the upper and lower compartment for Sequoyah;

4. Saturated or subcooled suppression pool for the BWRs;

5. Different radionuclide groups (radionuclide groups were classified together in many cases; the following radionuclide groups were classified together for some subcases: (a) tellurium, and ruthenium (b) the refractories, (c) the volatiles, (d) the nonvolatiles, (e) strontium, and lanthenum, and (f) lanthanum, cerium, and barium.

The data were entered into a computer program which interpolated linearly between the given points. For each value of FCONV or FCONC, the average fractile was calculated, and an average curve was constructed. The resultant distributions were used to select values for FCONV and FCONC for use in the SOR codes.

Aggregated Results

Logically grouped, the results of the calculations for all 82 cases are in Table 5.1 and Figures 5-1 to 5-34.

Table 5.1
Experts Interpolated Results and Aggregate for Each Case

C1:Z,DRY

	0.001	0.010	0.050	0.100	0.200	0.300	0.400	0.500	0.600	0.700	0.800	0.900	0.950	0.990	0.999
EXPERT A	0.089	0.091	0.100	0.111	0.133	0.156	0.178	0.200	0.289	0.378	0.467	0.556	0.600	0.763	0.800
EXPERT B	0.050	0.052	0.063	0.087	0.134	0.226	0.363	0.500	0.553	0.606	0.666	0.731	0.764	0.793	0.800
EXPERT C	0.001	0.001	0.003	0.005	0.008	0.024	0.052	0.080	0.100	0.120	0.164	0.232	0.267	0.294	0.300
EXPERT D	0.001	0.002	0.004	0.007	0.012	0.020	0.031	0.041	0.069	0.096	0.163	0.267	0.320	0.530	0.710
EXPERT E	0.020	0.031	0.080	0.100	0.140	0.176	0.208	0.240	0.284	0.328	0.383	0.447	0.480	0.660	0.701
AVERAGE	0.001	0.002	0.006	0.014	0.054	0.095	0.125	0.168	0.221	0.295	0.416	0.587	0.664	0.770	0.798

C1:Z,WET

EXPERT A	0.089	0.091	0.100	0.111	0.133	0.156	0.178	0.200	0.289	0.378	0.467	0.556	0.600	0.763	0.800
EXPERT B	0.050	0.052	0.063	0.087	0.134	0.226	0.363	0.500	0.553	0.606	0.666	0.731	0.764	0.793	0.800
EXPERT C	0.001	0.001	0.003	0.005	0.008	0.024	0.052	0.080	0.100	0.120	0.164	0.232	0.267	0.294	0.300
EXPERT D	0.002	0.004	0.011	0.021	0.040	0.068	0.104	0.140	0.212	0.284	0.408	0.582	0.670	0.830	0.920
EXPERT E	0.020	0.031	0.080	0.100	0.140	0.176	0.208	0.240	0.284	0.328	0.383	0.447	0.480	0.660	0.701
AVERAGE	0.001	0.003	0.009	0.032	0.082	0.114	0.148	0.192	0.254	0.334	0.457	0.594	0.685	0.783	0.840

C1:SU,DRY

EXPERT A	0.089	0.091	0.100	0.111	0.133	0.156	0.178	0.200	0.289	0.378	0.467	0.556	0.600	0.763	0.800
EXPERT B	0.050	0.052	0.063	0.087	0.134	0.226	0.363	0.500	0.553	0.606	0.666	0.731	0.764	0.793	0.800
EXPERT C	0.001	0.001	0.003	0.005	0.008	0.024	0.052	0.080	0.100	0.120	0.164	0.232	0.267	0.294	0.300
EXPERT D	0.001	0.002	0.004	0.007	0.014	0.023	0.034	0.045	0.071	0.097	0.168	0.282	0.340	0.550	0.730
EXPERT E	0.049	0.060	0.110	0.135	0.185	0.234	0.282	0.330	0.366	0.402	0.470	0.570	0.620	0.900	0.963
AVERAGE	0.001	0.002	0.007	0.016	0.057	0.098	0.131	0.180	0.249	0.337	0.451	0.585	0.682	0.786	0.935

C1:SU,WET

EXPERT A	0.089	0.091	0.100	0.111	0.133	0.156	0.178	0.200	0.289	0.378	0.467	0.556	0.600	0.763	0.800
EXPERT B	0.050	0.052	0.063	0.087	0.134	0.226	0.363	0.500	0.553	0.606	0.666	0.731	0.764	0.793	0.800
EXPERT C	0.001	0.001	0.003	0.005	0.008	0.024	0.052	0.080	0.100	0.120	0.164	0.232	0.267	0.294	0.300
EXPERT D	0.002	0.004	0.012	0.023	0.044	0.074	0.112	0.150	0.226	0.302	0.427	0.602	0.690	0.840	0.920
EXPERT E	0.049	0.060	0.110	0.135	0.185	0.234	0.282	0.330	0.366	0.402	0.470	0.570	0.620	0.900	0.963
AVERAGE	0.001	0.003	0.009	0.035	0.087	0.120	0.157	0.211	0.285	0.375	0.497	0.609	0.704	0.798	0.939

Table 5.1 (Continued)

C1:SQ,DRY

	0.001	0.010	0.050	0.100	0.200	0.300	0.400	0.500	0.600	0.700	0.800	0.900	0.950	0.990	0.999
EXPERT A	0.089	0.091	0.100	0.111	0.133	0.156	0.178	0.200	0.289	0.378	0.467	0.556	0.600	0.763	0.800
EXPERT B	0.050	0.052	0.063	0.087	0.134	0.226	0.363	0.500	0.553	0.606	0.666	0.731	0.764	0.793	0.800
EXPERT C	0.001	0.001	0.003	0.005	0.008	0.024	0.052	0.080	0.100	0.120	0.164	0.232	0.267	0.294	0.300
EXPERT D	0.001	0.003	0.007	0.013	0.026	0.043	0.066	0.089	0.141	0.194	0.300	0.480	0.540	0.740	0.870
EXPERT E	0.021	0.030	0.070	0.100	0.160	0.214	0.262	0.310	0.362	0.414	0.487	0.582	0.630	0.880	0.936
AVERAGE	0.001	0.002	0.008	0.025	0.070	0.107	0.143	0.189	0.259	0.357	0.479	0.596	0.691	0.789	0.911

C1:SQ,WET

EXPERT A	0.089	0.091	0.100	0.111	0.133	0.156	0.178	0.200	0.289	0.378	0.467	0.556	0.600	0.763	0.800
EXPERT B	0.050	0.052	0.063	0.087	0.134	0.226	0.363	0.500	0.553	0.606	0.666	0.731	0.764	0.793	0.800
EXPERT C	0.001	0.001	0.003	0.005	0.008	0.024	0.052	0.080	0.100	0.120	0.164	0.232	0.267	0.294	0.300
EXPERT D	0.003	0.008	0.022	0.041	0.081	0.132	0.196	0.260	0.368	0.476	0.608	0.752	0.840	0.930	0.970
EXPERT E	0.021	0.030	0.070	0.100	0.160	0.214	0.262	0.310	0.362	0.414	0.487	0.582	0.630	0.880	0.936
AVERAGE	0.001	0.003	0.009	0.044	0.092	0.125	0.169	0.227	0.304	0.410	0.526	0.643	0.740	0.867	0.954

C2:Z

EXPERT A	0.215	0.280	0.300	0.322	0.367	0.411	0.456	0.500	0.522	0.544	0.567	0.589	0.600	0.763	0.800
EXPERT B	0.150	0.154	0.175	0.212	0.287	0.399	0.550	0.700	0.738	0.775	0.815	0.857	0.878	0.896	0.900
EXPERT C	0.300	0.307	0.339	0.380	0.460	0.540	0.620	0.700	0.720	0.740	0.770	0.810	0.830	0.846	0.850
EXPERT D	0.002	0.020	0.100	0.200	0.400	0.540	0.620	0.700	0.760	0.820	0.875	0.925	0.950	0.980	0.987
EXPERT E	0.159	0.170	0.220	0.250	0.310	0.360	0.400	0.440	0.484	0.528	0.600	0.700	0.750	0.970	1.000
AVERAGE	0.010	0.100	0.212	0.282	0.356	0.428	0.500	0.550	0.615	0.712	0.765	0.835	0.883	0.959	0.989

C2:SU

EXPERT A	0.215	0.280	0.300	0.322	0.367	0.411	0.456	0.500	0.522	0.544	0.567	0.589	0.600	0.763	0.800
EXPERT B	0.150	0.154	0.175	0.212	0.287	0.399	0.550	0.700	0.738	0.775	0.815	0.857	0.878	0.896	0.900
EXPERT C	0.300	0.307	0.339	0.380	0.460	0.540	0.620	0.700	0.720	0.740	0.770	0.810	0.830	0.846	0.850
EXPERT D	0.002	0.020	0.100	0.200	0.400	0.540	0.620	0.700	0.760	0.820	0.875	0.925	0.950	0.980	0.987
EXPERT E	0.106	0.120	0.180	0.203	0.248	0.286	0.318	0.350	0.398	0.446	0.520	0.620	0.670	0.900	0.952
AVERAGE	0.010	0.100	0.193	0.253	0.328	0.399	0.474	0.541	0.598	0.707	0.761	0.833	0.880	0.951	0.984

Table 5.1 (Continued)

C3:Z

	0.001	0.010	0.050	0.100	0.200	0.300	0.400	0.500	0.600	0.700	0.800	0.900	0.950	0.990	0.999
EXPERT A	0.006	0.006	0.010	0.014	0.023	0.032	0.041	0.050	0.061	0.072	0.083	0.094	0.100	0.182	0.200
EXPERT B	0.000	0.000	0.000	0.000	0.000	0.000	0.000	0.000	0.000	0.000	0.000	0.000	0.000	0.000	0.000
EXPERT C	0.001	0.002	0.005	0.009	0.016	0.026	0.038	0.050	0.090	0.130	0.180	0.240	0.270	0.295	0.300
EXPERT D	0.000	0.000	0.001	0.002	0.004	0.007	0.012	0.016	0.028	0.041	0.080	0.147	0.180	0.360	0.500
EXPERT E	0.000	0.002	0.010	0.013	0.018	0.026	0.038	0.050	0.062	0.074	0.107	0.162	0.190	0.390	0.435
AVERAGE	0.000	0.000	0.000	0.000	0.000	0.008	0.016	0.028	0.042	0.062	0.087	0.149	0.206	0.305	0.450

C3:SU

EXPERT A	0.006	0.006	0.010	0.014	0.023	0.032	0.041	0.050	0.061	0.072	0.083	0.094	0.100	0.182	0.200
EXPERT B	0.000	0.000	0.000	0.000	0.000	0.000	0.000	0.000	0.000	0.000	0.000	0.000	0.000	0.000	0.000
EXPERT C	0.001	0.002	0.005	0.009	0.016	0.026	0.038	0.050	0.090	0.130	0.180	0.240	0.270	0.295	0.300
EXPERT D	0.000	0.000	0.001	0.002	0.004	0.007	0.012	0.016	0.028	0.041	0.080	0.147	0.180	0.360	0.500
EXPERT E	0.009	0.010	0.015	0.024	0.041	0.060	0.080	0.100	0.120	0.140	0.185	0.255	0.290	0.430	0.461
AVERAGE	0.000	0.000	0.000	0.000	0.000	0.009	0.019	0.034	0.050	0.078	0.110	0.174	0.243	0.341	0.460

C3:SQ

EXPERT A	0.006	0.006	0.010	0.014	0.023	0.032	0.041	0.050	0.061	0.072	0.083	0.094	0.100	0.182	0.200
EXPERT B	0.000	0.000	0.000	0.000	0.000	0.000	0.000	0.000	0.000	0.000	0.000	0.000	0.000	0.000	0.000
EXPERT C	0.001	0.002	0.005	0.009	0.016	0.026	0.038	0.050	0.090	0.130	0.180	0.240	0.270	0.295	0.300
EXPERT D	0.000	0.000	0.000	0.001	0.002	0.003	0.005	0.007	0.014	0.021	0.049	0.096	0.120	0.270	0.490
EXPERT E	0.014	0.030	0.100	0.145	0.235	0.312	0.376	0.440	0.488	0.536	0.588	0.642	0.670	0.730	0.743
AVERAGE	0.000	0.000	0.000	0.000	0.000	0.006	0.018	0.035	0.062	0.098	0.212	0.441	0.560	0.670	0.737

C4:SQ.LOWER

EXPERT A	0.389	0.391	0.400	0.411	0.433	0.456	0.478	0.500	0.567	0.633	0.700	0.767	0.800	0.882	0.900
EXPERT B	0.150	0.154	0.175	0.212	0.287	0.399	0.550	0.700	0.738	0.775	0.815	0.857	0.878	0.896	0.900
EXPERT C	0.300	0.307	0.339	0.380	0.460	0.540	0.620	0.700	0.760	0.820	0.860	0.880	0.890	0.898	0.900
EXPERT D	0.042	0.050	0.250	0.338	0.513	0.640	0.720	0.800	0.840	0.880	0.912	0.938	0.950	0.980	0.987
EXPERT E	0.178	0.270	0.660	0.738	0.853	0.920	0.940	0.960	0.968	0.976	0.984	0.991	0.995	0.999	1.000
AVERAGE	0.046	0.158	0.271	0.367	0.452	0.539	0.652	0.732	0.795	0.856	0.902	0.963	0.981	0.995	0.999

Table 5.1 (Continued)

	0.001	0.010	0.050	0.100	0.200	0.300	0.400	0.500	0.600	0.700	0.800	0.900	0.950	0.990	0.999
							C4:SQ,UPPER								
EXPERT A	0.389	0.391	0.400	0.411	0.433	0.456	0.478	0.500	0.567	0.633	0.700	0.767	0.800	0.882	0.900
EXPERT B	0.150	0.154	0.175	0.212	0.287	0.399	0.550	0.700	0.738	0.775	0.815	0.857	0.878	0.896	0.900
EXPERT C	0.300	0.307	0.339	0.380	0.460	0.540	0.620	0.700	0.760	0.820	0.860	0.880	0.890	0.898	0.900
EXPERT D	0.002	0.020	0.100	0.150	0.250	0.370	0.510	0.650	0.690	0.730	0.788	0.862	0.900	0.980	0.998
EXPERT E	0.041	0.140	0.580	0.615	0.685	0.736	0.768	0.800	0.820	0.840	0.868	0.903	0.920	0.940	0.945
AVERAGE	0.010	0.089	0.200	0.302	0.423	0.493	0.600	0.680	0.734	0.781	0.828	0.871	0.892	0.936	0.990
							C5:PB,SAT,2,3								
EXPERT A	0.378	0.382	0.400	0.422	0.467	0.511	0.556	0.600	0.644	0.689	0.733	0.778	0.800	0.882	0.900
EXPERT B	0.150	0.154	0.175	0.212	0.287	0.399	0.550	0.700	0.738	0.775	0.815	0.857	0.878	0.896	0.900
EXPERT C	0.300	0.307	0.339	0.380	0.460	0.540	0.620	0.700	0.760	0.820	0.870	0.910	0.930	0.946	0.950
EXPERT D	0.006	0.050	0.300	0.438	0.713	0.866	0.898	0.930	0.946	0.962	0.976	0.989	0.995	1.000	1.000
EXPERT E	0.217	0.280	0.560	0.630	0.770	0.860	0.900	0.940	0.956	0.972	0.983	0.988	0.990	0.999	1.000
AVERAGE	0.026	0.160	0.281	0.381	0.488	0.591	0.687	0.756	0.830	0.884	0.937	0.974	0.986	0.997	1.000
							C5:PD,SAT,4-9								
EXPERT A	0.378	0.382	0.400	0.422	0.467	0.511	0.556	0.600	0.644	0.689	0.733	0.778	0.800	0.882	0.900
EXPERT B	0.150	0.154	0.175	0.212	0.287	0.399	0.550	0.700	0.738	0.775	0.815	0.857	0.878	0.896	0.900
EXPERT C	0.300	0.307	0.339	0.380	0.460	0.540	0.620	0.700	0.720	0.740	0.770	0.810	0.830	0.846	0.850
EXPERT D	0.096	0.050	0.300	0.438	0.713	0.866	0.898	0.930	0.946	0.962	0.976	0.989	0.995	1.000	1.000
EXPERT E	0.217	0.280	0.560	0.630	0.770	0.860	0.900	0.940	0.956	0.972	0.983	0.988	0.990	0.999	1.000
AVERAGE	0.026	0.160	0.281	0.381	0.488	0.591	0.687	0.739	0.795	0.864	0.933	0.974	0.986	0.997	1.000
							C5:PB,SUB,2,3								
EXPERT A	0.378	0.382	0.400	0.422	0.467	0.511	0.556	0.600	0.644	0.689	0.733	0.778	0.800	0.882	0.900
EXPERT B	0.150	0.154	0.175	0.212	0.287	0.399	0.550	0.700	0.738	0.775	0.815	0.857	0.878	0.896	0.900
EXPERT C	0.300	0.307	0.339	0.380	0.460	0.540	0.620	0.700	0.760	0.820	0.870	0.910	0.930	0.946	0.950
EXPERT D	0.010	0.010	0.100	0.175	0.325	0.480	0.640	0.800	0.840	0.880	0.918	0.952	0.970	1.000	1.000
EXPERT E	0.217	0.280	0.560	0.630	0.770	0.860	0.900	0.940	0.956	0.972	0.983	0.988	0.990	0.999	1.000
AVERAGE	0.010	0.100	0.224	0.325	0.450	0.552	0.643	0.724	0.787	0.849	0.898	0.955	0.982	0.994	1.000

Table 5.1 (Continued)

	0.001	0.010	0.050	0.100	0.200	0.300	0.400	0.500	0.600	0.700	0.800	0.900	0.950	0.990	0.999
							C5:PB,SUB,4-9								
EXPERT A	0.378	0.382	0.400	0.422	0.467	0.511	0.556	0.600	0.644	0.689	0.733	0.778	0.800	0.882	0.900
EXPERT B	0.150	0.154	0.175	0.212	0.287	0.399	0.550	0.700	0.738	0.775	0.815	0.857	0.878	0.896	0.900
EXPERT C	0.300	0.307	0.339	0.380	0.460	0.540	0.620	0.700	0.720	0.740	0.770	0.810	0.830	0.846	0.850
EXPERT D	0.010	0.010	0.100	0.175	0.325	0.480	0.640	0.800	0.840	0.880	0.918	0.952	0.970	1.000	1.000
EXPERT E	0.217	0.280	0.560	0.630	0.770	0.860	0.900	0.940	0.956	0.972	0.983	0.988	0.990	0.999	1.000
AVERAGE	0.010	0.100	0.224	0.325	0.450	0.552	0.643	0.717	0.764	0.822	0.881	0.955	0.982	0.994	1.000
							C5:GG,SAT,2,3								
EXPERT A	0.378	0.382	0.400	0.422	0.467	0.511	0.556	0.600	0.644	0.689	0.733	0.778	0.800	0.882	0.900
EXPERT B	0.150	0.154	0.175	0.212	0.287	0.399	0.550	0.700	0.738	0.775	0.815	0.857	0.878	0.896	0.900
EXPERT C	0.300	0.307	0.339	0.380	0.460	0.540	0.620	0.700	0.760	0.820	0.870	0.910	0.930	0.946	0.950
EXPERT D	0.048	0.050	0.150	0.188	0.263	0.380	0.540	0.700	0.760	0.820	0.875	0.925	0.950	0.980	0.987
EXPERT E	0.006	0.040	0.190	0.245	0.355	0.448	0.524	0.600	0.660	0.720	0.788	0.862	0.900	0.990	1.000
AVERAGE	0.021	0.090	0.197	0.267	0.395	0.478	0.560	0.639	0.711	0.762	0.816	0.880	0.915	0.966	0.996
							C5:GG,SAT,4-9								
EXPERT A	0.378	0.382	0.400	0.422	0.467	0.511	0.556	0.600	0.644	0.689	0.733	0.778	0.800	0.882	0.900
EXPERT B	0.150	0.154	0.175	0.212	0.287	0.399	0.550	0.700	0.738	0.775	0.815	0.857	0.878	0.896	0.900
EXPERT C	0.300	0.307	0.339	0.380	0.460	0.540	0.620	0.700	0.720	0.740	0.770	0.810	0.830	0.846	0.850
EXPERT D	0.048	0.050	0.150	0.188	0.263	0.380	0.540	0.700	0.760	0.820	0.875	0.925	0.950	0.980	0.987
EXPERT E	0.006	0.040	0.190	0.245	0.355	0.448	0.524	0.600	0.660	0.720	0.788	0.862	0.900	0.990	1.000
AVERAGE	0.021	0.090	0.197	0.267	0.395	0.478	0.560	0.639	0.708	0.748	0.793	0.852	0.892	0.966	0.996
							C6:PB,SUB								
EXPERT A	0.193	0.196	0.200	0.206	0.217	0.228	0.239	0.250	0.328	0.406	0.483	0.561	0.600	0.783	0.800
EXPERT B	0.050	0.052	0.063	0.087	0.134	0.226	0.363	0.500	0.553	0.606	0.666	0.731	0.764	0.793	0.800
EXPERT C	0.010	0.013	0.025	0.046	0.082	0.120	0.160	0.200	0.280	0.360	0.440	0.520	0.561	0.593	0.600
EXPERT D	0.002	0.004	0.008	0.014	0.025	0.041	0.060	0.079	0.123	0.168	0.258	0.392	0.460	0.660	0.810
EXPERT E	0.045	0.070	0.180	0.215	0.285	0.346	0.398	0.450	0.498	0.546	0.615	0.705	0.750	0.998	1.000
AVERAGE	0.002	0.008	0.026	0.053	0.107	0.181	0.225	0.282	0.370	0.454	0.536	0.629	0.712	0.797	0.999

Table 5.1 (Continued)

	0.001	0.010	0.050	0.100	0.200	0.300	0.400	0.500	0.600	0.700	0.800	0.900	0.950	0.990	0.999
C6:FB,SAT															
EXPERT A	0.195	0.196	0.200	0.206	0.217	0.228	0.239	0.250	0.328	0.406	0.483	0.561	0.600	0.763	0.800
EXPERT B	0.050	0.052	0.063	0.087	0.134	0.226	0.363	0.500	0.553	0.606	0.666	0.731	0.764	0.793	0.800
EXPERT C	0.010	0.013	0.028	0.046	0.082	0.120	0.160	0.200	0.280	0.360	0.440	0.520	0.561	0.593	0.600
EXPERT D	0.004	0.009	0.024	0.043	0.079	0.120	0.165	0.210	0.318	0.426	0.558	0.713	0.790	0.900	0.950
EXPERT E	0.045	0.070	0.180	0.215	0.285	0.346	0.398	0.450	0.498	0.546	0.615	0.705	0.750	0.998	1.000
AVERAGE	0.006	0.017	0.051	0.081	0.148	0.208	0.245	0.326	0.408	0.489	0.561	0.668	0.727	0.874	0.999
C6:GG,SUB															
EXPERT A	0.195	0.196	0.200	0.206	0.217	0.228	0.239	0.250	0.328	0.406	0.483	0.561	0.600	0.763	0.800
EXPERT B	0.050	0.052	0.063	0.087	0.134	0.226	0.363	0.500	0.553	0.606	0.666	0.731	0.764	0.793	0.800
EXPERT C	0.010	0.013	0.028	0.046	0.082	0.120	0.160	0.200	0.280	0.360	0.440	0.520	0.561	0.593	0.600
EXPERT D	0.000	0.001	0.003	0.005	0.010	0.016	0.025	0.033	0.055	0.078	0.139	0.240	0.290	0.530	0.690
EXPERT E	0.113	0.120	0.150	0.163	0.188	0.210	0.230	0.250	0.278	0.306	0.368	0.462	0.510	0.900	0.988
AVERAGE	0.001	0.003	0.012	0.029	0.081	0.153	0.203	0.233	0.277	0.361	0.472	0.580	0.676	0.784	0.949
C6:GG,SAT															
EXPERT A	0.195	0.196	0.200	0.206	0.217	0.228	0.239	0.250	0.328	0.406	0.483	0.561	0.600	0.763	0.800
EXPERT B	0.050	0.052	0.063	0.087	0.134	0.226	0.363	0.500	0.553	0.606	0.666	0.731	0.764	0.793	0.800
EXPERT C	0.010	0.013	0.028	0.046	0.082	0.120	0.160	0.200	0.280	0.360	0.440	0.520	0.561	0.593	0.600
EXPERT D	0.001	0.003	0.008	0.015	0.030	0.052	0.081	0.110	0.178	0.246	0.370	0.550	0.640	0.810	0.910
EXPERT E	0.113	0.120	0.150	0.163	0.188	0.210	0.230	0.250	0.278	0.306	0.368	0.462	0.510	0.900	0.988
AVERAGE	0.002	0.008	0.030	0.059	0.121	0.181	0.216	0.245	0.302	0.396	0.498	0.595	0.695	0.792	0.953
C7:2,DRY,2,3															
EXPERT A	0.084	0.087	0.100	0.117	0.150	0.183	0.217	0.250	0.328	0.406	0.483	0.561	0.600	0.682	0.700
EXPERT B	0.050	0.052	0.063	0.087	0.134	0.226	0.363	0.500	0.553	0.606	0.666	0.731	0.764	0.793	0.800
EXPERT C	0.001	0.001	0.003	0.005	0.008	0.024	0.052	0.080	0.100	0.120	0.164	0.232	0.267	0.294	0.300
EXPERT D	0.001	0.002	0.004	0.007	0.012	0.020	0.031	0.041	0.069	0.096	0.163	0.267	0.320	0.530	0.710
EXPERT E	0.023	0.030	0.060	0.085	0.135	0.178	0.214	0.250	0.282	0.314	0.360	0.420	0.450	0.560	0.585
AVERAGE	0.001	0.002	0.006	0.014	0.053	0.092	0.127	0.180	0.236	0.299	0.412	0.562	0.652	0.784	0.797

Table 5.1 (Continued)

	0.001	0.010	0.050	0.100	0.200	0.300	0.400	0.500	0.600	0.700	0.800	0.900	0.950	0.990	0.999
							C7:Z,DRY,4-9								
EXPERT A	0.084	0.087	0.100	0.117	0.150	0.183	0.217	0.250	0.328	0.406	0.483	0.561	0.600	0.682	0.700
EXPERT B	0.050	0.052	0.063	0.087	0.134	0.226	0.363	0.500	0.553	0.606	0.666	0.731	0.764	0.793	0.800
EXPERT C	0.005	0.006	0.010	0.015	0.025	0.044	0.072	0.100	0.140	0.180	0.220	0.260	0.280	0.296	0.300
EXPERT D	0.001	0.002	0.004	0.007	0.012	0.020	0.031	0.041	0.069	0.096	0.163	0.267	0.320	0.530	0.710
EXPERT E	0.023	0.030	0.060	0.085	0.135	0.176	0.214	0.250	0.282	0.314	0.360	0.420	0.450	0.560	0.585
AVERAGE	0.001	0.004	0.011	0.023	0.059	0.098	0.143	0.192	0.242	0.300	0.412	0.562	0.652	0.784	0.797
							C7:Z,WET,2,3								
EXPERT A	0.084	0.087	0.100	0.117	0.150	0.183	0.217	0.250	0.328	0.406	0.483	0.561	0.600	0.682	0.700
EXPERT B	0.050	0.052	0.063	0.087	0.134	0.226	0.363	0.500	0.553	0.606	0.666	0.731	0.764	0.793	0.800
EXPERT C	0.001	0.001	0.003	0.005	0.008	0.024	0.052	0.080	0.100	0.120	0.164	0.232	0.267	0.294	0.300
EXPERT D	0.002	0.004	0.011	0.021	0.040	0.068	0.104	0.140	0.212	0.284	0.408	0.582	0.670	0.830	0.920
EXPERT E	0.023	0.030	0.060	0.085	0.135	0.176	0.214	0.250	0.282	0.314	0.360	0.420	0.450	0.560	0.585
AVERAGE	0.001	0.003	0.009	0.032	0.079	0.114	0.154	0.208	0.263	0.334	0.452	0.587	0.674	0.780	0.880
							C7:Z,WET,4-9								
EXPERT A	0.084	0.087	0.100	0.117	0.150	0.183	0.217	0.250	0.328	0.406	0.483	0.561	0.600	0.682	0.700
EXPERT B	0.050	0.052	0.063	0.087	0.134	0.226	0.363	0.500	0.553	0.606	0.666	0.731	0.764	0.793	0.800
EXPERT C	0.005	0.006	0.010	0.015	0.025	0.044	0.072	0.100	0.140	0.180	0.220	0.260	0.280	0.296	0.300
EXPERT D	0.002	0.004	0.011	0.021	0.040	0.068	0.104	0.140	0.212	0.284	0.408	0.582	0.670	0.830	0.920
EXPERT E	0.023	0.030	0.060	0.085	0.135	0.178	0.214	0.250	0.282	0.314	0.360	0.420	0.450	0.560	0.585
AVERAGE	0.003	0.007	0.020	0.039	0.085	0.124	0.169	0.217	0.267	0.334	0.452	0.587	0.674	0.780	0.880
							C7:SU,DRY,2,3								
EXPERT A	0.084	0.087	0.100	0.117	0.150	0.183	0.217	0.250	0.328	0.406	0.483	0.561	0.600	0.682	0.700
EXPERT B	0.050	0.052	0.063	0.087	0.134	0.226	0.363	0.500	0.553	0.606	0.666	0.731	0.764	0.793	0.800
EXPERT C	0.001	0.001	0.003	0.005	0.008	0.024	0.052	0.080	0.100	0.120	0.164	0.232	0.267	0.294	0.300
EXPERT D	0.001	0.002	0.004	0.007	0.014	0.023	0.034	0.045	0.071	0.097	0.167	0.282	0.340	0.550	0.730
EXPERT E	0.056	0.070	0.130	0.165	0.235	0.298	0.354	0.410	0.466	0.522	0.585	0.655	0.690	0.800	0.825
AVERAGE	0.001	0.002	0.007	0.016	0.058	0.099	0.141	0.205	0.278	0.384	0.507	0.612	0.682	0.777	0.815

Table 5.1 (Continued)

	0.001	0.010	0.050	0.100	0.200	0.300	0.400	0.500	0.600	0.700	0.800	0.900	0.950	0.99	0.999
							C7:SU,DRY,4-9								
EXPERT A	0.084	0.087	0.100	0.117	0.150	0.183	0.217	0.250	0.328	0.406	0.483	0.561	0.600	0.682	0.700
EXPERT B	0.050	0.052	0.063	0.087	0.134	0.226	0.363	0.500	0.553	0.606	0.666	0.731	0.764	0.793	0.800
EXPERT C	0.005	0.006	0.010	0.015	0.025	0.044	0.072	0.100	0.140	0.180	0.220	0.260	0.280	0.296	0.300
EXPERT D	0.001	0.002	0.004	0.007	0.014	0.023	0.034	0.045	0.071	0.097	0.167	0.282	0.340	0.550	0.730
EXPERT E	0.056	0.070	0.130	0.165	0.235	0.298	0.354	0.410	0.466	0.522	0.585	0.655	0.690	0.800	0.825
AVERAGE	0.001	0.004	0.012	0.024	0.064	0.107	0.158	0.217	0.281	0.384	0.507	0.612	0.682	0.777	0.815
							C7:SU,WET,2.3								
EXPERT A	0.084	0.087	0.100	0.117	0.150	0.183	0.217	0.250	0.328	0.406	0.483	0.561	0.600	0.682	0.700
EXPERT B	0.050	0.052	0.063	0.087	0.134	0.226	0.363	0.500	0.553	0.606	0.666	0.731	0.764	0.793	0.800
EXPERT C	0.001	0.001	0.003	0.005	0.008	0.024	0.052	0.080	0.100	0.120	0.164	0.232	0.267	0.294	0.300
EXPERT D	0.002	0.004	0.012	0.023	0.044	0.074	0.112	0.150	0.226	0.302	0.427	0.602	0.690	0.840	0.920
EXPERT E	0.056	0.070	0.130	0.165	0.235	0.298	0.354	0.410	0.466	0.522	0.585	0.655	0.690	0.800	0.825
AVERAGE	0.001	0.003	0.009	0.035	0.087	0.124	0.175	0.238	0.316	0.426	0.532	0.633	0.697	0.791	0.884
							C7:SU,WET,4-9								
EXPERT A	0.084	0.087	0.100	0.117	0.150	0.183	0.217	0.250	0.328	0.406	0.483	0.561	0.600	0.682	0.700
EXPERT B	0.050	0.052	0.063	0.087	0.134	0.226	0.363	0.500	0.553	0.606	0.666	0.731	0.764	0.793	0.800
EXPERT C	0.005	0.006	0.010	0.015	0.025	0.044	0.072	0.100	0.140	0.180	0.220	0.260	0.280	0.296	0.300
EXPERT D	0.002	0.004	0.012	0.023	0.044	0.074	0.112	0.150	0.226	0.302	0.427	0.602	0.690	0.840	0.920
EXPERT E	0.056	0.070	0.130	0.165	0.235	0.298	0.354	0.410	0.466	0.522	0.585	0.655	0.690	0.800	0.825
AVERAGE	0.003	0.007	0.021	0.044	0.094	0.138	0.189	0.245	0.316	0.426	0.532	0.633	0.697	0.791	0.884
							C7:SQ,DRY,2.3								
EXPERT A	0.084	0.087	0.100	0.117	0.150	0.183	0.217	0.250	0.328	0.406	0.483	0.561	0.600	0.682	0.700
EXPERT B	0.050	0.052	0.063	0.087	0.134	0.226	0.363	0.500	0.553	0.606	0.666	0.731	0.764	0.793	0.800
EXPERT C	0.001	0.001	0.003	0.005	0.008	0.024	0.052	0.080	0.100	0.120	0.164	0.232	0.267	0.294	0.300
EXPERT D	0.001	0.003	0.007	0.013	0.026	0.043	0.066	0.089	0.141	0.194	0.300	0.460	0.540	0.740	0.870
EXPERT E	0.025	0.030	0.050	0.078	0.132	0.184	0.232	0.280	0.324	0.368	0.437	0.532	0.580	0.840	0.899
AVERAGE	0.001	0.002	0.008	0.025	0.067	0.104	0.144	0.197	0.258	0.348	0.470	0.585	0.678	0.783	0.877

Table 5.1 (Continued)

	0.001	0.010	0.050	0.100	0.200	0.300	0.400	0.500	0.600	0.700	0.800	0.900	0.950	0.99	0.999
							C7:SQ,DRY,4-9								
EXPERT A	0.084	0.087	0.100	0.117	0.150	0.183	0.217	0.250	0.328	0.406	0.483	0.561	0.600	0.682	0.700
EXPERT B	0.050	0.052	0.063	0.087	0.134	0.226	0.363	0.500	0.553	0.606	0.666	0.731	0.764	0.793	0.800
EXPERT C	0.005	0.006	0.010	0.015	0.025	0.044	0.072	0.100	0.140	0.180	0.220	0.260	0.280	0.296	0.300
EXPERT D	0.001	0.003	0.007	0.013	0.026	0.043	0.066	0.089	0.141	0.194	0.300	0.460	0.540	0.740	0.870
EXPERT E	0.025	0.030	0.050	0.078	0.132	0.184	0.232	0.280	0.324	0.368	0.437	0.532	0.580	0.840	0.899
AVERAGE	0.002	0.006	0.017	0.030	0.073	0.114	0.158	0.207	0.264	0.348	0.470	0.585	0.678	0.783	0.877
							C7:SQ,WET,2,3								
EXPERT A	0.084	0.087	0.100	0.117	0.150	0.183	0.217	0.250	0.328	0.406	0.483	0.561	0.600	0.682	0.700
EXPERT B	0.050	0.052	0.063	0.087	0.134	0.226	0.363	0.500	0.553	0.606	0.666	0.731	0.764	0.793	0.800
EXPERT C	0.001	0.001	0.003	0.005	0.008	0.024	0.052	0.080	0.100	0.120	0.164	0.232	0.267	0.294	0.300
EXPERT D	0.003	0.008	0.022	0.041	0.081	0.132	0.196	0.260	0.368	0.476	0.605	0.762	0.840	0.930	0.970
EXPERT E	0.025	0.030	0.050	0.078	0.132	0.184	0.232	0.280	0.324	0.368	0.437	0.532	0.580	0.840	0.899
AVERAGE	0.001	0.003	0.009	0.042	0.068	0.125	0.175	0.231	0.300	0.398	0.518	0.636	0.730	0.857	0.952
							C7:SQ,WET,4-9								
EXPERT A	0.084	0.087	0.100	0.117	0.150	0.183	0.217	0.250	0.328	0.406	0.483	0.561	0.600	0.682	0.700
EXPERT B	0.050	0.052	0.063	0.087	0.134	0.226	0.363	0.500	0.553	0.606	0.666	0.731	0.764	0.793	0.800
EXPERT C	0.005	0.006	0.010	0.015	0.025	0.044	0.072	0.100	0.140	0.180	0.220	0.260	0.280	0.296	0.300
EXPERT D	0.003	0.008	0.022	0.041	0.080	0.132	0.196	0.260	0.368	0.476	0.608	0.762	0.840	0.930	0.970
EXPERT E	0.025	0.030	0.050	0.078	0.132	0.184	0.232	0.280	0.324	0.368	0.437	0.532	0.580	0.840	0.899
AVERAGE	0.004	0.009	0.024	0.050	0.095	0.139	0.188	0.238	0.300	0.398	0.518	0.636	0.730	0.857	0.952
							C8:Z,2,3								
EXPERT A	0.378	0.382	0.400	0.422	0.467	0.511	0.556	0.600	0.644	0.689	0.733	0.778	0.800	0.882	0.900
EXPERT B	0.150	0.154	0.175	0.212	0.287	0.399	0.550	0.700	0.738	0.775	0.815	0.857	0.878	0.896	0.900
EXPERT C	0.300	0.307	0.339	0.380	0.460	0.540	0.620	0.700	0.720	0.740	0.770	0.810	0.830	0.846	0.850
EXPERT D	0.013	0.020	0.050	0.100	0.200	0.300	0.400	0.500	0.580	0.660	0.738	0.813	0.850	0.950	0.973
EXPERT E	0.216	0.230	0.290	0.313	0.357	0.400	0.440	0.480	0.528	0.576	0.630	0.690	0.720	0.850	0.879
AVERAGE	0.016	0.050	0.186	0.275	0.376	0.442	0.509	0.576	0.645	0.708	0.750	0.808	0.843	0.894	0.962

Table 5.1 (Continued)

	0.001	0.010	0.050	0.100	0.200	0.300	0.400	0.500	0.600	0.700	0.800	0.900	0.950	0.99	0.999
							C8:SU,2,3								
EXPERT A	0.378	0.382	0.400	0.422	0.467	0.511	0.556	0.600	0.644	0.689	0.733	0.778	0.800	0.882	0.900
EXPERT B	0.150	0.154	0.175	0.212	0.287	0.399	0.550	0.700	0.738	0.775	0.815	0.857	0.878	0.896	0.900
EXPERT C	0.300	0.307	0.339	0.380	0.460	0.540	0.620	0.700	0.720	0.740	0.770	0.810	0.830	0.846	0.850
EXPERT D	0.013	0.020	0.050	0.100	0.200	0.300	0.400	0.500	0.580	0.660	0.738	0.813	0.850	0.950	0.973
EXPERT E	0.275	0.280	0.300	0.308	0.323	0.338	0.354	0.370	0.402	0.434	0.480	0.540	0.570	0.800	0.852
AVERAGE	0.016	0.050	0.186	0.284	0.344	0.404	0.467	0.539	0.620	0.705	0.746	0.806	0.842	0.894	0.962
							C8:Z,4-9								
EXPERT A	0.378	0.382	0.400	0.422	0.467	0.511	0.556	0.600	0.644	0.689	0.733	0.778	0.800	0.882	0.900
EXPERT B	0.150	0.154	0.175	0.212	0.287	0.399	0.550	0.700	0.738	0.775	0.815	0.857	0.878	0.896	0.900
EXPERT C	0.100	0.111	0.159	0.219	0.340	0.440	0.520	0.600	0.660	0.720	0.770	0.810	0.830	0.846	0.850
EXPERT D	0.013	0.020	0.050	0.100	0.200	0.300	0.400	0.500	0.580	0.660	0.738	0.813	0.850	0.950	0.973
EXPERT E	0.216	0.230	0.280	0.313	0.357	0.400	0.440	0.480	0.528	0.576	0.630	0.680	0.720	0.850	0.879
AVERAGE	0.016	0.050	0.165	0.237	0.348	0.426	0.492	0.559	0.626	0.692	0.750	0.808	0.843	0.894	0.962
							C8:SU,4-								
EXPERT A	0.378	0.382	0.400	0.422	0.467	0.511	0.556	0.600	0.644	0.689	0.733	0.778	0.800	0.882	0.900
EXPERT B	0.150	0.154	0.175	0.212	0.287	0.399	0.550	0.700	0.738	0.775	0.815	0.857	0.878	0.896	0.900
EXPERT C	0.100	0.111	0.159	0.219	0.340	0.440	0.520	0.600	0.660	0.720	0.770	0.810	0.830	0.846	0.850
EXPERT D	0.013	0.020	0.050	0.100	0.200	0.300	0.400	0.500	0.580	0.660	0.738	0.813	0.850	0.950	0.973
EXPERT E	0.275	0.280	0.300	0.308	0.323	0.338	0.354	0.370	0.402	0.434	0.480	0.540	0.570	0.800	0.852
AVERAGE	0.016	0.050	0.165	0.242	0.327	0.388	0.449	0.521	0.598	0.681	0.748	0.806	0.842	0.894	0.962
							C9:Z,2,3								
EXPERT A	0.005	0.046	0.050	0.056	0.067	0.078	0.089	0.100	0.111	0.122	0.133	0.144	0.150	0.191	0.200
EXPERT B	0.001	0.001	0.001	0.002	0.003	0.005	0.007	0.010	0.019	0.027	0.044	0.068	0.080	0.096	0.100
EXPERT C	0.001	0.002	0.005	0.009	0.018	0.026	0.038	0.050	0.090	0.130	0.180	0.240	0.270	0.225	0.300
EXPERT D	0.000	0.000	0.001	0.002	0.004	0.007	0.012	0.016	0.028	0.041	0.080	0.147	0.180	0.360	0.550
EXPERT E	0.066	0.100	0.250	0.275	0.325	0.360	0.380	0.400	0.416	0.432	0.453	0.477	0.490	0.590	0.613
AVERAGE	0.000	0.001	0.002	0.004	0.010	0.024	0.045	0.071	0.103	0.140	0.268	0.401	0.442	0.499	0.602

Table 5.1 (Continued)

	0.001	0.010	0.050	0.100	0.200	0.300	0.400	0.500	0.600	0.700	0.800	0.900	0.950	0.99	0.999
							CN:SU,2,3								
EXPERT A	0.045	0.046	0.050	0.056	0.067	0.078	0.089	0.100	0.111	0.122	0.133	0.144	0.150	0.191	0.200
EXPERT B	0.001	0.001	0.001	0.002	0.003	0.005	0.007	0.010	0.019	0.027	0.044	0.068	0.080	0.096	0.100
EXPERT C	0.001	0.002	0.005	0.009	0.016	0.026	0.038	0.050	0.090	0.130	0.180	0.240	0.270	0.295	0.300
EXPERT D	0.000	0.000	0.001	0.002	0.004	0.007	0.012	0.016	0.028	0.041	0.080	0.147	0.180	0.360	0.550
EXPERT E	0.139	0.150	0.200	0.220	0.260	0.296	0.328	0.360	0.384	0.408	0.442	0.487	0.510	0.600	0.620
AVERAGE	0.000	0.001	0.002	0.004	0.010	0.024	0.045	0.072	0.104	0.142	0.237	0.362	0.423	0.516	0.611
							C9:Z,4,6								
EXPERT A	0.045	0.046	0.050	0.056	0.067	0.078	0.089	0.100	0.111	0.122	0.133	0.144	0.150	0.191	0.200
EXPERT B	0.001	0.001	0.001	0.002	0.003	0.005	0.007	0.010	0.019	0.027	0.044	0.068	0.080	0.096	0.100
EXPERT C	0.020	0.021	0.024	0.028	0.036	0.072	0.136	0.200	0.240	0.280	0.340	0.420	0.461	0.493	0.500
EXPERT D	0.002	0.004	0.011	0.020	0.039	0.067	0.104	0.140	0.216	0.292	0.420	0.600	0.690	0.850	0.920
EXPERT E	0.066	0.100	0.250	0.275	0.325	0.360	0.380	0.400	0.416	0.432	0.453	0.477	0.490	0.590	0.613
AVERAGE	0.001	0.001	0.003	0.009	0.030	0.056	0.085	0.119	0.172	0.281	0.376	0.443	0.486	0.690	0.889
							C9:SU,4,6								
EXPERT A	0.045	0.046	0.050	0.056	0.067	0.078	0.089	0.100	0.111	0.122	0.133	0.144	0.150	0.191	0.200
EXPERT B	0.001	0.001	0.001	0.002	0.003	0.005	0.007	0.010	0.019	0.027	0.044	0.068	0.080	0.096	0.100
EXPERT C	0.020	0.021	0.024	0.028	0.036	0.072	0.136	0.200	0.240	0.280	0.340	0.420	0.461	0.493	0.500
EXPERT D	0.002	0.004	0.011	0.020	0.039	0.067	0.104	0.140	0.216	0.292	0.420	0.600	0.690	0.850	0.920
EXPERT E	0.139	0.150	0.200	0.220	0.260	0.296	0.328	0.360	0.384	0.408	0.442	0.487	0.510	0.600	0.620
AVERAGE	0.001	0.001	0.003	0.009	0.030	0.056	0.085	0.120	0.173	0.259	0.341	0.433	0.495	0.690	0.889
							C9:Z,5,7-9								
EXPERT A	0.045	0.046	0.050	0.056	0.067	0.078	0.089	0.100	0.111	0.122	0.133	0.144	0.150	0.191	0.200
EXPERT B	0.001	0.001	0.001	0.002	0.003	0.005	0.007	0.010	0.019	0.027	0.044	0.068	0.080	0.096	0.100
EXPERT C	0.010	0.010	0.012	0.014	0.018	0.036	0.068	0.100	0.140	0.180	0.220	0.260	0.280	0.296	0.300
EXPERT D	0.001	0.003	0.006	0.009	0.016	0.025	0.036	0.047	0.072	0.097	0.158	0.252	0.300	0.460	0.600
EXPERT E	0.066	0.100	0.250	0.275	0.325	0.360	0.380	0.400	0.416	0.432	0.453	0.477	0.490	0.590	0.613
AVERAGE	0.001	0.001	0.003	0.008	0.017	0.038	0.063	0.088	0.120	0.173	0.282	0.404	0.444	0.507	0.604

Table 5.1 (Continued)

	0.001	0.010	0.050	0.100	0.200	0.300	0.400	0.500	0.600	0.700	0.800	0.900	0.950	0.99	0.999
							C9:SH,5,7-9								
EXPERT A	0.045	0.046	0.050	0.056	0.067	0.078	0.089	0.100	0.111	0.122	0.133	0.144	0.150	0.191	0.200
EXPERT B	0.001	0.001	0.001	0.002	0.003	0.005	0.007	0.010	0.019	0.027	0.044	0.068	0.080	0.096	0.100
EXPERT C	0.010	0.010	0.012	0.014	0.018	0.036	0.068	0.100	0.140	0.180	0.220	0.260	0.280	0.296	0.300
EXPERT D	0.001	0.003	0.006	0.009	0.016	0.025	0.036	0.047	0.072	0.097	0.158	0.253	0.300	0.460	0.600
EXPERT E	0.139	0.150	0.200	0.220	0.260	0.296	0.328	0.360	0.384	0.408	0.442	0.487	0.510	0.600	0.620
AVERAGE	0.001	0.001	0.003	0.008	0.017	0.038	0.066	0.089	0.121	0.173	0.259	0.368	0.428	0.523	0.612
							C9:SQ,2,3								
EXPERT A	0.045	0.046	0.050	0.056	0.067	0.078	0.088	0.100	0.111	0.122	0.133	0.144	0.150	0.191	0.200
EXPERT B	0.001	0.001	0.001	0.002	0.003	0.005	0.007	0.010	0.019	0.027	0.044	0.068	0.080	0.096	0.100
EXPERT C	0.001	0.002	0.005	0.009	0.018	0.028	0.038	0.050	0.090	0.130	0.180	0.240	0.270	0.295	0.300
EXPERT D	0.000	0.000	0.000	0.001	0.002	0.003	0.005	0.007	0.014	0.021	0.049	0.096	0.120	0.270	0.490
EXPERT E	0.033	0.060	0.180	0.230	0.330	0.408	0.464	0.520	0.560	0.600	0.645	0.695	0.720	0.750	0.757
AVERAGE	0.000	0.000	0.001	0.003	0.008	0.019	0.041	0.067	0.097	0.134	0.243	0.520	0.620	0.720	0.754
							C9:SQ,4,6								
EXPERT A	0.045	0.046	0.050	0.056	0.067	0.078	0.089	0.100	0.111	0.122	0.133	0.144	0.150	0.191	0.200
EXPERT B	0.001	0.001	0.001	0.002	0.003	0.005	0.007	0.010	0.019	0.027	0.044	0.068	0.080	0.096	0.100
EXPERT C	0.020	0.021	0.024	0.028	0.036	0.072	0.136	0.200	0.240	0.280	0.340	0.420	0.461	0.493	0.500
EXPERT D	0.001	0.002	0.004	0.009	0.018	0.032	0.051	0.070	0.122	0.174	0.292	0.477	0.570	0.790	0.900
EXPERT E	0.033	0.060	0.180	0.230	0.330	0.408	0.464	0.520	0.560	0.600	0.645	0.695	0.720	0.750	0.757
AVERAGE	0.001	0.001	0.003	0.008	0.025	0.048	0.073	0.106	0.145	0.245	0.395	0.545	0.639	0.735	0.851
							C9:SQ,5,7-9								
EXPERT A	0.045	0.046	0.050	0.056	0.067	0.078	0.089	0.100	0.111	0.122	0.133	0.144	0.150	0.191	0.200
EXPERT B	0.001	0.001	0.001	0.002	0.003	0.005	0.007	0.010	0.019	0.027	0.044	0.068	0.080	0.096	0.100
EXPERT C	0.010	0.010	0.012	0.014	0.018	0.036	0.068	0.100	0.140	0.180	0.220	0.260	0.280	0.296	0.300
EXPERT D	0.000	0.001	0.002	0.004	0.007	0.011	0.017	0.023	0.038	0.053	0.099	0.173	0.210	0.380	0.560
EXPERT E	0.033	0.060	0.180	0.230	0.330	0.408	0.464	0.520	0.560	0.600	0.645	0.695	0.720	0.750	0.757
AVERAGE	0.001	0.001	0.003	0.006	0.014	0.027	0.054	0.080	0.113	0.153	0.262	0.521	0.620	0.720	0.754

Table 5.1 (Continued)

	0.001	0.010	0.050	0.100	0.200	0.300	0.400	0.500	0.600	0.700	0.800	0.900	0.950	0.99	0.999
C10:SQ,LOW,2,3															
EXPERT A	0.378	0.382	0.400	0.422	0.467	0.511	0.556	0.600	0.644	0.689	0.733	0.778	0.800	0.882	0.900
EXPERT B	0.150	0.154	0.175	0.212	0.287	0.399	0.550	0.700	0.738	0.775	0.815	0.857	0.878	0.896	0.900
EXPERT C	0.300	0.307	0.339	0.380	0.460	0.540	0.620	0.700	0.760	0.820	0.860	0.880	0.890	0.898	0.900
EXPERT D	0.005	0.050	0.250	0.338	0.513	0.640	0.720	0.800	0.840	0.880	0.912	0.938	0.950	0.980	0.987
EXPERT E	0.099	0.180	0.540	0.603	0.728	0.806	0.838	0.870	0.890	0.910	0.928	0.942	0.950	0.960	0.962
AVERAGE	0.025	0.155	0.265	0.363	0.473	0.572	0.655	0.726	0.784	0.833	0.874	0.911	0.936	0.959	0.984
C10:SQ,LOW,4-9															
EXPERT A	0.378	0.382	0.400	0.422	0.467	0.511	0.556	0.600	0.644	0.689	0.733	0.778	0.800	0.882	0.900
EXPERT B	0.150	0.154	0.175	0.212	0.287	0.399	0.550	0.700	0.738	0.775	0.815	0.857	0.878	0.896	0.900
EXPERT C	0.100	0.107	0.139	0.180	0.260	0.340	0.420	0.500	0.600	0.700	0.770	0.810	0.830	0.846	0.850
EXPERT D	0.005	0.050	0.250	0.338	0.513	0.640	0.720	0.800	0.840	0.880	0.912	0.938	0.950	0.980	0.987
EXPERT E	0.099	0.180	0.540	0.603	0.728	0.806	0.838	0.870	0.890	0.910	0.928	0.942	0.950	0.960	0.962
AVERAGE	0.025	0.118	0.196	0.279	0.422	0.526	0.620	0.703	0.763	0.812	0.858	0.911	0.936	0.959	0.984
C10:SQ,UP,2,3															
EXPERT A	0.378	0.382	0.400	0.422	0.467	0.511	0.556	0.600	0.644	0.689	0.733	0.778	0.800	0.882	0.900
EXPERT B	0.150	0.154	0.175	0.212	0.287	0.399	0.550	0.700	0.738	0.775	0.815	0.857	0.878	0.896	0.900
EXPERT C	0.300	0.307	0.339	0.380	0.460	0.540	0.620	0.700	0.760	0.820	0.860	0.880	0.890	0.898	0.900
EXPERT D	0.002	0.020	0.100	0.150	0.250	0.370	0.510	0.650	0.690	0.730	0.788	0.862	0.900	0.980	0.998
EXPERT E	0.067	0.110	0.300	0.350	0.450	0.520	0.560	0.600	0.632	0.664	0.695	0.725	0.740	0.790	0.801
AVERAGE	0.010	0.089	0.195	0.293	0.409	0.494	0.563	0.628	0.683	0.727	0.777	0.851	0.878	0.906	0.990
C10:SQ,UP,4-9															
EXPERT A	0.378	0.382	0.400	0.422	0.467	0.511	0.556	0.600	0.644	0.689	0.733	0.778	0.800	0.882	0.900
EXPERT B	0.150	0.154	0.175	0.212	0.287	0.399	0.550	0.700	0.738	0.775	0.815	0.857	0.878	0.896	0.900
EXPERT C	0.100	0.107	0.139	0.180	0.260	0.340	0.420	0.500	0.600	0.700	0.770	0.810	0.830	0.846	0.850
EXPERT D	0.002	0.020	0.100	0.150	0.250	0.370	0.510	0.650	0.690	0.730	0.788	0.862	0.900	0.980	0.998
EXPERT E	0.067	0.110	0.300	0.350	0.450	0.520	0.560	0.600	0.632	0.664	0.695	0.725	0.740	0.790	0.801
AVERAGE	0.010	0.088	0.185	0.229	0.359	0.452	0.530	0.600	0.662	0.711	0.758	0.814	0.852	0.904	0.990

Table 5.1 (Continued)

	0.001	0.010	0.050	0.100	0.200	0.300	0.400	0.500	0.600	0.700	0.800	0.900	0.950	0.99	0.999
C11:PB,SAT,2,3															
EXPERT A	0.189	0.191	0.200	0.211	0.233	0.256	0.278	0.300	0.367	0.433	0.500	0.567	0.600	0.845	0.900
EXPERT B	0.054	0.052	0.063	0.087	0.134	0.226	0.363	0.500	0.553	0.606	0.666	0.731	0.764	0.793	0.800
EXPERT C	0.010	0.013	0.028	0.046	0.082	0.120	0.160	0.200	0.280	0.360	0.440	0.520	0.561	0.583	0.600
EXPERT D	0.004	0.009	0.024	0.043	0.080	0.120	0.165	0.210	0.318	0.426	0.558	0.712	0.790	0.900	0.950
EXPERT E	0.039	0.050	0.100	0.117	0.153	0.186	0.218	0.250	0.290	0.330	0.390	0.470	0.510	0.993	1.000
AVERAGE	0.006	0.017	0.051	0.078	0.133	0.188	0.232	0.281	0.345	0.433	0.521	0.628	0.730	0.865	0.997
C11:PB,SAT,4-8															
EXPERT A	0.189	0.191	0.200	0.211	0.233	0.256	0.278	0.300	0.367	0.433	0.500	0.567	0.600	0.845	0.900
EXPERT B	0.050	0.052	0.063	0.087	0.134	0.226	0.363	0.500	0.553	0.606	0.666	0.731	0.764	0.793	0.800
EXPERT C	0.010	0.011	0.018	0.026	0.042	0.060	0.080	0.100	0.140	0.180	0.240	0.320	0.361	0.393	0.400
EXPERT D	0.004	0.009	0.024	0.043	0.080	0.120	0.165	0.210	0.318	0.426	0.558	0.712	0.790	0.900	0.950
EXPERT E	0.039	0.050	0.100	0.117	0.153	0.186	0.218	0.250	0.290	0.330	0.390	0.470	0.510	0.993	1.000
AVERAGE	0.006	0.014	0.036	0.060	0.107	0.159	0.208	0.256	0.309	0.389	0.500	0.628	0.730	0.865	0.997
C11:GG,SAT,2,3															
EXPERT A	0.189	0.191	0.200	0.211	0.233	0.256	0.278	0.300	0.367	0.433	0.500	0.567	0.600	0.845	0.900
EXPERT B	0.050	0.052	0.063	0.087	0.134	0.226	0.363	0.500	0.553	0.606	0.666	0.731	0.764	0.793	0.800
EXPERT C	0.010	0.013	0.028	0.046	0.082	0.120	0.160	0.200	0.280	0.360	0.440	0.520	0.561	0.583	0.600
EXPERT D	0.001	0.003	0.008	0.015	0.030	0.052	0.081	0.110	0.178	0.248	0.370	0.550	0.640	0.810	0.910
EXPERT E	0.059	0.070	0.120	0.132	0.157	0.180	0.200	0.220	0.244	0.268	0.330	0.430	0.480	0.700	0.749
AVERAGE	0.002	0.008	0.030	0.059	0.115	0.167	0.211	0.251	0.299	0.397	0.500	0.593	0.689	0.789	0.892
C11:GG,SAT,4-8															
	0.001	0.010	0.050	0.100	0.200	0.300	0.400	0.500	0.600	0.700	0.800	0.900	0.950	0.990	0.999
EXPERT A	0.189	0.191	0.200	0.211	0.233	0.256	0.278	0.300	0.367	0.433	0.500	0.567	0.600	0.845	0.900
EXPERT B	0.050	0.052	0.063	0.087	0.134	0.226	0.363	0.500	0.553	0.606	0.666	0.731	0.764	0.793	0.800
EXPERT C	0.010	0.011	0.018	0.026	0.042	0.060	0.080	0.100	0.140	0.180	0.240	0.320	0.361	0.393	0.400
EXPERT D	0.001	0.003	0.008	0.015	0.030	0.052	0.081	0.110	0.178	0.248	0.370	0.550	0.640	0.810	0.910
EXPERT E	0.059	0.070	0.120	0.132	0.157	0.180	0.200	0.220	0.244	0.268	0.330	0.430	0.480	0.700	0.749
AVERAGE	0.002	0.008	0.024	0.046	0.089	0.141	0.192	0.231	0.272	0.348	0.462	0.581	0.689	0.789	0.892

Table 5.1 (Continued)

	0.001	0.010	0.050	0.100	0.200	0.300	0.400	0.500	0.600	0.700	0.800	0.900	0.950	0.99	0.999
C12:PB,SUB,2,3															
EXPERT A	0.184	0.187	0.200	0.217	0.250	0.283	0.317	0.350	0.406	0.461	0.517	0.572	0.600	0.845	0.900
EXPERT B	0.050	0.052	0.063	0.087	0.134	0.226	0.363	0.500	0.553	0.606	0.666	0.731	0.764	0.793	0.800
EXPERT C	0.010	0.013	0.028	0.046	0.082	0.120	0.160	0.200	0.280	0.360	0.440	0.520	0.561	0.593	0.600
EXPERT D	0.002	0.004	0.008	0.014	0.025	0.041	0.060	0.079	0.123	0.168	0.257	0.392	0.460	0.660	0.810
EXPERT E	0.029	0.060	0.200	0.260	0.380	0.472	0.536	0.600	0.660	0.720	0.785	0.855	0.890	0.990	1.000
AVERAGE	0.002	0.008	0.026	0.053	0.107	0.182	0.255	0.331	0.421	0.508	0.583	0.707	0.783	0.895	0.996
C12:PB,SUB,4-9															
EXPERT A	0.184	0.187	0.200	0.217	0.250	0.283	0.317	0.350	0.406	0.461	0.517	0.572	0.600	0.845	0.900
EXPERT B	0.050	0.052	0.063	0.087	0.134	0.226	0.363	0.500	0.553	0.606	0.666	0.731	0.764	0.793	0.800
EXPERT C	0.010	0.011	0.018	0.026	0.042	0.060	0.080	0.100	0.140	0.180	0.240	0.320	0.361	0.393	0.400
EXPERT D	0.002	0.004	0.008	0.014	0.025	0.041	0.060	0.079	0.123	0.168	0.257	0.392	0.460	0.660	0.810
EXPERT E	0.029	0.060	0.200	0.260	0.380	0.472	0.536	0.600	0.660	0.720	0.785	0.855	0.890	0.990	1.000
AVERAGE	0.002	0.008	0.022	0.041	0.080	0.142	0.217	0.283	0.374	0.483	0.579	0.707	0.783	0.895	0.996
C12:GG,SUB,2,3															
EXPERT A	0.184	0.187	0.200	0.217	0.250	0.283	0.317	0.350	0.406	0.461	0.517	0.572	0.600	0.845	0.900
EXPERT B	0.050	0.052	0.063	0.087	0.134	0.226	0.363	0.500	0.553	0.606	0.666	0.731	0.764	0.793	0.800
EXPERT C	0.010	0.013	0.028	0.046	0.082	0.120	0.160	0.200	0.280	0.360	0.440	0.520	0.561	0.593	0.600
EXPERT D	0.000	0.001	0.003	0.005	0.010	0.016	0.025	0.033	0.055	0.078	0.139	0.240	0.290	0.500	0.690
EXPERT E	0.044	0.060	0.130	0.160	0.220	0.268	0.304	0.340	0.380	0.420	0.472	0.537	0.570	0.700	0.729
AVERAGE	0.001	0.003	0.012	0.029	0.079	0.150	0.219	0.280	0.342	0.417	0.504	0.583	0.672	0.779	0.876
C12:GG,SUB,4-9															
EXPERT A	0.184	0.187	0.200	0.217	0.250	0.283	0.317	0.350	0.406	0.461	0.517	0.572	0.600	0.845	0.900
EXPERT B	0.050	0.052	0.063	0.087	0.134	0.226	0.363	0.500	0.553	0.606	0.666	0.731	0.764	0.793	0.800
EXPERT C	0.010	0.011	0.018	0.026	0.042	0.060	0.080	0.100	0.140	0.180	0.240	0.320	0.361	0.393	0.400
EXPERT D	0.000	0.001	0.003	0.005	0.010	0.016	0.025	0.033	0.055	0.078	0.139	0.240	0.290	0.500	0.690
EXPERT E	0.044	0.060	0.130	0.160	0.220	0.268	0.304	0.340	0.380	0.420	0.472	0.537	0.570	0.700	0.729
AVERAGE	0.001	0.003	0.012	0.025	0.062	0.113	0.188	0.251	0.310	0.379	0.478	0.577	0.672	0.779	0.876

Table 5.1 (Continued)

	0.001	0.010	0.050	0.100	0.200	0.300	0.400	0.500	0.600	0.700	0.800	0.900	0.950	0.99	0.999
							C13:PB,SAT,2,3								
EXPERT A	0.378	0.382	0.400	0.422	0.467	0.511	0.556	0.600	0.644	0.689	0.733	0.778	0.800	0.882	0.900
EXPERT B	0.150	0.154	0.175	0.212	0.287	0.399	0.550	0.700	0.738	0.775	0.815	0.857	0.878	0.896	0.900
EXPERT C	0.300	0.307	0.339	0.380	0.460	0.540	0.620	0.700	0.760	0.820	0.870	0.910	0.930	0.946	0.950
EXPERT D	0.006	0.050	0.300	0.438	0.713	0.866	0.898	0.930	0.946	0.962	0.976	0.989	0.995	1.000	1.000
EXPERT E	0.157	0.220	0.500	0.575	0.725	0.822	0.866	0.910	0.930	0.950	0.965	0.975	0.980	0.995	0.998
AVERAGE	0.026	0.160	0.276	0.379	0.491	0.584	0.680	0.752	0.819	0.876	0.925	0.964	0.978	0.996	1.000
							C13:PB,SAT,4-9								
EXPERT A	0.378	0.382	0.400	0.422	0.467	0.511	0.556	0.600	0.644	0.689	0.733	0.778	0.800	0.882	0.900
EXPERT B	0.150	0.154	0.175	0.212	0.287	0.399	0.550	0.700	0.738	0.775	0.815	0.857	0.878	0.896	0.900
EXPERT C	0.010	0.017	0.047	0.086	0.162	0.260	0.380	0.500	0.560	0.620	0.680	0.740	0.770	0.795	0.800
EXPERT D	0.006	0.050	0.300	0.438	0.713	0.866	0.898	0.930	0.946	0.962	0.976	0.989	0.995	1.000	1.000
EXPERT E	0.157	0.220	0.500	0.575	0.725	0.822	0.866	0.910	0.930	0.950	0.965	0.975	0.980	0.995	0.998
AVERAGE	0.011	0.041	0.161	0.251	0.426	0.533	0.622	0.708	0.774	0.853	0.918	0.964	0.978	0.996	1.000
							C13:GG,SAT,2,3								
EXPERT A	0.378	0.382	0.400	0.422	0.467	0.511	0.556	0.600	0.644	0.689	0.733	0.778	0.800	0.882	0.900
EXPERT B	0.150	0.154	0.175	0.212	0.287	0.399	0.550	0.700	0.738	0.775	0.815	0.857	0.878	0.896	0.900
EXPERT C	0.300	0.307	0.339	0.380	0.460	0.540	0.620	0.700	0.760	0.820	0.870	0.910	0.930	0.946	0.950
EXPERT D	0.027	0.050	0.150	0.188	0.263	0.380	0.540	0.700	0.760	0.820	0.875	0.925	0.950	0.980	0.987
EXPERT E	0.295	0.360	0.650	0.700	0.800	0.860	0.880	0.900	0.908	0.916	0.930	0.950	0.960	0.990	0.997
AVERAGE	0.038	0.148	0.218	0.309	0.440	0.541	0.643	0.719	0.773	0.835	0.882	0.916	0.940	0.974	0.994
							C13:GG,SAT,4-9								
EXPERT A	0.378	0.382	0.400	0.422	0.467	0.511	0.556	0.600	0.644	0.689	0.733	0.778	0.800	0.882	0.900
EXPERT B	0.150	0.154	0.175	0.212	0.287	0.399	0.550	0.700	0.738	0.775	0.815	0.857	0.878	0.896	0.900
EXPERT C	0.010	0.017	0.047	0.086	0.162	0.260	0.380	0.500	0.560	0.620	0.680	0.740	0.770	0.795	0.800
EXPERT D	0.027	0.050	0.150	0.188	0.263	0.380	0.540	0.700	0.760	0.820	0.875	0.925	0.950	0.980	0.987
EXPERT E	0.295	0.360	0.650	0.700	0.800	0.860	0.880	0.900	0.908	0.916	0.930	0.950	0.960	0.990	0.997
AVERAGE	0.013	0.042	0.153	0.214	0.379	0.490	0.585	0.675	0.737	0.791	0.864	0.910	0.936	0.974	0.994

Table 5.1 (Continued)

	0.001	0.010	0.050	0.100	0.200	0.300	0.400	0.500	0.600	0.700	0.800	0.900	0.950	0.99	0.999
C14:PB,SUB,2,3															
EXPERT A	0.367	0.373	0.400	0.433	0.500	0.567	0.633	0.700	0.722	0.744	0.767	0.789	0.800	0.882	0.900
EXPERT B	0.150	0.154	0.175	0.212	0.287	0.399	0.550	0.700	0.738	0.775	0.815	0.857	0.878	0.896	0.900
EXPERT C	0.300	0.307	0.339	0.380	0.460	0.540	0.620	0.700	0.760	0.820	0.870	0.910	0.930	0.946	0.950
EXPERT D	0.010	0.010	0.100	0.175	0.325	0.480	0.640	0.800	0.840	0.880	0.918	0.952	0.970	1.000	1.000
EXPERT E	0.504	0.560	0.810	0.845	0.915	0.956	0.968	0.980	0.984	0.988	0.992	0.996	0.998	0.999	0.999
AVERAGE	0.010	0.100	0.225	0.332	0.468	0.588	0.703	0.755	0.810	0.867	0.929	0.981	0.991	0.998	1.000
C14:PB,SUB,4-9															
EXPERT A	0.367	0.373	0.400	0.433	0.500	0.567	0.633	0.700	0.722	0.744	0.767	0.789	0.800	0.882	0.900
EXPERT B	0.150	0.154	0.175	0.212	0.287	0.399	0.550	0.700	0.738	0.775	0.815	0.857	0.878	0.896	0.900
EXPERT C	0.010	0.020	0.067	0.125	0.242	0.340	0.420	0.500	0.580	0.660	0.730	0.790	0.820	0.845	0.850
EXPERT D	0.010	0.010	0.100	0.175	0.325	0.480	0.640	0.800	0.840	0.880	0.918	0.952	0.970	1.000	1.000
EXPERT E	0.504	0.560	0.810	0.845	0.915	0.956	0.968	0.980	0.984	0.988	0.992	0.996	0.998	0.999	0.999
AVERAGE	0.010	0.040	0.163	0.247	0.406	0.529	0.648	0.729	0.781	0.936	0.917	0.981	0.991	0.998	1.000
C14:GG,SUB,2,3															
EXPERT A	0.367	0.373	0.400	0.433	0.500	0.567	0.633	0.700	0.722	0.744	0.767	0.789	0.800	0.882	0.900
EXPERT B	0.150	0.154	0.175	0.212	0.287	0.399	0.550	0.700	0.738	0.775	0.815	0.857	0.878	0.896	0.900
EXPERT C	0.300	0.307	0.339	0.380	0.460	0.540	0.620	0.700	0.760	0.820	0.870	0.910	0.930	0.946	0.950
EXPERT D	0.027	0.050	0.150	0.188	0.263	0.380	0.540	0.700	0.760	0.820	0.875	0.925	0.950	0.980	0.987
EXPERT E	0.437	0.500	0.780	0.820	0.900	0.948	0.964	0.980	0.982	0.984	0.986	0.989	0.990	0.999	1.000
AVERAGE	0.038	0.148	0.218	0.310	0.452	0.571	0.691	0.743	0.789	0.851	0.913	0.980	0.985	0.990	1.000
C14:GG,SUB,4-9															
EXPERT A	0.367	0.373	0.400	0.433	0.500	0.567	0.633	0.700	0.722	0.744	0.767	0.789	0.800	0.882	0.900
EXPERT B	0.150	0.154	0.175	0.212	0.287	0.399	0.550	0.700	0.738	0.775	0.815	0.857	0.878	0.896	0.900
EXPERT C	0.010	0.020	0.067	0.125	0.242	0.340	0.420	0.500	0.580	0.660	0.730	0.790	0.820	0.845	0.850
EXPERT D	0.027	0.050	0.150	0.188	0.263	0.380	0.540	0.700	0.760	0.820	0.875	0.925	0.950	0.980	0.987
EXPERT E	0.437	0.500	0.780	0.820	0.900	0.948	0.964	0.980	0.982	0.984	0.986	0.989	0.990	0.999	1.000
AVERAGE	0.015	0.054	0.169	0.238	0.391	0.511	0.631	0.720	0.767	0.817	0.892	0.980	0.985	0.990	1.000

Table 5.1 (Continued)

	0.001	0.010	0.050	0.100	0.200	0.300	0.400	0.500	0.600	0.700	0.800	0.900	0.950	0.99	0.999
							C15:PB,2,3								
EXPERT A	0.045	0.046	0.050	0.056	0.067	0.078	0.089	0.100	0.111	0.122	0.133	0.144	0.150	0.191	0.200
EXPERT B	0.001	0.001	0.001	0.002	0.003	0.005	0.007	0.010	0.019	0.027	0.044	0.068	0.080	0.096	0.100
EXPERT C	0.002	0.002	0.004	0.005	0.008	0.014	0.022	0.030	0.045	0.062	0.090	0.130	0.150	0.166	0.170
EXPERT D	0.000	0.000	0.000	0.000	0.000	0.000	0.000	0.001	0.001	0.002	0.006	0.012	0.015	0.052	0.155
EXPERT E	0.007	0.010	0.025	0.034	0.051	0.068	0.084	0.100	0.124	0.148	0.183	0.227	0.250	0.320	0.336
AVERAGE	0.000	0.000	0.000	0.001	0.003	0.009	0.021	0.042	0.062	0.084	0.112	0.143	0.173	0.250	0.329
							C15:PB,4,6								
EXPERT A	0.045	0.046	0.050	0.056	0.067	0.078	0.089	0.100	0.111	0.122	0.133	0.144	0.150	0.191	0.200
EXPERT B	0.001	0.001	0.001	0.002	0.003	0.005	0.007	0.010	0.019	0.027	0.044	0.068	0.080	0.096	0.100
EXPERT C	0.005	0.006	0.010	0.015	0.025	0.044	0.072	0.100	0.140	0.180	0.260	0.381	0.441	0.489	0.500
EXPERT D	0.000	0.000	0.000	0.001	0.001	0.003	0.004	0.006	0.013	0.020	0.052	0.108	0.136	0.349	0.650
EXPERT E	0.007	0.010	0.025	0.034	0.051	0.068	0.084	0.100	0.124	0.148	0.183	0.227	0.250	0.320	0.336
AVERAGE	0.000	0.000	0.001	0.003	0.008	0.020	0.041	0.063	0.083	0.107	0.135	0.192	0.273	0.449	0.541
							C15:PB,5,7								
EXPERT A	0.045	0.046	0.050	0.056	0.067	0.078	0.089	0.100	0.111	0.122	0.133	0.144	0.150	0.191	0.200
EXPERT B	0.001	0.001	0.001	0.002	0.003	0.005	0.007	0.010	0.019	0.027	0.044	0.068	0.080	0.096	0.100
EXPERT C	0.005	0.006	0.008	0.011	0.017	0.026	0.038	0.050	0.070	0.090	0.180	0.341	0.421	0.486	0.500
EXPERT D	0.000	0.000	0.000	0.000	0.000	0.001	0.001	0.002	0.004	0.005	0.013	0.026	0.032	0.090	0.220
EXPERT E	0.007	0.010	0.025	0.034	0.051	0.068	0.084	0.100	0.124	0.148	0.183	0.227	0.250	0.320	0.336
AVERAGE	0.000	0.000	0.001	0.002	0.005	0.013	0.028	0.049	0.069	0.089	0.119	0.162	0.235	0.421	0.494
							C15:PB,8,9								
EXPERT A	0.045	0.046	0.050	0.056	0.067	0.078	0.089	0.100	0.111	0.122	0.133	0.144	0.150	0.191	0.200
EXPERT B	0.001	0.001	0.001	0.002	0.003	0.005	0.007	0.010	0.019	0.027	0.044	0.068	0.080	0.096	0.100
EXPERT C	0.005	0.006	0.008	0.011	0.017	0.026	0.038	0.050	0.070	0.090	0.180	0.341	0.421	0.486	0.500
EXPERT D	0.000	0.000	0.000	0.000	0.000	0.001	0.001	0.002	0.004	0.005	0.013	0.026	0.032	0.090	0.220
EXPERT E	0.007	0.010	0.025	0.034	0.051	0.068	0.084	0.100	0.124	0.148	0.183	0.227	0.250	0.320	0.336
AVERAGE	0.000	0.000	0.001	0.002	0.005	0.013	0.029	0.056	0.077	0.101	0.132	0.185	0.256	0.441	0.495

Table 5.1 (Continued)

	0.001	0.010	0.050	0.100	0.200	0.300	0.400	0.500	0.600	0.700	0.800	0.900	0.950	0.99	0.999
							C15:GG,2,3								
EXPERT A	0.045	0.046	0.050	0.056	0.067	0.078	0.089	0.100	0.111	0.122	0.133	0.144	0.150	0.191	0.200
EXPERT B	0.001	0.001	0.001	0.002	0.003	0.005	0.007	0.010	0.019	0.027	0.044	0.068	0.080	0.096	0.100
EXPERT C	0.002	0.002	0.004	0.005	0.008	0.014	0.022	0.030	0.046	0.062	0.090	0.130	0.150	0.166	0.170
EXPERT D	0.000	0.000	0.000	0.000	0.001	0.001	0.002	0.003	0.005	0.008	0.020	0.040	0.050	0.137	0.310
EXPERT E	0.026	0.040	0.100	0.120	0.160	0.194	0.222	0.250	0.282	0.314	0.375	0.465	0.510	0.780	0.841
AVERAGE	0.000	0.000	0.001	0.002	0.005	0.010	0.027	0.052	0.077	0.111	0.145	0.251	0.330	0.510	0.814
							C15:GG,4,6								
EXPERT A	0.045	0.046	0.050	0.056	0.067	0.078	0.089	0.100	0.111	0.122	0.133	0.144	0.150	0.191	0.200
EXPERT B	0.001	0.001	0.001	0.002	0.003	0.005	0.007	0.010	0.019	0.027	0.044	0.068	0.080	0.096	0.100
EXPERT C	0.005	0.006	0.010	0.015	0.025	0.044	0.072	0.100	0.140	0.180	0.260	0.381	0.441	0.489	0.500
EXPERT D	0.000	0.000	0.001	0.003	0.006	0.011	0.019	0.026	0.050	0.074	0.151	0.281	0.346	0.613	0.820
EXPERT E	0.026	0.040	0.100	0.120	0.160	0.194	0.222	0.250	0.282	0.314	0.375	0.465	0.510	0.780	0.841
AVERAGE	0.000	0.001	0.002	0.005	0.015	0.030	0.058	0.082	0.113	0.147	0.218	0.320	0.423	0.595	0.820
							C15:GG,5,7								
EXPERT A	0.045	0.046	0.050	0.056	0.067	0.078	0.089	0.100	0.111	0.122	0.133	0.144	0.150	0.191	0.200
EXPERT B	0.001	0.001	0.001	0.002	0.003	0.005	0.007	0.010	0.019	0.027	0.044	0.068	0.080	0.096	0.100
EXPERT C	0.005	0.008	0.008	0.011	0.017	0.026	0.038	0.050	0.070	0.090	0.180	0.341	0.421	0.486	0.500
EXPERT D	0.000	0.000	0.001	0.001	0.002	0.004	0.006	0.008	0.014	0.021	0.042	0.079	0.097	0.212	0.390
EXPERT E	0.026	0.040	0.100	0.120	0.160	0.194	0.222	0.250	0.282	0.314	0.375	0.465	0.510	0.780	0.841
AVERAGE	0.000	0.001	0.002	0.003	0.008	0.019	0.040	0.063	0.087	0.120	0.178	0.293	0.392	0.510	0.814
							C15:GG,8,9								
EXPERT A	0.045	0.046	0.050	0.056	0.067	0.078	0.089	0.100	0.111	0.122	0.133	0.144	0.150	0.191	0.200
EXPERT B	0.001	0.001	0.001	0.002	0.003	0.005	0.007	0.010	0.019	0.027	0.044	0.068	0.080	0.096	0.100
EXPERT C	0.005	0.006	0.008	0.011	0.017	0.026	0.068	0.100	0.140	0.180	0.260	0.381	0.441	0.489	0.500
EXPERT D	0.000	0.000	0.001	0.001	0.002	0.004	0.006	0.008	0.014	0.021	0.042	0.079	0.097	0.212	0.390
EXPERT E	0.026	0.040	0.100	0.120	0.160	0.194	0.222	0.250	0.282	0.314	0.375	0.465	0.510	0.780	0.841
AVERAGE	0.000	0.001	0.002	0.003	0.008	0.019	0.047	0.072	0.100	0.135	0.192	0.304	0.404	0.510	0.814

Table 5.1 (Continued)

	0.001	0.010	0.050	0.100	0.200	0.300	0.400	0.500	0.600	0.700	0.800	0.900	0.950	0.99	0.999
C16:PB,2,3															
EXPERT A	0.039	0.041	0.050	0.061	0.083	0.106	0.128	0.150	0.161	0.172	0.183	0.194	0.200	0.241	0.250
EXPERT B	0.001	0.001	0.001	0.002	0.003	0.005	0.007	0.010	0.019	0.027	0.044	0.068	0.080	0.096	0.100
EXPERT C	0.020	0.020	0.022	0.024	0.028	0.058	0.114	0.170	0.202	0.234	0.264	0.292	0.306	0.317	0.320
EXPERT D	0.000	0.000	0.000	0.000	0.001	0.001	0.002	0.003	0.006	0.009	0.024	0.049	0.062	0.170	0.360
EXPERT E	0.008	0.010	0.020	0.035	0.065	0.094	0.122	0.150	0.178	0.206	0.235	0.265	0.280	0.330	0.341
AVERAGE	0.014	0.014	0.018	0.024	0.036	0.053	0.075	0.097	0.113	0.129	0.150	0.175	0.186	0.223	0.234
C16:PB,4,6															
EXPERT A	0.039	0.041	0.050	0.061	0.083	0.106	0.128	0.150	0.161	0.172	0.183	0.194	0.200	0.241	0.250
EXPERT B	0.001	0.001	0.001	0.002	0.003	0.005	0.007	0.010	0.019	0.027	0.044	0.068	0.080	0.096	0.100
EXPERT C	0.060	0.061	0.068	0.076	0.092	0.180	0.340	0.500	0.600	0.700	0.790	0.870	0.911	0.947	0.950
EXPERT D	0.000	0.001	0.002	0.004	0.008	0.014	0.023	0.032	0.059	0.086	0.175	0.325	0.400	0.670	0.850
EXPERT E	0.008	0.010	0.020	0.035	0.065	0.094	0.122	0.150	0.178	0.206	0.235	0.265	0.280	0.330	0.341
AVERAGE	0.000	0.001	0.003	0.006	0.019	0.044	0.071	0.085	0.143	0.181	0.242	0.531	0.755	0.911	0.947
C16:PB,5,7-9															
EXPERT A	0.039	0.041	0.050	0.061	0.083	0.105	0.128	0.150	0.161	0.172	0.183	0.194	0.200	0.241	0.250
EXPERT B	0.001	0.001	0.001	0.002	0.003	0.005	0.007	0.010	0.019	0.027	0.044	0.068	0.080	0.096	0.100
EXPERT C	0.040	0.042	0.052	0.064	0.088	0.160	0.280	0.400	0.540	0.680	0.790	0.870	0.911	0.943	0.950
EXPERT D	0.000	0.000	0.003	0.003	0.004	0.005	0.007	0.010	0.018	0.025	0.057	0.097	0.120	0.280	0.450
EXPERT E	0.008	0.010	0.020	0.035	0.065	0.094	0.122	0.150	0.178	0.206	0.235	0.265	0.280	0.330	0.341
AVERAGE	0.000	0.001	0.003	0.004	0.010	0.027	0.057	0.085	0.123	0.169	0.212	0.404	0.750	0.911	0.947
C16:OG,2,3															
EXPERT A	0.039	0.041	0.050	0.061	0.083	0.106	0.128	0.150	0.161	0.172	0.183	0.194	0.200	0.241	0.250
EXPERT B	0.001	0.001	0.001	0.002	0.003	0.005	0.007	0.010	0.019	0.027	0.044	0.068	0.080	0.096	0.100
EXPERT C	0.020	0.020	0.022	0.024	0.028	0.058	0.114	0.170	0.202	0.234	0.264	0.292	0.306	0.317	0.320
EXPERT D	0.000	0.000	0.000	0.001	0.002	0.003	0.006	0.008	0.015	0.022	0.050	0.096	0.120	0.280	0.490
EXPERT E	0.023	0.030	0.060	0.078	0.112	0.146	0.178	0.210	0.258	0.306	0.383	0.488	0.540	0.930	1.000
AVERAGE	0.000	0.000	0.002	0.003	0.009	0.024	0.050	0.084	0.126	0.169	0.202	0.281	0.338	0.540	0.969

Table 5.1 (Continued)

	0.001	0.010	0.050	0.100	0.200	0.300	0.400	0.500	0.600	0.700	0.800	0.900	0.950	0.99	0.999
							C16:GG,4,6								
EXPERT A	0.039	0.041	0.050	0.061	0.082	0.106	0.128	0.150	0.161	0.172	0.183	0.194	0.200	0.241	0.250
EXPERT B	0.001	0.001	0.001	0.002	0.003	0.005	0.007	0.010	0.019	0.027	0.044	0.068	0.080	0.096	0.100
EXPERT C	0.060	0.061	0.068	0.078	0.092	0.180	0.340	0.500	0.600	0.700	0.790	0.870	0.911	0.943	0.950
EXPERT D	0.000	0.001	0.002	0.004	0.008	0.014	0.023	0.032	0.059	0.066	0.175	0.325	0.400	0.670	0.850
EXPERT E	0.023	0.030	0.060	0.078	0.112	0.146	0.178	0.210	0.258	0.306	0.383	0.487	0.540	0.930	1.000
AVERAGE	0.000	0.001	0.003	0.006	0.021	0.052	0.078	0.107	0.159	0.186	0.316	0.571	0.775	0.926	0.973
							C16:GG,5,7-9								
EXPERT A	0.039	0.041	0.050	0.061	0.083	0.108	0.128	0.150	0.161	0.172	0.183	0.194	0.200	0.24[illegible]	0.250
EXPERT B	0.001	0.001	0.001	0.002	0.003	0.005	0.007	0.010	0.019	0.027	0.044	0.068	0.080	0.09[illegible]	0.100
EXPERT C	0.040	0.042	0.052	0.064	0.088	0.160	0.280	0.400	0.540	0.680	0.790	0.870	0.911	0.[illegible]	0.950
EXPERT D	0.000	0.000	0.003	0.003	0.004	0.005	0.007	0.010	0.018	0.025	0.052	0.097	0.120	0.260	0.450
EXPERT E	0.023	0.030	0.060	0.078	0.112	0.146	0.178	0.210	0.258	0.306	0.383	0.487	0.540	0.930	1.000
AVERAGE	0.000	0.001	0.003	0.004	0.010	0.030	0.065	0.094	0.143	0.183	0.268	0.510	0.771	0.920	0.973

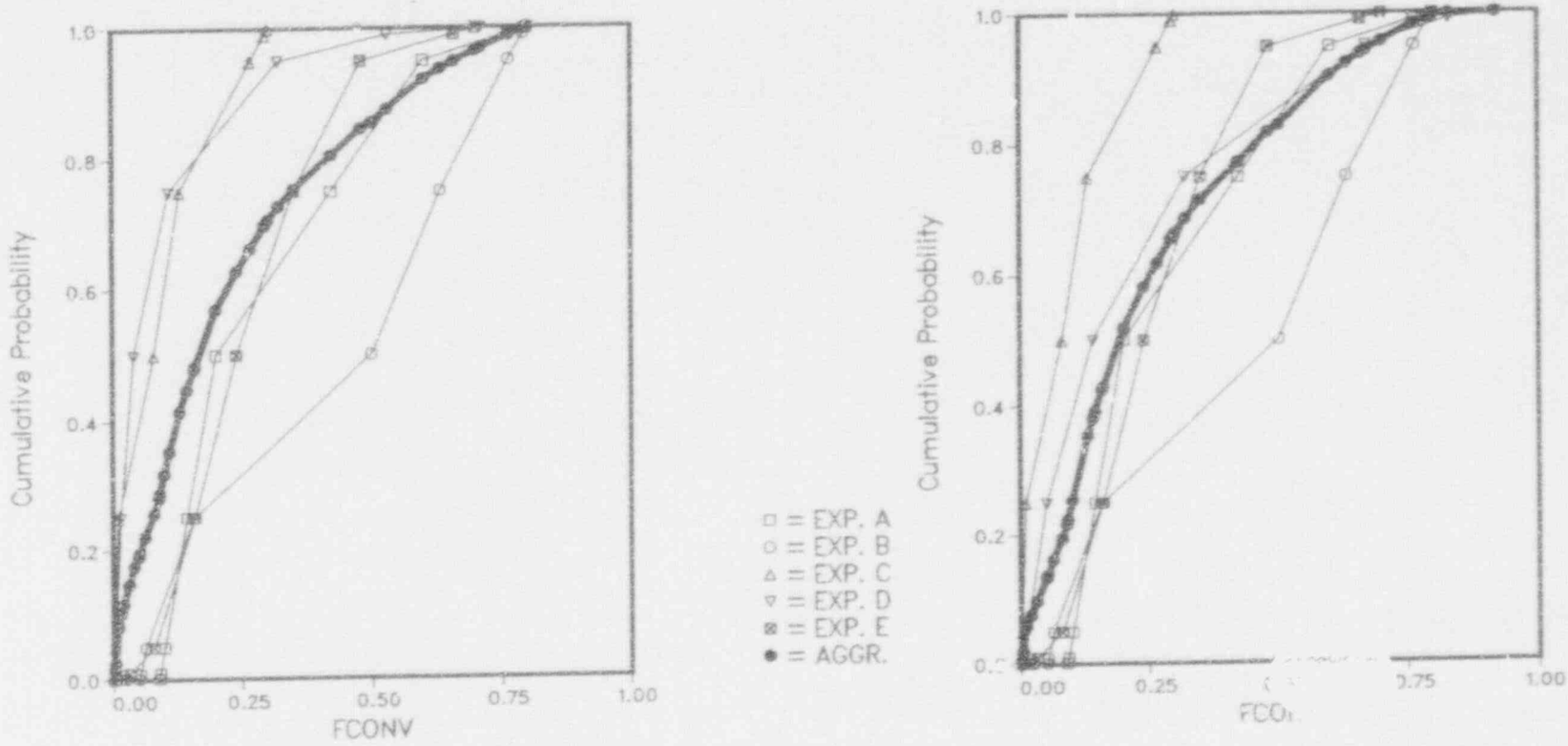

Figure 5-1. Case 1: Zion, Dry Cavity (left) and Wet Cavity (right).

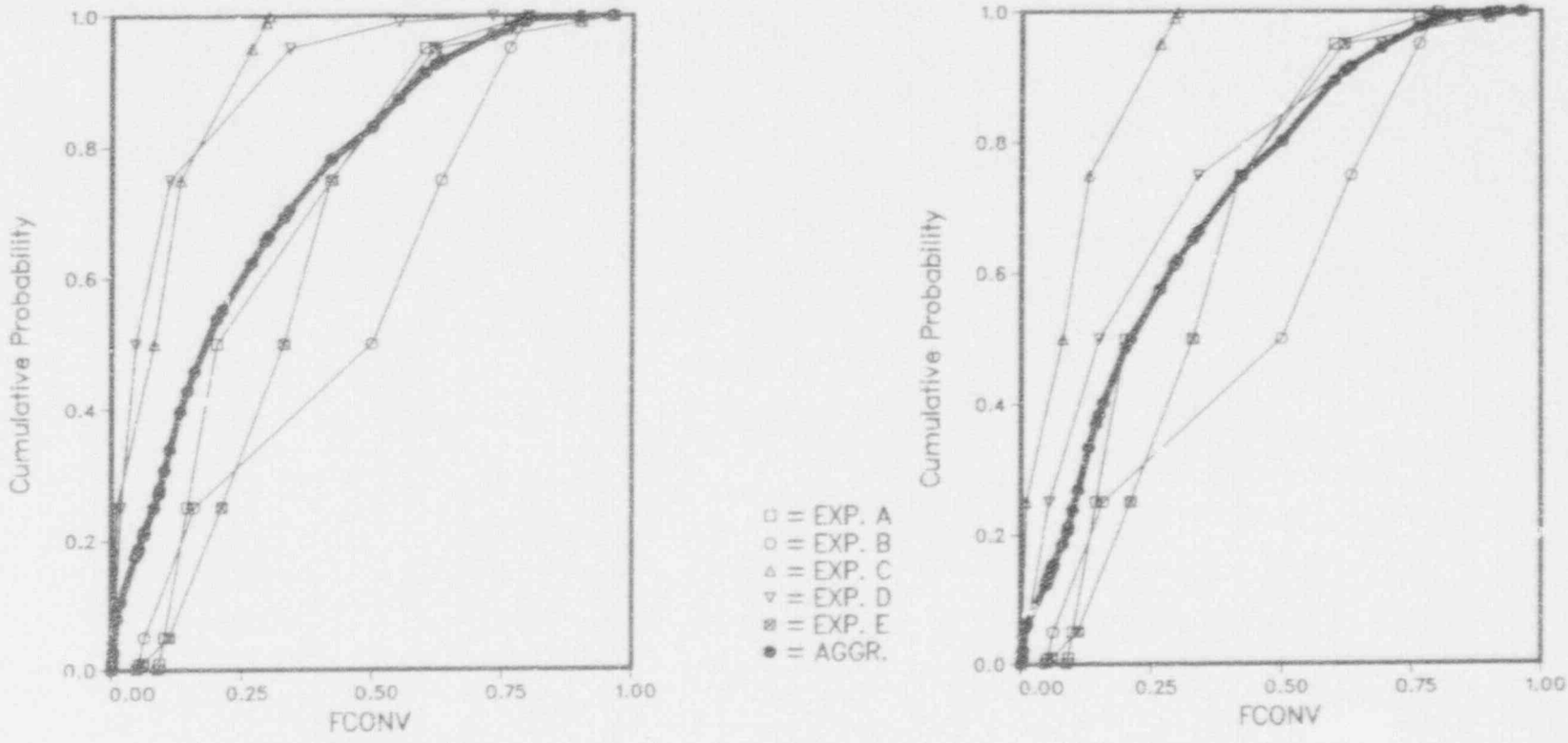

Figure 5-2. Case 1: Surry, Dry Cavity (left) and Wet Cavity (right).

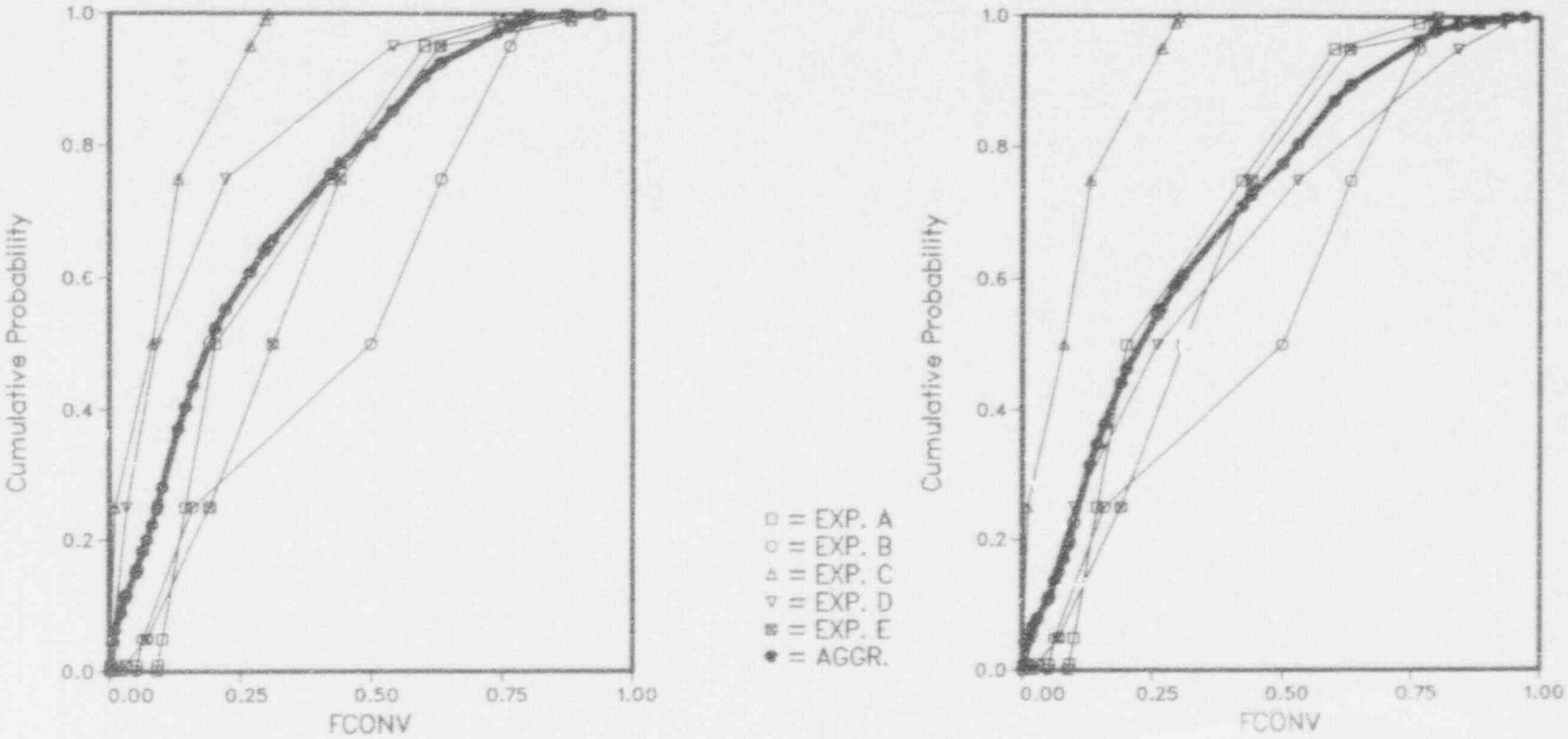

Figure 5-3. Case 1: Sequoyah, Dry Cavity (left) and Wet Cavity (right).

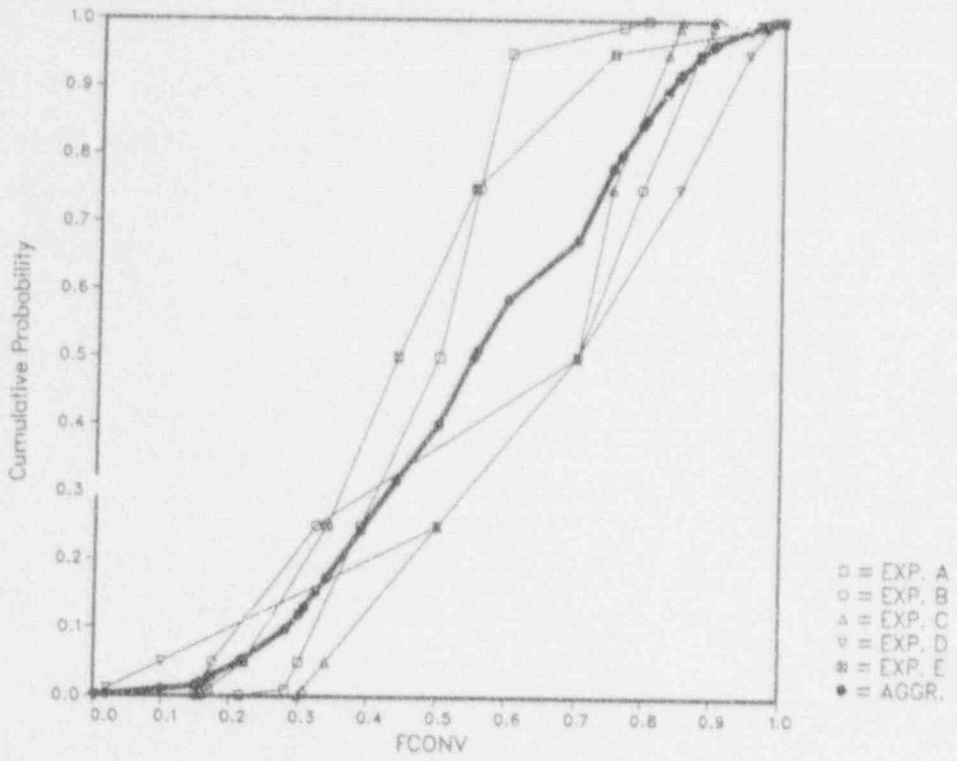

Figure 5-4. Case 2: Zion.

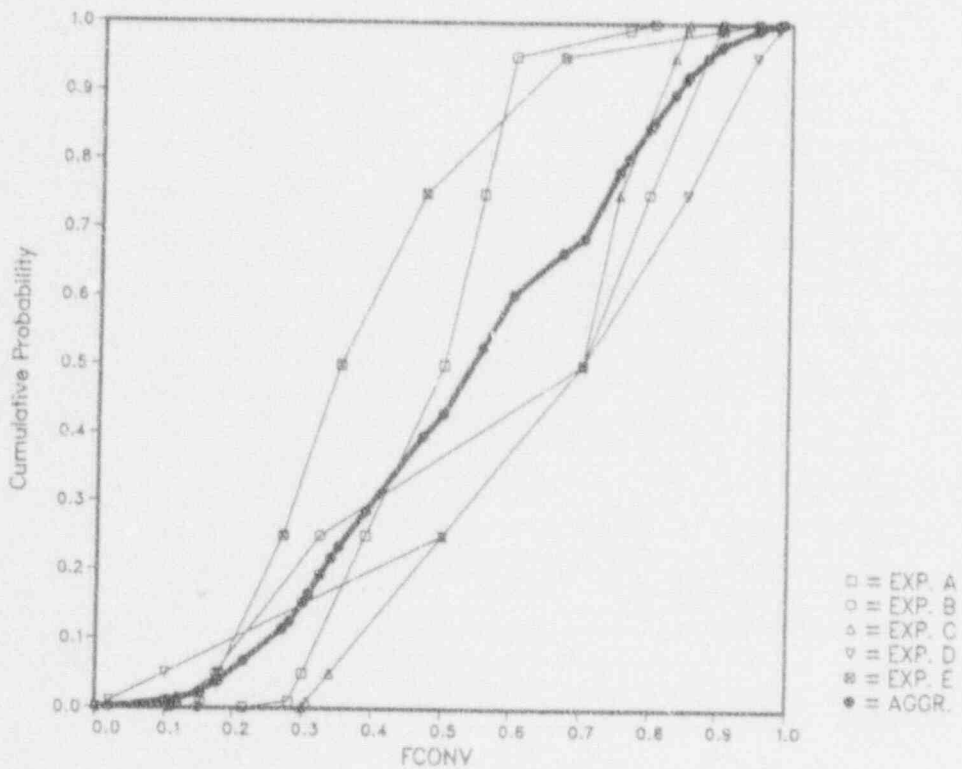

Figure 5-5. Case 2: Surry.

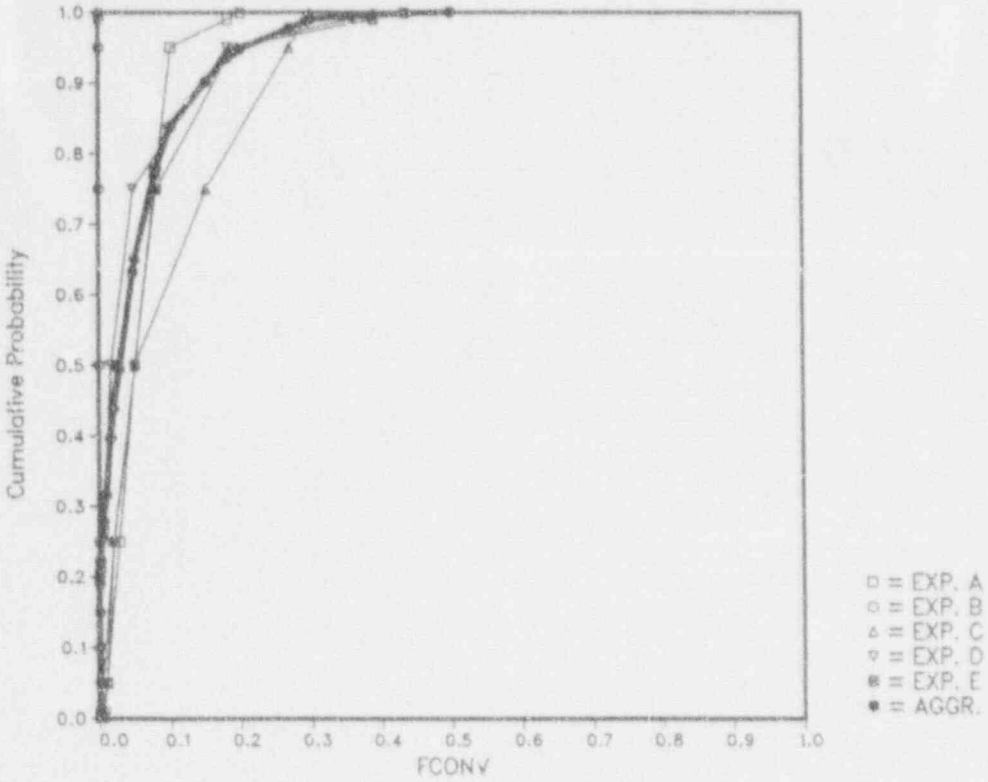

Figure 5-6. Case 3: Zion.

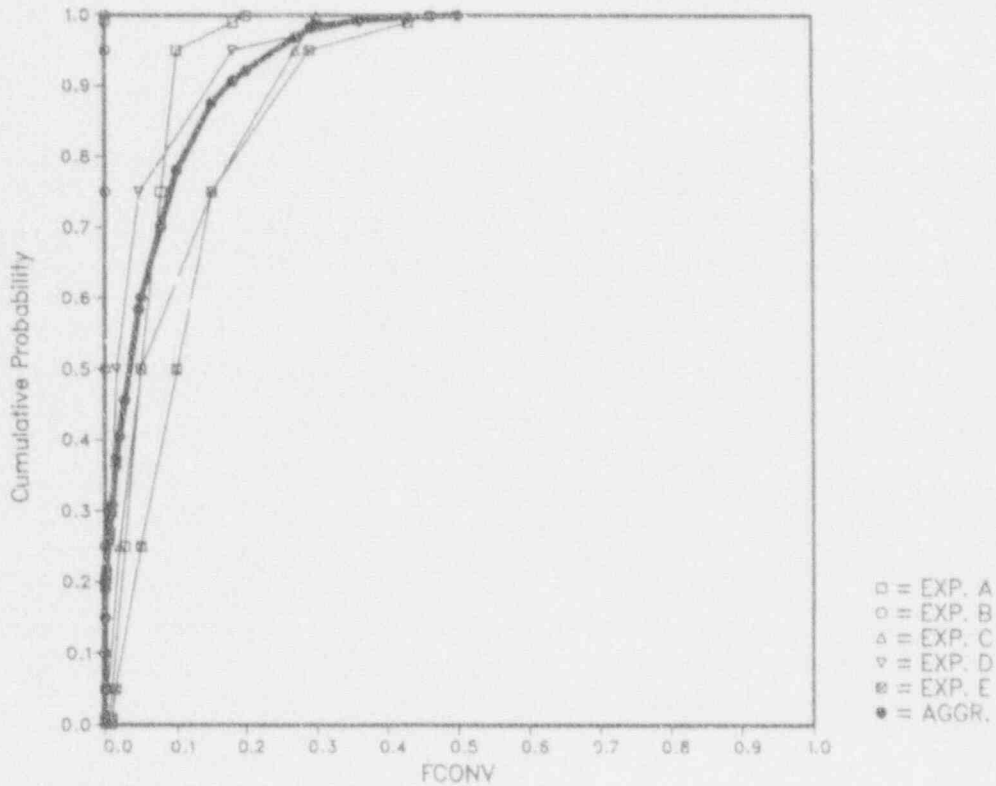

Figure 5-7. Case 3: Surry.

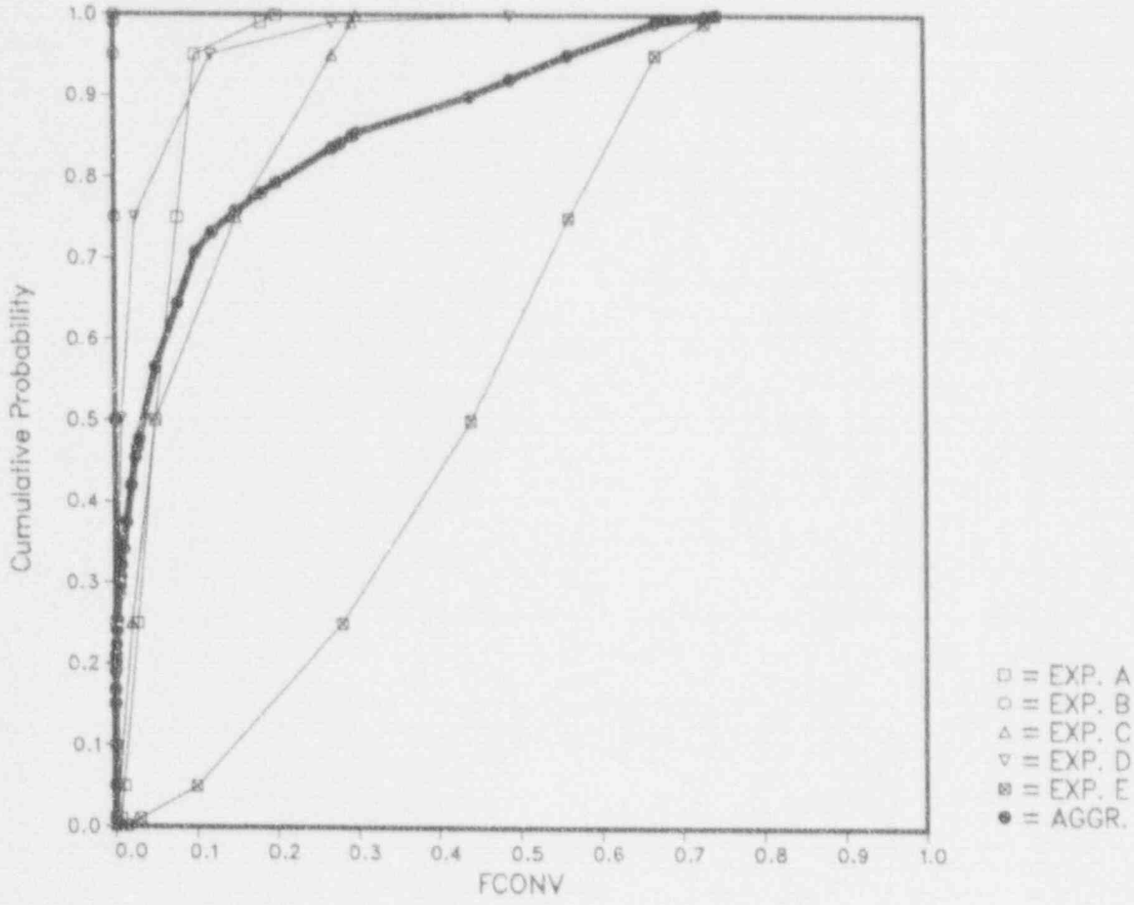

Figure 5-8. Case 3: Sequoyah.

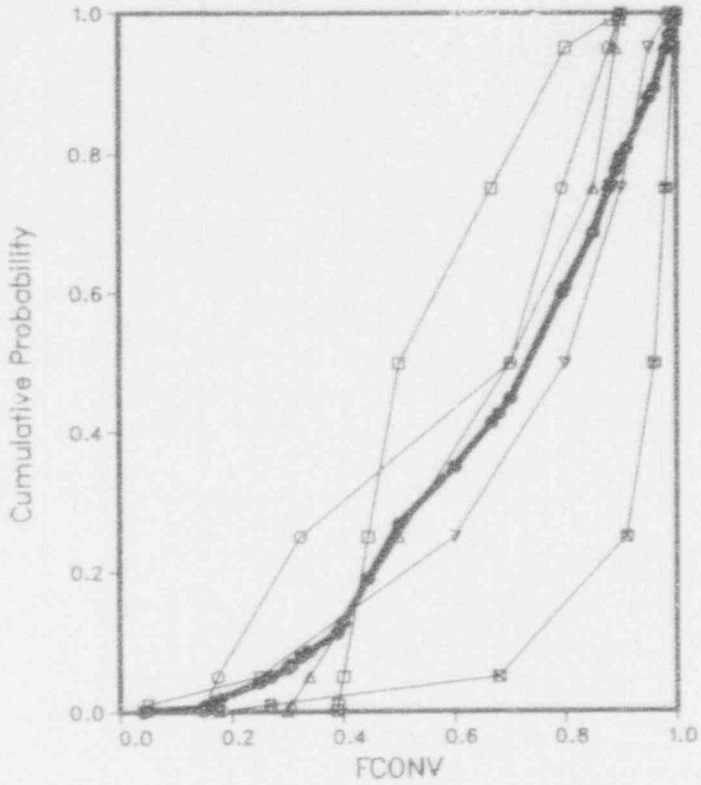

Figure 5-9. Case 4: Sequoyah, Lower Compartment.

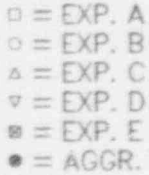

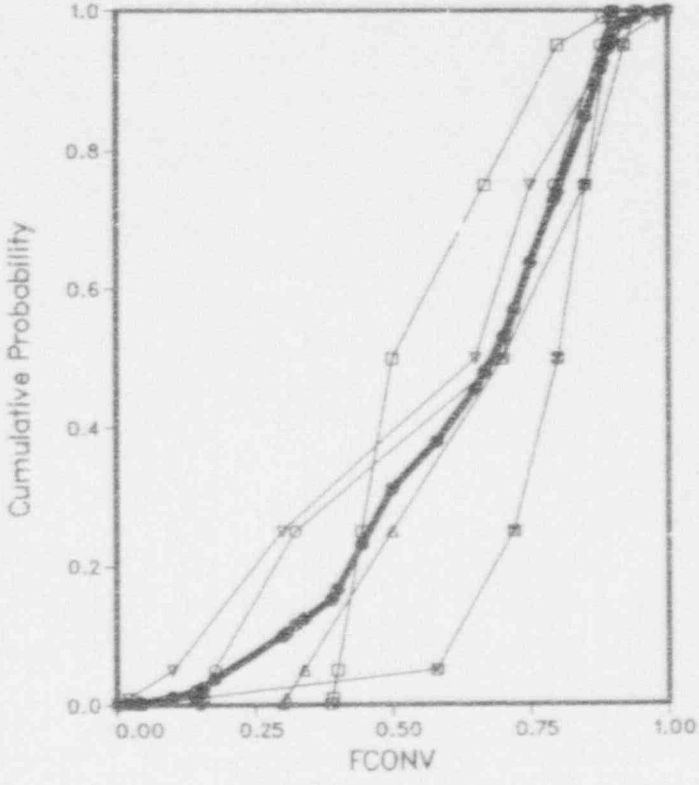

Figure 5-10. Case 4: Sequoyah, Upper Compartment.

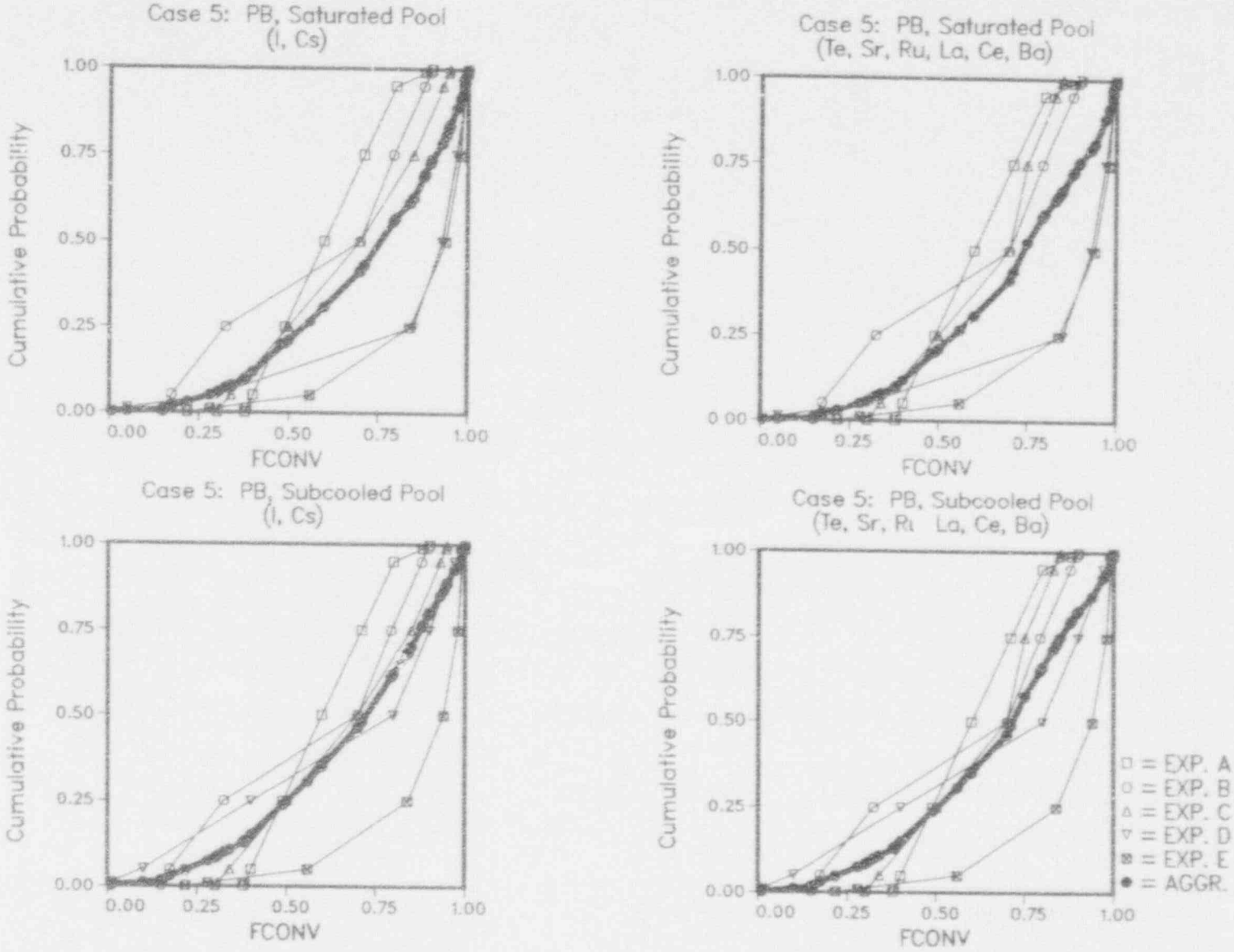

Figure 5-11. Case 5: Peach Bottom, Saturated Pool (top) and Subcooled Pool (bottom).

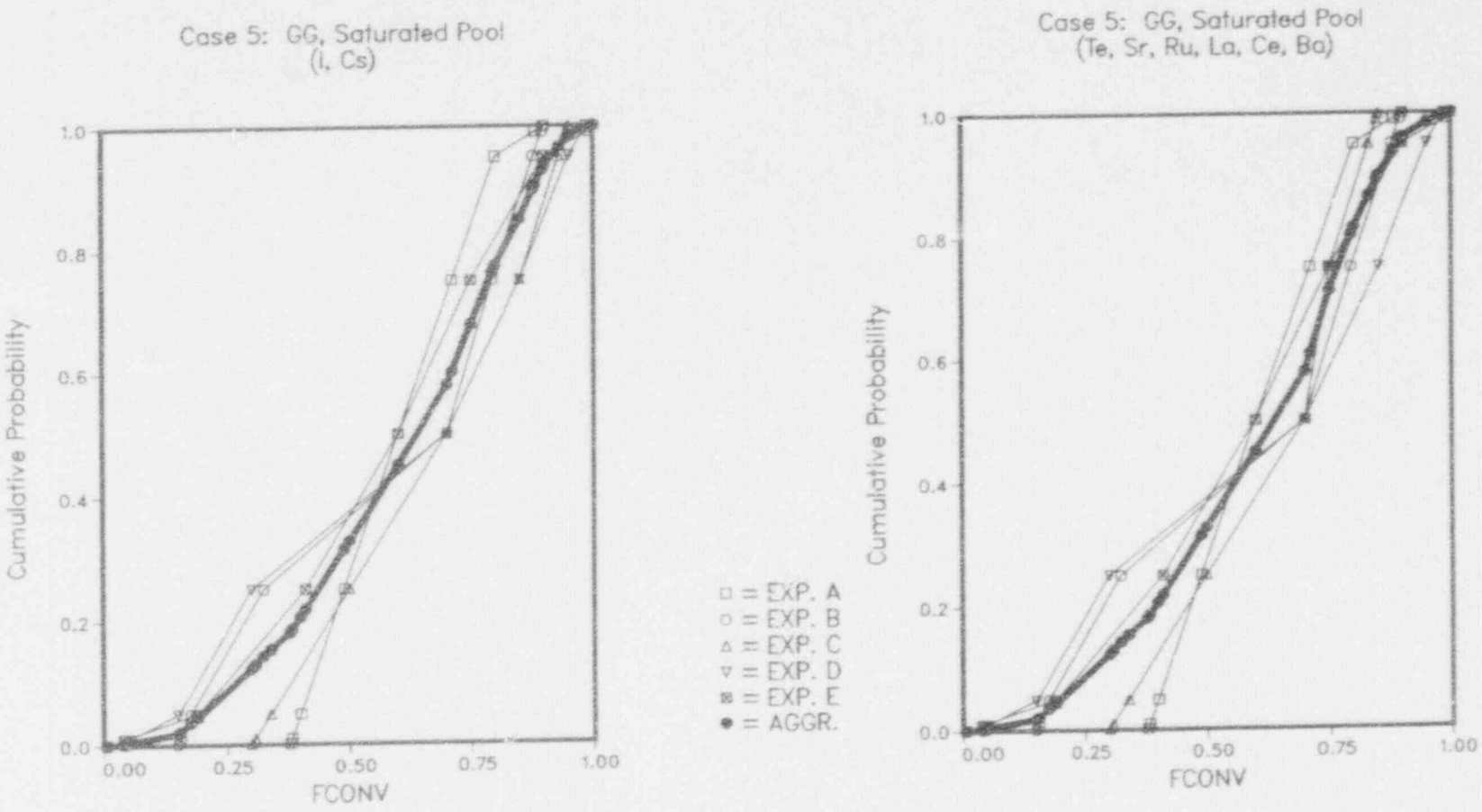

Figure 5-12. Case 5: Grand Gulf, Saturated Pool.

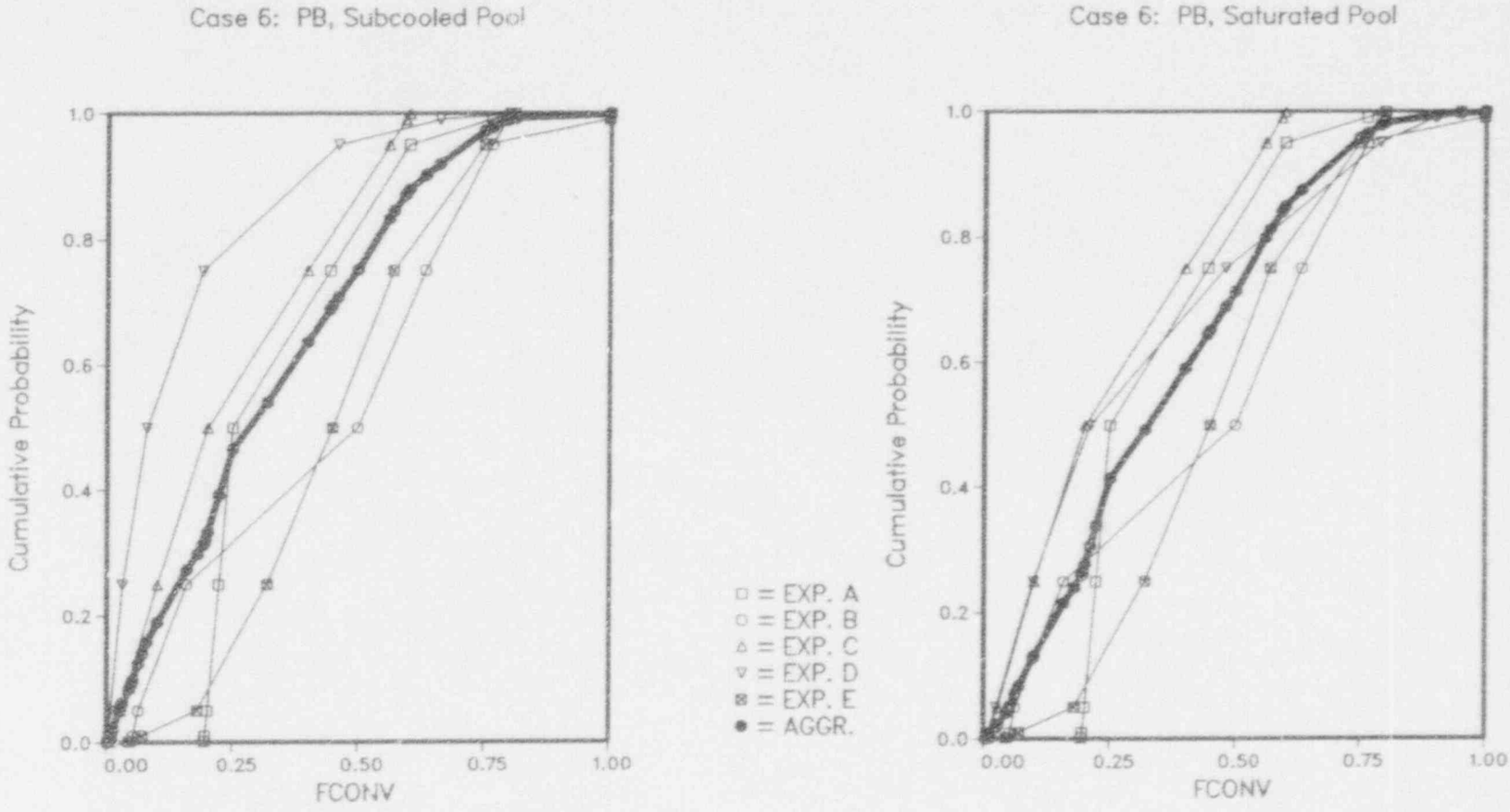

Figure 5-13. Case 6: Peach Bottom, Subcooled Pool (left) and Saturated Pool (right).

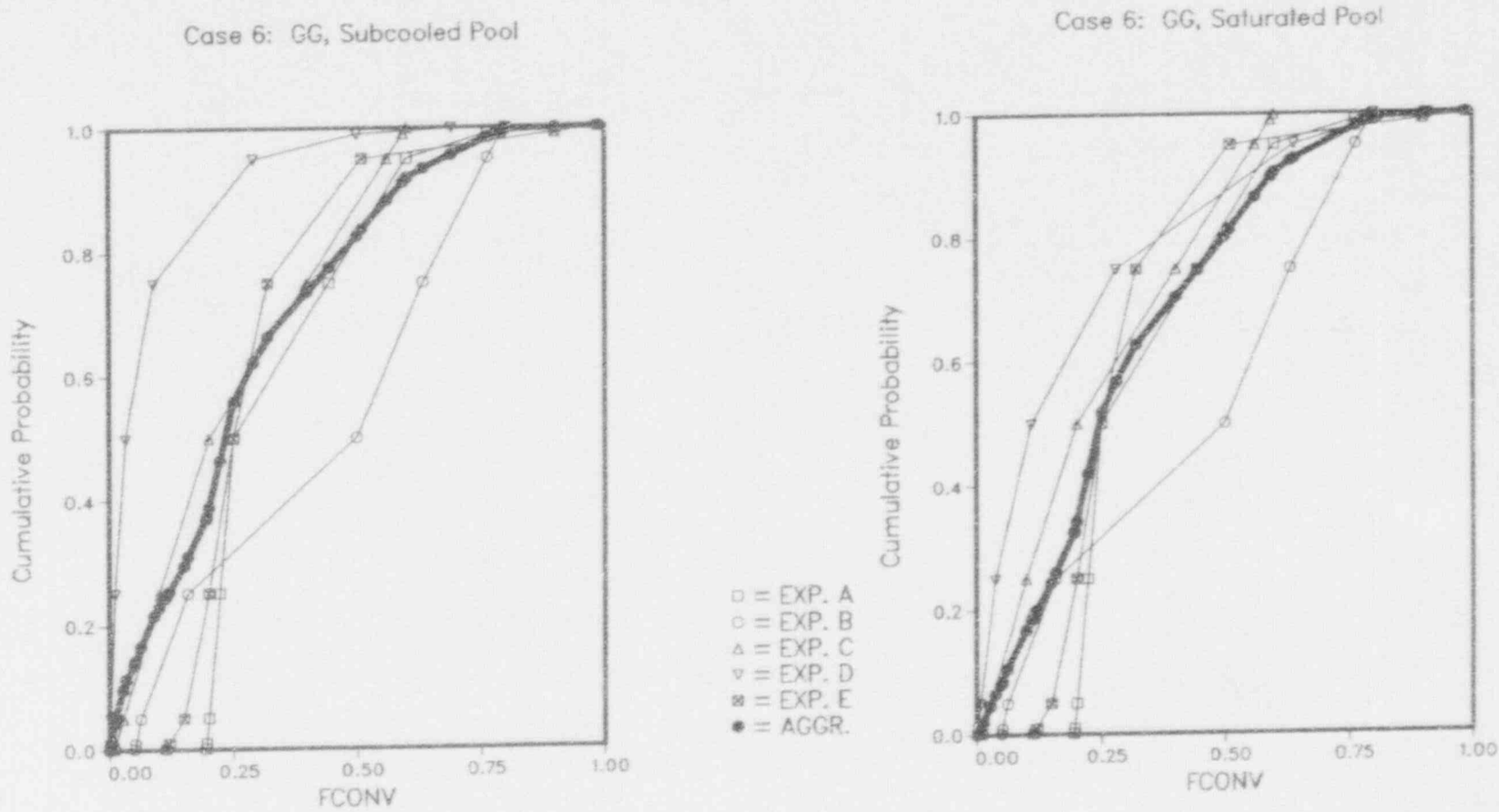

Figure 5-14. Case 6: Grand Gulf, Subcooled Pool (left); Saturated Pool (right).

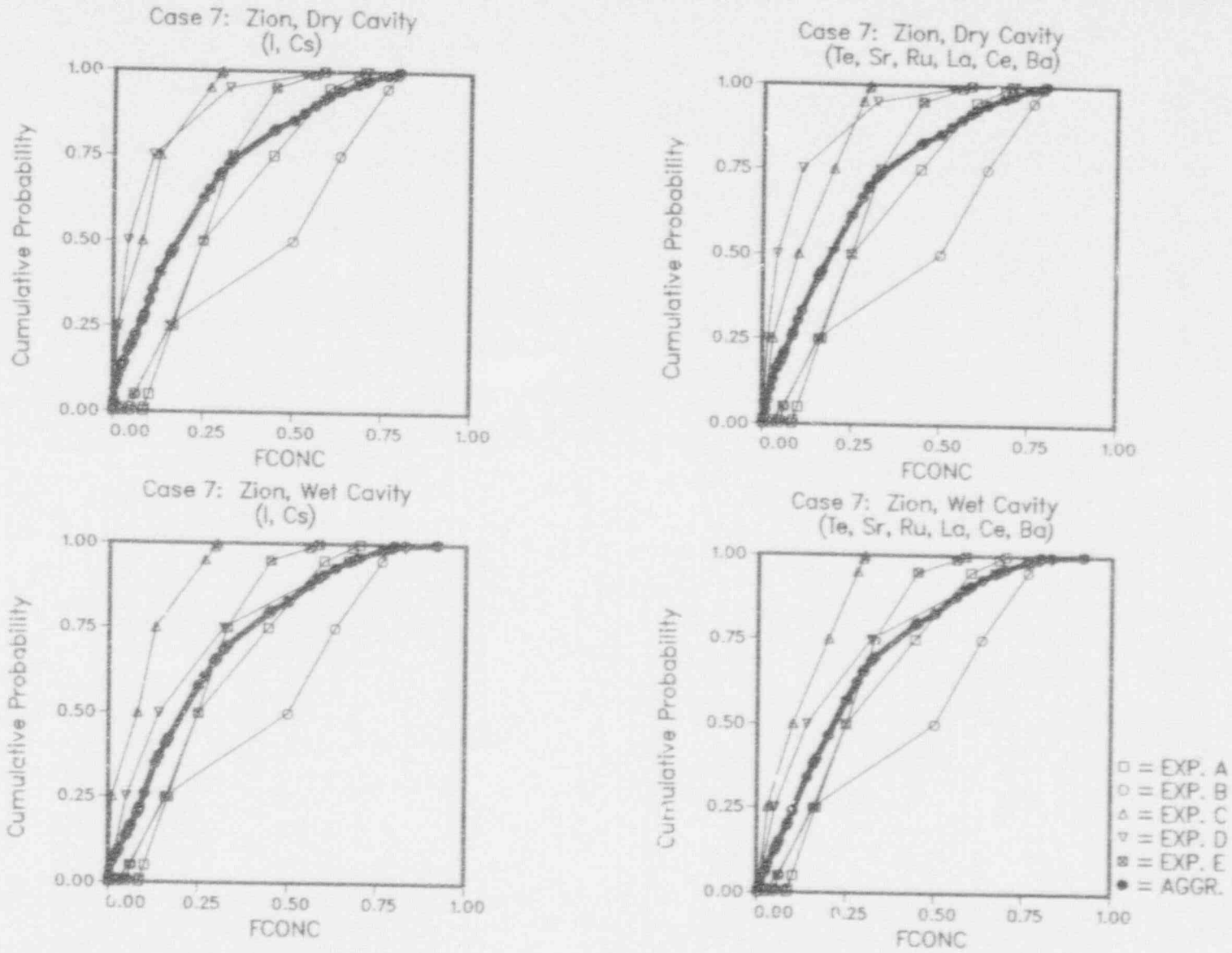

Figure 5-15. Case 7: Zion, Dry and Wet Cavity.

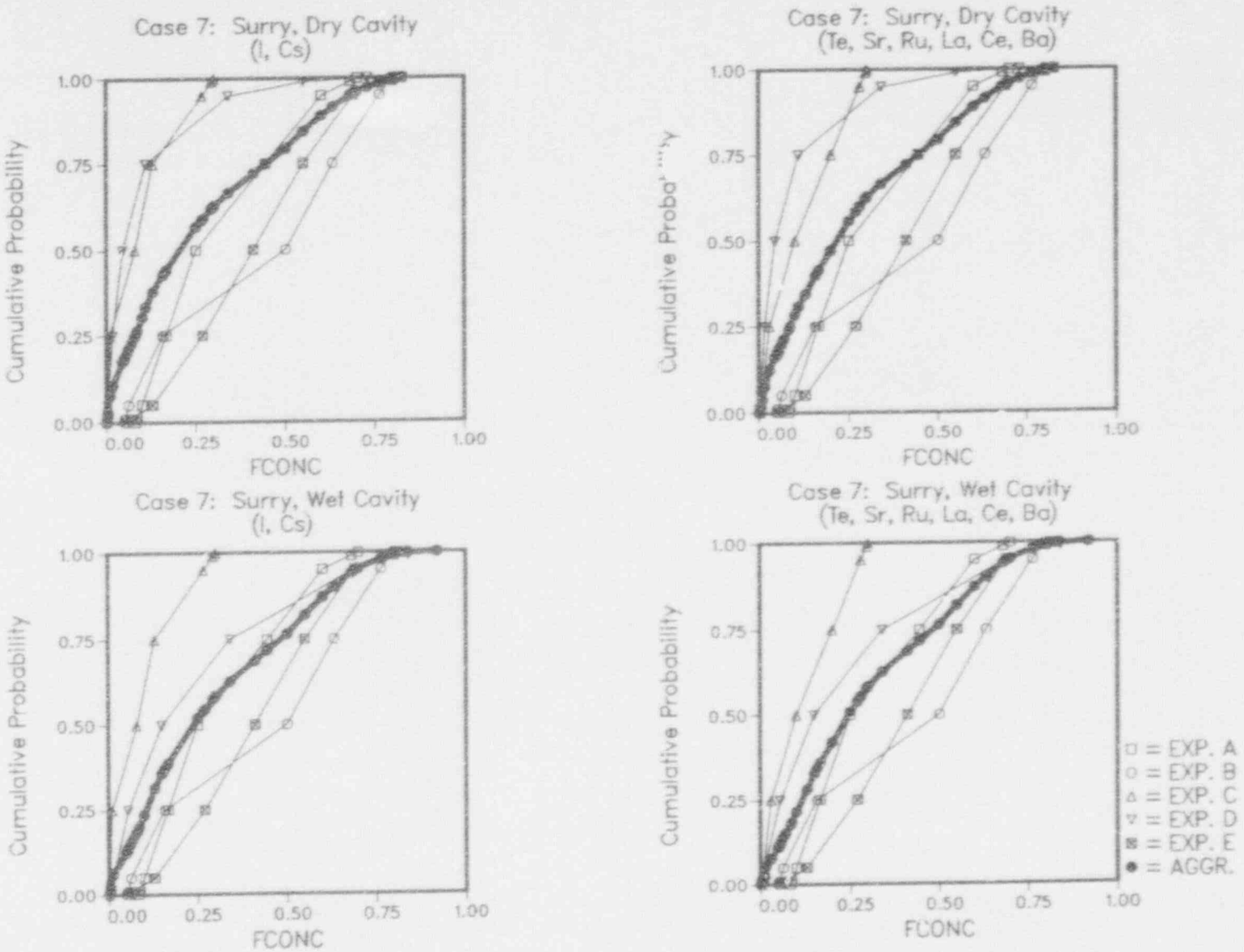

Figure 5-16. Case 7: Surry, Dry and Wet Cavity.

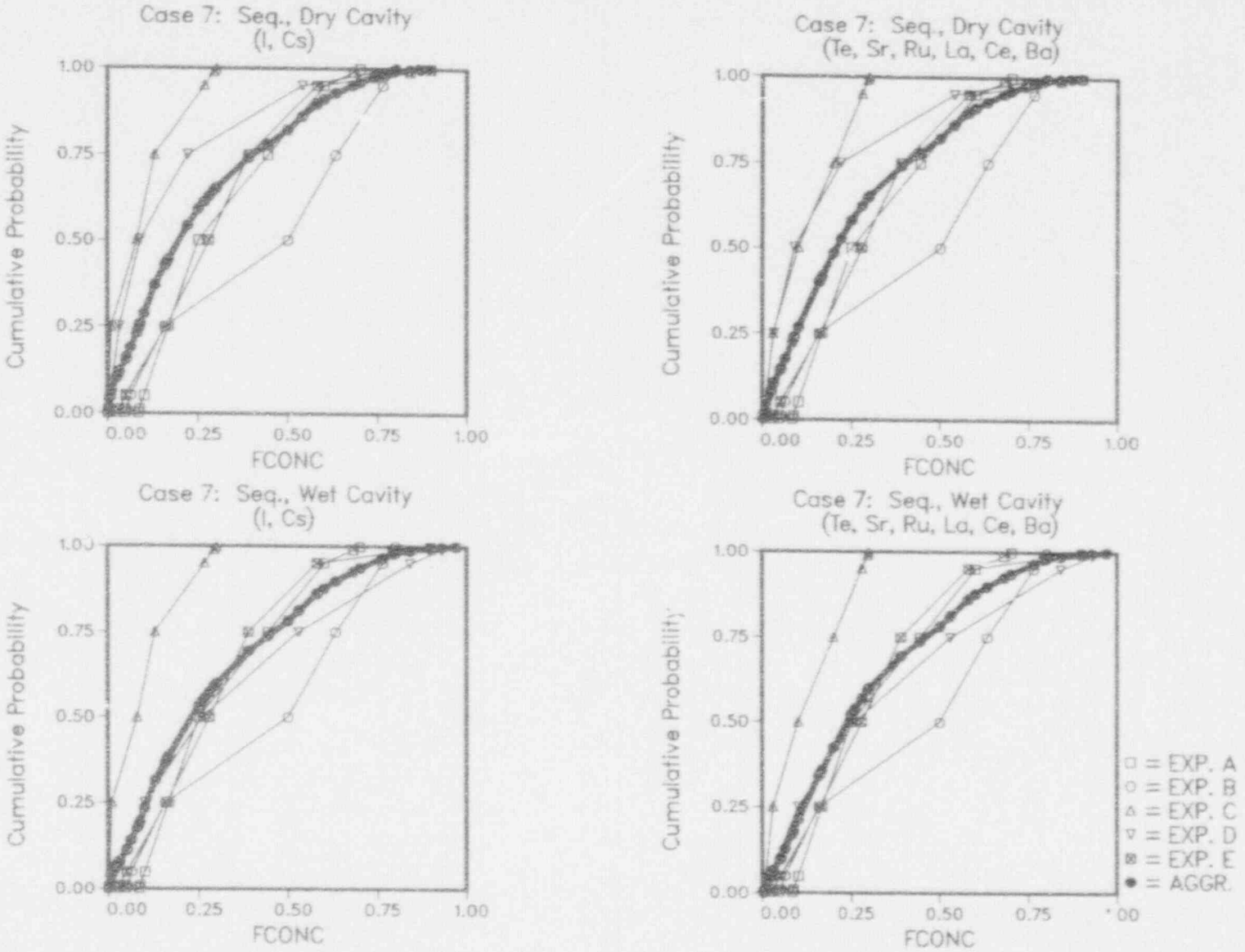

Figure 5-17. Case 7: Sequoyah, Dry and Wet Cavity.

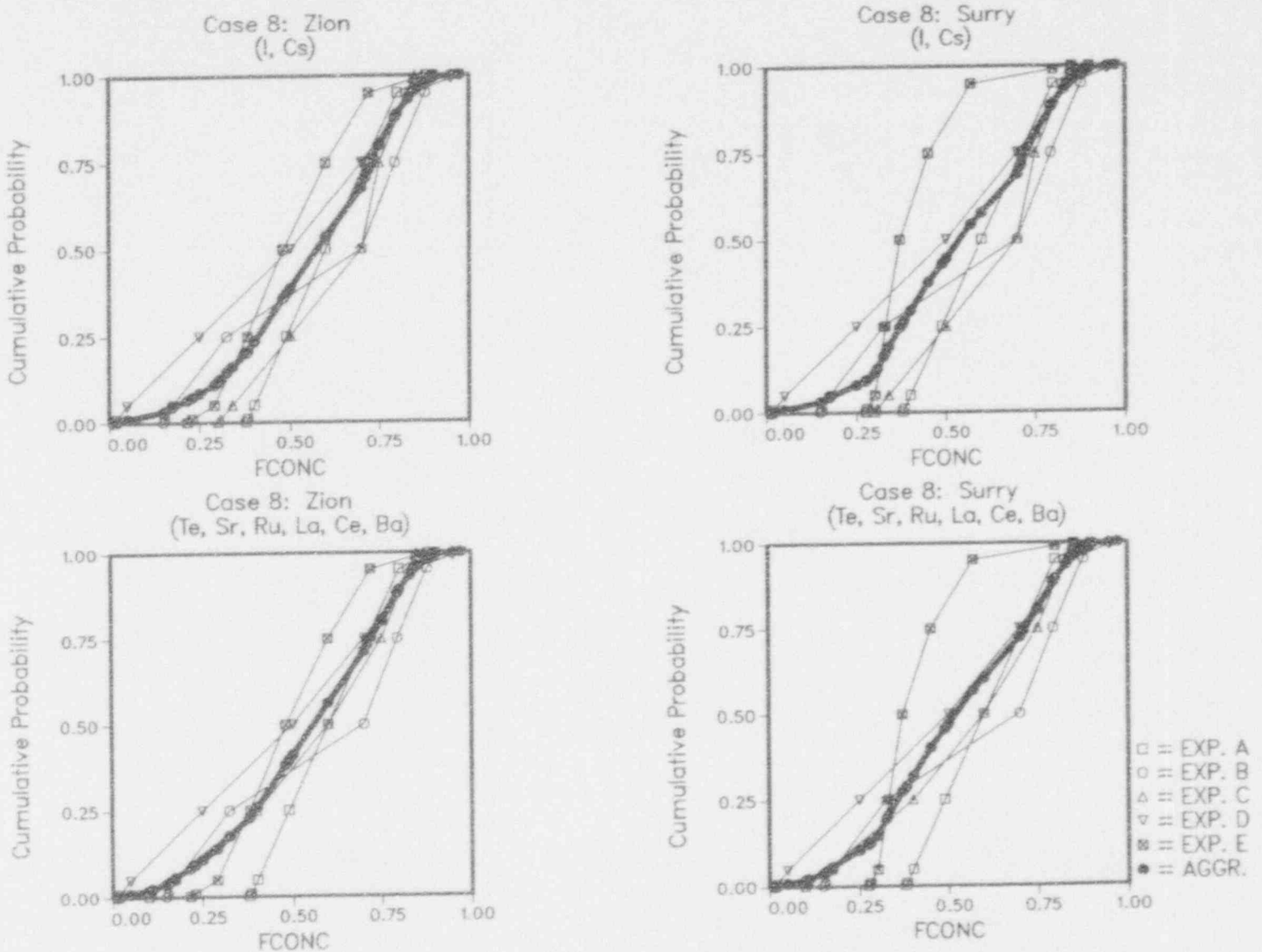

Figure 5-18. Case 8: Zion (left) and Case 8: Surry (right).

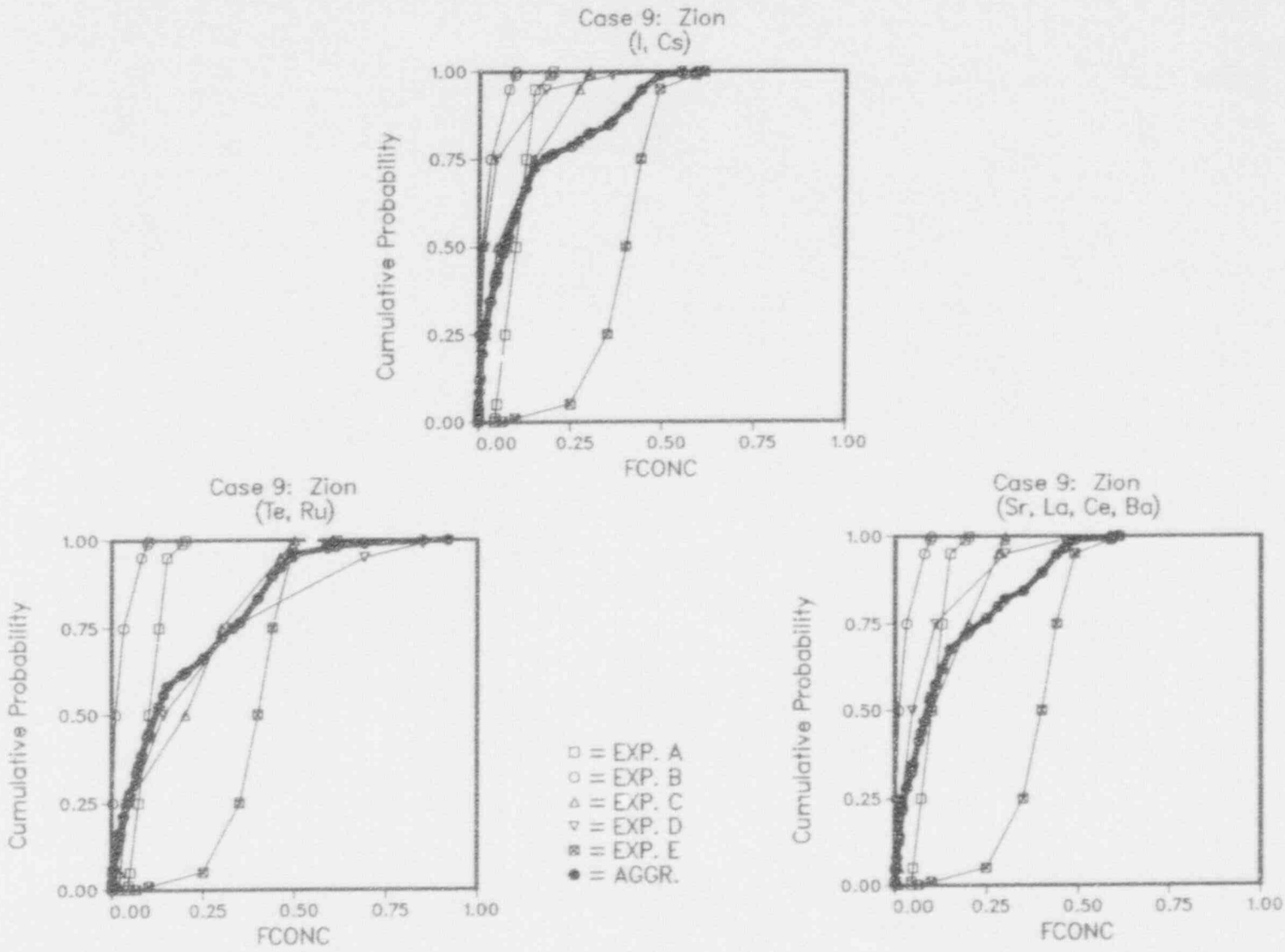

Figure 5-19. Case 9: Zion.

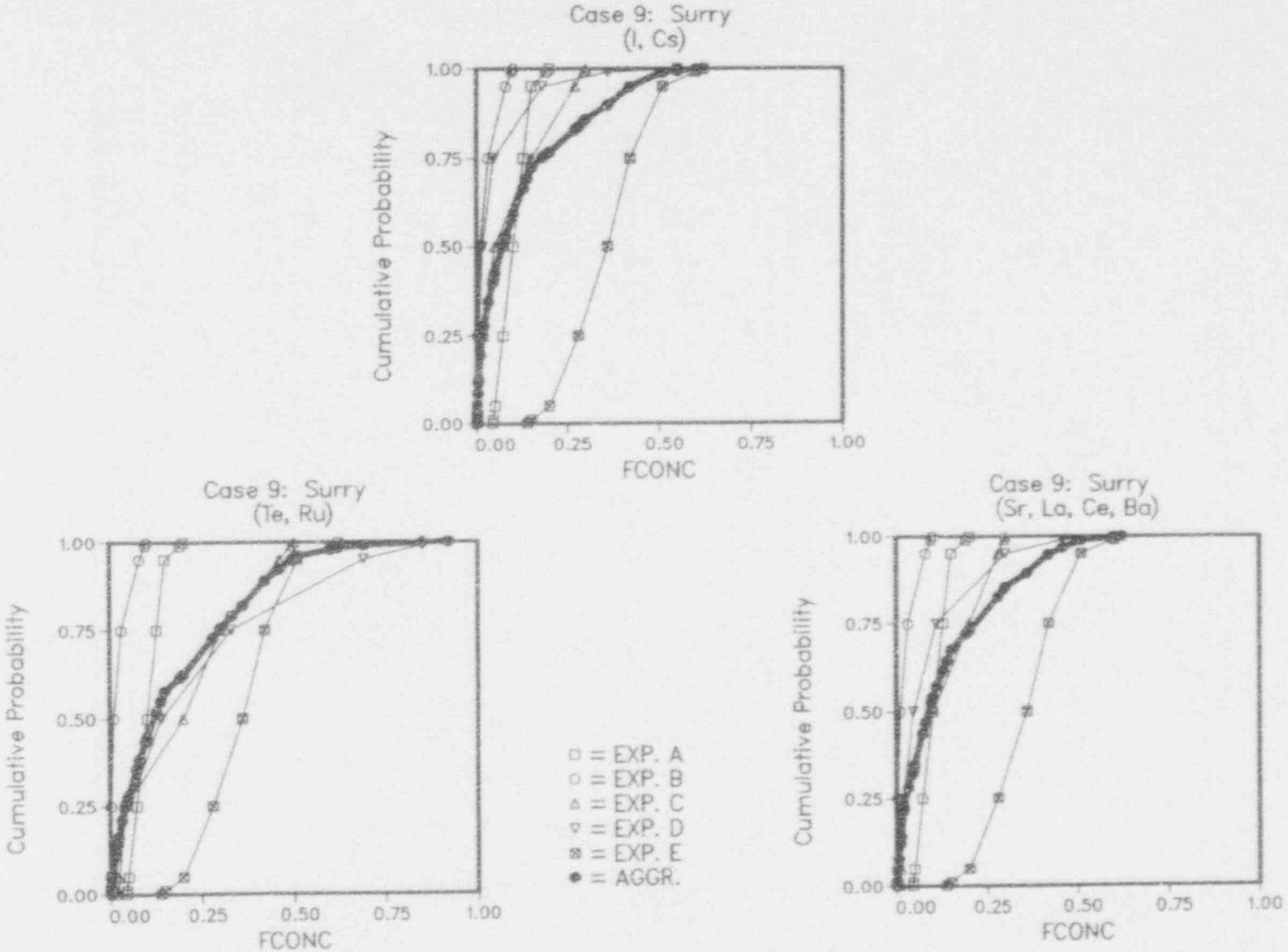

Figure 5-20. Case 9: Surry.

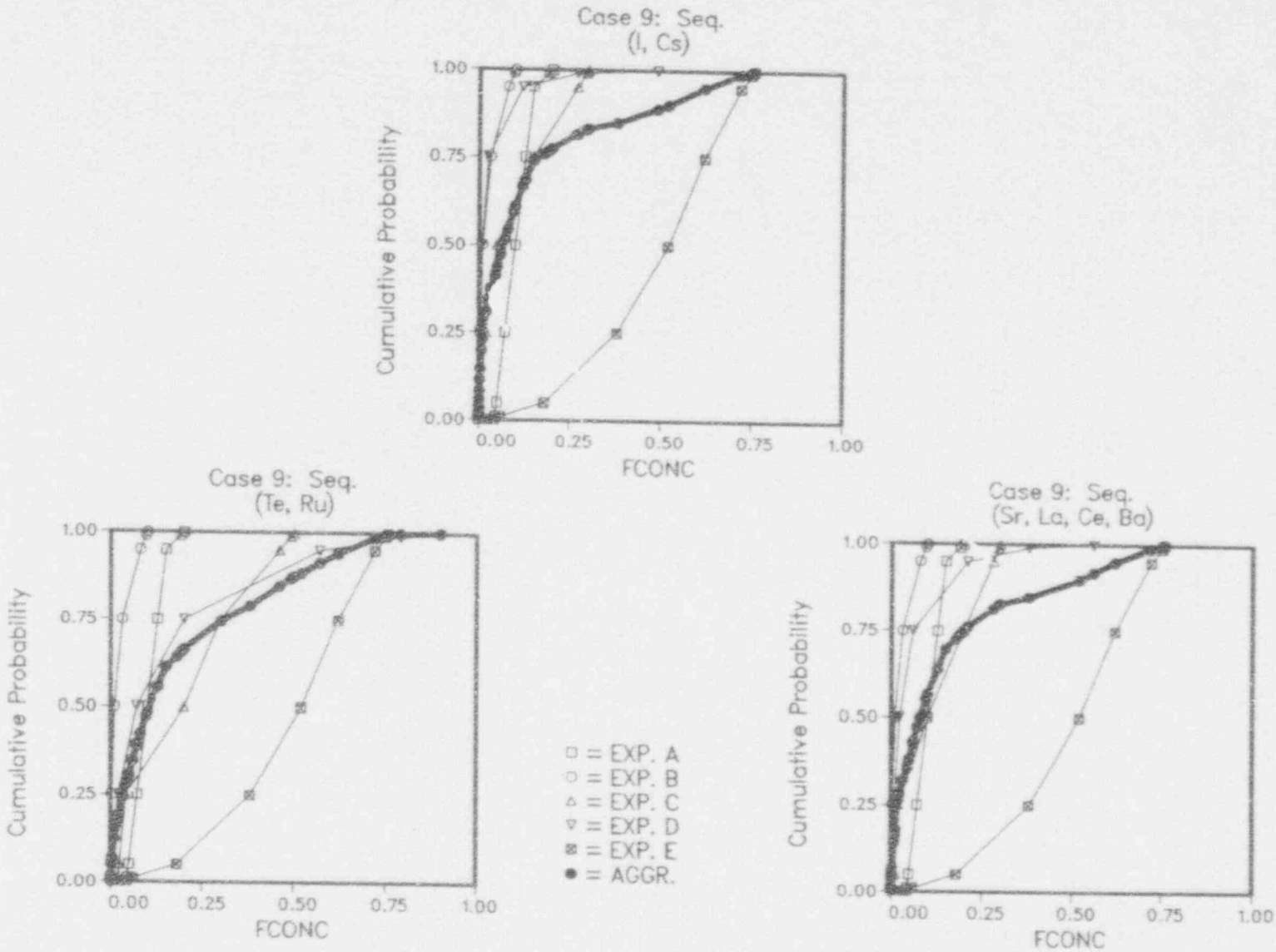

Figure 5-21. Case 9: Sequoyah.

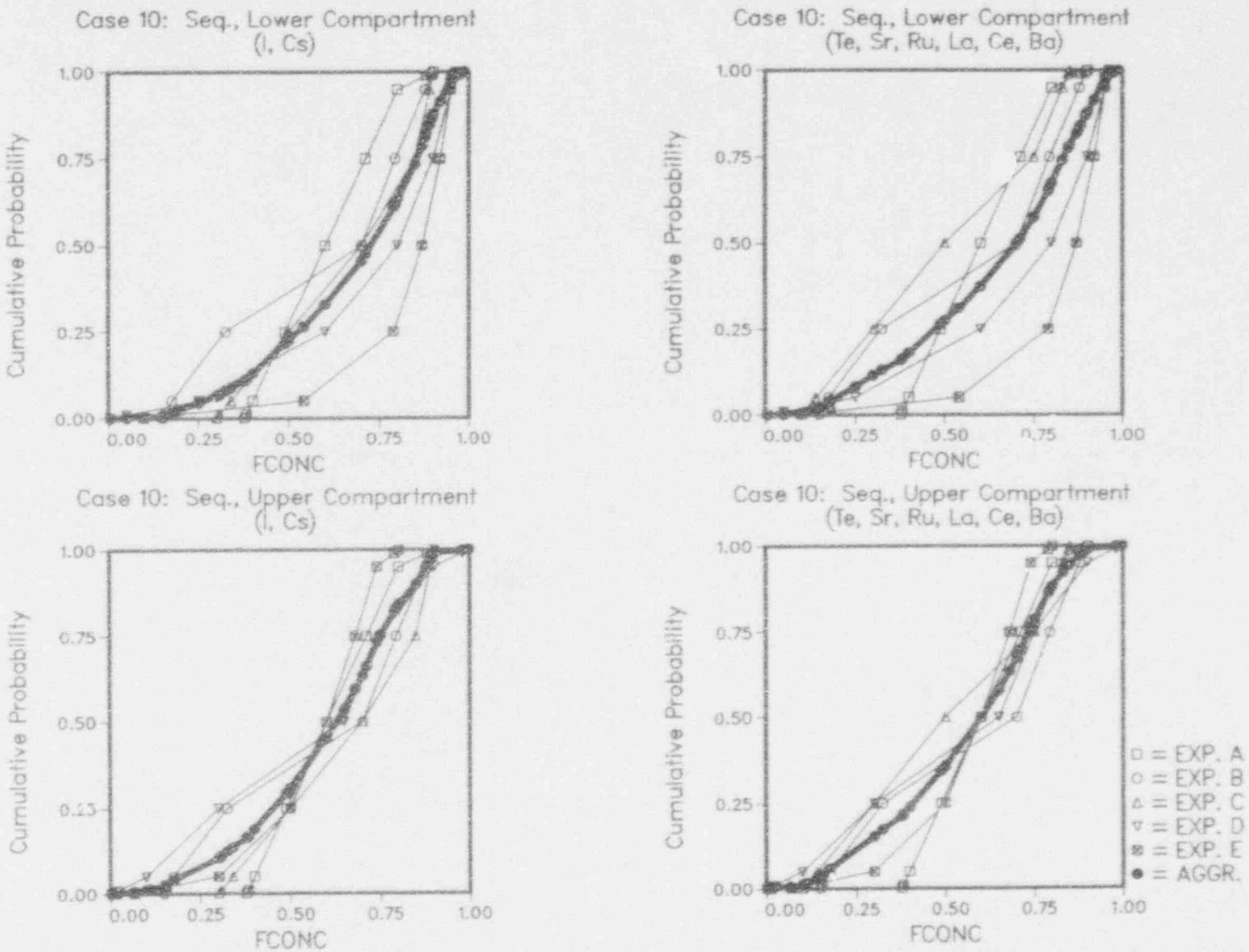

Figure 5-22. Case 10: Sequoyah. Lower Compartment (top), and Upper Compartment (bottom).

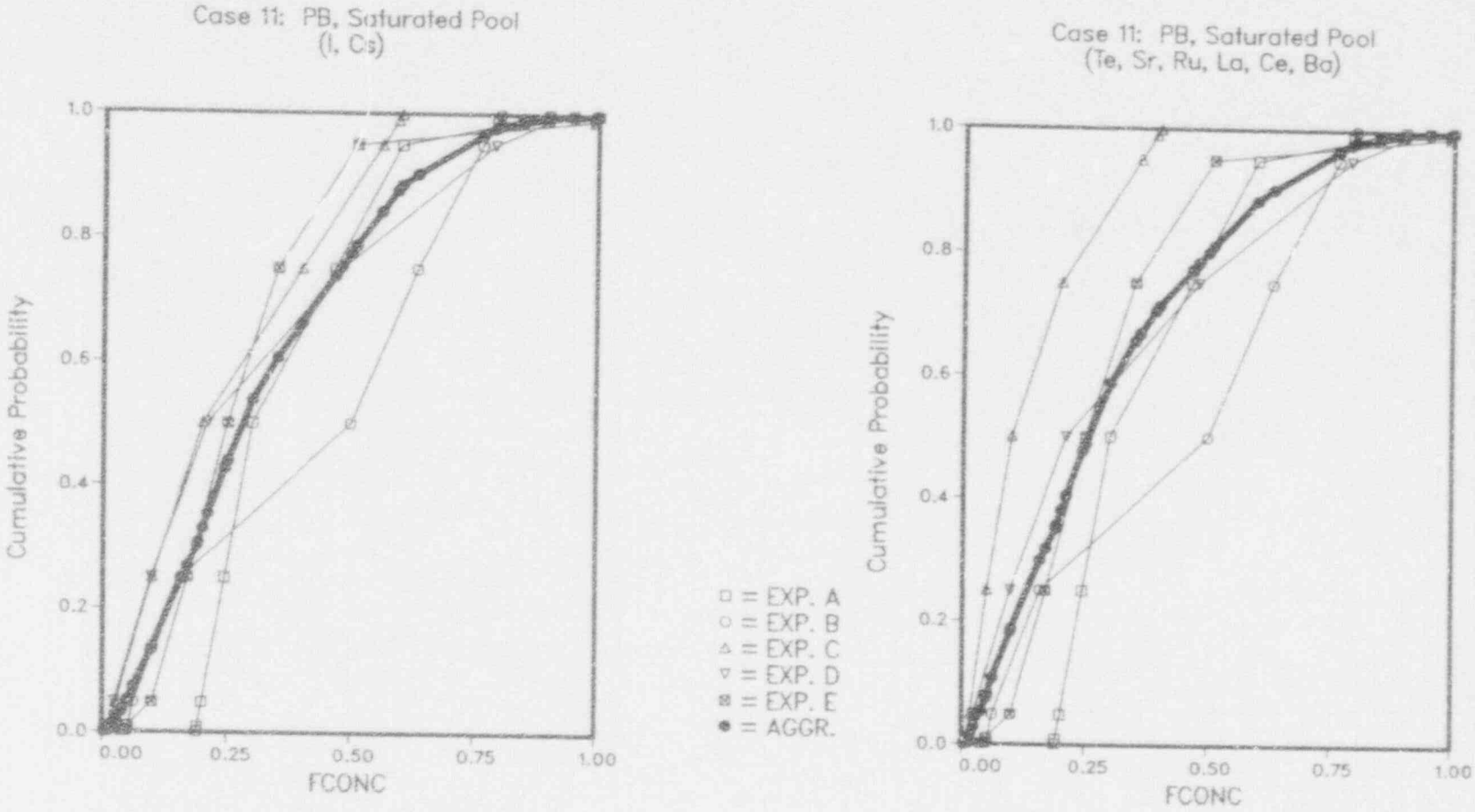

Figure 5-23. Case 11: Peach Bottom, Saturated Pool.

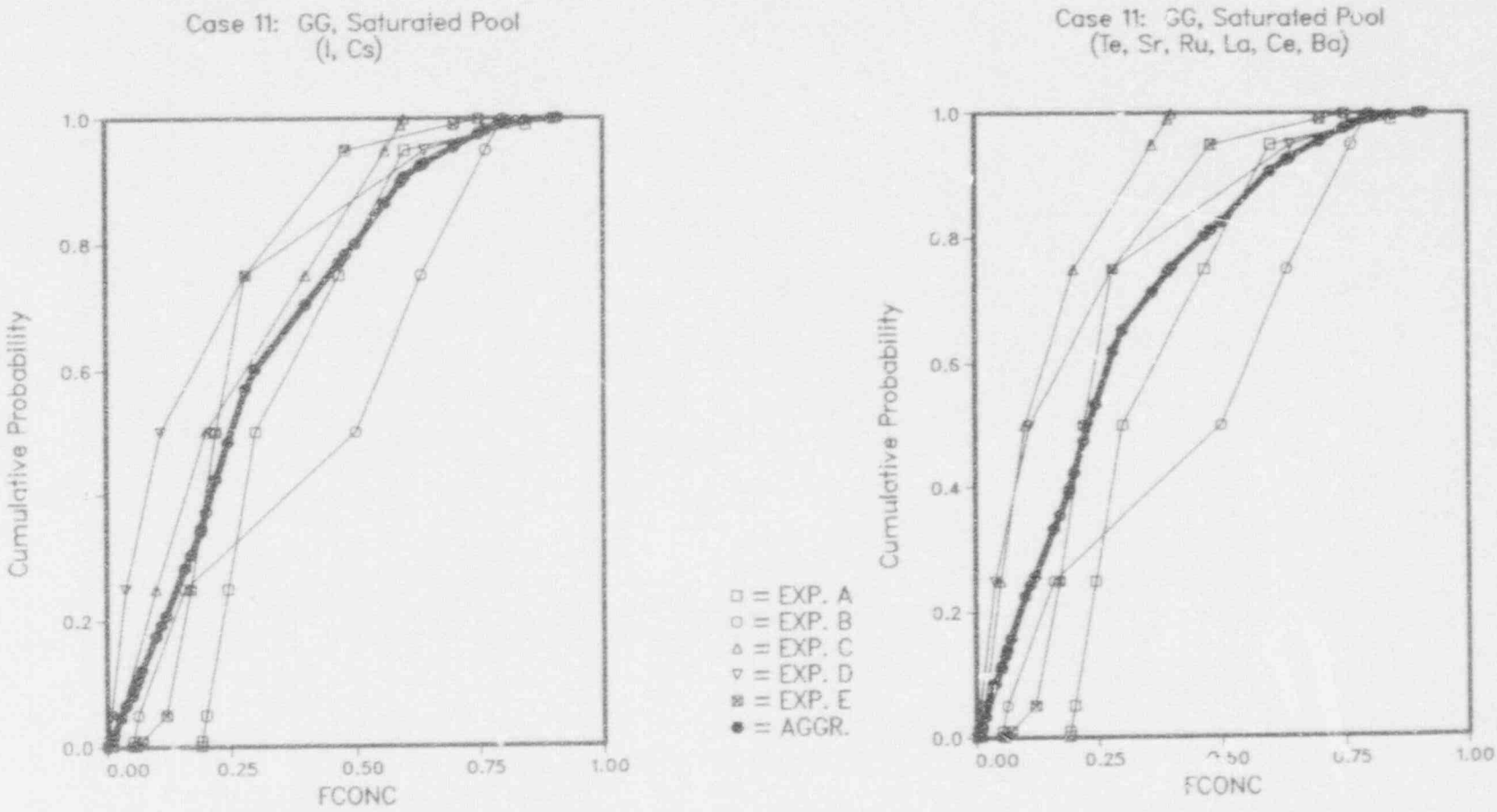

Figure 5-24. Case 11: Grand Gulf, Saturated Pool.

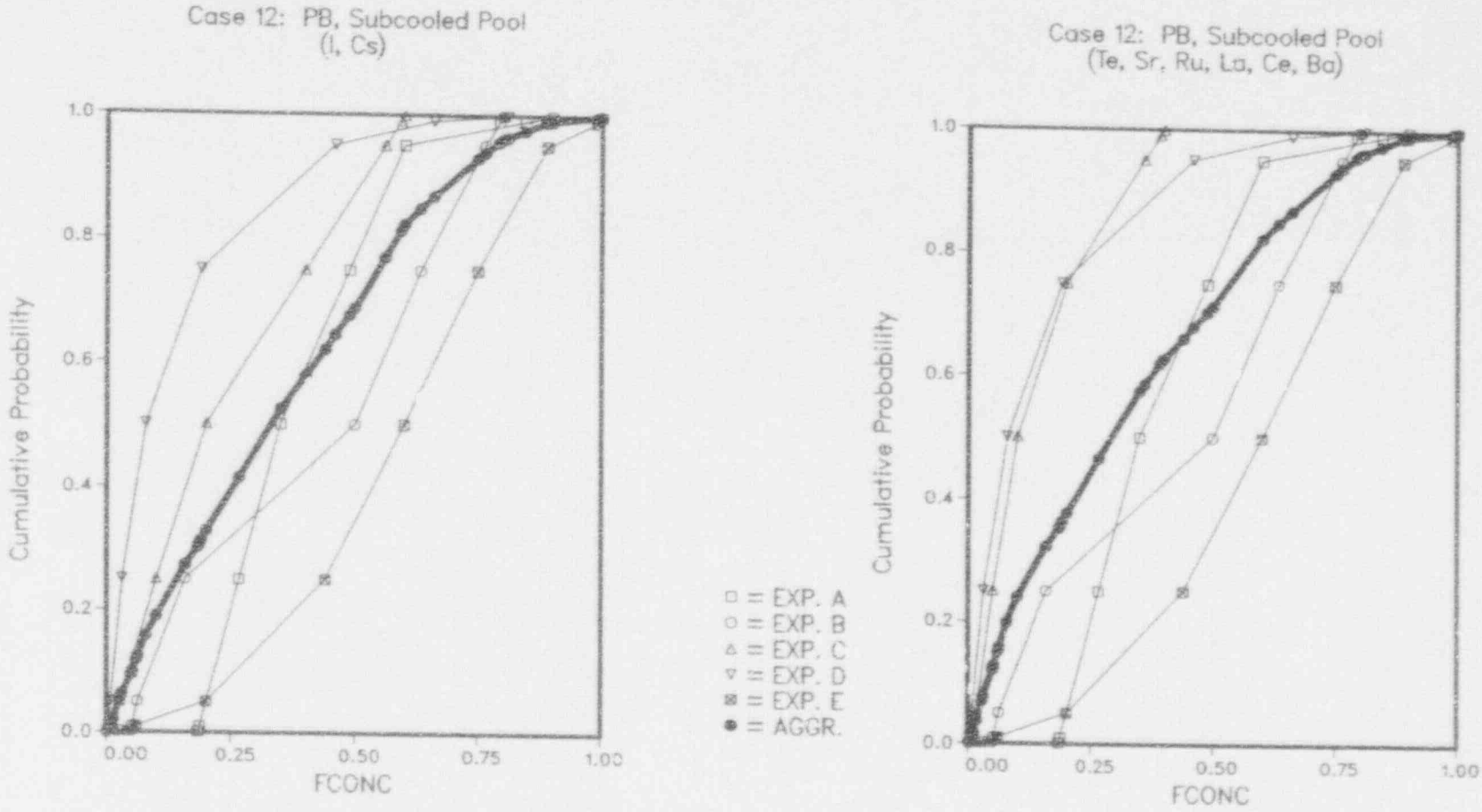

Figure 5-25. Case 12: Peach Bottom, Subcooled Pool.

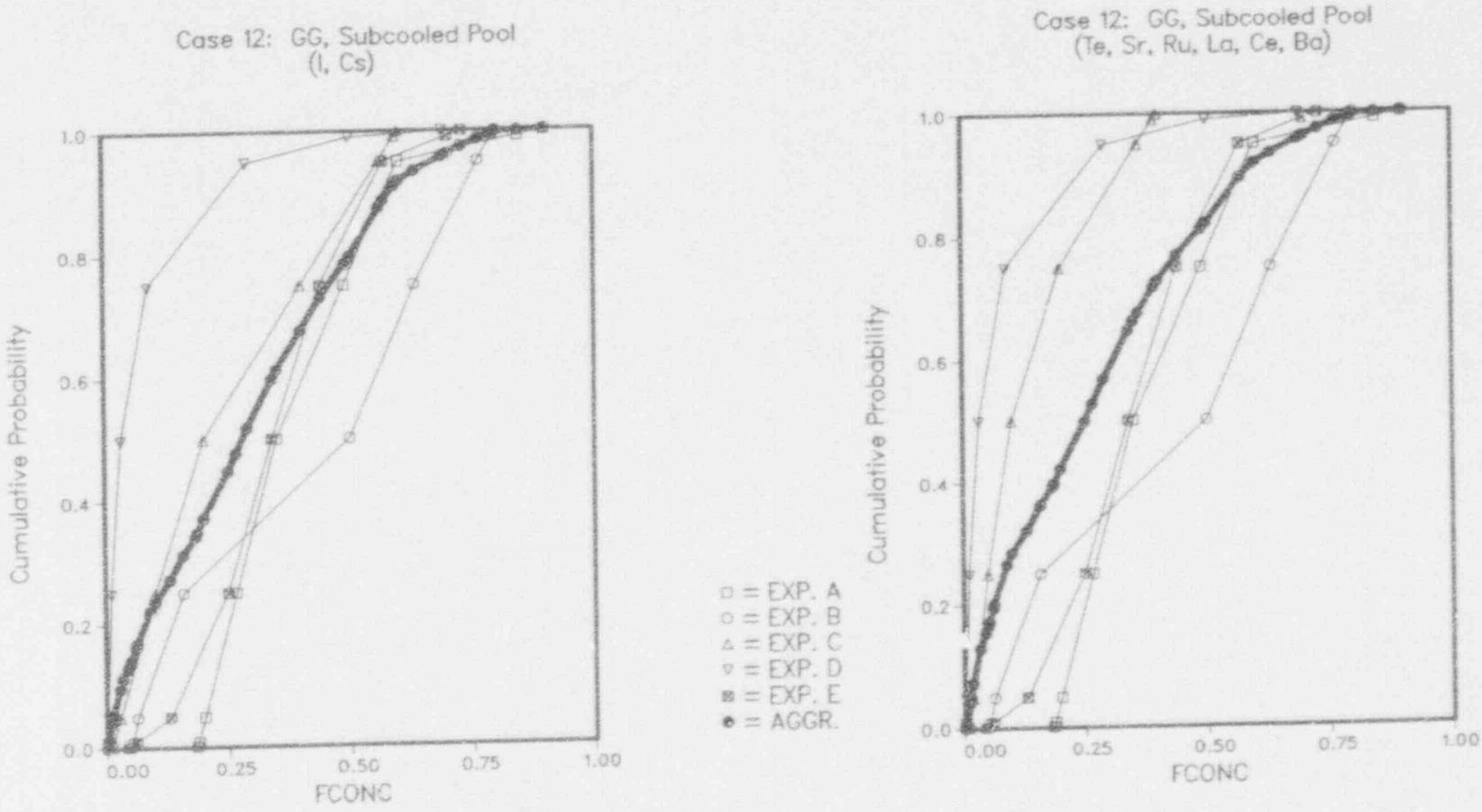

Figure 5-26. Case 12: Grand Gulf, Subcooled Pool.

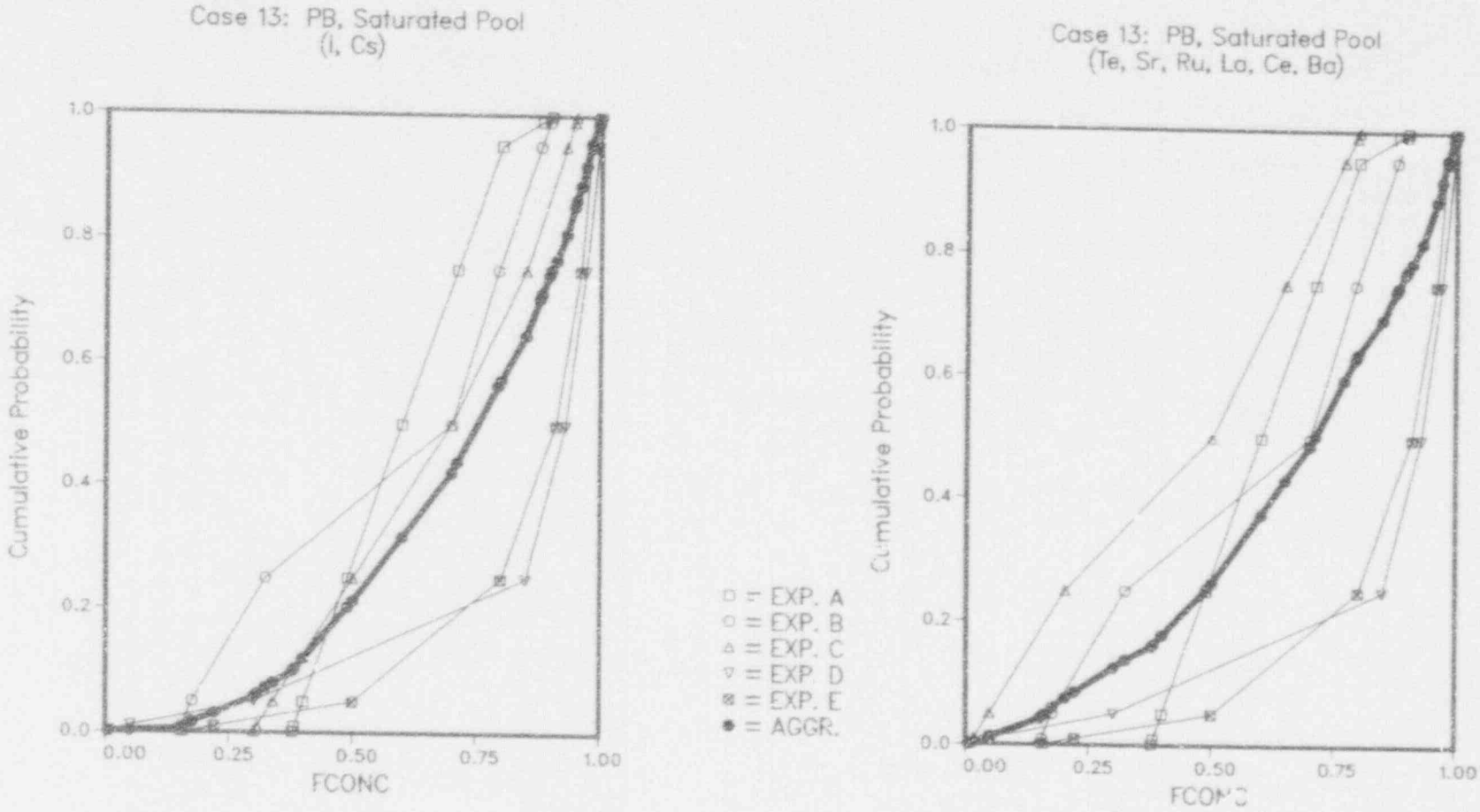

Figure 5-27. Case 13: Peach Bottom, Saturated Pool.

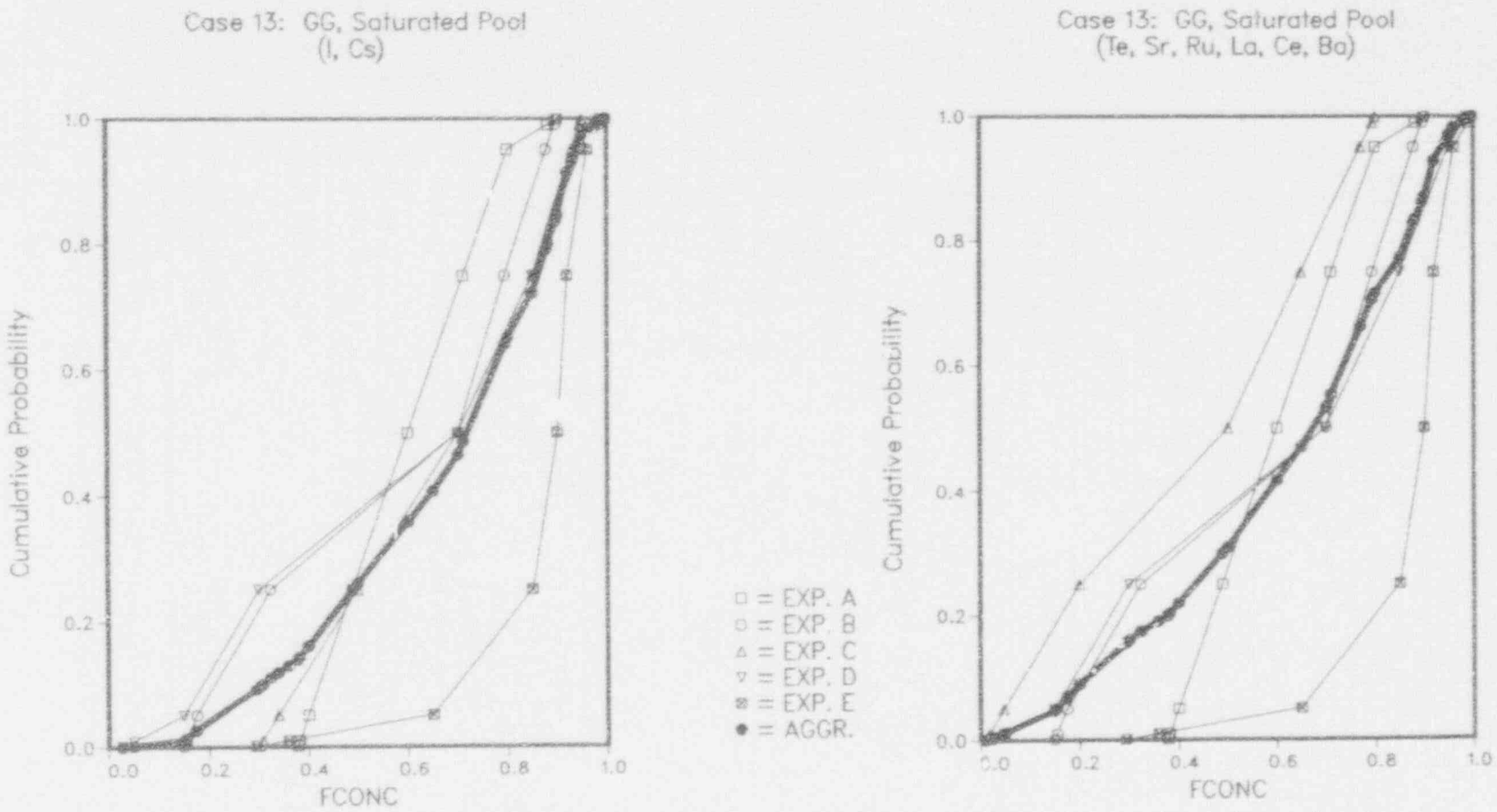

Figure 5-28. Case 13: Grand Gulf, Saturated Pool.

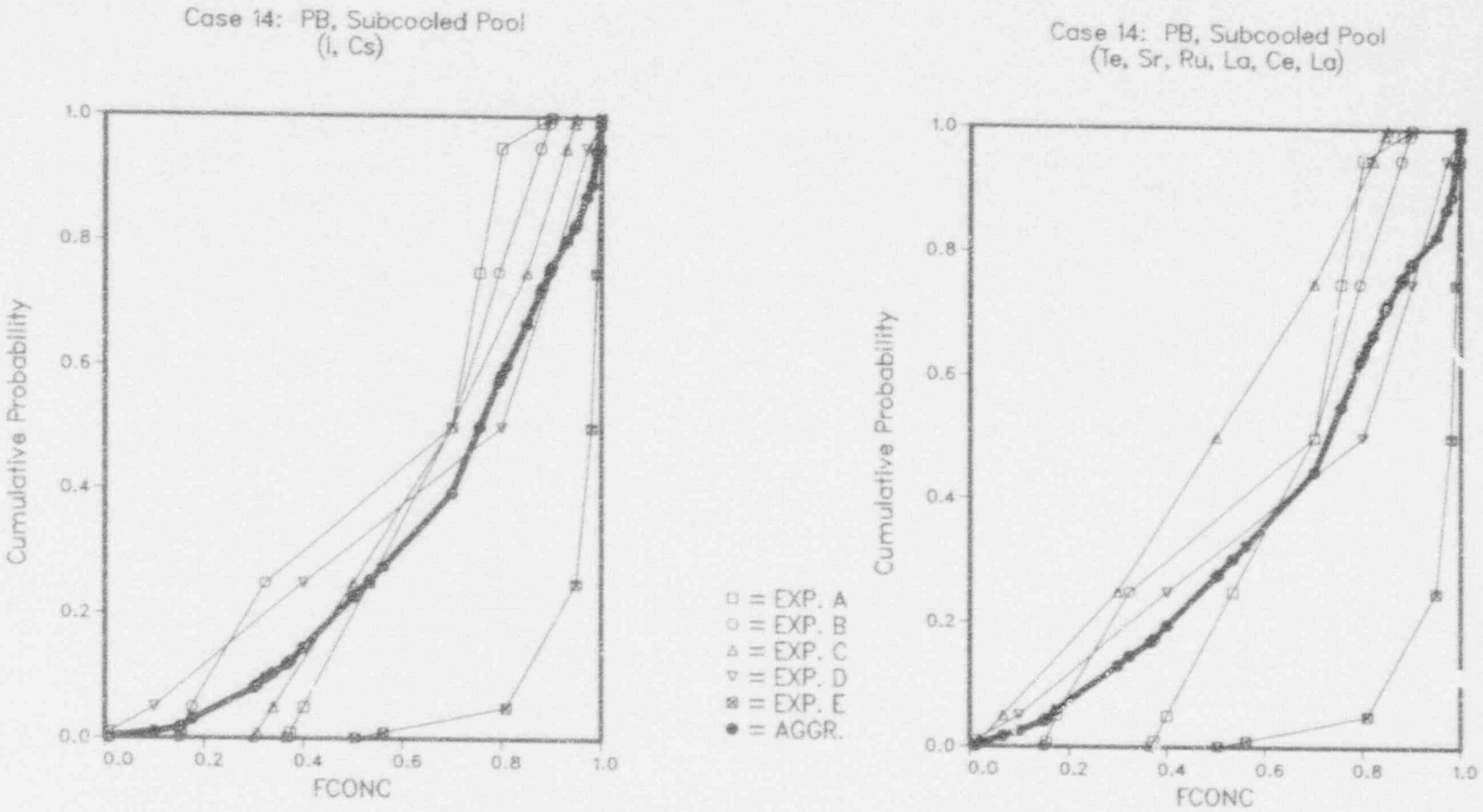

Figure 5-29. Case 14: Peach Bottom, Subcooled Pool.

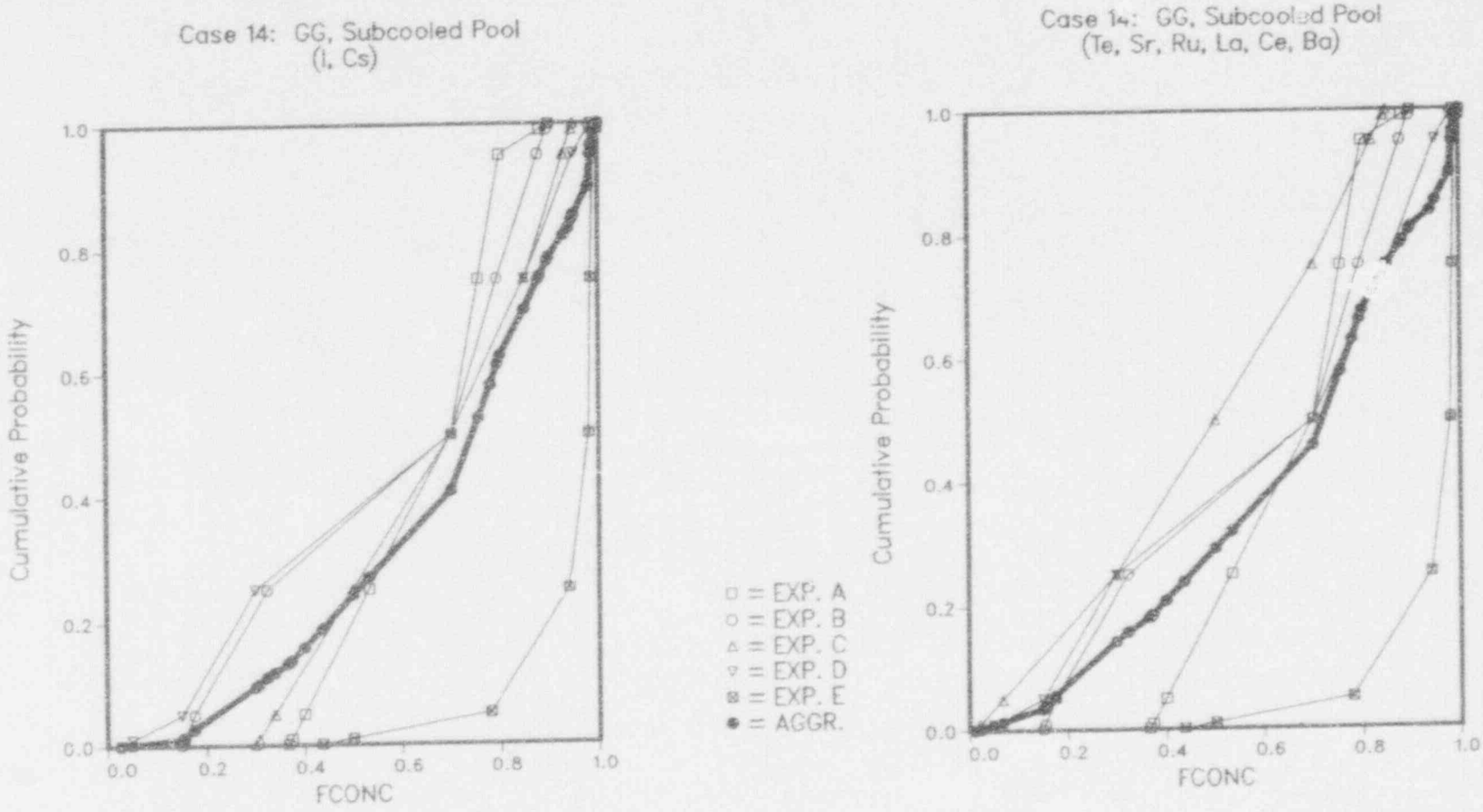

Figure 5-30. Case 14: Grand Gulf, Subcooled Pool.

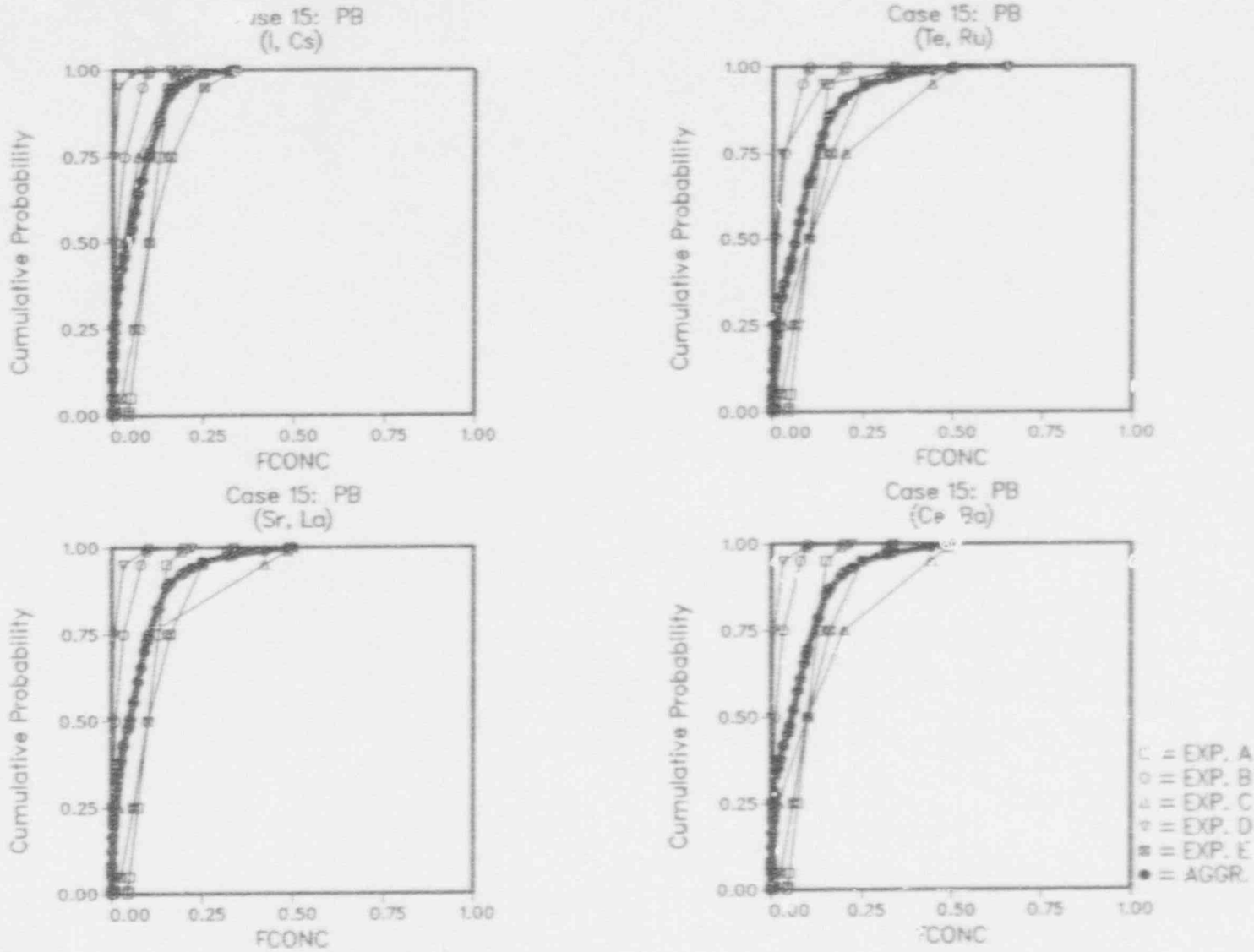

Figure 5-31. Case 15: Peach Bottom.

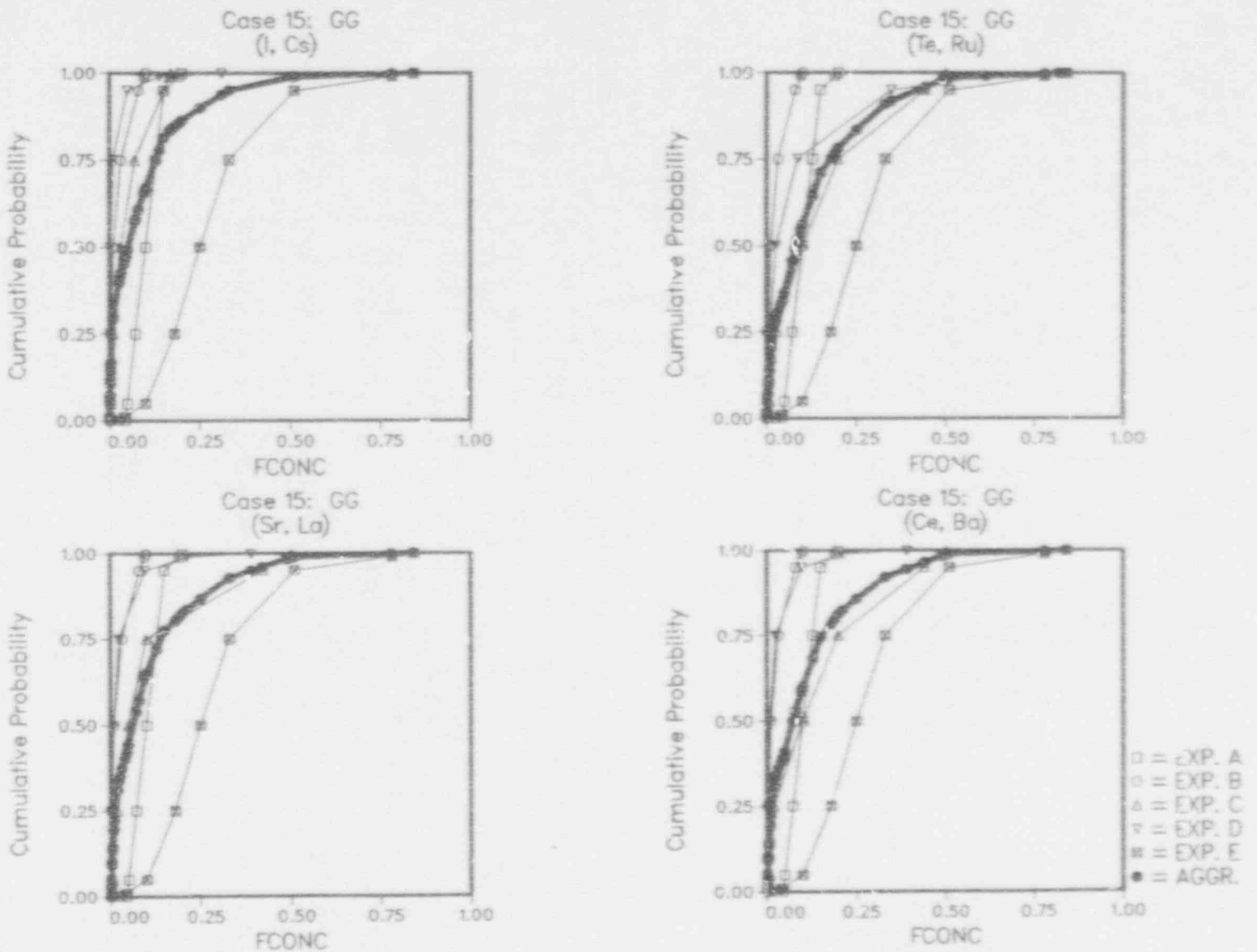

Figure 5-32. Case 15: Grand Gulf.

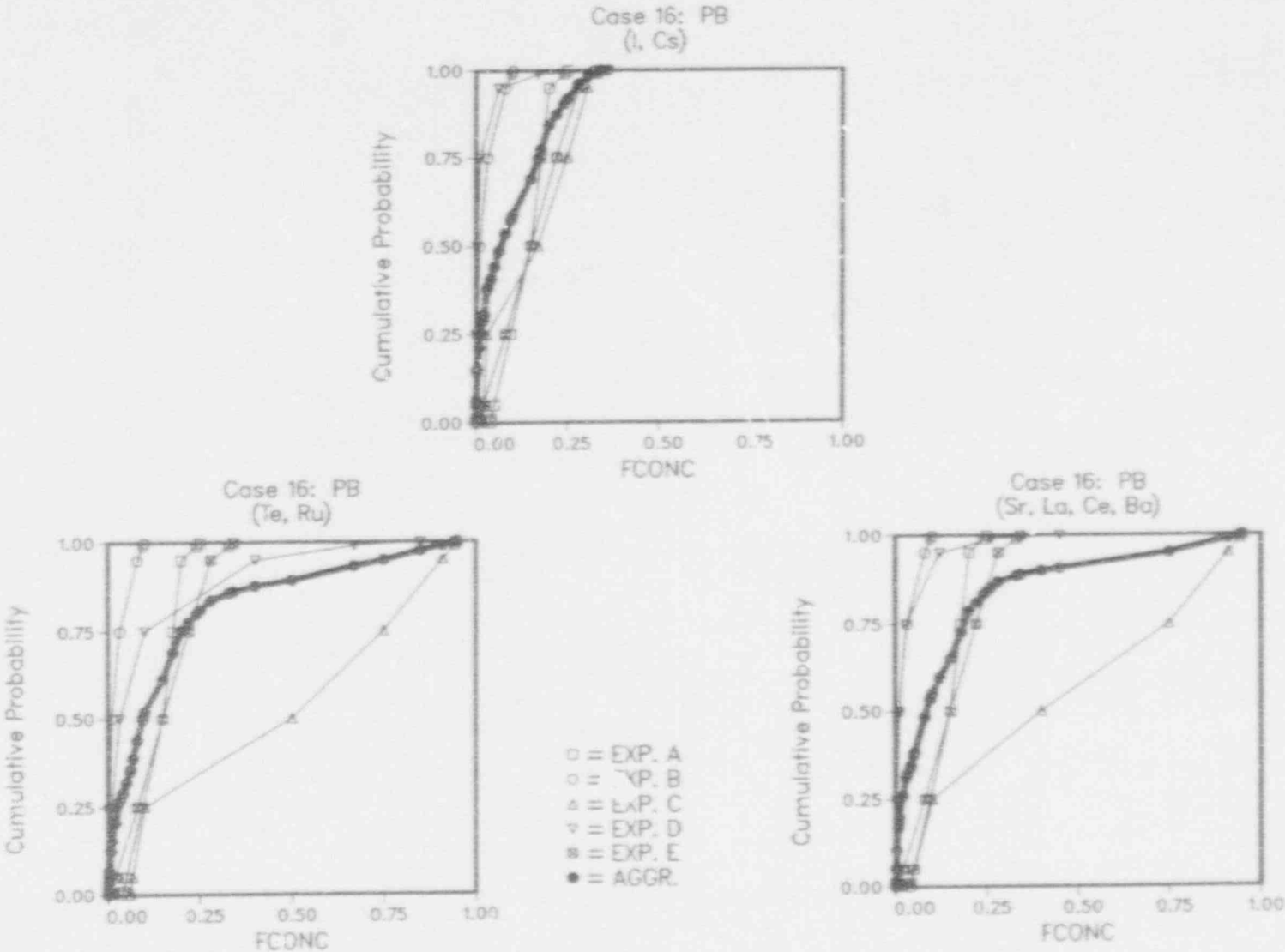

Figure 5-33. Case 16: Peach Bottom.

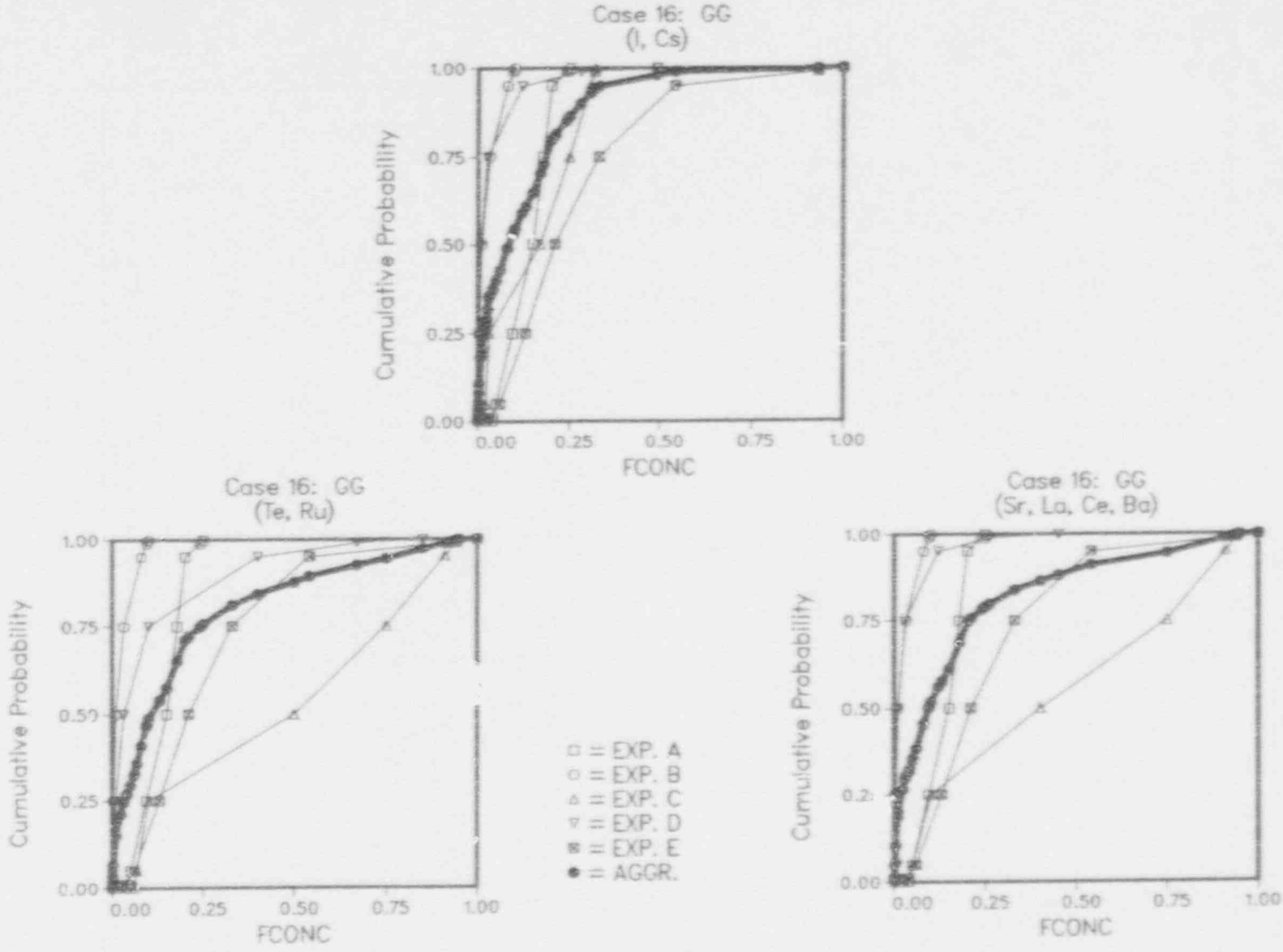

Figure 5-34. Case 16: Grand Gulf.

Individual Elicitations for Issue 5

Expert A's Elicitation

Release of Fission Products from Containment for Surry, Zion, Sequoyah, Peach Bottom, and Grand Gulf FCONV and FCONC

Description of Expert A's Rationale/Methodology

Expert A thinks that the dynamic shape factor has canceling effects. "Fluffy" particles have higher settling rates, but they do not coagulate as quickly as do smaller particles. Small particles do not get resuspended, but do get coagulated and do not settle out. The most important factor in determining this issue is thus the residence time of the aerosols in the containment. Everytning else is subsidiary, including the size of the containment failure.

The expert relied on A Reference Guide on Severe Accidents for much of his understanding of severe accident conditions and used BMI-2104[A-1] and BMI-2139[A-2] for estimates of the event timing and thus residence times. The expert also grouped all the radionuclides together.

Expert A estimated the values of FCONC at probabilities of 0.001, 0.5, and 0.999. The 0.25 and 0.75 fractiles are to be calculated by the project as the geometric averages of the adjacent 0.001 and 0.5, and 0.5 and 0.999 values, respectively. An implication of taking geometric averages is that some probability distributions for the value of FCONC or FCONV are bimodal. The expert felt that this was a reasonable representation of his judgment.

Cases 1 & 2. The only difference between Cases 1 and 2 is the depressurization time and thus the residence time. The expert estimated that the release rate would be increased, so FCONV would be increased. Cesium, iodine, and cesium iodide are more volatile than the other fission products and will come out of the fuel earlier. They would then be deposited in the vessel. After that, those fission products that are more difficult to remove from the fuel come out of the containment, but they are deposited in the vessel more slowly. Thus, no distinction was made between the volatiles and the refractory group. The values of FCONV and FCONC are the same.

Case 3. Failure is some hours after vessel breach. Expert A assumed 24 h. Although it was explained to the expert that 4 to 12 h is more typical, he did not think ths difference was important. The aerosol concentrations drop dramatically in 1 to 2 h and do not change much thereafter. The most important parameter is timing.

Case 4. The expert believed that the results should be the same as those for Case 2.

Case 5. Differences between this case and others for the presence of water were pointed out to the expert. He believed that the additional humidity does not make much difference in FCONC. The humidity makes particles

compact, and they settle out faster; but they do not agglomerate as fast. Differences in containment construction do not make much difference.

Case 6: The expert believed that the results should be the same as those for Case 5.

Cases 11 to 16: Fission product releases should be similar in BWRs and in PWRs.

Results of Expert A's Elicitation

The results of the Expert's elicitations are given in Table A-1.

Table A-1
Expected Value of FCONC,FCONV

	Cumulative Probability				
Case	0.001	0.250	0.500	0.750	0.999
1	0.05	0.15	0.5	0.63	0.8
2	0.15	0.32	0.7	0.79	0.9
3	1.E-6	3.2E-6	1.E-5	3.2E-5	1.E-4
4	0.15	0.32	0.7	0.79	0.9
5	0.15	0.32	0.7	0.79	0.9
6	0.05	0.15	0.5	0.63	0.8
7	0.05	0.15	0.5	0.63	0.8
8	0.15	0.32	0.7	0.79	0.9
9	1.E-3	3.2E-3	1.E-2	3.2E-2	0.1
10	0.15	0.32	0.7	0.79	0.9
11	0.05	0.15	0.5	0.63	0.8
12	0.05	0.15	0.5	0.63	0.8
13	0.15	0.32	0.7	0.79	0.9
14	0.15	0.32	0.7	0.79	0.9
15	1.E-3	3.2E-3	1.E-2	3.2E-2	0.1
16	1.E-3	3.2E-3	1.E-2	3.2E-2	0.1

Sources of Uncertainty

The timing of events, especially the time of rupture, is the most important source of uncertainty.

Correlations with Other Variables

Correlations with variables other than the timing of important events was not discussed.

Suggested Methods for Reducing Uncertainty

Code calculations that resolve the timing of events would significantly decrease the expert's uncertainty in the fission product release.

REFERENCES

A-1. J. A. Gieseke et al., "Radionuclide Release Under Specific LWR Accident Conditions," Vol. IV: PWR Ice Condenser Design, BMI-2104, Battelle Memorial Institute, 1984.

A-2. R. S. Denning et al., "Radionuclide Release Calculations for Selected Severe Accident Scenarios," Vols. I-V, NUREG/CR-4624, BMI-2139, Battelle Memorial Institute, 1986.

Expert B's Elicitation

Release of Fission Products from Containment for Surry, Zion, Sequoyah, Peach Bottom, and Grand Gulf FCONV and FCONC

Description of Expert B's Rationale/Methodology

Expert B provided the following description of his methodology for assessing FCONV and FCONC:

"Used as main basis NAUA calculations done in conjunction with STCP calculations. Took numbers from NAUA output as well as reports.

To distinguish between FCONC and FCONV, values for PI (particle source in vessel) and PE (particle source ex-vessel) which NAUA provides were considered. Also values for Ce which are entirely from CCI release.

For practical considerations, only Xe, I, Cs, and Te are considered for RCS release (FCONV), and only Te, St, Ru, La, Ce, and Ba are considered for ex-vessel (CCI) release (FCONC).

Took into account Brookhaven uncertainty study, Ed Fuller calculation for Peach Bottom (letter to Dave Williams dated 3/14/88), calculations noted Cases 54 and 55 from revised Dave Williams calculations with CONTAIN, and SAND86-2129C report on MELCOR calculations.

Ranges are intended to include uncertainties from:

1. Surface area (deposition area or compartment height);
2. Natural circulation;
3. Hygroscopic nature of aerosols (primarily I and Cs groups);
4. Particle shape factors (not big effect);
5. H_2 burn;
6. Residence time."

Results of Expert B's Elicitation

The results of the elicitation are given in Tables B-1 to B-16.

Sources of Uncertainty

The expert indicated that his uncertainty ranges were intended to include surface area (deposition area or compartment height), natural circulation, hygroscopic nature of aerosols (primarily iodine and cesium groups), particle shape factors (not a big effect), hydrogen burns, and residence time (a factor of 2 effect).

Correlations with Other Variables

Within each of the 16 cases, all variables are assumed to have a rank correlation of 1. No other correlations were indicated.

Suggested Methods for Reducing Uncertainty

No specific suggestions were made for reducing the uncertainty in the elicited variables.

Table B-1
Elicitation Results for Case 1: FCONV, PWR, Early Containment Leak*

	Quantiles				
Release Classes	0.001	0.25	0.50	0.75	0.999
Xe, Kr	1.00	1.00	1.00	1.00	1.00
I, Br	0.001	0.01	0.08	0.13	0.30
Cs, Rb	0.001	0.01	0.08	0.13	0.30
Te, Sb, Se	0.001	0.01	0.08	0.13	0.30
Sr**	0.001	0.01	0.08	0.13	0.30
Ru, Rh**	0.001	0.01	0.08	0.13	0.30
La, Zr**	0.001	0.01	0.08	0.13	0.30
Ce, Pu**	0.001	0.01	0.08	0.13	0.30
Ba**	0.001	0.01	0.08	0.13	0.30

*Particular consideration given to following NAUA calculations from BMI-2104, Vol. 8: Zion TMLB' high leak, Surry TMLB' high leak, Sequoyah TMLB'$_{\gamma}$.[B-1]
**Quantiles not supplied by expert; assumed to be same as for 1.

Table B-2
Elicitation Results for Case 1: FCONV, PWR, Early Containment Rupture*

	Quantiles				
Release Classes	0.001	0.25	0.50	0.75	0.999
Xe, Kr	1.00	1.00	1.00	1.00	1.00
I, Br	0.30	0.50	0.70	0.75	0.85
Cs, Rb**	0.30	0.50	0.70	0.75	0.85
Te, Sb, Se**	0.30	0.50	0.70	0.75	0.85
Sr**	0.30	0.50	0.70	0.75	0.85
Ru, Rh**	0.30	0.50	0.70	0.75	0.85
La, Zr**	0.30	0.50	0.70	0.75	0.85
Ce, Pu**	0.30	0.50	0.70	0.75	0.85
Ba**	0.30	0.50	0.70	0.75	0.85

*Particular consideration given to following calculations: Zion $S_2DCF\gamma$ (NUREG/CR-4624),[B-2] Surry AGδ (NUREG/CR-4624), Surry TMLB'δ_e (special calculation done with STCP but condensation turned off, used BMI-2104 input for NAUA).
**Quantiles not supplied by expert; assumed to be same as for I.

Table B-3
Elicitation Results for Case 3: FCONV, PWR, Late Containment Rupture*

	Quantiles				
Release Classes	0.001	0.25	0.50	0.75	0.999
Xe, Kr	1.00	1.00	1.00	1.00	1.00
I, Br	0.001	0.02	0.05	0.15	0.30
Cs, Rb	0.001	0.02	0.05	0.15	0.30
Te, Sb, Se	0.001	0.02	0.05	0.15	0.30
Sr**	0.001	0.02	0.05	0.15	0.30
Ru, Rh**	0.001	0.02	0.05	0.15	0.30
La, Zr**	0.001	0.02	0.05	0.15	0.30
Ce, Pu**	0.001	0.02	0.05	0.15	0.30
Ba**	0.001	0.02	0.05	0.15	0.30

*Particular consideration given to following NAUA calculations from NUREG/CR-4624:[B-2] Zion $S_2DCFS_\swarrow$, Zion $S_2DCS_\swarrow$.
**Quantiles not supplied by expert; assumed to be same as for I.

Table B-4
Elicitation Results for Case 4: FCONV, Sequoyah, Early Rupture in Lower Compartment of Ice Condenser*

	Quantiles				
Release Classes	0.001	0.25	0.50	0.75	0.999
Xe, Kr	1.00	1.00	1.00	1.00	1.00
I, Br	0.30	0.50	0.70	0.85	0.90
Cs, Rb	0.30	0.50	0.70	0.85	0.90
Te, Sb, Se	0.30	0.50	0.70	0.85	0.90
Sr**	0.30	0.50	0.70	0.85	0.90
Ru, Rh**	0.30	0.50	0.70	0.85	0.90
La, Zr**	0.30	0.50	0.70	0.85	0.90
Ce, Pu**	0.30	0.50	0.70	0.85	0.90
Ba**	0.30	0.50	0.70	0.85	0.90

*Particular consideration given to following calculations: S_3B_7 (NUREG/CR-5062),[B-3] S_3B (Cases 54 and 55 in CONTAIN calculations performed by Dave Williams).
**Quantiles not specified by expert; assumed to be same as for I.

Table B-5
Elicitation Results for Case 5: FCONV, BWR, Early Containment Rupture*

	Quantiles				
Release Classes	0.001	0.25	0.50	0.75	0.999
Xe, Kr	1.00	1.00	1.00	1.00	1.00
I, Br	0.30	0.50	0.70	0.85	0.95
Cs, Rb	0.30	0.50	0.70	0.85	0.95
Te, Sb, Se	0.30	0.50	0.70	0.75	0.85
Sr**	0.30	0.50	0.70	0.75	0.85
Ru, Rh**	0.30	0.50	0.70	0.75	0.85
La, Zr**	0.30	0.50	0.70	0.75	0.85
Ce, Pu**	0.30	0.50	0.70	0.75	0.85
Ba**	0.30	0.50	0.70	0.75	0.85

*Particular consideration given to following NAUA calculations from NUREG/CR-4624:[B-2] Grand Gulf TC26, Peach Bottom TC1.
**Quantiles not specified by expert; assumed to be same as for Te.

Table B-6
Elicitation Results for Case 6: FCONV, BWR, Early Containment Leak*

	Quantiles				
Release Classes	0.001	0.25	0.50	0.75	0.999
Xe, Kr	1.00	1.00	1.00	1.00	1.00
I, Br	0.01	0.10	0.20	0.40	0.60
Cs, Rb	0.01	0.10	0.20	0.40	0.60
Te, Sb, Se	0.01	0.10	0.20	0.40	0.60
Sr**	0.01	0.10	0.20	0.40	0.60
Ru, Rh**	0.01	0.10	0.20	0.40	0.60
La, Zr**	0.01	0.10	0.20	0.40	0.60
Ce, Pu**	0.01	0.10	0.20	0.40	0.60
Ba**	0.01	0.10	0.20	0.40	0.60

*Particular consideration given to NAUA calculations for Grand Gulf S_2E-leak failure (BMI-2104, Vol.8).[B-1]
**Quantiles not specified by expert; assumed to be same as for I.

Table B-7
Elicitation Results for Case 7: FCONC, PWR, Early Containment Leak*

	Quantiles				
Release Classes	0.001	0.25	0.50	0.75	0.999
Xe, Kr**	1.00	1.00	1.00	1.00	1.00
I, Br***	0.001	0.01	0.08	0.13	0.30
Cs, Rb***	0.001	0.01	0.08	0.13	0.30
Te, Sb, Se	0.005	0.03	0.10	0.20	0.30
Sr	0.005	0.03	0.10	0.20	0.30
Ru, Rh	0.005	0.03	0.10	0.20	0.30
La, Zr	0.005	0.03	0.10	0.20	0.30
Ce, Pu	0.005	0.03	0.10	0.20	0.30
Ba	0.005	0.03	0.10	0.20	0.30

*Expert considered Cases 1 and 8 in developing this case.
**Quantiles not specified by expert.
***Quantiles not specified by expert; assigned values for I from Case 1 (i.e., FCONV, PWR, early containment leak).

Table B-8
Elicitation Results for Case 8: FCONC, PWR, Early Containment Rupture*

	Quantiles				
Release Classes	0.001	0.25	0.50	0.75	0.999
Xe, Kr**	1.00	1.00	1.00	1.00	1.00
I, Br***	0.30	0.50	0.70	0.75	0.85
Cs, Rb***	0.30	0.50	0.70	0.75	0.85
Te, Sb, Se	0.10	0.40	0.60	0.75	0.85
Sr	0.10	0.40	0.60	0.75	0.85
Ru, Rh	0.10	0.40	0.60	0.75	0.85
La, Zr	0.10	0.40	0.60	0.75	0.85
Ce, Pu	0.10	0.40	0.60	0.75	0.85
Ba	0.10	0.40	0.60	0.75	0.85

*Particular consideration given to following NAUA calculations: Zion TMLU, Zion $S_2DCF\gamma$ and Surry AGδ from NUREG/CR-4624[B-2] and special calculation for Surry TMLB'δ_e indicated in Case 2.
**Quantiles not specified by expert.
***Quantiles not specified by expert; assigned values for I from Case 2 (FCONV, PWR, early containment rupture).

Table B-9
Elicitation Results for Case 9: FCONC, PWR, Late Containment Rupture*

	Quantiles				
Release Classes	0.001	0.25	0.50	0.75	0.999
Xe, Kr**	1.00	1.00	1.00	1.00	1.00
I, Br***	0.001	0.02	0.05	0.15	0.30
Cs, Rb***	0.001	0.02	0.05	0.15	0.30
Te, Sb, Se	0.02	0.04	0.20	0.30	0.50
Sr	0.01	0.02	0.10	0.20	0.30
Ru, Rh	0.02	0.04	0.20	0.30	0.50
La, Zr	0.01	0.02	0.10	0.20	0.30
Ce, Pu	0.01	0.02	0.10	0.20	0.30
Ba	0.01	0.02	0.10	0.20	0.30

*Particular consideration given to following calculations from NUREG/CR-4624:[B-2] Zion $S_2DCF\delta\sigma b\surd$, Zion $S_2DC_r\delta\surd$.
**Quantiles not supplied by expert.
***Quantiles not supplied by expert; assigned values for I from Case 3 (FCONV, PWR, late containment rupture).

Table B-10
Elicitation Results for Case 10: FCONC, Sequoyah, Early Rupture in Lower Compartment of Ice Condenser*

	Quantiles				
Release Classes	0.001	0.25	0.50	0.75	0.999
Xe, Kr**	1.00	1.00	1.00	1.00	1.00
I, Br***	0.30	0.50	0.70	0.85	0.90
Cs, Rb***	0.30	0.50	0.70	0.85	0.90
Te, Sb, Se	0.10	0.30	0.50	0.75	0.85
Sr	0.10	0.30	0.50	0.75	0.85
Ru, Rh	0.10	0.30	0.50	0.75	0.85
La, Zr	0.10	0.30	0.50	0.75	0.85
Ce, Pu	0.10	0.30	0.50	0.75	0.85
Ba	0.10	0.30	0.50	0.75	0.85

*Particular consideration given to the calculation for $S_3B\gamma$ from NUREG/CR-5062.[B-3]
**Quantiles not specified by expert.
***Quantiles not specified by expert; assigned values for I from Case 4 (Sequoyah, early rupture in lower compartment of ice condenser).

Table B-11
Elicitation Results for Case 11: FCONC, BWR, Early Containment Leak, Saturated Pool*

	Quantiles				
Release Classes	0.001	0.25	0.50	0.75	0.999
Xe, Kr**	1.00	1.00	1.00	1.00	1.00
I, Br***	0.01	0.10	0.20	0.40	0.60
Cs, Rb***	0.01	0.10	0.20	0.40	0.60
Te, Sb, Se	0.01	0.05	0.10	0.20	0.40
Sr	0.01	0.05	0.10	0.20	0.40
Ru, Rh	0.01	0.05	0.10	0.20	0.40
La, Zr	0.01	0.05	0.10	0.20	0.40
Ce, Pu	0.01	0.05	0.10	0.20	0.40
Ba	0.01	0.05	0.10	0.20	0.40

*Expert considered Cases 16, 15 and 12 in developing this case.
**Quantiles not specified by expert.
***Quantiles not specified by expert; assigned values for I from Case 6 (FCONV, BWR, early containment leak).

Table B-12
Elicitation Results for Case 12: FCONC, BWR,
Early Containment Leak Subcooled Pool*

	Quantiles				
Release Classes	0.001	0.25	0.50	0.75	0.999
Xe, Kr**	1.00	1.00	1.00	1.00	1.00
I, Br***	0.01	0.10	0.20	0.40	0.60
Cs, Rb***	0.01	0.10	0.20	0.40	0.60
Te, Sb, Se	0.01	0.05	0.10	0.20	0.40
-	0.01	0.05	0.10	0.20	0.40
, Rh	0.01	0.05	0.10	0.20	0.40
La, Zr	0.01	0.05	0.10	0.20	0.40
Ce, Pu	0.01	0.05	0.10	0.20	0.40
Ba	0.01	0.05	0.10	0.20	0.40

*Expert considered Cases 16, 15, and 11 in developing this case.
**Quantiles not specified by expert.
***Quantiles not specified by expert; assigned values for I from Case 6 (FCONV, BWR, early containment leak).

Table B-13
Elicitation Results for Case 13: FCONC, BWR,
Early Containment Rupture, Saturated Pool*

	Quantiles				
Release Classes	0.001	0.25	0.50	0.75	0.999
Xe, Kr**	1.00	1.00	1.00	1.00	1.00
I, Br***	0.30	0.50	0.70	0.85	0.95
Cs, Rb***	0.30	0.50	0.70	0.85	0.95
Te, Sb, Se	0.01	0.20	0.50	0.65	0.80
Sr	0.01	0.20	0.50	0.65	0.80
Ru, Rh	0.01	0.20	0.50	0.65	0.80
La, Zr	0.01	0.20	0.50	0.65	0.80
Ce, Pu	0.01	0.20	0.50	0.65	0.80
Ba	0.01	0.20	0.50	0.65	0.80

*Particular consideration was given to following NAUA calculations from NUREG/CR-4624:[B-2] Grand Gulf TC2 (or TCγ) and Peach Bottom TC1.
**Quantiles not specified by expert.
***Quantiles not specified by expert; assigned values for I from Case 5 (FCONV, BWR, early containment rupture).

Table B-14
Elicitation Results for Case 14: FCONC, BWR, Early Containment Rupture, Subcooled Pool*

	Quantiles				
Release Classes	0.001	0.25	0.50	0.75	0.999
Xe, Kr[b]	1.00	1.00	1.00	1.00	1.00
I, Br[c]	0.30	0.50	0.70	0.85	0.95
Cs, Rb[c]	0.30	0.50	0.70	0.85	0.95
Te, Sb, Se	0.01	0.30	0.50	0.70	0.85
Sr	0.01	0.30	0.50	0.70	0.85
Ru, Rh	0.01	0.30	0.50	0.70	0.85
La, Zr	0.01	0.30	0.50	0.70	0.85
Ce, Pu	0.01	0.30	0.50	0.70	0.85
Ba	0.01	0.30	0.50	0.70	0.85

*Expert considered Cases 13 and 10 in developing this case.
**Quantiles not specified by expert.
***Quantiles not specified by expert; assigned values for I from Case 5 (FCONV, BWR, early containment rupture).

Table B-15
Elicitation Results for Case 15: FCONC, BWR, Late Leak*

	Quantiles				
Release Classes	0.001	0.25	0.50	0.75	0.999
Xe, Kr**	1.00	1.00	1.00	1.00	1.00
I, Br***	0.002	0.01	0.03	0.07	0.17
Cs, Rb***	0.002	0.01	0.03	0.07	0.17
Te, Sb, Se	0.005	0.03	0.10	0.20	0.50
Sr	0.005	0.02	0.05	0.10	0.50
Ru, Rh	0.005	0.03	0.10	0.20	0.50
La, Zr	0.005	0.02	0.05	0.10	0.50
Ce, Pu	0.005	0.02	0.10	0.20	0.50
Ba	0.005	0.02	0.10	0.20	0.50

*Expert considered Cases 16, 12, and 11 in developing this case.
**Quantiles not specified by expert.
***Quantiles not specified by expert; used values for Te divided by 3. I and Cs are released early in CCI and then scavenged (e.g., TB1 sequence in NUREG/CR-4624, Vol. 1).[B-2]

Table B-16
Elicitation Results for Case 16: FCONC, BWR, Late Rupture*

	Quantiles				
Release Classes	0.001	0.25	0.50	0.75	0.999
Xe, Kr**	1.00	1.00	1.00	1.00	1.00
I, Br***	0.02	0.03	0.17	0.25	0.32
Cs, Rb***	0.02	0.03	0.17	0.25	0.32
Te, Sb, Se	0.06	0.10	0.50	0.75	0.95
Sr	0.04	0.10	0.40	0.75	0.95
Ru, Rh	0.06	0.10	0.50	0.75	0.95
La, Zr	0.04	0.10	0.40	0.75	0.95
Ce, Pu	0.04	0.10	0.40	0.75	0.95
Ba	0.04	0.10	0.40	0.75	0.95

*Particular consideration given to following calculations: Peach Bottom TBγ (NUREG/CR-4624),[B-2] estimates from Fuller-Table 3 (based on MAAP[B-5] and other EPRI codes), TB sequence (MELCOR, SAND86-2129C).[B-4]
**Quantiles not specified by expert.
***Quantiles not specified by expert; used values for Te divided by 3. I and Cs are released early in CCI and then scavenged (e.g., TB1 sequence in NUREG/CR-4624, Vol. 1).[B-2]

REFERENCES

B-1. J. A. Gieseke et al., "Radionuclide Release Under Specific LWR Accident Conditions," Vol. IV: PWR Ice Condenser Design, BMI-2104, Battelle Memorial Institute, 1984.

B-2. R. S. Denning et al., "Radionuclide Release Calculations for Selected Severe Accident Scenarios," Vols. I-V, NUREG/CR-4624, BMI-2139, Battelle Memorial Institute, 1986.

B-3. M. T. Leonard et al., "Supplemental Radionuclide Release Calculations for Selected Severe Accident Scenarios," NUREG/CR-5062, BMI-2160, Battelle Memorial Institute, 1987.

B-4 S. E. Dingman et al., "Analysis of Peach Bottom Station Blackout With MELCOR," SAND86-2129C, Sandia National Laboratories, 1986.

B-5 Industry Degraded Core Rulemaking Program, "Modular Accident Analysis Program (MAAP) User's Manual," IDCOR Technical Report on Subtasks 16.2 and 16.3, Fauske & Associates, Inc., for the Atomic Industrial Forum, Bethesda, MD, 1987.

Expert C's Elicitation

Release of Fission Products from Containment
for Surry, Zion, Sequoyah, and Grand Gulf
FCONV and FCONC

Description of Expert C's Rationale/Methodology

Expert C stated that his rationale for the FCONV and FCONC issues was essentially the same as that used in Expert B's assessment of the Peach Bottom reactor building DF issue (Issue 7). Hence, only a brief summary is given here; the description of Expert B's treatment of the reactor building DF should be consulted for additional details. In what follows, the term FCON will be used when the discussion applies equally to FCONV and FCONC.

Expert C felt that the methodology for developing uncertainty distributions should meet two basic requirements: it should incorporate the results of detailed code calculations (when available) as directly as possible, and it should also account for uncertainties not adequately represented by the range of code results, including the effects of modeling uncertainties in the codes themselves. To meet these requirements, Expert C devised a two-step process for developing uncertainty distributions for FCON. The first step was to develop what he called a "base distribution" using the results of code calculations. The second step was to make substantial changes to the base distribution to take into account additional uncertainties that he believed could have potentially important effects upon the code calculations.

Development of Base Distributions

The expert relied primarily upon calculations performed with the STCP and with its precursor codes,[C-1,C-2] and upon CONTAIN calculations.[C-3] When relevant calculations of FCON itself were not available, he used applicable code calculations of thermal-hydraulic conditions (e.g., generation rates of gases and/or steam) and aerosol generation rates together with the aerosol systematics discussed in Appendix N of Reference C-3 to estimate base distributions for FCON. He also performed a small number of CONTAIN calculations to evaluate the impact of certain specific effects, for example, uncertainty in the areas available for aerosol settling.

Modification of Base Distributions

Expert C felt that there were a number of uncertainties that his base distributions did not adequately reflect. These arise both from modeling uncertainties in the codes and from variations in accident scenarios not adequately represented by the available code calculations. He decomposed these uncertainties into the following subcategories:

1. Flow rates of steam and gas into the containment, which act to sweep aerosols and radionuclides out of the containment. High flows favor high FCON.

2. Aerosol generation rates, especially during CCI. High aerosol generation rates result in high aerosol densities that favor rapid agglomeration and aerosol deposition and, therefore, favor reduced FCON values.

3. Effect of containment volume. Since insufficient code calculations existed to permit the direct definition of a base distribution for all cases and all containments, the expert sometimes extrapolated results for one containment to the analogous case for other containments. He used aerosol behavior systematics to allow for the effect of volume differences and, in some cases, included some additional uncertainty when there was a need to extrapolate.

4. Containment pressure in leakage failure cases. When the containment undergoes a leakage failure, it may not depressurize completely (by definition of the leakage cases, it does not depressurize fully within 2 h.) Instead, pressure may decline until it reaches a quasi-steady state in which inflow of steam and gas equals the leakage rate. The higher this quasi-steady pressure is for a given gas inflow rate, the longer the gas residence time and, hence, the lower the FCON values. In estimating the effect of this uncertainty, the expert assumed that the quasi-steady pressure could be anything from near ambient up to the containment failure pressure.

5. Uncertainties in aerosol agglomeration and deposition rates associated with aerosol shape factors, turbulent agglomeration, steam condensation on aerosols (including hygroscopic aerosol effects), and uncertainty in areas of surfaces available for aerosol settling.

Expert C noted that, during CCI, cesium and iodine were released early, while release of tellurium (and the ruthenium group, insofar as it is released at all) tends to persist into late times. The refractory oxide species (strontium, lanthanum, cerium, and barium) show an intermediate behavior. He believed these differences in timing could have significant effects upon FCONC for late containment failures, but would be less important for early failures. Hence, he divided the radionuclides into three groups in estimating FCONC for late failures, with different distributions for each group. These groups consisted of cesium and iodine; tellurium and ruthenium; and strontium, lanthanum, cerium, and barium.

To incorporate the estimated effects of the five uncertainty subcategories above into his distributions, the expert used a simple conceptual model in which the release from the containment is controlled by competition between aerosol deposition, represented by a fractional deposition rate λ_a, versus transport out of the containment by the flow of steam and gas, represented by the fractional transport rate λ_g. FCON is then equal to $\lambda_g/(\lambda_g + \lambda_a) = 1/(1 + RP)$, where $RP = \lambda_a/\lambda_g$ is a release parameter that the Expert defined and used in his analysis. The expert converted his base distributions for FCON into distributions for RP, and then estimated how each of the uncertainties discussed above might introduce additional uncertainty into λ_a and/or λ_g and, hence, into RP. He then calculated the effect of the

combined uncertainties noted above upon his initial distribution for RP using a decomposition tree, which allowed for all possible combinations of the various assumptions he made concerning the possible effects of the uncertainties individually. The resulting distributions for RP were then converted back into distributions for FCON to obtain the final results the expert gave in his elicitation. The methodology was identical to that used by Expert B in analyzing Issue 7 (BWR reactor building DFs), and several of the uncertainty subcategories listed above are also similar. Hence, the summary of Expert B's elicitation for Issue 7 may be consulted for additional details.

Expert C noted that for several of the cases involving early rupture failure, available code calculations gave large ($\geq$0.5) FCON values. These results were considered physically reasonable for these cases, and the existing uncertainties were not believed great enough to reverse the conclusion that FCON would be relatively large. He believed that it would not be useful to attempt to apply the detailed procedure outlined above to these cases and, therefore, developed subjective distributions for these cases directly from the available code calculations.

Results of Expert C's Elicitation

The results of the elicitation are summarized in Tables C-1 to C-16.

The results in Tables C-2, C-4, C-5, C-8, C-13, and C-14 were constructed by the expert directly from the consideration of code calculations (primarily STCP and CONTAIN).

The results in Tables C-1, C-3, C-6, C-7, C-9, and C-16 were constructed by developing a base distribution and then modifying this distribution for factors that the expert felt were not adequately represented in available code calculations, as was described in the preceding discussion of the Expert's rationale.

Sources of Uncertainty

The five uncertainty subcategories that the expert included in his decomposition tree are those that he felt to be most important. He also believed that significant uncertainty was introduced by the need to group together a range of accident scenarios in a single case; however, he doubted that this was the dominant source of uncertainty. He did not assign great importance to the uncertainty in the surface areas available for aerosol settling, as CONTAIN calculations he had performed indicated this would be important only when aerosol densities were quite low.

Correlation with Other Variables

Expert C believed that, other things being equal, high FCCI values would be correlated with high aerosol densities in containment, which he believed would favor enhanced agglomeration and settling rates. Hence, he believed

there might be some inverse correlation between FCCI and FCON. For similar reasons, he believed that there might be an inverse correlation between FCON and pool DFs in those scenarios in which aerosols would be subject to scrubbing in pools before release of the aerosols to the containment. However, he believed that substantial additional effort would be needed to define such correlations quantitatively (if it could be done) and that simply guessing at the correlations could do more harm than good. Hence, Expert C did not specify any correlations between FCON and other variables.

Suggested Methods for Reducing Uncertainty

Expert C believed that uncertainties in FCON might be significantly reduced if it were possible to define the dominant accident scenarios more accurately and then perform detailed code calculations, with a carefully designed nodalization of the containment, for the specific scenarios of interest. Appropriate sensitivity studies would have to be a part of these calculations. Even if they failed to yield substantial reductions in the uncertainties, they would put the assessment of the uncertainty distributions on a firmer basis. Aerosol modeling improvements needed to include better definition of shape factors, turbulent agglomeration (including models for turbulent intensities), and improved modeling of steam condensation on aerosols, especially hygroscopic aerosols. On the whole, however, he felt that uncertainties in the thermal-hydraulic conditions (and perhaps uncertainty in the aerosol sources) were probably more important than the uncertainty in the aerosol modeling, given accurate thermal-hydraulics and aerosol sources. Finally, he felt that the most important uncertainty affecting FCON in a given accident sequence was the uncertainty in the accident progression, that is, in the mode and timing of containment failure. (In the present study, this uncertainty was represented primarily by the case structure, rather than by the distributions the experts gave for a specified case.) Unless this uncertainty can be reduced (e.g., by detailed code calculations and improved models for containment loads and performance where needed), he believed that uncertainties in FCON for a specified accident sequence are not likely to be greatly reduced by improved aerosol modeling or by reducing the range of accident sequences grouped together into a single case.

Elicitation Results for Case 1: FCONC, PWR, Early Containment Leak

These results are presented individually for Zion, Surry, and Sequoyah. Furthermore, cases involving a dry and wet cavity are presented. Identical results are assumed to hold for FCONC in Case 7. The differences between the wet and dry cavity cases results from three sources: reduced aerosol concentration, increased gas flow out of the containment, and the potential for steam condensation.

Table C-1(a)
Zion, Dry Cavity
FCONV and FCONC for Early Leak

Cumulative Weight	Final Distribution
1.000E-02	5.256E-01
5.000E-02	3.198E-01
1.000E-01	2.197E-01
1.500E-01	1.673E-01
2.000E-01	1.294E-01
2.500E-01	1.059E-01
3.000E-01	8.679E-02
3.500E-01	7.108E-02
4.000E-01	5.926E-02
4.500E-01	4.971E-02
5.000E-01	4.144E-02
5.500E-01	3.442E-02
6.000E-01	2.860E-02
6.500E-01	2.362E-02
7.000E-01	1.923E-02
7.500E-01	1.540E-02
8.000E-01	1.205E-02
8.500E-01	9.054E-03
9.000E-01	6.382E-03
9.500E-01	3.794E-03
9.900E-01	1.532E-03

Table C-1(b)
Zion, Wet Cavity
FCONV and FCONC for Early Leak

Cumulative Weight	Final Distribution
1.000E-02	8.313E-01
5.000E-02	6.667E-01
1.000E-01	5.427E-01
1.500E-01	4.495E-01
2.000E-01	3.779E-01
2.500E-01	3.207E-01
3.000E-01	2.692E-01
3.500E-01	2.288E-01
4.000E-01	1.944E-01
4.500E-01	1.638E-01
5.000E-01	1.373E-01
5.500E-01	1.151E-01
6.000E-01	9.565E-02
6.500E-01	7.835E-02
7.000E-01	6.336E-02
7.500E-01	5.034E-02
8.000E-01	3.877E-02
8.500E-01	2.864E-02
9.000E-01	1.954E-02
9.500E-01	1.124E-02
9.900E-01	4.139E-03

Table C-1(c)
Surry, Dry Cavity
FCONV and FCONC for Early Leak

Cumulative Weight	Final Distribution
1.000E-02	5.478E-01
5.000E-02	3.396E-01
1.000E-01	2.354E-01
1.500E-01	1.801E-01
2.000E-01	1.398E-01
2.500E-01	1.146E-01
3.000E-01	9.414E-02
3.500E-01	7.720E-02
4.000E-01	6.445E-02
4.500E-01	5.410E-02
5.000E-01	4.514E-02
5.500E-01	3.752E-02
6.000E-01	3.119E-02
6.500E-01	2.578E-02
7.000E-01	2.099E-02
7.500E-01	1.681E-02
8.000E-01	1.316E-02
8.500E-01	9.892E-03
9.000E-01	6.974E-03
9.500E-01	4.148E-03
9.900E-01	1.675E-03

Table C-1(d)
Surry, Wet Cavity
FCONV and FCONC for Early Leak

Cumulative Weight	Final Distribution
1.000E-02	8.435E-01
5.000E-02	6.862E-01
1.000E-01	5.648E-01
1.500E-01	4.717E-01
2.000E-01	3.991E-01
2.500E-01	3.405E-01
3.000E-01	2.872E-01
3.500E-01	2.449E-01
4.000E-01	2.088E-01
4.500E-01	1.764E-01
5.000E-01	1.483E-01
5.500E-01	1.245E-01
6.000E-01	1.037E-01
6.500E-01	8.505E-02
7.000E-01	6.887E-02
7.500E-01	5.479E-02
8.000E-01	4.224E-02
8.500E-01	3.123E-02
9.000E-01	2.133E-02
9.500E-01	1.227E-02
9.900E-01	4.524E-03

Table C-1(e)
Sequoyah, Dry Cavity
FCONV and FCONC for Early Leak

Cumulative Weight	Final Distribution
1.000E-02	7.436E-01
5.000E-02	5.432E-01
1.000E-01	4.136E-01
1.500E-01	3.296E-01
2.000E-01	2.661E-01
2.500E-01	2.201E-01
3.000E-01	1.823E-01
3.500E-01	1.517E-01
4.000E-01	1.273E-01
4.500E-01	1.064E-01
5.000E-01	8.865E-02
5.500E-01	7.377E-02
6.000E-01	6.110E-02
6.500E-01	5.001E-02
7.000E-01	4.041E-02
7.500E-01	3.220E-02
8.000E-01	2.490E-02
8.500E-01	1.842E-02
9.000E-01	1.265E-02
9.500E-01	7.346E-03
9.900E-01	2.762E-03

Table C-1(f)
Sequoyah, Wet Cavity
FCONV and FCONC for Early Leak

Cumulative Weight	Final Distribution
1.000E-02	9.272E-01
5.000E-02	8.360E-01
1.000E-01	7.465E-01
1.500E-01	6.659E-01
2.000E-01	5.946E-01
2.500E-01	5.274E-01
3.000E-01	4.647E-01
3.500E-01	4.083E-01
4.000E-01	3.559E-01
4.500E-01	3.075E-01
5.000E-01	2.642E-01
5.500E-01	2.249E-01
6.000E-01	1.888E-01
6.500E-01	1.565E-01
7.000E-01	1.277E-01
7.500E-01	1.017E-01
8.000E-01	7.825E-02
8.500E-01	5.757E-02
9.000E-01	3.881E-02
9.500E-01	2.170E-02
9.900E-01	7.629E-03

Table C-2
Zion and Surry
Elicitation Results for Case 2: FCONV, PWR,
Early Containment Rupture

Quantile	FCONV
0.99	0.98
0.95	0.95
0.75	0.85
0.50	0.70
0.25	0.50
0.05	0.10
0.01	0.02

Elicitation Results, Case 3: FCONV, PWR, Late Containment Rupture

Results are presented for Zion and Surry and also for Sequoyah. The results for FCONV for all species are assumed to be the same as those presented in Table C-9 for FCONC for iodine and cesium in Case 9.

Table C-3(a)
Surry and Zion
Late Rupture 'FCONC' for Cesium, Iodine
Late Rupture FCONV, All Species

Cumulative Weight	Final Distribution
1.000E-02	3.561E-01
5.000E-02	1.823E-01
1.000E-01	1.146E-01
1.500E-01	8.087E-02
2.000E-01	6.048E-02
2.500E-01	4.667E-02
3.000E-01	3.674E-02
3.500E-01	2.944E-02
4.000E-01	2.376E-02
4.500E-01	1.926E-02
5.000E-01	1.566E-02

Table C-3(a) (Continued)

Cumulative Weight	Final Distribution
5.500E-01	1.273E-02
6.000E-01	1.029E-02
6.500E-01	8.262E-03
7.000E-01	6.561E-03
7.500E-01	5.121E-03
8.000E-01	3.888E-03
8.500E-01	2.841E-03
9.000E-01	1.928E-03
9.500E-01	1.112E-03
9.900E-01	4.324E-04

Table C-3(b)
Sequoyah: Late Rupture 'FCONC' for Cesium, Iodine
Extrapolation From Surry and Zion,
Late Rupture FCONV, All Species

Cumulative Weight	Final Distribution
1.000E-02	2.716E-01
5.000E-02	1.177E-01
1.000E-01	6.810E-02
1.500E-01	4.578E-02
2.000E-01	3.295E-02
2.500E-01	2.471E-02
3.000E-01	1.900E-02
3.500E-01	1.486E-02
4.000E-01	1.175E-02
4.500E-01	9.334E-03
5.000E-01	7.441E-03

Table C-3(b) (Continued)

Cumulative Weight	Final Distribution
5.500E-01	5.930E-03
6.000E-01	4.706E-03
6.500E-01	3.709E-03
7.000E-01	2.889E-03
7.500E-01	2.209E-03
8.000E-01	1.638E-03
8.500E-01	1.163E-03
9.000E-01	7.596E-04
9.500E-01	4.128E-04
9.900E-01	1.455E-04

Elicitation Results, Case 4: FCONV, Sequoyah, Early Rupture in Lower Compartment of Ice Condenser

Results are given for ruptures in both the lower and upper compartments of the ice condenser. Identical results are assumed to hold for FCONC in Case 10.

Table C-4
FCONV, Sequoyah, Early Rupture in Lower and Upper Compartments

Quantile	Lower Compartment FCONV = FCONC	Upper Compartment FCONV = FCONC
0.99	0.98	0.98
0.95	0.95	0.90
0.75	0.90	0.75
0.50	0.80	0.65
0.25	0.60	0.30
0.05	0.25	0.10
0.01	0.05	0.02

Elicitation Results, Case 5: FCONV, BWR, Early Containment Rupture

Results are presented for Peach Bottom and for Grand Gulf. Further, cases involving saturated and subcooled pools are presented. Identical results are assumed to hold for FCONC in Case 13 (saturated pool) and Case 14 (subcooled pool) for Peach Bottom.

Table C-5
FCONV, BWR, Early Containment Rupture

	Peach Bottom		Grand Gulf
Quantile	Saturated	Subcooled	Subcooled & Saturated
0.99	1.00	1.00	0.98
0.95	0.99	0.97	0.95
0.75	0.97	0.90	0.85
0.50	0.93	0.80	0.70
0.25	0.85	0.40	0.30
0.05	0.30	0.10	0.15
0.01	0.05	0.01	0.05

Elicitation Results, Case 6: FCONV, BWR, Early Containment Leak

Results are presented individually for Peach Bottom, and Grand Gulf. Further, the results are subdivided by whether the pool is subcooled or saturated. Identical results are assumed to hold for FCONC in Case 11 (saturated pool) and Case 12 (subcooled pool).

Table C-6(a)
Peach Bottom, Subcooled Pool
FCONV and FCONC for Early Leak

Cumulative Weight	Final Distribution
1.000E-02	6.632E-01
5.000E-02	4.631E-01
1.000E-01	3.473E-01
1.500E-01	2.744E-01
2.000E-01	2.245E-01
2.500E-01	1.856E-01
3.000E-01	1.549E-01
3.500E-01	1.309E-01
4.000E-01	1.107E-01
4.500E-01	9.325E-02
5.000E-01	7.913E-02

Table C-6(a) (Continued)

Cumulative Weight	Final Distribution
5.500E-01	6.695E-02
6.000E-01	5.609E-02
6.500E-01	4.670E-02
7.000E-01	3.860E-02
7.500E-01	3.129E-02
8.000E-01	2.474E-02
8.500E-01	1.894E-02
9.000E-01	1.351E-02
9.500E-01	8.295E-03
9.900E-01	3.521E-03

Table C-6(b)
Peach Bottom, Saturated Pool
FCONV and FCONC for Early Leak

Cumulative Weight	Final Distribution
1.000E-02	8.968E-01
5.000E-02	7.867E-01
1.000E-01	6.910E-01
1.500E-01	6.097E-01
2.000E-01	5.400E-01
2.500E-01	4.754E-01
3.000E-01	4.199E-01
3.500E-01	3.687E-01
4.000E-01	3.213E-01
4.500E-01	2.798E-01
5.000E-01	2.418E-01
5.500E-01	2.068E-01
6.000E-01	1.756E-01
6.500E-01	1.474E-01
7.000E-01	1.216E-01
7.500E-01	9.831E-02
8.000E-01	7.733E-02
8.500E-01	5.822E-02
9.000E-01	4.075E-02
9.500E-01	2.402E-02
9.900E-01	9.405E-03

Elicitation Results, Case 7: FCONC, PWR, Early Containment Leak

See Table C-1. The results for FCONC in Case 7 are identical to the results specified for FCONV in Case 1.

Table C-7
Grand Gulf, Subcooled Pool and Dry Cavity
FCONV and FCONC for Early Leak

Cumulative Weight	Final Distribution
1.000E-02	4.978E-01
5.000E-02	2.916E-01
1.000E-01	1.971E-01
1.500E-01	1.457E-01
2.000E-01	1.129E-01
2.500E-01	8.947E-02
3.000E-01	7.253E-02
3.500E-01	5.915E-02
4.000E-01	4.855E-02
4.500E-01	4.004E-02
5.000E-01	3.310E-02
5.500E-01	2.728E-02
6.000E-01	2.236E-02
6.500E-01	1.822E-02
7.000E-01	1.467E-02
7.500E-01	1.158E-02
8.000E-01	8.918E-03
8.500E-01	6.604E-03
9.000E-01	4.517E-03
9.500E-01	2.594E-03
9.900E-01	9.716E-04

Table C-7 (Continued)

Cumulative Weight	Final Distribution
1.000E-02	8.142E-01
5.000E-02	6.356E-01
1.000E-01	5.056E-01
1.500E-01	4.098E-01
2.000E-01	3.384E-01
2.500E-01	2.802E-01
3.000E-01	2.334E-01
3.500E-01	1.945E-01
4.000E-01	1.622E-01
4.500E-01	1.351E-01
5.000E-01	1.120E-01
5.500E-01	9.241E-02
6.000E-01	7.571E-02
6.500E-01	6.134E-02
7.000E-01	4.896E-02
7.500E-01	3.832E-02
8.000E-01	2.913E-02
8.500E-01	2.107E-02
9.000E-01	1.409E-02
9.500E-01	7.782E-03
9.900E-01	2.677E-03

Elicitation Results, Case 8: FCONC, PWR, Early Containment Rupture

The results presented are for Zion and Surry. For Sequoyah, the results are the same as for FCONV (Table C-4).

Table C-8
Zion and Surry

Quantile	FCONC
0.99	0.95
0.95	0.85
0.75	0.70
0.50	0.50
0.25	0.25
0.05	0.05
0.01	0.02

Elicitation Results, Case 9: FCONC, PWR, Late Containment Rupture

Results are presented for Zion and Surry and also for Sequoyah. The expert gave different groups of radionuclides: cesium and iodine; tellurium and ruthenium (including molybdenum); and refractories (lanthanum, cesium, strontium, barium). The results for iodine and cesium are the same as those presented in Table C-3 for FCONV, all species.

Table C-9(a)
Surry and Zion, Cesium, Iodine
Extrapolated From Surry and Zion,
Late Rupture FCONV, All Species

Cumulative Weight	Final Distribution
1.000E-02	3.561E-01
5.000E-02	1.823E-01
1.000E-01	1.146E-01
1.500E-01	8.087E-02
2.000E-01	6.048E-02
2.500E-01	4.667E-02
3.000E-01	3.674E-02
3.500E-01	2.944E-02
4.000E-01	2.376E-02
4.500E-01	1.926E-02
5.000E-01	1.566E-02
5.500E-01	1.273E-02
6.000E-01	1.029E-02
6.500E-01	8.262E-03
7.000E-01	6.561E-03
7.500E-01	5.121E-03
8.000E-01	3.888E-03
8.500E-01	2.841E-03
9.000E-01	1.928E-03
9.500E-01	1.112E-03
9.900E-01	4.324E-04

Table C-9(b)
Surry and Zion, Tellurium, Ruthenium
Late Rupture 'FCONC' for Tellurium, Ruthenium

Cumulative Weight	Final Distribution
1.000E-02	8.469E-01
5.000E-02	6.904E-01
1.000E-01	5.641E-01
1.500E-01	4.680E-01
2.000E-01	3.916E-01
2.500E-01	3.287E-01
3.000E-01	2.761E-01
3.500E-01	2.327E-01
4.000E-01	1.957E-01
4.500E-01	1.642E-01
5.000E-01	1.373E-01
5.500E-01	1.142E-01
6.000E-01	9.420E-02
6.500E-01	7.690E-02
7.000E-01	6.195E-02
7.500E-01	4.895E-02
8.000E-01	3.756E-02
8.500E-01	2.770E-02
9.000E-01	1.895E-02
9.500E-01	1.101E-02
9.900E-01	4.308E-03

Table C-9(c)
Surry and Zion, Refractories
Late Rupture 'FCONC' for Refractories

Cumulative Weight	Final Distribution
1.000E-02	4.591E-01
5.000E-02	2.963E-01
1.000E-01	2.151E-01
1.500E-01	1.673E-01
2.000E-01	1.349E-01
2.500E-01	1.107E-01
3.000E-01	9.199E-02
3.500E-01	7.718E-02
4.000E-01	6.513E-02
4.500E-01	5.515E-02
5.000E-01	4.673E-02
5.500E-01	3.955E-02
6.000E-01	3.340E-02
6.500E-01	2.809E-02
7.000E-01	2.335E-02
7.500E-01	1.912E-02
8.000E-01	1.542E-02
8.500E-01	1.206E-02
9.000E-01	8.844E-03
9.500E-01	5.763E-03
9.900E-01	2.694E-03

Table C-9(d)
Sequoyah, Cesium, Iodine
Late Rupture 'FCONC' for Cesium, Iodine
Late Rupture FCONV, All Species

Cumulative Weight	Final Distribution
1.000E-02	2.716E-01
5.000E-02	1.177E-01
1.000E-01	6.810E-02
1.500E-01	4.578E-02
2.000E-01	3.295E-02
2.500E-01	2.471E-02
3.000E-01	1.900E-02
3.500E-01	1.486E-02
4.000E-01	1.175E-02
4.500E-01	9.334E-03
5.000E-01	7.441E-03
5.500E-01	5.930E-03
6.000E-01	4.706E-03
6.500E-01	3.709E-03
7.000E-01	2.889E-03
7.500E-01	2.209E-03
8.000E-01	1.638E-03
8.500E-01	1.163E-03
9.000E-01	7.596E-04
9.500E-01	4.128E-04
9.900E-01	1.455E-04

Table C-9(e)
Sequoyah, Tellurium, Ruthenium
Late Rupture 'FCONC' for Tellurium, Ruthenium

Cumulative Weight	Final Distribution
1.000E-02	7.885E-01
5.000E-02	5.715E-01
1.000E-01	4.222E-01
1.500E-01	3.242E-01
2.000E-01	2.541E-01
2.500E-01	2.021E-01
3.000E-01	1.623E-01
3.500E-01	1.311E-01
4.000E-01	1.062E-01
4.500E-01	8.611E-02
5.000E-01	6.974E-02
5.500E-01	5.629E-02
6.000E-01	4.515E-02
6.500E-01	3.589E-02
7.000E-01	2.185E-02
7.500E-01	2.166E-02
8.000E-01	1.614E-02
8.500E-01	1.151E-02
9.000E-01	7.544E-03
9.500E-01	4.113E-03
9.900E-01	1.453E-03

Table C-9(f)
Sequoyah, Refractories
Late Rupture 'FCONC' for Refractories

Cumulative Weight	Final Distribution
1.000E-02	3.828E-01
5.000E-02	2.103E-01
1.000E-01	1.386E-01
1.500E-01	1 011E-01
2.000E-01	7.761E-02
2.500E-01	6.140E-02
3.000E-01	4.942E-02
3.500E-01	4.036E-02
4.000E-01	3.320E-02
4.500E-01	2.742E-02
5.000E-01	2.268E-02
5.500E-01	1.873E-02
6.000E-01	1.543E-02
6.500E-01	1.265E-02
7.000E-01	1.026E-02
7.500E-01	8.168E-03
8.000E-01	6.377E-03
8.500E-01	4.777E-03
9.000E-01	3.349E-03
9.500E-01	2.023E-03
9.900E-01	8.451E-04

Elicitation Results, Case 10: FCONC, Sequoyah, Early Rupture in Lower Compartment of Ice Condenser

See Table C-4. The results for FCONC in Case 10 are identical to the results specified for FCONV in Case 4.

Elicitation Results, Case 11: FCONC, BWR, Early Containment Leak, Saturated Pool

See Table C-6. The results for FCONC in Case 11 are identical to those specified for FCONV in Case 6 for the saturated pool case.

Elicitation Results, Case 12: FCONC, BWR, Early Containment Leak, Subcooled Pool

See Table C-6. The results for FCONC in Case 12 are identical to those specified for FCONV in Case 6 for the subcooled pool case.

Elicitation Results, Case 13: FCONC, BWR, Early Containment Rupture, Saturated Pool

See Table C-5. The results for FCONC in Case 13 for Peach Bottom are identical to the results specified for FCONV in Case 5 for the saturated pool case.

Table C-13
Elicitation for Case 13: FCONC, BWR,
Early Containment Rupture, Saturated Pool

Quantiles	Peach Bottom	Grand Gulf
0.99	1.00	0.95
0.95	0.99	0.87
0.75	0.97	0.80
0.50	0.93	0.75
0.25	0.85	0.50
0.05	0.30	0.25
0.01	0.05	0.05

Elicitation Results, Case 14: FCONC, BWR, Early Containment Rupture, Subcooled Pool

See Table C-5. The results for FCONC in Case 14 are identical to those specified for FCONV in Case 5 for the subcooled pool case. Furthermore, in absence of other information, the same values are used for Grand Gulf as for the saturated case.

Table C-14
Elicitation for Case 14: FCONC, BWR,
Early Containment Rupture, Subcooled Pool.

Quantiles	Peach Bottom	Grand Gulf
0.99	1.00	0.95
0.95	0.97	0.87
0.75	0.90	0.80
0.50	0.80	0.75
0.25	0.40	0.50
0.05	0.10	0.25
0.01	0.01	0.05

Table C-15(a)
Elicitation Results for Case 15:
Peach Bottom: Late Leak FCONC for Cesium, Iodine
Extrapolated from Surry & Zion

Cumulative Weight	Final Distribution
1.000E-02	5.153E-02
5.000E-02	1.550E-02
2.500E-01	2.395E-03
5.000E-01	6.274E-04
7.500E-01	1.672E-04
9.500E-01	2.749E-05
9.900E-01	8.887E-06

Table C-15(b)
Elicitation Results for Case 15:
Peach Bottom: Late Leak FCONC for Tellurium, Ruthenium
Extrapolated from Surry & Zion

Cumulative Weight	Final Distribution
1.000E-02	3.498E-01
5.000E-02	1.363E-01
2.500E-01	2.342E-02
5.000E-01	6.238E-03
7.500E-01	1.667E-03
9.500E-01	2.753E-04
9.900E-01	8.899E-05

Table C-15(c)
Elicitation Results for Case 15:
Peach Bottom: Late Leak FCONC for Refractories

Cumulative Weight	Final Distribution
1.000E-02	8.999E-02
5.000E-02	3.228E-02
2.500E-01	6.252E-03
5.000E-01	1.926E-03
7.500E-01	6.073E-04
9.500E-01	1.304E-04
9.900E-01	5.148E-05

Table C-15(d)
Elicitation Results for Case 15:
Grand Gulf: Late Leak FCONC for Cesium, Iodine

Cumulative Weight	Final Distribution
1.000E-02	1.366E-01
5.00E-02	5.019E-02
2.500-01	9.353E-03
5.000E-01	2.678E-03
7.500E-01	7.611E-04
9.500E-01	1.341E-04
9.900E-01	4.406E-05

Table C-15(e)
Elicitation Results for Case 15:Grand Gulf:
Late Leak FCONC for Tellurium, Ruthenium

Cumulative Weight	Final Distribution
1.000E-02	6.127E-01
5.00E-02	3.457E-01
2.500-01	8.627E-02
5.000F-01	2.615E-02
7.500E-01	7.359E-03
9.500E-01	1.340E-03
9.900E-01	4.404E-04

Table C-15(f)
Elicitation Results for Case 15:Grand Gulf:
Late Leak FCONC for Refractories

Cumulative Weight	Final Distribution
1.000E-02	2.120E-01
5.00E-02	9.714E-02
2.500-01	2.392E-02
5.000E-01	8.242E-03
7.500E-01	2.815E-03
9.500E-01	6.453E-04
9.900E-01	2.532E-04

Elicitation Results, Case 16: FCONC, BWR, Late Rupture

These results are presented for Peach Bottom and for Grand Gulf. Separate results are given for these radionuclide groups: cesium and iodine; tellurium and ruthenium (including molybdenum) and refractories (lanthanum, cerium, strontium, barium). The values specified for iodine and cesium could also be used for FCONV for late containment rupture, all species.

Table C-16(a)
Peach Bottom: Cesium, Iodine
Late Rupture 'FCONC' for Cesium, Iodine
Late Rupture FCONV All Species

Cumulative Weight	Final Distribution
1.000E-02	1.661E-01
5.000E-02	6.196E-02
1.000E-01	3.377E-02
1.500E-01	2.208E-02
2.000E-01	1.565E-02
2.500E-01	1.158E-02
3.000E-01	8.805E-03
3.500E-01	6.820E-03
4.000E-01	5.351E-03
4.500E-01	4.228E-03
5.000E-01	3.353E-03
5.500E-01	2.660E-03
6.000E-01	2.102E-03
6.500E-01	1.651E-03
7.000E-01	1.281E-03
7.500E-01	9.770E-04
8.000E-01	7.259E-04
8.500E-01	5.124E-04
9.000E-01	3.356E-04
9.500E-01	1.827E-04
9.900E-01	6.557E-05

Table C-16(b)
Peach Bottom: Tellurium, Ruthenium
Late Rupture 'FCONC' for Tellurium, Ruthenium

Cumulative Weight	Final Distribution
1.000E-02	6.657E-01
5.000E-02	3.978E-01
1.000E-01	2.590E-01
1.500E-01	1.842E-01
2.000E-01	1.371E-01
2.500E-01	1.048E-01
3.000E-01	8.158E-02
3.500E-01	6.425E-02
4.000E-01	5.105E-02
4.500E-01	4.073E-02
5.000E-01	3.254E-02
5.500E-01	2.598E-02
6.000E-01	2.063E-02
6.500E-01	1.627E-02
7.000E-01	1.267E-02
7.500E-01	9.685E-03
8.000E-01	7.212E-03
8.500E-01	5.100E-03
9.000E-01	3.346E-03
9.500E-01	1.842E-03
9.900E-01	6.554E-04

Table C-16(c)
Peach Bottom: Refractories
Late Rupture 'FCONC' for Refractories

Cumulative Weight	Final Distribution
1.000E-02	2.562E-01
5.000E-02	1.182E-01
1.000E-01	7.232E-02
1.500E-01	5.071E-02
2.000E-01	3.782E-02
2.500E-01	2.934E-02
3.000E-01	2.325E-02
3.500E-01	1.873E-02
4.000E-01	1.525E-02
4.500E-01	1.248E-02
5.000E-01	1.025E-02
5.500E-01	8.422E-03
6.000E-01	6.895E-03
6.500E-01	5.612E-03
7.000E-01	4.528E-03
7.500E-01	3.594E-03
8.000E-01	2.793E-03
8.500E-01	2.099E-03
9.000E-01	1.477E-03
9.500E-01	8.996E-04
9.900E-01	3.927E-04

Table C-16(d)
Grand Gulf: Cesium, Iodine
Late Rupture 'FCONC' for Cesium, Iodine
late Rupture FCONV All Species

Cumulative Weight	Final Distribution
1.000E-02	2.763E-01
5.000E-02	1.205E-01
1.000E-01	7.020E-02
1.500E-01	4.730E-02
2.000E-01	3.420E-02
2.500E-01	2.564E-02
3.000E-01	1.977E-02
3.500E-01	1.549E-02
4.000E-01	1.225E-02
4.500E-01	9.753E-03
5.000E-01	7.784E-03
5.500E-01	6.209E-03
6.000E-01	4.963E-03
6.500E-01	3.893E-03
7.000E-01	3.034E-03
7.500E-01	2.320E-03
8.000E-01	1.725E-03
8.500E-01	1.225E-03
9.000E-01	8.046E-04
9.500E-01	4.363E-04
9.900E-01	1.519E-04

Table C-16(e)
Grand Gulf: Refractories
Late Rupture 'FCONC' for Refractories

Cumulative Weight	Final Distribution
1.000E-02	3.848E-01
5.000E-02	2.140E-01
1.000E-01	1.422E-01
1.500E-01	1.043E-01
2.000E-01	8.021E-02
2.500E-01	6.361E-02
3.000E-01	5.136E-02
3.500E-01	4.196E-02
4.000E-01	3.458E-02
4.500E-01	2.864E-02
5.000E-01	2.373E-02
5.500E-01	1.965E-02
6.000E-01	1.621E-02
6.500E-01	1.328E-02
7.000E-01	1.076E-02
7.500E-01	8.603E-03
8.000E-01	6.724E-03
8.500E-01	5.042E-03
9.000E-01	3.547E-03
9.500E-01	2.147E-03
9.900E-01	8.946E-04

Table C-16(f)
Grand Gulf: Tellurium, Ruthenium
Late Rupture 'FCONC' for Tellurium, Ruthenium

Cumulative Weight	Final Distribution
1.000E-02	7.925E-01
5.000E-02	5.782E-01
1.000E-01	4.302E-01
1.500E-01	3.318E-01
2.000E-01	2.615E-01
2.500E-01	2.084E-01
3.000E-01	1.679E-01
3.500E-01	1.359E-01
4.000E-01	1.103E-01
4.500E-01	8.996E-02
5.000E-01	7.274E-02
5.500E-01	5.881E-02
6.000E-01	4.726E-02
6.500E-01	3.761E-02
7.000E-01	2.953E-02
7.500E-01	2.272E-02
8.000E-01	1.699E-02
8.500E-01	1.212E-02
9.000E-01	7.988E-03
9.500E-01	4.346E-03
9.900E-01	1.517E-03

REFERENCES

C-1 J. A. Gieseke et al., "Radionuclide Release Under Specific LWR Accident Conditions," Vol. IV: PWR Ice Condenser Design, BMI-2104, Battelle Memorial Institute, 1984.

C-2 R. S. Denning et al., "Radionuclide Release Calculations for Selected Severe Accident Scenarios," Vols. I-V, NUREG/CR-4624, BMI-2139, Battelle Memorial Institute, 1986.

C-3 R. J. Lipinski, D. R. Bradley, J. E. Brockmann et al., Appendix N of "Uncertainty in Radionuclide Release Under Specific LWR Accident Conditions," Vol.II, SAND84-0410, Sandia National Laboratories, 1984.

Expert D's Elicitation

Release of Fission Products From Containment
for Surry, Zion, Sequoyah, Peach Bottom, and Grand Gulf
FCONV/FCONC

Description of Expert D's Rationale/Methodology

A. First, Expert D assessed the factors affecting FCONV AND FCONC:

1. Aerosol Characteristics

- Shape factors
- Distribution
- Density

2. Residence Time

- Size of breach
- Timing of breach

3. Multicompartmentation

4. Effective Height

5. Thermodynamic State of the Atmosphere

- Superheated
- Saturated (condensing)

6. Hygroscopicity

7. H_2 Burn (affects 2 and 5 above)

B. Expert D then assessed the location of release of the radionuclide:

1. FCONV - cesium, iodine, some tellurium;

2. FCONC - nonvolatiles, tellurium.

C. Expert D then examined each of the individual factors listed under A and evaluated their effect on FCONV and FCONC.

1. Shape Factors

- Evolutionary chain of particles: crystallites → agglomerates → flocks.[D-1] Sharp-edged aerosols are not produced.

- STEP experiment suggests spherical shapes.[D-2]

- Even traces of soluble fission products will absorb some moisture to create spherelike shapes.

- Stone & Webster parametric study with NAUA-MOD4.
- Conclusion: range of shape factors = 1.0 - 1.5.

2. Residence Time

- ANS source term parametric study[D-3] shows that for a 2-h delay in containment breach, the airborne aerosol decreases by a factor of 10.

3. Multicompartmentation

- Reference D-3 assigns to this effect a factor of 1.6. Analysis of DEMONA experiments[D-4] confirms the effect, qualitatively of the same order.
- Conclusion: factor of 1.5

4. Effective Height

- All STCP and Stone & Webster analysis underestimate settling areas by a factor of 2 to 5 for PWRs and BWRs, respectively. IDCOR analyses show the effect is significant.
- Conclusion: factor of 2.0 to 5.0

5. Hygroscopicity

- If the effect can be present, it will be dominant (see expert's detailed notes), as confirmed by LACE experiments LA2, LA4, and LA6 (unpublished results). Detailed discussion of the phenomena is in Reference D-5.
- Conclusion: FCONV affected by a factor of 10 for saturated, late cases and by 2 to 3 for superheated, early cases. FCONC affected by a factor of 1.1 to 1.2 in either case.

6. H_2 Burns

- Duration of burn: about 10 s. (100 ft/10 ft/s)
- Critical flow of steam at 100 psia (Moody): G_{crit} = 250 lb/ft^2-s

- e.g. V =2E + 6 ft^3, A = 7 ft^2, ρ = .03 lb/ft^3
- V_m/V = 7*250/(.03*2E + 6) = .03 s^{-1} → T_{res} = 30 s
- For ρ = .05 → T_{res} = 60 s
- For A = 1 ft^2 → T_{res} = 400 s.

- Conclusion: H_2 burn increases leakage by a factor of 2

D. The available calculations used by Expert D where

1. CREST Exercise (Reference D-5)

   - Surry, AB sequence, no condensation on particles
   - FCON = .5 - .6

2. Sandia Analysis[D-6]

   - Containment Releases for Peach Bottom (TB)

	CS	Te	Ba	La
MELCOR	.44	.63	.76	.77
STCP	.55	.83	.90	.43

3. ANS Report[D-3]

Surry individual factors affecting containment releases:

	AB	TMLB	Comment
DRY	.43	.75	No diffusiophoresis, no condensation on aerosol
DP_H	.69	.76	Diffusiophoresis
"Suspended Liquid"	.44	.65	Treated as combined effect of condensation on aerosol and hygroscopicity
Multicompart-mentation	.60	.60	

Propagating the uncertainties results in the following distribution (see expert's detailed notes).

AB: $P(FCON<.5) = .8$, $P(.5 < FCON < .7) = .2$

TMLB: $P(FCON<.5) = .6$, $P(.5 < FCON < .8) = .4$

Built-in conservatism: equal probability assigned to each bin.

Results of Expert D's Elicitation

All release classes have approximately the same FCONV or FCONC.

Case	.05	.50	.95	UB
1	.1	.2	.6	.8
2	.3	.5	.6	.8
3	.01	.05	.1	.2
4	.4	.5	.8	.9
5	.4	.6	.8	.9
6	.2	.25	.6	.8
7	.1	.25	.6	.7
8	.4	.6	.8	.9
9	.05	.1	.15	.2
10	.4	.6	.8	.9
11	.2	.3	.6	.9
12	.2	.35	.6	.9
13	.4	.6	.8	.9
14	.4	.7	.8	.9
15	.05	.1	.15	.2
16	.05	.15	.2	.25
17	.001	.01	.1	.2
18	.01	.05	.1	.2

Sources of Uncertainty

Expert D listed the factors contributing to the uncertainty in the result in his analysis of this issue presented above and assessed their effects.

Correlations with Other Variables

No correlations were specified with variables from other issues. Because only one distribution was given for all release classes in a particular case, no correlation need be specified for variables within the issue.

Suggested Methods for Reducing Uncertainty

No suggestions were made for reducing the uncertainty.

REFERENCES

D-1 C. E. Lapple, "Particle-Size Analysis and Analyzers," Chemical Engineering, May 20, 1968.

D-2 B. J. Schlenger et al., "Characteristics of Releases from TREAT Source Term Experiment STEP-1," ANS Winter Meeting, Washington DC., November 1986.

D-3 "Report of the Special Committee on Source Terms," American Nuclear Society, September 1984.

D-4 W. Schock, "General Valuation of the Results of the DEMONA Program," Laboratorium fur Aerosolphysik und Filtertechnik Kernforschungszentrum Karlsruhe, DEMONA Final Colloquium, Kernforschungszentrum Karlsruhe, June 1, 1987.

D-5 A. Drozd and J. Baron, "Hygroscopic Aerosol Growth at Near Saturation Conditions," Aerosol Codes Workshop, Brussels, September 9-11, 1987.

D-6 S. E. Dingman et al., "Analysis of Peach Bottom Station Blackout with MELCOR," SAND86-2129C, Sandia National Laboratories, Albuquerque, NM, 1986.

Expert E's Elicitation

Release of Fission Products from Containment
for Surry, Zion, Sequoyah, Peach Bottom and Grand Gulf
FCONV/FCONC

Description of Expert E's Rationale/Methodology

This elicitation outlines Expert E's "decomposition" procedure that he used to arrive at uncertainty distributions for FCONV and FCONC. A basic assumption in the decomposition was that FCONV and FCONC for fission products are the same as the respective fractions of total aerosols from those sources, and therefore, FCONV applies uniformly to all fission products from the RCS (except for noble gases) and FCONC applies uniformly to fission products released during MCCI.

To develop an uncertainty distribution, the Expert E believed it necessary either to use some existing sensitivity analysis based on a comprehensive aerosol code or some simplified aerosol algorithm and conduct an independent uncertainty analysis. He opted for the latter because the existing sensitivity analyses did not lend themselves to easy interpretation in terms of the sources of uncertainty that he believed to be controlling.

The simplified aerosol algorithm selected for this decomposition was that of the EPRI-modified FAI aerosol correlation. This selection was made because of the correlation's availability, simplicity, flexibility, and general applicability for describing containment aerosol behavior. The algorithm is very well outlined in EPRI NP-4974.[E-1] The algorithm was programmed for solution on a PC via a forward marching in time finite difference procedure.

Inspection of the FAI correlation reveals that the following parameters can be directly varied in an uncertainty analysis that uses the algorithm:

1. Containment leak rates (including condensation on walls);

2. Aerosol source rates;

3. Geometry (particularly effective containment height and containment volume);

4. Aerosol form factors (gamma and chi).

In the expert's opinion, the above parameters can be used to scope the uncertainties in FCONV and FCONC and are listed in their order of importance as major contributors to the uncertainties (timing of containment failure is the major source of uncertainty and is implicitly included under item 1 above). It is also believed that the level of turbulence in containment, as it affects agglomeration, is an important uncertainty. However, there did not seem to be a convenient means of incorporating that uncertainty into this analysis. Consequently, that contribution was not an explicit part of this decomposition.

SELECTION OF UNCERTAINTY VALUES FOR PARAMETERS

1. Containment Failure Time and Leak Rates

Expert E felt that, by far, the most significant contributors to the uncertainty in FCONV and FCONC are the timing and mode of containment failure. The containment failure time is loosely specified as part of the guidance on sequence definition, that is, early and late. He chose to define early as coincident with the time of reactor vessel (RV) failure. While this choice is expected to have a relatively large influence on FCONV, FCONC should prove to be relatively insensitive to it. The guidance on the meaning of late containment failure time was "after the bulk of MCCI release is over." He chose to quantify this specifically as meaning after 90% of MCCI release is over. This should be a good representation of the intent of the definition of a late containment failure.

The selection of the failure hole size (which translates into leak rate) was more difficult. Little data exist on the containment response to overpressure events (whether there is gross rupture or if cracks develop that are sufficient to relieve the pressure before gross rupture) and how the response might be related to containment type and rate of pressurization.

Two qualitatively different failure modes, "leak" and "rupture," were suggested in the guidance on sequence definition. The guidance defined rupture as "failures that would depressurize containment in 2 h or less. These failures are typically characterized by an equivalent area of 0.1 ft^2 to 7 ft^2. Leaks were defined as "failures so small that pressurization would be arrested but depressurization would not occur within 2 h. These failures are typically characterized by an equivalent area of less than 0.1 ft^2. A further qualification of the definition of leak included failures so small that containment would not be depressurized and that such leaks were "characterized by equivalent hole areas of a few square inches."

Based on this guidance, he chose the following uncertainty ranges for failure hole size:

Failure Mode	Minimum (ft^2)	Maximum (ft^2)	Best Guess (ft^2)
Rupture	.10	7.00	1.00
Leak	.01	.1	.05

To develop a distribution with his decomposition, a best guess value was needed as well as the extremes of the ranges. The distribution could then be developed as a simple smoothed curve through the points. Without additional criteria, he chose the simple average as the best guess leak size. However, Expert E's opinion is that gross ruptures are unlikely for containments that derive their strength from concrete lined with steel for leak tightness, and most of the containments considered in this study are of this type. Therefore, he chose a best guess rupture value of 1 ft^2 that is somewhat less than the simple average. There is little

basis for this particular selection other than opinion and the fact that it is near the log-mean of the range as well as being a size that is the lowest that can be chosen without significantly affecting the values for FCONC for early-rupture sequences. (That this is so was determined via a sensitivity analysis varying rupture size for the Surry plant.)

2. Leak Rates for Selected Hole Sizes

During most of the depressurization period, the flow out of the break is assumed to be choked. Therefore, an appropriate relation for the flow rate is given by the sonic velocity equation:

$$Q = A \sqrt{kgRT} .$$

The leak rate from containment following failure is an output of the STCP and was reported in the BMI-2104 (Reference 1) series of reports. Rather than directly using the above sonic velocity equation, it was decided to be consistent with the STCP and use the maximum value of 14.7 volume fraction reported for the Surry AB-gamma sequence for a 7 ft^2 opening (which converts to 2.083×10^8 cm^3/s). The values for all other hole sizes were scaled from this value (Q ~ A) to give:

Hole Size (ft^2)	Choked Flow Rate (cm^3/s)
.01	2.976×10^5
.05	1.488×10^6
.10	2.976×10^6
1.00	2.976×10^7
7.00	2.083×10^8

As a further simplification, the above values were assumed to apply for all sequences and all plants. That this is a reasonable simplification was confirmed by inspection of BMI-2104 [5-2] which did show remarkably similar values for the various plants in their calculated depressurization flows at containment failure time, despite expected differences in the assumed containment failure pressures.

3. Depressurization Times

In the absence of additional sources of heat and/or mass, the containment depressurization was assumed to be adiabatic-isentropic for which

$$P/\rho^k = \text{constant} = C = P_0 /(P_0/Rf_0)^k .$$

By definition,

$$\rho = M/V \text{ or } \frac{d\rho}{dt} = \frac{1}{V}\frac{dm}{dt} .$$

For sonic flow

$$\frac{dm}{dt} = -A \sqrt{kgC}\ \rho^{(k+1)/2} .$$

Therefore,

$$\frac{d\rho}{dt} = -(A/V)\sqrt{kgC}\ \rho^{(k+1)/2}$$

Integration and substitution gives for the time, T, for depressurization from some P_0 down to P_1:

$$T = \frac{\left[\frac{P_0}{RT_0(P_0/P_1)^{(1-k)/2}}\right]^{(1-k)/2} \cdot \left[\frac{P_0}{RT_0}\right]^{(1-k)/2}}{\left(\frac{k-2}{2}\right)\frac{A}{V}\sqrt{kg\frac{P_0}{(P_0/RT_0)^k}}} \quad (1)$$

Application of Eq. (1) for Surry with P_0 (failure pressure) of 85 psia, T_0 (saturated) of 710 R, and P_1 of 14.7 psia for a .1 ft^2 opening gave a depressurization time of 16629 s (using values of k and R for steam). To be consistent with the general guidance that a .1 ft^2 hole depressurizes in exactly 2 hours (7200 s), the above equation for the depressurization was modified for use as

$$T' = \left(\frac{7200}{16629}\right) T$$

With this modification, the following were developed for the "nominal" depressurization times in seconds for the various plants and hole sizes:

Hole Size (ft^2)	Surry	Zion	GG	PB	Seq
.01	72000	102240	53280	49619	38837
.05	14400	20448	10656	9924	7767
.1	7200	10224	5328	4962	3884
1	720	1022	533	496	388
7	103	146	76	71	55

The above values for depressurization times do not include any consideration of additional mass being added during depressurization that might, for example, come from the flashing of saturated water pools (such as the suppression pool for BWRs). For such sequences where flashing is considered to occur, the depressurization time can be greatly extended. An analysis assuming the pool flashes at a rate to maintain saturation shows that a good approximation to the depressurization time under these conditions can be obtained by simply adding to the original (no flashing) time, T_0, an additional time increment given by M_f/W_1 where M_f = the total mass of water flashed over the time period and W_1 = the containment choked flow mass leak rate.

Therefore, for saturated pool sequences only, the depressurization time was approximated simply as

$$T = T_0 + M_f/W_1,$$

and the leak rate was assumed constant at the "choked" value over the entire period.

The values for M_f were obtained as follows. The water pool is assumed to flash adiabatically (i.e., no external heat supply or losses). Therefore, the mass fraction of the water converted to steam, X, is calculated by

$$X = \frac{H_1 - H_2}{H_{fg}}.$$

For example, if the Grand Gulf containment is assumed to fail at 75 psia and depressurization occurs all the way down to atmospheric (14.7 psia), the quantity of steam produced is determined as follows:

From the steam tables

At 75 psia saturated	$H_1 = 277.43$ BTU/lb
At 14.7 psia	$H_1 = 180.07$ BTU/lb
	$H_g = 1150.4$ BTU/lb

Therefore,

$$X = \frac{277.43 - 180.07}{1150.4 - 180.07} \approx 0.1,$$

or 10% of the pool water will convert to vapor.

For a suppression pool inventory of 136,000 ft^3, this becomes

$$M_f = (136000)(62.4)(.1)(454) = 3.87 \times 10^8 \text{ grams}.$$

PROCEDURE FOR USING THE POOL FLASHING AND THE DEPRESSURIZATION TIME EXTENSION IN THE UNCERTAINTY ANALYSIS

The water that flashes from saturated pools as depressurization occurs can have at least three fates. It can blow out through the leak path, condense onto aerosols in the containment atmosphere, or condense onto containment surfaces.

An analysis shows that if the initial condition at the start of depressurization is uniform structure and gas temperature, then the atmosphere would be generally cooler than the structure during the depressurization. Therefore, it would be unlikely that condensation onto structures would occur. The most likely fate for the steam under these circumstances is for it to condense heterogeneously onto the aerosols as well as to leak out the failure hole. If condensation does occur, then the full extension to the depressurization time will not be manifested. Under conditions where

containment failure is assumed to occur following a hydrogen burn, the atmosphere will be superheated, which will tend to suppress all condensation.

In the absence of a detailed mechanistic methodology for addressing such thermal-hydraulic considerations, the following procedure was adopted.

The maximum calculated values for FCON for saturated pool sequences would be expected to result by using the full flashing time extension and by not permitting any steam condensation. The minimum FCON would be calculated by assuming all the steam condenses onto the aerosols and that there is no extension to the depressurization time because of flashing. The "best guess" value was arbitrarily chosen as the average of these two FCON extremes for the "best guess" hole size.

1. Leak Rates Before Containment Failure

The BMI-2104 series also reported leak rates from containment before failure. For consistency in this study, the BMI-2104 values were generally used with one modification. For late failure sequences, the influx of steam and MCCI gases could enhance the normal unfailed containment leak rates. Therefore, for cases intended to maximize the FCON values, the unfailed containment leak rate taken from BMI-1204 was arbitrarily increased by a factor of 10 after the time of reactor vessel failure.

2. Leak Rates after Depressurization

After depressurization and in the absence of hydrogen burns, the leak rate from a failed containment should be driven by the gases evolved from MCCI. For such periods, the MCCI-driven leak rates were taken directly from BMI-2104 and used as the containment leak rates unless these values exceeded the choked flow rate. For periods of hydrogen burns, the leak rate was assumed to be the choked flow values previously determined (although it is realized that this may be inconsistent with the actual temperature achieved during such burns). An average duration of 300 s for hydrogen burns was taken from the BMI-2104 results and used in this analysis. The number of hydrogen burns chosen depended on the containment type and whether FCON values were to be minimized or maximized. The maximum number of hydrogen burns was for Sequoyah, which had three hydrogen burns equally spaced at 2000 s apart.

3. Steam Condensation On Walls

In the present analysis, the effect (on removing aerosols) of steam condensation onto the containment structures was treated as if it were a leakage flow. The various sequence volumetric rates of steam condensation reported in BMI-2104 were averaged for each plant and used in this analysis. The values and timing were generally obtained for three different time periods: before reactor vessel failure during boiloff, during depressurization of the containment, and during boiloff of cavity water. For maximized cases, wall condensation was not included as an aerosol attenuation process, but it was included for both "best guess" and minimum cases.

AEROSOL SOURCES

Three types of sources of aerosols were considered in this decomposition:

- Direct from RCS (or after passing through a suppression pool in the cases for BWRs)
- MCCI releases
- Flashed saturated pool water.

1. RCS Aerosol Source Rates

For the aerosols coming directly from the RCS during the core heatup and meltdown processes, the values in BMI-2104 served as the basis for developing this source in this study. For a given plant, the reported RCS total release values for the different sequences were averaged. However, the CORSOR model on which these are based is known from recent ORNL data to generally overpredict the release by an average factor that is judged to be about 2. For the expert's best guess cases, then, he used the averaged BMI-2104 results divided by 2. For the maximized cases, he used the minimum value for any sequence for that plant, and for the minimized cases, he used the maximum value. The source times (to get a rate) were taken as the BMI-2104 times from start of core melt to the time of core collapse. For BWR cases, it was assumed that all RCS releases first passed through the suppression pool before entering containment. Therefore, the source rates into containment were markedly reduced for these cases through the use of two different suppression pool decontamination factors. The DF values for saturated and for subcooled pools were estimated from the BMI-2104 sequence results to be respectively: ~1000 and ~3000 for Grand Gulf; ~430 and ~1300 for Peach Bottom.

2. MCCI Aerosol Source Rates

Once again, BMI-2104 was relied on for guidance and for quantification of the magnitude and timing of aerosol sources generated by MCCI. For the "generalized" sequences used in this uncertainty analysis, the following adaptations were made of the BMI-2104 results.

For each plant, a "representative" sequence was selected to serve as a surrogate for all MCCI sources for that plant. The selected "representative" sequence was TMLB' for PWRs and TC for BWRs. The BMI-2104 calculated aerosol sources for these sequences were plotted and represented for input into the present PC algorithm as a series of straight line segments. These were used as the best guess values. For the uncertainty variations in the MCCI aerosol source rates, the VANESA sensitivity study reported in QUEST[E-3] indicated that for Surry TMLB' the upper bound case was generally less than three times the base case and that the lower bound case was generally greater than a factor of ~7 below the base case.

Therefore, in the algorithm, all minimum FCONC cases used the best guess MCCI source multiplied by 3 (a higher source rate gives a smaller FCONC). For the "maximized" cases, the best guess values were reduced by a factor of 7.

3. Water Aerosol Source Rates

Under the section on depressurization time, it was noted that water evaporated from flashing pools would be expected to condense onto aerosols. This phenomenon could not be readily included in the FAI aerosol correlation. Consequently, condensation onto aerosols was simulated in minimization cases by treating the steam as a separate source of aerosols that were permitted to co-agglomerate with the RCS and the MCCI aerosols. The total source of water that was input as a pseudo-aerosol source included the amount that was expected to condense out of the saturated environment on depressurization as well as the amount flashed.

Best guess and minimum cases used identical water aerosol sources, whereas no water source was input for maximum cases.

GEOMETRY UNCERTAINTIES

The FAI algorithm permits the variation of the containment volume and the effective containment height for aerosol settling. The compartment volumes, as taken from BMI-2104, were considered to be subject to very little uncertainty. However, it was the expert's opinion that there is significant uncertainty associated with the effective height because of the lack of accurate knowledge of the horizontal surface area available for gravitational fallout.

Based on a study of the containment equipment drawings, some previous walkthroughs of actual containments, and personal communication with other experts, Expert E felt that an appropriate "best guess" for the horizontal area could be represented by the mean cross-sectional area multiplied by 2. For the uncertainty variation, it was judged that this factor could be as high as 3 and that it could be no lower than 1.0. The factor of 3 is expert opinion only and cannot be further justified at this time.

AEROSOL FORM FACTORS

The FAI aerosol correlation also conveniently allows for variation in the aerosol form factors, gamma and chi. The values used in this analysis were taken from the QUEST reports.

In this analysis, it was assumed that gamma = chi = 1.0 for the "best guess" cases and the maximized cases (smaller values for gamma and chi result in larger FCON values). The minimized cases used gamma = chi = 4.0.

SPECIAL CONSIDERATIONS FOR SEQUOYAH

The case guidance for Sequoyah specified that differentiation be made between failures in the lower compartment and failures in the upper compartment for early rupture cases. To accommodate this differentiation, the following strategy was adopted.

1. Upper Compartment Failures

The aerosol source rates were reduced by a DF equal to 3 or 1 depending on whether ice is present or absent (these values were estimated from the BMI-2104 results). The full volume of both compartments and the associated overall effective height were used.

2. Lower Compartment Failures

The RCS release before containment failure was treated exactly like the above upper-compartment cases.

3. After Containment Failure

After containment failure, the aerosol sources were no longer reduced by the ice-condenser DF. Only the effective height of the lower compartment was used although the full volume of both compartments was allowed to influence the depressurization time. Melted ice was assumed available to flash. The best guess cases for Sequoyah were assumed to include three hydrogen burns.

Results of Expert E's Elicitation

The results of the elicitation are summarized in Table E-1. The expert gave the .01, .25, .50, .75, and .99 probability values, which were linearly interpolated to get the .05 and .95 values.

Sources of Uncertainty

The expert listed the factors contributing to the uncertainty in the result in his analysis of this issue presented above and assessed their effects.

Correlation with Other Variables

Within each of the 16 cases, all variables are assumed to have a rank correlation of 1. No other correlations were indicated.

Suggested Methods for Reducing Uncertainty

No specific suggestions were made for reducing the uncertainties in the elicited variables.

Results of Expert E's Elicitation

Table E-1
Elicitation results for Expert E
(All release classes have approximately the same FCONV or FCONC)

	Fractile									Plant
	.001	.01	.05	.25	.50	.75	.95	.99	.999	
Case 1		.06	.11	.21	.33	.42	.62	.90		Surry
		.031	.08	.16	.24	.35	.48	.66		Zion
		.03	.07	.19	.31	.44	.63	.88		Sequoyah
Case 2		.12	.18	.27	.35	.47	.67	.90		Surry
		.17	.22	.34	.44	.55	.75	.97		Zion
Case 3		.01	.015	.05	.10	.15	.29	.43		Surry
		.002	.01	.02	.05	.08	.19	.39		Zion
		.03	.10	.28	.44	.56	.67	.73		Sequoyah
Case 4		.27	.68	.91	.96	.98	.995	.999		Sequoyah Lower
		.14	.58	.72	.80	.85	.92	.94		Sequoyah Upper
Case 5		.04	.19	.41	.60	.75	.90	.99		Grand Gulf
		.28	.56	.84	.94	.98	.99	.999		Peach Bottom
Case 6		.12	.15	.20	.25	.32	.51	.90		Grand Gulf
		.07	.18	.32	.45	.57	.75	.998		Peach Bottom
Case 7:		.07	.13	.27	.41	.55	.69	.80		Surry
		.03	.06	.16	.25	.3	.45	.56		Zion
		.03	.05	.16	.28	.39	.58	.84		Sequoyah
Case 8:		.28	.30	.33	.37	.45	.57	.80		Surry
		.23	.29	.38	.48	.60	.72	.85		Zion
Case 9:		.15	.20	.28	.36	.42	.51	.60		Surry
		.10	.25	.35	.40	.44	.49	.59		Zion
		.06	.18	.38	.52	.62	.72	.75		Sequoyah
Case 10:		.18	.54	.79	.87	.92	.95	.96		Sequoyah Lower
		.11	.30	.50	.60	.68	.74	.79		Sequoyah Upper
Case 11:		.07	.12	.17	.22	.28	.48	.70		Grand Gulf
		.05	.10	.17	.25	35	.51	.993		Peach Bottom
Case 12:		.06	.13	.25	.34	.44	.57	.70		Grand Gulf
		.06	.20	.44	.60	.75	.89	.99		Peach Bottom
Case 13:		.36	.65	.85	.90	.92	.96	.99		Grand Gulf
		.22	.50	.80	.91	.96	.98	.995		Peach Bottom

Table E-1 (Continued)

	Fractile									Plant
	.001	.01	.05	.25	.50	.75	.95	.99	.999	
Case 14:		.50	.78	.94	.98	.985	.99	.999		Grand Gulf
		.56	.81	.95	.98	.99	.998	.999		Peach Bottom
Case 15:		.04	.10	.18	.25	.33	.51	.78		Grand Gulf
		.01	.025	.06	.10	.16	.25	.32		Peach Bottom
Case 16:		.03	.06	.13	.21	.33	.54	.93		Grand Gulf
		.01	.02	.08	.15	.22	.28	.33		Peach Bottom

REFERENCES

E-1 "Evaluation of Empirical Aerosol Correlations," EPRI NP-4974, Electric Power Research Institute, December 1986.

E-2 J. A. Gieseke et al., "Radionuclide Release Under Specific LWR Accident Conditions." Vol IV: PWR Ice Condenser Design, BMI-2104, Battelle Memorial Institute, Columbus, OH, 1984.

E-3 R. J. Lipinski et al., Appendix N of "Uncertainty in Radionuclide Release Under Specific LWR Accident Conditions," Vol. II, SAND84-0410, Sandia National Laboratories, 1985.

5.6 Issue 6. BWR Late Iodine Release from the Suppression Pool and Reactor Cavity Water

Summary and Aggregation of Source Term Issue 6--Late Iodine

Experts Consulted: Thomas Kress, Oak Ridge National Laboratory; Dana Powers Sandia National Laboratories, Richard Vogel, Electric Power Research Institute.

Issue Description

This issue has two parts. Part 1 considers the release of iodine from a BWR suppression pool following containment failure. Part 2 considers the release of iodine from water in the RPV pedestal during CCI. Iodine that is released is assumed to be in a volatile form and not subject to subsequent retention (because of pool scrubbing, spray operation, or aerosol deposition) in the containment.

Part 1

What distributions characterize the uncertainty in the release of volatile iodine from the suppression pool after the containment has failed? Two cases were considered:

1. A subcooled suppression pool is maintained throughout the sequence (as would occur in a short-term station blackout). The pool temperature at vessel breach is 350 K. The maximum temperature attained during the period of interest is approximately 370 K. Substantial surface evaporation is expected but no bulk boiling.

2. A saturated suppression pool is maintained throughout the sequence (as would result from a long-term station blackout). The maximum pool temperature attained is approximately 415 K. Substantial flashing of the pool would accompany containment failure.

Part 2

What distributions characterize the uncertainty in the release of volatile iodine from water that overlies the core debris in the RPV pedestal? Two cases were to be considered:

1. The drywell is flooded at vessel breach and CCI proceeds underwater.

2. The RPV pedestal contains water at the time of vessel breach but most of this water (about 290,000 kg) boils away during CCI.

Summary of Rationale

Expert A formulated a model of the physical and chemical processes that lead to rerelease of iodine from water pools. Uncertain parameters in the model are identified and uncertainty ranges for these parameters are defined. The model is then repetitively exercised by randomly varying the values of uncertain parameters within their uncertainty ranges. Predictions of the model obtained in these multiple runs are used to formulate a probability density function for the fraction of iodine entrapped by the water that is subsequently released.

Two iodine release mechanisms were considered by the Expert A: mechanical release and release as a result of iodine chemistry.

The mechanical release is due to entrainment when gases sparge through the water pool. Correlations of entrainment for the churn-turbulent flow regime were used by this expert.

Uncertain mechanical release parameters considered by the expert were:

1. Pool parameters (decontamination factors, pressure over, temperature, surface tension);
2. Aerosol generation (from core concrete generation and during core degradation);
3. Gas generation (during CCI);
4. Moles of steam and hydrogen discharge to pool;
5. Viscosity of gases sparging the pool;
6. Area for superficial gas velocity.

The revaporization release of iodine as a result of chemical processes is conventionally described in terms of a partition coefficient defined as

$$PC = \frac{\text{concentration of iodine in the aqueous phase}}{\text{concentration of iodine in the gaseous phase}}$$

Uncertain revaporization release parameters considered by the expert were:

1. Equilibrium constants (tri-iodide, I_2 hydrolysis, hypoiodous acid);
2. Moles CH_4 generated;
3. HOI partition coefficient;
4. Radiation dose rate;

5. Factors affecting pH;

6. Iodine parameters (fraction cesium iodide in pool, iodine discharge to pool, iodine available for ex-vessel release, in-vessel release rate);

7. Cesium parameters (Cesium discharge to pool);

8. Boric acid discharge to pool.

Expert B assumed that the release of iodine from the pools could be calculated from the following equation:

Release Rate = (Gas Flux from Water) x (Concentration Iodine in Water) x (Iodine Partition Coefficient).

Expert B considered a pool of water with a gas flux off (or near) the surface. Based on the definition of the iodine partition coefficient (IPC) and assuming equilibrium is established, the expert obtained the following equation for release fraction (RF):

$$RF = 1 - \exp(-V_g/(V_w IPC)) \qquad (1)$$

where V_g is the volume of gas evolved, V_w is the volume of water, and IPC is the iodine partition coefficient. Expert A felt that the IPC depended primarily on the concentration of iodine in the water, the pool pH, and the irradiation. However, he assumed that enough fission products had been released to drive the IPC essentially to its lowest value for a given pH.

In general, the maximum release fraction in Expert B's distribution corresponded to the minimum pH value and was also based on the assumption that all of the water and gas were effective in the removal process. The median value corresponded to the expert's best guess value for the pH and was based on the assumption that only 50% of the water was effective in the removal process. The minimum RF in the distribution was based mostly on the expert's judgment.

Expert C estimated the pH of the suppression pool for Part 1 at about 9.5. He referenced Beahm and showed that at high pH, I_2 could be converted into nonvolatile forms by radiation. Beahm indicated to the expert that at pHs in the neighborhood of 10, the formation of I_2 by radiation would be extremely slow, if at all. Expert C concluded that very little of the iodide would be converted to I_2 in the suppression pool for the particular cases presented to the expert review group. The expert also indicated that the formation of organic iodides was not of serious concern because of the low conversion of I- to CH_3I at high pH.

Expert C used data developed by Beahm at a pH = 9 to get a log partition coefficient of 3.5 to calculate the fraction of iodine released. Expert C used the same definition for partition coefficients as Expert A.

The concentration of iodine in the aqueous phase was assumed to be 2.9 x 10^{-5} moles/L. Therefore, the concentration in the gas phase will be 9.2 x 10^{-9} g-atoms/L. Assuming that 1.28 x 10^{7} L (100°C, 1 atm) of H_2 goes through the suppression pool, then the total gram atoms of iodine removed would be 0.11. The total gram atoms of iodine in the pool is 111.6. This fraction of iodine lost from the suppression pool would be 1.1 x 10^{-3}. Expert C stated that this was a conservative calculation that assumed equilibrium.

For Part 2, Expert C concluded that the pH of the overlying solution will be roughly 8.3. For a pH of 8.3, the log partition coefficient from Beahm's data can be estimated to be 3.

To convert the partition coefficient in an amount of iodine released, Expert C had to estimate the amount of gas that will sparge through the water. H_2 will be released for about 2 h because of the zirconium-water reaction. Expert C stated that under such reducing conditions, no I_2 will be released. Sparging by steam, which might be effective in removing I_2, will occur from the boiling of the water. Expert C assumed that the boildown of 2.4 x 10^{8} lb of water to 1.7 x 10^{8} lb of water results in all the steam going through the water. The volume of steam resulting was estimated to be 5.4 x 10^{8} L (assuming 1 atm and 373 K). This results in an iodine concentration in the steam of 1.31 x 10^{-9} moles/L. Assuming a sparging flow of 5.4 x 10^{8} L through the solution, the amount of iodine released would be 0.71 moles of I_2, or 179 grams of iodine that could be released. The fraction of iodine released would then be 0.62.

Expert C developed his distributions around the above estimates.

Method of Aggregation

Assumptions Used to Average Distributions

Three experts were elicited on this issue. Each provided a cumulative distribution function for the four cases for this issue:

Case 1. A subcooled suppression pool is maintained throughout the sequence (as would occur in a short-term station blackout). The pool temperature at vessel breach is 350 K. The maximum temperature attained during the period of interest is approximately 370 K. Substantial surface evaporation is expected but no bulk boiling.

Case 2. A saturated suppression pool is maintained throughout the sequence (as would result from a long-term station blackout). The maximum pool temperature attained is approximately 415 K. Substantial flashing of the pool would accompany containment failure.

Case 3. The drywell is flooded at the time of vessel breach and CCI proceeds underwater over the period of interest.

Case 4. The RPV pedestal contains water at the time of vessel breach but most of this water (about 290,000 kg) is boiled away during CCI.

Aggregated Results

Table 6-1
Case 1. Subcooled Suppression Pool

	Cumulative Probability			
Release Fraction	Average	Expert A	Expert B	Expert C
0.000	0.073	0.000	0.000	0.220
1.0E-06	0.127	1.0E-05	0.000	0.380
1.0E-05	0.183	1.0E-04	0.000	0.550
1.0E-04	0.224	0.001	0.000	0.670
5.0E-04	0.254	0.005	0.050	0.706
1.0E-03	0.337	0.010	0.250	0.750
1.1E-03	0.421	0.011	0.500	0.751
2.0E-03	0.578	0.020	0.950	0.763
5.0E-03	0.618	0.050	1.000	0.803
0.010	0.657	0.100	1.000	0.870
0.020	0.713	0.200	1.000	0.940
0.025	0.737	0.250	1.000	0.960
0.030	0.760	0.300	1.000	0.980
0.050	0.831	0.500	1.000	0.993
0.060	0.867	0.600	1.000	1.000
0.075	0.917	0.750	1.000	1.000
0.100	1.000	1.000	1.000	1.000

If an expert did not provide a parameter value at the 0 or the 1 fractile, parameters at these two levels were obtained by linear extrapolation from the two closest points. Linear interpolation was used to obtain values between assessed points. The three distributions for each case were averaged arithmetically to obtain the average distribution.

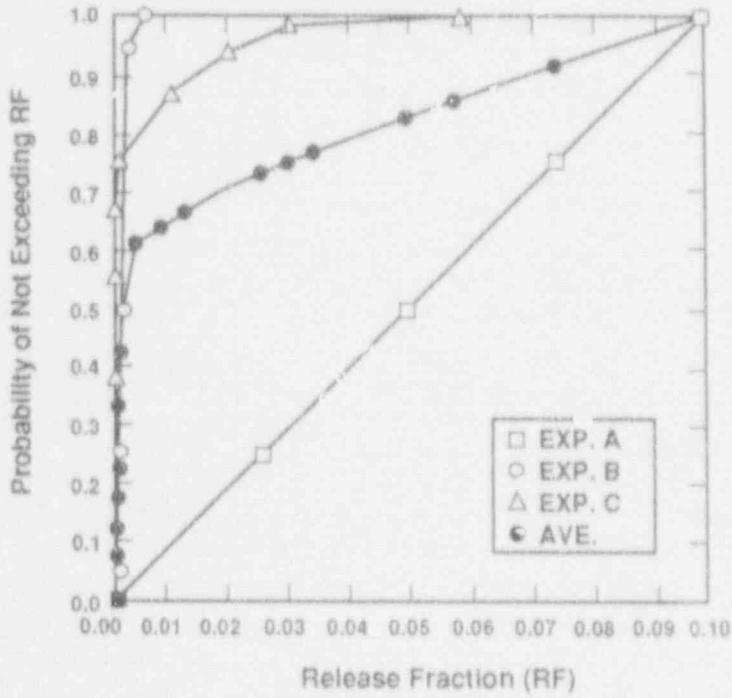

Figure 6-1. Subcooled Suppression Pool.

Table 6-2
Case 2. Saturated Suppression Pool

	Cumulative Probability			
Release Fraction	Average	Expert A	Expert B	Expert C
0.000	0.000	0.000	0.000	0.000
1.0E-06	0.010	0.000	0.000	0.029
1.0E-05	0.033	0.000	0.000	0.098
1.0E-04	0.083	0.000	0.000	0.249
5.0E-04	0.125	0.000	0.050	0.326
9.0E-04	0.218	0.000	0.250	0.403
1.0E-03	0.307	0.000	0.500	0.422
2.0E-03	0.465	0.003	0.950	0.442
5.0E-03	0.505	0.013	1.000	0.501
0.010	0.543	0.030	1.000	0.600
0.050	0.604	0.163	1.000	0.650
0.100	0.663	0.330	1.000	0.660

Table 6-2 (Continued)

	Cumulative Probability			
Release Fraction	Average	Expert A	Expert B	Expert C
0.150	0.723	0.500	1.000	0.670
0.200	0.783	0.670	1.000	0.680
0.400	0.870	0.900	1.000	0.710
0.600	0.912	0.967	1.000	0.770
0.700	0.940	1.000	1.000	0.820
0.800	0.957	1.000	1.000	0.870
0.900	0.973	1.000	1.000	0.920
0.950	0.990	1.000	1.000	0.970
1.000	1.000	1.000	1.000	1.000

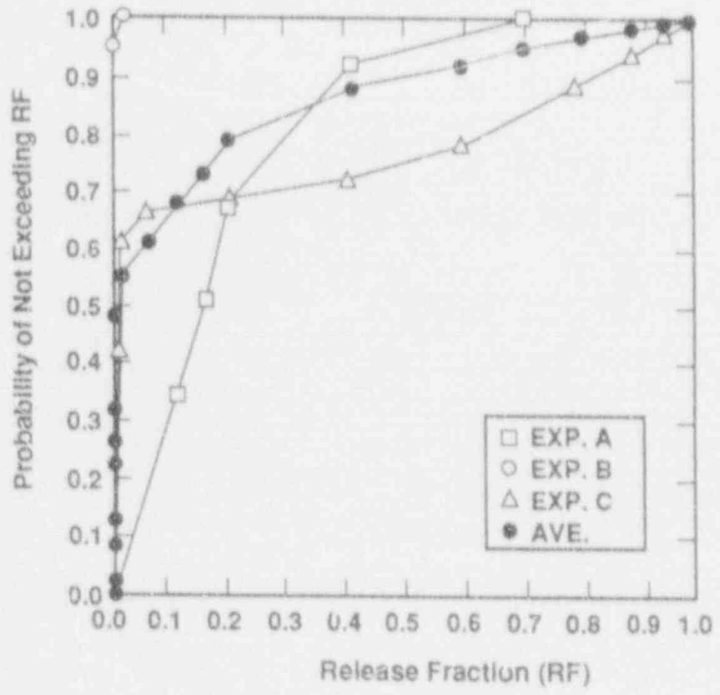

Figure 6-2. Saturated Suppression Pool.

Table 6-3
Case 3. Flooded Pedestal Cavity

	Cumulative Probability			
Release Fraction	Average	Expert A	Expert B	Expert C
0.004	0.000	0.000	0.000	0.000
0.010	0.002	0.000	0.000	0.006
0.020	0.005	0.000	0.000	0.016
0.040	0.010	0.000	0.000	0.029
0.050	0.012	0.000	0.000	0.035
0.063	0.019	0.013	0.000	0.043
0.080	0.026	0.030	0.000	0.049
0.100	0.039	0.050	0.000	0.066
0.125	0.070	0.125	0.000	0.085
0.200	0.180	0.350	0.050	0.140
0.250	0.255	0.500	0.083	0.183
0.400	0.481	0.950	0.183	0.310
0.500	0.535	0.975	0.250	0.380
0.600	0.645	1.000	0.500	0.434
0.630	0.700	1.000	0.650	0.450
0.650	0.739	1.000	0.750	0.468
0.800	0.823	1.000	0.870	0.600
0.900	0.917	1.000	0.950	0.800
0.963	0.975	1.000	1.000	0.925
1.000	1.000	1.000	1.000	1.000

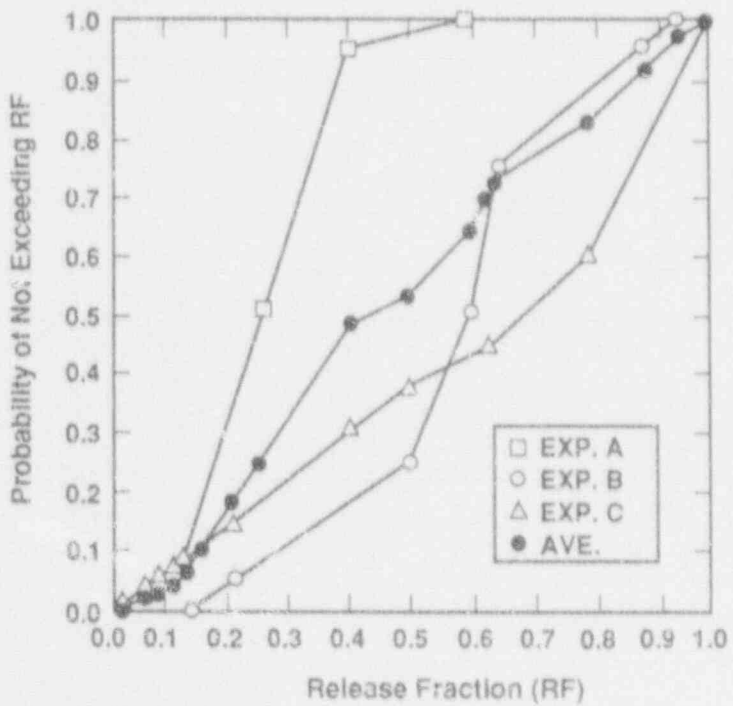

Figure 6-3. Flooded Pedestal Cavity.

Table 6-4
Case 4. Wet Pedestal Cavity

	Cumulative Probability			
Release Fraction	Average	Expert A	Expert B	Expert C
0.080	0.000	0.000	0.000	0.000
0.100	0.002	0.000	0.000	0.005
0.140	0.038	0.000	0.100	0.015
0.160	0.057	0.000	0.150	0.020
0.200	0.094	0.000	0.250	0.033
0.250	0.180	0.000	0.500	0.040
0.300	0.210	0.000	0.583	0.047
0.400	0.272	0.000	0.750	0.067
0.500	0.301	0.000	0.813	0.090
0.600	0.333	0.000	0.875	0.125
0.700	0.366	0.000	0.938	0.160
0.800	0.400	0.000	1.000	0.200
0.850	0.507	0.250	1.000	0.270
0.900	0.613	0.500	1.000	0.340
0.950	0.710	0.750	1.000	0.380
1.000	1.000	1.000	1.000	1.000

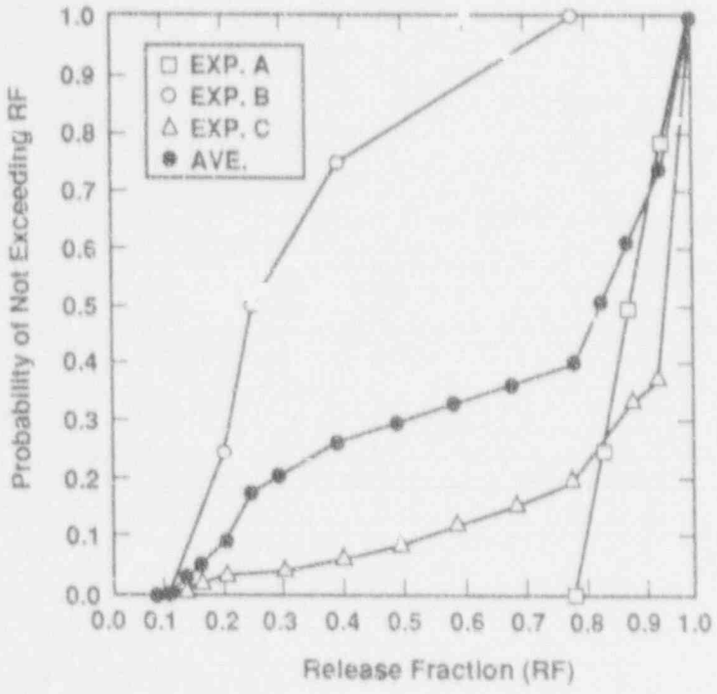

Figure 6-4. Wet Pedestal Cavity.

Individual Elicitations for Issue 6

Expert A's Elicitation

BWR Late Iodine Release from the Suppression Pool and Reactor Cavity Water

Description of Expert A's Rationale/Methodology

Expert A has documented his approach in a written report.* A brief overview of his rationale and methodology is provided here.

The approach used by the expert was to first formulate a model of the physical and chemical processes that lead to rerelease of iodine from water pools. Uncertain parameters in the model are identified and uncertainty ranges for these parameters are defined. These parameters and their ranges used in the calculations are listed in the document footnoted below. The model is then repetitively exercised by randomly varying the values of uncertain parameters within their uncertainty ranges. Predictions of the model in these multiple runs are used to formulate a probability density function for the fraction of iodine entrapped by the water that is subsequently released.

This approach was chosen by the expert because it focuses attention on microscopic parameters that could and often have been studied in a variety of contexts. Because research has been done, or at least could be done, on the parametric quantities, there is some transparent and defendable basis for defining the uncertainty ranges. This contrasts with the situation created when uncertainty ranges, based on judgments, are sought for the release process, which has not been investigated experimentally. The approach does, however, depend on a quantitatively articulated model. Uncertainty in the revaporization process based on a qualitative intuition concerning the current state of understanding or research is not admitted in this approach.

Two iodine release mechanisms were considered by Expert A: (1) mechanical release and (2) release as a result of iodine chemistry.

The mechanical release is because of entrainment when gases sparge through the water pool. Correlations of entrainment for the churn-turbulent flow regime were used by the expert.

The revaporization release of iodine as a result of chemical processes is conventionally described in terms of a partition coefficient defined as

$$PC = \frac{\text{concentration of iodine in the aqueous phase}}{\text{concentration of iodine in the gaseous phase}}$$

---

*D. A. Powers, "Uncertainty in Revolatilization of Iodine from Water Pools," in NUREG/CR-4551, Rev. 1, "Evaluation of Severe Accident Risks," Vol. 2, Pt. 5, Sandia National Laboratories, Albuquerque, New Mexico, (unpublished).

Here the partition coefficient is defined as:

$$PC = \frac{3[I_3^-] + 2[I_2] + [HOI] + [I^-] + [IO_3^-]}{(I_2 : g) + (HOI : g)},$$

where brackets indicate aqueous species and parentheses indicate gaseous species. In addition, a release from the formation of organic iodides is considered.

Results of Expert A's Elicitation

Case 2: Iodine Revolatilization from a Saturated Suppression Pool

Table A-1 and Figure A-1 show the cumulative probability distribution of iodine revolatilization release for this case. It appears that the distribution skews to the lower release fraction. The median of the distribution is about 5*10^{-}, which is much less than the arithmetic mean of 0.232. The number of model calculations in this case is 562.

Table A-1
Cumulative Probability Distribution of
Late Iodine Release Fraction from Water Pool
Case 2. Saturated Suppression Pool

Cumulative Probability (*)	Iodine Release Fraction
3	1.0E-06
10	1.0E-05
25	1.0E-04
42	1.0E-03
60	0.01
65	0.05
68	0.2
71	0.4
77	0.6
87	0.8
92	0.9
97	0.95
100	1.0

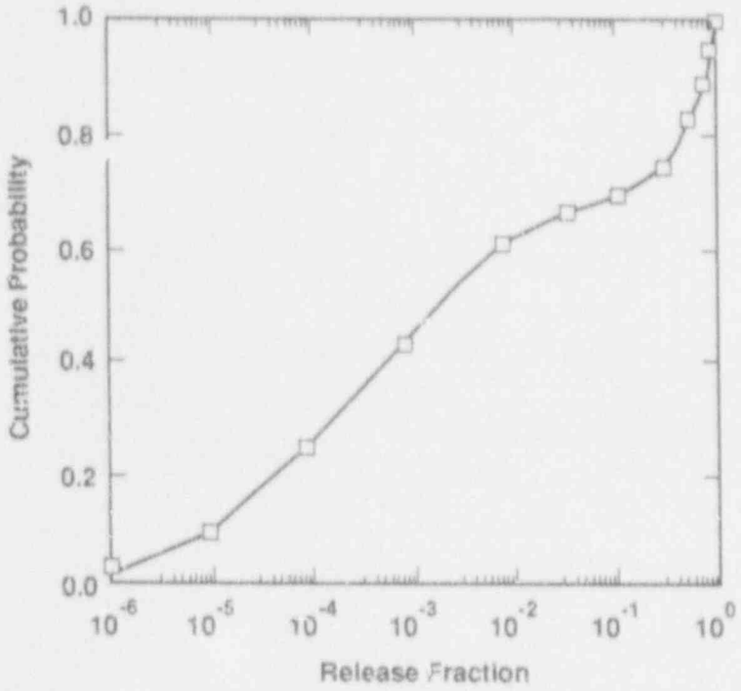

Figure A-1. Case 2: Saturated Suppression Pool.

Case 1: Iodine Revolatilization from a Subcooled Suppression Pool

Case 1 is similar to Case 2 except that the mass flow through the subcooled water pool is only that caused by hydrogen. Any steam in the gas discharged to the suppression pool is condensed. Because Case 1 has much less sparging gas through the suppression pool, the iodine revolatilization release for this case is much less than that of Case 2. The cumulative probability distribution of iodine release for Case 1 is shown in Table A-2 and Figure A-2. The iodine release for this case is much lower than that for Case 2. The median of the distribution is estimated to be about $8*10^{-6}$. These results were obtained from 750 iterations of the model.

The hydrogen ion concentrations in the steam suppression pool are, according this model, quite variable. A probability density function for the pH (negative of the base 10 logarithm of the hydrogen ion concentration) is shown in Figure A-2b. The density function of pH is distinctly bimodal with modes at somewhat more than 8 and somewhat more than 4. Despite the high hydrogen ion concentrations (i.e., low pH values) that develop in the suppression pool, iodine releases remain low. It is inferred from this that iodine release is determined to a significant extent by the sparging rate of hydrogen through the pool. Entrainment by the hydrogen gas is essentially negligible. Chemistry in the pool determines how much iodine partitions into the sparging gas.

Table A-2
Cumulative Probability Distribution of
Late Iodine Release Fraction from Water Pool
Case 1. Subcooled Suppression Pool

Cumulative Probability (%)	Iodine Release Fraction
22	1.0E-07
38	1.0E-06
55	1.0E-05
67	1.0E-04
75	1.0E-03
87	0.01
94	0.02
98	0.03
100	0.06

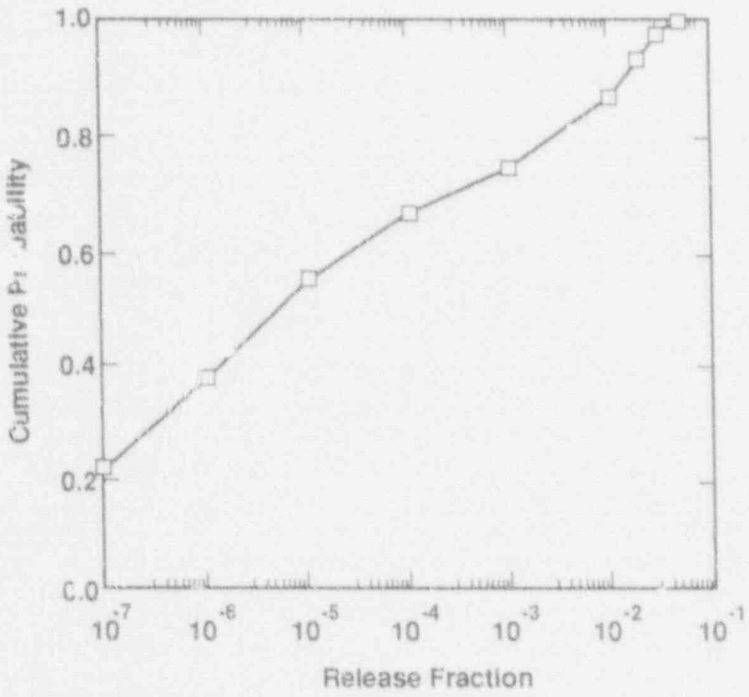

Figure A-2a. Case 1: Iodine Revolatilization.

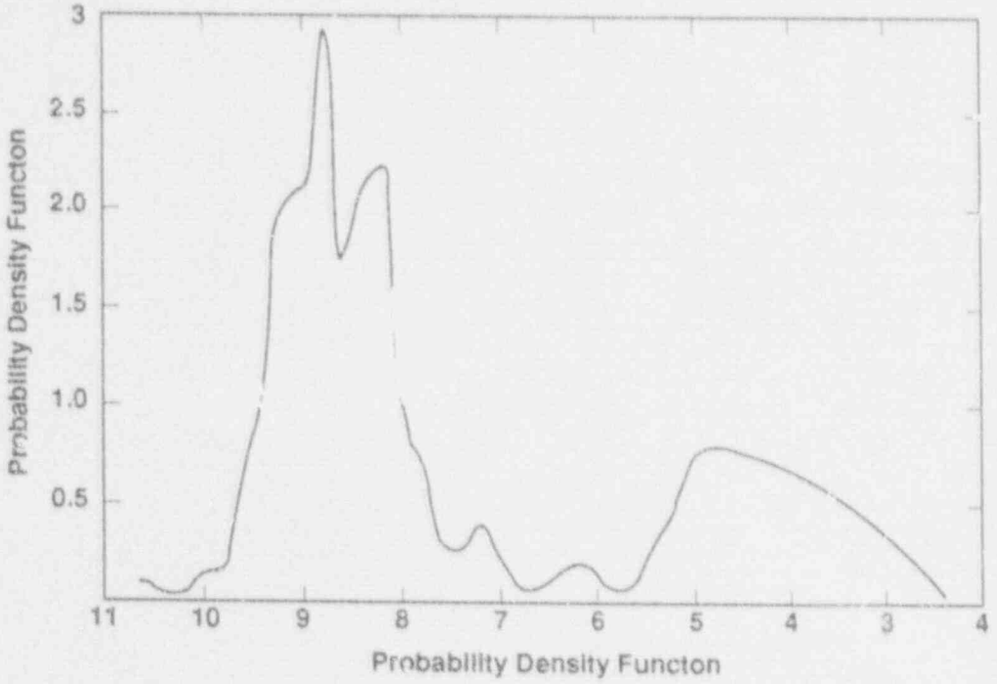

Figure A-2b. Probability Density Function for Water (pH).

Case 3. Iodine Revolatilization from a Flooded Reactor Cavity Pedestal

Both Cases 3 and 4 are dominated by the tremendous rate of gas sparging. Gas sparging brought on by the attack of melt on concrete is actually a small part of the sparging. Most of the gas flow through the water pool (in these two cases, water overlying the debris) is caused by the boiling of water. Because the large sparging rates, the results for Cases 3 and 4 are relatively insensitive to the details of aerosus iodine chemistry or the nature of water entrainment in the gas flow. The results will be sensitive to the boiloff rate specified in the problem.

The cumulative probability distributions of iodine release in Case 3 are shown in Table A-3 and Figure A-3 based on the results of 486 iterations of the model. The first column shows the calculation time of 36,000 s specified by the problem. Because the release fractions after 36,000 s are so high, it was thought useful to also show the probability distributions for 18,000 s of core debris interaction with concrete.

The mean release fractions after 36,000 and 18,000 s are 0.581 and 0.484, respectively. The median release fractions for these two calculation times are about 0.7 and 0.4. This indicates that much of the iodine release occurs in the early stages of the core debris interaction with concrete.

Table A-3
Cumulative Probability Distribution of
Late Iodine Release Fraction from Water Pool
Case 3. Flooded Reactor Cavity Pedestal

Cumulative Probability (%)		Iodine Release Fraction
36,000 s	18,000 s	
0.6	0.8	0.01
1.6	2.5	0.02
2.9	4.3	0.04
4.3	6.0	0.063
4.9	7.6	0.08
6.6	11	0.10
14	23	0.20
31	42	0.40
38	52	0.50
45	65	0.63
60	75	0.80

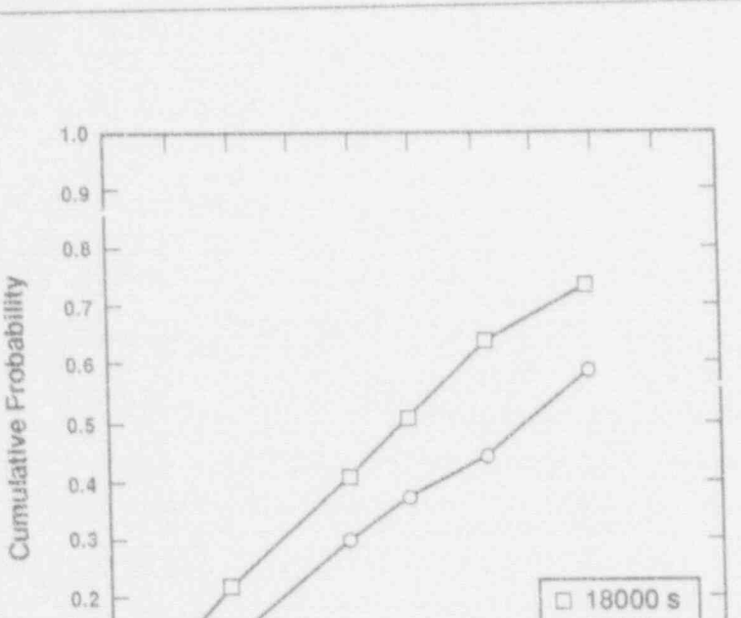

Figure A-3. Case 3: Flooded Reactor Cavity.

Case 4. Iodine Revolatilization from a Wet Reactor Cavity Pedestal

Case 4 is the most unusual because the water pool has evaporated nearly to dryness, as specified by the problem. In fact, were the calculation extended slightly beyond the prescribed time, the water pool would be completely evaporated. Consequently, Expert A concluded that the iodine release fraction in Case 4 is 1.0 (i.e., complete release) if the calculation time were slightly extended beyond 36,000 s. Again two calculation times (36,000 s and 18,000 s) were used in Case 4 to derive the probability distributions.

Table A-4 and Figure A-4 show the cumulative probability distribution for Case 4. The mean value of iodine release fraction for 36,000-s running time is 0.86 and the median release fraction is almost 1.0. Reducing the time period to 18,000 s leads to a mean release fraction of 0.71 and a median release fraction of 0.87.

Sources of Uncertainty

Since Expert A used a model to derive his uncertainty distribution of iodine release fraction, the sources of uncertainty in his model are explicitly identified and the ranges of uncertainty parameters were used in his iteration calculations of the model.

Table A-4
Cumulative Probability Distribution of
Late Iodine Release Fraction from Water Pool
Case 4. Wet Reactor Cavity Pedestal

Cumulative Probability (%)		Iodine Release Fraction
36,000 s	18,000 s	
0.5	5.5	0.10
1.5	8.5	0.14
2.0	9.3	0.16
3.3	11	0.20
4.7	17	0.30
6.7	21	0.40
9.0	27	0.50
12.5	32	0.60
16	38	0.70
20	44	0.80
34	53	0.90
38	57	0.95

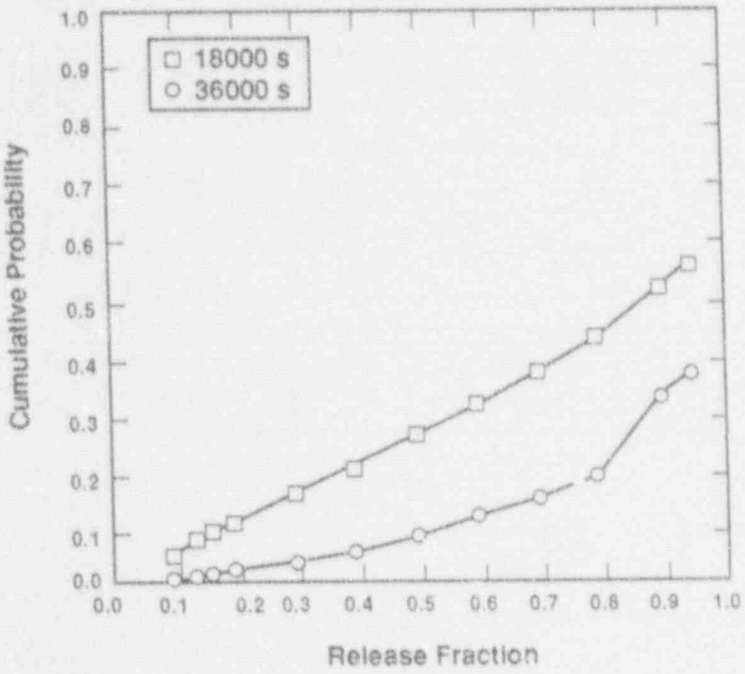

Figure A-4. Case 4: Wet Reactor Cavity Pedestal.

The following uncertain parameters in the mechanical release model were identified by the expert:

1. Density of liquid;
2. Liquid surface tension;
3. Density of gas sparging the pool;
4. Viscosity of gases;
5. Superficial gas velocity;
6. Correlations of entrainment rates.

For iodine release as a result of iodine chemistry, the expert identified the following factors affecting the partition coefficient:

1. Tri-iodide formation;
2. Overall hydrolysis reaction;
3. Hypoiodous acid formation constant;
4. Gas phase concentrations of organic species;
5. Organic iodine formation;

6. Iodate ion stability under irradiation;

7. Hydrogen ion concentration in steam condensate;

8. Iodine discharge rate and chemical form to the suppression pool;

9. Iodine available for ex-vessel release;

10. Discharge of cesium to suppression pool;

11. Chemical form of discharged cesium;

12. Boric acid discharge to suppression pool;

13. Duration of the analysis for Cases 1 and 2.

Though these were sources of uncertainty, not all of them greatly affected the results of iodine revaporization calculations.

Correlations with Other Variables

According to Expert A's model, the iodine revaporization release from the suppression pool is correlated with the following other source term variables:

- Total iodine and cesium releases from the vessel into the suppression pool (in-vessel release and deposition) and the chemical forms of these materials;

- Amount of hydrogen gas discharged into the suppression pool (in-vessel hydrogen production).

The iodine release from the reactor cavity pedestal water is correlated with the following other source term variables:

- Amount of gas release during core debris interaction with concrete.

Suggested Methods for Reducing Uncertainty

None.

Expert B's Elicitation

BWR Late Iodine Release from the Suppression Pool and Reactor Cavity Water

Description of Expert B's Rationale/Methodology

Expert B assumed the release of iodine from the pools could be calculated from the following equation:

Release Rate = (Gas Flux from Water) x (Concentration Iodine in Water) x (Iodine Partition Coefficient).

He considered a pool of water with a gas flux either off or near the surface. Based on the definition of the IPC and assuming equilibrium is established, the following equation was obtained for RF:

$$RF = 1 - \exp(-V_g/(V_w IPC)), \qquad EQ\ (1)$$

where V_g is the volume of gas evolved, V_w is the volume of water, and IPC is the iodine partition coefficient. Expert B felt that the iodine partition coefficient depended primarily on the concentration of iodine in the water, the pool pH, and the irradiation. However, he assumed that enough fission products had been released essentially to drive the IPC to its lowest value for a given pH.

In general, the maximum release fraction in the Expert B's distribution corresponded to the minimum pH value and was also based on the assumption that all the water and gas were effective in the removal process. The median value corresponded to the expert's best guess value for the pH and was based on the assumption that only 50% of the water was effective in the removal process. The minimum RF in the distribution was based mostly on his judgment.

Part 1

For Cases 1 and 2 Expert B used a water volume (V_w) of 3.9 ML. To obtain the gas volume (V_g) for Case 1 the expert assumed 50% of the in-vessel zirconium was oxidized and was released to the suppression pool as hydrogen. He calculated a gas volume of 26.5 ML. Furthermore, for Case 1, he assumed that no water was vaporized during this process. For Case 2, there is a substantial amount of pool flashing, and therefore, the expert neglected the amount of H_2 that is passed through the pool for this case. He assumed that 8% of the pool volume is boiled away. Based on the ratio of the steam-specific volume to the liquid-specific volume, he calculated that V_g/V_w is 128 for Case 2 (compared to 6.8 for Case 1). To calculate the pool pH, the expert assumed that the fission product inventory of iodine was 17.7 kg and the original pH of the water was 7.2. As a lower bound, the expert assumed that all the iodine enters the pool as HI. Based on this assumption, he calculated a minimum pool pH of 4.5. However, the expert's best guess was that the pool pH would not change much because he

felt that the HI would be counterbalanced by CsOH. Thus, his best guess was that the pool pH would be approximately 7. Expert B used Figure B-1 to obtain the IPC for different pH values. For pH values of 4.6 and 7, he indicated that the IPCs would be 100 and 316, respectively. In selecting the IPCs the assumption was made that the irradiation dose to the pool was sufficient to convert [I^-] into [I^2] at low pH values. The values for V_g/V_w and IPC were then used with Eq. (1) to calculate the maximum release fractions, which for Cases 1 and 2 were 0.07 and .72, respectively.

Part 2

Expert B felt that because the cavity water boils at the bottom surface, the gas probably would be in equilibrium with the water. For Cases 3 and 4, the expert did not consider the amount of iodine in the cavity water. Additionally, the expert did not include the effect that the boil-down process has on the iodine concentraton. Based on experiments, the expert's best guess was that the cavity water would have a pH of 9. The IPC, which corresponds to a pH of 9, is 3160. These experiments did not, however, include B_4C, which would tend to lower the pH. Taking this into account, the expert estimated that the cavity water could have a pH as low as 8.5, which leads to an IPC of approximately 1000. For Cases 3 and 4, the gases come from CCI and from boiling away of the cavity water. If only the gases released from CCI are considered, the release fraction for Case 3 is negligible. However, if one considers the boiling-off process, the release fractions are quite significant. For Case 3, the expert assumed 33% of the water has boiled off, which results in a maximum release fraction of 0.41 (pH of 8.5 and an IPC of 1000).

For Case 4 essentially all the water has boiled out of the cavity and, therefore, the expert felt that the release fraction could be as high as 1. However, it was the expert's opinion that release fractions as low as 0.8 were credible.

Results of Expert B's Elicitation

Part 1

The results for Cases 1 and 2 are presented in Tables B-1 and B-2, respectively.

Part 2

The results for Cases 3 and 4 are presented in Tables B-3 and B-4, respectively.

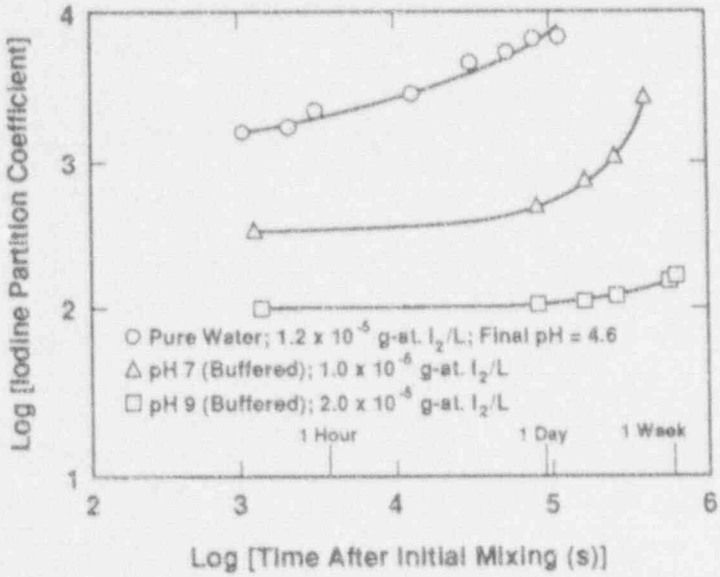

Figure B-1. Iodine Partition Coefficient versus Mixing Time; pH Effect at 298 K. (from E. G. Beauheim et al., "Chemistry and Transport of Iodine in containment; NUREG/CR-4697, ORNL-TM-10135, Oak Ridge National Laboratory, Oak Ridge, TN, Oct. 1986).

Table B-1
Release Fractions, Case 1 (Subcooled SP)

Release Fraction	Cumulative Probability
0.000	0.00
0.025	0.25
0.050	0.50
0.075	0.75
0.100	1.00

Table B-2
Release Fractions, Case 2 (Saturated SP)

Release Fraction	Cumulative Probability
0.001	0.00
0.100	0.33
0.150	0.50
0.200	0.67
0.400	0.90
0.700	1.00

Table B-3
Release Fractions, Case 3 (Flooded Cavity)

Release Fraction	Cumulative Probability
0.050	0.00
0.100	0.05
0.250	0.50
0.400	0.95
0.600	1.00

Table B-4
Release Fractions, Case 4 (Wet Cavity)

Release Fraction	Cumulative Probability
0.800	0.00
0.850	0.25
0.900	0.50
0.950	0.75
1.000	1.00

Sources of Uncertainty

The major sources of uncertainty were the IPC and the volume of gases passed through the pool. The uncertainty in IPC was judged to be a function of the uncertainties of pool pH, the concentration of iodine in the water, and the effects of irradation. However, it was the expert's opinion that the irradation field was strong enough to drive the IPC to its lowest value for a given pH. The uncertainty the pH stemmed from an uncertainty in the chemical species present and an uncertainty in the concentration of iodine in the water. The expert indicated that even if the uncertainty in the input chemical species was reduced, a significant amount of uncertainty would still exist because of the complex chemistry taking place in the pool.

Expert C's Elicitation

BWR Late Iodine Release from the Suppression Pool and Reactor Cavity Water

Description of Expert C's Rationale/Methodology

Expert C provided a detailed written explanation of his analysis of this issue. This analysis lead to the calculation of the median values for late iodine release. The written explanation is reproduced below with minor editorial changes and additions by the substantive assistant.

Part 1: Release from the Suppression Pool

Expert C assumed the following pool conditions before the accident occurs:

1. pH 7.2 to 7.4;
2. Water volume 3.9×10^6 L;
3. Temperature--ambient.

Further assumptions were made about the progression of the accident which led Expert C to an evaluation of the pool conditions during the time period of interest. These assumptions were

1. In the TBUX sequence (short-term station blackout with the RPV maintained at high pressure) boron [from standby liquid control (SLC)] is not discharged into the RPV.

2. Boron will enter the suppression pool only as a result of the oxidation of B_4C (contained in the control blades) in the amount suggested by Parker's experiments (0.72% according to Beahm).

3. The total iodine inventory in core is 17.7 kg. Source Term Code Package (STCP) calculations show that 80% will be retained in suppression pool.

4. Iodine enters pool as CsI. In the absence of boric acid it is not clear that much HI will be formed.) However, as a separate extreme assumption, take it that all iodine is in the form of HI.

5. 180 kg of cesium would be deposited in the pool, as either CsI or CsOH.

6. 1000 kg of structural material is deposited in the pool. This is mainly tin from zircaloy.

7. Water addition to the pool over the course of the accident amounts to approximately a 10% increase in volume. This increase can be neglected.

8. With regard to H_2, the TB sequence calculated by STCP[C-1] arrives at 30% of the zircaloy clad reacted. Assuming 64,100 kg of cladding, Expert C calculated that 4.22×10^5 moles (gram) of hydrogen would be released to the pool. This is equivalent to 1.28×10^7 L at 100°C and 1 atmosphere.

Based on these assumptions, Expert C calculated the pH of the solution in the pool.

For Assumption Set A he assumed that the iodine was all in the form of CsI. The calculated pH was 10.4.

For Assumption Set B he assumed that CsI is converted to HI in the RPV and that the Cs that is left behind is converted to CsOH. He further assumed that the HI will neutralize a part of the OH-, thus resulting in 860.3 moles CsOH being deposited in the suppression pool. The pH of the resulting solution was calculated to be 10.3. Thus, whether it is CsI or HI makes essentially no difference with regard to pH. Assumptions A and B were not distinguished by Expert C.

The effect of boron entering the suppression pool was reflected in the pH assessment. Beahm[C-2] suggests a formula for calculating pH based on the ratio of hydroxide to boric acid. The application of the formula to this problem is outside the range of the experimental data. According to Parker, 0.72% of the B_4C in a BWR is volatilized as boric acid. Thus, about 5×10^2 gram atoms of boron are produced. Expert C applied Beahm's formula and estimated the pool pH to be 9.36. At the request of Expert C, Ed Beahm measured the pH of an appropriate mixture. He quoted from a letter from Beahm giving his results:

> "To simulate the conditions that we discussed: 180 kg of Cs and 0.72% of the B_4C inventory of boron in 3.9×10^6 L, I used 0.3 mL of 1 M NaOH and 10 mg of H_3BO_3 in 2 L of pure water. The pH was 9.5. This is close to the value expected from Eq. (8) of NUREG/CR-4697."

Expert C also considered the possible effects of tin on the pool's pH. He concluded that the concentration (0.0022 moles/L) was too low to influence pH. Possible effects on pH from other sources were also addressed. It has been said that the effect of radiation on nitrogen (N_2) dissolved in the water is that it will cause nitric acid (HNO_3) to be formed and will make the suppression pool acid. Expert C felt that H_2 bubbling through the pool would sweep the N_2 out. In addition, he felt that the question of whether the N_2 is present or not is not germane because nitric acid is formed only very slowly at high pHs under irradiation which is indicated by Beahm's work as discussed below.

Beahm[C-3] says that at high pH, I_2 could be converted into nonvolatile forms by radiation. In a private communication between Expert C and Beahm, Beahm indicated that at pHs in the neighborhood of 10, the formation of I_2 by radiation would be extremely slow, if at all.

The trend toward less formation of I_2 at higher pH can be seen by the data presented in Table C-1. This work was done at an I- concentration of 10^{-4} m/L.

Table C-1
Effect of pH on the Formation of I_2 Under Irradiation

	% Conversion to I_2		
Radiation Dose	pH 6.8	pH 6.1	pH 3.05
2 M rad	0.3	0.33	72

Furthermore, Beahm has estimated the radiation level in the suppression pool as being 0.02 megarad/h. He described an experiment in a letter* to Lisa Chan in which the liberation of I_2 from aqueous solutions was measured. At an iodide concentration of 10^{-4} moles/L, a pH of 8.5 (borate buffered system) and an irradiation level of 0.5 megarad/h, 0.03% of the oxide was converted to I_2 in about 2 h.

From these data, Expert C concluded that very little of the iodide would be converted to I_2 in the suppression pool for the particular cases presented to the expert review group.

In Sandia presentations of this issue, the question of the possible formation of organic iodides was raised. Expert C argued that the pH of the water in the suppression pool will be alkaline (in the range of 10.4 to 9.4). He explained that Beahm has done experiments at a pH of 9.0 in which methane in a carrier gas was bubbled through a solution containing I- in an irradiation field of 0.7 M rad/h.[C-4] Less than 1.2×10^{-4} % of the methane was converted to methyl iodide and about 6.2×10^{-3} % of the I- was converted to organic iodide in the gas phase in 1.4 h. In consideration of this low conversion of I- to CH_3I at a high pH, Expert C concluded that the formation of organic iodides was a serious concern.

Expert C performed a calculation to establish his best-estimate (median) value for iodine revolatilization from the suppression pool. He assumed that the pH would be 9.5 and that radiation does not form extra I_2. An estimate of what the partition coefficient would be under these conditions was made.

The overall reaction of particular importance is

$$3I_2 + 3H_2O \rightarrow 5I^- + IO_3^- + 6H^+.$$

Expert C quoted Beahm's statement that "under basic conditions (in the presence of radiation), H_2O_2 can convert I_2 to I^-." It was also clear to the expert, based on the equation above, that basic conditions do not favor keeping the iodine in the form of I_2. The data developed by Beahm are

*E. C. Beahm to Lisa Chan, NRC, Letter on measuring the liberation of I_2 from aqueous solutions, August 13, 1987.

generally at a low pH. However, Figure C-1 does include data at pH = 9. The "partition coefficient" as used by Beahm is defined as

$$IPC = \frac{\text{Concentration iodine in aq. phase}}{\text{Concentration iodine in gas phase}}$$

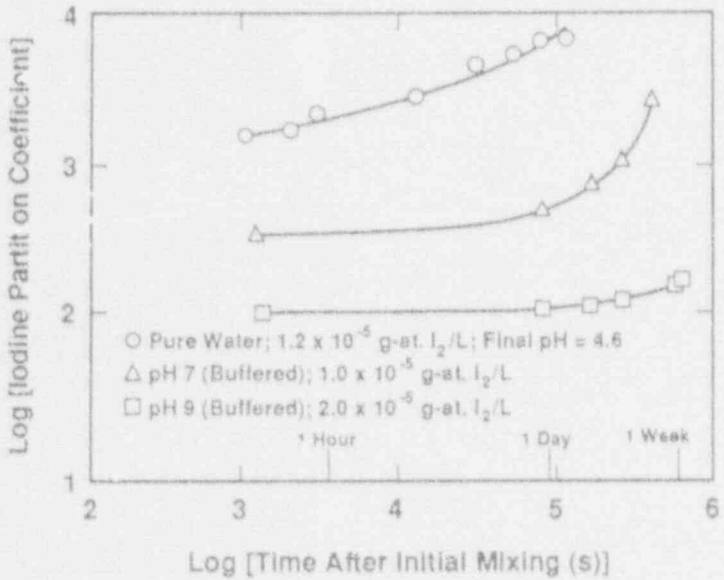

Figure C-1. Iodine Partition Coefficient vs. Mixing Time; pH Effect at 298 K.

Expert C noted that log (IPC) at pH of 9 starts at 3 and within one day climbs to 4. It seemed appropriate to Expert C, since this pH is 9.5, to assume a log (IPC) of 3.5 and calculate what the released fraction will be.

The concentration of iodide in the aqueous phase was assumed to be 2.9×10^{-5} moles/L. Therefore, the concentration in the gas phase will be 9.2×10^{-9} g-atoms/L. Assuming 1.28×10^{7} L (100°C, 1 atm) of H_2 go through the suppression pool, then the total gram atoms of iodine removed would be 0.11. The total gram atoms of iodine in the pool is 111.6. This fraction of iodine from the suppression pool would be 1.1×10^{-3}. Expert C stated that this was a conservative calculation that assumed equilibrium.

For Case 2, it seemed to Expert C that the amount released will not be much different. The suppression pool temperature was assumed to be 142°C rather than 100°C. The vaporization of 8% of the water at containment failure leads to a much smaller volume of steam than was assumed in Case 1.

Furthermore, according to Beahm[C-5] for at least at a pH of 7 (buffered), a higher temperacure gives a higher partition coefficient (i.e., favors the aqueous phase more). Beahm points out that it may not be intuitively obvious why high aqueous phase temperatures give lower iodine volatility. He mentions that this effect is due to the more rapid iodine hydrolyses which produces nonvolatile products I- and IO_3 and thus prevents the rapid formation of volatile species. Based on this information, Expert C stated that a slight reduction in the iodine release over the case for a subcooled pool was appropriate.

Part 2: Release from Water in the RPV Pedestal

Case 1: Flooded Reactor Cavity

Expert C made the following assumptions:

1. There is 1.1×10^6 kg of water in the reactor cavity at time of vessel breach; 7.7×10^5 kg remain in the reactor cavity after 10 h.

2. The core and associated debris are discharged to the reactor cavity. The STCP assumed (probably erroneously) that 100% of the core and assorted structural material go through the bottom of the reactor. Expert C took the STCP results as the basis for his assumptions with regard to core debris composition. In Reference C-1, pages 4-78 and 4-79, the composition and amounts of the melt at the time of failure are given (for the TB sequence). Some of the important ingredients are shown in Table C-2. The total weight of the core debris adds up to 334,375 kg not including the B_4C or B_2O_3 in Reference C-1.

Table C-2
Assumed Composition (Partial) of Core Debris

Constituent	Mass (kg)
Cesium (Cs)	3,48
Iodine (I)	0,289
Tellurium (Te)	23
Barium (Ba)	109.7
Tin (Sn)	1,065
UO_2	166,200
Zirconium (Zr) (structural)	57,798
Iron (Fe)	59,068
ZrO_2	28,700
B_4C	2,500

generally at a low pH. However, Figure C-1 does include data at pH = 9. The "partition coefficient" as used by Beahm is defined as

$$IPC = \frac{\text{Concentration iodine in aq. phase}}{\text{Concentration iodine in gas phase}}$$

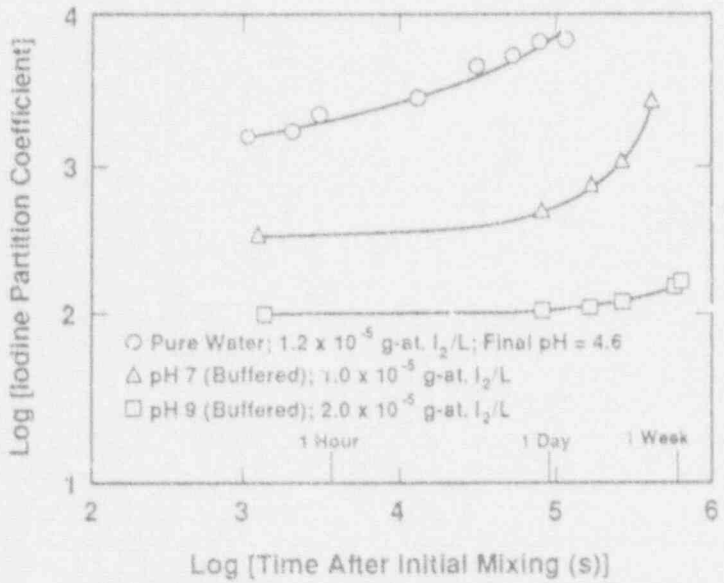

Figure C-1. Iodine Partition Coefficient vs. Mixing Time; pH Effect at 298 K.

Expert C noted that log (IPC) at pH of 9 starts at 3 and within one day climbs to 4. It seemed appropriate to Expert C, since this pH is 9.5, to assume a log (IPC) of 3.5 and calculate what the released fraction will be.

The concentration of iodide in the aqueous phase was assumed to be 2.9×10^{-5} moles/L. Therefore, the concentration in the gas phase will be 9.2×10^{-9} g-atoms/L. Assuming 1.28×10^{7} L (100°C, 1 atm) of H_2 go through the suppression pool, then the total gram atoms of iodine removed would be 0.11. The total gram atoms of iodine in the pool is 111.6. This fraction of iodine from the suppression pool would be 1.1×10^{-3}. Expert C stated that this was a conservative calculation that assumed equilibrium.

For Case 2, it seemed to Expert C that the amount released will not be much different. The suppression pool temperature was assumed to be 142°C rather than 100°C. The vaporization of 8% of the water at containment failure leads to a much smaller volume of steam than was assumed in Case 1.

Furthermore, according to Beahm[C-5] for at least at a pH of 7 (buffered), a higher temperature gives a higher partition coefficient (i.e., favors the aqueous phase more). Beahm points out that it may not be intuitively obvious why high aqueous phase temperatures give lower iodine volatility. He mentions that this effect is due to the more rapid iodine hydrolyses which produces nonvolatile products I^- and IO_3 and thus prevents the rapid formation of volatile species. Based on this information, Expert C stated that a slight reduction in the iodine release over the case for a subcooled pool was appropriate.

Part 2: Release from Water in the RPV Pedestal

Case 1: Flooded Reactor Cavity

Expert C made the following assumptions:

1. There is 1.1×10^6 kg of water in the reactor cavity at time of vessel breach; 7.7×10^5 kg remain in the reactor cavity after 10 h.

2. The core and associated debris are discharged to the reactor cavity. The STCP assumed (probably erroneously) that 100% of the core and assorted structural material go through the bottom of the reactor. Expert C took the STCP results as the basis for his assumptions with regard to core debris composition. In Reference C-1, pages 4-78 and 4-79, the composition and amounts of the melt at the time of failure are given (for the TB sequence). Some of the important ingredients are shown in Table C-2. The total weight of the core debris adds up to 334,375 kg not including the B_4C or B_2O_3 in Reference C-1.

Table C-2
Assumed Composition (Partial) of Core Debris

Constituent	Mass (kg)
Cesium (Cs)	3.48
Iodine (I)	0.289
Tellurium (Te)	23
Barium (Ba)	109.7
Tin (Sn)	1,065
UO_2	166,200
Zirconium (Zr) (structural)	57,798
Iron (Fe)	59,068
ZrO_2	28,700
B_4C	2,500

3. Assumptions with regard to what gets into the water phase are particularly important. In Reference C-6, data are given on the aerosols released for TQUV. This is a transient with loss-of-makeup water. Expert C assumed that the data are not too different for TBUX. By very crude integration, the amount of aerosol and the composition of potential basic and acidic components were estimated. The results are shown in Table C-3.

Table C-3
Estimate of Aerosols Released During CCI

Species	Fraction of Total (%)*
Na_2O	2.8
K_2O	34.7
SiO_2	24.9
BaO	1.9
SrO	2.5
CaO	22.0

*Total aerosol released = 2,805,600 g.

To estimate the pH of the solution overlying the core debris, Expert C assumed that all the aerosols were trapped by the water. He saw this as a key assumption in his analysis.

4. Expert C stated that another important aspect of the situation is the oxidation potential of the solution. For approximately the first 2 h, H_2 will be bubbling through the water due to the zirconium-water reaction. Under these conditions, Expert C felt that I_2 will not be appreciably released. However, after the H_2 evolution stops, the oxidation potential of the solution is not clearly reduced so that estimates of pH become relevant.

5. Expert C estimated the volume of water available based on the geometry of the Grand Gulf plant. The pedestal at Grand Gulf has an inside diameter of 6.25 m. The volume of the reactor cavity up to the level of the door for CRD removal (2.9 m above the floor) and access was calculated to be 8.95×10^4 L.

Under item 3 above it was estimated that the total mass of core debris is 334,375 kg. Expert C estimates the debris volume assuming a density of 4 g/cc as 8.36×10^4 L. He concluded that the core debris will essentially fill the reactor cavity. The 1.1×10^6 kg of water assumed present in the drywell to start with, would have a volume of 1.09×10^6 L.

The total volume of the reactor cavity, including the volume of the overflow area up to the top of the wire was calculated to be 9.55×10^5 L. Expert C assumed that the CRD access door was a circular personnel hatch and calculated a volume of 2.9×10^4 L. (It is actually a rectangular doorway with a volume of about 3,000 L.)

The volume of the reactor pedestal up to the level of the top of the wire wall was calculated to be 1.52×10^3 L. (The actual volume is approximately 1.8×10^5 L.) The total volume of a pool on the drywell floor was estimated as 9.55×10^5 L. The volume of water plus core debris was estimated at 1.17×10^6 L.

Expert C concluded that water would flow over the wire and that vigorous gas generation would occur in the pedestal. He assumed that there is sufficient leakage around the reactor vessel skirt such that the pedestal would not pressurize sufficiently to force the water down to the level of the access opening where venting from the cavity could occur. He thus concluded that there would be 8.72×10^5 L of water present in the drywell at the start of CCI.

Based on the above assumptions, Expert C proceeded to calculate the pH of the overlying water layer, both before and after the boil-off due to heat transfer from the debris. The composition of important aerosols released from CCI (Table C-3) were assumed to control the acidity. B_2O_3 (or H_3BO_3) was not included in the aerosol released but Expert C stated that it probably should be. The amount of B_4C from the control blades that would be converted to B_2O_3 or H_3BO_3 was assumed to be about 2,500 kg. There is a slightly soluble compound of boron and calcium called Colemanite (a mineral), $2CaO\text{-}3B_2O_3\text{-}5H_2O$; its solubility at 25°C is 0.1%. Expert C felt that this should be involved in the considerations. However, he found that the concentration of calcium would not be high enough to ensure precipitation. Based on the assumptions above, the total amount of boron available would be 1.95×10^6 g. Based on the information given in Table C-3, the amount of calcium available for dissolution would be 4.41×10^5 g. Thus Expert C calculated that the concentration of Ca^{++} would be 0.0126 moles/L. The boron concentration was calculated to be 0.22 moles/L.

In the calculation of the concentration of other species that would influence the pH, based on Table C-3, Expert C calculated aerosol concentration based on the amount of water available at the beginning of boil-down. The results are shown in Table C-4.

Table C-4
Concentration of Aerosols In Overlying Water

Species (%)	Fraction in Aerosol	Mass in Water Assuming Aerosol Dissolves (g)	Equivalent of Base (OH/L)
Na_2O	2.8	7.84×10^4	0.0029
K_2O	34.7	9.72×10^5	0.0 ,6
BaO	1.89	5.29×10^4	0.000792
SrO	2.49	6.97×10^4	0.001542
CaO	22	0.0252	
		Total	0.0540

Since Na_2O, K_2O, BaO and SrO all are potentially strong bases, Expert C used the Beahm's equation to calculate the initial pH (again assuming no water boil-off). The calculated value was 8.3.

As the water boils down from 1.1×10^6 kg to 7.7×10^5 kg the volume of the water would be reduced to 6.18×10^5 L. However, the ratio of base to boric acid would stay essentially the same so the pH will remain at 8.3.

Expert C felt that it was reasonable to question the assumption that the aerosols released in the dry case constitute the solute in the case when there is overlying water. He stated that it is possible that leaching of constituents could occur such that they might not form aerosols. The listing of the constituents for the TB sequence[C-1] does not indicate any potential materials that would lower the pH if they were leached. Expert C felt that Cs would probably be leached but that compared with the amount of CaO, Na_2O, K_2O, etc., coming from the concrete, the increase in pH would be insignificant. Thus, Expert C stated that although the logic in assuming that the aerosols become the solute may be a bit surprising, it seemed workable.

Expert C suggested that one mechanism that could be suggested for making the solution more acidic than predicted is the formation of nitric acid by radiation. The water may be saturated with nitrogen, since it is exposed to air (although the solution will be boiling and thus would remove most of the nitrogen). Referring to the previous discussion on Part 1 of this issue (suppression pool release), it was pointed out that at high pHs, iodine can be converted into more volatile forms by radiation.[C-7] Beahm has indicated that at a pH of 10, the formation of I_2 by radiation would be extremely slow, if it occurred at all. It was stated that a pH of 8.5 and a radiation level of 0.5 megarad/h 0.03% of the iodine was converted to I_2 in about 2 h. At a pH of 8.3, it seems very unlikely therefore that appreciable amounts of nitric acid formation would occur. In summary, Expert C concluded that the pH of the overlying solution will be roughly 8.3. For a pH of 8.3, the log partition coefficient, Figure C-1, can be estimated to be 3.

In order to convert the partition coefficient in an amount of iodine released, Expert C had to guess at the amount of gas which will sparge through the water. H_2 will be released for about 2 h due to the $Zr\text{-}H_2O$ reaction. Expert C stated that under such reducing conditions, no I_2 will be released. Sparging by steam, which might be effective in removing I_2, will occur due to the boiling of the water. Expert C assumed that the boil-down of 2.4×10^8 lb of water to 1.7×10^6 lb of water results in all that steam going through the water. The volume of steam resulting was estimated to be 5.4×10^8 L (assuming 1 atm and 373 K).

It was further assumed that the log of the partition coefficient would be 3. This would result in an iodine concentration in the steam of 1.31×10^{-9} moles/L.

Assuming a sparging flow of 5.4×10^8 L through the solution, the amount of iodine released would be 0.71 moles of I_2 or 179 g of iodine that could be released. The fraction of iodine released would then be 0.62.

Expert C cited several items that would argue for a lower release. These were:

1. Equilibrium between the aqueous solution and the steam would not be achieved;

2. The concentration of the iodine in the aqueous phase would be consistently decreasing; thus, the concentration in the gas phase would be similarly decreasing instead of being constant as was assumed.

Case 2: Wet Reactor Cavity

In this particular case, the core debris is assumed to be covered by 2.72×10^5 L of water. Ten hours after vessel breach, the solution above the core has boiled down to 59 L. As this boil-down occurs, much of the solute material would precipitate. The solution would have been concentrated by a factor of 4600. Expert C felt that the solution could be said to have evaporated to dryness.

The initial concentrations were assumed similar to those of Case 1 and the ratio of base to boric acid was taken to be the same. Therefore, the starting pH would be as previously calculated: 8.3. However, at the end of the boil-down, a large amount of wet solids would be left. Based on Expert C's assumptions of Case 1, the 59 L will be mixed 2800 kg of solids.

Wisbey[C-8] evaporated a solution of pH 9 with 10^{-4} M CsI dissolved in it to dryness. The total irradiation dose was 2.1 megarads. Twenty-two percent of the iodine was converted to a volatile form. The final pH was 8.5. Since this seemed to be a pertinent experiment, Expert C used this result as the basis for his results.

Results of Expert C's Elicitation

The results are tabulated in Table C-5. Figures C-2 and C-3 show the distributions for Parts 1 and 2 of this issue, respectively. Values for iodine release calculated for each case were used as the median of the distribution. Expert C based the distributions on his knowledge of the issues involved and on engineering judgment.

Sources of Uncertainty

Part 1 - Release from the Suppression Pool

Expert C felt that these values could be reliably calculated based on available information with relatively little uncertainty. However, the results of his calculation would be sensitive to the quantity of cesium retained by the suppression pool (through the pool pH). Cesium retention would be affected by in-vessel retention (FVES). In the range of 90 to 180 kg of cesium in the pool, Expert C felt that his results would be appropriate.

Table C-5
Summary of Iodine Release Distributions

Case	Fractile of Distribution						
	0	0.05	0.25	0.50	0.75	0.95	1.0
Subcooled Pool (Part 1, Case 1)	10^{-4}	5×10^{-4}	10^{-3}	1.1×10^{-3}		2×10^{-3}	5×10^{-3}
Saturated Pool (Part 1, Case 2)	10^{-4}	5×10^{-4}	9×10^{-4}	1.0×10^{-3}		2×10^{-3}	5×10^{-3}
Flooded Drywell (Part 2, Case 1)	--	0.2	0.5	0.6	0.65	0.9	--
Wet Drywell (Part 2, Case 2)	0.1	--	0.2	0.25	0.4	--	0.8

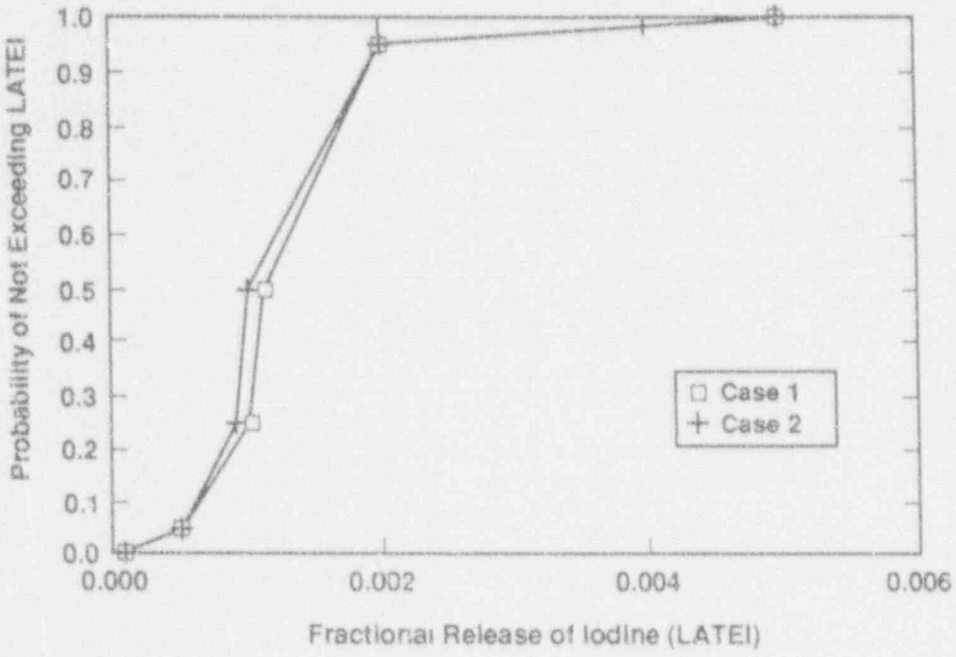

Figure C-2. Part 1. From the Suppression Pool.

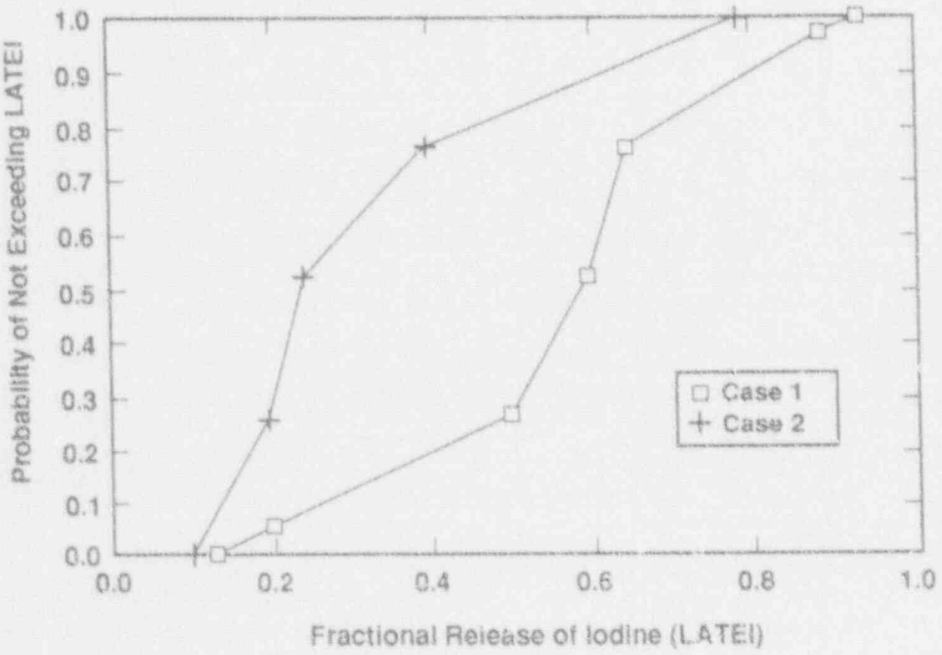

Figure C-3. Part 2. From the Drywell Floor Pool.

Part 2 - Release from Water in the RPV Pedestal

Expert C felt that there was considerably more uncertainty in these results. The retention of CCI aerosol by the water pool was identified as being the dominant contributor to uncertainty. This involves both production in the melt and subsequent scrubbing by the water.

REFERENCES

C-1. R. S. Denning et al., "Supplemental Radionuclide Release Calculations for Selected Severe Accident Scenarios," Vol. 4, NUREG/CR-4624, BMI-2139, Battelle Memorial Institute, 1986.

C-2. E. C. Beahm et al., "Chemistry and Transport of Iodine in Containment," NUREG/CR-4697, ORNL/TM-10135, October 1986.

C-3. Ibid., p. 15.

C-4. Ibid., p. 26

C-5. Ibid., p. 12.

C-6. J. A. Gieseke et al., "Radionuclide Release Under Specific LWR Accident Conditions." Volume IV: PWR Ice Condenser Design, BMI-2104, Battelle Memorial Institute, 1984, pp. 6-93 to 6-94.

C-7. E. C. Beahm et al., "Chemistry and Transport of Iodine in Containment," NUREG/CR-4697, p. 15, ORNL/TM-10135, October 1986.

C-8. S. Wisbey et al., "Iodine Behavior in Containment Under LWR Accident Conditions," NUREG/CP-0078, p. 6-29, Oak Ridge National Laboratory, September 1986.

5.7 Issue 7. Peach Bottom Reactor Building Decontamination Factor

Summary of Expert Panel's Assessment of Source Term Issue 7

Experts consulted: J. Gieseke, Battelle Memorial Institute; David Williams, Sandia National Laboratories; Andrzej Drozd, Stone & Webster Engineering Corporation; Ben Y. H. Liu, University of Minnesota.

Issue Description

The experts were asked to quantify the uncertainty in the decontamination factor (DF) of the reactor building for radionuclides released from the Peach Bottom drywell. The variable that was elicited was the reactor building DF.

The reactor building DF is defined as the ratio of the amount of fission products released into the reactor building to the amount released out of the reactor building (to the environment). The value of the reactor building DF should be greater than or equal to 1. A reactor building DF value of 1 means no retention by the reactor building.

This issue is concerned only with the cases for which the reactor building structure is intact after containment failure. It is assumed that the reactor building blow-out panels are open after containment failure. The reactor building DF may be evaluated for each of nine radionuclide groups: noble gas, iodine, cesium, tellurium, strontium, ruthenium, lanthanum, cerium, and barium.

There are six cases for Peach Bottom reactor building DF:

1. Drywell rupture and a subcooled suppression pool;
2. Drywell rupture and a saturated suppression pool;
3. Drywell shell melt-through and a subcooled pool;
4. Drywell shell melt-through and a saturated pool;
5. Drywell head seal leakage and a subcooled pool;
6. Drywell head seal leakage and a saturated pool.

Summary of Rationale

Expert A based reactor building DF distributions on NAUA calculations with adjustments for neglected phenomena. He also considered calculations performed by the SNL staff and the Brookhaven staff. He estimated the effects of the following parameters: hygroscopic aerosols, circulation patterns in the reactor building, residence time (containment leak size), and reactor building surface area.

Expert A assumed that the location of the containment failure had a small effect on reactor building DF except in the case of drywell shell melt-through after contact with core debris. Containment failure due to drywell

shell meltthrough was estimated to result in about twice the deposition rate in the reactor building compared to other containment failure locations, since the pathway is extended and there is more surface area for deposition.

Expert B defined a simple model in terms of the release parameters and varied the input based on uncertainties in the underlying parameters. When possible, code results furnished a base distribution. (He used existing CORCON, VANESSA, CONTAIN runs to establish the base distributions.) He shifted the base distributions to account for modeling uncertainties, parameter uncertainties, and calculation-induced uncertainties.

He used MAAP code results to define the distribution for reactor DF that included the effect of having two holes in the reactor building and setting up a convective flow between them (chimney effect). He constructed base distributions assuming a 0.5 chance of the chimney effect.

Expert C's approach to this issue was to determine which parameters were important, to perform a scoping study on the important parameters to estimate the DFs associated with these parameters, and to estimate the range of credible DFs for the reactor building.

He felt that aerosol behavior, residence time, removal mechanisms, and the building compartmentalization would be important parameters that would affect the decontamination factors. Both chemistry effects and chimney effects would probably be negligible in the secondary containment.

Parameters important to aerosol behavior were the shape factor, particle density, concentration, initial distribution, and agglomeration. Parameters that would affect the residence time were the gas flow rates and the presence of hydrogen burns. Important removal mechanisms were gravitational settling and diffusiophoresis. Factors cited that would affect gravitational settling were atmospheric dryness or condensing and hygroscopic effects.

Expert C estimated the DFs associated with five additional parameters: (1) diffusiophoresis, (2) condensation on particles, (3) hygroscopic effect, (4) multi-volume effect, (5) and hydrogen burn.

Expert D used reactor building DF values calculated by the STCP in BMI-2104 and BMI-2139 to assess the mean values of reactor building DF. He used his experience in experimental aerosol transport to set the upper and lower bound values of reactor building DF.

The mean residence time of an aerosol inside the reactor building is considered by Expert D to be the main variable in determining the reactor building DF value, which in turn is dominated by the volume of the reactor building.

No retention or deposition in the reactor building is considered for the noble gas group. The remaining eight groups were treated the same, because other uncertainties overwhelm the difference among different radionuclide groups.

Method of Aggregation

Expert D did not distinguish among radionuclide groups (other than the noble gas group). The other three experts established different distributions for the volatile species (iodine and cesium) and for the nonvolatile species. The iodine and cesium distributions developed by Expert A were only slightly different. Expert C presented a distribution for the tellurium group that is only slightly different from his nonvolatile distribution. Based on the results of all four experts, the eight nuclide groups were classified into two categories for the reactor building DF issue: volatile (iodine and cesium) and nonvolatile (all the others, except noble gases).

Assumptions Used in Averaging Distributions

1. Linear extrapolation obtained endpoint probabilities (0 and 1) for those experts who did not assign values for the two endpoint probabilities.

2. The arithmetic mean was used for calculating the average frequency among different experts for a given value of revolatilization fraction.

3. Linear interpolation was used to obtain the values between the experts' assessed points.

Aggregated Results

Table 7-1 gives the aggregate results for each Peach Bottom case.

Table 7-1
Reactor Building Decontamination Factor
Aggregate for Case 1

	Quantile								
Radionuclides	0.000	0.040	0.050	0.250	0.500	0.750	0.950	0.990	1.000
Cesium, Iodine	1.0	1.042	1.099	1.409	2.297	4.277	9.878	56.175	470.000
Aerosols	1.0	1.055	1.113	1.480	2.621	4.905	10.157	63.900	507.000
				Aggregate for Case 2					
Cesium, Iodine	1.0	1.042	1.141	1.66[illegible]	2.836	4.936	10.885	77.375	428.000
Aerosols	1.0	1.060	1.129	1.577	2.610	5.[illegible]83	12.795	81.776	461.000
				Aggregate for Case 3					
Cesium, Iodine	1.0	1.061	1.158	1.830	2.955	4.803	11.140	74.900	594.000
Aerosols	1.0	1.0[illegible]	1.147	1.978	3.446	5.713	13.313	85.050	634.000
				Aggregate for Case 4					
Cesium, Iodine	1.0	1.056	1.228	2.293	4.049	6.860	14.488	87.919	551.000
Aerosols	1.0	1.079	1.250	2.221	4.023	6.812	17.009	92.074	590.000
				Aggregate for Case 5					
Cesium, Iodine	1.0	1.00	1.020	1.11	1.35	1.731	6.656	9.639	361
Aerosols	1.0	1.00	1.020	1.11	1.41	1.881	6.656	9.639	361
				Aggregate for Case 6					
Cesium, Iodine	1.0	1.00	1.020	1.11	1.46	2.57	6.65[illegible]	9.639	361
Aerosols	1.0	1.00	1.020	1.11	1.48	2.57	6.656	9.639	361

Individual Elicitations for Issue 7

Expert A's Elicitation

Peach Bottom Reactor Building Decontamination Factor

Description of Expert A's Rationale/Methodology

Expert A considered the dependent parameters DF, 1/DF (penetration), and 1-1/DF (decontamination efficiency) to understand the effects of the important parameters on the result. He used a conversion table for distributions. Median values were determined from code calculations referenced below. For all noble gases (xenon, krypton, etc.) DF = 1. For all drywell rupture and shell melt-through cases, the minimum DF ($F_{.001}$) is very near 1.0, and the maximum DF ($F_{.999}$) is estimated to be 10. For the drywell head leak case, the range is from 1.0 to 1.4.

The expert based his judgments largely on NAUA calculations with adjustments for neglected phenomena. The NAUA code is well baselined against experiments: DEMONA, LACE, and numerous dry aerosol studies. Sequences or parts of sequences that matched conditions specified by the case definition for this issue were used. Reactor building DFs were calculated from the Brookhaven sensitivity study to support the median values selected for Case 1 and to evaluate the effects of input parameter values. The calculations performed by the SNL staff were also considered. The expert assumed a small effect from varying the break location except for drywell liner melt-through at Peach Bottom, which was estimated to result in about twice the deposition rate since the pathway is extended and there is more surface area to pass. The expert estimated the effects for uncalculated parameters as follows:

1. Hygroscopic aerosols < 2x for median
   < 5x for upper bound

2. Circulation patterns < 2x
   (natural circulation)

3. Residence time (leak size) < 2x

4. Surface area (general) 2 - 4x.

For flow patterns, the general conclusions are that Peach Bottom may have more direct flow paths out than were considered in NUREG/CR-4624.

Results of Expert A's Elicitation

The result for each case are given below.

Case 1: Peach Bottom

	Fractile				
	.001	.25	.50	.75	.999
Xe, Kr	1	1	1	1	1
I, Br	1.05	1.2	1.4	1.8	10
Cs, Rb	1.05	1.2	1.5	3	10
All others	1.05	1.2	1.5	3	10

The results of the pertinent calculations are:

	NUREG/CR-4624 Low cond. in sec. containment	NUREG/CR-5062 Wetwell fail. with very subcooled pool		NUREG/CR-4624 High cond. in sec. containment	
	TB1	TRUX	Brookhaven Min - Med - High	TC1	TC3
GR1 (Xe/Kr)	1.00	1.00	- - -	1.0	1.0
GR2 (I)	1.12	1.66	1.2 - 1.40 - 2.60	2.0	1.9
GR3 (Cs)	1.64	1.68	1.0 - 1.30 - 1.70	2.03	2.01
GR4 (Te)	1.45	5.00	1.1 - 1.20 - 1.30	1.21	1.72
GR5 (Sr)	1.35	3.32	1.0 - 1.14 - 1.30	1.27	1.65
GR6 (Ru)	1.58	4.10	1.2 - 1.50 - 1.70	1.37	1.68
GR7 (La)	1.58	3.11	1.0 - 1.20 - 1.34	1.43	1.72
GR8 (Le)	1.42	3.31	1.1 - 1.25 - 1.25	1.33	1.67
GR9 (Ba)	1.43	3.96	1.0 - 1.116 -1.20	1.22	1.68

Case 2: Peach Bottom

	Fractile				
	.001	.25	.50	.75	.999
Xe, Kr	1	1	1	1	1
I, Br	1.1	1.7	2	4	10
Cs, Rb	1.1	1.7	2	4	10
All others	1.1	1.2	1.8	2.5	10

Case 3: Peach Bottom

	Fractile				
	.001	.25	.50	.75	.999
Xe, Kr	1	1	1	1	1
I, Br	1.1	1.3	1.8	3	10
Cs, Rb	1.1	1.2	2.0	5	10
All others	1.1	1.2	2.0	5	10

This case is comparable to case 1, but the leak location is different. Assume about 50% more deposition.

Case 4: Peach Bottom

	Fractile				
	.001	.25	.50	.75	.999
Xe, Kr	1	1	1	1	1
I, Br	1.2	2.0	3.0	6.0	10
Cs, Rb	1.2	2.0	3.0	6.0	10
All others	1.2	1.5	2.5	4.0	10

This case is comparable to case 2 Peach Bottom but the leak location is different. Assume 1.5 to 2 times deposition.

Case 5: Peach Bottom

	Fractile				
	.001	.25	.50	.75	.999
Xe, Kr	1	1	1	1	1
I, Br	1.0	-	1.1	-	1.4
Cs, Rb	1.0	-	1.1	-	1.4
All others	1.0	-	1.1	-	1.4

Case 6: Peach Bottom

	Fractile				
	.001	.25	.50	.75	.999
Xe, Kr	1	1	1	1	1
I, Br	1.0	-	1.1	-	1.4
Cs, Rb	1.0	-	1.1	-	1.4
All others	1.0	-	1.1	-	1.4

Sources of Uncertainty

Expert A considered break location, building flow patterns, uncertainties in building parameters, and modeling deficiencies to be the main sources of uncertainty.

Correlations with Other Variables

Expert A specified no correlations with other variables.

Suggested Methods for Reducing Uncertainty

Expert A made no suggestions for reducing the uncertainty.

Expert B's Elicitation

Peach Bottom Reactor Building Decontamination Factor

Description of Expert B's Rationale/Methodology

Expert B's approach attempted to meet what he felt to be two basic requirements for his analysis:

1. A number of calculations with mechanistic accident analysis codes (the STCP, MAAP, etc.) have been performed for various accident sequences, at least for the Peach Bottom plant. Expert B believed that these codes combine evaluation of the boundary and initial conditions for radionuclide transport and deposition within the reactor building, together with treatments of many of the phenomenologies involved, to a degree that no simple standalone separate-effects calculations could ever do. Hence, he believed that any uncertainty methodology should incorporate the information represented by the code calculations as directly as possible.

2. A number of important uncertainties in the code calculations were believed to exist, in part because of phenomenological uncertainties in code modeling. Hence, any uncertainty methodology should explicitly account for the more important modeling uncertainties that might affect the code results. Since these uncertainties can involve limitations of the code models themselves, some of them are not readily investigated simply by performing sensitivity studies with the codes, even if it were feasible to perform any desired number of such sensitivity studies.

To meet these needs, Expert B devised a two-step process for developing uncertainty distributions for the reactor building DF. The first step was to develop what he called a "base distribution" using the results of code calculations. The second step was to make substantial changes to the base distribution to account for the uncertainties that he believed could have potentially important effects upon the code calculations.

Development of Base Distributions

Expert B relied primarily upon the following code calculations in constructing his base distributions:

- MAAP results for Peach Bottom[B-1], which gave a wide range of DFs, 1.3 to about 50. When there were two openings to the reactor building, one to the refueling bay and one to the steam tunnel, a "chimney" effect developed in the MAAP calculations and the DFs were quite small, 1.3 to 2.8. When only one of the two paths was open, the DFs were much larger, 6.8 to 63. In addition, DFs were somewhat smaller for cesium and iodine than for other species.

- STCP calculations[B-2] using a single-volume representation of the reactor building, which gave small DFs, 1.1 to 2.9. Hydrogen burns played an important role in making the DFs small.

- Calculations by P. Bieniarz using the RMA code* (a modified version of the STCP), which gave DFs in the range 2 to 6, with most results in the range 4 to 6, and with DFs for cesium and iodine somewhat smaller than for other species in some (not all) cases. The assumptions made in these analyses reduced the importance of hydrogen burns in comparison with the STCP results, which may be the principal reason for the larger DFs.

- A MELCOR calculation[B-3] yielded DFs in the range 2 to 4. A "reverse chimney" effect developed in this calculation.

The expert relied heavily upon the MAAP calculations and the sensitivity to the chimney effect these calculations displayed, which he considered to be physically realistic. He therefore developed two subdistributions for his base distribution, one assuming a chimney effect developed and one assuming that it did not. The first was derived by broadening somewhat the distribution of MAAP results in which a chimney effect was involved and included DFs ranging from about 1.05 to about 3. The second was based upon all the other results, including the MAAP results without a chimney effect, and spanned a range of about 1.1 to 25. He was uncertain whether a chimney effect actually would develop in the risk-dominant accident scenarios; so, he combined these distributions with equal weight to derive his base distribution. He expressed his distribution in terms of a release parameter RP = DF-1 (this release parameter is discussed further below). He believed RP should be logarithmically distributed and defined a probability density function (pdf) for ln(RP). He defined one pdf for cesium and iodine and another for all other species; these pdfs did not differ greatly. His base distributions are

DF	ln(RP)	p (Cs,I)	p (others)
1.025	-3.69	0.0	0.0
1.05	-3.00	0.16	0.0
1.1	-2.30	0.16	0.179
1.2	-1.61	0.297	0.307
2.0	0.0	0.297	0.307
3.0	0.69	0.08	0.09
15.0	2.64	0.03	0.09
25	3.22	0.0	0.0

Modification of the Base Distributions

Expert B felt that there were a number of uncertainties that his base distributions did not adequately reflect. These arise both from modeling uncertainties in the codes and from variations in accident scenarios not adequately represented by the available code

*P. Bieniarz, presentation to Source Term Panel on 1/13/88, including handout of report describing work done for the NY Power Authority (Fitzpatrick Plant).

calculations. He decomposed these uncertainties into the following subcategories:

1. Flows of steam and gas into the reactor building, which act to sweep aerosols and radionuclides out of the building. High flows favor low DFs; saturated pools favor high flows. Most available code calculations are for saturated pools. Comparisons with unsaturated pools were based, in part, upon various calculations of steam flow rates (saturated pools) versus CCI gas generation rates.

2. Aerosol generation rates, especially during CCI. High aerosol generation favors rapid agglomeration and aerosol deposition; hence, high DFs. Uncertainties in aerosol generation were estimated from assessments of uncertainties in STCP calculations and converted into uncertainties in aerosol deposition rates using aerosol behavior systematics discussed in Appendix N of Reference B-4.

3. Location of release to the reactor building (at the knuckle versus the torus room) in Peach Bottom. Effective building volume is smaller for knuckle release, favoring somewhat lower DFs.

4. Uncertainties in aerosol agglomeration and deposition rates for aerosol shape factors, turbulent agglomeration, and uncertainty in areas of surfaces available for aerosol settling. Dry atmospheres (subcooled pools) could favor enhanced deposition rates because larger effects of shape factors and turbulent agglomeration upon deposition rates, while wet atmospheres (saturated pools) could result in enhanced deposition rates from steam condensation effects, especially for hygroscopic aerosols. He felt that the steam condensation effects had the largest potential for enhanced DFs associated with rapid aerosol deposition; he therefore believed that enhanced deposition rates were more likely to contribute to increasing the DF for saturated pools than for unsaturated pools.

5. Hydrogen burn uncertainties. Dry atmospheres (subcooled pools) are more favorable to vigorous burns that could sweep aerosols out of the building and, hence, lower the DFs.

To incorporate the estimated effects of these uncertainties into his distributions, Expert B used a simple conceptual model in which the release from the building is controlled by competition between aerosol deposition, represented by a fractional deposition rate λ_a, versus transport out of the building by the flow of steam and gas, represented by the fractional transport rate λ_g. The fraction released from the containment is equal to $\lambda_g/(\lambda_g + \lambda_a)$, and the DF is the inverse of this, $DF = 1 + \lambda_a/\lambda_g = 1 + \tau_g/\tau_a$, where the characteristic time constants (τ's) are the inverse of the λ's. Since the expert believed that the various uncertainties could cause both λ_a and λ_g to vary substantially, he felt that logarithmic distributions would be suitable for describing them and, hence, for describing the distribution of their ratio, which he defined to be his "release parameter" $RP = \lambda_a/\lambda_g = DF - 1$. He therefore converted his

base distributions for the DF into base distributions for RP, assessed the effects of the various uncertainties upon the distribution for RP, and converted back to a distribution for DF to obtain his final results. Note that large values of the release parameter correspond to large values of the DF and, hence, to small values of the release.

For each uncertainty considered, Expert B defined a small number (usually two to four) of discrete levels; that is, he selected two or more values that a parameter representing the uncertainty could take on. For the reactor building DF analysis, this parameter was the factor R by which the uncertainty could alter λ_s or λ_g and, hence, alter RP. He then assigned a weight W to each level; that is, a subjective probability that the parameter R would actually take on a value close to the value representing each level.

The R values developed by Expert B are multiplication factors, that may be applied directly to the RP distributions he derived from the code calculations. He converted the base pdf for RP that was given above into a cumulative distribution function and then modified the base CDF for RP using a "decomposition tree" structure that allowed for all possible combinations of the levels defined for all the uncertainties considered. Each of the endpoints of the tree yields a reproduction of the base CDF for RP shifted by an amount equal to the product of the R values assigned to the branches corresponding to the particular path taken through the tree. The weight assigned to this endpoint is equal to the product of the W values assigned to each of the branch points. The final distribution for RP was formed by combining the weighted distributions for all the tree end points. This distribution was then converted back to a distribution for RP using Eq. (1).

Expert B's decomposition tree is illustrated schematically in Figure B-1. The figure is drawn for a case in which five uncertainties are considered, with four levels being defined for the first uncertainty and three levels for the other four uncertainties, yielding 324 endpoints for the entire tree. (Most of the decomposition trees the expert used for the reactor building DF issue had somewhat fewer branches than the example shown in the figure.) Each branch point is associated with an (R,W) pair. The superscripts in the figure refer to the 1st to 5th uncertainties considered. The subscript refers to the level chosen for that uncertainty. A given path through the tree can be represented by the five numbers (jklmn), where

j = level chosen for uncertainty 1,
k = level chosen for uncertainty 2,
l = level chosen for uncertainty 3,
m = level chosen for uncertainty 4,
n = level chosen for uncertainty 5.

In Figure B-1, complete paths and the corresponding (jklmn) values are shown schematically for nine of the 324 endpoints of the tree.

In principle, dependencies between the uncertainties could be accounted for by allowing the R values and/or the W values assigned at any branch point to depend upon which branch had been taken at the previous branch points.

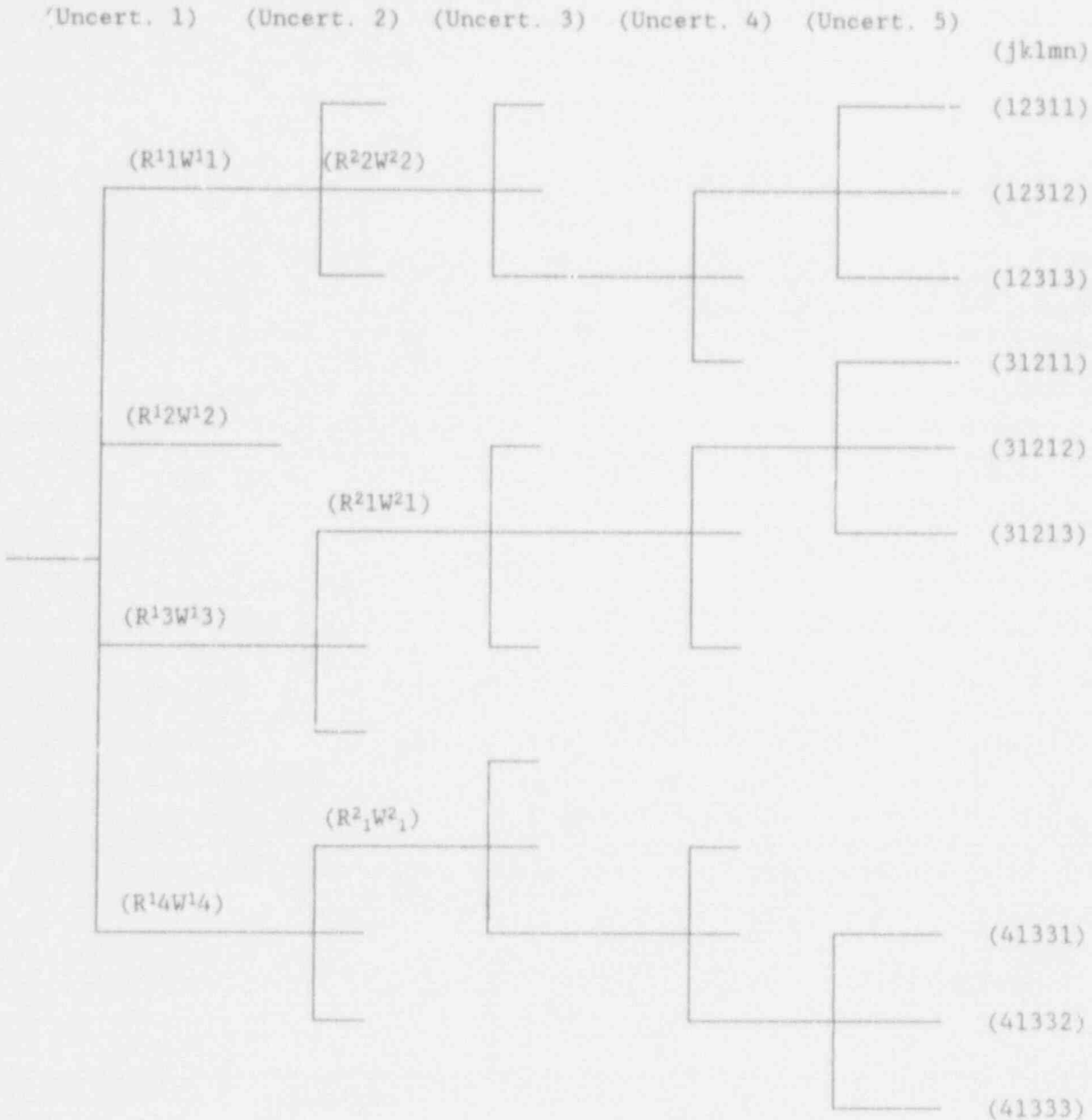

Figure B-1. Schematic of Decomposition Tree Used by Expert B

Practical considerations imposed severe limits upon the degree to which this could actually be done, however. Except where otherwise noted in the discussion of the elicitation results, the various uncertainties were assumed to be phenomenologically independent.

For each endpoint of the tree, a CDF for RP can be generated. This CDF is

$$RP^N(P) = R^1_j R^2_k R^3_l R^4_m R^5_n RP^0(P), \quad (1)$$

where $RP^0(P)$ is the value of release parameter corresponding to the Pth fractile of the base distribution, while $RP^N(P)$ is the value of the release parameter corresponding to the Pth fractile of the distribution for the Nth endpoint of the tree. The weight assigned to this particular result (tree endpoint) is given by:

$$W^N = W^1_j W^2_k W^3_l W^4_m W^5_n. \quad (2)$$

To obtain the final combined distributions, Expert B inverted the endpoint distributions and summed the resulting weighted probabilities corresponding to a given value of RP. Thus:

$$P(RP) = \sum_N W^N P^N(RP). \quad (3)$$

Here, $P^N(RP)$ is the probability that the release parameter will be less than RP for the Nth endpoint distribution, and P(RP) is the probability that the release parameter will be less than RP in the combined distribution. Finally, Expert B converted the combined distribution back into a distribution for the DF, as noted previously.

Expert B's base distributions are given above. The R and W values that he applied to modify his distributions were as follows.

For flow rate uncertainties, subcooled pools:

W = 0.15 0.35 0.35 0.15
R = 1.0 2.5 5.0 10.0

For flow rate uncertainties, saturated pools:

W = .25 0.50 0.25
R = .333 1.0 3.0

For aerosol generation rates:

W = .20 0.35 0.30 0.15
R = .577 1.0 1.73 3.162

For release to the knuckle:

W =	0.5	0.5
R =	0.5	1.0

For uncertainties in aerosol agglomeration and deposition rates:

Subcooled pools:

W =	0.4	0.4	0.2
R =	1.0	2.0	5.0

Saturated pool:

W =	0.3	0.4	0.2	0.1
R =	1.0	2.0	5.0	10.0

For H_2 burns, subcooled pools:

W =	.33	.34	0.33
R =	.30	.50	1.0

Refueling Bay DF

The expert also offered DF distributions for the refueling bay, for use in cases in which the release was directly from the drywell to the refueling bay, bypassing the reactor building. He based these distributions upon two STCP calculations, both of which showed very small DFs (<1.1)[B-2,B-5]. He believed these results were physically reasonable. He believed that it would not be useful to attempt to apply the detailed procedure described above to the refueling bay DF and therefore developed subjective distributions for the refueling bay DF directly from the STCP calculations.

Finally, Expert B emphasized that despite the use of the formalism described here, his distributions should still be viewed as being fundamentally subjective: the W values, in particular, represent subjective probabilities, and even the R values include subjective elements despite the use of code results, experimental results, and stand-alone aerosol calculations where these were available and applicable. Since the expert did consider these distributions to be subjective, he therefore made revisions to the final results when he considered them to be unreasonable in some respect. In general, these revisions were limited to adjustments to the tails of the distributions to modify release fractions he considered to be excessively high or excessively low.

Results of Expert B's Elicitation

The final results are given below.

Case 1: Peach Bottom

	Fractile								
	.01	.05	.1	.25	.50	.75	.9	.95	.99
Gr 2,3*	1.02	1.05	1.09	1.27	1.99	4.88	15.5	32.9	126
Gr 4-9**	1.03	1.08	1.14	1.38	2.27	5.79	18.3	38.2	141

Case 2: Peach Bottom

Gr 2,3*	1.02	1.05	1.09	1.25	1.90	4.56	14.3	30.0	116
Gr 4-9**	1.03	1.07	1.13	1.34	2.15	5.38	16.8	35.0	129

Case 3: Peach Bottom

Gr 2,3*	1.03	1.08	1.14	1.40	2.39	6.36	20.7	44.2	167
Gr 4-9**	1.05	1.12	1.21	1.54	2.78	7.62	24.7	51.4	186

Case 4: Peach Bottom

Gr 2,3*	1.03	1.07	1.13	1.36	2.27	5.92	19.1	40.5	154
Gr 4-9**	1.04	1.11	1.19	1.50	2.62	7.04	22.6	47.1	172

*GR 2, 2 = iodine, cesium

**GR4-9 = tellurium, strontium, ruthenium, lanthanum, cerium, barium.

Refueling Bay DF

For cases in which the release was directly from the drywell head to the refueling bay, Expert B gave the following distribution:

Frac.	0.01	0.05	0.25	0.50	0.75	0.95	0.99
DF	1.001	1.01	1.05	1.1	1.5	3.0	10.0

(All cases: saturated or subcooled pool, Peach Bottom)

Sources of Uncertainty

The R values and W values directly reflect the importance Expert B assigned to the uncertainties that he explicitly included in his decomposition tree, discussed in connection with Figure B-1. He thought uncertainties reflected in his base distributions were important, including especially the question of whether there would or would not be a chimney effect. Unlike the situation for a number of other issues, he believed that uncertainty resulting from the need to group together a range of accident scenarios in a single "case" could be quite important for this issue. He did not assign great importance to the uncertainty in the surface areas available for settling, as CONTAIN calculations he had performed indicated this would be important only when aerosol densities were quite low.

Correlation with Other Variables

Expert B believed that other things being equal, high FCCI values would correlate with high aerosol densities in the reactor building. Since he believed that high aerosol densities favored larger DFs, other things being equal, he expected that there would be some positive correlation between the DF and FCCI. However, he believed that substantial additional effort would be needed to define such correlations quantitatively (if it could be done at all) and that simply guessing at the correlations could do more harm than good. Hence, Expert B did not specify any correlations between the reactor building DF and other variables.

Suggested Methods for Reducing Uncertainty

Expert B believed that uncertainties in the reactor building DF could be significantly reduced if it were possible to define the dominant accident scenarios more accurately and then perform detailed code calculations, with a carefully designed nodalization of the reactor building, for the specific scenarios of interest. Determining whether there would be one or two openings to the reactor building would be especially helpful, because the chimney effect requires two openings, and he believed this to be one of the more important uncertainties. Improved modeling of counter-current flow through a single, large opening is also needed (the NRC codes do not directly model counter-current gas flows, although MAAP does.) Aerosol modeling improvements needed include better definition of shape factors, turbulent agglomeration (including models for turbulent intensities), and improved modeling of steam condensation on aerosols, especially hygroscopic aerosols. On the whole, however, he felt that uncertainties in the thermal-hydraulic conditions (and perhaps uncertainty in the aerosol sources) were probably more important than the uncertainty in the aerosol modeling, given accurate thermal-hydraulics and aerosol sources.

REFERENCES

B-1. Ed Fuller to D. C. Williams, Letter on Peach Bottom MAAP analysis for Station Blackout, March 14, 1988.

B-2. R. S. Denning et al., "Radionuclide Release Calculations for Selected Severe Accident Scenarios," Vols. I-V, NUREG/CR-4624, BMI-2139, Battelle Memorial Institute, 1986.

B-3. S. E. Dingmon et al., "Analysis of Peach Bottom Station Blackout with MELCOR," SAND86-2129C, Sandia National Laboratories, 1986.

B-4. R. J. Lipinski, D. R. Bradley, J. E. Brockman et al., Appendix N of "Uncertainty in Radionuclide Release Under Specific LWR Accident Conditions," Vol. II, SAND84-0410, Sandia National Laboratories, 1985.

B-5. M. T. Leonard et al., "Supplemental Radionuclide Release Calculations for Selected Severe Accident Scenarios," NUREG/CR-5062, BMI-2160, Battelle Memorial Institute, 1987.

Expert C's Elicitation

Peach Bottom Reactor Building Decontamination Factor

Description of Expert C's Rationale/Methodology

Expert C collapsed the nine radionuclide groups in the previous section into the following three groups: cesium and iodine, tellurium, and nonvolatiles. The expert's approach was to determine which parameters were important, to perform a scoping study on the important parameters to estimate the DFs for them, and to estimate the range of credible DFs for the reactor building. This information was then used as a starting point for the six cases in this issue. The values were then adjusted based on attributes for each case.

Expert C felt that aerosol behavior, residence time, removal mechanisms, and the building compartmentation would be important parameters affecting decontamination factors. On the other hand, the expert assumed that both chemistry and chimney effects would be negligible in the secondary containment.

Parameters that the expert felt were important to aerosol behavior were the shape factor, particle density, concentration, initial distribution, and agglomeration. It was the expert's opinion that the size of the particulates is less than or equal to "classical" laminar sublayer, which would lead the particle to behave as a sphere. The expert bases his opinion on Reference C-1, which indicates that the formation of crystallites-to-agglomerates-to-flocs does not produce "sharp-edge" aerosols. In addition, the expert referenced results from the STEP experiment,* which suggest that the aerosols had spherical shapes. He felt the shape factor would range from 1 to 1.5. However, parametric studies by Stone and Webster with NAUA-MOD 4 showed no significant effect on leakage for shape factors in the range from 1 to 2. Expert C thought that the particle density would range from the density of water to the density of structural material with a particle porosity of 50%. That is, the density would range from 1 g/cc to 4 g/cc. He felt that the aerosol entering the reactor building would be "aged" and, therefore, would have a stable distribution. Calculated standard deviations in GREST[C-2] range from 1.8 to 2.2. Thus, the standard deviation of the distribution would be approximately 2.

Parameters that Expert C felt would affect the residence time were the gas flow rates and the presence of hydrogen burns.

Removal mechanisms that were important were gravitational settling and diffusiophoresis. Factors cited that would affect gravitational settling were atmospheric dryness or condensing and hygroscopic effects.

---

*B. J. Schlenger et al., "Characteristics of Releases from TREAT Source-Term Experiment STEP-1," presented at the ANS Winter Meeting, Washington D.C., November 1986.

To estimate the decontamination factor of the various parameters Expert C performed a scoping study. His approach was to establish a base case, evaluate base parameters, and then consider the effects of additional parameters that were not analyzed in the base case. In the base case, it was assumed that there was no condensation on the particles, no Stephan flow, and no hydrogen burns. Also, the reactor building was modeled with a single volume. Three base parameters were evaluated that included the DF for a simple aerosol, DF_A, the DF attributed to settling height, DF_H, and the DF attributed to residence time, DF_R. The base parameters were evaluated using Stone and Webster's modified version of NAUA-4. The base case was evaluated for four sets of input variations. The base case inputs for the four subcases are shown in Table C-1 along with the calculated DFs. Based on these calculations the expert estimated that DF_A is 1.5, DF_H is 3 and DF_R is 1.5. He felt, furthermore, that based on these results the effect of aerosol loading was negligible.

Table C-1
Base Case Input Parameters and Calculated DFs

Input Parameter	Case 1	Case 2	Case 3	Case 4
Containment Volume (m^3)	5000	5000	5000	5000
Analysis Time (h)	10.0	10.0	10.0	10.0
Geometric Radius (μ)	0.2	0.5	0.5	0.5
Standard Deviation	1.65	2.1	2.1	2.1
Particle Density (g/cm^3)	2.0	3.0	3.0	3.0
Height (m)	10.0	3.3	3.3	3.3
Source* (g/s)	10.0	10.0	10.0	30.0
Leakage**	Type 1	Type 1	Type 2	Type 2
Decontamination Factor (DF)	1.5	4.7	7.0	7.5

*Source rate is for 1 h.
**Leakage terms :

Type 1		Type 2	
Time (h)	Leakage (% Vol/Day)	Time (h)	Leakage (% Vol/Day)
0.0	10000	0.0	1000
0.5	1000	5.0	100
1.0	1000	10.0	100
10.0	1000		
Average residence time in 5 h:			
1.75		4.3	

Next, Expert C estimated the DFs for five additional parameters. The five parameters were diffusiophoresis (DF_D), condensation on particles (DF_c), hygroscopic effect (DF_{Hy}), multi-volume effect (DF_m), and hydrogen burn (DF_{HB}).

Diffusiophoresis aerosol removal is always "competing" with leakage and gravitational settling. From Stone and Webster's parametric studies, in support of Reference C-3, the expert was able to single out the effect of diffusiophoresis and concluded DF_D would be in the range from 1.2 to 1.4. Furthermore, he cites GREST calculations[C-2] that show diffusiophoresis is significant but is not the dominant removal term. Therefore, DF_D will probably be approximately 1.3.

Expert C indicated that for particles above a critical radius (1 to 2 μ), condensation on them causes fast growth. As the particle grows from 1 to 10 μ, the settling velocity (in air) increases by a factor of 20. Additionally, the expert stated that results from various experiments have indicated that condensing atmospheres substantially increased the rate of gravitational settling. Thus, the expert estimated that DF_c would be 2.

The expert believed hygroscopicity affected aerosol removal behavior in two ways: it reduced the critical radius below 0.01 μ, and it substantially accelerated the condensation rate. To support this position, he referred to conclusions from Reference C-4, which indicated that for CsOH solutions, condensation can occur in even highly superheated conditions and that near-saturated conditions particle growth and settling is rapid. The expert assigned a value of 10 to DF_{Hy}.

The DF attributed to the multi-volume effect was assigned a value of 1.5 in Reference C-3. The expert agreed with this conclusion.

Expert C indicated that a hydrogen burn has the potential of removing all airborne aerosols. However, he believed that stripping off the aerosols already settled out probably would not happen. Based on Reference C-5, the estimated saltation velocity is on the order of 100 ft/s. He believed it was very unlikely to have such conditions in a closed volume. He assigned DF_{HB} a value of 0.5, which reflects his belief that not more than 50% of the fission products will be airborne during a hydrogen burn.

The estimated values of the parameters (i.e., DF_A, DF_B, etc.) were treated as maximums, and thus, the parameter could vary from 1 to its maximum value. The overall DF was obtained by multiplying all the individual DFs together. To do this, the expert created a tree that had a branch point for each DF. The minimum value (1) was on one branch and the maximum value (the value of the individual DF) on the other branch. The expert assumed each branch was equally likely. Thus, he was able to propagate the uncertainty for each DF through the tree. He grouped the result from each branch endpoint and generated a probability distribution function, pdf, for the reactor building DF. The pdf for the reactor building DF is presented in Table C-2.

Table C-2
Reactor Building DF Likelihood
(Based On Scoping Study)

Likelihood	Rx Bldg DF
0.13	1.5
0.16	2.0
0.55	5.0
0.16	>10

Expert C used the results from the scoping study to assess which parameters were important to this issue, to determine the magnitude of the DF associated with the various parameters, and to indicate the range that the reactor building DF should be in.

Results of Expert C's Elicitation

Expert C provided distributions for the cesium and iodine group first and then gave results for the nonvolatile group. He had no reasoning for tellurium but felt that it would be between cesium/iodine and the nonvolatiles. The median value for the tellurium group is the average of the cesium/iodine group median value and the nonvolatile group median value. The minimum value for the tellurium group corresponds to the minimum value for the cesium/iodine group. Similarly, the maximum value for the tellurium group corresponds to the maximum value for the non volatile group.

The DFs for the cesium/iodine group are lower than the DFs for the nonvolatile group because the cesium/iodine group is released earlier and at a higher flow rate than the nonvolatile cesium/iodine group. The nonvolatiles follow the volatiles by approximately half an hour and therefore have a long residence time.

The cases that have saturated steam conditions benefit from condensation and therefore have higher DFs than the subcooled cases. For the subcooled cases the expert assumed that the concentration of steam in the reactor building at the rupture location was less than 10%. For the saturated cases, he assumed that the steam concentration at the rupture location was 90% or more.

Cases in which the rupture occurs in a location such that there are several compartments to go through before being released to the atmosphere will have higher DFs than cases that have a relatively short path to the atmosphere. Therefore, cases with ruptures that lead directly to the refueling bay have very little chance of having a large DF, whereas ruptures that lead to the torus room, and must travel a more tortuous path, have correspondingly higher DFs.

The results for Cases 1 through 6 are presented in Table C-3.

Table C-3
Reactor Building DFs

Case	Quantiles 0.00	0.05	0.50	0.95	1.00
			Cesium and Iodine Group		
1	1.5	2.0	3.0	5.0	8.0
2	1.5	2.0	4.0	6.0	100.0
3	1.5	2.0	3.0	4.0	10.0
4	2.0	3.0	5.0	10.0	100.0
5	1.0	1.2	1.5	1.8	2.0
6	1.0	1.5	2.0	2.5	3.0
			Tellurium Group		
1	1.5	2.0	3.5	6.0	10.0
2	1.5	2.0	4.5	8.0	100.0
3	1.5	2.0	3.5	6.0	10.0
4	2.0	3.0	5.5	10.0	100.0
5	1.0	1.3	1.7	2.0	2.5
6	1.0	2.0	2.5	3.0	3.5
			Nonvolatile Group		
1	1.5	3.0	4.0	6.0	10.0
2	1.5	3.0	5.0	10.0	100.0
3	1.5	2.0	4.0	5.0	10.0
4	2.0	4.0	6.0	10.0	100.0
5	1.0	1.5	2.0	2.5	3.0
6	1.0	2.0	3.0	3.5	4.0

Sources of Uncertainty

Expert C felt that the major sources of uncertainty were the rather coarsely defined initial conditions, the flow rates of the carrier gas (affects residence time) and the effects of a hydrogen burn.

REFERENCES

C-1. C. E. Lapple, "Particle-size Analysis and Analyzers," Chemical Engineering, May 20, 1968.

C-2. H. A. Morewitz et al., "Results of GREST Code Comparison Exercise," SINDOC(85)157, August 19, 1985.

C-3. American Nuclear Society, "Report of the Special Committee on Source Terms," American Nuclear Society, LaGrange, Illinois, September 1984.

C-4. A. Drozd and J. Baron, "Hygroscopic Aerosol Growth at Near Saturated Conditions," in Proceedings of Water-Cooled Reactor Aerosol Code Evaluation and Uncertainty Assessment Workshop, pp. 291-302, Brussels, Belgium, September 9-11, 1987.

C-5. F. A. Zenz, "Conveyability of Materials of Mixed Particle Size," Industrial and Engineering Chem. Fund., Vol. 3, p. 65, 1964.

Expert D's Elicitation

Peach Bottom Reactor Building Decontamination Factor

Description of Expert D's Rationale/Methodolgy

No retention or deposition in the reactor building is considered for the noble gas group. Therefore, the reactor building DF for noble gases is set to 1.0 for all cases.

The mean residence time of an aerosol inside the reactor building is considered to be the main variable in determining the reactor building DF value, which in turn is dominated by the volume of reactor building. For the case PB-3, the aerosol is assumed to be released from the containment into the torus room. It goes up the elevator shaft, which could connect with all floors of the reactor building, goes up to the refueling bay, and then is released into the environment. Expert D estimated that for the PB-3 case, the reactor building volume would be about 50% larger than that for PB-1 case.

The remaining eight groups are treated the same because other uncertainties overwhelm the differences among different radionuclide groups. The suppression pool is subcooled or saturated at the time of containment failure and is treated the same as the DF values of the reactor building because the uncertainties of other phenomena are more important than the suppression temperature.

Reactor building DF values calculated by the STCP in BMI-2104 and BMI-2139 are used by the expert as the references for assessing the mean values of reactor building DF. The expert also used his experience in experimental data on aerosol transports to set the upper and lower bound values of reactor building DF.

Results of Expert D's Elicitation

PB-1: Drywell Rupture and Suppression Pool Subcooled

The expert used this as the "base case." The median value (50th percentile) of 2 is based on the range of reactor building DF values in BMI reports (1.2 to 5). The first percentile value of 1.1 is based on the expert's personal experience and the observation that in most aerosol deposition experiments with reasonable flow, the aerosol loss is unlikely to be less than 10%. The lower bound reflects the smaller particle size, the chimney effect, and the large flow rate and resuspension from hydrogen burn. It also reflects the uncertainty in aerosol size distribution and the belief that at least 10% of the aerosol entering the reactor building is in a size range that makes it easily removable by deposition on building surfaces. The 99th percentile value of DF = 10 is based on the belief that the upper bound is unlikely to be more than a factor of 2 larger than that (DF = 5) calculated in the BMI reports.

This upper bound reflects the large particle size and about 50% humidity assumptions. The estimate is also consistent with the expert's personal experience and with the observation that in most practical situations with aerosols of a nonuniform size distribution, at least 10% of the aerosol mass would be in a size range that would make it difficult to remove by deposition. The 25th and 75th percentile values are interpolated using a geometrical method. Table D-1 and Figure D-1 show the cumulative distribution function of reactor building DF for this case.

Table D-1
Cumulative Probability Distribution for Reactor Building DF
Peach Bottom Case PB-1

Cumulative Probability (%)	Reactor Building DF
1	1.1
25	1.5
50	2
75	5
99	10

PB-2: Drywell Rupture and Suppression Pool Saturated

Same as that for PB-1.

PB-3: Drywell Shell Melt-Through and Suppression Pool Subcooled

Table D-2 and Figure D-2 show the cumulative distribution function of reactor building DF for the PB-3 case. The rationales for the upper bound and the lower bound for this case are the same as those for PB-1. However, the median value of reactor building DF for this case was assessed to be a factor two larger than that of PB-1. The expert reasoned that the aerosol would have to travel through a larger volume before being released to the environment, since the release path for this case would be from the drywell into the torus room first. Since the retention fraction increases as a square of volume, the expert assigned the 50th percentile value of 4 for PB-3.

Pb-4: Drywell Shell Melt-Through and Suppression Saturated

Same as that for PB-3.

PB-5: Drywell Head Leakage and Suppression Pool Subcooled

Same as that for PB-1.

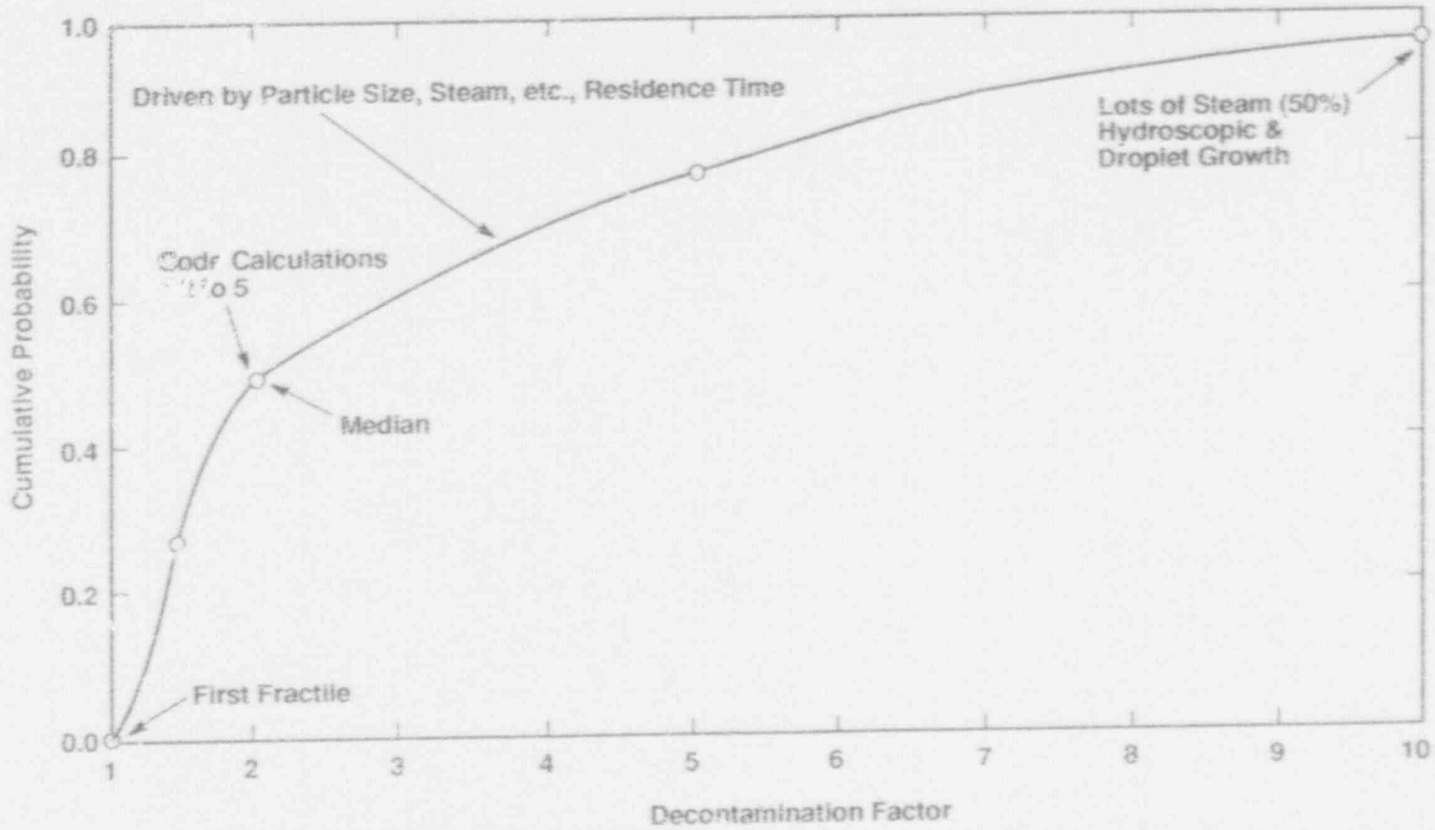

Figure D-1. Cumulative Distribution Function for Reactor Building Case PB-1.

The expert cited the following two reasons for assigning PB-5 the same as PB-1.

1. Since PB-5 involves a leakage instead of a catastrophic rupture, its source rate of aerosol from drywell into the refueling bay would be smaller than that of PB-1. Therefore, the mean residence time of PB-5 would be larger than that of PB-1. On the other hand, the volume of the refueling bay is smaller than that of PB-1; so, the mean residence time would be smaller. These two factors counteract each other.

2. The other uncertainties considered by the expert would tend to overwhelm the differences between PB-1 and PB-5.

PB-6: Drywell Head Leakage and Suppression Pool Saturated

Same as that for PB-1.

Table D-2
Cumulative Probability Distribution for
Reactor Building DF; Peach Bottom Case PB-3

Cumulative Probability (%)	Reactor Building DF
1	1.1
25	3.
50	4
75	6.6
99	10

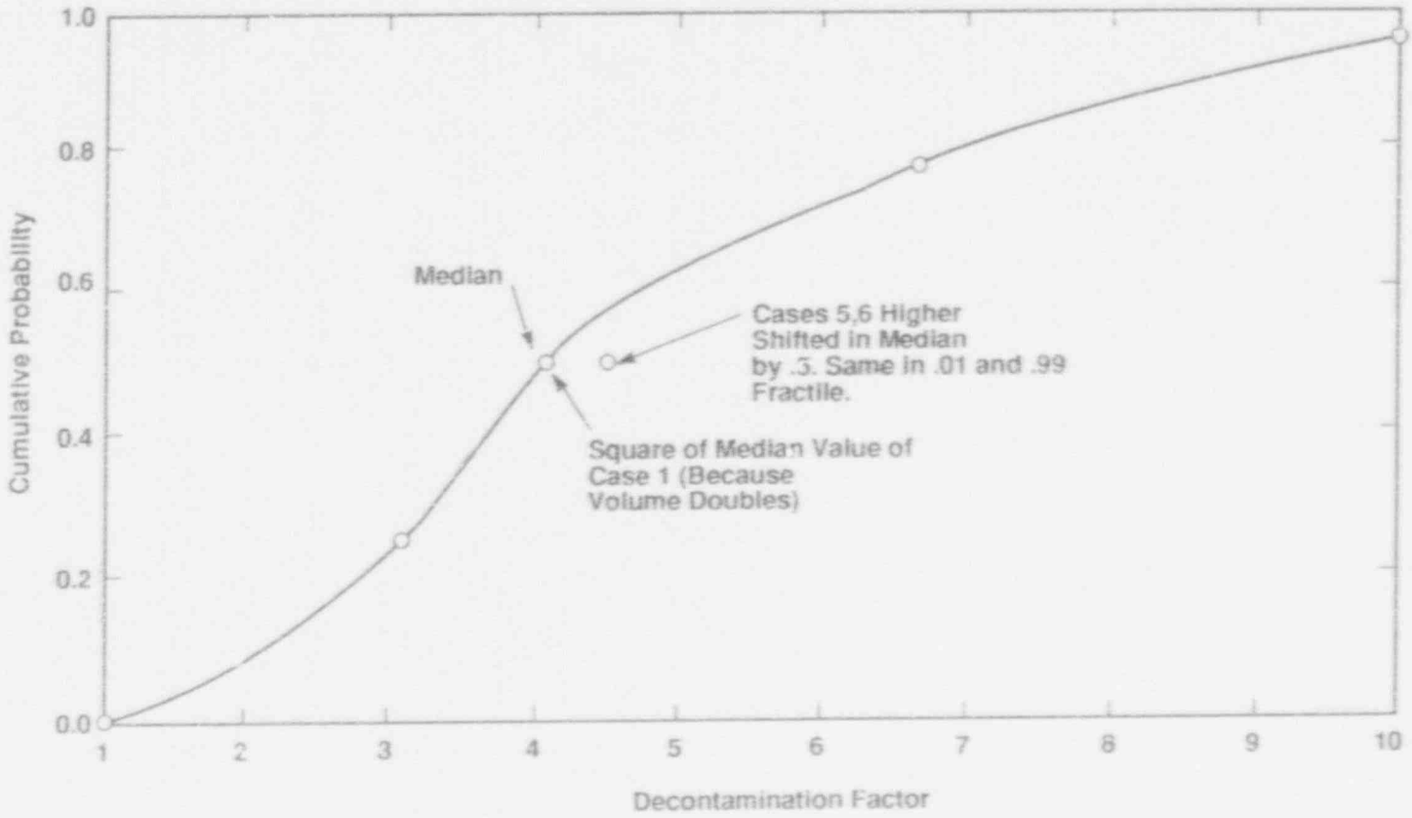

Figure D-2. Cumulative Distribution Function for Reactor Building Case PB-3.

Sources of Uncertainty

The sources of uncertainty considered are the occurrence and effects of hydrogen burn, the aerosol size distributions, and the potential presence of chimney effect from opening of both blow-out panels at the refueling bay and reactor building/turbine building.

Correlations with Other Variables

None.

5.8 Radionuclide Release Associated with Pressure Driven Melt Expulsion from the Reactor Coolant System.

Summary and Aggregation of Source Term Issue 8
FDCH

Experts consulted: Robert Henry, Fauske and Associates; Ben Y. H. Liu, University of Minnesota; David Williams, Sandia National Laboratories.

Issue Description

This issue characterizes the current uncertainty in the radionuclide release for the pressure-driven expulsion of melt from the RCS and subsequent dispersal of the core debris. These characteristics are described by the parameter FDCH in the parametric source term model. $FDCH_i$ is defined as the fraction of the inventory of radionuclide group i present in melt participating in pressure-driven melt expulsion that is released to containment as a result of pressure-driven melt expulsion. The quantity added to the in-containment source term is

$$(1.0-FCOR_i)*(FME)*(FDCH_i)$$

where

$FCOR_i$ = fraction of the initial inventory of nuclide i that is released from the fuel to the vessel before vessel breach

FME = fraction of core debris participating in pressurized melt ejection.

Summary of Rationale

Expert A constructed distributions that were based on a model he developed. This model considered the following first-order terms: (1) mass of material (debris) ejected, (2) RPV failure size, (3) primary system pressure, (4) containment geometry, and (5) extent of entrainment of the debris into the gas flow from vessel breach. In this model the expert assumed isothermal choked flow from the vessel breach and calculated the lower bound gas velocity necessary to entrain debris using a critical Weber number criterion. He also assumed that all entrainment occurs within the cavity and occurs within 1 s.

Expert B constructed a base distribution using results calculated with three different models for the DCH release of thermochemical vaporization:

> Model 1 estimated release fractions based on the rate of vaporization of each species and the residence time of debris particles within each containment volume, assumed that the debris particles maintained a constant temperature within each of three compartments, and assumed a vaporization rate with an Arrhenius dependence upon temperature.

Model 2 estimated release fractions based on the rate of vaporization of each species and the residence time of debris particles within each containment volume, accounted for transient heatup and cooldown of particles following ejection, and integrated the vaporization rate over the particles' thermal history.

Model 3 assumed equilibrium conditions rather than relying on rate calculations; each compartment was assumed to saturate at the relevant temperature by each fission product species. The rate at which new (unsaturated) gas entered the compartment, thereby permitting additional vaporization to occur, was taken into account.

The CONTAIN code was used to supply thermal-hydraulic boundary conditions for the calculations.

He then modified the base distribution to incorporate additional uncertainties: (1) the temperature of the core debris, (2) the oxygen potential experienced by the reacting debris, (3) miscellaneous model parameters (residence time of a debris particle in the containment atmosphere, particle size, and the mass transfer effectiveness), (4) the free energy for formation of rare species for which little or no data are available, and (5) the activity coefficients for the various species of interest. The distributions were also modified to account for aerosolization by mechanical fragmentation processes.

Expert C cited three possible aerosolization processes for fission products: (1) effervescence, (2) punch through, and (3) atomization by gas rushing of the melt. These processes produce particle sizes in three ranges (10 μ, 10 μ to 500 μ, and 500 μ to 1 mm). The particles in the largest size range would be expected to fall out of the containment atmosphere. The Expert took the sizes of the particles into account in formulating his distribution.

Expert C felt that chemical processes were not important in FDCH because the event occurs so rapidly that diffusion/mixing rates limit the amount of oxidation. He also felt that the material atomized later would scrub out earlier atomized material because of the confined volume. The expert felt that the high release fractions observed experimentally would not scale to reactor size.

Method of Aggregation

The following assumptions were made to reform Expert A's results for aggregation:

1. Figure A-1 in the individual elicitation narrative was used to represent the Zion and the Surry high pressure cases (17 MPa) and the BWR case.

2. Figure A-2 was used to represent the Zion and the Surry low pressure cases (7 MPa) and the Sequoyah high pressure case (17 MPa).

3. Figure A-3 was used to represent the Sequoyah low pressure case (7 MPa).

4. The release fractions from Figures A-1, A-2, and A-3 were assumed to be appropriate for all radionuclides except the noble gases and cesium and iodine.

5. The release fraction for the noble gases and cesium and iodine were assumed to be 1.0.

The following assumptions were made to reform Expert B's results for aggregation:

1. The values were assumed to be valid for all scenarios and all plants.

2. The release fraction for the noble gases was assumed to be 1.0. (The expert disagreed with this assumption and values were changed in the elicitation. Unfortunately for timing reasons, the original assumption was propagated through the analyses.)

The following assumptions were made to reform Expert C's results for aggregation:

1. The values presented in the elicitation were taken to be valid for all scenarios and all plants.

2. The release fractions for cesium and iodine were assumed to be 1.0.

All assumptions were approved by the experts (except for Expert B, assumption 2.)

Aggregated Results

Table 8-1 through 8-7 on the following pages present the aggregated results.

Table 8-1
FDCH Aggregate: Zion, High Primary Pressure Case, 17 MPa

Radionuclides	Quantile										
	0.000	0.010	0.050	0.100	0.250	0.500	0.750	0.900	0.950	0.990	1.000
Ce	0.00001	0.00004	0.00023	0.00047	0.00144	0.00576	0.02241	0.05168	0.07421	0.19284	0.35927
La	0.00001	0.00004	0.00023	0.00047	0.00144	0.00576	0.02241	0.05166	0.07381	0.14545	0.24162
Ba	0.00001	0.00004	0.00023	0.00047	0.00170	0.00895	0.04014	0.08675	0.42799	0.66000	1.00000
Sr	0.00001	0.00004	0.00023	0.00047	0.00144	0.00692	0.02713	0.08111	0.30899	0.77000	1.00000
Te	0.00008	0.00013	0.00042	0.00080	0.00400	0.00753	0.01333	0.04579	0.06562	0.09333	0.10357
Ru, Mo	0.00001	0.00008	0.00032	0.00067	0.00329	0.01476	0.05143	0.17170	0.35000	0.70000	1.00000
Cs, I	0.00669	0.03000	0.15000	0.35000	0.90000	0.93571	0.97143	0.99286	1.00000	1.00000	1.00000
Noblas	1.00000	1.00000	1.00000	1.00000	1.00000	1.00000	1.00000	1.00000	1.00000	1.00000	1.00000

Table 8-2
FDCH Aggregate: Zion, Low Primary Pressure Case, 7 MPa

Radionuclides	Quantile										
	0.000	0.010	0.050	0.100	0.250	0.500	0.750	0.900	0.950	0.990	1.000
Ce	0.00001	0.00004	0.00016	--	0.00071	0.00319	0.01583	--	0.06677	0.19284	0.35927
La	0.00001	0.00004	0.00016	--	0.00071	0.00319	0.01583	--	0.06641	0.14545	0.24162
Ba	0.00001	0.00004	0.00016	--	0.00171	0.00556	0.02737	--	0.42799	0.86000	1.00000
Sr	0.00001	0.00004	0.00016	--	0.00071	0.00323	0.02044	--	0.30899	0.77000	1.00000
Te	0.00009	0.00011	0.00020	--	0.00100	0.00601	0.00964		0.09000	0.09333	0.10574
Ru, Mo	0.00001	0.00008	0.00018	--	0.00091	0.01077	0.04377	--	0.35000	0.70000	1.00000
Cs, I	0.00669	0.03000	0.15000	--	0.90000	0.93571	0.97143	--	1.00000	1.00000	1.00000
Nobles	1.00000	1.00000	1.00000	--	1.00000	1.00000	1.00000	--	1.00000	1.00000	1.00000

Table 8-3
FDCH Aggregate: Surry, High Primary Pressure Case, 17 MPa

Radionuclides	Quantile										
	0.000	0.010	0.050	0.100	0.250	0.500	0.750	0.900	0.950	0.990	1.000
Ce	0.00001	0.00004	0.00023	--	0.00144	0.00567	0.02241	--	0.07421	0.19284	0.35927
La	0.00001	0.00004	0.00023	--	0.00144	0.00567	0.02241	--	0.07381	0.14545	0.24162
Ba	0.00001	0.00004	0.00023	--	0.00170	0.00695	0.04014	--	0.42799	0.86000	1.00000
Sr	0.00001	0.00004	0.00023	--	0.00144	0.00692	0.02713	--	0.30899	0.77000	1.00000
Te	0.00008	0.00013	0.00042	--	0.00400	0.02461	0.20000	--	0.87500	0.97500	1.00000
Ru, Mo	0.00001	0.00008	0.00032	--	0.00329	0.01476	0.05143	--	0.35000	0.70000	1.00000
Cs, I	0.00669	0.03000	0.15000	--	0.90000	0.93571	0.97143	--	1.00000	1.00000	1.00000
Nobles	1.00000	1.00000	1.00000	--	1.00000	1.00000	1.00000	--	1.00000	1.00000	1.00000

Table 8-4
FDCH Aggregate: Surry, Low Primary Pressure Case, 7 MPa

Radionuclides	Quantile										
	0.000	0.010	0.050	0.100	0.250	0.500	0.750	0.900	0.950	0.990	1.000
Ce	0.00001	0.00004	0.00016	--	0.00071	0.00391	0.01583	--	0.06677	0.19284	0.35927
La	0.00001	0.00004	0.00016	--	0.00071	0.00391	0.01583	--	0.06641	0.14545	0.24162
Ba	0.00001	0.00004	0.00016	--	0.00071	0.00535	0.02737	--	0.42799	0.86000	1.00000
Sr	0.00001	0.00004	0.00016	--	0.00071	0.00323	0.02044	--	0.30899	0.77000	1.00000
Te	0.00009	0.00011	0.00020	--	0.00100	0.01635	0.20000	--	0.87500	0.97500	1.00000
Ru, Mo	0.00001	0.00008	0.00018	--	0.00091	0.01077	0.04377	--	0.35000	0.70000	1.00000
Cs, I	0.00669	0.03000	0.15000	--	0.90000	0.93571	0.97143	--	1.00000	1.00000	1.00000
Nobles	1.00000	0.00000	1.00000	--	1.00000	1.00000	1.00000	--	1.00000	1.00000	1.00000

Table 8-5
FDCH Aggregate: Sequoyah High Primary Pressure Case, 17 MPa

Radionuclides	Quantile										
	0.000	0.010	0.050	0.100	0.250	0.500	0.750	0.900	0.950	0.990	1.000
Ce	0.00001	0.00004	0.00016	--	0.00071	0.00319	0.01583	--	0.06677	0.19284	0.35927
La	0.00001	0.00004	0.00016	--	0.00071	0.00319	0.01583	--	0.06641	0.14545	0.24162
Ba	0.00001	0.00004	0.00016	--	0.00071	0.00556	0.02737	--	0.42799	0.86000	1.00000
Sr	0.00001	0.00004	0.00016	--	0.00071	0.00323	0.02044	--	0.30899	0.77000	1.00000
Te	0.00009	0.00011	0.00020	--	0.00100	0.01635	0.20000		0.87500	0.97500	1.00000
Ru, Mo	0.00001	0.00008	0.00018	--	0.00091	0.01077	0.04377	--	0.35000	0.70000	1.00000
Cs, I	0.00669	0.03000	0.15000	--	0.90000	0.93571	0.97143	--	1.00000	1.00000	1.00000
Noblas	1.00000	1.00000	1.00000	--	1.00000	1.00000	1.00000	--	1.00000	1.00000	1.00000

Table 8-6
FDCH Aggregate: Sequoyah Low Primary Pressure Case, 7 MPa

Radionuclides	Quantile										
	0.000	0.010	0.050	0.100	0.250	0.500	0.750	0.900	0.950	0.990	1.000
Ce	0.00001	0.00004	0.00016	--	0.00071	0.00280	0.01056	--	0.06677	0.19284	0.35927
La	0.00001	0.00004	0.00016	--	0.00071	0.00280	0.01056	--	0.06641	0.14545	0.24162
Ba	0.00001	0.00004	0.00016	--	0.00071	0.00448	0.02609	--	0.42799	0.86000	1.00000
Sr	0.00001	0.00004	0.00016	--	0.00071	0.00280	0.01851	--	0.30899	0.77000	1.00000
Te	0.00009	0.00011	0.00020	--	0.00100	0.01000	0.20000		0.87500	0.97500	1.00000
Ru, Mo	0.00001	0.00008	0.00018	--	0.00091	0.00731	0.04351	--	0.35000	0.70000	1.00000
Cs, I	0.00669	0.03000	0.15000	--	0.90000	0.93571	0.97143	--	1.00000	1.00000	1.00000
Noblas	1.00000	1.00000	1.00000	--	1.00000	1.00000	1.00000	--	1.00000	1.00000	1.00000

Table 8-7
FDCH Aggregate: BWR Case: 7 MPs

Radio-nuclides	Quantile										
	0.000	0.010	0.050	0.100	0.250	0.500	0.750	0.900	0.950	0.990	1.000
Ce	0.00001	0.00004	0.00023	--	0.00144	0.00576	0.02241	--	0.07421	0.19284	0.35927
La	0.00001	0.00004	0.00023	--	0.00144	0.00578	0.002241	--	0.07381	0.14545	0.24162
Ba	0.00001	0.00004	0.00023	--	0.00170	0.00895	0.04014	--	0.42799	0.86000	1.00000
Sr	0.00001	0.00004	0.00023	--	0.00144	0.00892	0.02713	--	0.30899	0.77000	1.00000
Te	0.00008	0.00013	0.00042	--	0.00400	0.02461	0.20000		0.87500	0.97500	1.00000
Ru, Mo	0.00001	0.00008	0.00032	--	0.00329	0.01476	0.05143	--	0.35000	0.70000	1.00000
Cs, I	0.00669	0.03000	0.15000	--	0.90000	0.93571	0.97143	--	1.00000	1.00000	1.00000
Nobles	1.00000	1.00000	1.00000	--	1.00000	1.00000	1.00000	--	1.00000	1.00000	1.00000

Individual Elicitations for Issue 8

Expert A's Elicitation

Radionuclide Release Associated with Pressure-Driven Melt Expulsion from the Reactor Coolant System.

Description of Expert A's Rationale/Methodology

Expert A developed a model to calculate best estimates of the release fractions for the nonvolatile fission products. He assumed that the volatile fission products and the noble gases had already escaped from the core. He then provided cumulative distribution functions (CDFs) for the nonvolatile release fractions with the best estimates representing the median value of the distributions.

Model Developed to Calculate Best Estimate Releases

The model developed by the expert considered the following first order terms:

- Mass of material (debris) ejected,
- RPV failure size,
- Primary system pressure,
- Containment geometry, and
- Extent of entrainment of the debris into the gas flow from vessel breach.

Some of the equations used to perform the calculations to address this issue and some of the assumptions made during the calculations are presented below.

1. The gas flow rate in the cavity is calculated assuming isothermal choked flow from the orifice in the vessel using the following relations:

$$M_g = \frac{P_o A_v}{2} \sqrt{\frac{M_w}{RT}} \qquad (1)$$

where

M_g = Mass flow rate of gas (kg),

P_o = Pressure in reactor pressure vessel (Pa),

M_w = Molecular weight,

R = Universal gas constant,

T = Temperature, and

A_v = Area of vessel breach (m^2).

2. The gas velocity in the cavity is calculated using the geometry of the cavity as follows.

$$U_c = \frac{P_o A_v}{2 P_c A_c} \sqrt{\frac{RT}{M_w}}, \qquad (2)$$

where

A_c = surface area of cavity (m^2),
U_c = gas velocity in cavity (m/s).

3. The entrainment is limited by the kinetic energy in the gas available to overcore the surface tension in the debris allowing particulates from the debris to become available for entrainment into the gas flow. The lower bound gas velocity to entrain debris is calculated using a critical Weber number criterion:

$$d = \frac{10 \sigma}{\rho_g U_c^2} \qquad (3)$$

where

g = gravitational acceleration,
σ = surface tension, and
ρ_g = density of gas.

4. The mass of material ejected in the PWR cases is assumed to be 50,000 kg (approximately 40% of the core), and in the BWR cases is 70,000 kg (approximately 30% of the core).

5. The RPV failure size is in the range of 0.1 to 0.3 m in diameter.

6. The primary system pressure is from 2 to 17 MPa (290 to 2470 psi).

. The containment geometry is plant-specific; no generic assumptions can be made.

8. All entrainment occurs in the cavity; outside the cavity, the gas velocities are too low for further entrainment (deentrainment could occur).

9. All activity within the cavity occurs within 1 s.

Results of Expert A's Elicitation

PWR Base Case Calculation

Expert A used the Zion containment geometry to make base case calculations:

1. The gas velocity in the cavity was calculated using Eq. (2) and the following parameters:

   P_o = vessel pressure = 17 MPa

   A_v = area of vessel breach = 0.07 m^2 (from an assumed failure diameter of 0.3 m)

   A_c = surface area of cavity = 12 m^2 (Zion)

   P_c = assumed containment pressure = 0.3 MPa

   $(R*T/M_w)^{0.5}$ = sonic velocity at RPV breach orifice = 500 m/s (R: universal gas constant, T: temperature, M_w: molecular weight)

   U_c = gas velocity in cavity = $[(17*10^6 * 0.07)/(2* 0.3*10^6 * 12)] * 500$ = 80 m/s

2. An energy balance was then performed to calculate how much debris could be entrained; for the debris to be entrained in the gas stream, the gas flowing with a velocity of 80 m/s would accelerate debris particulates at rest to essentially the velocity of the gas stream. This results in a decrease of the gas velocity. It was assumed that the minimum gas velocity to continue the entrainment process would be 30 m/s.

   Energy required to entrain all 50,000 kg of the debris = [50,000 kg * $(30 m/s)^2$] = 23 MJ.

   Mass of gas required to generate 23 MJ by slowing down from 80 m/s to 30 m/s = $Mass_{gas}$ = $(2 * 23 MJ * 10^6)/(80^2 - 30^2)$ = 8400 kg.

   M_g = 1240 kg/s (calculated from Eq.(1)).

   In 1 s, 1240 kg of gas has flowed over the debris; this is about 15% of the mass flow necessary to entrain the entire 50,000 kg of debris. Therefore, about 15% of the debris could be entrained.

3. The expert felt that 10% of the fission products in the material entrained in the gas flow could be released to the containment. The fission products released would be in vapor form initially but would quickly be condensed to an aerosol and would be part of the containment aerosol loading. Debris entrained by the gas stream would be far larger than most aerosols and would quickly settle out.

4. The release fraction of the nonvolatiles, with respect to the initial core inventory, can be estimated as follows:

   $RF = 0.4 * 0.15 * 0.1 = 6*10^{-3}$

   (.4: 40% of core released from vessel; 0.15: 15% of available debris entrained in gas flow from RPV blowdown; and 0.1: amount of fission products in the entrained debris that is released to the containment atmosphere.)

5. A special calculation was made for tellurium; tellurium can be bound within the vessel by zirconium. The release fraction of tellurium can be calculated as follows:

   $RF_{Te} = 0.15 * 0.15 * 0.5 = 1*10^{-2}$

   (0.15: 15% of the debris is entrained into the gas stream (as calculated previously); 0.15: 15% zirconium in the debris (15% of the core is clad), and 0.5: 50% of the Te has reacted with the zirconium.)

   The value is close to that calculated for the nonvolatiles. Tellurium will therefore be considered using the same distributions as the nonvolatiles.

6. It is assumed that the noble gases and the volatiles (cesium and iodine) have already been released.

Zion Calculation Using a Primary Pressure of 7 MPa

A calculation was made using a primary pressure of 7 MPa--all of the other parameters remained the same as in the previous calculation. A gas velocity of about 30 m/s was calculated. From this the expert concluded that a negligible amount of fine scale fragmentation will occur and practically no radionuclides will be released to the containment in this process.

Calculation Using the Sequoyah Cavity Dimensions

Using the methodology already developed:

P_o = 17 MPa

A_v = 0.07 m^2

A_c = 30 m^2

P_c = 0.3 MPa

U_c = 32 m/s

$Mass_r$ = 3.7 * 10^5 kg

$Mass_{entrained}$ < 1 % of mass dispersed

Release fraction = 0.4 * 0.01 * 0.1 = 4 * 10^{-4}

Calculations for BWRs

The expert calculated release fractions only for the BWR high pressure case (7 MPa). This corresponds to a failure of the Automatic Depressurization System (ADS) scenario. The BWR lower pressure scenarios do not produce velocities in the cavity high enough to entrain a significant amount of debris. The parameters used are presented below:

P_o = 7 MPa

A_v = 0.07 m^2

D = 0.3 m

A_c = 3 m^2

P_c = 0.3 MPa

U_c = (7 * 10^6 * 0.07 * 500)/(2 * 0.3 * 10^6 * 3) = 140 m/s

Debris mass is assumed to be 70,000 kg (about 30 %).

Kinetic energy of debris necessary for a velocity of 30 m/s:

KE = (70,000 kg * $(30 m/s)^2$)/2 = 32 MJ,

$Mass_{gas}$ = (2 * 32 * 10^6)/(140^2 - 30^2) = 3420 kg required to entrain 70,000 kg of debris

M_g = 510 kg/s.

In 1 s, 510 kg of gas would have flowed out of the vessel; this is about 15% of the mass necessary to entrain the entire 70,000 kg of debris. About 15% of the debris will be entrained. The mass of debris entrained is 10,400 kg.

The release fraction (percent of core inventory) for the nonvolatiles can be calculated as follows:

$RF = 0.3 * 0.15 * 0.1 = 5 * 10^{-3}$

Release fraction from debris ejected:

$r = 0.15 * 0.1 = 0.015.$

The results are similar to those calculated for the Zion high RPV pressure case. The distribution that applies to the Zion 17 MPa calculation will therefore be used to represent the BWR nonvolatile release fraction.

Development of Cumulative Distribution Functions

The above calculations provided the basis to construct the CDFs found in Figures A-1 to A-3. The values calculated served as medians for the CDFs. The CDFs in Figures A-1 to A-3 represent the release fractions for all radionuclides except the noble gases, cesium and iodine--those are assumed to have already escaped. Tellurium was considered as a special case and is included in the CDFs.

The CDFs do not include the effect of water. The expert felt that water would bring the release fractions down. He suggested a factor of two credit for water cases.

Figure A-1 shows the release fractions for Zion with the primary system at high pressure (17 MPa) and the BWRs with the vessel at 7 MPa. Figure A-2 shows Zion with a primary pressure of 7 MPa and Sequoyah with a primary pressure of 17 MPa. Figure A-3 shows Sequoyah with a primary pressure of 7 MPa.

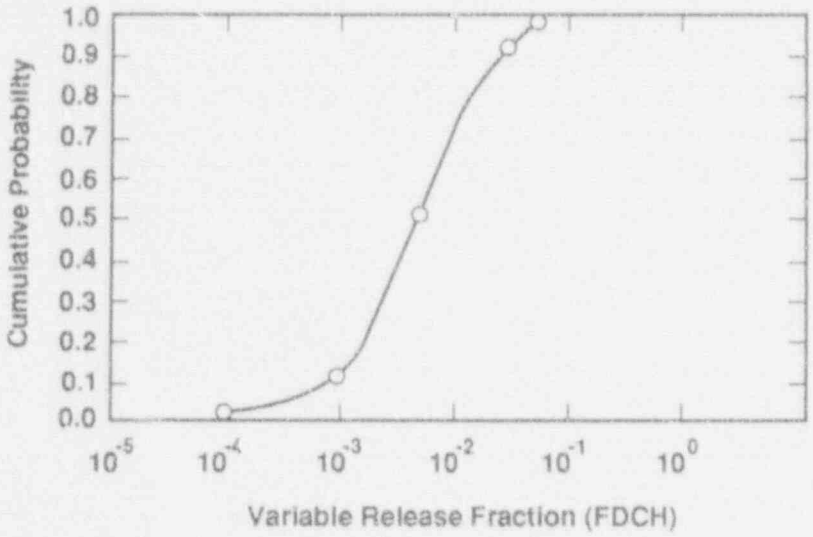

Figure A-1. Zion, No Water, High Pressure.

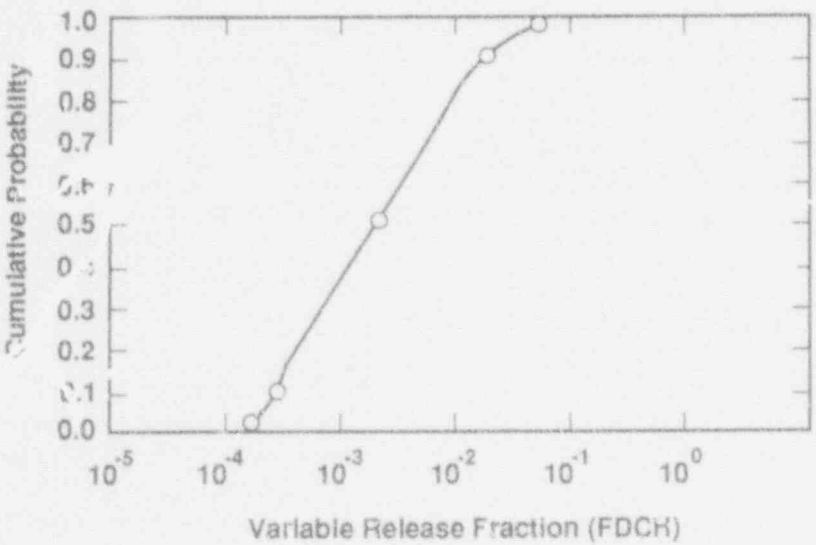

Figure A-2. Zion, Low Pressure.

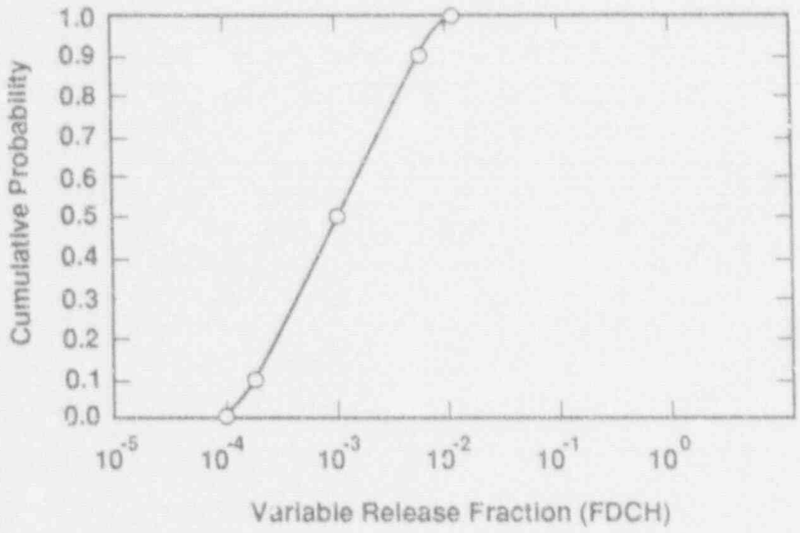

Figure A-3. Sequoyah, Low Pressure.

Expert B's Elicitation

Radionuclide Release Associated with Pressure-Driven Melt Expulsion from the Reactor Coolant System

Description of Expert B's Rationale/Methodology

Expert B considered both thermochemical vaporization and mechanical aerosolization processes in evaluating the release for pressure-driven melt expulsion. Of the two, he believed that only vaporization had the potential to yield large release fractions, and it was also the process that he felt was more amenable to detailed analysis. Hence, he devoted most of his efforts to assessing the vaporization release.

The experts dealing with this issue discussed possible case structures, but no consensus was reached as to its structure; hence, no case structure was provided to the experts for this issue, and it was up to them to decide upon what cases, if any, they consider. Expert B concluded that defining a case structure would not be useful for this issue because he did not feel that the characteristics that might be used to define it would represent the dominant uncertainties; that is, he felt that all cases would be subject to a similar range of phenomenological uncertainties and that these uncertainties were large when compared with possible differences between the various cases. In support of this view he offered the following observations concerning some of the suggestions that were made for defining a case structure:

1. Water that might be in the cavity below the vessel before vessel breach (VB) might be blown out of the cavity before it underwent substantial interaction with the debris. In this event, the distribution for a wet-cavity case would be virtually the same as that for a dry-cavity case. Alternatively, substantial debris-water interaction would possibly occur, in which case Expert B believed that reduced temperatures would result in a reduction in the releases for vaporization. Hence, Expert B, if he were to have defined a wet-cavity case, would have defined two subcases, depending upon whether the water was or was not blown out before substantial interaction, and then combined them to obtain the final wet-cavity case. Since he would have assigned considerable weight (about 50%) to the hypothesis that the water would be blown out of the cavity, the final composite distribution still would not have differed greatly from the dry-cavity case.

2. Expert B agreed that the degree of RCS pressurization could indeed affect the degree to which the debris would be fragmented and dispersed and that this could affect the amount of release. However, he believed that the HPME release would be risk-significant only when the associated DCH loads were sufficient to result in containment failure at the time of DCH; otherwise, even

if containment failure did occur later, most of the aerosol in DCH would have been deposited within containment and would not be released to the environment. Expert B felt that reduced RCS pressure would result in reduced probabilities for containment failure but given the containment failure, conditions corresponding to a relatively severe DCH event had probably developed. These conditions would be similar for intermediate and high RCS pressures. (For similar reasons, Expert B based his entire elicitation upon the assumption that the events of interest were primarily those for which DCH loads were severe enough to threaten containment.)

3. Expert B believed that the amount of unoxidized zirconium in the melt was potentially significant because it could affect both the temperature and the oxygen potential of reacting debris. However, he noted that these effects would be most important for radionuclides that were physically located in the same reacting drop that contained the zirconium. Expert B believed that oxidic species and metallic species would tend to segregate in the vessel and that, for the most part, they would not be found in the same drop; that is, he felt most individual debris drops would be either largely oxide or largely metal, rather than mixed. He believed, therefore, that zirconium content would not have a large effect upon the vaporization of the oxidic species. Of the important metallic species, all except tellurium are very refractory under strongly reducing conditions and would undergo little vaporization until the zirconium had been oxidized. As for tellurium, he believed that it would tend to have large release fractions in any case and that these could not be greatly enhanced by a high zirconium content. Hence, Expert B did not define separate cases based upon zirconium content or upon PWRs vs. BWRs. Instead, he "internalized" the uncertainties for zirconium content in that they were among the factors considered when he assessed the effects of the uncertainties in oxygen potential and temperature upon radionuclide vaporization.

Expert B therefore considered only one case for this issue, except that he provided distributions for Mo and Ru for the PWR large, dry containments that were different from those provided for Sequoyah and the BWRs, for reasons to be noted below.

For the vaporization contribution to FDCH, Expert B constructed what he referred to as a "base distribution" based upon CONTAIN-DCH code results and three simple models for DCH release that he had developed. (CONTAIN-DCH is a version of the CONTAIN 1.1 code[B-1] which has been modified to include models for DCH phenomena.)[B-2,B-3] This distribution is a CDF for each radionuclide group considered. The distribution was constructed using CONTAIN code calculations for the Surry plant[B-3] to supply boundary conditions for the three simple models for DCH release. The base distributions were basically defined to span the ranges given by the three models, except that tails were added to the distributions to acknowledge the existence of alternative modeling assumptions that would have given results larger or smaller than any of those explicitly considered.

These models were based upon the assumption that the vaporization rate would be given by:

$$dN/dt = D\ Sh\ S_d\ (C_0 - C_b)\ /\ d \tag{1a}$$

$$Sh = 2.0 + 0.6\ (Re^{1/2})(Sc^{1/3}) \tag{1b}$$

$$C = P_v/RT \tag{1c}$$

$$P_v = \sum_i \nu_i P_{vi} \tag{1d}$$

In the above, N is the number of moles of the radionuclide species of interest that are vaporized, D is the diffusivity of the radionuclide vapors in the gas phase, Sh is the Sherwood number, S_d is the available surface area of the debris, C_0 and C_b are the gas-phase molar concentrations of radionuclide vapors at the debris drop surface and in the bulk gas, respectively, d is the diameter of the debris drop, and Re and Sc are the Reynolds and Schmidt numbers, respectively. The effective total vapor pressure of the radionuclide P_v is obtained by summing the partial pressures p_{vi} of the various vapor molecular species contributing to the vaporization of the radionuclide, with each vapor species weighted by ν_i, which is the number of atoms of the radionuclide per molecule of the ith vapor species. Total vaporization is obtained by integrating Eq. 1 over time.

In the first of the three models, the integral of Eq. 1 over time was estimated by noting that in many CONTAIN-DCH calculations, the heat capacity of the gas mixed with the debris was initially considerably less than that of the debris and, hence, the gas was calculated to be quickly heated to a temperature close to the debris initial temperature, with the debris cooling relatively little. (Chemical reaction energy also contributed to keeping the debris temperatures high.) In such cases, the calculated debris temperatures remained close to the initial temperature until the debris was transported downstream to compartments further removed from the reactor cavity. In the first model, therefore, the integral of Eq. 1 was estimated by using the temperatures of the high-temperature compartments closer to the cavity and the residence times in these compartments, as calculated by the CONTAIN-DCH code. In addition, it was assumed that $C_b << C_0$, an assumption discussed below.

In some of the CONTAIN-DCH calculations, gas temperatures never reached values as high as the initial debris temperatures. For example, this was true in cases involving co-dispersed water or very large steam supplies, as could arise when a large vessel failure size was assumed. Since vaporization is strongly temperature dependent, the vaporization in these cases would be dominated by the transient period before the drop cooled to the gas temperature. Since the duration of this transient was generally shorter than the compartment residence times considered in the first model, a second model was constructed in which the integral of Eq. 1 was estimated based upon the drop transient thermal response. The latter was estimated from CONTAIN-DCH separate-effects calculations in which it was assumed that

debris drops of various compositions were introduced into a steam-hydrogen atmosphere, and the drop thermal response was calculated. The cases considered included cases in which a high zirconium content resulted in substantial initial temperature increases, before the onset of cooling.

In both of the first two models, it was assumed that C_b, the radionuclide vapor pressure in the bulk gas, was negligible in comparison with the vapor pressure at the particle surface. This will be true whenever the total vaporization is less than that required to saturate the gas, or whenever processes exist that remove vapor from the atmosphere fast enough to maintain $C_b << C_0$. The latter will generally be the case in scenarios for which the second model is applicable, since the lower gas temperatures usually result in vapor recondensation before the vapor partial pressures approach those corresponding to the debris drop vapor pressure. Even when the gas and debris temperatures are about equal, some processes may remove vapor from the bulk gas (for example, the bulk gas and debris surface thermochemical environments (oxygen potentials, etc.) and may be quite different, so the equilibrium vapor pressure in the gas can be lower than that at the drop surface, leading to recondensation in the gas.

When the first model was applied, the amounts vaporized were typically calculated to be greater than the amounts required to saturate the atmosphere in the high-temperature compartments, which were generally relatively small (<1000 m^3) in volume. Since processes rapidly removing the vapor from the atmosphere might not exist, a third model was constructed in which it was assumed that vaporization could initially proceed only until the volumes of the high-temperature compartments were saturated with the radionuclide vapor. Additional vaporization was assumed to occur only at the rate at which the saturated gas was swept out of the compartment and replaced with fresh, unsaturated gas. Again, the various parameters required to apply the model were based upon the CONTAIN-DCH calculations for the Surry plant.

In all three models, the radionuclide vapor pressures required were calculated using the thermochemical data base incorporated into the VANESA code for core-concrete interactions.[B-4] Vaporization processes involving chemical reaction were considered in addition to congruent vaporization processes. That is, in addition to congruent processes such as

$$Ru(d) \longrightarrow Ru(g) \qquad (2a)$$

$$SrO(d) \longrightarrow SrO(g), \qquad (2b)$$

consideration was given to processes in which chemical reaction leads to enhanced vapor pressures, such as

$$Ru(d) + xH_2O \longrightarrow RuO_x(g) + xH_2, \qquad (3a)$$

$$SrO(d) + H_2 \longrightarrow Sr(g) + H_2O, \text{ and} \qquad (3b)$$

$$BaO(d) + H_2O \longrightarrow Ba(OH)_2(g). \qquad (3c)$$

Here, the d and g refer to species in the debris and in the gas phase, respectively. The various chemical reactions considered were essentially those considered in the VANESA code, except that only species in the metal-oxygen-hydrogen systems were considered.

Expert B stated that vaporization of refractory metals and refractory oxides was generally slight except when reactions such as those illustrated in Eq. (3a,b,c) were important. He thus ascribed considerable importance to uncertainties in the oxygen potential at the surfaces of the debris drops.

He then substantially modified his base distributions to allow for uncertainties not included in either the CONTAIN-DCH calculations or in his three DCH vaporization models. The following additional uncertainties were considered:

1. Temperature of the debris during the time of maximum vaporization. This uncertainty includes uncertainty in debris temperature at vessel breach but also includes other factors: heat generation by zirconium-rich debris, the possible need to transport debris to a more oxidizing environment before significant molybdenum and ruthenium vaporization can occur, etc.

2. The oxygen potential at the surface of the reacting/vaporizing debris drops.

3. Miscellaneous model parameters including residence time of a debris particle in the high-temperature environment, particle size, and the mass transfer effectiveness (expressed as the product of the vapor diffusivity and the Sherwood number).

4. The free energy of formation of the various chemical species, for some of which the available data are very limited.

5. The activity coefficients of the various species of interest in the debris.

For each of these five uncertainties, Expert B defined three or more discrete levels (i.e., he selected three or more values that a parameter representing that uncertainty could take on). For the DCH analysis, this parameter was the factor R by which the uncertainty could alter the integral of (Eq. 1). He then assigned a weight W to each level, that is, a subjective probability that the parameter R would actually take on a value close to the value representing each level.

The R values developed by Expert B are multiplication factors, which may be applied directly to the time integrals of (Eq. 1) as evaluated using the three vaporization models. When release fractions are small, these R values could be used to multiply the vaporization fractions themselves. This is not the case when vaporization fractions are large, since doing so would neglect the reduction in vaporization rates as the debris drop becomes depleted in the vaporizing species. In all cases of interest, Expert B found that vapor pressures were approximately proportional to the

concentration remaining in the debris drop. This leads to a simple exponential decay in vaporization rate with time, and the other parameters remaining constant. Hence, Expert B defined a "release parameter" $RDCH_i$, related to $FDCH_i$ by

$$FDCH_i = 1 - \exp(-RDCH_i). \quad (4)$$

He then converted his base distribution for $FDCH_i$ into an equivalent distribution for $RDCH_i$ and applied the R factors to the latter.

The base CDF for $RDCH_i$ was modified using a "decomposition tree" structure, which allowed for all possible combinations of the levels defined for the five uncertainties that were enumerated above. Each of the endpoints of the tree yields a reproduction of the base CDF for $RDCH_i$ shifted by an amount equal to the product of the five R values assigned to the branches corresponding to the particular path taken through the tree. The weight assigned to this end point is equal to the product of the W values assigned to each of the branch points. The final distribution for $RDCH_i$ was formed by combining the weighted distributions obtained for all the tree endpoints. This distribution was then converted back to a distribution for $FDCH_i$ using (Eq. 4).

Expert B's decomposition tree is illustrated schematically in Figure B-1. Each branch point is associated with an (R,W) pair. The superscripts in the figure refer to the first through the fifth uncertainty considered. The subscript refers to the level chosen for that uncertainty. The tree is drawn for the case of the metallic species for which four temperature levels were defined, with three levels being defined for each of the other uncertainties, yielding 324 endpoints for the entire tree. (For the oxidic species, three levels were defined for all five uncertainties, yielding 243 endpoints.) A given path through the tree can be represented by the five numbers (jklmn), where

j = level chosen for uncertainty 1
k = level chosen for uncertainty 2
l = level chosen for uncertainty 3
m = level chosen for uncertainty 4
n = level chosen for uncertainty 5.

In Figure B-1, complete paths and the corresponding (jklmn) values are shown schematically for nine of the 324 endpoints of the tree.

In principle, dependencies between the uncertainties could be taken into account by allowing the R values and/or the W values assigned at any branch point to depend upon which branch had been taken at the previous branch points. Practical considerations imposed severe limits upon the degree to which this could actually be done, however. The only dependency that Expert B considered was a correlation between temperature and oxygen potential for

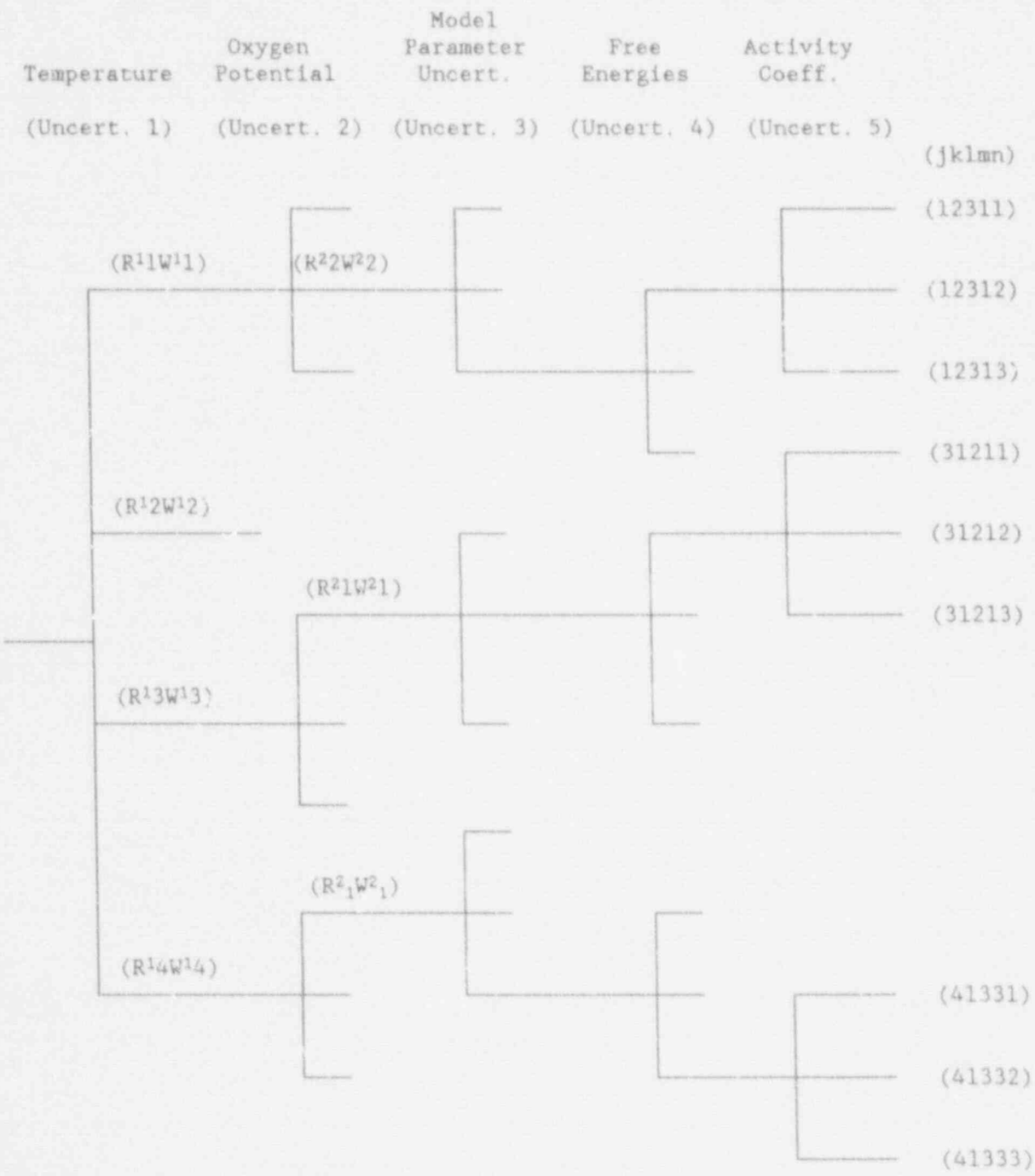

Figure B-1. Schematic of Decomposition Tree Used by Expert B

some radionuclides. (He believed that high zirconium content could tend to yield high temperatures and low oxygen potentials, and that this could result in a negative correlation between these two parameters.) In all other cases, the various uncertainties were assumed to be phenomenologically independent.

For each endpoint of the tree, a CDF for $RDCH_i$ can be generated. This CDF is

$$RDCH_i^N(P) = R^1{}_j R^2{}_k R^3{}_l R^4{}_m R^5{}_n RDCH_i^0(P), \tag{5}$$

where $RDCH_i^0(P)$ is the value of release parameter [defined by Eq. (4)] for group i corresponding to the Pth fractile of the base distribution, while $RDCH_i^N(P)$ is the value of the release parameter corresponding to the Pth fractile of the distribution for the Nth endpoint of the tree. The weight assigned to this particular result (tree endpoint) is given by

$$W^N = W^1{}_j W^2{}_k W^3{}_l W^4{}_m W^5{}_n. \tag{6}$$

To obtain the final combined distributions, Expert B inverted the endpoint distributions and summed the resulting weighted probabilities corresponding to a given value of $RDCH_i$, thus:

$$P(RDCH_i) = \sum_N W^N P^N(RDCH_i). \tag{7}$$

Here, $P^N(RDCH_i)$ is the probability that the release parameter will be less than $RDCH_i$ for the Nth endpoint distribution, and $P(RDCH_i)$ is the probability that the release parameter will be less than $RDCH_i$ in the combined distribution. Finally, Expert B converted the combined distribution back into a distribution for $FDCH_i$, using Eq. 4.

Although Expert B used these procedures to develop distributions for ruthenium and molybdenum in addition to the other radionuclides considered, he mistrusted the results because the volatility of these species is enhanced so greatly in strongly oxidizing atmospheres that he believed the amount of vaporization could well be determined primarily by the amount of debris that could be transported to a strongly oxidizing environment. He therefore modified the distributions for these species to account for this factor. He believed that the ice condenser in Sequoyah and the suppression pool in the BWRs would serve as barriers to the transport of debris to those portions of the containment richest in oxygen. Hence, he defined two distributions for these species, one for the PWR large, dry containments and one for Sequoyah and the BWRs. CONTAIN-DCH calculations for Surry and Sequoyah, were used in estimating the amounts of debris that might reach strongly oxidizing environments.

The decomposition tree discussed above applies only to the distribution of release fractions of vaporization. In addition, Expert B gave some consideration to aerosol formation by mechanical fragmentation. For this process, the expert assumed that the release fractions for all species would be the same. He based his distribution for mechanical aerosolization upon experimental results obtained from the Surtsey experiments DCH-1, DCH-2, and DCH-3.[B-5] The measured releases for the various species would include both vaporization and mechanical contributions in these experiments, and thus would provide an upper bound to the contribution of the mechanical aerosol generation alone. Expert B based his mechanical aerosolization distributions primarily upon the measured distributions for lanthenum which is expected to be the least volatile of the species considered and had the lowest measured release fractions. Expert B defined his distribution so that the 25% and 75% points roughly corresponded to the range of lanthanum releases deduced from the Surtsey experiments. (In some cases, only very preliminary Surtsey data were available, and the expert considered the relation between his distributions and the experimental results to be quite accurate.) He then filled in the remainder of the distribution in an essentially subjective manner. His distributions for mechanical aerosol generation are given in Table B-6.

In developing the final distribution for $FDCH_i$, for each fractile Expert B used the higher of the vaporization value or the mechanical aerosolization value corresponding to his distributions. In practice, the mechanical aerosolization releases dominated the distributions for the least volatile species (lanthanum and cerium) but had little impact upon the distributions for the other species except to increase release fractions at the low end of the range in some instances. Expert B believed that the risk-significance of mechanical aerosol generation in his distributions would not be great.

Finally, Expert B emphasized that despite the formalism described here, his distributions should still be viewed as being fundamentally subjective: the W values, in particular, represent subjective probabilities and even the R values include subjective elements despite the use of code results, experimental results, and thermochemical calculations where these were available and applicable. Since the expert considered these distributions to be subjective, he therefore revised the final results when he considered them to be unreasonable in some respect. In general, these revisions were limited to adjustments to the tails of the distributions to modify release fractions he considered to be excessively high or excessively low.

Results of Expert B's Elicitation

Tables B-1 through B-5 provide the levels assigned to each uncertain parameter considered by Expert B, the R value (multiplication factor) that corresponds to that level of the parameter and the weight assigned to that level. Table B-6 gives his distribution for mechanical aerosol generation. Table B-7 provides the final distribution for each radionuclide group.

Table B-1
Multiplication Factors (R) and Subjective Weights (W)
Used in Obtaining Distributions for FDCH
Uncertainty 1: Temperature

Nonmetals	Level 1	Level 2	Level 3	Level 4
Value (k)	2000	2500*	3000	3500
Weight	0.35	0.45	0.2	0.0
		R Values		
Cerium	7×10^{-3}	1.0	28.0	--
Lanthanum	0.016	1.0	36.0	--
Barium	0.26	1.0	3.0	--
Strontium	0.18	1.0	3.0	--
Cesium iodide	0.14	1.0	2.3	--
Metals				
Weight	0.25	0.4	0.25	0.1
		R Values		
Tellurium	0.13	1.0	3.9	10.3
Ruthenium	8.1×10^{-4}	1.0	118.0	3630.0
Molybdenum	0.123	1.0	14.0	142.0

*Base case

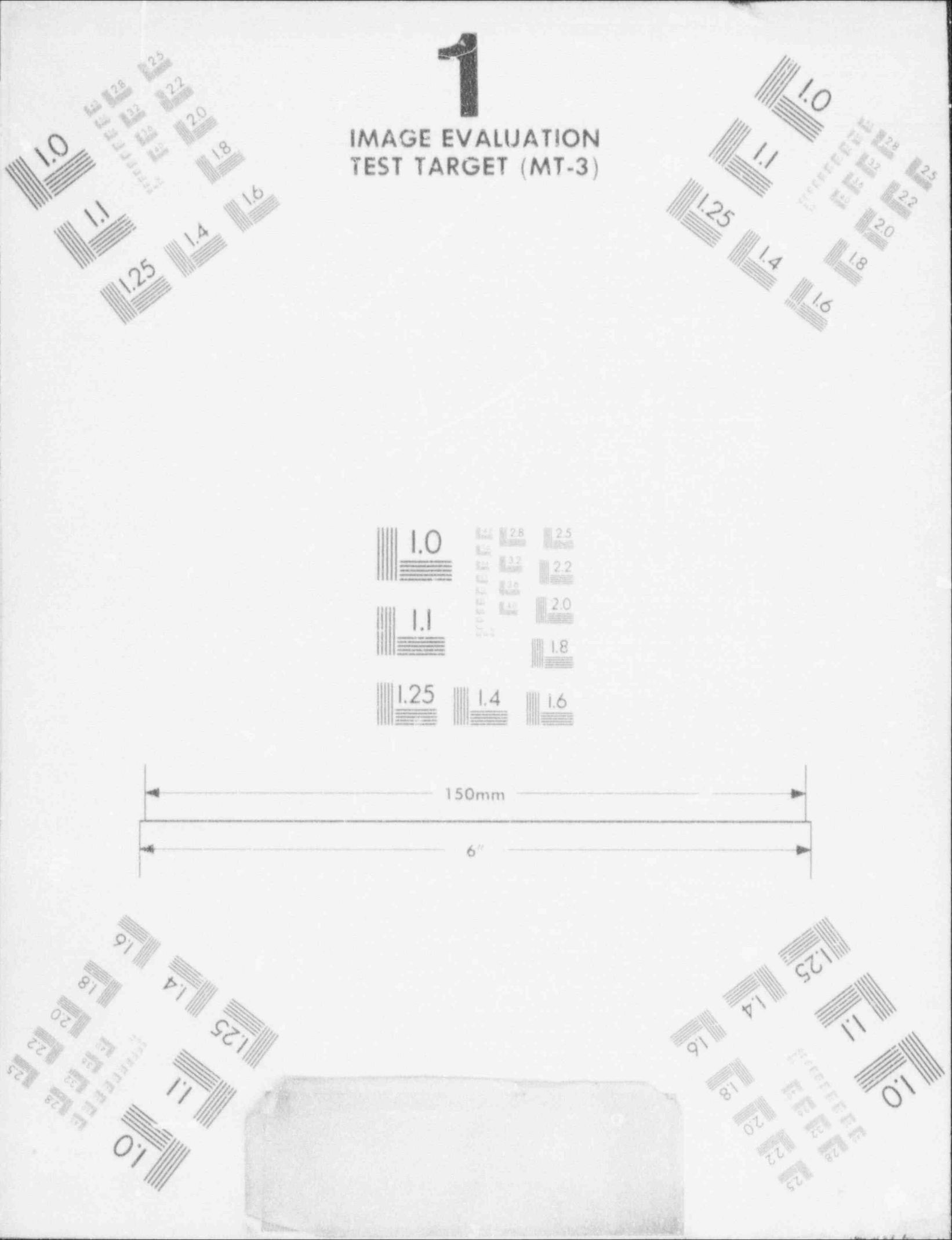
1
IMAGE EVALUATION
TEST TARGET (MT-3)
1.0
1.1
1.25
1.4
1.6
1.8
2.0
2.2
2.5
2.8
3.2
3.6
4.0
150mm
6"

1

IMAGE EVALUATION
TEST TARGET (MT-3)

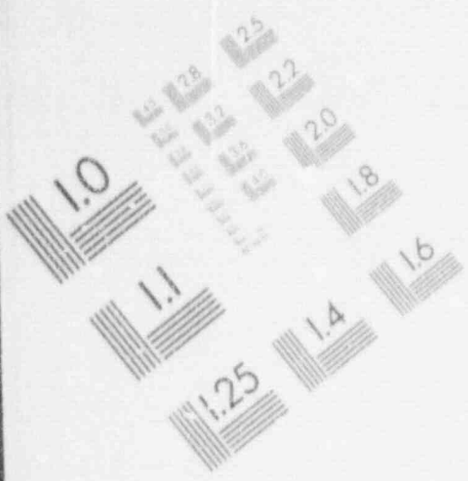

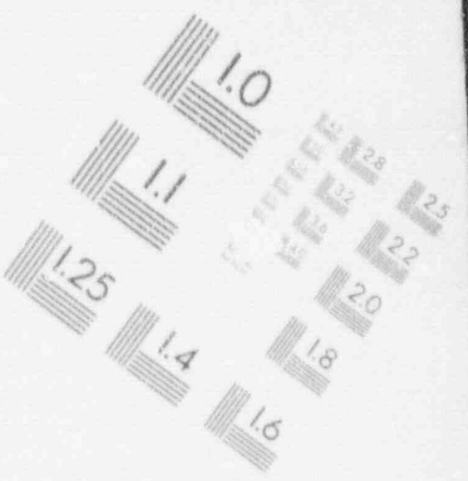

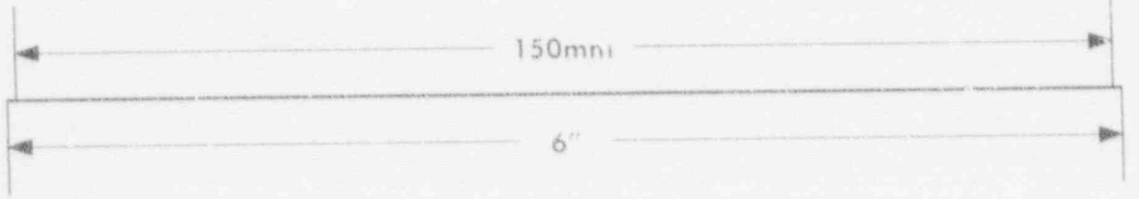

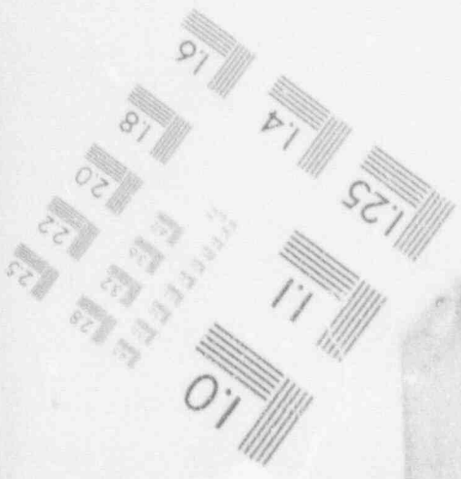

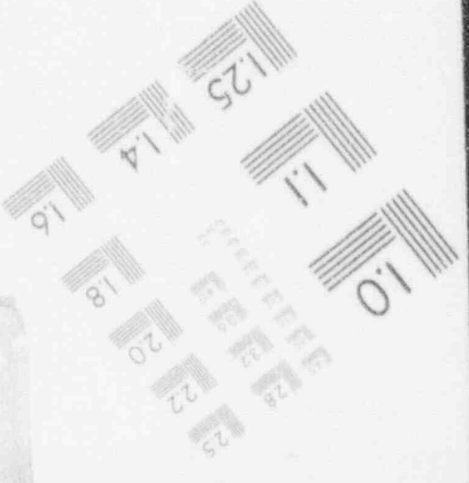

Table B-2
Multiplication Factors (R) and Subjective Weights (W)
Uncertainty 2: Oxygen Potential

Value	Level 1 Low[1]	Level 2 Medium[2]	Level 3 High[3]
Debris Temperature < 2500 K			
Weight	0.2	0.5	0.3
	R Values		
Ce	0.5	1.0	4.8
La	18	1.0	0.3
Ba	4.5	0.8	2.4
Sr	64	1.0	2.2
Te	1.0	1.0	2.0
Ru	0.25	1.0	7.0
Mo	1.9×10^{-4}	1.0	166.0
Debris Temperature > 2500 K			
Weight	0.5	0.35	0.15

[1]Low: Chemical equilibrium assuming metallic composition of debris calculated in BMI-2104 for the Surry 'MLB' sequence;

[2]Medium: Base case, $H_2/H_2O = 2$, corresponding to chemical equilibrium for the steam-iron reaction, with a minor modification for vaporization of Ba species.

[3]High: $H_2/H_2O \leq 0.1$.

Table B-3
Multiplication Factors (R) and Subjective Weights (W)
Used in Obtaining Distributions for FDCH
Uncertainty 3: Miscellaneous Model Parameters

	Level 1 Low	Level 2 Medium	Level 3 High
Weight	0.3	0.4	0.3
	R Values--All Species		
	0.32	1.0	3.2

Table B-4
Multiplication Factors (R) and Subjective Weights (W)
Used in Obtaining Distributions for FDCH
Uncertainty 4: Free Energy of Formation

	Level 1 Low	Level 2 Medium	Level 3 High
Weight	0.25	0.5	0.25
R Values--All Species			
	0.1	1.0	10.0

Table B-5
Multiplication Factors (R) and Subjective Weights (W)
Used in Obtaining Distributions for FDCH
Uncertainty 5: Activity Coefficients

	Level 1 Low	Level 2 Medium	Level 3 High
Weight	0.25	0.5	0.25
R Values			
Oxides	0.03	0.3	3.0
Cesium Iodide	0.03	0.3	3.0
Metals	0.32	1.0	3.2

Mechanical Aerosol Generation

The expert believed that radionuclide release from mechanical aerosol generation would be approximately independent of the radionuclide species. He provided the distribution for this component of the release in Table B-6.

Table B-6
Distribution for Mechanical Aerosol Generation

	Fractile						
Distribution	0.01	0.05	0.25	0.50	0.75	0.95	0.99
All species	10^{-5}	10^{-4}	10^{-3}	3×10^{-3}	0.01	0.05	0.20

Table B-7
Results for FDCH

Distribution Fractile	0.01	0.05	0.25	0.50	0.75	0.95	0.99
Cerium	1×10^{-5}	1×10^{-4}	1×10^{-3}	3×10^{-3}	0.01	0.05	0.28
Lanthanum	1×10^{-5}	1×10^{-4}	1×10^{-3}	3×10^{-3}	0.01	0.05	0.20
Barium	1×10^{-5}	1×10^{-4}	1×10^{-3}	0.012	0.084	0.74	0.98
Strontium	1×10^{-5}	1×10^{-4}	1×10^{-3}	3×10^{-3}	0.029	0.56	0.96
Cesium iodide	0.01	0.05	0.25	0.75	0.90	1.0	1.0
Tellurium	0.01	0.05	0.20	0.60	0.80	0.95	1.0
Ruthenium	1×10^{-5}	2×10^{-3}	0.015	0.04	0.15	0.40	0.75
Molybdenum	2×10^{-4}	0.002	0.05	0.15	0.43	0.80	0.98
Ruthenium & Molybdenum*	2×10^{-5}	4×10^{-4}	0.02	0.05	0.20	0.50	0.90

*Sequoyah and BWRs

Sources of Uncertainty

The R values and W values directly reflect the importance Expert B assigned to the five uncertainties that he explicitly included in the decomposition tree discussed in connection with Fig. B-1. In addition, he considered the uncertainties represented by the differences between the three models he used to define his base distribution to be fairly important. These latter factors alone would yield somewhat over an order of magnitude uncertainty range in most cases (based upon the ratio of the 0.95 fractile release to the 0.05 fractile release).

Correlation with Other Variables

Expert B did not specify any correlations between FDCH and other variables.

Suggested Methods for Reducing Uncertainty

Expert B believed that small-scale thermochemical experiments could prove useful in reducing the uncertainties of free energies of formation and those of activity coefficients. The other uncertainties (including those

reflected in the base distribution) reflect primarily uncertainties in the thermochemical boundary conditions imposed upon the vaporizing debris. Reducing these uncertainties will require improved mechanistic models for DCH processes, coupling of these models with vaporization modeling, and reductions of uncertainties in the in-vessel accident progression analysis. Experimentation such as the Surtsey program will be needed to validate the mechanistic modeling; prototypical thermochemical environments (e.g., steam-driven melts containing unoxidized zirconium metal) will be required for optimum validation. Such experiments will also be useful in reducing the uncertainties of mechanical aerosol generation.

REFERENCES

B-1. K. K. Murata et al., "User's Manual for CONTAIN 1.1, A Computer Code for Severe Nuclear Reactor Accident Containment Analysis," NUREG/CR-5026, SAND87-2309, Sandia National Laboratories, September 1989.

B-2. D. C. Williams et al., "Containment Loads Due to Direct Containment Heating and Associated Hydrogen Behavior: Analysis and Calculations with the CONTAIN Code," NUREG/CR-4896, SAND87-0633, Sandia National Laboratories, May 1987.

B-3. D. C. Williams and D. L. Y. Louie, "CONTAIN Analyses of Direct Containment Heating Events in the Surry PLant," Proceedings of the Thermal Hydraulics Division of the 1988 ANS/ENS Winter Meeting, Washington, D.C., Oct. 31 - Nov. 4 1988.

B-4. D. A. Powers, J. E. Brockmann, and A. W. Shiver, "VANESA: A Mechanistic Model of Radionuclide Release and Aerosol Generation During Core Debris Interactions with Concrete," NUREG/CR-4308, SAND85-1370, Sandia National Laboratories, July 1986.

B-5. W. W. Tarbell et al., "Direct Containment Heating and Aerosol Generation During High Pressure Melt Ejection Experiments," SAND88-1504C, Proceedings of the Thermal Hydraulics Division of the 1988 ANS/ENS Winter Meeting, Washington, D.C., Oct. 31 - Nov. 4 1988.

Expert C's Elicitation

Radionuclide Release Associated with Pressure-Driven Melt Expulsion From the Reactor Coolant System.

Description of Expert C's Rationale/Methodology

The expert did not distinguish among any cases. He believed that the information supplied concerning the possible types of accidents does not allow him to distinguish among cases or reactor types. He grouped all the radionuclides together for this issue except for the noble gases. The noble gas release rates were estimated to be 1.0.

During DCH there are three possible aerosolization processes for fission products: (1) effervescence (gas bubble bursting), (2) punch through and (3) atomization by gas rushing by the melt. These processes produce particles whose sizes fall into three ranges: about 10 μ, 10 μ to 500 μ, and 500 μ to 1 mm. In the first size category, the particles are all volatilized or aerosolized. In the third size category, the particles are not aerosolized because they fall with velocities of meters per second. The expert has considered the size of the particles for each process to predict fission product release rates.

The expert estimates that the most probable value of FDCH is about 1%, which agrees with the results of the DCH experiments. For aerosolization process (3) the geometry of contact between liquid and gas will cause FDCH to have an upper bound of about 15%.

The expert thinks that a value for FDCH of 30% is absurd. Later atomized material will scrub out earlier atomized material because of the confined volume. Thus, single particle atomization fractions are not appropriate to use. The existing data from experiments seem to contradict the expert's intuition. In addition, he does not think the results of the experiments will scale up to the reactor size. Chemical processes limit atomization in the time scales of the DCH event. Events occur so rapidly that he does not believe chemical processes can be important. In other words, diffusion/mixing rates limit the chemical reaction rates so that there will be little oxidation. His judgment is that the maximum aerosolization density would correspond to a solid fraction of about 2%. This is about the same density as cigarette smoke. At larger solid fractions, the particles would start to agglomerate and settle.

Results of Expert C's Elicitation

For noble gases, FDCH would be 1.0. For the other radionuclides, the cumulative probability distribution is given in Figure C-1 and Table C-1.

Table C-1
Cumulative Probability Distribution of
Radionuclide Release With Pressure Driven Melt
Expulsion from RCS (FDCH)

Cumulative Probability	FDCH
0.00	0.0001
0.25	0.001
0.50	0.01
0.75	0.03
1.00	0.10

Sources of Uncertainty

Uncertainties in pressure and plant type are not large compared to the uncertainties in the aerosolization mechanism.

Correlations With Other Variables

Correlations with other variables were not made, because the basic aerosolization mechanism is the dominant uncertainty and is poorly understood.

DISTRIBUTION:

Frank Abbey
U. K. Atomic Energy Authority
Wigshaw Lane, Culcheth
Warrington, Cheshire, WA3 4NE
ENGLAND

Kiyoharu Abe
Department of Reactor Safety
Research
Nuclear Safety Research Center
ToKai Research Establishment
JAERI
Tokai-mura, Naga-gun
Ibaraki-ken,
JAPAN

Ulvi Adalioglu
Nuclear Engineering Division
Cekmece Nuclear Research and
Training Centre
P.K.1, Havaalani
Istanbul
TURKEY

Bharat Agrawal
USNRC-RES/AEB
MS: NL/N-344

Kiyoto Aizawa
Safety Research Group
Reactor Research and Development
Project
PNC
9-13 1-Chome Akasaka
Minatu-Ku
Tokyo
JAPAN

Oguz Akalin
Ontario Hydro
700 University Avenue
Toronto, Ontario
CANADA M5G 1X6

David Aldrich
Science Applications International
Corporation
1710 Goodridge Drive
McLean, VA 22102

Agustin Alonso
University Politecnica De Madrid
J Gutierrez Abascal, 2
28006 Madrid
SPAIN

Christopher Amos
Science Applications International
Corporation
2109 Air Park Road SE
Albuquerque, NM 87106

Richard C. Anoba
Project Engr., Corp. Nuclear Safety
Carolina Power and Light Co.
P. O. Box 1551
Raleigh, NC 27602

George Apostolakis
UCLA
Boelter Hall, Room 5532
Los Angeles, CA 90024

James W. Ashbar
Boston Edison Company
800 Boylston Street
Boston, MA 02199

Donald H. Ashton
Bechtel Power Corporation
P.O. Box 2166
Houston, TX 77252-2166

J. de Assuncao
Cabinete de Proteccao e Seguranca
Nuclear
Secretario de Estado de Energia
Ministerio da Industria
av. da Republica, 45-6°
1000 Lisbon
PORTUGAL

Mark Averett
Florida Power Corporation
P.O. Box 14042
St. Petersburg, FL 33733

Raymond O. Bagley
Northeast Utilities
P.O. Box 270
Hartford, CT 06141-0270

Juan Bagues
Consejo de Seguridad Nucleare
Sarangela de la Cruz 3
28020 Madrid
SPAIN

George F. Bailey
Washington Public Power Supply System
P. O. Box 968
Richland, WA 99352

H. Bairiot
Belgonucleaire S A
Rue de Champ de Mars 25
B-1050 Brussels
BELGIUM

Louis Baker
Reactor Analysis and Safety Division
Building 207
Argonne National Laboratory
9700 South Cass Avenue
Argonne, IL 60439

H-P. Balfanz
TUV-Norddeutschland
Grosse Bahnstrasse 31,
2000 Hamburg 54
FEDERAL REPUBLIC OF GERMANY

Patrick Baranowsky
USNRC-NRR/OEAB
MS: 11E-22

H. Bargmann
Dept. de Mecanique
Inst. de Machines Hydrauliques et de Mecaniques des Fluides
Ecole Polytechnique de Lausanne
CH-1003 Lausanne
M E. (ECUBLENS)
CH. 1015 Lausanne
SWITZERLAND

Robert A. Bari
Brookhaven National Laboratory
Building 130
Upton, NY 11973

Richard Barrett
USNRC-NRR/PRAB
MS: 10A-2

Kenneth S. Baskin
S. California Edison Company
P.O. Box 800
Rosemead, CA 91770

J. Basselier
Belgonucleaire S A
Rue du Champ de Mars 25, B-1050
Brussels
BELGIUM

Werner Bastl
Gesellschaft Fur Reaktorsicherheit
Forschungsgelande
D-8046 Garching
FEDERAL REPUBLIC OF GERMANY

Anton Bayer
BGA/ISH/ZDB
Postfach 1108
D-8042 Neuherberg
FEDERAL REPUBLIC OF GERMANY

Ronald Bayer
Virginia Electric Power Co.
P. O. Box 26666
Richmond, VA 23261

Eric S. Beckjord
Director
USNRC-RES
MS: NL/S-007

Bruce B. Beckley
Public Service Company
P.O. Box 330
Manchester, NH 03105

William Beckner
USNRC-RES/SAIB
MS: NL/S-324

Robert M. Bernero
Director
USNRC-NMSS
MS: 6A-4

Ronald Berryman [2]
Virginia Electric Power Co.
P. O. Box 26666
Richmond, VA 23261

Robert C. Bertucio
NUS Corporation
1301 S. Central Ave, Suite 202
Kent, WA 98032

John H. Bickel
EG&G Idaho, Inc.
P.O. Box 1625
Idaho Falls, ID 83415

Peter Bieniarz
Risk Management Association
2309 Dietz Farm Road, NW
Albuquerque, NM 87107

Adolf Birkhofer
Gesellschaft Fur Reaktorsicherheit
Forschungsgelande
D-8046 Garching
FEDERAL REPUBLIC OF GERMANY

James Blackburn
Illinois Dept. of Nuclear Safety
1035 Outer Park Drive
Springfield, IL 62704

Dennis C. Bley
Pickard, Lowe & Garrick, Inc.
2260 University Drive
Newport Beach, CA 92660

Roger M. Blond
Science Applications Int. Corp.
20030 Century Blvd., Suite 201
Germantown, MD 20874

Simon Board
Central Electricity Generating
Board
Technology and Planning Research
Division
Berkeley Nuclear Laboratory
Berkeley Gloucestershire, GL139PB
UNITED KINGDOM

Mario V. Bonace
Northeast Utilities Service Company
P.O. Box 270
Hartford, CT 06101

Gary J. Boyd
Safety and Reliability Optimization
Services
9724 Kingston Pike, Suite 102
Knoxville, TN 37922

Robert J. Breen
Electric Power Research Institute
3412 Hillview Avenue
Palo Alto, CA 94303

Charles Brinkman
Combustion Engineering
7910 Woodmont Avenue
Bethesda, MD 20814

K. J. Brinkmann
Netherlands Energy Res. Fdtn.
P.O. Box 1
1755ZG Petten NH
NETHERLANDS

Allan R. Brown
Manager, Nuclear Systems and
Safety Department
Ontario Hydro
700 University Ave.
Toronto, Ontario M5G1X6
CANADA

Robert G. Brown
TENERA L.P.
1340 Saratoga-Sunnyvale Rd.
Suite 206
San Jose, CA 95129

Sharon Brown
EI Services
1851 So. Central Place, Suite 201
Kent, WA 98031

Ben Buchbinder
NASA, Code QS
600 Maryland Ave. SW
Washington, DC 20546

R. H. Buchholz
Nutech
6835 Via Del Oro
San Jose, CA 95119

Robert J. Budnitz
Future Resources Associates
734 Alameda
Berkeley, CA 94707

Gary R. Burdick
USNRC-RES/DSR
MS: NL/S-007

Arthur J. Buslik
USNRC-RES/PRAB
MS: NL/S-372

M. Bustraan
Netherlands Energy Res. Fdtn.
P.O. Box 1
1755ZG Petten NH
NETHERLANDS

Nigel E. Buttery
Central Electricity Generating Board
Booths Hall
Chelford Road, Knutsford
Cheshire, WA168QG
UNITED KINGDOM

Jose I. Calvo Molins
Probabilistic Safety Analysis Group
Consejo de Seguridad Nuclear
Sor Angela de la Cruz 3, Pl. 6
28020 Madrid
SPAIN

J. F. Campbell
Nuclear Installations Inspectorate
St. Peters House
Balliol Road, Bootle
Merseyside, L20 3LZ
UNITED KINGDOM

Kenneth S Canady
Duke Power Company
422 S. Church Street
Charlotte, NC 28217

Lennart Carlsson
IAEA A-1400
Wagramerstrasse 5
P.O. Box 100
Vienna, 22
AUSTRIA

Annick Carnino
Electricite de France
32 Rue de Monceau 8EME
Paris, F5008
FRANCE

G. Caropreso
Dept. for Envir. Protect. & Hlth.
ENEA Cre Casaccia
Via Anguillarese, 301
00100 Roma
ITALY

James C. Carter, III
TENERA L.P.
Advantage Place
308 North Peters Road
Suite 280
Knoxville, TN 37922

Eric Cazzoli
Brookhaven National Laboratory
Building 130
Upton, NY 11973

John G. Cesare
SERI
Director Nuclear Licensing
5360 I-55 North
Jackson, MS 39211

S. Chakraborty
Radiation Protection Section
Div. De La Securite Des Inst. Nuc
5303 Wurenlingen
SWITZERLAND

Sen-I Chang
Institute of Nuclear Energy Research
P.O. Box 3
Lungtan, 325
TAIWAN

J. R. Chapman
Yankee Atomic Electric Company
1671 Worcester Road
Framingham, MA 01701

Robert F. Christie
Tennessee Valley Authority
400 W. Summit Hill Avenue, W10D190
Knoxville, TN 37902

T. Cianciolo
BWR Assistant Director
ENEA DISP TX612167 ENEUR
Rome
ITALY

Thomas Cochran
Natural Resources Defense Council
1350 New York Ave. NW, Suite 300
Washington, D.C. 20005

Frank Coffman
USNRC-RES/HFB
MS: NL/N-316

Larry Conradi
NUS Corporation
16835 W. Bernardo Drive
Suite 202
San Diego, CA 92127

Peter Cooper
U.K. Atomic Energy Authority
Wigshaw Lane, Culcheth
Warrington, Cheshire, WA3 4NE
UNITED KINGDOM

C. Allin Cornell
110 Coquito Way
Portola Valley, CA 94025

Michael Corradini
University of Wisconsin
1500 Johnson Drive
Madison, WI 53706

E. R. Corran
Nuclear Technology Division
ANSTO Research Establishment
Lucas Heights Research Laboratories
Private Mail Bag 7
Menai, NSW 2234
AUSTRALIA

James Costello
USNRC-RES/SSEB
MS: NL/S-217A

George R. Crane
1570 E. Hobble Creek Dr.
Springville, UT 84663

Mat Crawford
SERI
5360 I-55 North
Jackson, MS 39211

Michael C. Cullingford
Nuclear Safety Division
IAEA
Wagramerstrasse, 5
P.O. Box 100
A-1400 Vienna
AUSTRIA

Garth Cummings
Lawrence Livermore Laboratory
L-71, Box 808
Livermore, CA 94526

Mark A. Cunningham
USNRC-RES/PRAB
MS: NL/S-372

James J. Curry
7135 Salem Park Circle
Mechanicsburg, PA 17055

Peter Cybulskis
Battelle Columbus Division
505 King Avenue
Columbus, OH 43201

Peter R. Davis
PRD Consulting
1935 Sabin Drive
Idaho Falls, ID 83401

Jose E. DeCarlos
Consejo de Seguridad Nuclear
Sor Angela de la Cruz 3, Pl. 8
28016 Madrid
SPAIN

M. Marc Decroton
Department Technologie
CEN/SCK
Boeretang 200
B-2400 Mol
BELGIUM

Richard S. Denning
Battelle Columbus Division
505 King Avenue
Columbus, OH 43201

Vernon Denny
Science Applications Int. Corp.
5150 El Camino Real, Suite 3
Los Altos, CA 94303

J. Devooget
Faculte des Sciences Appliques
Universite Libre de Bruxelles
av. Franklin Roosevelt
B-1050 Bruxelles
BELGIUM

R. A. Diederich
Supervising Engineer
Environmental Branch
Philadelphia Electric Co.
2301 Market St.
Philadelphia, PA 19101

Raymond DiSalvo
Battelle Columbus Division
505 King Avenue
Columbus, OH 43201

Mary T. Drouin
Science Applications International
Corporation
2109 Air Park Road S.E.
Albuquerque, NM 87106

Andrzej Drozd
Stone and Webster
Engineering Corp.
243 Summer Street
Boston, MA 02107

N. W. Edwards
NUTECH
145 Martinville Lane
San Jose, CA 95119

Ward Edwards
Social Sciences Research Institute
University of Southern California
Los Angeles, CA 90089-1111

Joachim Ehrhardt
Kernforschungszentrum Karlsruhe/INR
Postfach 3640
D-7500 Karlsruhe 1
FEDERAL REPUBLIC OF GERMANY

Adel A. El-Bassioni
USNRC-NRR/PRAB
MS: 10A-2

J. Mark Elliott
International Energy Associates,
Ltd., Suite 600
600 New Hampshire Ave., NW
Washington, DC 20037

Farouk Eltawila
USNRC-RES/AEB
MS: NL/N-344

Mike Epstein
Fauske and Associates
P. O. Box 1625
16W070 West 83rd Street
Burr Ridge, IL 60521

Malcolm L. Ernst
USNRC-RGN II

F. R. Farmer
The Long Wood, Lyons Lane
Appleton, Warrington
WA4 5ND
UNITED KINGDOM

P. Fehrenback
Atomic Energy of Canada, Ltd.
Chalk River Nuclear Laboratories
Chalk River Ontario, K0J1P0
CANADA

P. Ficara
ENEA Cre Casaccia
Department for Thermal Reactors
Via Anguillarese, 301
00100 ROMA
ITALY

A. Fiege
Kernforschungszentrum
Postfach 3640
D-7500 Karlsruhe
FEDERAL REPUBLIC OF GERMANY

John Flack
USNRC-RES/SAIB
MS: NLS-324

George F. Flanagan
Oak Ridge National Laboratory
P.O. Box Y
Oak Ridge, TN 37831

Karl N. Fleming
Pickard, Lowe & Garrick, Inc.
2260 University Drive
Newport Beach, CA 92660

Terry Foppe
Rocky Flats Plant
P. O. Box 464, Building T886A
Golden, CO 80402-0464

Joseph R. Fragola
Science Applications International Corporation
274 Madison Avenue
New York, NY 10016

Wiktor Frid
Swedish Nuclear Power Inspectorate
Division of Reactor Technology
P. O. Box 27106
S-102 52 Stockholm
SWEDEN

James Fulford
NUS Corporation
910 Clopper Road
Gaithersburg, MD 20878

Urho Fulkkinen
Technical Research Centre of Finland
Electrical Engineering Laboratory
Otakaari 7 B
SF-02150 Espoo 15
FINLAND

J. B. Fussell
JBF Associates, Inc.
1630 Downtown West Boulevard
Knoxville, TN 37919

John Garrick
Pickard, Lowe & Garrick, Inc.
2260 University Drive
Newport Beach, CA 92660

John Gaunt
British Embassy
3100 Massachusetts Avenue, NW
Washington, DC 20008

Jim Gieseke
Battelle Columbus Division
505 King Avenue
Columbus, OH 43201

Frank P. Gillespie
USNRC-NRR/PMAS
MS: 12G-18

Ted Ginsburg
Department of Nuclear Energy
Building 820
Brookhaven National Laboratory
Upton, NY 11973

James C. Glynn
USNRC-RES/PRAB
MS: NL/S-372

P. Govaerts
Departement de la Surete Nucleaire
Association Vincotte
avenue du Roi 157
B-1060 Bruxelles
BELGIUM

George Greene
Building 820M
Brookhaven National Laboratory
Upton, NY 11973

Carrie Grimshaw
Brookhaven National Laboratory
Building 130
Upton, NY 11973

H. J. Van Grol
Energy Technology Division
Energieonderzoek Centrum Nederland
Westerduinweg 3
Postbus 1
NL-1755 Petten ZG
NETHERLANDS

Sergio Guarro
Lawrence Livermore Laboratories
P. O. Box 808
Livermore, CA 94550

Sigfried Hagen
Kernforschungzentrum Karlsruhe
P. O. Box 3640
D-7500 Karlsruhe 1
FEDERAL REPUBLIC OF GERMANY

L. Hammar
Statens Karnkraftinspektion
P.O. Box 27106
S-10252 Stockholm
SWEDEN

Stephen Hanauer
Technical Analysis Corp.
6723 Whittier Avenue
Suite 202
McLean, VA 22101

Brad Hardin
USNRC-RES/TRAB
MS: NL/S-169

R. J. Hardwich, Jr.
Virginia Electric Power Co.
P.O. Box 26666
Richmond, Va 23261

Michael R. Haynes
UKAEA Harwell Laboratory
Oxfordshire
Didcot, Oxon., OX11 ORA
ENGLAND

Michael J. Hazzan
Stone & Webster
3 Executive Campus
Cherry Hill, NJ 08034

A. Hedgran
Royal Institute of Technology
Nuclear Safety Department
Bunellvagen 60
10044 Stockholm
SWEDEN

Sharif Heger
UNM Chemical and Nuclear
Engineering Department
Farris Engineering
Room 209
Albuquerque, NM 87131

Jon C. Helton
Dept. of Mathematics
Arizona State University
Tempe, AZ 85287

Robert E. Henry
Fauske and Associates, Inc.
16W070 West 83rd Street
Burr Ridge, IL 60521

P. M. Herttrich
Federal Ministry for the
Environment, Preservation of
Nature and Reactor Safety
Husarenstrasse 20
Postfach 120629
D-5300 Bonn 1
FEDERAL REPUBLIC OF GERMANY

F. Houser
Giesellschaft Pur Reaktorsicherheit
Forschurgsgelande
D-8046 Garching
FEDERAL REPUBLIC OF GERMANY

E. F. Hicken
Giesellschaft Fur Reaktorsicherheit
Forschungsgelande
D-8046 Garching
FEDERAL REPUBLIC OF GERMANY

D. J. Higson
Radiological Support Group
Nuclear Safety Bureau
Australian Nuclear Science and
Technology Organisation
P.O. Box 153
Rosebery, NSW 2018
AUSTRALIA

Daniel Hirsch
University of California
A. Stevenson Program on
Nuclear Policy
Santa Cruz, CA 95064

H. Hirschmann
Hauptabteilung Sicherheit und
Umwelt
Swiss Federal Institute for
Reactor Research (EIR)
CH-5303 Wurenlingen
SWITZERLAND

Mike Hitchler
Westinghouse Electric Corp.
Savanna River Site
Aiken, SC 29808

Richard Hobbins
EG&G Idaho, Inc.
P. O. Box 1625
Idaho Falls, ID 83415

Steven Hodge
Oak Ridge National Laboratory
P.O. Box Y
Oak Lidge, TN 37831

Lars Hoegberg
Office of Regulation and Research
Swedish Nuclear Power Inspectorate
P. O. Box 27106
S-102 52 Stockholm
SWEDEN

Lars Hoeghort
IAEA A-1400
Wagranerstraase 5
P.O. Box 100
Vienna, 22
AUSTRIA

Edward Hofer
Giesellschaft Fur Reaktorsicherheit
Forschurgsgelande
D-8046 Garching
FEDERAL REPUBLIC OF GERMANY

Peter Hoffmann
Kernforschingszentrum Karlsruhe
Institute for Material
Und Festkorperforsching I
Postfach 3640
D-7500 Karlsruhe 1
FEDERAL REPUBLIC OF GERMANY

N. J. Holloway
UKAEA Safety and Reliability
Directorate
Wigshaw Lane, Culcheth
Warrington, Cheshire, WA34NE
UNITED KINGDOM

Stephen C. Hora
University of Hawaii at Hilo
Division of Business Administration
and Economics
College of Arts and Sciences
Hilo, HI 96720-4091

J. Peter Hoseman
Swiss Federal Institute for
Reactor Research
CH-5303, Wurenlingen
SWITZERLAND

Thomas G. Houghton
KMC, Inc.
1747 Pennsylvania Avenue, NW
Washington, DC 20006

Dean Houston
USNRC-ACRS
MS: P-315

Der Yu Hsia
Taiwan Atomic Energy Council
67, Lane 144, Keelung Rd.
Sec. 4
Taipei
TAIWAN

Alejandro Huerta-Bahena
National Commission on Nuclear
Safety and Safeguards (CNSNS)
Insurgentes S. y N. 1776
Col. Florida
C. P. 04270 Mexico, D.F.
MEXICO

Kenneth Hughey [2]
SERI
5360 I-55 North
Jackson, MS 39211

Won-Guk Hwang
Kzunghee University
Yongin-Kun
Kyunggi-Do 170-23
KOREA

Michio Ichikawa
Japan Atomic Energy Research
Institute
Dept. of Fuel Safety Research
Tokai-Mura, Naka-Gun
Ibaraki-Ken, 319-1
JAPAN

Sanford Israel
USNRC-AEOD/ROAB
MS: MNBB-9715

Krishna R. Iyengar
Louisiana Power and Light
200 A Huey P. Long Avenue
Gretna, LA 70053

Jerry E. Jackson
USNRC-RES
MS: NL/S-302

R. E. Jaquith
Combustion Engineering, Inc.
1000 Prospect Hill Road
M/C 9490-2405
Windsor, CT 06095

S. E. Jensen
Exxon Nuclear Company
2101 Horn Rapids Road
Richland, WA 99352

Kjell Johannson
Studsvik Energiteknik AB
S-611 82, Nykoping
SWEDEN

Richard John
SSM, Room 102
927 W. 35th Place
USC, University Park
Los Angeles, CA 90089-0021

D. H. Johnson
Pickard, Lowe & Garrick, Inc.
2260 University Drive
Newport Beach, CA 92660

W. Reed Johnson
Department of Nuclear Engineering
University of Virginia
Reactor Facility
Charlottesville, VA 22901

Jeffery Julius
NUS Corporation
1301 S. Central Ave, Suite 202
Kent, WA 98032

H. R. Jun
Korea Adv. Energy Research Inst.
P.O. Box 7, Daeduk Danju
Chungnam 300-31
KOREA

Peter Kafka
Gesellschaft Fur Reaktorsicherheit
Forschungsgelande
D-8046 Garching
FEDERAL REPUBLIC OF GERMANY

Geoffrey D. Kaiser
Science Application Int. Corp.
1710 Goodridge Drive
McLean, VA 22102

William Kastenberg
UCLA
Boelter Hall, Room 5532
Los Angeles, CA 90024

Walter Kato
Brookhaven National Laboratory
Associated Universities, Inc.
Upton, NY 11973

M. S. Kazimi
MIT, 24-219
Cambridge, MA 02139

Ralph L. Keeney
101 Lombard Street
Suite 704W
San Francisco, CA 94111

Henry Kendall
Executive Director
Union of Concerned Scientists
Cambridge, MA

Frank King
Ontario Hydro
700 University Avenue
Bldg. H11 G5
Toronto
CANADA M5G1X6

Oliver D. Kingsley, Jr.
Tennessee Valley Authority
1101 Market Street
GN-38A Lookout Place
Chattanooga, TN 37402

Stephen R. Kinnersly
Winfrith Atomic Energy
Establishment
Reactor Systems Analysis Division
Winfrith, Dorchester
Dorset DT2 8DH
ENGLAND

Ryohei Kiyose
University of Tokyo
Dept. of Nuclear Engineering
7-3-1 Hongo Bunkyo
Tokyo 113
JAPAN

George Klopp
Commonwealth Edison Company
P.O. Box 767, Room 35W
Chicago, IL 60690

Klaus Koberlein
Gesellschaft Fur Reaktorsicherheit
Forschungsgelande
D-8046 Garching
FEDERAL REPUBLIC OF GERMANY

E. Kohn
Atomic Energy Canada Ltd.
Candu Operations
Mississauga
Ontario, L5K 1B2
CANADA

Alan M. Kolaczkowski
Science Applications International
Corporation
2109 Air Park Road, S.E.
Albuquerque, NM 87106

S. Kondo
Department of Nuclear Engineering
Facility of Engineering
University of Tokyo
3-1, Hongo 7, Bunkyo-ku
Tokyo
JAPAN

Herbert J. C. Kouts
Brookhaven National Laboratory
Building 179C
Upton, NY 11973

Thomas Kress
Oak Ridge National Laboratory
P.O. Box Y
Oak Ridge, TN 37831

W. Kroger
Institut fur Nukleare
Sicherheitsforschung
Kernforschungsanlage Julich GmbH
Postfach 1913
D-5170 Julich 1
FEDERAL REPUBLIC OF GERMANY

Greg Krueger [3]
Philadelphia Electric Co.
2301 Market St.
Philadelphia, PA 19101

Bernhard Kuczera
Kernforschungzentrum Karlsruhe
LWR Safety Project Group (PRS)
P. O. Box 3640
D-7500 Karlsruhe 1
FEDERAL REPUBLIC OF GERMANY

Jeffrey L. LaChance
Science Applications International
Corporation
2109 Air Park Road S.E.
Albuquerque, NM 87106

H. Larsen
Risø National Laboratory
Postbox 49
DK-4000 Roskilde
DENMARK

Wang L. Lau
Tennessee Valley Authority
400 West Summit Hill Avenue
Knoxville, TN [illegible]

Timothy J. Leahy
ET Services
1851 South Central Place, Suite 201
Kent, WA 98031

John C. Lee
University of Michigan
North Campus
Dept. of Nuclear Engineering
Ann Arbor, MI 48109

Tim Lee
USNRC-RES/RPSB
MS: NL/N-353

Mark T. Leonard
Science Applications International Corporation
2109 Air Park Road, SE
Albuquerque, NM 87106

Leo Lesage
Director, Applied Physics Div.
Argonne National Laboratory
Building 208, 9700 South Cass Ave.
Argonne, IL 60439

Milton Levenson
Bechtel Western Power Company
50 Beale St.
San Francisco, CA 94119

Librarian
NUMARC/USCEA
1776 I Street NW, Suite 400
Washington, DC 80006

Eng Lin
Taiwan Power Company
242, Roosevelt Rd., Sec. 3
Taipei
TAIWAN

N. J. Liparulo
Westinghouse Electric Corp.
P. O. Box 355
Pittsburgh, PA 15230

Y. H. (Ben) Liu
Department of Mechanical Engineering
University of Minnesota
Minneapolis, MN 55455

Bo Liwnang
IAEA A-1400
Swedish Nuclear Power Inspectorate
P.O. Box 27106
S-102 52 Stockholm
SWEDEN

J. P. Longworth
Central Electric Generating Board
Berkeley Gloucester
GL13 9PB
UNITED KINGDOM

Walter Lowenstein
Electric Power Research Institute
3412 Hillview Avenue
P. O. Box 10412
Palo Alto, CA 94303

William J. Luckas
Brookhaven National Laboratory
Building 130
Upton, NY 11973

Hans Ludewig
Brookhaven National Laboratory
Building 130
Upton, NY 11973

Robert J. Lutz, Jr.
Westinghouse Electric Corporation
Monroeville Energy Center
EC-E-371, P. O. Box 355
Pittsburgh, PA 15230-0355

Phillip E. MacDonald
EG&G Idaho, Inc., Inc.
P.O. Box 1625
Idaho Falls, ID 83415

Jim Mackenzie
World Resources Institute
1735 New York Ave. NW
Washington, DC 20006

Richard D. Fowler
Idaho Nat. Engineering Laboratory
P.O. Box 1625
Idaho Falls, ID 83415

A. P. Malinauskas
Oak Ridge National Laboratory
P.O. Box Y
Oak Ridge, TN 37831

Giuseppe Mancini
Commission European Comm.
CEC-JRC Eraton
Ispra Varese
ITALY

Lasse Mattila
Technical Research Centre of
Finland
Lonnrotinkatu 37, P. O. Box 169
SF-00181 Helsinki 18
FINLAND

Roger J. Mattson
SCIENTECH Inc.
11821 Parklawn Dr.
Rockville, MD 20852

Donald McPherson
USNRC-NRR/DONRR
MS: 12G-18

Jim Metcalf
Stone and Webster Engineering
Corporation
245 Summer St.
Boston, MA 02107

Mary Meyer
A-1, MS F600
Los Alamos National Laboratory
Los Alamos, NM 87545

Ralph Meyer
USNRC-RES/AEB
MS: NL/N-344

Charles Miller
8 Hastings Rd.
Monsey, NY 10952

Joseph Miller
Gulf States Utilities
P. O. Box 220
St. Francisville, LA 70775

William Mims
Tennessee Valley Authority
400 West Summit Hill Drive.
W10D199C-K
Knoxville, TN 37902

Jocelyn Mitchell
USNRC-RES/SAIB
MS: NL/S-324

Kam Mohktarian
CBI Na-Con Inc.
800 Jorie Blvd.
Oak Brook, IL 60521

James Moody
P.O. Box 641
Rye, NH 03870

S. Mori
Nuclear Safety Division
OECD Nuclear Energy Agency
38 Blvd. Suchet
75016 Paris
FRANCE

Walter B. Murfin
P.O. Box 550
Mesquite, NM 88048

Joseph A. Murphy
USNRC-RES/DSR
MS: NL/S-007

V. I. Nath
Safety Branch
Safety Engineering Group
Sheridan Park Research Community
Mississauga, Ontario L5K 1B2
CANADA

Susan J. Niemczyk
1541 18th St. NW, #112
Washington, DC 20036

Pradyot K. Niyogi
USDOE-Office of Nuclear Safety
Washington, DC 20545

Paul North
EG&G Idaho, Inc.
P. O. Box 1625
Idaho Falls, ID 83415

Edward P. O'Donnell
Ebasco Services, Inc.
2 World Trade Center, 89th Floor
New York, NY 10048

David Okrent
UCLA
Boelter Hall, Room 5532
Los Angeles, CA 90024

Robert L. Olson
Tennesree Valley Authority
400 West Summit Hill Rd.
Knoxville, TN 37902

Simon Ostrach
Case Western Reserve University
418 Glenman Bldg.
Cleveland, OH 44106

D. Paddleford
Westinghouse Electric Corporation
Savanna River Site
Aiken, SC 29808

Robert L. Palls, Jr.
USNRC-NRR/PRAB
MS: 10A-2

Chang K. Park
Brookhaven National Laboratory
Building 130
Upton, NY 11973

Michael C. Parker
Illinois Department of Nuclear
Safety
1035 Outer Park Dr.
Springfield, IL 62704

Gareth Parry
NUS Corporation
910 Clopper Road
Gaithersburg, MD 20878

J. Pelce
Departement de Surete Nucleaire
IPSN
Centre d'Estudes Nucleaires du CEA
B.P. no. 6, Cedex
F-92260 Fontenay-aux-Roses
FRANCE

G. Petrangeli
ENEA Nuclear Energy ALT Disp
Via V. Brancati, 48
00144 Rome
ITALY

Marty Plys
Fauske and Associates
16W070 West 83rd St.
Burr Ridge, IL 60521

Mike Podowski
Department of Nuclear Engineering
and Engineering Physics
RPI
Troy, NY 12180-3590

Robert D. Pollard
Union of Concerned Scientists
1616 P Street, NW, Suite 310
Washington, DC 20036

R. Potter
UK Atomic Energy Authority
Winfrith, Dorchester
Dorset, DT2 8DH
UNITED KINGDOM

William T. Pratt
Brookhaven National Laboratory
Building 130
Upton, NY 11973

M. Preat
Chef de Service Surete Nucleaire et
Assurance Qualite
TRACTEBEL
Bd. du Regent 8
B-100 Bruxells
BELGIUM

David Pyatt
USDOE
MS: EH-332
Washington, DC 20545

William Raisin
NUMAEC
1726 M St. NW
Suite 904
Washington, DC 20036

Joe Rashid
ANATECH Research Corp.
3344 N. Torrey Pines Ct.
Suite 1020
La Jolla, CA 90237

Dale M. Rasmuson
USNRC-RES/PRAB
MS: NL/S-372

Ingvard Rasmussen
Riso National Laboratory
Postbox 49
DK-4000, Roskilde
DENMARK

Norman C. Rasmussen
Massachusetts Institute of Technology
77 Massachusetts Avenue
Cambridge, MA 02139

John W. Reed
Jack R. Benjamin & Associates, Inc.
444 Castro St., Suite 501
Mountain View, CA 94041

David B. Rhodes
Atomic Energy of Canada, Ltd.
Chalk River Nuclear Laboratories
Chalk River, Ontario K0J1P0
CANADA

Dennis Richardon
Westinghouse Electric Corporation
P.O. Box 355
Pittsburgh, PA 15230

Doug Richeard
Virginia Electric Power Co.
P.O.Box 26666
Richmond, VA 23261

Robert Ritzman
Electric Power Research Institute
3412 Hillview Avenue
Palo Alto, CA 94304

Richard Robinson
USNRC-RES/PRAB
MS: NL/S-372

Jack E. Rosenthal
USNRC-AEOD/ROAB
MS: MNBB-9715

Denwood F. Ross
USNRC-RES
MS: NL/S-007

Frank Rowsome
9532 Fern Hollow Way
Gaithersburg, MD 20879

Wayne Russell
SERI
5360 I-55 North
Jackson, MS 39211

Jorma V. Sandberg
Finnish Ctr. Rad. Nucl. and Safety
Department of Nuclear Safety
P.O. Box 268
SF-00101 Helsinki
FINLAND

G. Saponaro
ENEA Nuclear Engineering Alt.
Zia V Bra atati 4B
00144 ROME
ITALY

M. Sarran
United Engineers
P. O. Box 8223
30 S 17th Street
Philadelphia, PA 19101

J. Schroeder
EG&G Idaho, Inc.
P. O. Box 1625
Idaho Falls, ID 83415

Marty Sattison
EG&C Idaho, Inc.
P. O. Box 1625
Idaho Falls, ID 83415

George D. Sauter
Electric Power Research Institute
3412 Hillview Avenue
Palo Alto, CA 94303

Jorge Schulz
Bechtel Western Power Corporation
50 Beale Street
San Francisco, CA 94119

B. R. Sehgal
Electric Power Research Institute
3412 Hillview Avenue
Palo Alto, CA 94303

Subir Sen
Bechtel Power Corp.
15740 Shady Grove Road
location 1A-7
Gaithersburg, MD 20877

S. Serra
Ente Nazionale per l'Energia
Electtrica (ENEL)
via G. B. Martini 3
Rome
ITALY

Bonnie J. Shapiro
Science Applications International
Corporation
360 Bay Street
Suite 200
Augusta, GA 30901

H. Shapiro
Licensing and Risk Branch
Atomic Energy of Canada Ltd.
Sheridan Park Research Community
Mississauga, Ontario L5K 1B2
CANADA

Dave Sharp
Westinghouse Savannah River Co.
Building 773-41A, P. O. Box 616
Aiken, SC 29802

John Sherman
Tennessee Environmental Council
1719 West End Avenue, Suite 227
Nashville, TN 37203

Brian Sheron
USNRC-RES/DSR
MS: NL/N-007

Rick Sherry
JAYCOR
P. O. Box 85154
San Diego, CA 92138

Steven G. Sholly
MNB Technical Associates
1723 Hamilton Avenue, Suite K
San Jose, CA 95125

Louis M. Shotkin
USNRC-RES/RPSB
MS: NL/N-353

M. Siebertz
Chef de la Section Surete' des
Reacteurs
CEN/SCK
Boeretang, 200
B-2400 Mol
BELGIUM

Melvin Silberberg
USNRC-RES/DE/WNB
MS: NL/S-260

Gary Smith
SERI
5360 I-55 North
Jackson, MS 39211

Gary L. Smith
Westinghouse Electric Corporation
Hanford Site
Box 1970
Richland, WA 99352

Lanny N. Smith
Science Applications International
Corporation
2109 Air Park Road SE
Albuquerque, NM 87106

K. Soda
Japan Atomic Energy Res. Inst.
Tokai-Mura Naka-Gun
Ibaraki-Ken 319-11
JAPAN

David Sommers
Virginia Electric Power Company
P. O. Box 26666
Richmond, VA 23261

Herschel Spector
New York Power Authority
123 Main Street
White Plains, NY 10601

Themis P. Speis
USNRC-RES
MS: NL/S-007

Klaus B. Stadie
OECD-NEA, 38 Bld. Suchet
75016 Paris
FRANCE

John Stetkar
Pickard, Lowe & Garrick, Inc
2216 University Drive
Newport Beach, CA 92660

Wayne L. Stiede
Commonwealth Edison Company
P.O. Box 767
Chicago, IL 60690

William Stratton
Stratton & Associates
2 Acoma Lane
Los Alamos, NM 87544

Soo-Pong Suk
Korea Advanced Energy Research Institute
P. O. Box 7
Daeduk Danji, Chungnam 302-31
KOREA

W. P. Sullivan
GE Nuclear Energy
175 Curtner Ave., M/C 789
San Jose, CA 95125

Tony Taig
U.K. Atomic Energy Authority
Wigsha · Lane, Culcheth
Warrington, Cheshire, WA3 4NE
UNITED KINGDOM

John Taylor
Electric Power Research Institute
3412 Hillview Avenue
Palo Alto, CA 94303

Harry Teague
U.K. Atomic Energy Authority
Wigshaw Lane, Culcheth
Warrington, Cheshire, WA3 4NE
UNITED KINGDOM

Technical Library
Electric Power Research Institute
P.O. Box 10412
Palo Alto, CA 94304

Mark I. Temme
General Electric, Inc.
P.O. Box 3508
Sunnyvale, CA 94088

T. G. Theofanous
University of California, S.B.
Department of Chemical and Nuclear Engineering
Santa Barbara, CA 93106

David Teolis
Westinghouse-Bettis Atomic Power Laboratory
P. O. Box 79, ZAP 34N
West Mifflin, PA 15122-0079

Ashok C. Thadani
USNRC-NRR/SAD
MS: 7E-4

Garry Thomas
L-499 (Bldg. 490)
Lawrence Livermore National Laboratory
7000 East Ave.
P.O. Box 808
Livermore, CA 94550

Gordon Thompson
Institute for Research and Security Studies
27 Ellworth Avenue
Cambridge, MA 02139

Grant Thompson
League of Women Voters
1730 M. Street, NW
Washington, DC 20036

Arthur Tingle
Brookhaven National Laboratory
Building 130
Upton, NY 11973

Rich Toland
United Engineers and Construction
30 S. 17th St., MS 4V7
Philadelphia, PA 19101

Brian J. R. Tolley
DG/XII/D/1
Commission of the European Communities
Rue de la Loi, 200
B-1049 Brussels
BELGIUM

David R. Torgerson
Atomic Energy of Canada Ltd.
Whiteshell Nuclear
Research Establishment
Pinawa, Manitoba, ROE 1LO
CANADA

Alfred F. Torri
Pickard, Lowe & Garrick, Inc.
191 Calle Magdalena, Suite 290
Encinitas, CA 92024

Klau Trambauer
Gesellschaft Fur Reaktorsicherheit
Forschungsgelande
D-8046 Garching
FERERAL REPUBLIC OF GERMANY

Nicholas Tsoulfanidis
Nuclear Engineering Dept.
University of Missouri-Rolla
Rolla, MO 65401-0249

Chao-Chin Tung
c/o H.B. Bengelsdorf
ERC Environmental Services Co.
P. O. Box 10130
Fairfax, VA 22030

Brian D. Turland
UKAEA Culham Laboratory
Abingdon, Oxon OX14 3DB
ENGLAND

Takeo Uga
Japan Institute of Nuclear Safety
Nuclear Power Engineering Test
Center
3-6-2, Toranomon
Minato-ku, Tokyo 108
JAPAN

Stephen D. Unwin
Battelle Columbus Division
505 King Avenue
Columbus, OH 43201

A. Valeri
DISP
ENEA
Via Vitaliano Brancati, 48
I-00144 Rome
ITALY

Harold VanderMolen
USNRC-RES/PRAB
MS: NL/S-372

G. Bruce Varnado
ERC International
1717 Louisiana Blvd. NE, Suite 202
Albuquerque, NM 87110

Jussi K. Vaurio
Imatran Voima Oy
Loviisa NPS
SF-07900 Loviisa
FINLAND

William E. Vesely
Science Applications International
Corporation
2929 Kenny Road, Suite 245
Columbus, OH 43221

J. I. Villadoniga Zallon
Div. of Analysis and Assessment
Consejo de Seguridad Nuclear
c/ Sor Angela de la Cruz, 3
28020 Madrid
SPAIN

Willem F. Vinck
Kapellestract 25
1980
Tervuren
BELGIUM

R. Virolainen
Office of Systems Integration
Finnish Centre for Radiation and
Nuclear Safety
Department of Nuclear Safety
P.O. Box 268
Kumpulantie 7
SF-00520 Helsinki
FINLAND

Raymond Viskanta
School of Mechanical Engineering
Purdue University
West Lafayette, IN 47907

S. Visweswaran
General Electric Company
175 Curtner Avenue
San Jose, CA 95125

Truong Vo
Pacific Northwest Laboratory
Battelle Blvd.
Richland, WA 99352

Richard Vogel
Electric Power Research Institute
P. O. Box 10412
Palo Alto, CA 94303

G. Volta
Engineering Division
CEC Joint Research Centre
CP No. 1
I-21020 Ispra (Varese)
ITALY

Ian B. Wall
Electric Power Research Institute
3412 Hillview Avenue
Palo Alto, CA 94303

Adolf Walser
Sargent and Lundy Engineers
55 E. Monroe Street
Chicago, IL 60603

Edward Warman
Stone & Webster Engineering Corp.
P.O. Box 2325
Boston, MA 02107

Norman Weber
Sargent & Lundy Co.
55 E. Monroe Street
Chicago, IL 60603

Lois Webster
American Nuclear Society
555 N. Kensington Avenue
La Grange Park, IL 60525

Wolfgang Werner
Gesellschaft Fur Reaktorsicherheit
Forschungsgelande
D-8046 Garching
FEDERAL REPUBLIC OF GERMANY

Don Wesley
IMPELL
1651 East 4th Street
Suite 210
Santa Ana, CA 92701

Detlof von Winterfeldt
Institute of Safety and Systems Management
University of Southern California
Los Angeles, CA 90089-0021

Pat Worthington
USNRC-RES/AEB
MS: NL/N-344

John Wreathall
Science Applications International Corporation
2929 Kenny Road, Suite 245
Columbus, OH 43221

D. J. Wren
Atomic Energy of Canada Ltd.
Whiteshell Nuclear Research Establishment
Pinawa, Manitoba, ROE 1LO
CANADA

Roger Wyrick
Inst. for Nuclear Power Operations
1100 Circle 75 Parkway, Suite 1500
Atlanta, GA 30339

Kun-Joong Yoo
Korea Advanced Energy Research Institute
P. O. Box 7
Daeduk Danji, Chungnam 300-31
KOREA

Faith Young
Energy People, Inc.
Dixou Springs, TN 37057

Jonathan Young
R. Lynette and Associates
15042 Northeast 40th St.
Suite 206
Redmond, WA 98052

C. Zaffiro
Division of Safety Studies
Directorate for Nuclear Safety and Health Protection
Ente Nazionale Energie Alternative
Via Vitaliano Brancati, 48
I-00144 Rome
ITALY

Mike Zentner
Westinghouse Hanford Co.
P. O. Box 1970
Richland, WA 99352

X. Zikidis
Greek Atomic Energy Commission
Agia Paraskevi, Attiki
Athens
GREECE

Bernhard Zuczera
Kernforschungszentrum
Postfach 3640
D-7500 Karlsruhe
FEDERAL REPUBLIC OF GERMANY

8523 Document Processing
3141 S. A. Landenberger [5]
3151 G. C. Claycomb
5214 D. B. Clauss
6344 E. D. Gorham
6411 D. D. Carlson
6411 R. J. Breeding
6411 D. M. Kunsman
6400 N. R. Ortiz
6410 D. A. Dahlgren
6412 A. L. Camp
6412 S. L. Daniel
6412 T. M. Hake
6413 L. A. Miller
6412 L. B. Mitchell
5412 A. C. Payne, Jr.
6613 T. T. Sype
6321 T. A. Wheeler
6412 D. W. Whitehead
6413 T. D. Brown
6413 F. T. Harper [2]
6613 R. M. Cranwell
6412 W. R. Cramond [3]
6613 R. L. Iman
6418 S. L. Thompson
6411 K. J. Maloney
6419 M. P. Bohn
6419 J. A. Lambright
5420 D. A. Powers
6402 K. D. Bergeron
4343 J. J. Gregory
6402 D. C. Williams
6453 J. S. Philbin
6460 J. V. Walker
6460A M. Berman
6463 M. P. Sherman
6471 L. D. Bustard
6473 W. A. von Riesemann
8524 J. A. Wackerly

NRC FORM 335 (2-89) NRCM 1102, 3201, 3202

U.S. NUCLEAR REGULATORY COMMISSION

BIBLIOGRAPHIC DATA SHEET

(See instructions on the reverse)

1. REPORT NUMBER (Assigned by NRC, Add Vol., Supp., Rev., and Addendum Numbers, If any.)

NUREG/CR-4551
SAND86-1309
Vol. 2, Rev. 1, Part 4

2. TITLE AND SUBTITLE

Evaluation of Severe Accident Risks:
Quantification of Major Input Parameters

Experts' Determination of Source Term Issues

3. DATE REPORT PUBLISHED

MONTH: June
YEAR: 1992

4. FIN OR GRANT NUMBER

A1322

5. AUTHOR(S)

F.T. Harper, R.J. Breeding, T.D. Brown, J.J. Gregory,
H.N. Jow, A.C. Payne, E.D. Gorham, C.N. Ames,* J.C. Helton,**
G. Boyd ***

6. TYPE OF REPORT

Technical

7. PERIOD COVERED (Inclusive Dates)

8. PERFORMING ORGANIZATION - NAME AND ADDRESS (If NRC, provide Division, Office or Region, U.S. Nuclear Regulatory Commission, and mailing address; if contractor, provide name and mailing address.)

Sandia National Laboratories
Albuquerque, NM 87185-5800

* Science Applications International Corp.
** Arizona State University
*** Safety and Reliability Optimization Services, Inc.

9. SPONSORING ORGANIZATION - NAME AND ADDRESS (If NRC, type "Same as above"; if contractor, provide NRC Division, Office or Region, U.S. Nuclear Regulatory Commission, and mailing address.)

Division of Safety Issue Resolution
Office of Nuclear Regualtory Research
U.S. Nuclear Regulatory Commission
Washington, DC 20555

10. SUPPLEMENTARY NOTES

11. ABSTRACT (200 words or less)

In support of the Nuclear Regulatory Commission's (NRC's) assessment of the risk from severe accidents at commercial nuclear power plants in the U.S. reported in NUREG-1150, the Severe Accident Risk Reduction Program (SAARP) has completed a revised calculation of the risk to the general public from severe accidents at five nuclear power plants: Surry, Sequoyah, Zion, Peach Bottom and Grand Gulf.

The emphasis in this risk analysis was not on determining a point estimate of risk, but to determine the distribution of risk, and to assess the uncertainties that account for the breadth of this distribution. Off-site risk initiation by events, both internal to the power station and external to the power station.

Much of the important input to the logic models was generated by expert panels. This document presents the distributions and the rationale supporting the distributions for the questions posed to the Source Term Panel.

12. KEY WORDS/DESCRIPTORS (List words or phrases that will assist researchers in locating the report.)

Probabilistic Risk Assessment, Reactor Safety, Severe Accidents, Source Terms, Fission Product Transport, Decontamination Factors, Revolatilization, Core Concrete Interaction Release, Fission Product Release, Late Iodine Sources

13. AVAILABILITY STATEMENT

Unlimited

14. SECURITY CLASSIFICATION

(This Page)
Unclassified

(This Report)
Unclassified

15. NUMBER OF PAGES

16. PRICE

THIS DOCUMENT WAS PRINTED USING RECYCLED PAPER

UNITED STATES
NUCLEAR REGULATORY COMMISSION
WASHINGTON, D.C. 20555-0001

OFFICIAL BUSINESS
PENALTY FOR PRIVATE USE, $300

SPECIAL FOURTH-CLASS RATE
POSTAGE AND FEES PAID
USNRC
PERMIT NO. G-67

UNITED STATES
NUCLEAR REGULATORY COMMISSION
WASHINGTON, D.C. 20555-0001

OFFICIAL BUSINESS
PENALTY FOR PRIVATE USE, $300

SPECIAL FOURTH-CLASS RATE
POSTAGE AND FEES PAID
USNRC
PERMIT NO. G-67

120555139531 1 1AN
US NRC-OADM
DIV FOIA & PUBLICATIONS SVCS
TPS-PDR-NUREG
P-211
WASHINGTON DC 20555